Altered Lipid Metabolism Associated With Insulin Resistance And Obesity Is A Major Contributor To The Onset And Progression Of Type 2 Diabetes

By

Michael James CHRISTOPHER
Bachelor of Applied Science (Applied Biology)
Graduate Diploma (Biomolecular Technologies)
Bachelor of Science (Applied Biology/Biotechnology) Honours 1st Class

In fulfillment of the degree of Doctor of Philosophy (PhD) for the Department of Medicine, Monash University

Date submitted: Friday November 21st, 2014

This thesis is dedicated to my father, the late, Henry (Bonn) Christopher and my mother, Frances Christopher.

With special dedications to Professor Frank Alford, a truly great mentor who introduced me to the world of diabetes research; and to my extraordinary partner, Marion Oakley.

TABLE OF CONTENTS

ACKNOWLEDGMENTS ..... **XV**

ABBREVIATIONS (GENERAL) ..... **XVIII**

CHAPTER 1 LITERATURE REVIEW 1

1.1 INTRODUCTION **1**

1.1.1 Link between obesity, type 2 diabetes and dyslipidaemia 1

1.2 MASS SPECTROMETRY AND LIPIDOMICS **1**

1.2.1 The quantification of lipid species using mass spectrometry 1

1.2.2 Targeted lipid profiling 2

1.2.3 Lipid biomarkers improve disease prediction and classification 4

1.2.4 Lipid nomenclature 5

1.3 LIPID ABNORMALITIES ASSOCIATED WITH OBESITY, INSULIN RESISTANCE AND TYPE 2 DIABETES **5**

1.3.1 Changing lipid profiles with progression to type 2 diabetes 5

1.3.2 Role of fatty acids, sphingolipids and diacylglyerols in insulin resistance 6

1.3.3 Elevated glycerolipids and cholesteryl esters are markers of obesity 8

1.3.4 Diet influences hepatic *de novo* lipogenesis and lipid profiles 9

1.3.5 Role of lysophosphocholines in obesity and insulin resistance 10

1.3.6 Lipid abnormalities associated with early onset insulin resistance 11

1.3.7 Other lipids implicated in the pathogenesis of type 2 diabetes 12

1.3.8 Limitations associated with human lipidomic studies 13

1.4 THE LEPTIN RECEPTOR-DEFICIENT *DB/DB* MOUSE MODEL **13**

1.4.1 Characteristics of the C57BL/KsJ obese/diabetic *db/db* mouse 13

1.4.2 Lipid and metabolic defects in *db/db* mice 14

1.4.3 Treatments targeting lipid and metabolic defects in *db/db* mice 15

1.4.4 Comparison of genetically obese *db/db* and *ob/ob* mouse models 17

1.5 RELATIONSHIP BETWEEN GENE EXPRESSION AND LIPID PROFILES IN OBESITY, INSULIN RESISTANCE AND TYPE 2 DIABETES **19**

1.5.1 Hepatic gene expression profiling and metabolic defects in *db/db* mice 19
1.5.2 Gene candidates associated with obesity, insulin resistance and type 2 diabetes . 20

1.6 STATEMENT OF THE RESEARCH PROBLEM(S) 20
1.7 CENTRAL HYPOTHESIS 21
1.8 PRIMARY GOAL 21
1.9 SPECIFIC AIMS 22

CHAPTER 2 GENERAL METHODS 23

2.1 PLASMA AND TISSUE COLLECTION FROM STUDIES 23

2.1.1 Obese/diabetic *db/db* mouse study 23
2.1.2 Human insulin resistance and obesity study 23

2.2 PREPARATION OF MOUSE LIVER FOR LIPID EXTRACTIONAND GENE EXPRESSION 24

2.2.1 Cryomilling of mouse liver 24
2.2.2 Reconstitution and sonication of mouse liver powder 24
2.2.3 Determination of total protein content in mouse liver homogenates 24

2.3 PREPARATION OF MOUSE SKELETAL MUSCLE, LEFT-VENTRICLE AND ADIPOSE TISSUE FOR LIPID EXTRACTION 25

2.3.1 Cutting, homogenisation and sonication 25
2.3.2 Determination of total protein content 25

2.4 PREPARATION OF HUMAN SKELETAL MUSCLE FOR LIPID EXTRACTION 26

2.4.1 Homogenisation, sonication and determination of protein content 26

2.5 LIPID EXTRACTION OF MOUSE AND HUMAN PLASMA AND TISSUE STOCK HOMOGENATES 26

2.5.1 Lipid extraction protocol 26
2.5.2 Lipid extraction method 27
2.5.3 Established targeted lipid profiling methodology 27
2.5.4 Acquisition of comparative lipidomic data 28

2.6 STATISTICAL ANALYSES **30**

CHAPTER 3 ESTABLISHMENT OF TARGETED LIPID PROFILING METHODOLOGY TO CHARACTERISE LIPID SPECIES IMPLICATED IN THE PATHOGENESIS OF TYPE 2 DIABETES 31

3.1 INTRODUCTION **31**

3.1.1 Expansion of established targeted lipid profiling methodology 31
3.1.2 Evidence that phosphatidylethanolamines, ether-phospholipids and lysophospholipids are associated with type 2 diabetes 31
3.1.3 Chemical and structural features of cardiolipins 34
3.1.4 Role of cardiolipins in mitochondrial dysfunction and diabetes 35
3.1.5 Measurement of cardiolipin species by mass spectrometry in positive ion mode 36

3.2 MATERIALS AND METHODS **37**

3.2.1 Optimisation of mass spectrometer acquisition parameters for lipid standards 37
3.2.2 Identification of phosphatidylethanolamine, ether-phospholipid and lysophospholipid species in human plasma 38
3.2.3 Identification of cardiolipin species in human plasma and mouse tissues 41

3.3 RESULTS **42**

3.3.1 Optimal API 4000 Q/TRAP mass spectrometer acquisition parameters and voltages for lipid standards 42
3.3.2 Phosphatidylethanolamine, ether-phospholipid and lysophospholipid species identified in human plasma 45
3.3.3 Fatty acid composition of lipid species in human plasma 50
3.3.4 Cardiolipin species identified in human plasma and mouse tissues 53
3.3.5 Full coverage of the 20 most abundant cardiolipin species in mouse tissues 53

3.4 DISCUSSION **60**

3.4.1 Targeted lipid profiling of PE, PE(O), PE(P) and LPE species 63
3.4.2 Targeted lipid profiling of CL species in positive ion mode 64
3.4.3 Conclusion 65

CHAPTER 4 CHARACTERISATION OF PLASMA AND TISSUE LIPID PROFILES IN A MOUSE MODEL OF TYPE 2 DIABETES 67

4.1 INTRODUCTION **67**

4.1.1 The *db/db* genetic mouse model 67
4.1.2 Progression of disease in the homozygous C57BL/KsJ *db/db* mouse 67
4.1.3 Other metabolic abnormalities associated with the *db/db* mice 68
4.1.4 Lipidomic analysis of plasma and metabolic tissues in obesity, insulin resistance and type 2 diabetes 69

4.2 MATERIALS AND METHODS **69**

4.2.1 Mouse genotypes 69
4.2.2 Diet, health monitoring and metabolic tests 70
4.2.3 Collection of plasma and tissues from mice at time of cull 70
4.2.4 Laboratory Analyses 72
4.2.5 Lipid analysis of mouse tissues and plasma 72
4.2.6 Statistical analyses 73

4.3 RESULTS **75**

4.3.1 Body composition, biochemical and metabolic characteristics in female mice 75
4.3.2 Body composition, biochemical and metabolic characteristics in male mice 78
4.3.3. Assay performance of lipid measurements 82
4.3.4 Early changes in plasma and tissue lipid profiles in *db/h* mice 85
4.3.5 Dominant effect of genotype, and not gender or age, on global lipid profiles 88
4.3.6 Relationship between gender and global lipid profiles 88
4.3.7 Relationship between age and global lipid profiles 92
4.3.8 Relationship between genotype and global lipid profiles 94
4.3.9 Comparison of lipid classes and species in *db/db* vs. *H/H* mice 97
4.3.10 Fatty acid composition of elevated triacylglycerol species in *db/db* mice 122
4.3.11 Role of hepatic *de novo* lipogenesis in the supply of circulating fatty acids 124

4.4 DISCUSSION **128**

4.4.1 The *db/db* mouse represents a progressive model of type 2 diabetes 128

4.4.2 Genotype, rather than gender or age, is the dominant effect on mouse lipid profiles 129
4.4.3 Higher inter-animal variance in lipid levels in male *db/db* mice prevents detection of early lipid abnormalities in tissues 130
4.4.4 Metabolic pathway maps for plasma, liver and left-ventricle in male *db/db* mice 131
4.4.5 Differential elevation of glycerolipids and cholesteryl esters in plasma and tissues of *db/db* mice 131
4.4.6 Relationship between saturated fatty acids, inflammation, sphingolipid synthesis and insulin resistance 140
4.4.7 Differential regulation of the major glycerophospholipids in plasma and liver of *db/db* mice 143
4.4.8 Cardiolipin remodelling is associated with oxidative stress, obesity and diabetes 149
4.4.9 Ether- and vinyl ether-linked phospholipids are differentially regulated in plasma and tissues of *db/db* mice 151
4.4.10 Early elevation of lysophospholipids in plasma of *db/db* mice 153
4.4.11 Conclusion 156

CHAPTER 5 RELATIONSHIP BETWEEN GLOBAL GENE EXPRESSION AND LIPID PROFILES IN A MOUSE MODEL OF TYPE 2 DIABETES 160

5.1 INTRODUCTION 160

5.1.1 The genetic *db/db* mouse model resembles human type 2 diabetes 160
5.1.2 Identification of genes associated with lipid abnormalities in *db/db* mice 160
5.1.3 Role of the liver in the pathogenesis of type 2 diabetes 161
5.1.4 Gene expression profiling tracks hepatic metabolic defects in type 2 diabetes 161
5.1.5 Tracking of gene expression and lipid profiling abnormalities in *db/db* mice 162

5.2 MATERIALS AND METHODS 163

5.2.1 Global gene expression profiling in mouse liver using DNA microarrays 163
5.2.2 Preparation of mouse liver samples for total RNA extraction 163
5.2.3 Mouse whole-genome gene expression direct hybridization assay 164
5.2.4 Liver gene expression profiling and data analysis 169

5.2.5 Strategy linking liver gene expression and lipid profiling abnormalities.....170

5.3 RESULTS.....170

5.3.1 Differential liver gene expression in all male *db/db* versus male *H/H* mice.....170
5.3.2 Differential liver gene expression in male *db/db* mice at each age.....173
5.3.3 Effect of ageing on differential liver gene expression in male *db/db* and male H/H mice.....174
5.3.4 Liver genes associated with lipid pathway/diabetes-specific disease states in all male *db/db* mice.....177
5.3.5 Liver genes associated with lipid pathway/diabetes-specific disease states in male *db/db* mice at 10 and/or 16 weeks of age.....177
5.3.6 Twenty-one liver genes are associated with lipid pathway/diabetes-specific disease states in male *db/db* mice at both 10 and 16 weeks of age.....180
5.3.7 Correlation of lipid classes/subclasses with differentially expressed genes linked to lipid pathway/diabetes-specific disease states in male *db/db* mice.....182

5.4 DISCUSSION.....185

5.4.1 Biomarker genes associated with metabolic defects in male *db/db* mice at 6 weeks of age.....185
5.4.2 Upregulation of hepatic fatty acid oxidation, lipogenesis, glycerolipid and glycerophospholipid synthesis in male *db/db* mice at 10 weeks of age.....186
5.4.3 Upregulation of hepatic fatty acid oxidation/storage is linked to impaired insulin signalling and inflammation in male *db/db* mice at 16 weeks of age.....188
5.4.4 Upregulation of fatty acid and glucose metabolic pathways is associated with stimulation of glucocorticoids in male *db/db* mice.....189
5.4.5 Correlations between liver lipid classes/subclasses and differentially expressed genes associated with lipid pathways in male *db/db* mice.....190
5.4.6 Differentially expressed mouse genes in male *db/db* mice are candidate genes for human obesity and type 2 diabetes.....191
5.4.7 Conclusion.....192

CHAPTER 6 CHARACTERISATION OF PLASMA AND SKELETAL MUSCLE LIPID PROFILES IN HUMAN INSULIN RESISTANCE AND OBESITY.....194

6.1 INTRODUCTION 194

6.1.1 Insulin resistance, obesity and lipid abnormalities contribute to type 2 diabetes 194
6.1.2 Early metabolic defects in the pathogenesis of type 2 diabetes 194
6.1.3 Plasma lipid abnormalities associated with insulin resistance, obesity and type 2 diabetes 195
6.1.4 The Human insulin resistance and obesity study 196

6.2 MATERIALS AND METHODS 197

6.2.1 Classification of study participants 197
6.2.2 Anthropometric, body composition and insulin clamp measurements 198
6.2.3 Blood collection and muscle biopsies 199
6.2.4 Biochemical analysis 200
6.2.5 Plasma and skeletal muscle lipid analysis 200
6.2.6 Statistical analyses 200

6.3 RESULTS 203

6.3.1 Subject characteristics at baseline and during steady-state insulin clamp 203
6.3.2 Assay performance of lipid measurements 205
6.3.3 Lipids associated with obesity, insulin resistance and type 2 diabetes 205
6.3.4 Lipids associated with measures of insulin sensitivity 207
6.3.5 Lipids associated with body mass index and measures of glycaemia 209
6.3.6 Comparison of steady-state clamp and fasting plasma lipids 210

6.4 DISCUSSION 210

6.4.1 Different lipid abnormalities are associated with obesity and insulin resistance 210
6.4.2 Lipid abnormalities associated with obesity 212
6.4.3 Lipid abnormalities associated with insulin resistance 213
6.4.4 Lipid abnormalities associated with combined obesity and insulin resistance ... 214
6.4.5 Lipid abnormalities associated with type 2 diabetes 216
6.4.6 Obesity-induced lipid abnormalities drive insulin resistance and type 2 diabetes 219
6.4.7 Plasma triacylglycerol species are predictive of insulin resistance 220

6.4.8 Plasma triacylglycerol species are predictive of combined obesity/insulin resistance and type 2 diabetes 222
6.4.9 Steady-state clamp plasma glycerolipids and cholesteryl esters are associated with insulin resistance 222
6.4.10 Insulin clamp-induced suppression of plasma lipid classes/subclasses differs in obesity, insulin resistance and type 2 diabetes 223
6.4.11 Conclusion 224

CHAPTER 7 GENERAL DISCUSSION 227

7.1 DISCUSSION 227

7.1.1 Identification and characterisation of altered lipid metabolism in type 2 diabetes using a systems biology approach 227
7.1.2 Global lipid profiles and gene expression are associated with different stages of obesity insulin resistance and type 2 diabetes 227
7.1.3 Early elevation of hepatic *de novo* lipogenesis in *db/db* mice and humans 228
7.1.4 Triacylglycerol species are potential risk factors for obesity, insulin resistance and type 2 diabetes 231
7.1.5 Phosphatidylcholine species are potential risk factors for obesity, insulin resistance and type 2 diabetes in *db/db* mice 232
7.1.6 Early pathological cardiolipin remodelling and possible drug intervention strategies 234
7.1.7 Comparison of lipid abnormalities associated with obesity in humans and *db/db* mice 235
7.1.8 Comparison of lipid abnormalities associated with insulin resistance in humans and *db/db* mice 236
7.1.9 Liver genes linked to lipid metabolic pathway/diabetes-specific disease states in male *db/db* mice 237
7.1.10 Final thesis synopsis 238

REFERENCES 240
APPENDICES 254

ABSTRACT

The Australian population and indeed most of the developed world are facing an obesity epidemic, which is associated with a dramatic increase in the incidence of type 2 diabetes (T2D). Obesity and insulin resistance (IR) are strong predictors of the development of T2D. Dyslipidaemia as assessed by "traditional" measures (raised plasma triglycerides and/or decreased high-density lipoprotein cholesterol) is also a major risk factor for the onset and progression of T2D. However, the measurement of a few circulating "classical" lipids and lipoproteins alone does not adequately represent the hundreds of lipids in the circulation and tissues that may be associated with the pathogenesis of T2D.

Initially, targeted lipid profiling methodology was developed to characterise lipid species that are implicated in the pathogenesis of T2D. These methods resulted in 60 species from the phosphatidylethanolamine, alkylphosphatidylethanolamine, alkenylphosphatidylethanolamine, lysophosphatidylethanolamine and cardiolipin classes/subclasses being added to the ~270 lipid species representing 20 lipid classes/subclasses that are routinely measured in our laboratory using reverse phase high performance liquid chromatography combined with electrospray ionization tandem mass spectrometry (LC ESI-MS/MS) and established multiple reaction monitoring experiments in positive ion mode.

Comprehensive lipidomic analysis was then performed to compare temporal (6, 10 and 16 weeks of age) and tissue-specific (plasma, liver, skeletal muscle, left-ventricle and adipose) lipid abnormalities in male and female leptin receptor-deficient homozygous *db/db* mice with a C57BL/KsJ background (an established monogenic model of diabetes) and their less affected heterozygous (*db/h*) and control (*H/H*) littermates. The independent effect of the *db/db* genotype on plasma and tissue lipid abnormalities was clearly superior to the separate effects of gender and age. There was a myriad of temporal and tissue-specific lipid abnormalities in *db/db* mice (versus corresponding *H/H* mice) associated with early elevations of surrogate measures of hepatic *de novo* lipogenesis and cardiolipin remodelling, but also with increasing oxidative stress and severity of disease. Using DNA microarray analysis with mouse whole-genome gene expression WG-6 version 2.0 BeadChips, 68 differentially expressed genes in the livers of male *db/db* mice (versus male *H/H* mice, with ages combined) were found to be linked to lipid pathway/diabetes-specific disease states. Correlation analyses revealed that elevated triacylglycerol and lysophosphaethanolamine classes/subclasses were significantly correlated

with 24 and 20 genes respectively, and that many of these differentially expressed liver genes have been identified as candidate genes for human T2D.

Finally, in a human study in which 80 adults were classified as lean, overweight-to-obese and insulin sensitive, overweight-to-obese and insulin resistant, or T2D, there was a gradation of fasting plasma lipid abnormalities associated with obesity, IR and combined obesity/IR, but ~85% of the lipid abnormalities in T2D subjects (versus lean group) were already present in the combined obesity/IR group prior to the onset of T2D. Some of these lipid abnormalities also occurred in the *db/db* mice.

Taken together, these studies improve our understanding of the biological interplay that exists between lipid abnormalities, obesity and IR, and provide more opportunities to identify new therapeutic targets and possible lipid biomarkers for early detection and prevention of disease progression.

DECLARATION

I declare that the thesis comprises only my original work and all other materials used are duly acknowledged in the thesis. The thesis is not more than 100,000 words in length.

_____

Michael James CHRISTOPHER

ACKNOWLEDGMENTS

I am deeply indebted to my supervisor Associate Professor Peter Miekle (Head of Metabolomics – Baker IDI) for his guidance and critique throughout the course of my research and writing of this thesis and giving me this opportunity to extend my skills and knowledge within the diabetes/obesity paradigm . This gratitude I also extend to my co-supervisor Professor Josephine Forbes (Glycation and Diabetes Laboratory – Baker IDI and Mater Medical Institute Queensland University) for her experienced comments and background and contribution of the research material (subjects) for this thesis and to Dr. Brooke Harcourt for her supporting role.

To Dorit Samocha-Bonet (Group Leader, Diabetes & Metabolism Division – Garvan Institute of Medical Research) I am indebted for the opportunity to collaborate in the Human Study and for her comments during the writing of this thesis.

Together with their friendship, I thank Dr.Chris Barlow and Jacqui Weir for imparting all their expert knowledge on the machinations of the mass spectrometer and all its intricacies.

To the staff of the Genomics and Systems Biology laboratory led by Dr. Kiymet Bozaoglu thank you for your supporting role in teaching me the finer, 'glassier' points of gene expression.

A special thank you goes to Dr. Ross Lazarus (Computational Biology) for sharing his knowledge and understanding of the complexities of the gene expression results and to Dr. Gerard Wong and Dr. Piyushkumar Mundra (Metabolomics) for their commitment (friendship) and support with the statistical analyses.

The following people also provided assistance with either statistics or laboratory support to whom I am equally grateful: Kevin Huynh and Ricardo Tan; and Dr. Clinton Bruce (Cellular and Molecular Metabolism).

To all my other colleagues from the Metabolomics Department thank you for your friendship and support which sustained me throughout: (Michelle Cinel and Natalie Mellett; Zahir Alshehry and Anmar Anwar).

To my family, Louise, Shane, Ben and Glenda – thank you all for your undying support and for willing me on across the finish line, and, to Marion who lit the tunnel throughout.

PUBLICATIONS

Peter J. Meikle and Michael J. Christopher (2011) Lipidomics is providing new insight into the metabolic syndrome and its sequelae. Current Opinion in Lipidology 22:210–215

Peter J. Meikle, Gerard Wong, Despina Tsorotes, Christopher K. Barlow, Jacquelyn M. Weir, Michael J. Christopher, Gemma L. MacIntosh, Benjamin Goudey, Linda Stern, Adam Kowalczyk, Izhak Haviv, Anthony J. White, Anthony M. Dart, Stephen J. Duffy, Garry L. Jennings and Bronwyn A. Kingwell (2011) Plasma Lipidomic Analysis of Stable and Unstable Coronary Artery Disease. Arterioscler Thromb Vasc Biol 31:2723-2732

Leonie K Heilbronn, Adelle CF Coster, Lesley V Campbell, Jerry R Greenfield, Kylie Lange, Michael J Christopher, Peter J Meikle and Dorit Samocha-Bonet (2013) The effect of short term overfeeding on serum lipids inhealthy humans. Obesity 21:E649–E659

Part of the work in the thesis was presented at the following meetings:

PRESENTATIONS AT CONFERENCES

2nd Australian Symposium on Metabolomics. The Sebel, Albert Park, Melbourne, 3-5 October 2010

The 1st Frontiers in Obesity and Diabetes Research (sponsored by Monash University and Diabetes Institute). Royal Society of Victoria, Melbourne, 18-20 September 2011

ABBREVIATIONS (GENERAL)

ANCOVA, analysis of covariance
AMPK, AMP-dependent protein kinase
BMI, body mass index
CollE, collision energy
CXP, collision exit potential
CID, collision-induced dissociation
DP, declustering potential
DHA, docosahexaenoic acid
DEXA, dual energy X-ray absorptiometry
EPA, eicosapentaenoic acid
EP, entrance potential
FA, fatty acid
FFA, free fatty acids
FFM, fat-free mass
GIR, glucose infusion rate
HDL, high density lipoprotein
HFD, high-fat diet
HOMA-IR, homeostasis model assessment of insulin resistance
11β-HSD1, 11β-hydroxysteroid dehydrogenase type 1
IL-6, interleukin-6
IMTG, intramyocellular triglyceride
IR, insulin resistant
IS, insulin sensitive
KEGG, Kyoto Encyclopaedia of Genes and Genomes
LC, liquid chromatography
LC ESI-MS/MS, liquid chromatography electrospray ionisation tandem mass spectrometry
LDL, low density lipoprotein
Lean/IS, lean insulin-sensitive
MRM, multiple reaction monitoring
MS, mass spectrometry
NAFLD, non-alcoholic fatty liver disease
NL, neutral loss
NGT, normal glucose tolerant
NEFA, non-esterified fatty acid
NS, non-significant
OGTT, oral glucose tolerance test
Ov-ob/IS, overweight-to-obese, insulin sensitive
Ov-ob/IR, overweight-to-obese, insulin resistant
PBS, phosphate buffered saline
%CV, percent coefficient of variance
PPAR, peroxisome proliferator-activated receptor
PCA, principal component analysis
PUFA, polyunsaturated fatty acid
Q1, first quadrupole
Q2, second quadrupole
Q3, third quadrupole
QC, quality control
ROS, reactive oxygen species

STAT3, signal-transducer and activator of transcription 3
SS, steady-state
SCD1, stearoyl CoA desaturase 1
T2D, type 2 diabetes
TNF-α, tumour necrosis factor-α
VLDL, very low density lipoprotein
WHR, waist-to-hip ratio

ABBREVIATIONS (LIPID CLASSES AND SUBCLASSES)

BMP, bis(monoacylglycerol)phosphate
Cer, ceramide
CE, cholesteryl ester
CL, cardiolipin
COH, free cholesterol
DG, diacylglycerol
dhCer, dihydroceramide
DHC, dihydrosylceramide
GM3, ganglioside
LPC, lysophosphatidylcholine
LPC(O), lysoalkylphosphatidylcholine
LPE, lysophosphatidylethanolamine
MHC, monohydrosylceramide
PC, phosphatidylcholine
PC(O), alkylphosphatidylcholine
PC(P), alkenylphosphatidylcholine
PE, phosphatidylethanolamine
PE(O), alkylphosphatidylethanolamine
PE(P), alkenylphosphatidylethanolamine
PG, phosphatidylglycerol
PI, phosphatidylinositol
PS, phosphatidylserine
SM, sphingomyelin
TG, triacylglycerol
THC, trihydrosylceramide

CHAPTER 1 LITERATURE REVIEW

1.1 INTRODUCTION

1.1.1 Link between obesity, type 2 diabetes and dyslipidaemia

The Australian population and indeed most of the developed world are facing an obesity epidemic, which is associated with a dramatic increase in the incidence of type 2 diabetes (T2D) and its precursors, impaired fasting glucose and/or impaired glucose tolerance. Global estimates of the prevalence of diabetes indicate that there were 285 million adults with diabetes in the year 2010, which is expected to rise to 439 million by 2030 [1]. These figures include type 1 and type 2, diagnosed and undiagnosed diabetes, and relate to adults aged 20-79. If the current rates of mortality and diabetes incidence continue, the prevalence of diabetes in Australia is projected to rise from 7.6% in 2000 to 11.4% by 2025, with the number of cases of diabetes doubling from one million in 2010 to two million by 2025 [2]. Obesity and insulin resistance (IR) are strong predictors of the development of diabetes in many populations [3].

Dyslipidaemia as assessed by "traditional" measures [raised plasma triglycerides and low-density lipoprotein (LDL)-cholesterol, and decreased high-density lipoprotein (HDL)-cholesterol] is not only a major risk factor for the onset and progression of diabetes, but is also associated with inflammation and/or oxidative stress [4,5]. Dyslipidaemia is known to be caused by obesity, a high-fat diet, physical inactivity, smoking, hypothyroidism, and several inherited genetic disorders. However, the measurement of these "classical" lipids and lipoproteins alone does not adequately represent the complex lipid abnormalitiesin the circulation and tissues that may be associated with the pathogenesis of T2D.

1.2 MASS SPECTROMETRY AND LIPIDOMICS

1.2.1 The quantification of lipid species using mass spectrometry

Lipidomics is a branch of metabolomics that involves the characterisation and quantification of all lipid molecular species within a biological system [6]. Mass spectrometry is capable of analysing hundreds of lipid species from a single sample collected from blood, tissues, cells or

organelles [7,8]. One study designed to systematically map the mammalian plasma lipidome using high-resolution liquid and gas chromatography coupled with mass spectrometry (MS) was able to quantify almost 600 distinct "non-classical" lipid species in human plasma [8]. Among these were 73 glycerolipid species and 36 sterol lipid species which contribute to the measurements of total triglycerides and total cholesterol respectively.

Essentially, a mass spectrometer measures the mass of molecules that have been electrically charged (ions), and a "lipid profile" is a mass spectrum of all the measured lipids contained in a lipid extract. More particularly, well-established separation techniques such as gas chromatography and high pressure liquid chromatography (HPLC), combined with advances in soft-ionisation mass spectrometry such as electrospray ionisation tandem mass spectrometry (ESI-MS/MS), have enabled the rapid and sensitive detection of a large number of lipid species (including low abundance lipids) with minimal sample preparation [6].

In a multisector mass spectrometer, such as a triple quadrupole instrument, the most common methods of analysing lipid molecules are product ion scanning, precursor ion scanning and neutral loss ion scanning [6]. Product ion scanning (daughter scan) is used to analyse the masses of the fragments generated from collision-induced dissociation (occurs in the second quadrupole) of a selected parent ion of interest. Opposite in action to product ion scanning, precursor ion scanning (parent scan) is used to analyse the mass-to-charge ratio (*m/z*) of precursor ions that generate a selected daughter ion (fragment) of interest. A similar type of analysis is neutral loss scanning, whereby the second mass analyzer (third quadrupole) detects daughter ions that are a specified mass smaller than the parent ion scanned in the first mass analyzer (first quadrupole).

1.2.2 Targeted lipid profiling

Targeted lipid profiling combines liquid chromatography with multiple reaction monitoring (MRM) experiments and stable isotope or non-physiological internal standards to potentially quantify hundreds of known lipids with known fragmentation profiles with high sensitivity, precision and accuracy [6,7,8]. With any MRM experiment, the first mass analyser remains static at the *m/z* for a known parent ion (e.g. the protonated parent ion, phosphatidylethanolamine 34:2$[M+H]^+$, has a *m/z* value of 716.5), and the second mass analyser remains static at a known $[M+H]^+$ daughter ion with a *m/z* value of 575.5 (generated by the

neutral loss of 141.0 Da, equivalent to the mass of the phosphoethanolamine head group). MRM experiments can be performed on multiple parent and daughter ion combinations in a single HPLC run. Stable isotopes or non-physiological standards representing the same lipid class/subclass that have a different parent ion mass but the same fragmentation profile are used as internal standards for quantitative analysis. A typical MRM experiment (using tandem mass spectrometry) on a triple quadrupole instrument is shown in Figure 1.1.

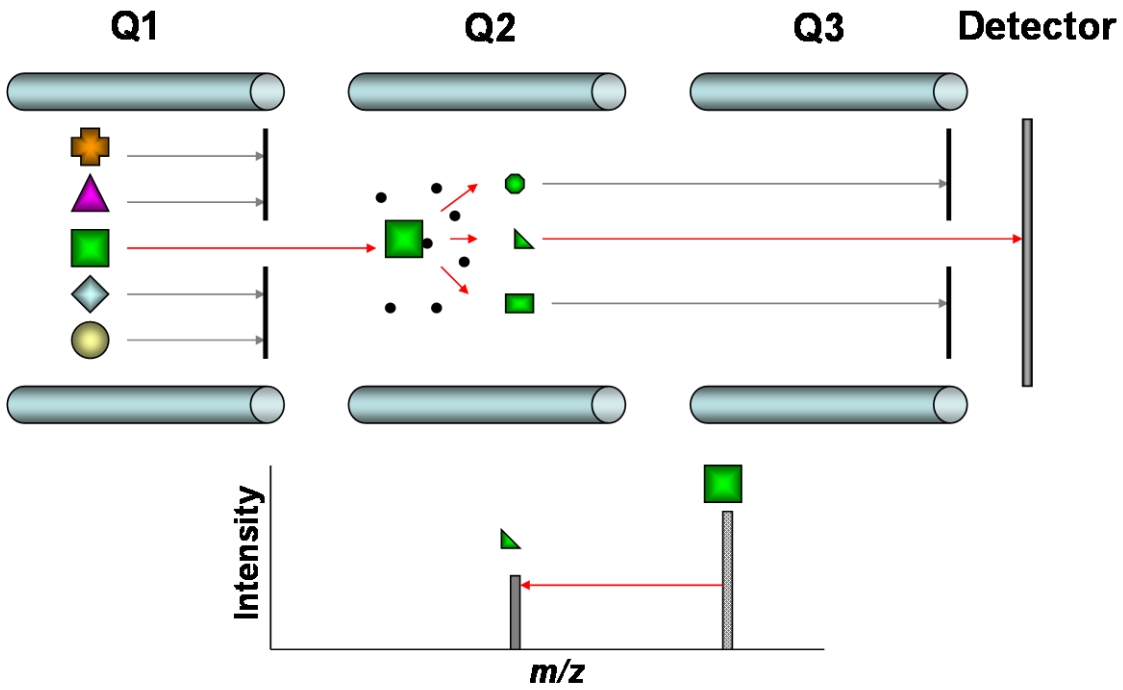

Figure 1.1 A typical multiple reaction monitoring experiment to analyse lipids on a triple quadrupole mass spectrometer. The first mass analyser (first quadruple, Q1) remains static at the *m/z* for a selected parent ion. This parent ion undergoes collision-induced dissociation in the second quadrupole (Q2). The second mass analyser (third quadruple, Q3) remains static at the *m/z* of a selected daughter ion, and a signal is detected.

LC ESI-MS/MS and MRM experiments have been used in our laboratory to identify and characterise 259-312 individual lipid species representing 20-23 classes/subclasses in human plasma samples at least to the bond type level (i.e., according to whether the species has an acyl, alkyl or alkenyl bond linkage to the glycerol backbone) using neutral loss and precursor ion scans [9,10,11]. While product ion scans in negative mode can provide additional information on the fatty acid chain length and number of double bonds present in each fatty acyl chain (e.g. diacylglycerol (DG) 16:1/18:1, triacylglycerol (TG) 16:1/18:1/18:2), they do not provide

empirical evidence on either the position of the acyl chains on the glycerol backbone (i.e., *sn*-1, *sn*-2 or *sn*-3) or the position of the double bonds within the acyl chain (e.g. 9Z or 11Z). Recently, mass spectrometry-based experiments have successfully been developed to obtain further structural information on both these points [12]. Despite the limitations of individual lipidomic analyses, the quantification of lipid classes/subclasses and individual lipid species containing different fatty acids associated with each lipid glycerol backbone by LC ESI-MS/MS allows comparison of the levels of saturated, monounsaturated and polyunsaturated fatty acids in each lipid pool [11].

1.2.3 Lipid biomarkers improve disease prediction and classification

One of the benefits of measuring multiple lipid species using mass spectrometry is that the incorporation of lipid biomarkers into classification models can better predict or classify specific disease states than traditional measures. Meikle *et al.* revealed that classification models incorporating the top 20 ranked features from "non-classical" circulating lipid species and traditional risk factors for coronary artery disease provided improved classification of unstable coronary artery disease from stable coronary artery disease than models containing only 11 traditional risk factors (including cholesterol, HDL-cholesterol, triglycerides and the very strong determinants, C-reactive protein and systolic blood pressure) [10]. Another study found that particular lipid species (mainly TG) with lower carbon number and double bond content were associated with increased risk of T2D, and correlated with IR [13].

Therefore, plasma lipid profiling, defined as the quantification of multiple individual lipid species, provides the opportunity to focus on individual lipid species or groups of lipids as potential biomarkers for disease classification and as risk factors for specific disease states (for example, T2D). In this regard, improved risk assessment tools could be developed to predict an individual's risk of developing T2D, and to allow early detection and implementation of early lifestyle and pharmaceutical intervention to prevent or reduce the risk of progression to T2D [14,15]. The measurement of changes in the levels of multiple "non-classical" lipid classes and species in plasma and tissues with the onset and progression of T2D, combined with an understanding of the underlying changes in lipid metabolism, pathways and biological functions will provide the necessary foundation for the development of new tests to identify those individuals at increased risk of developing T2D.

1.2.4 Lipid nomenclature

It is impractical to attempt to fully elucidate the composition of every isomeric lipid species when high throughput targeted lipid profiling is required to perform comparative lipidomic analysis of large population cohorts. The limited structural elucidation of lipid species identified and characterised in our laboratory is reflected in the nomenclature. We have tried to remain consistent with the nomenclature proposed by the International Lipid Classification and Nomenclature Committee [16], which was updated in 2009 [17] and is available online on the LIPID MAPS website (http://www.lipidmaps.org). Although some ambiguity may exist with the nomenclature, particularly the abbreviated names given to some lipid classes/subclasses, we have tried to follow the rule of reflecting the structural information obtained in the particular experiment. For example, phospatidylcholine (PC) species are reported at the level of bond type level (i.e., acyl, alkyl or alkenyl), with the sum of the number of carbons in the two esterified fatty acids and the sum number of double bonds (e.g. PC 36:3). In addition, DG and TG species are reported at the fatty acyl/alkyl level (DG 16:1/18:1, TG 16:1/18:1/18:2), but not at the fatty acyl/alkyl position level. In the case of sphingomyelin (SM) species, we assumed that the major sphingoid backbone in SM species was dihydroxy (d18:1) sphingosine, even though the precursor ion scan of *m/z* 184.1 for SM analysis was only indicative of the phosphocholine head group (e.g. SM 38:1). The abbreviations used for the measured lipid class/subclasses are shown in the Abbreviations section of this thesis.

1.3 LIPID ABNORMALITIES ASSOCIATED WITH OBESITY, INSULIN RESISTANCE AND TYPE 2 DIABETES

1.3.1 Changing lipid profiles with progression to type 2 diabetes

When performing lipidomic analysis to determine lipid abnormalities associated with obesity, IR and/or T2D, there are many variables that may explain the differences observed in the relative abundance and direction of change in some lipid classes/subclasses and individual species between groups. It is likely that the severity of disease in each individual, along with genetic background, gender, age, environmental factors (diet, physical activity, lifestyle and medications), use of appropriate control groups, heterogenous nature of the disease, number of subjects, and type of statistical tests may influence whether a particular lipid species is significantly elevated or reduced in obese/IR subjects compared with a lean healthy control

group. Therefore, it is critical to reduce the influence of confounding variables on lipidomic analyses by matching each group closely for clinical measures [e.g. age, sex, genotype, body mass index (BMI)], and using an appropriate but stringent statistical test that adjusts for appropriate covariates and corrects the *P*-value for multiple comparisons (e.g. the number of measured lipids).

Even with all of these safeguards in place, the same lipid species may be significantly reduced with acute IR to protect the cell against the initial metabolic insult, but gradually increase with chronic exposure to IR. Most studies compare one-off samples in treatment and control groups, effectively determining lipid abnormalities that occur at a snapshot in time in the disease process. The power of comparing multiple lipid abnormalities in sequential samples from plasma and different tissues before and during the onset and progression of IR and T2D cannot be underestimated, as it allows investigation of the complex relationships that exist between lipid dysregulation, lipid metabolic pathways and disease progression.

1.3.2 Role of fatty acids, sphingolipids and diacylglyerols in insulin resistance

Despite the complexity of the metabolic phenotype associated with the development of obesity, IR and T2D, the mechanism of action and direction of change of some lipid classes/subclasses with disease progression is well understood. There are two mechanisms by which the oversupply of nutrients (obesity) antagonizes insulin action in peripheral tissues. Firstly, when adipocytes exceed their storage capacity, fats begin to accumulate in ectopic tissues (e.g. liver, skeletal muscle, heart, pancreatic β-cells), leading to the formation of putative intermediates [long-chain fatty acyl-CoA, ceramide (Cer), DG] that inhibit insulin signal transduction. Secondly, obesity triggers a chronic inflammatory state and cytokines, released from adipocytes and/or macrophages that infiltrate adipose tissue, antagonize insulin action [18]. However, not all obese patients develop IR, and many are normal glucose tolerant (NGT) with a low risk of developing T2D.

Circulating factors associated with obesity [e.g. increased saturated fatty acids (FA) such as palmitate (16:0) and stearate (18:0), and inflammatory cytokines such as tumour necrosis factor (TNF)-α and interleukin (IL)-6] selectively induce enzymes that synthesise sphingolipids (e.g. Cer and/or its derivatives GM3 gangliosides and sphingosine), which antagonize insulin signalling, induce oxidative stress, inhibit glucose uptake and storage [19], and contribute to

pancreatic β-cell failure, cardiomyopathy, hypertension, diabetes and atherosclerosis [20]. There are two distinct mechanisms by which Cer accumulation in insulin-sensitive tissues can inhibit insulin action. Firstly, Cer specifically blocks the translocation of Akt/PKB to the plasma membrane, and secondly, Cer stimulates the dephosphorylation of Akt/PKB by protein phosphatase 2 [21]. However, pharmacological inhibition of *de novo* Cer synthesis (by myriocin or fumonisin B1) ameliorates the IR induced by corticosteroids, saturated fats, and genetic models of obesity [19]. In contrast, unsaturated FAs [e.g. linoleate (18:2)] induce IR by Cer-independent mechanisms involving, for example, DG-activated protein kinase C isoforms or phosphatidic acid [22]. Notably, in Wistar rats fed either standard rat chow, high-polyunsaturated FA diet or high-saturated FA diet for 5 weeks ad libitum, the Cer content did not change in any muscle in the polyunsaturated FA diet group, but increased by 46% and 52% respectively in the soleus and red gastrocnemius (and was unchanged in white gastrocnemius) in the high-saturated FA diet group [23]. Therefore, the regulation of Cer levels depends on the diet (FA composition) and type of skeletal muscle.

In NGT male subjects, a strong negative correlation was found between fasting skeletal muscle total Cer (and several Cer species) content and insulin sensitivity, independently of BMI, waist-to-hip ratio, percent body fat, and fasting plasma glucose, insulin, FFA, cholesterol and triglyceride levels [24]. In contrast, there were marked positive correlations between fasting skeletal muscle total SM and BMI, waist-to-hip ratio, and percent body fat, but no association with insulin sensitivity. Moreover, Haus *et al.* showed that elevated fasting plasma levels of total Cer and several Cer species in obese/T2D subjects compared with lean healthy subjects may contribute to IR through activation of inflammatory mediators, such as TNF-α [25].

Using logistic regression analyses, adjusted for multiple covariates, Meikle *et al.* found that both prediabetes and T2D were positively associated with the Cer, dihydroceramide (dhCer), DG, TG, cholesteryl ester (CE), phosphatidylethanolamine (PE), phosphatidylglycerol (PG) and phosphatidylinositol (PI) classes/subclasses in fasting plasma, and negatively associated with the dihexosylceramide (DHC), trihexosylceramide (THC) and alkylphosphatidylcholine (PC(O)) subclass in two large human cohorts (versus NGT subjects) [9]. However, there was no association of other sphingolipid subclasses [i.e., monohexosylceramide (MHC), GM3 ganglioside or SM)] with prediabetes (i.e., patients with impaired fasting glucose and/or impaired glucose tolerance) and T2D. These findings suggest that there was an upregulation of

de novo Cer synthesis, most likely driven by elevated free FAs (FFA), which play a key role in the dysregulation of lipid homeostasis associated with T2D [9].

1.3.3 Elevated glycerolipids and cholesteryl esters are markers of obesity

Elevated circulating TG, DG and CE levels are established markers of obesity [26,27,28,29,30], prediabetes [9] and T2D [9,13]. The FA composition (total FA-carbon number and total FA double bond number) are critical in determining whether a particular circulating TG species is positively or negatively associated with obesity, IR and T2D [26,30,31]. Generally, circulating TG species containing low total FA-carbon number (≤ 52) and low total FA double bond number (≤ 2) are associated with IR and increased risk of T2D, whereas TG species containing higher total FA-carbon number and higher total FA double bond number are associated with decreased risk of T2D, and are not correlated with IR. Notably, diet-induced weight loss in obese individuals led to a reduction in circulating saturated and short-chain FA-containing TG species, which was associated with improved insulin sensitivity [30]. Furthermore, 13 fasting plasma TG species with high total FA-carbon number and high total FA double bond number, along with CE 18:2, were upregulated in active compared with inactive same-sex co-twins who had been discordant for leisure-time physical activity for 30 years [32]. These plasma TG species were also positively associated with insulin sensitivity.

These studies demonstrate the power of targeted plasma lipid profiling of TG species for determining the severity of disease (i.e., increasing obesity and IR) at any point in time, and provides the opportunity to identify one or more circulating TG species (biomarkers) that can accurately predict an individual's risk of developing T2D. Meikle *et al.* found that multivariate classification models incorporating lipid species (including TG 14:0/16:0/18:2) and traditional risk factors provided improved classification of unstable coronary artery disease from stable coronary artery disease compared with models containing only traditional risk factors [10]. In contrast to the TG findings in plasma, metabolically active long-chain fatty acyl-CoA lipids are considered better predictors of insulin sensitivity than the relatively inert TG lipids in skeletal muscle [33,34]. Also of interest was the finding that intramyocellular triglycerides (IMTG) levels were markedly elevated in both obese/IR and endurance-trained/insulin sensitive humans compared with lean subjects, but the lipid peroxidation/IMTG ratio was 4.2-fold higher in the obese subjects [35]. This suggests that endurance training protects against IMTG peroxidation, and that there is a link between lipid peroxidation/IMTG ratio and IR.

Some DG species also appear to be highly associated with obesity and IR, and predictive of T2D. Chronic high-fat diet induced obesity in male C57BL/6J mice was associated with markedly elevated fasting plasma 16:0, 18:0 or 18:1 FA-containing TG and DG species [26], and only low abundant skeletal muscle DG species that contained an unsaturated FA on both positions (e.g. DG 16:1/18:1) were significantly elevated in obese/sedentary subjects compared with both normal weight/sedentary and normal weight/endurance trained athletes [36]. Moreover, skeletal muscle 18:1 FA-containing DG species and saturated Cer content were elevated in obese and T2D subjects compared with lean subjects [37]. In the same study, the ratio of diacylglycerol hydrolase-to-triacylglycerol hydrolase activity (an index of incomplete TG hydrolysis) correlated with both total DG and total Cer content, and skeletal muscle total DG content was the main determinant of IR [37]. In lean healthy men who underwent either a 6 h hyperinsulinaemic-euglycaemic clamp or clamp combined with intralipid (Liposyn II)/heparin infusion, there was a ~4-fold increase in plasma FFA levels (versus clamp alone), which resulted in a marked reduction in IR [38]. In addition, the intralipid infusion induced striking increases in skeletal muscle protein kinase C (PKC) activity, DG mass and membrane-associated PKC-βII and PKC-δ abundance, and a 70% reduction in IκB-α mass, an inhibitor of NF-κB, all of which contribute to IR [38].

As the proportions of fatty acids in circulating CEs reflect the amount of fatty acids in the diet [39], certain CE species are considered biomarkers of obesity and T2D. Fasting serum CE species containing high proportions of 16:0, 16:1 and 18:0 FAs are positively associated with obesity and T2D, and CE species containing a low proportion of 18:2 FA are negatively associated with obesity [40] and T2D [41,42,43]. Therefore, obesity and T2D are to a large extent driven by altered lipid metabolism resulting from the oversupply of FFA in many Western diets.

1.3.4 Diet influences hepatic *de novo* lipogenesis and lipid profiles

Stearoyl CoA desaturase 1 (SCD1) belongs to the delta-9 desaturase family, and is a crucial lipogenic endoplasmic reticulum-bound enzyme that converts saturated FAs (primarily 16:0 and 18:0), the end-products of lipogenesis, to monounsaturated FAs (16:1 and 18:1). Monounsaturated FAs derived from the activity of SCD1 are predominantly incorporated into TG, CE and phospholipids [44]. It would appear counter-intuitive that increased SCD1 protein

expression and activity promotes multiple aspects of the metabolic syndrome [45] given that saturated fats are incorporated into DG and Cer, which promote IR. The inhibition of SCD1 with 20 weeks antisense oligonucleotide treatment in mice protected against saturated fat diet-induced obesity, IR, and hepatic steatosis, but also strongly promoted aortic atherosclerosis, independently of obesity and IR, which could not be reversed by dietary oleate (18:2) [46]. Therefore, there appear to be detrimental effects associated with the prolonged upregulation of hepatic *de novo* lipogenesis and sustained accumulation of saturated fats.

It is also important to note that dietary fat and carbohydrate composition can greatly influence hepatic *de novo* lipogenesis [47] and lipidomic profiles [26,48,49]. Hepatic *de novo* lipogenesis is activated by low-fat/high-carbohydrate diets, and high levels of circulating insulin and carbohydrate [47]. Long-chain FAs (16:0, 16:1, 18:0 and 18:1) derived from increased hepatic *de novo* lipogenesis are released into the circulation as VLDL-bound triglyceride [50] to maintain normal 16:1/16:0 and 18:1/18:0 ratios in metabolic tissues [47]. Conversely, high-fat diets provide plentiful long-chain saturated and monounsaturated FAs, thereby inhibiting hepatic *de novo* lipogenesis and delta-9 desaturase activity [47]. Therefore, mouse models of high fat diet-induced obesity are likely to generate some differences in plasma and tissue lipidomic profiles compared with genetic mouse models of obesity (e.g. *db/db* and *ob/ob*), in which mice are fed an unrestricted low-fat/high-carbohydrate (standard chow) diet. However, the development of obesity and IR in mice may induce hepatic *de novo* lipogenesis in the presence of a high-fat diet [51,52].

1.3.5 Role of lysophosphocholines in obesity and insulin resistance

There is no solid consensus as to whether the association of lysophosphocholine (LPC) lipids with obesity and insulin resistance is beneficial or detrimental to lipid metabolism and glucose homeostasis. In favour of the former notion, decreased fasting plasma LPC levels have been found in glucose intolerant and insulin resistant individuals [13,53], the elevation in IR observed in healthy adults in response to 28 days overfeeding was accompanied by reductions in many fasting plasma LPC species [54], and LPC lipids from full-fat dairy diets were positively associated with insulin sensitivity and inversely associated with IR [55]. Recent evidence suggests that LPC may be a novel insulin-independent signal that regulates blood glucose levels [56]. In addition, Barber *et al.* showed a significant reduction in many fasting plasma LPC species in obese/insulin sensitive and obese/T2D subjects compared with lean healthy subjects,

and found that fasting circulating LPCs were negatively associated with both BMI, but were not associated with IR or T2D *per se* [26].

In contrast, Pietilainen *et al.*found that young adult monozygotic obese co-twins had increased levels of five fasting serum LPC species compared with non-obese co-twins, and that LPC 16:0 and LPC 20:4 were negatively correlated with insulin sensitivity, independent of genetic factors [29]. Another study showed that elevated LPC levels in young pigs with early obesity were associated with endothelial dysfunction and oxidative stress [57], and Kim *et al.* found that dietary fatty acid composition influenced the relative abundances of LPC species in overweight/obese IR men (with a higher fat intake) compared with age-matched lean healthy men [48]. Notably, LPCs can increase plasminogen activator inhibitor-1, a potent prothrombotic and proatherogenic protein [58], induce endothelial cell expression of cell adhesion molecules [59], and inhibit hepatic fatty acid oxidation in mitochondria [60].

As mentioned earlier, the contrasting LPC results in the studies described above may be attributable to the severity of disease in each individual, combined with differences in gender, age, genetic background, environmental factors (especially diet), species-type, and the robustness of the statistical tests. More consistent LPC results may be achieved by sequentially tracking the changes in LPC levels in plasma and metabolic tissues with the onset and progression of T2D using a genetic mouse model of obesity/diabetes (i.e., *db/db* with C57BL/KsJ background) with known metabolic consequences, a controlled dietary intake, and less intra-genotype variation in metabolic and lipidomic measurements.

1.3.6 Lipid abnormalities associated with early onset insulin resistance

Although the onset of human obesity and IR usually overlap, it would be invaluable to discover which lipid abnormalities are associated early in the development of IR, independent of obesity, both from a diagnostic and therapeutic viewpoint. It is also of interest to know the relative contributions of ectopic lipid accumulation (lipotoxicity) or inflammation to the early onset of IR. Time course studies in high-fat fed obese rodent models have shed some light on these issues. In male C57BL/6J mice fed a high-fat diet (HFD; 60% kcal from fat) for 3 days, 1 week, 2 weeks, 5 weeks or 10 weeks, body weight, adipose tissue mass and IR was already significantly increased by 3 days HFD, as was liver and skeletal muscle TG, non-esterified FA, DG and Cer content, but plasma adiponectin was reduced compared with low-fat fed control

mice [61]. The study concluded that different mechanisms appear to evolve over the 10 week HFD period; i.e., early onset (as early as 3 days) IR is more likely related to acute tissue lipid overload (lipotoxicity), whereas the more chronic state of IR in established obesity is largely mediated by macrophage-induced proinflammatory actions (i.e., the secretion of adipocytokines such as IL-6 and TNF-α from both adipose tissue and infiltrating macrophages) [61].

In another study, female Sprague-Dawley rats fed either a chow diet (12% kcal from fat; control group) or HFD (60% kcal from lard) for 3 days, 2 wk, or 4 wk, adiponectin significantly stimulated FA oxidation and acetyl-CoA carboxylase phosphorylation in isolated soleus muscle in low-fat fed control rats, but not the HFD group (i.e., as early as 3 days) [62]. After 2 wks HFD, plasma membrane FA transporters, skeletal muscle DG and Cer increased, and insulin-stimulated phosphorylation of both protein kinase B and protein kinase B substrate 160 were significantly blunted compared with control rats. After 4 wk of HFD, maximal insulin-stimulated glucose transport was impaired compared with control rats. Therefore, early loss of adiponectin's stimulatory effect on FA oxidation with 3 days HFD preceded an increase in plasmalemmal FA transporters (i.e., increased rate of FA uptake), accumulation of skeletal muscle DG and Cer and blunted insulin signalling (by 2 weeks), and ultimately impaired maximal insulin-stimulated glucose transport in skeletal muscle (by 4 weeks) [62]. These findings suggest that early onset adiponectin resistance may have contributed to the development of IR. These high-fat fed obese rodent studies give a valuable insight into the mechanisms responsible for the early onset and progression of IR, including adiponectin resistance, lipotoxicity and inflammation in the presence of obesity.

1.3.7 Other lipids implicated in the pathogenesis of type 2 diabetes

Despite the large number of lipid species that have been shown to be associated with obesity, IR and/or T2D (section 1.3) there is also evidence that lipid species from other lipid subclasses may be implicated in the pathogenesis ofobesity, IR, T2D and coronary artery disease. These lipids include other PE species, and lipids from the alkylphosphatidylethanolamine (PE(O)), alkenylphosphatidylethanolamine (PE(P)), lysophosphatidylethanolamine (LPE) and cardiolipin (CL) subclasses [9,10,29,54,63,64,65,66,67]. These lipids are described in greater detail in Chapter 3 (sections 3.1.2 to 3.1.4).

1.3.8 Limitations associated with human lipidomic studies

Although many studies have revealed lipidomic abnormalities associated with human obesity, IR and T2D, they are generally restricted by specific limitations in experimental design and lipid measurement capabilities, including the collection of one-off samples (usually plasma) to compare the levels of a modest number of lipid species representing one or two lipid classes/subclasses in two groups of subjects (e.g. obese versus lean controls) [25,28,29,66,67,68,69]. Lipid abnormalities associated with animal models of obesity, IR and T2D offer certain advantages over human studies, including the capacity to relate lipid abnormalities in the circulation to those observed in different tissue beds, and to compare global gene expression profiling with lipid profiling in the same individuals. To date, few studies have sequentially tracked the lipid abnormalities in plasma and metabolic tissues that occur with disease progression in animal models over a relatively short time-frame and/or compared global gene expression and targeted lipid profiling in the same individual [65,70,71].

1.4 THE LEPTIN RECEPTOR-DEFICIENT *DB/DB* MOUSE MODEL

1.4.1 Characteristics of the C57BL/KsJ obese/diabetic *db/db* mouse

The diabetes *db* gene mutation (autosomal recessive mutation on chromosome 4 with complete penetrance) occurred spontaneously in the C57BL/KsJ strain of mice from the Jackson Laboratory (Bar Harbor, ME, USA), resulting in global deficiency in the protein expression of the leptin receptor and the development of T2D in homozygous (*db/db*) mice [72]. The diabetic phenotype of *db/db* mice is determined by the genetic background on which the mutation is expressed. In this regard, homozygous *db/db* mice with a C57BL/KsJ genetic background exhibit a more severe diabetic phenotype with obesity due to hyperphagia, and eventual islet degeneration and secretory deficit compared with *db/db* mice with a C57BL/6J background, which is characterised by pancreatic hyperplasia [73]. The diabetic *db/db* genetic mouse (C57BL/KsJ background) serves as a good monogenic model of IR, obesity and T2D, and closely resembles disease progression to T2D in humans, in which hyperinsulinaemia and IR is followed by progressive hyperglycaemia and gradual pancreatic insufficiency [74,75]. The time-frame of disease progression in C57BL/KsJ *db/db* mice is described in more detail in Chapter 4 (section 4.1.2).

1.4.2 Lipid and metabolic defects in *db/db* mice

As the *db/db* genetic mouse model closely resembles the development of human obesity, IR and T2D, the lipid abnormalities in the *db/db* mice may be similar to those observed in comparable models of animal obesity and human cohort studies. Ussher *et al.* found that TG and long-chain fatty acyl-CoA (total and 16:0) levels were elevated, but DG and Cer levels were not found to be significantly higher in gastrocnemius muscle of 6 week old *db/db* versus age-matched *db/h* lean mice on unrestricted standard chow diet [76]. Similar to chronic high-saturated fat-fed C57BL/6 mice, both respiratory exchange ratio and whole-body oxygen consumption were significantly lower in *db/db* versus *db/h* lean mice, confirming increased fat oxidation. Treatment with myriocin (an inhibitor of serine palmitoyl transferase-1, the rate-limiting enzyme of *de novo* Cer synthesis) for 4 weeks had no effect on gastrocnemius muscle TG, long-chain fatty acyl-CoA or DG levels, but significantly reduced Cer levels in *db/db* mice, which was associated with an improvement in fasting glucose, glucose and insulin tolerance, insulin sensitivity and insulin-signalling [76].

Recently, DeMarco *et al.* found significant elevations in the levels of total TG and DG levels (and increased number of lipid droplets) in the left ventricle of 12- and 15-week old obese/IR male *db/db* mice compared with age-matched *db/*wild-type mice, which included an increase in the relative abundance of TG and DG species containing low total FA-carbon number and low total FA double bond number in *db/db* mice at 15 weeks of age [77]. In addition, total FAs, Cer, SM, PC, LPC, PE and PC/PE ratio were significantly elevated in 12 week old *db/db* mice, and total FAs, SM, PC and PC/PE ratio remained elevated at 15 weeks of age compared with age-matched *db/*wild-type mice. These lipid abnormalities in the left-ventricle of male *db/db* mice corresponded to a worsening of non-dipping blood pressure pattern, persistent mitochondrial ultrastructural abnormalities, increased capacity for mitochondrial FA oxidation, and increased nitrosative and oxidative stress (generation of reactive oxygen species (ROS)), resulting in the development of diastolic dysfunction [77].

Furthermore, defects in hepatic insulin signalling (decreased gene expression of hepatic insulin receptor substrates-1 and 2, and decreased insulin-stimulated Akt-phosphorylation) occurred in primary hepatocytes from C57BLKS/J-*db*/*db* mice at one month of age [78]. Kimura *et al.* showed that obesity associated endoplasmic reticulum stress in 8-10 week old male C57BLKs/J background *db/db* mice inhibited signal-transducer and activator of transcription 3 (STAT3)-

dependent suppression of hepatic gluconeogenic enzymes, resulting in increased hepatic glucose production [79]. In agreement with these findings, increased expression of hepatic gluconeogenic enzyme genes have been demonstrated in *db/db* mice [80], and increased hepatic glycogenolytic and gluconeogenic enzyme activities contributed to the chronic hyperglycaemia found in *db/db* mice [81]. A summary of the key metabolic and lipid abnormalities observed in C57BL/KsJ *db/db* mice compared with IR and/or T2D humans is shown in Table 1.1.

1.4.3 Treatments targeting lipid and metabolic defects in *db/db* mice

Treatment of obese *db/db* mice with specific drugs or genetic ablation of enzymes can give insights into the metabolic pathways that may be responsible for aberrant lipid profiles, glucose homeostasis and insulin sensitivity, and how best to ameliorate these metabolic defects in human obesity and/or T2D.

Treatment of 9 week old C57BL/KsJ male *db/db* mice with metformin (an insulin-sensitising and glucose-lowering drug that improves hepatic IR and inhibits hepatic gluconeogenesis and glycogenolysis) for 4 weeks significantly decreased body weight, epididymal fat mass, fasting glucose and insulin levels [82]. However, only fasting glucose was significantly decreased by 4 weeks of intensive insulin treatment, and neither treatment significantly increased serum or adipose adiponectin levels. Treatment of obese 9 week old male C57BL/KsJ *db/db* mice (and *ob/ob* mice) with berberine for 3 weeks [a glucose-lowering drug that improves glucose tolerance and insulin action by activating AMP-dependent protein kinase (AMPK), a key sensor of cellular energy status and stress] significantly decreased body weight and respiratory quotient, and significantly increased energy expenditure, with no change in food intake [83]. Notably, berberine reversed the dyslipidaemia (i.e., decreased plasma TG, FFA, and cholesterol levels) and fatty liver (decreased hepatic TG) in male C57BL/KsJ *db/db* mice by promoting hepatic and skeletal muscle AMPK-activation of FA oxidation via upregulation of FA oxidation genes and downregulation of lipogenic genes.

In another study, combination therapy with peroxisome proliferator-activated receptor (PPAR)-α and PPAR-γ agonists (insulin-sensitising drugs that enhance the synthesis and secretion of adipose adiponectin, a key regulator of insulin sensitivity) significantly reduced body weight and plasma glucose, insulin, triglyceride and FFA levels, and increased plasma adiponectin and glucose-stimulated insulin secretion in obese diabetic C57BL/KsJ *db/db* mice [84]. In 10 week

Table 1.1 Summary of the key metabolic and lipid abnormalities in C57BL/KsJ *db/db* mice compared with IR[a] and/or T2D[b] humans

Major findings in *db/db* mice	Ref.	Major findings in IR and/or T2D humans	Ref.
The **diabetes *db* gene mutation** led to global deficiency in the protein expression of the leptin receptor, resulting in: **Decreased energy expenditure and excess caloric intake,** which is manifested primarily by obesity (hyperphagia), followed by hyperinsulinaemia, IR, hyperlipidaemia (raised FFA and triglycerides), progressive hyperglycaemia, and eventual islet degeneration and secretory deficit (vs. *db/h* mice)	[72-75]	The **oversupply of nutrients (obesity)** antagonizes insulin action in peripheral tissues by two mechanisms: **1)** When **adipocytes exceed their storage capacity**, fats accumulate in ectopic tissues (liver, skeletal muscle, heart, pancreatic β-cells), leading to the formation of putative intermediates (long-chain fatty acyl-CoA, Cer, DG) that inhibit insulin signal transduction; **2)** Obesity triggers a **chronic inflammatory state** and cytokines, released from adipocytes and/or macrophages that infiltrate adipose tissue, antagonize insulin action	[18]
Gastrocnemius muscle: Increased TG[c], long-chain fatty acyl-CoA (total and 16:0); decreased RER[d] and whole-body oxygen consumption; increased FA oxidation; glucose and insulin intolerance, IR and decreased insulin signalling at 6 weeks of age (vs. lean *db/h* mice)	[76]		
Left ventricle: Increased total FA, TG, DG, Cer, SM, PC, LPC, PE levels and PC/PE ratio at 12 weeks of age, and total TG, DG, FAs, SM, PC and PC/PE ratio remained elevated at 15 weeks of age, which corresponded to increased FA oxidation, nitrosative and oxidative stress (reactive oxygen species generation), persistent mitochondrial ultrastructural abnormalities and diastolic dysfunction (vs. *db/*wild-type mice	[77]	**Circulating lipids:** Elevated TG, DG and CE levels are established markers of obesity Both pre-diabetes and T2D are positively associated with Cer, dhCer, TG, DG, CE, PE, PG and PI, and negatively associated with DHC, THC and PC(O)	[26-30] [9,13]
Adipose tissue: Decreased total Cer and SM, but increased mRNA levels of genes encoding key enzymes involved in adipose Cer generation	[70]	**TG species** with lower FA carbon number (≤ 52) and lower double bond content (≤ 2) are associated with increased risk of T2D, and correlate with IR	[13]
Liver: Increased endoplasmic reticulum stress and hepatic glucose production; decreased STAT3[d]-dependent suppression of gluconeogenic enzymes, and increased mRNA expression of genes encoding gluconeogenic enzymes	[79,80]	Elevated **saturated FAs** (16:0; 18:0) and cytokines (TNF-α; IL-6) selectively induce the synthesis of sphingolipids (Cer, GM3 gangliosides), which inhibit insulin action and glucose uptake, and induce oxidative stress	[19]

[a] IR, insulin resistant
[b] T2D, type 2 diabetes
[c] Abbreviations for lipid classes and subclasses are shown in Abbreviations section of thesis
[d] STAT3, signal-transducer and activator of transcription 3

old obese C57BL/KsJ *db/db* mice either untreated or treated with phlorizin (which selectively lowers blood glucose) or bezafibrate (which selectively lowers plasma non-esterified FA and triglycerides) for 2 weeks, abnormalities in glucose-induced insulin secretion and gene expression relating to β-cell differentiation and stress response mediators in pancreatic β-cells were normalised by phlorizin but unchanged by bezafibrate [85]. Therefore, hyperglycemia (in the presence of hyperinsulinaemia), independent of plasma hyperlipidemia, is sufficient for the gradual loss of β-cell differentiation and secretory function in *db/db* mice. Importantly, similar mechanisms may be responsible for β-cell dysfunction in human T2D [86].

Furthermore, treatment with resolvin D1 (an endogenous lipid mediator of homeostasis after an inflammatory insult) for 8 or 16 days in 8 week old male obese B6.BKS(D) *db/db* mice improved glucose tolerance, and decreased fasting blood glucose and homeostasis model assessment of IR (HOMA-IR) [87]. Additionally, adiponectin production, insulin-stimulated Akt/protein kinase B phosphorylation and alternatively activated macrophages were increased, but IL-6 expression and $F4/80^{+}CD11c^{+}$ inflammatory macrophages were reduced in adipose tissue.

The improvements in lipid profiles and glucose homeostasis induced by treatments targeting specific metabolic pathways in *db/db* mice were similar to those observed with comparable treatments in other animal models of obesity, IR and T2D [88,89,90], and provide strong evidence that these beneficial outcomes may also occur in comparable human cohorts.

1.4.4 Comparison of genetically obese *db/db* and *ob/ob* mouse models

The genetic leptin-deficient *ob/ob* mouse model is an alternative to the genetic leptin receptor-deficient *db/db* mouse model. The C57BL/6J-*ob/ob* mouse originated from the Jackson Laboratory in Bar Harbor, ME, USA [91]. Mutation of the *ob* gene on chromosome 6 caused a defect in leptin production, resulting in glucocorticoid-dependent obesity and diabetes [92]. The *ob/ob* mouse develops morbid obesity, hyperinsulinemia and hyperglycemia by 8 weeks of age [93,94], but is less hyperglycaemic than the *db/db* mouse [95]. They also manifest hepatic steatosis due to excessive *de novo* lipogenesis driven by the low fat/high carbohydrate chow diet and chronic hyperinsulinaemia [96]. Both *ob/ob* and *db/db* mice genetic models closely resemble the onset of obesity and IR observed in humans, but circulating leptin levels are elevated in *db/db* mice, reflecting severe leptin resistance [97,98], and *db*/*db* mice are insensitive to leptin

due to a mutation in the leptin receptor [99]. Therefore, central or peripheral administration of recombinant leptin has no effect on food intake or body weight in C57BL/KsJ *db/db* mice [100]. Furthermore, leptin treatment reversed the metabolic defects associated with impaired activity and mRNA expression of the glucocorticoid regulator, hepatic 11β-hydroxysteroid dehydrogenase type 1 (11β-HSD1), in *ob/ob* mice, but did not influence hepatic 11β-HSD1 expression in *db*/*db* mice, indicating that the effects of leptin on hepatic 11β-HSD1 are mediated by the leptin receptor [101]. However, a lack of leptin signaling also results in elevated liver triglycerides in *db/db* mice (hepatosteatosis), and larger, more triglyceride-rich very-LDL (VLDL) particles [102]. In skeletal muscle, leptin stimulates FA oxidation via AMPK, resulting in a decrease of lipid accumulation in skeletal muscle [103]. In human populations, nonalcoholic fatty liver disease (NAFLD) is associated with obesity, abnormal glucose tolerance, elevated circulating triglyceride levels, IR and diabetes, and has been described as the hepatic manifestation of the metabolic syndrome [104].

Importantly, however, the increases in mRNA levels of genes encoding key enzymes involved in adipose Cer generation and hydrolysis, and the changes in sphingolipid levels in adipose tissues (i.e., significant reduction in both total Cer and SM levels) were similar in obese C57BL-*ob/ob* mice at 14–16 weeks of age and obese *db/db* mice compared with their corresponding lean counterparts [70]. These findings give confidence that gene expression and lipid abnormalities associated with sphingolipid metabolism in these genetically distinct obese mouse models are very similar, despite differences in genetic background and severity of disease. This pattern of adipose sphingolipid metabolism was also similar to that observed in obese non-diabetic and obese/T2D human subjects, in which elevated mRNA expression and increased activity of most key enzymes responsible for adipose Cer metabolism corresponded to significantly lower adipose total Cer content compared with lean subjects [105].

In contrast to adipose tissue, plasma levels of total Cer and SM were elevated in *ob/ob* mice compared with lean mice [70]. This was also similar to the elevation of fasting plasma total Cer and several Cer species observed in obese/T2D subjects compared with lean healthy subjects [25], and the finding that both prediabetes and T2D were positively associated with total Cer and dhCer levels [9]. These results reinforce the notion that lipid abnormalities and gene expression of key enzymes in the sphingolipid metabolic pathway in genetically obese/diabetic *db/db* and *ob/ob* mouse models may be translatable to comparable human cohort studies.

1.5 RELATIONSHIP BETWEEN GENE EXPRESSION AND LIPID PROFILES IN OBESITY, INSULIN RESISTANCE AND TYPE 2 DIABETES

1.5.1 Hepatic gene expression profiling and metabolic defects in *db/db* mice

Comparison of gene expression profiles and simultaneous lipid abnormalities associated with obesity, IR and the progression to T2D can help to define the underlying mechanisms and metabolic pathways involved in the pathogenesis of T2D. In particular, the liver is crucial in maintaining glucose homeostasis, and impaired hepatic glucose metabolism, including an increased rate of hepatic gluconeogenesis, leads to the development of T2D [74,75,106]. Additionally, impaired hepatic FA oxidation, synthesis and storage contributes to the development of T2D [107,108,109].

Recently, Zhang *et al.* used high-throughput RNA sequencing to compare gene expression profiling in the livers of 9 week old male wild-type C57BL/6 and male diabetic *db/db* mice, and found that the upregulated genes were mainly associated with lipid and FA metabolic processes, and the downregulated genes were mainly associated with immune-related processes in male diabetic *db/db* mice [110]. Detailed pathway network analyses revealed that genes associated with hepatic glucose metabolism (specifically glycolysis, gluconeogenesis and glycogenolysis) and FA metabolism (specifically FA oxidation and storage) were upregulated in male diabetic *db/db* mice [110].

Gene expression profiling is also a powerful tool for examining which hepatic metabolic pathways are enhanced by specific drug treatments to overcome the metabolic defects associated with T2D. A single dose of the hypoglycaemic agent, metformin, not only reduced blood glucose levels and hepatic glucose-6-phosphatase gene expression and enzyme activity (a key rate-limiting enzyme in gluconeogenesis) in the livers of 8 week old obese diabetic male C57BL/KsJ-*db/db* mice, but also significantly altered the gene expression profiles of ten metabolic pathways, including those involved in glycolysis/gluconeogenesis, the citrate cycle, FA and glycerolipid metabolism, and amino acid metabolism [111]. In support of these findings, the expression of genes encoding enzymes involved in hepatic lipogenesis, gluconeogenesis and FA β-oxidation were upregulated in 12 week old male C57BL/6J-*ob/ob* mice compared with their lean counterparts, which was accompanied by increased body weight and plasma glucose, insulin and glucosylceramide levels, as well as increased hepatic steatosis [112]. Most of these

gene expression and metabolic/lipidomic defects were restored by 5 weeks treatment with an inhibitor of the enzyme glucosylceramide synthase, suggesting that the pharmacological lowering of glycosphingolipids improves insulin signalling, glucose homeostasis and hepatic steatosis in *ob/ob* mice at the transcriptional level [112].

1.5.2 Gene candidates associated with obesity, insulin resistance and type 2 diabetes

Global gene expression studies have been performed in obese and/or T2D humans to identify candidate genes associated with these disease states [113]. In a study that examined seven independent modelling methods used to select the most likely candidate genes for human obesity and T2D from data obtained from genome-wide linkage analysis and association studies, seven of the nine primary candidate genes identified for human T2D alone were involved in the processing of metabolites in the glycolytic and mitochondrial oxidative phosphorylation pathways [113]. These findings confirm that the diabetic *db/db* mouse model is a suitable model for tracking gene expression profiling in obesity, IR and T2D, and may identify specific gene candidates or lipid classes/species as potential therapeutic targets for early prevention or treatment in comparable human disease cohorts.

1.6 Statement of the research problem(s)

Dyslipidaemia as assessed by standard measures (raised plasma triglycerides and LDL-cholesterol, and decreased HDL-cholesterol) is an important independent risk factor for IR and T2D in the adult population. However, the measurement of these "classical" lipids alone does not adequately represent the complex lipid abnormalities in the circulation and tissues that are associated with the pathogenesis of T2D. At present, there is a lack of understanding of the biological interplay that exists between abnormalities in lipid metabolism and the pathogenesis of T2D. Further to this, the contribution of lipid abnormalities to the onset and progression of T2D is unclear. Numerous studies have successfully employed a variety of "lipid profiling" approaches using MS techniques to identify and quantify a limited number of individual molecular lipid species in models of obesity, IR and/or T2D. However, there are specific limitations relating to the measurement of these lipid abnormalities regarding 1) the number of individual lipid species able to be quantified in a single patient sample; 2) the lack of large cohorts consisting of sequential samples in individuals before and during the onset and progression of IR and T2D; 3) the ability to relate the lipid abnormalities in the circulation to

those observed in different tissue beds; 4) the ability for meaningful comparisons between the dyslipidaemia and abnormal lipid metabolism observed with obesity, IR and/or T2D in animal models versus human cohorts; and 5) the capacity to associate global gene expression profiling with lipid profiling in the same individual.

My PhD research project will address these specific limitations using comprehensive experimental designs in suitable animal models and human diabetic cohorts, and high-throughput targeted lipid profiling employing reverse phase LC ESI-MS/MS. A more complete understanding of the relationship that exists between lipid abnormalities and the onset and progression of T2D will provide the opportunity to identify new therapeutic targets and possible lipid biomarkers that can accurately predict an individual's risk of developing T2D.

1.7 Central hypothesis

Altered lipid metabolism in the circulation and tissues is a major contributor to the onset and progression of type 2 diabetes

1.8 Primary goal

Lipidomics offers a global view of lipid metabolism, providing a solid platform to investigate the complex relationship between changing lipid levels and multiple metabolic and gene expression pathways associated with the pathogenesis of T2D. The wealth of information derived from lipidomic studies will identify new avenues for research into T2D, leading to hypothesis-driven targets for the development of new treatments and the discovery of lipid biomarkers that can accurately predict an individual's risk of developing T2D in a clinical setting.

The primary goal is to improve our understanding of the relationship between lipid metabolism and the pathogenesis of T2D by employing targeted lipid profiling techniques to map out the abnormal lipid metabolism in different tissue beds and resultant changes in plasma lipids over time in the *db/db* (leptin-receptor deficient) diabetic mouse model. I will then integrate this lipid profiling with global gene expression profiling to define the metabolic pathways involved. These findings will be compared with plasma and skeletal muscle lipid profiling in comparable human cohort studies.

1.9 Specific aims

1) Develop targeted lipid profiling methodology to characterise lipid species that are thought to contribute to the pathogenesis of T2D.

2) Characterise the lipid abnormalities in the circulation and tissues associated with the onset and progression of T2D in the *db/db* (leptin-receptor deficient) mouse model.

3) Compare the lipid abnormalities in the circulation and tissues observed in the *db/db* diabetic mouse model with that observed in comparable human cohort studies.

4) Perform global gene expression profiling on selected tissue(s) from *db/db* mice to define associations between gene expression and the progressive lipid abnormalities associated with T2D.

CHAPTER 2 GENERAL METHODS

2.1 PLASMA AND TISSUE COLLECTION FROM STUDIES

2.1.1 Obese/diabetic *db/db* mouse study

The Obese/diabetic *db/db* mouse study, in which male and female leptin receptor-deficient *H/H*, *db/h*, and *db/db* mice (C57BL/KsJ background) were placed on an unrestricted standard chow diet (8% energy from fat) with free access to water for either 6, 10 or 16 weeks (7-12 mice per group) is described in Chapter 4 of this thesis (Materials and Methods, section 4.2). A total of 170 mice completed the study, which resulted in the collection of 165 plasma, 167 liver, 166 skeletal muscle (gastrocnemius), 168 heart (left-ventricle), and 162 adipose (omental) samples at the time of cull (after a 6 h fast) for subsequent targeted lipidomic and selective gene expression profiling (liver only). This study was in collaboration with Professor Josephine Forbes and Brooke Harcourt, Glycation and Diabetes Laboratory, Baker IDI Heart & Diabetes Institute, Melbourne, and Mater Research, University of Queensland, Brisbane.

2.1.2 Human insulin resistance and obesity study

The Human insulin resistance and obesity study, in which 80 adult participants were classified into the four groups according to BMI, homeostasis model assessment of insulin resistance (HOMA-IR) and diabetic status, and underwent procedures for the measurement of insulin sensitivity (hyperinsulinemic-euglycemic clamp), body composition (dual energy X-ray absorptiometry), abdominal fat distribution (computed tomography) and plasma and skeletal muscle lipidomic analysis (mass spectrometry) is described in chapter 6 of this thesis (Materials and Methods, section 6.2). For lipidomic analysis, a total of 160 paired fasting baseline and steady-state hyperinsulinaemic-euglycaemic clamp blood samples were collected into EDTA tubes from 80 subjects on the metabolic study day. In addition, a total of 144 skeletal muscle (vastus lateralis) biopsy samples were obtained from 77 of the 80 subjects (77 samples at fasting baseline, and 67 samples at 150 min steady-state clamp). This study was a collaboration with Dorit Samocha-Bonet, Katherine Tonks, and Jerry Greenfield, Diabetes and Obesity Research Program, Garvan Institute of Medical Research, Sydney.

2.2 PREPARATION OF MOUSE LIVER FOR LIPID EXTRACTIONAND GENE EXPRESSION

2.2.1 Cryomilling of mouse liver

As part of the Obese/diabetic *db/db* mouse study, frozen mouse liver samples were powdered using a cryomilling procedure in preparation for lipid extraction (targeted lipid profiling) and any subsequent whole-mouse genome DNA microarray gene expression profiling analysis. Each frozen mouse liver sample (wet weight range 0.4-1.8 g; approximately three-quarters of the liver) was placed in a cryomill canister (in a liquid nitrogen bath) containing a 10 mm diameter ballbearing, fastened to the Cryomill Dismembranator (Sartorius 'Mikro-Dismembranator S', Stedim Biotech) and dismembranated for 1.0 min at 2,000 rpm to form a fine homogenous powder. The canister containing the liver powder was immediately returned to the liquid nitrogen bath, and one flat spoonful of liver powder (weighing ~30-70 mg) was scooped into a 1.5 ml eppendorf tube (for subsequent lipidomic analysis), and placed on dry ice. The remaining mouse liver powder was scooped into a 2.0 ml DNase-free and RNase-free tube (for any subsequent gene expression analysis), and placed on dry ice. Both tubes were stored at -80°C for later analysis.

2.2.2 Reconstitution and sonication of mouse liver powder

The frozen mouse liver powder collected for lipidomic analysis was stored on dry ice, accurately weighed on a weighing balance (Mettler Toledo), and reconstituted in 10 volumes of ice-cold 1 x phosphate buffered saline (PBS), pH 7.5, with vigorous vortexing for 30-60 sec. Each mouse liver 'homogenate' was sonicated on ice for 15 sec at amplitude 23° using a digital probe-sonifier (Branson).

2.2.3 Determination of total protein content in mouse liver homogenates

Each sonicated mouse liver homogenate was diluted 1:25 with milliQ water, vortexed thoroughly and assayed in duplicate using the bicinchoninic acid (BCA) Protein Assay (Pierce Biotechnology BCA™ Protein Assay Kit) according to manufacturer's kit instructions [114]. The mean total protein content calculated for the 167 mouse liver homogenates was 13.3 ± 0.3 (SEM) mg protein/ml homogenate. Each mouse liver homogenate was diluted to a final stock

concentration of 5.0 mg protein/ml with ice-cold PBS (pH 7.5) and stored at -80°C. In addition, liver homogenate quality control (QCs) samples were prepared for the liver lipid extraction run by pooling equal volumes from at least five stock mouse liver homogenates, and dividing the mixture into suitable aliquots.

2.3 PREPARATION OF MOUSE SKELETAL MUSCLE, LEFT-VENTRICLE AND ADIPOSE TISSUE FOR LIPID EXTRACTION

2.3.1 Cutting, homogenisation and sonication

Each frozen piece of mouse tissue (skeletal muscle, left-ventricle or adipose) was placed on dry ice, cut into a suitable size (~30-70 mg wet weight) with a sterile scalpel blade/handle, placed into a 2.0 ml graduated flat-bottomed micro-centrifuge tube (Astral Scientific) on dry ice, accurately weighed on a weighing balance, and stored at -80°C for subsequent electric homogenisation, sonication, protein determination, and lipid extraction.

On the day of homogenisation, each frozen tissue sample was homogenised in 10 volumes of ice-cold PBS (pH 7.5) for 10-15 sec at 30,000 rpm with a PT 3100 Electric Homogeniser **(**Polytron). Between each homogenisation, the homogeniser probe was washed consecutively in distilled water, 70% w/v ethanol, and distilled water at 30,000 rpm for 3-5 sec. The tissue homogenates were sonicated on ice as previously described for liver homogenates (section 2.2.2), and kept on ice.

2.3.2 Determination of total protein content

Each sonicated mouse skeletal muscle and left-ventricle homogenate was diluted 1:25, and each sonicated mouse adipose homogenate was diluted 1:4 with milliQ water, vortexed thoroughly, and assayed in duplicate using the BCA Protein Assay as previously described for liver homogenates (section 2.2.3). These dilutions were required to ensure that the protein content of each tissue homogenate was comfortably detected on the quadratic-polynomial equation-generated standard curve (range 1.25-25 μg protein/well). The mean protein content calculated for 166 mouse skeletal muscle homogenates, 168 left-ventricle homogenates and 162 adipose homogenates was 12.7 ± 0.2, 10.9 ± 0.2, and 4.4 ± 0.2 mg protein/ml respectively. Each mouse skeletal muscle and left-ventricle homogenate was diluted to a final stock concentration of 5.0

mg protein/ml homogenate, and each mouse adipose homogenate was diluted to a final stock concentration of 2.0 mg protein/ml homogenate with the appropriate volume of ice-cold PBS (pH 7.5), and stored at -80°C. Furthermore, separate skeletal muscle, left-ventricle and adipose homogenate QCs were prepared for the corresponding lipid extraction run as previously described for stock mouse liver homogenates (section 2.2.3).

2.4 PREPARATION OF HUMAN SKELETAL MUSCLE FOR LIPID EXTRACTION

2.4.1 Homogenisation, sonication and determination of protein content

As part of the Human insulin resistance and obesity study, a total of 144 frozen human skeletal muscle biopsy samples were received on dry ice from the Garvan Institute of Medical Research. Each frozen piece of skeletal muscle weighed 20-45 mg wet weight. The electric homogenisation, sonication, total protein determination, and preparation of human skeletal muscle stock homogenates (5.0 mg protein/ml homogenate) for subsequent lipid extraction was performed as previously described for mouse skeletal muscle (sections 2.3.1 and 2.3.2). The mean total protein content calculated for the human skeletal muscle homogenates was 10.2 ± 0.2 mg protein/ml. In addition, 2 µl of the antioxidant butylhydroxytoluene (50 mM in ethanol) was added per ml of stock homogenate (final concentration 100 µM), and the stock homogenates were stored at -80°C.

2.5 LIPID EXTRACTION OF MOUSE AND HUMAN PLASMA AND TISSUE STOCK HOMOGENATES

2.5.1 Lipid extraction protocol

Prior to lipid extraction, 1 µl of the antioxidant butylhydroxytoluene (20 mM in ethanol) was added to 200 µl aliquots of plasma samples obtained from the human cohort study (final concentration 100 µM) to prevent the oxidation of lipids. A total of eight lipid extraction runs were performed for the mouse and human cohort studies, with separate lipid extraction runs performed for plasma and each of the tissues for the mouse and human studies.

For each lipid extraction run, plasma or tissue stock homogenate samples were randomised using the random number generator website: www.psychicscience.org. In tube order, each extraction

assay consisted of a “reagent blank” tube (10 µl milliQ water, but no internal standards), a “sample blank + internal standards” tube repeated every 40 tubes throughout the assay, a “Tamm-Horsfall protein-1 (THP-1) monocyte QC” tube (2 mg protein/ml), specific QC tubes corresponding to plasma or tissue samples being extracted (repeated every 15 tubes throughout the assay), and an “unextracted internal standards” tube, which does not undergo lipid extraction (and can be used to calculate the recovery of lipid internal standards from the extraction procedure).

2.5.2 Lipid extraction method

A mixture of 16 different internal standards (50-1000 pmol, 15 µl; Table 2.1) dissolved in chloroform:methanol (1:1 v/v) was added to 10 µl plasma or tissue stock homogenate (2-5 mg protein/ml) samples in a 1.5 ml eppendorf tube. Lipids were extracted in 20 volumes chloroform/methanol (2:1 v/v, 200 µl) using a single-phase extraction method [10,11,115]. Briefly, samples were vortexed for 3-5 sec, mixed for 10 min on a rotation mixer, sonicated for 30 min, and left to stand at room temperature for a further 20 min. Extracts were centrifuged at 13,000 rpm (16,200 g) for 10 min (Heraeus Fresco 17 centrifuge, Thermo Electron Corporation), the supernatant was transferred to a 96-well plate, and dried under nitrogen at 40^{o}C for 45 min. Lipids were then reconstituted in 50 µl water-saturated butanol, sonicated for 10 min, and 50 µl methanol containing 10 mM ammonium formate was added. The extracts were centrifuged at 4,000 rpm (3,041 g) for 5 min (Heraeus multifuge 1S-R, Thermo Electron Corporation). The supernatant (200 µl) was transferred to a 300 µl glass insert placed in a 2.0 ml glass vial with a Teflon lined cap (Agilent Technologies) designed to sit in a 54-well plate of an auto-sampler attached to a API 4000 Q/TRAP (triple quadrupole) mass spectrometer (Applied Biosystems PE Sciex).

2.5.3 Established targeted lipid profiling methodology

Prior to the commencement of my PhD project, targeted lipid profiling methodology was already established in the Metabolomics Laboratory at Baker IDI Heart & Diabetes Institute, Melbourne (headed by A/Prof Peter Meikle) for the routine measurement of ~270 lipid species (representing 20-25 classes/subclasses) in human plasma samples (Table 2.1). [11]. The separation of extracted lipids was performed using rapid resolution, reverse phase high pressure liquid chromatography (HPLC) using 1.8 µm (particle size), 50 × 2.1 mm (internal diameter) Zorbax

C18 columns (Agilent Technologies) with gradients of water/methanol/tetrahydrofuran combined with electrospray ionisation-tandem mass spectrometry (ESI-MS/MS) and established multiple reaction monitoring (MRM) experiments in positive ion-mode. Two solvents were prepared for HPLC, with solvents A and B consisting of tetrahydrofuran:methanol:water in the ratios 30:20:50 and 75:20:5 by volume respectively, both containing 10 mM ammonium formate. In the first chromatography run lasting 14 min, all measured lipid species (5 µl injection) except diacylglycerol (DG) and triacylglycerol (TG) species were separated under gradient conditions (300 µl/min) as follows: 0% solvent B to 100% solvent B over 8.0 min, then 100% solvent B for 2.5 min, a return to 0% solvent B over 0.5 min, and 0% solvent B for 2.5 min prior to the next injection. Columns were heated to 50°C and the auto-sampler regulated to 25°C. In the second chromatography run, ~70 DG and TG species (1 µl injection) were separated using an isocratic flow (100 µl/min) of 85% solvent B over 6 min. The MS default settings were: Curtain gas, 10 psi; Turbo-ion spray source, 5000 volts and 350°C; Ion source gas 1, 40 psi; and Ion source gas 2, 40 psi. Internal standards were commercially available for most lipid classes and subclasses investigated. These lipid standards were either commercially available stable isotope-labelled (deuterated) or non-physiological (very low abundance in biological fluids) (Table 2.1) [11].

LC ESI-MS/MS quantification assays were developed to target many lipid classes, subclasses and individual species in plasma, including sphingolipids [dihydroceramide (dhCer), ceramide (Cer), monohydrosylceramide (MHC), dihydrosylceramide (DHC), trihydrosylceramide (THC) sphingomyelin (SM) and ganglioside (GM3)], glycerophospholipids [phosphatidylcholine (PC), phosphatidylethanolamine (PE), phosphatidylinositol (PI), phosphatidylserine (PS), phosphatidylglycerol (PG) and bis(monoacylglycerol)phosphate (BMP)], ether-phospholipids [alkylphosphatidylcholine (PC(O)) and alkenylphosphatidylcholine (PC(P))], lysophospholipids [lysophosphatidylcholine (LPC) and lysoalkylphosphatidylcholine (LPC(O)], sterol lipids [cholesteryl ester (CE) and free cholesterol (COH)], and the glycerolipids, DG and TG [9,10,11].

2.5.4 Acquisition of comparative lipidomic data

Lipid analysis of the chromatographically separated lipids was performed using Analyst 1.5 and Multiquant data systems. Lipid peak integration was performed using AB Sciex MultiQuant software v1.2. Comparative lipid abundances were calculated by relating the peak area of each species to the peak area of the corresponding internal standard. Not all lipid species were

Table 2.1 Established methodology for measurement of lipid species using liquid chromatography electrospray ionisation tandem mass spectrometry in positive ion mode.

Lipid class or subclass[a]	No. of species	Internal Standard[b]	Pmol[c]	Parent ion	Experiment[d]
dhCer	6	dhCer 8:0	100	$[M+H]^+$	PI, *m/z* 284.3
Cer	6	Cer 17:0	100	$[M+H]^+$	PI, *m/z* 264.3
MHC	6	MHC 16:0 d_3	50	$[M+H]^+$	PI, *m/z* 264.3
DHC	6	DHC 16:0 d_3	50	$[M+H]^+$	PI, *m/z* 264.3
THC	6	THC 17:0	50	$[M+H]^+$	PI, *m/z* 264.3
GM3	6	THC 17:0	50	$[M+H]^+$	PI, *m/z* 264.3
SM	12	SM 30:1	200	$[M+H]^+$	PI, *m/z* 184.1
PC	35	PC 13:0/13:0	100	$[M+H]^+$	PI, *m/z* 184.1
PC(O)	16	PC 13:0/13:0	100	$[M+H]^+$	PI, *m/z* 184.1
LPC	19	LPC 13:0	100	$[M+H]^+$	PI, *m/z* 184.1
LPC(O)	3	LPC 13:0	100	$[M+H]^+$	PI, *m/z* 285. 2
PE	18	PE 17:0/17:0	100	$[M+H]^+$	NL, 141 Da
PI	17	PE 17:0/17:0	100	$[M+NH_4]^+$	PI, *m/z* 184.1
PS	7	PS 17:0/17:0	100	$[M+H]^+$	NL, 185 Da
PG	4	PG 17:0/17:0	100	$[M+NH_4]^+$	NL, 189 Da
BMP	1	BMP 14:0/14:0	100	$[M+NH_4]^+$	PI, *m/z* 339.3
CE	31	CE 18:0 d_6	1000	$[M+NH_4]^+$	PI, *m/z* 369.3
COH	1	COH d_7	1000	$[M+NH_4]^+$	PI, *m/z* 369.3
DG	27	DG 15:0/15:0	200	$[M+NH_4]^+$	NL, fatty acid
TG	44	TG 17:0/17:0/17:0	100	$[M+NH_4]^+$	NL, fatty acid

[a] For definition of abbreviated lipid class or subclass, see section 2.5.3.
[b] Amount of internal standard per sample. d_3, d_6 and d_7, deuterated
[c] Amount of internal standard per sample.
[d] This methodology was established within the Metabolomics laboratory prior to the commencement of this candidature. PI, precursor ion; NL, neutral loss

observed in all plasma and tissue samples. The criteria for accepting lipid species for further statistical analyses were:

1) The signal was at least three times greater than the average background concentration of the "blank + internal standards" tubes.
2) The lipid species was detected in at least 93% of mouse samples; and
3) The percent coefficient of variance (%CV) of the lipid species (measured in 12-14 specific QC samples spaced evenly throughout the lipid extraction assay) was less than 30%.

Lipid levels were calculated as pmol/ml of plasma or pmol/mg protein in tissues. The total abundance of each lipid class was calculated as the sum of individual lipid species within that class [11].

2.6 Statistical Analyses

The statistical analyses used to compare body composition, biochemical, metabolic and lipidomic data between groups is fully described for the Obese/diabetic *db/db* mouse study in Chapter 4 (section 4.2.6), and for the Human insulin resistance and obesity study in Chapter 6 (section 6.2.7). Each statistical test was chosen to best suit the unique features of the data being analysed, taking into account the distribution and variance of the data, the number of subjects in each group, and the question being addressed.

CHAPTER 3 ESTABLISHMENT OF TARGETED LIPID PROFILING METHODOLOGY TO CHARACTERISE LIPID SPECIES IMPLICATED IN THE PATHOGENESIS OF TYPE 2 DIABETES

3.1 INTRODUCTION

3.1.1 Expansion of established targeted lipid profiling methodology

As previously described in Chapter 2 (section 2.5.3), the Metabolomics Laboratory at Baker IDI Heart & Diabetes Institute, Melbourne (headed by A/Prof Peter Meikle) already had established targeted lipid profiling methodology for the routine measurement of ~270 lipid species in human plasma samples using liquid chromatography electrospray ionisation tandem mass spectrometry **(**LC ESI-MS/MS) and established multiple reaction monitoring (MRM) experiments in positive ion mode. These lipid species represented 20 different lipid classes and subclasses (Table 2.1).

Despite this comprehensive lipid profiling capability, a number of lipid classes and subclasses were not covered by the existing methodology. Furthermore, the measurement of phosphatidylethanolamine (PE) species was limited to the measurement of 18 species containing a total of 32-40 even-numbered carbons and 0-7 double bonds in the two acyl-linked fatty acids.

In this chapter, I describe the development of targeted lipid profiling methodology and MRM experiments to characterise lipids implicated in the pathogenesis of type 2 diabetes (T2D), including additional PE species, and species representing the alkylphosphatidylethanolamine (PE(O)), alkenylphosphatidylethanolamine (PE(P)), lysophosphatidylethanolamine (LPE) and cardiolipin (CL) subclasses.

3.1.2 Evidence that phosphatidylethanolamines, ether-phospholipids and lysophospholipids are associated with type 2 diabetes

Targeted lipid profiling using MS techniques quantifies multiple individual lipid species in plasma, tissues, and cell culture samples. Using this approach, a number of lipids from various classes/subclasses have been linked to the pathogenesis of T2D, including free fatty acids (FFA),

the glycerophospholipids phosphatidylcholine (PC) and PE, the sphingolipids ceramide (Cer) and sphingomyelin (SM), and the glycerolipids diacylglycerol (DG) and triacylglycerol (TG) [9,25,28,29,65,66,67,68,69].

However, there is evidence that other lipids may be implicated in the pathogenesis of T2D, including other species representing PE, its ether-phospholipid and lysophospholipid subclasses, and CL (see below). The chemical structure of lipid species representing the PE class, and the PE(P), LPE, alkylphosphatidylcholine (PC(O)) and lysophosphatidylcholine (LPC) subclasses are shown in Figure 3.1. The PE and PC glycerophospholipid classes are classified according to whether the polar head group attached to the phosphate ester group at the *sn*-3 position of the glycerol backbone is ethanolamine or choline respectively. The ether-phospholipid subclasses are further divided into alkyl- and alkenyl-phospholipids [i.e., PE(O) and PE(P)] according to whether an alkyl chain is linked to the glycerol backbone via an ether- or vinyl-ether bond at the *sn*-1 position respectively]. Lysophospolipids are classified by the attachment of a single fatty acid to the glycerol backbone (e.g. LPE and LPC) (Figure 3.1).

PE is an abundant class of phospholipids that are key building blocks of membrane bilayers in animal and plants, especially in mitochondria. Graessler *et al.* showed that some PE species were significantly elevated in obese men compared with a group of leaner men [28], and Meikle *et al.* showed that prediabetes and T2D were positively associated with fasting plasma total PE and most PE species in two large human cohorts, independent of obesity [9]. In another study, Meikle *et al.* also found that stable coronary artery disease was positively associated with total PE and most PE species [10]. Some PE lipids are a source of arachidonic acid for the production of proinflammatory eicosanoids.

Some PE(P) species are required for intracellular cholesterol transport and signalling in animal tissues [116]. PE(P) deficiency has been implicated in ageing and various degenerative diseases. In one study, circulating levels of the eight identified PE(P) species, especially the 20:4 and 22:6 FA-containing PE(P) species, were significantly reduced in clinical dementia subjects compared with normal-cognitive controls, and the magnitude of this decrease correlated with the severity of the dementia [117]. Furthermore, young adult monozygotic obese co-twins had decreased levels of fasting serum ether-linked PC(O) and PE(O) phospholipids compared with non-obese co-twins [29], and both prediabetes and T2D were negatively associated with fasting plasma PC(O) and alkenylphosphatidylcholine (PC(P)) subclasses [9]. The vinyl ether linkage of the

A.PE 16:1/16:1

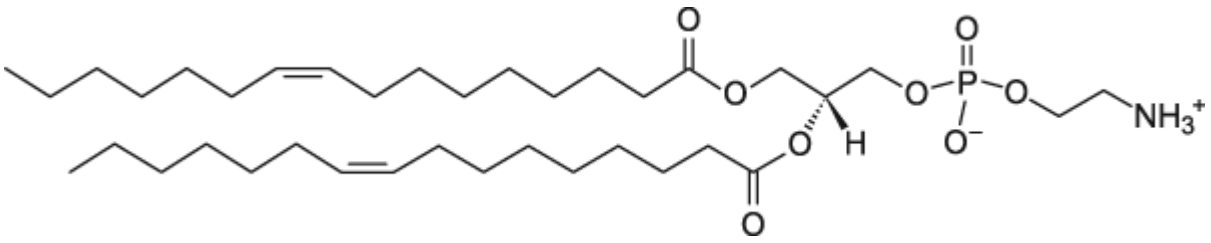

B.PE(P-18:0/18:1)

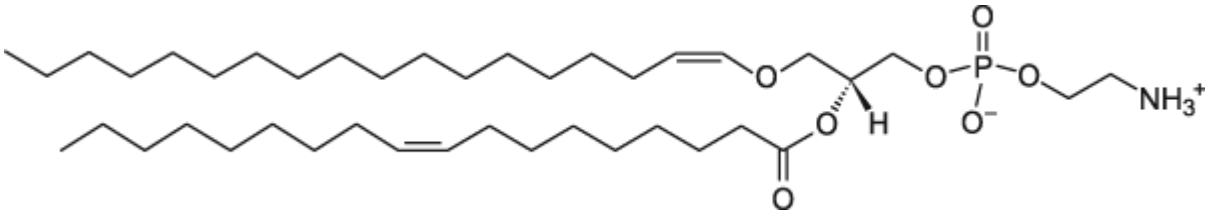

C.LPE 18:1

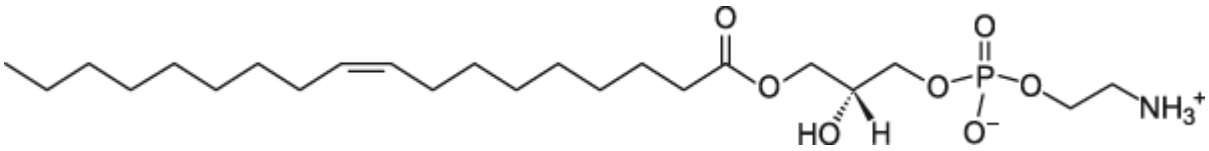

D.PC(O-18:1/18:1)

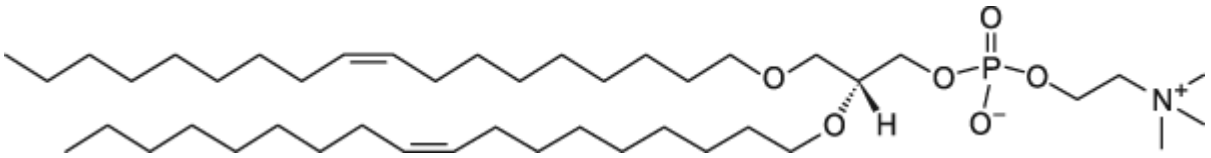

E.LPC 18:1

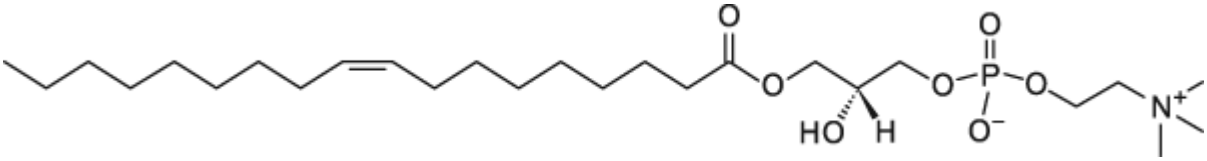

Figure 3.1 Chemical structures of glycerophospholipid species. Lipid species representing the phosphatidylethanolamine (PE) class (A), and alkenylphosphatidylethanolamine plasmalogen (PE(P)) (B), lysophosphoethanolamine (LPE) (C), alkylphosphatidylcholine (PC(O)) (D) and lysophosphatidylcholine (LPC) (E) subclasses. Source: **www.avantilipids.com**

PE(P) and PC(P) plasmalogens is susceptible to oxidation by reactive oxygen species [118,119], and the double bonds associated with polyunsaturated fatty acids in ether-linked PE(O) and PC(O) phospholipids are susceptible to oxidative modification [9].

In contrast, Donovan *et al.* found that five PC(O) species and the plasmalogen PE(P-18:0/20:4) were elevated in morbidly obese subjects compared with lean subjects, and that the treatment of human coronary artery endothelial cells with the PE(P-18:0/20:4) induced expression of cell adhesion molecules, indicative of endothelial cell activation and atherogenesis [63]. Heilbronn *et al.* also observed elevations in fasting plasma PE(P) and PE(O) subclasses in response to 28 days overfeeding by 1250 kcal/day (45% total energy as fat) in healthy adults [54]. These mixed findings highlight the uncertainty of the role of ether-linked phospholipids as antioxidants and/or anti-inflammatory molecules. It is likely that disease severity and the heterogenous nature of the populations may account for the large discrepancy in relative abundance, pattern of change, and phenotypes associated with individual ether-linked phospholipid species.

Although very little is known about the role of LPE lipids in obesity, insulin resistance (IR) and T2D, both LPC and LPE are derived from the oxidation of polyunsaturated (particularly 20:4 and 22:6) FA-containing vinyl ether-linked plasmalogens, PC(P) and PE(P), but are also products of PC and PE hydrolysis by secretory phospholipases [54,63]. In subjects with myocardial infarction or unstable ischemic attack fed a fatty fish diet for 8 weeks, the significant increase in the percentage of the omega n-3 series FAs [eicosapentaenoic acid (20:5n-3), docosahexaenoic acid (22:6n-3) and α-linolenic acid (18:3n-3)] in fasting plasma proved beneficial, resulting in a significant decrease in lipids from the LPE, LPC, Cer and DG classes/subclasses that are potential mediators of IR and inflammation [120]. In agreement with these findings, logistic regression analysis revealed that the LPE subclass, and particularly LPE 20:4 and LPE 22:6 were positively associated with stable coronary artery disease (versus healthy controls), which was likely due to the degradation of PE(P) species (i.e., elimination of the vinyl ether linkage) by reactive oxygen species [10].

3.1.3 Chemical and structural features of cardiolipins

Cardiolipins (CL) or diphosphatidylglycerols (1,3-diphosphatidyl-*sn*-glycerol) are complex anionic phospholipids containing two negative charges, with a dimeric structure consisting of two phosphatidyl moieties, three distinct glycerol backbones, and four FA side-chains (Figure

3.2). CLs are found predominantly in the mitochondrial inner membrane of eukaryotic cells, but also in the mitochondria of higher plants, yeasts, and bacteria, with genetic ancestry traced back to bacterial membranes [121]. In mammals, CL is most abundant in heart, in which 80-90% of the FA chains are linoleate [18:2(n-6)], with lesser amounts of 18:1, 20:4 and 22:6, and tetralinoleoyl-CL (CL 18:2/18:2,18:2/18:2) is the most abundant species [122]. In fact, there is a very limited array of fatty acids involved in the biosynthesis of CL species, and the FA composition of CL is highly specific to species, organ and cell-type [123]. This highly restrictive FA pattern is believed to confer structural uniformity and molecular symmetry across species [122]. The predominant 18:2-rich FA composition within CL species is believed to be achieved by an acyl chain remodelling process [124].

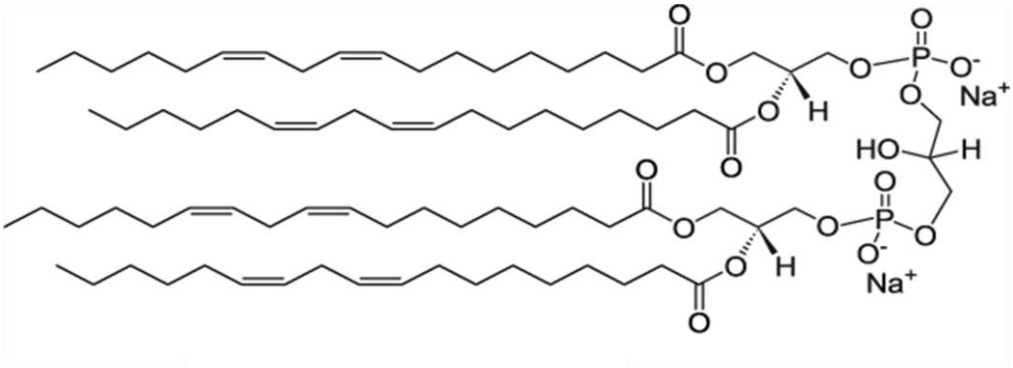

Figure 3.2 Chemical structure of tetralinoleoyl-cardiolipin, CL 18:2/18:2,18:2/18:2.

3.1.4 Role of cardiolipins in mitochondrial dysfunction and diabetes

CL is also required for the proper structure and activity of mitochondrial respiratory chain supercomplexes involved in oxidative phosphorylation [125], and maintains inner membrane fluidity, osmotic stability and potential by interacting with numerous mitochondrial proteins [126]. A loss of CL content, alterations in FA chain composition and/or CL peroxidation can result in mitochondrial dysfunction leading to a number of pathological conditions including ischemia, hypothyroidism, ageing, and heart failure [127].

CL has also been implicated in the pathogenesis of diabetes and cardiovascular disease. Within days after the induction of streptozotocin-induced diabetes in C57BL/6 wild-type mice, there was dramatic loss of the two most abundant CL molecular species present in heart, CL 18:2/18:2,18:2/18:2 and CL 18:1/18:2,18:2/18:2, and a profound remodelling of the remaining

CL molecular species, including a 16-fold increase in the content of CL 18:2/22:6,18:2/22:6, which preceded the TG accumulation in the diabetic myocardium [64]. Similar alterations in CL molecular species were seen in the 4 months old C57BL/6 *ob/ob* mice (hyperglycaemic diabetic state) compared with wild-type mice, but even at 2 months of age (IR, but not hyperglycaemic), there were higher quantities of CL 16:1/18:2,18:2/18:2, CL 20:3/18:2,18:2/18:2 and CL 20:3/18:2,22:6/18:2 in the *ob/ob* mouse heart compared with wild-type mice [64]. These findings are consistent with a role for early (pre-diabetic) alterations in CL species content contributing to mitochondrial dysfunction in diabetic cardiomyopathy.

Due to the high content of unsaturated FAs in CL species, and its location near the site of reactive oxygen species production, CL is particularly susceptible to peroxidative attack by reactive oxygen species. CL peroxidation has been shown to play a critical role in several pathophysiological situations, including human and experimental heart failure [128], non-alcoholic fatty liver [129], and neurodegeneration [130]. Using negative ion mode electrospray ionization mass spectrometry, it was found that the major cardiac CL species, CL 18:2/18:2,18:2/18:2, decreased significantly in failing hearts from spontaneously hypertensive male rats, whereas minor species containing a 20:3, 20:4 or 22:6 FA side-chain were significantly increased [131]. However, despite the importance of CL in mitochondrial function and the pathogenesis of disease states, few studies have quantified individual CL molecular species compared with other cellular lipid classes.

3.1.5 Measurement of cardiolipin species by mass spectrometry in positive ion mode

The majority of studies using LC ESI-MS/MS technology have quantified individual CL species by measuring negatively charged ions [64,121,123]. Impressively, Han *et al.* used shotgun lipidomics in negative ion mode to identify and quantitate cardiolipin molecular species from lipid extracts of mouse heart, liver, and skeletal muscle [123], but this is incompatible with the quantification of many other lipid species that use positive ion mode. Therefore, it was important to develop targeted profiling methodology for the measurement of CL species using optimal LC ESI-MS/MS conditions and established MRM experiments in positive ion mode so that they could be measured in a single experiment with the other lipid species of interest. Crucially, Hsu *et al.* was able to structurally characterise CL species isolated from *E. coli* by detecting sodiated adduct ions $[M-2H+3Na]^+$ using multiple-stage ion-trap mass spectrometric methods in positive ion mode [132].

Given the potentially crucial roles that PE, LPE, PE(O), PE(P) and CL lipid species play in the pathogenesis of T2D, it was important to identify and characterise as many of these species as possible in human and mouse plasma and tissue extracts, so that targeted lipid profiling could be developed to measure species of interest in mouse and human studies examining obesity, IR, and diabetes. The measurement of these biologically important lipids would complement the list of ~270 other lipids that are already routinely quantified in our laboratory using LC ESI-MS/MS and established MRM experiments in positive ion mode.

3.2 MATERIALS AND METHODS

3.2.1 Optimisation of mass spectrometer acquisition parameters for lipid standards

To develop targeted lipid profiling methodology for the measurement of PE, LPE, PE(O), PE(P) and CL species using LC ESI-MS/MS, it was necessary to optimise the MS settings for each lipid class and subclass. Acquisition parameters for PE 16:1/16:1 (exact mass = 687.5 Da), PE(P-18:0/18:1) (exact mass = 729.6 Da) and CL 14:0/14:0,14:0/14:0 (exact neutral mass = 1240.9 Da; purchased as a diammonium salt) lipid standards **(**Avanti Polar Lipids, Alabaster, AL) were optimised in both positive- and negative ion mode on an API 4000 Q/TRAP triple quadrupole mass spectrometer (Applied Biosystems) using a combination of Q1 (first quadrupole) ion scans, product ion scans, and precursor ion scans.

For each standard, a 20 μM stock solution was initially prepared in chloroform/methanol (1:1 v/v), and 200 nM working solutions were prepared on the day of the experiments with methanol/10 mM ammonium formate. Each 200 nM working solution was infused separately into the mass spectrometer at 20 μl/min. For each lipid standard, Q1 ion scans were acquired over 1 min using manual and/or auto tuning to identify distinct molecular parent ion(s) and adducts both in positive- and negative ion mode. The Edit Ramp feature was ramped from 0 to 400 volts to identify the lowest declustering potential (DP) voltage that produced maximum signal intensity of the selected parent ion peak in the Q1 ion scan, with the entrance potential (EP) set at 10 volts or -10 volts for positive and negative ion modes respectively.

Using the assigned optimal voltages for DP and EP and medium collision gas setting, product ion scans were acquired to identify distinct daughter ions in Q3 (third quadrupole) generated from the fragmentation of the selected parent ion in the collision cell (Q2, second quadrupole). Based on the signal intensity and confirmed identification of the daughter ion fragments (from isotopic masses), the Edit Ramp feature was used to optimise the collision energy (CollE) voltage and subsequently the collision exit potential (CXP) voltage to produce maximum signal intensity of the selected daughter ion. In the case of the protonated CL 14:0/14:0,14:0/14:0[M+H]$^+$parent ion, no product ion peaks were initially detected in the product ion scan, but the improved resolution obtained with enhanced product ion scans resulted in the detection and identification of distinct daughter ion fragments in both positive and negative ion mode.

At the time of method development, no suitable LPE standard was available. However, during this developmental period, many LPE species were detected in the plasma and tissue extracts by MRM experiments incorporating the neutral loss (NL) of mass 141.0 Da (equivalent to the mass of the phosphoethanonolamine head group) using the optimal voltages applied to the internal standard PE 17:0/17:0. Subsequently, LPE 14:0 became available, was purchased from Avanti Polar Lipids, and was included as an internal standard for plasma and tissue samples obtained from the Obese/diabetic *db/db* mouse study (Chapter 4), the Human insulin resistance and obesity study (Chapter 6), and the Human short-term overfeeding study [54] using the PE 17:0/17:0 internal standard for the quantification of LPE species [11].

3.2.2 Identification of phosphatidylethanolamine, ether-phospholipid and lysophospholipid species in human plasma

3.2.2.1 Identification of species in human plasma using neutral loss scans

NL scans were performed by LC ESI-MS/MS on a 10 µL human plasma extract from a healthy volunteer containing 100 pmol of PE 17:0/17:0 as internal standard using the acquisition parameters and optimal voltages determined for the PE 16:1/16:1 standard in positive ion mode (Table 1), combined with LC conditions as described previously (section 2.5.3). Three separate experiments (5 µl injections) were performed in positive ion mode to identify [M+H]$^+$parent ions that underwent a NL of mass 141.0 Da in the ranges 400-600 *m/*z, 600-800 *m/*z, and 800-1000 *m/z*.

3.2.2.2 Identification of species in human plasma using stepwise unscheduled multiple reaction monitoring experiments

To perform a comprehensive search for other PE, PE(O), PE(P) or LPE species present in the same human plasma extract, a total of 16 acquisition methods consisting of stepwise unscheduled MRM assignments were constructed, with Q1 values ranging from 451-850 *m/z*. Each acquisition method consisted of 25 paired MRM assignments covering a Q1 range of 25 *m/z* units, with each Q1 *m/z* value corresponding to a potential protonated ($[M+H]^+$) parent ion. Each Q1 *m/z* value was paired with two Q3 values representing a NL of mass 141.0 or 142.0 Da respectively. MRM experiments were performed by LC ESI-MS/MS using the acquisition parameters determined for the PE 16:1/16:1 standard in positive ion mode (Table 3.1), combined with LC conditions as described previously (section 2.5.3). The stepwise design of these 16 acquisition methods enabled the detection of any PE, PE(O), PE(P) or LPE $[M+H]^+$ parent ions and their corresponding $[M+1]^+$ and $[M+2]^+$ isotopologues (containing one or two ^{13}C-atoms respectively in the biological range 451-850 *m/z* (cut-off < 500 cps peak height). As lipids have a distribution of masses driven primarily by ^{13}C atoms (accounting for ~1% of the total lipid abundance), the scanning of NL of mass 142.0 Da will detect non-monoisotopic lipids containing at least one ^{13}C-atom. As we are only interested in the signal arising from a NL of mass 141.0 Da for monoisotopic lipids, this method allows monoisotopic lipids to be chromatographically distinguished from non-monoisotopic lipids.

3.2.2.3 Determination of fatty acid composition of species in human plasma

To confirm the identity and chemical structure of the 65 PE, PE(O) and PE(P) species detected in human plasma, it was important to determine the FA-chain composition of each species in the same human plasma extract by established LC ESI-MS/MS using the acquisition parameters determined for the PE 16:1/16:1 standard in negative ion mode (Table 3.1). A total of 16 acquisition methods consisting of unscheduled MRM experiments were designed to detect these 65 species using 46 different Q1 *m/z* values corresponding to negatively charged $[M-H]^-$

Table 3.1 Optimised acquisition parameters for lipid standards on an API 4000 Q/TRAP mass spectrometer.

Lipid Standard[a]	Ion mode	Selected parent ion	Q1 *m/z*	Selected daughter ion	Q3 *m/z*	Voltage settings (volts)			
						DP	EP	CollE	CXP
PE 16:1/16:1	Positive	$[M+H]^+$	688.5	NL, 141.0 Da	547.5	80	10	30	14
	Negative	$[M-H]^-$	686.5	Fatty acid 16:1$[M-H]^-$	253.2	-120	-10	-50	-14
PE(P-18:0/18:1)	Positive	$[M+H]^+$	730.6	NL, 141.0 Da	589.6	55	10	21	8
	Negative	$[M-H]^-$	728.5	Fatty acid 18:1$[M-H]^-$	281.3	-120	-10	-50	-14
CL 14:0/14:0,14:0/14:0	Positive	*$[M+H]^+$	1242.0	DG 14:0/14:0$[M+H]^+$ -H_2O	495.5	130	10	39	12
	Negative	$[M-H]^-$	1239.8	Distinct ion at *m/z* 525.0	525.0	NM	NM	NM	NM

[a] Mass spectrometer default settings: Curtain gas, 10 psi ; Turbo-ion spray source, 5000 or -5000 volts, 350°C; Ion source gas 1, 40 psi; Ion source gas 2, 40 psi

PE, phospatidylethanolamine; PE(P), alkenylphosphatidylethanolamine; CL, cardiolipin; Q1, first quadrupole; Q3, third quadrupole; NL, neutral loss; DG, diglyceride; DP, declustering potential; EP, entrance potential; CollE, collision energy; CXP, collision cell exit potential; NM, not measured

***** Distinct parent ions were also detected at *m/z* 1258.9 for $[M+NH_4]^+$ and *m/z* 1264.0 for $[M+Na]^+$

parent ions. Each acquisition method consisted of three Q1 $[M-H]^-$ parent ion *m/z* values, with each Q1 value assigned to 13 different Q3 $[M-H]^-$ daughter ion *m/z* values corresponding to the most abundant FAs found in human plasma, namely 14:0, 15:0, 16:0, 16:1, 17:0, 18:0, 18:1, 18:2, 18:3, 20:3, 20:4, 22:5 and 22:6.

3.2.3 Identification of cardiolipin species in human plasma and mouse tissues

3.2.3.1 Identification of species in human plasma using unscheduled multiple reaction monitoring

Initially, an acquisition method using unscheduled MRM experiments consisting of $CL[M+H]^+$ parent ions (Q1) and their paired diglyceride (DG) adduct daughter ions, $DG[M+H]^+ -H_2O$ (Q3), were constructed to identify major CL species [64,121,123,128,131] in positive ion mode using the optimal acquisition voltage settings and parameters determined for the CL 14:0/14:0,14:0/14:0 standard (Table 3.1). Initially, a 10 µl human plasma extract from a healthy volunteer containing 50 pmol CL 14:0/14:0,14:0/14:0 as internal standard was analysed using established LC ESI-MS/MS conditions in positive ion mode.

3.2.3.2 Identification of species in mouse heart using precursor ion scans

Four separate precursor ion scan experiments (5 µl injections) were performed on a 10 µl wild-type C57BL/6 mouse heart extract containing 50 pmol CL 14:0/14:0,14:0/14:0 as internal standard using the acquisition parameters determined for the CL 14:0/14:0,14:0/14:0 standard in positive ion mode (Table 3.1). These experiments were constructed to identify $CL[M+H]^+$ parent ions that generated the major daughter ions DG 18:2/18:2$[M+H]^+ -H_2O$, DG 18:2/18:1$[M+H]^+ -H_2O$, DG 18:2/20:4$[M+H]^+ -H_2O$ or DG 18:2/22:6$[M+H]^+ -H_2O$ (with Q3 *m/z* values of 599.5, 601.5, 623.5 and 647.5 respectively).

3.2.3.3 Identification of species in different mouse tissues using unscheduled multiple reaction monitoring experiments

An acquisition method with unscheduled MRM assignments in positive ion mode was constructed to quantify the 16 CL species identified in the four precursor ion scans in the mouse heart extract. Another acquisition method with unscheduled MRM assignments in positive ion

mode was then constructed to identify further CL species [123] in 10 µl wild-type C57BL/6 mouse heart, skeletal muscle, liver and adipose tissue extracts (two samples from each tissue-type) containing 50 pmol CL 14:0/14:0,14:0/14:0 as internal standard using the acquisition parameters determined for the CL 14:0/14:0,14:0/14:0 standard in positive ion mode (Table 3.1). From the 31 CL species tested, 20 CL species were identified and quantified in wild-type C57BL/6 mouse heart, with a lesser number of CL species detected in the liver, skeletal muscle and adipose tissue extracts. An acquisition method with unscheduled MRM assignments in positive ion mode was designed and tested in the same wild-type C57BL/6 mouse heart, skeletal muscle, liver and adipose tissue extracts to capture all the DG adduct daughter ions generated from each of these 20 abundant CL$[M+H]^+$ parent ions, ensuring full coverage of measurements (Table 3.5).

3.2.3.4 Quantification of the 20 most abundant cardiolipin species in mouse heart

Finally, an acquisition method with scheduled MRM assignments was constructed to quantify the 20 most abundant CL species found in mouse heart extracts. This acquisition method was designed so that each CL$[M+H]^+$ parent ion was assigned to one of the paired Q3 DG$[M+H]^+$ - H_2O adduct daughter ions generated from each isomer within that CL species (Table 3.6). This method was used for subsequent measurement of these 20 CL species in plasma and tissue samples obtained from the Obese/diabetic *db/db* mouse study (Chapter 4), the Human insulin resistance and obesity study (Chapter 6), and the Human short-term overfeeding study [54] using the same optimal voltage settings applied to the CL 14:0/14:0,14:0/14:0 standard in positive ion mode.

3.3 RESULTS

3.3.1 Optimal API 4000 Q/TRAP mass spectrometer acquisition parameters and voltages for lipid standards

The optimal API 4000 Q/TRAP triple quadrupole MS acquisition parameters obtained for PE 16:1/16:1, PE(P-18:0/18:1), and CL 14:0/14:0,14:0/14:0 lipid standards in both positive- and negative ion modes are shown in (Table 3.1). In positive ion mode, Q1 ion scans showed distinct $[M+H]^+$ parent ions for all three standards, and CL 14:0/14:0,14:0/14:0 also generated distinct

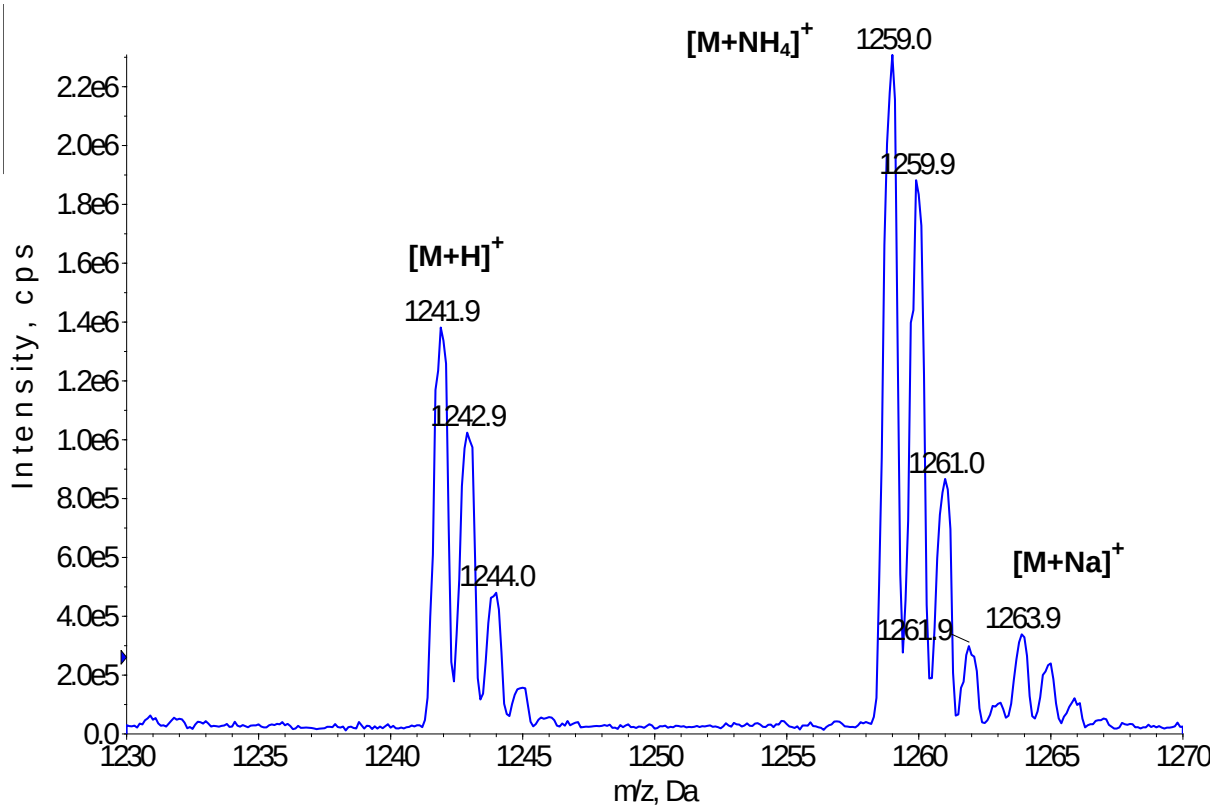

Figure 3.3 Q1 spectra of a cardiolipin standard, CL 14:0/14:0,14:0/14:0. A 200 nM working solution of CL 14:0/14:0,14:0/14:0 was prepared in methanol/10 mM ammonium formate and infused into the API 4000 Q/TRAP mass spectrometer at 20 ul/min. Q1 ion scans were performed in positive ion mode over 1 min using default settings: Curtain gas, 10 psi ; Turbo-ion spray, 5000 volts, 350°C; Ion source gas 1, 40 psi; Ion source gas 2, 40 psi.

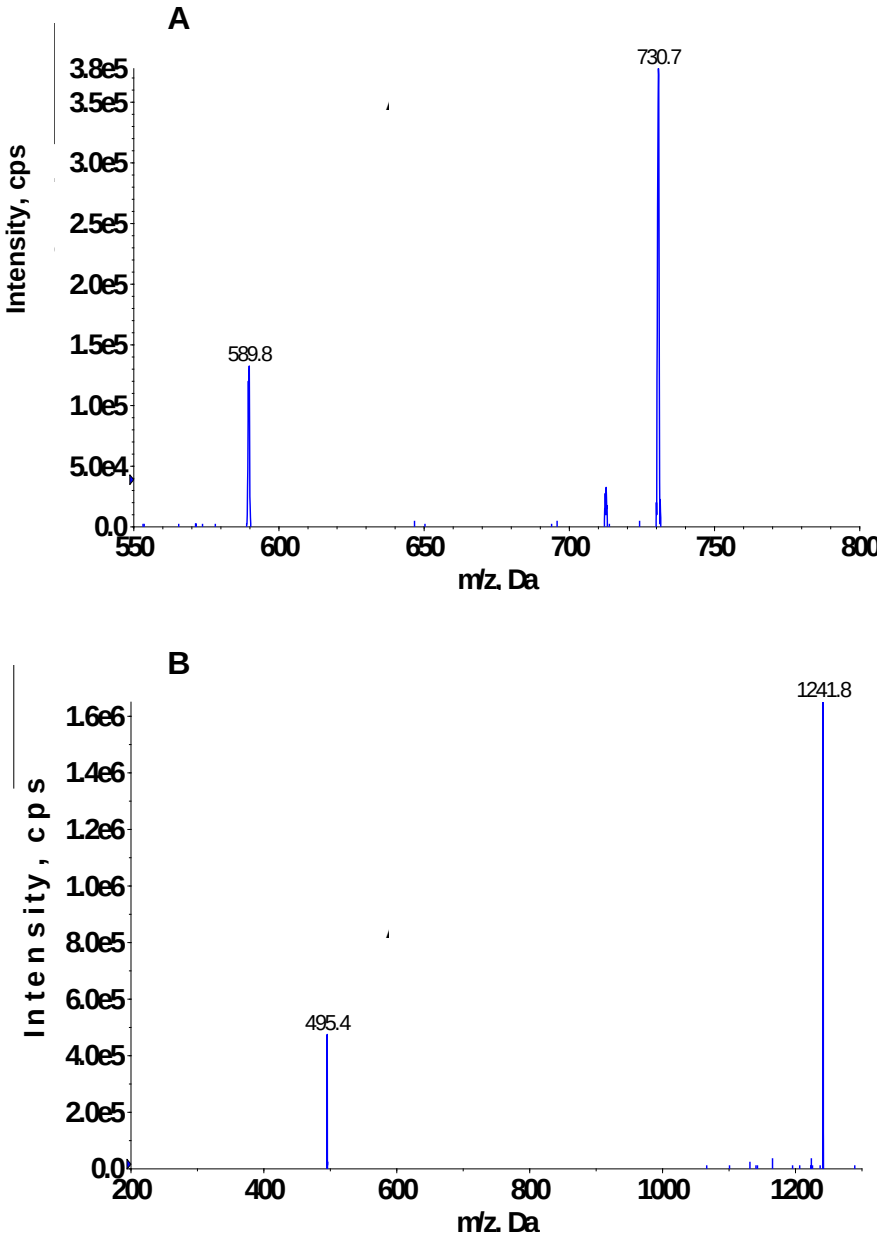

Figure 3.4 Product ion spectra of alkenylphosphatidylethanolamine plasmalogen and cardiolipin standards. Working solutions (200 nM) of the lipid standards were prepared in methanol/10 mM ammonium formate, and infused separately into the API 4000 Q/TRAP mass spectrometer at 20 µl/min. A product ion scan of PE(P-18:0/18:1)$[M+H]^+$ (A) or enhanced product ion scan of CL 14:0/14:0,14:0/14:0$[M+H]^+$ (B) were performed in positive ion mode over 1 min using optimal voltages and default settings (Table 3.1).
NL, neutral loss; DG, diglyceride

$[M+NH_4]^+$ and $[M+Na]^+$ parent ions at *m/z* 1259.0 and 1263.9 respectively (Figure 3.3). Product ion scans revealed that the parent ions PE 16:1/16:1$[M+H]^+$ and PE(P-18:0/18:1)$[M+H]^+$ generated distinct daughter ions at *m/z* 547.5 and 589.6 respectively, indicating a NL of 141.0 Da, equivalent to the mass of the phosphoethanolamine head group. The product ion spectra of PE(P-18:0/18:1) is shown in Figure 3.4A. An enhanced product ion scan of CL 14:0/14:0,14:0/14:0$[M+H]^+$ showed a distinct daughter ion peak corresponding to DG 14:0/14:0$[M+H]^+$ -H_2O at *m/z* 495.4 (Figure 3.4B). In negative ion mode, Q1 ion scans showed that all three lipid standards generated a distinct $[M-H]^-$ parent ion. Product ion scans revealed that the parent ions PE 16:1/16:1$[M-H]^-$ and PE(P-18:0/18:1)$[M-H]^-$ generated distinct daughter ions corresponding to fatty acid 16:1$[M-H]^-$ and fatty acid 18:1$[M-H]^-$ at *m/z* 253.2 and *m/z* 281.3 respectively, whereas CL 14:0/14:0,14:0/14:0$[M-H]^-$ generated an unidentified ion fragment at *m/z* 525.0.

3.3.2 Phosphatidylethanolamine, ether-phospholipid and lysophospholipid species identified in human plasma

The NL of 141.0 Da scan of a plasma extract from a healthy volunteer using LC ESI-MS/MS identified 42 species, including 7 PE, 8 PE(O), 8 PE(P) and 4 LPE species (intensity cut-off > 1.0 % of the major species detected). The lipids were initially characterised according to their isotopic masses and comparison of retention times with other closely related species (Figure 3.5). The resolution of the LC is sufficient enough to obtain separate peaks for lipid species with identical isotopic masses, and allows identification of these species based on retention times [11].

The sensitivity of MRM experiments is superior to that achieved by NL scans, enabling the detection of other PE, PE(O), PE(P) and LPE species in the same human plasma extract. A total of 13 LPE and 65 PE, PE(O) and PE(P) species were detected and identified in the human plasma extract from a healthy volunteer by stepwise unscheduled MRM experiments (Q1 values ranging from 451-850 *m/z*) according to isotopic mass and comparison of retention times with other closely related species (Table 3.2). For example, the isomeric lipid species PE 36:6, PE(O-37:6) and PE(P-37:5) were detected using the same ion pair (736.6/595.6), but they were able to be separated chromatographically at the bond type level (i.e., acyl, alkyl or alkenyl) [133], with distinct peaks generated at retention times of 5.91, 6.20 and 6.35 min respectively.

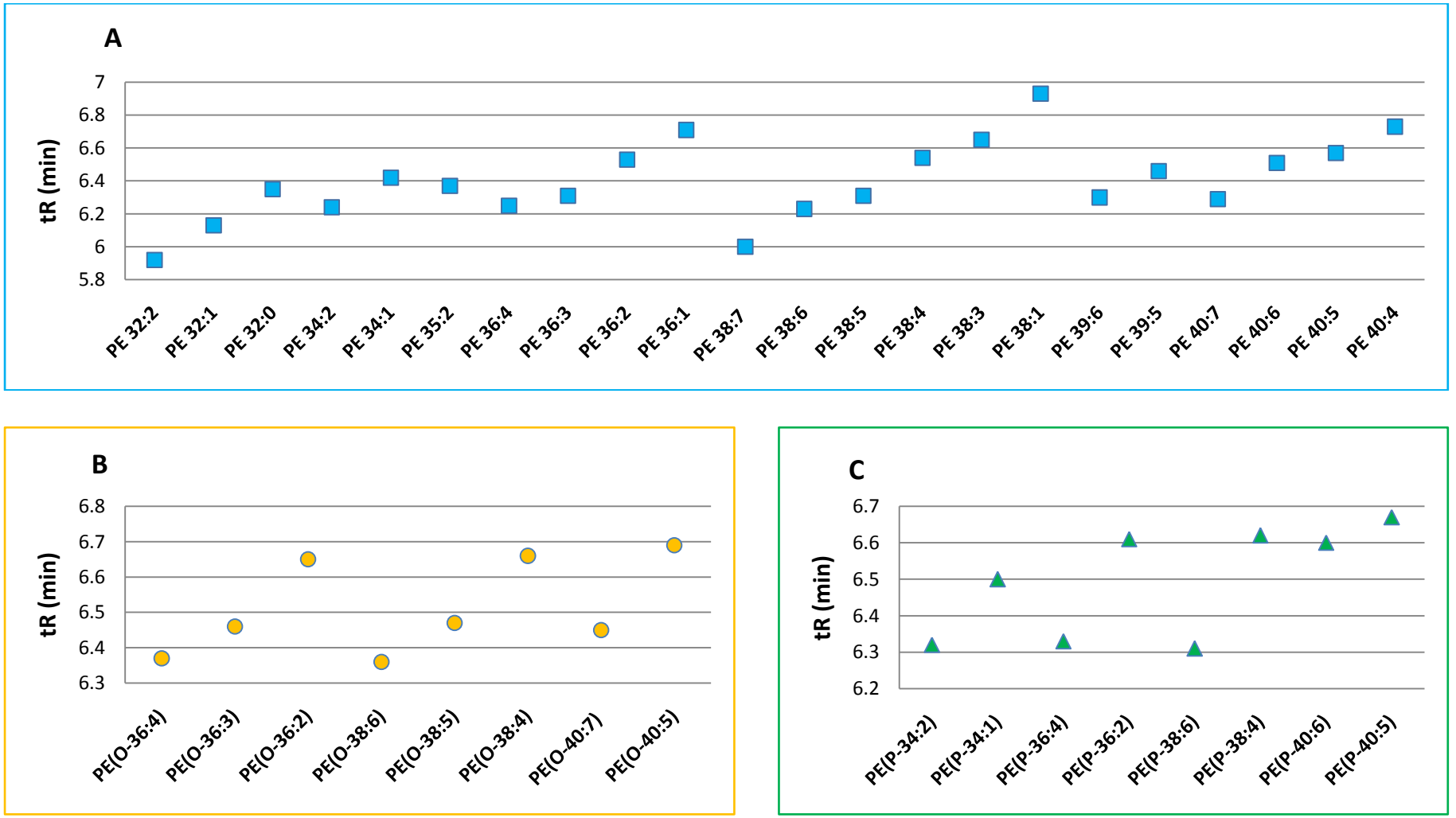

Figure 3.5 Identification of phosphatidylethanolamine, alkylphosphatidylethanolamine and alkenylphosphatidylethanolamine species in human plasma. Neutral loss of 141.0 Da scans were performed in positive ion mode on a API 4000 Q/TRAP mass spectrometer using optimal voltages and default settings (Table 3.1). Species of phosphatidylethanolamine (A), alkylphosphatidylethanolamine (B) and alkenylphosphatidylethanolamine (C) were identified according to isotopic mass and comparison of retention times with other closely related species.

Table 3.2 Identification of 78 phosphatidylethanolamine, ether-phospholipid and lysophospholipid species in human plasma.

No.	Lipid species[a]	Q1 *m/z* of $[M+H]^+$ parent ion	Q3 *m/z* of $[M+H]^+$ daughter ion[b]	Retention time (min)
1	LPE 16:1	452.3	311.2	1.53
2	LPE 16:0	454.3	313.2	2.48
3	LPE 18:3	476.3	335.2	1.63
4	LPE 18:2	478.3	337.2	2.01
5	LPE 18:1	480.3	339.2	2.9
6	LPE 18:0	482.3	341.2	3.69
7	LPE 20:4	502.4	361.3	2.13
8	LPE 20:3	504.4	363.3	2.59
9	LPE 20:2	506.4	365.3	2.47
10	LPE 20:1	508.4	367.3	3.27
11	LPE 22:6	526.4	385.3	2.25
12	LPE 22:5	528.4	387.3	2.32
13	LPE 22:4	530.4	389.3	2.52
14	PE 32:2	688.5	547.4	5.88
15	PE 32:1	690.5	549.4	6.12
16	PE 32:0	692.5	551.4	6.35
17	PE(P-34:2)	700.5	559.4	6.33
18	PE(O-34:2)	702.5	561.4	6.37
19	PE(P-34:1)	702.5	561.4	6.5
20	PE 33:1	704.5	563.4	6.27
21	PE(O-34:1)	704.5	563.4	6.55
22	PE(O-34:0)	706.5	565.4	6.79
23	PE 34:4	712.5	571.4	5.92
24	PE(O-35:4)	712.5	571.4	6.22
25	PE 34:3	714.5	573.4	6.03
26	PE(O-35:3)	714.5	573.4	6.48
27	PE 34:2	716.5	575.4	6.22
28	PE 34:1	718.5	577.4	6.43
	PE 17:0/17:0 (IS)	720.5	579.4	6.64
29	PE(O-36:6)	722.5	581.4	6.17
30	PE(O-36:5)	724.5	583.4	6.2
31	PE(P-36:4)	724.5	583.4	6.34
32	PE(O-36:4)	726.6	585.5	6.39
33	PE 35:3	728.6	587.5	6.2
34	PE(O-36:3)	728.6	587.5	6.5
35	PE(P-36:2)	728.6	587.6	6.65
36	PE 35:2	730.6	589.5	6.4
37	PE(O-36:2)	730.6	589.5	6.66
38	PE 35:1	732.6	591.5	6.6
39	PE 35:0	734.6	593.5	6.81
40	PE 36:6	736.6	595.5	5.91
41	PE(O-37:6)	736.6	595.5	6.2
42	PE(P-37:5)	736.6	595.6	6.35
43	PE 14:0/22:5	738.6	597.5	6.07

No.	Lipid species[a]	Q1 *m/z* of $[M+H]^+$ parent ion	Q3 *m/z* of $[M+H]^+$ daughter ion[b]	Retention time (min)
44	PE(P-37:4)	738.6	597.5	6.49
45	PE 36:4	740.6	599.5	6.26
46	PE(P-37:3)	740.6	599.5	6.5
47	PE 36:3	742.6	601.5	6.31
48	PE(P-37:2)	742.6	601.5	6.65
49	PE 36:2	744.6	603.5	6.54
50	PE 36:1	746.6	605.5	6.72
51	PE(P-38:6)	748.6	607.5	6.32
52	PE 36:0	748.6	607.5	6.94
53	PE(O-38:6)	750.6	609.5	6.38
54	PE(O-38:5)	752.6	611.5	6.44
55	PE(P-38:4)	752.6	611.5	6.65
56	PE(O-38:4)	754.6	613.5	6.68
57	PE(O-38:3)	756.6	615.5	6.92
58	PE 38:7	762.6	621.5	6
59	PE(P-39:6)	762.6	621.5	6.48
60	PE 38:6	764.6	623.5	6.23
61	PE 38:5	766.6	625.5	6.32
62	PE 38:4	768.6	627.5	6.56
63	PE 38:3	770.6	629.5	6.63
64	PE 38:2	772.6	631.5	6.76
65	PE(O-40:7)	776.6	635.5	6.48
66	PE(P-40:6)	776.6	635.5	6.63
67	PE 39:6	778.6	637.5	6.38
68	PE(O-40:6)	778.6	637.5	6.49
69	PE(P-40:5)	778.6	637.5	6.67
70	PE(O-40:5)	780.6	639.5	6.73
71	PE(P-40:4)	780.6	639.5	6.94
72	PE(O-40:4)	782.6	641.5	6.88
73	PE(O-40:3)	784.6	643.5	7.18
74	PE 40:7	790.6	649.5	6.32
75	PE 40:6	792.6	651.5	6.53
76	PE 40:5	794.6	653.5	6.69
77	PE 40:4	796.6	655.5	6.75
78	PE(O-42:7)	804.7	663.6	7.54

[a] The 11 LPE species highlighted in blue were added to the list of ~270 lipid species routinely measured using liquid chromatography electrospray ionisation-tandem mass spectrometry and established multiple reaction monitoring experiments **(**MRM) in positive ion mode (Table 2.1).

[b] MRM experiments (incorporating NL of 141.0 Da) were performed in positive ion mode on a API 4000 Q/TRAP mass spectrometer using optimal voltages and default settings (Table 3.1)

Q1, first quadrupole; Q3, third quadrupole; LPE, lysophosphatidylethanolamine; PE, phosphatidylethanolamine; PE(O), alkylphosphatidylethanolamine; PE(P), alkenylphosphatidylethanolamine; NL, neutral loss; IS, internal standard

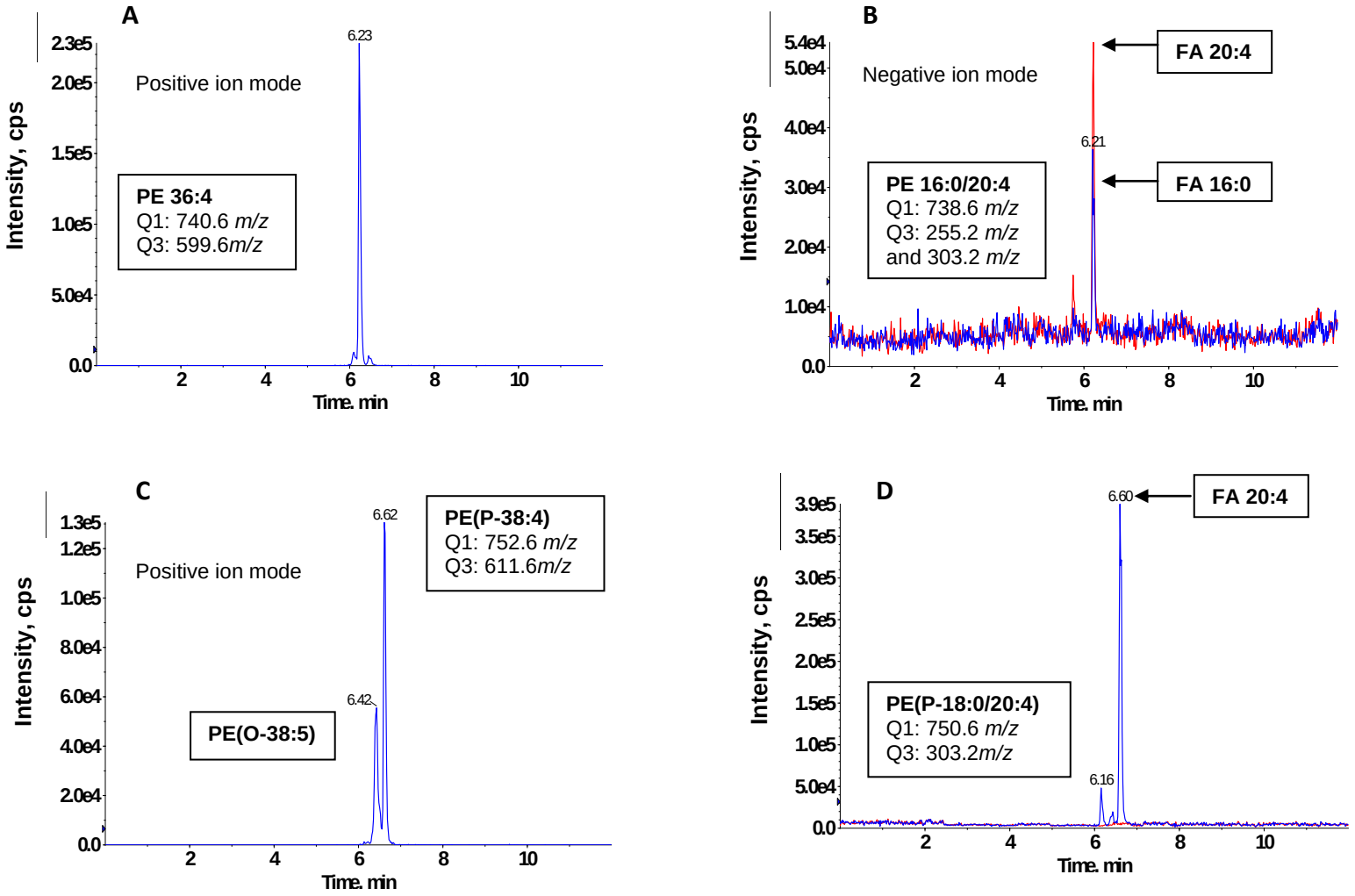

Figure 3.6 Determination of fatty acid composition in lipid species in human plasma. Typical spectra for PE 36:4 (Panels A and B) and PE(P-38:4) (Panels C and D) in positive ion mode (by neutral loss of mass 141.0 Da) and in negative ion mode (by detection of selected fatty-acid daughter ions) respectively on a API 4000 Q/TRAP mass spectrometer using optimal voltages and default settings (Table 3.1).
PE, phosphatidylethanolamine; PE(O), alkylphosphatidylethanolamine; PE(P), alkenylphosphatidylethanolamine

3.3.3 Fatty acid composition of lipid species in human plasma

Full or partial fatty acyl-chain composition was determined in 36 of the 65 PE, PE(O) and PE(P) species previously identified by stepwise unscheduled MRM experiments in positive ion mode. Typical spectra showing the matching retention times of the peaks detected for PE 36:4 and PE(P-38:4) in positive ion mode (incorporating NL of 141.0 Da) and negative ion mode (unscheduled MRM experiments incorporating the detection of selected fatty acid daughter ions) respectively under optimal LC ESI-MS/MS conditions are shown in Figure 3.6. In positive ion mode, the Q1 parent ion PE 36:4$[M+H]^+$ (*m/z* 740.6) generated a Q3 daughter ion (*m/z* 599.6) with a retention time of 6.23 min (Figure 3.6A). In negative ion mode, the Q1 parent ion PE 36:4$[M-H]^-$ (*m/z* 738.6) generated two Q3 daughter ions, fatty acid 16:0$[M-H]^-$ (*m/z* 255.2) and fatty acid 20:4$[M-H]^-$ (*m/z* 303.2), with the same retention time of 6.21 min (Figure 3.6B). Subsequent examination of the fatty acid product corresponding to 18:2 or other possible fatty acids failed to produce a signal at the specified retention time. These findings indicate that PE 36:4 consists primarily of fatty acids 16:0 and 20:4, allowing re-identification at the fatty acyl/alkyl level as PE 16:0/20:4 [133]. Using the same steps, fatty acid 20:4 was detected as the only product of PE(P-38:4) with a retention time of 6.60 min (Figures 3.6C and D). As plasmalogens do not have a fatty acid in the vinyl ether-linked sn-1 position, we deduced that this lipid corresponded to PE(P-38:4), and could be re-defined as PE(P-18:0/20:4). Overall, full or partial fatty-acyl chain composition was detected in 36 of the 65 PE, PE(O) and PE(P) species (Table 3.3). In cases where more than two fatty acids were detected in the same species (e.g. 18:0, 18:1 and 18:2 were detected in PE 36:2), the possible isomers were identified (i.e., PE 18:1/18:1 and PE 18:0/18:2), and the relative abundance was measured, but the nomenclature remained at the less specific bond type level (PE 36:2).

From the list of 13 LPE and 65 PE, PE(O) and PE(P) species that were identified in the human plasma extract using LC ESI-MS/MS and stepwise unscheduled MRM experiments in positive ion mode (section 3.3.2), 40 species, including 11 LPE species (highlighted in blue in Table 3.2), along with 5 PE, 14 PE(O) and 10 PE(P) species (highlighted in blue in Table 3.3) were added to the list of ~270 lipid species routinely measured using LC ESI-MS/MS and established MRM experiments in positive ion mode as part of a targeted lipid profiling strategy. Despite determining the fatty acid composition of 17 of the 29 selected PE, PE(O) and PE(P) species (Table 3.3), the nomenclature used for these species in future mouse and human studies examining the pathogenesis of T2D remained at the less specific bond type level (e.g., PE 34:2),

Table 3.3 Fatty acid composition of phosphatidylethanolamine and ether-phospholipid species in human plasma.

	Positive ion mode		Negative ion mode		
No.	Q1 *m/z* of $[M+H]^+$ parent ion	Lipid species[a, c]	Q1 *m/z* of $[M-H]^-$ parent ion	Q3 $[M-H]^-$ fatty acids detected[b]	Possible lipid species
1	688.5	PE 32:2	686.5	None	PE 32:2
2	690.5	PE 32:1	688.5	None	PE 32:1
3	692.5	PE 32:0	690.5	None	PE 32:0
4	700.5	PE(P-34:2)	698.5	18:2	PE(P-16:0/18:2)
5	702.5	PE(O-34:2)	700.5	None	PE(O-34:2)
6	702.5	PE(P-34:1)	700.5	18:1	PE(P-16:0/18:1)
7	704.5	PE 33:1	702.5	None	PE 33:1
8	704.5	PE(O-34:1)	702.5	None	PE(O-34:1)
9	706.5	PE(O-34:0)	704.5	None	PE(O-34:0)
10	712.5	PE 34:4	710.5	None	PE 34:4
11	712.5	PE(O-35:4)	710.5	None	PE(O-35:4)
12	714.5	PE 34:3	712.5	None	PE 34:3
13	714.5	PE(O-35:3)	712.5	18:2	PE(O-17:1/18:2)
14	716.5	PE 34:2	714.5	16:0, 18:2	PE 16:0/18:2
15	718.5	PE 34:1	716.5	16:0, 18:1	PE 16:0/18:1
	720.5	PE 17:0/17:0 (IS)	718.5	17:0	PE 17:0/17:0 (IS)
16	722.5	PE(O-36:6)	720.5	None	PE(O-36:6)
17	724.5	PE(O-36:5)	722.5	None	PE(O-36:5)
18	724.5	PE(P-36:4)	722.5	20:4	PE(P-16:0/20:4)
19	726.6	PE(O-36:4)	724.6	18:2	PE(O-18:2/18:2)
20	728.6	PE 35:3	726.6	18:2	PE 17:1/18:2
21	728.6	PE(O-36:3)	726.6	18:1	PE(O-18:1/18:2)
22	728.6	PE(P-36:2)	726.6	18:2	PE(P-18:0/18:2)
23	730.6	PE 35:2	728.6	None	PE 35:2
24	730.6	PE(O-36:2)	728.6	18:2	PE(O-18:0 /18:2)
25	732.6	PE 35:1	730.6	None	PE 35:1
26	734.6	PE 35:0	732.6	None	PE 35:0
27	736.6	PE 36:6	734.6	None	PE 36:6
28	736.6	PE(O-37:6)	734.6	None	PE(O-37:6)
29	736.6	PE(P-37:5)	734.6	None	PE(P-37:5)
30	738.6	PE 36:5	736.6	14:0	PE 14:0/22:5
31	738.6	PE(P-37:4)	736.6	20:4	PE(P-17:0/20:4)
32	740.6	PE 36:4	738.6	16:0, 20:4	PE 16:0/20:4
33	740.61	PE(P-37:3)	738.6	None	PE(P-37:3)
34	742.6	PE 36:3	740.6	18:1, 18:2	PE 18:1/18:2
35	742.6	PE(P-37:2)	740.6	None	PE(P-37:2)
36	744.6	PE 36:2	742.6	18:0, 18:1, 18:2	PE 18:1/18:1; PE 18:0/18:2
37	746.6	PE 36:1	744.6	18:0, 18:1	PE 18:0/18:1
38	748.6	PE(P-38:6)	746.6	22:6	PE(P-16:0/22:6)
39	748.6	PE 36:0	746.6	None	PE 36:0
40	750.6	PE(O-38:6)	748.6	20:4, 22:5	PE(O-18:2/20:4); PE(O-16:1/22:5)

No.	Positive ion mode		Negative ion mode		
	Q1 *m/z* of $[M+H]^+$ parent ion	Lipid species[a, c]	Q1 *m/z* of $[M-H]^-$ parent ion	Q3 $[M-H]^-$ fatty acids detected[b]	Possible lipid species
41	752.6	PE(O-38:5)	750.6	20:3, 22:5	PE(O-18:2/20:3); PE(O-16:0/22/5
42	752.6	PE(P-38:4)	750.6	20:4	PE(P-18:0/20:4)
43	754.6	PE(O-38:4)	752.6	20:3	PE(O-18:1/20:3)
44	756.6	PE(O-38:3)	754.6	18:2	PE(O-20:1/18:2)
45	762.6	PE 38:7	760.6	None	PE 38:7
46	762.6	PE(P-39:6)	760.6	None	PE(P-39:6)
47	764.6	PE 38:6	762.6	16:0, 18:0, 22:6	PE 16:0/22:6
48	766.6	PE 38:5	764.6	16:0, 18:1, 20:4, 22:5	PE 18:1/20:4; PE 16:0/22:5
49	768.6	PE 38:4	766.6	18:0, 20:4	PE 18:0/20:4
50	770.6	PE 38:3	768.6	20:3	PE 18:0/20:3
51	772.6	PE 38:2	770.6	None	PE 38:2
52	776.6	PE(O-40:7)	774.6	22:5	PE(O-18:2/22:5)
53	776.6	PE(P-40:6)	774.6	22:6	PE(P-18:0/22:6)
54	778.6	PE 39:6	776.6	None	PE 39:6
55	778.6	PE(O-40:6)	776.6	None	PE(O-40:6)
56	778.6	PE(P-40:5)	776.6	22:5	PE(P-18:0/22:5)
57	780.6	PE(O-40:5)	778.6	22:5	PE(O-18:0/22:5)
58	780.6	PE(P-40:4)	778.6	20:4	PE(P-20:0/20:4)
59	782.6	PE(O-40:4)	780.6	None	PE(O-40:4)
60	784.6	PE(O-40:3)	782.6	18:2	PE(O-22:1/18:2)
61	790.6	PE 40:7	788.6	18:1	PE 18:1/22:6
62	792.6	PE 40:6	790.6	18:0, 22:6	PE 18:0/22:6
63	794.6	PE 40:5	792.6	None	PE 40:5
64	796.6	PE 40:4	794.6	18:0	PE 18:0/22:4
65	804.7	PE(O-42:7)	802.7	None	PE(O-42:7)

[a] The identity of 65 PE, PE(O) and PE(P) species was initially determined using liquid chromatography electrospray ionisation-tandem mass spectrometry (LC ESI-MS/MS) and stepwise unscheduled multiple reaction monitoring **(**MRM) experiments (incorporating NL of 141.0 Da) in positive ion mode on a API 4000 Q/TRAP mass spectrometer using optimal voltages and default settings (Table 3.1).

[b] The fatty acid composition of lipid species was determined using unscheduled MRM experiments in negative ion mode (by detection of selected fatty acid daughter ions)

[c] The 29 PE, PE(O) and PE(P) species highlighted in blue were added to the list of ~270 lipid species routinely measured using LC ESI-MS/MS and established **(**MRM) in positive ion mode (Table 2.1).

Q1, first quadrupole; Q3, third quadrupole; PE, phosphatidylethanolamine; PE(O) alkylphosphatidylethanolamine; PE(P), alkenylphosphatidylethanolamine; NL, neutral loss; IS, internal standard

as the abundance of specific isomers of these lipids was likely to vary in human versus mouse plasma, and in different tissues.

3.3.4 Cardiolipin species identified in human plasma and mouse tissues

Using unscheduled MRM experiments consisting of Q1 $[M+H]^+$ parent ions coupled to Q3 DG adduct daughter ions ($DG[M+H]^+ -H_2O$) in positive ion mode, only two CL species, namely CL 18:2/18:2,18:2/18:2 and CL 18:2/18:2,18:2/18:1, were identified in a human plasma extract. Using precursor ion scans, a total of 16 individual CL species were identified that generated the major daughter ions DG 18:2/18:2$[M+H]^+$-H_2O, DG 18:2/18:1$[M+H]^+$-H_2O, DG18:2/20:4$[M+H]^+$ -H_2O or DG 18:2/22:6$[M+H]^+$ -H_2O in a C57BL/6 wild-type mouse heart extract (Figure 3.7 and Table 3.4).

Using more sensitive unscheduled MRM experiments, at least 11 of the 31 CL species tested were detected in all C57BL/6 wild-type mouse tissue (heart, liver, skeletal muscle, and adipose) extracts. The mean percent abundance of the 20 most abundant CL species across the four mouse tissues is shown in Figure 3.8, with the distribution of the six most abundant CL species in each of the tissues shown in Figure 3.9. These six CL species contributed at least 85% to the total CL content in all mouse tissue extracts. The total CL content was highest in the heart, with the liver, skeletal muscle and adipose tissue containing 31%, 13% and 5% of the heart content respectively. Interestingly, CL species containing at least one 22:6 FA chain contributed 24% and 21% to the total CL content in heart and skeletal muscle respectively, but only ~2% in liver and adipose tissue. The two most abundant CL species in all tissues tested were CL 18:2/18:2,18:2/18:2 and CL 18:2/18:2,18:2/18:1, combining to contribute 64%, 77%, 52% and 77% to the total CL content in heart, liver, skeletal muscle and adipose tissue respectively.

3.3.5 Full coverage of the 20 most abundant cardiolipin species in mouse tissues

An acquisition method consisting of unscheduled MRM experiments designed to capture all DG adduct daughter ions ($DG[M+H]^+ -H_2O$) generated from the 20 most abundant CL species in 10 µL C57BL/6 wild-type mouse tissue extracts (heart, liver, skeletal muscle and adipose) is shown in Table 3.5. These 20 CL species consisted of 33 isomers, requiring 63 MRM experiments to cover all possible combinations of Q3 DG $[M+H]^+ -H_2O$ daughter ions obtained from collision-

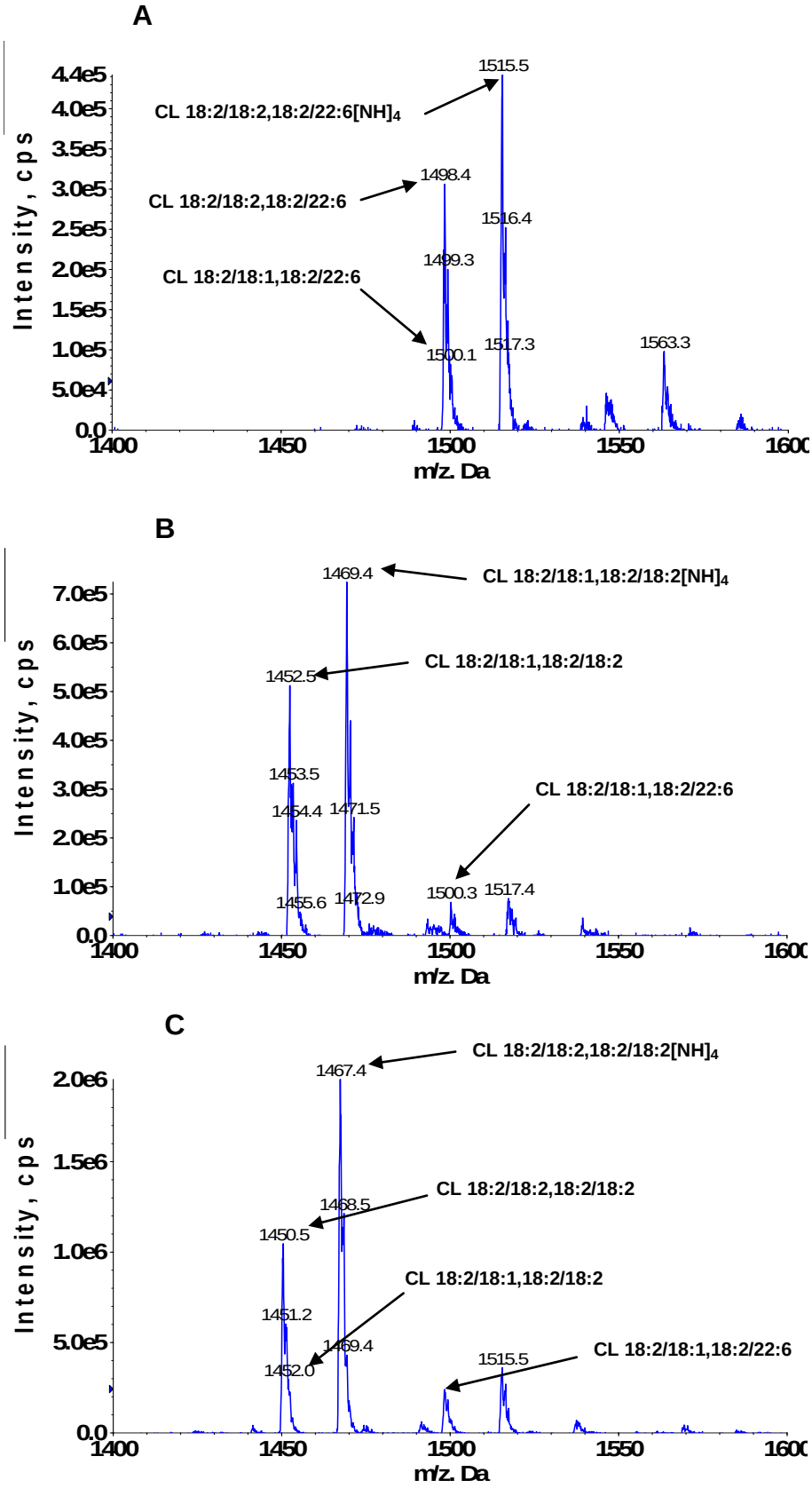

Figure 3.7 Precursor ion spectra to identify CL species in C57BL/6 wild-type mouse heart. A total lipid extract from mouse heart was infused into the mass spectrometer at 20 ul/min. Precursor ion scans were performed in positive ion mode over 30 sec in mass-correlated acceleration mode using optimal voltages and default settings (Table 3.1). Precursor ion scans of *m/z* 647.5 corresponding to DG 18:2/22:6$[M+H]^+$ -H_2O (A), *m/z* 601.5 corresponding to DG 18:2/18:1$[M+H]^+$-H_2O (B), and *m/z* 599.5 corresponding to DG 18:2/18:2$[M+H]^+$ -H_2O (C) were acquired to identify CL species.

Table 3.4 Identity of cardiolipin species in C57BL/6 wild-type mouse heart using precursor ion scans in positive ion mode.

No.	CL species[a]	Q1 *m/z* of $[M+H]^+$ parent ion	Retention time (min)	% of total CL content
1	CL 18:2/18:2,18:2/16:1	1423.9	7.47	3.0[b]
2	CL 18:2/18:1,18:2/16:1	1426.0	7.6	1.1
3	CL 18:2/18:1,18:1/16:1	1428.0	7.73	0.5
4	CL 18:2/18:2,18:2/18:3	1448.0	7.40	0.4
5	CL 18:2/18:2,18:2/18:2	1450.0	7.51	27.9[b]
6	CL 18:2/18:2,18:2/18:1	1452.0	7.63	26.9[b]
7	CL 18:2/18:1,18:2/18:1	1454.0	7.75	7.0[b]
8	CL 18:2/18:2,18:2/20:3	1476.0	7.57	1.2
9	CL 18:2/18:1,18:2/20:3	1478.0	7.67	1.3
10	CL 18:2/18:1,18:2/20:2	1480.0	7.78	1.2
11	CL 18:2/22:6,18:2/18:3	1496.0	7.38	1.8
12	CL 18:2/18:2,18:2/22:6	1498.0	7.48	15.9[b]
13	CL 18:2/18:1,18:2/22:6	1500.0	7.59	8.8[b]
14	CL 18:2/18:1,18:2/22:5	1502.0	7.73	0.4
15	CL 18:2/22:6,18:1/20:4	1524.0	7.58	0.8
16	CL 18:2/22:6,18:2/22:6	1546.0	7.47	1.8

[a] Precursor ion scans that generated the major daughter ions DG 18:2/18:2$[M+H]^+$ -H_2O, DG 18:2/18:1$[M+H]^+$ -H_2O, DG 18:2/20:4$[M+H]^+$ -H_2O or DG 18:2/22:6$[M+H]^+$ -H_2O were performed on a mouse heart lipid extract in positive ion mode on a API 4000 Q/TRAP mass spectrometer using optimal voltages and default settings (Table 3.1).
[b] the six most abundant CL species
CL, cardiolipin; %, percent

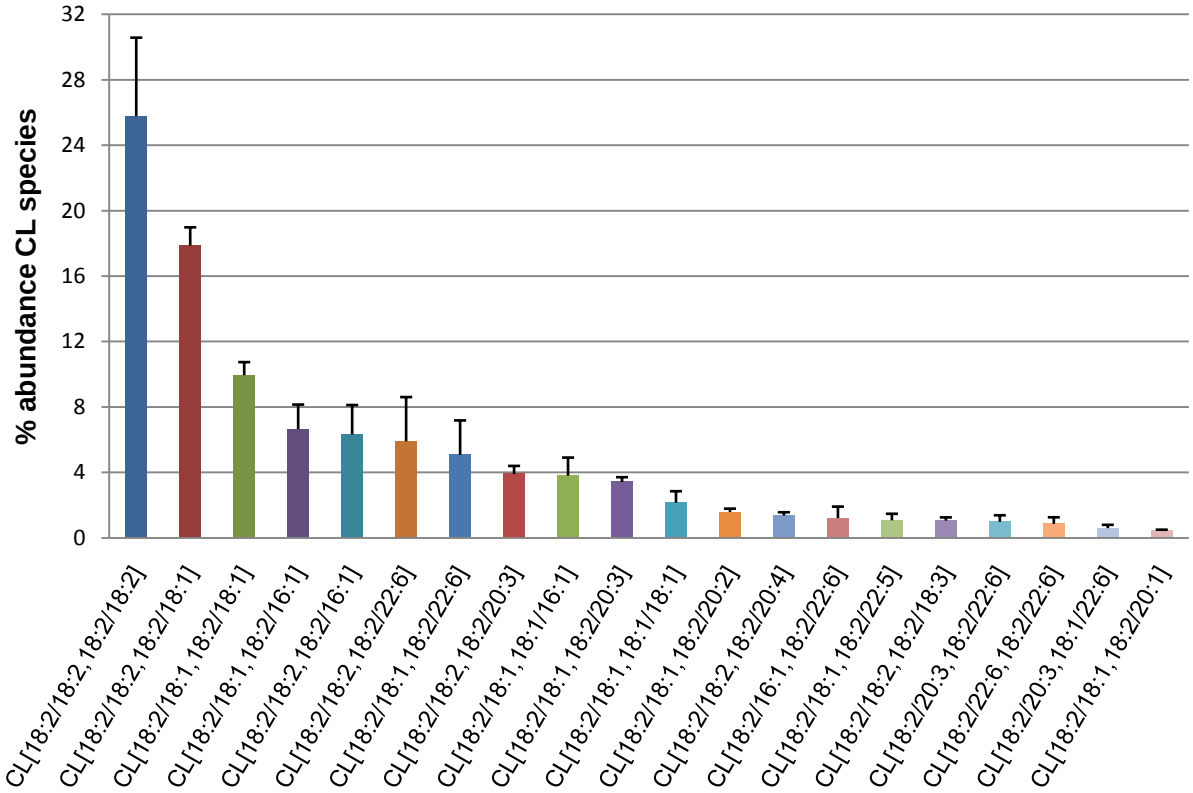

Figure 3.8 The 20 most abundant cardiolipin species in C57BL/6 wild-type mouse tissues. Liquid chromatography electrospray ionisation-tandem mass spectrometry and unscheduled multiple reaction monitoring experiments were performed on mouse tissue extracts (two each from heart, liver, skeletal muscle and adipose) in positive ion mode on a API 4000 Q/TRAP mass spectrometer using optimal voltages and default settings (Table 3.1). CL data is expressed as mean % abundance ± SEM. At least 11 of the CL species tested were detected in all mouse tissues.
CL, cardiolipin; %, percent

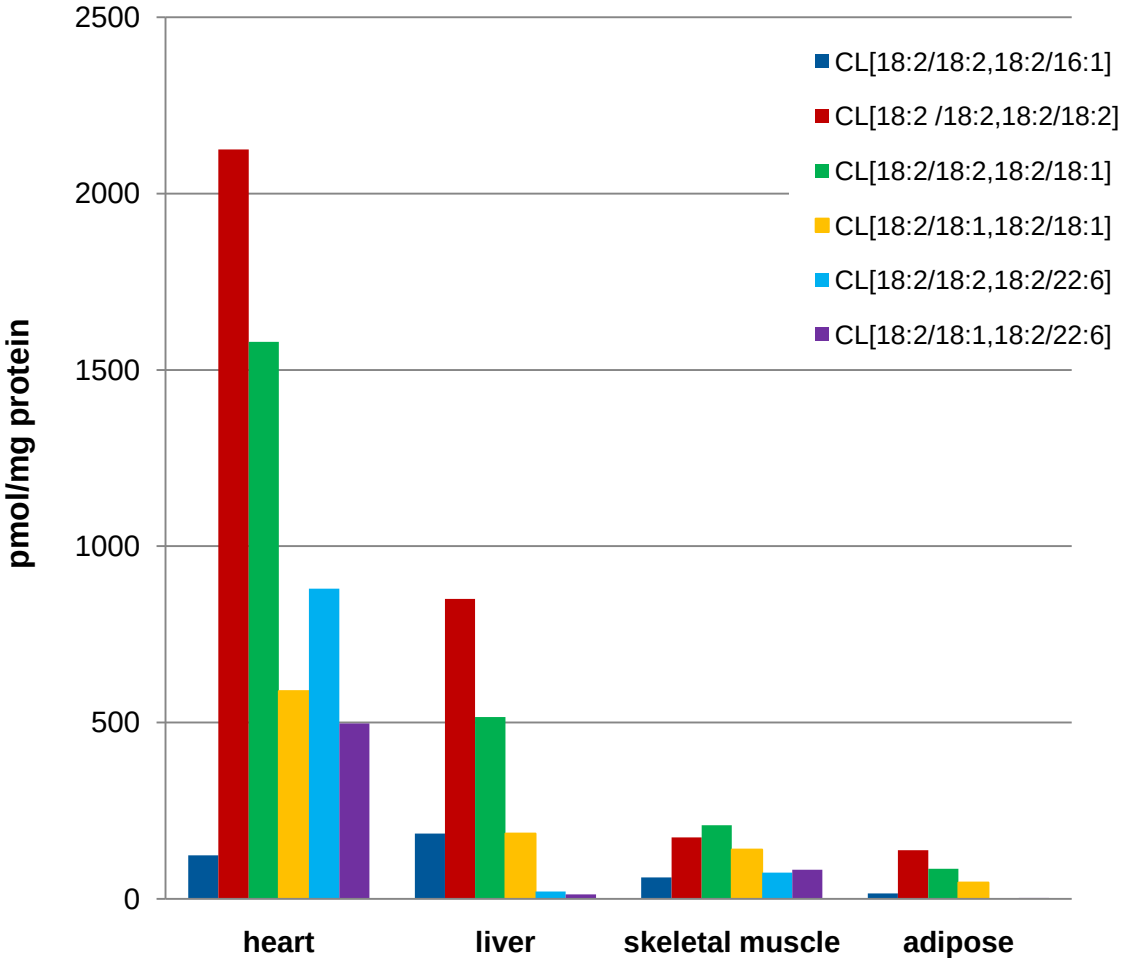

Figure 3.9 Content and distribution of the six most abundant cardiolipin species in C57BL/6 wild-type mouse tissue. Liquid chromatography electrospray ionisation-tandem mass spectrometry and unscheduled multiple reaction monitoring experiments were performed on mouse tissue extracts (two each from heart, liver, skeletal muscle and adipose) in positive ion mode on a API 4000 Q/TRAP mass spectrometer using optimal voltages and default settings (Table 3.1). CL data is expressed as mean species content (pmol/mg protein). Only two lipid extracts were obtained for each tissue-type. Hence, no error bars were generated.
CL, cardiolipin

Table 3.5 Full coverage acquisition method to quantify the 20 most abundant cardiolipin species (and corresponding isomers) in C57BL/6 wild-type mouse tissue.

CL Species[a]	Q1 *m/z* $[M+H]^+$ parent ion	DG $[M+H]^+$ -H_2O daughter ion	Q3 *m/z*
CL 14:0/14:0,14:0/14:0 (IS)	1242.0	DG 14:0/14:0	495.5
CL 18:2/16:1,18:2/18:2	1423.9	DG 18:2/16:1	573.5
CL 18:2/18:2,18:2/16:1	1423.9	DG 18:2/18:2	599.5
CL 18:2/16:1,18:2/18:1	1426.0	DG 18:2/16:1	573.5
CL 18:1/16:1,18:2/18:2	1426.0	DG 18:1/16:1	575.5
CL 18:2/18:2,18:1/16:1	1426.0	DG 18:2/18:2	599.5
CL 18:2/18:1,18:2/16:1	1426.0	DG 18:2/18:1	601.5
CL 18:2/16:1,18:1/18:1	1428.0	DG 18:2/16:1	573.5
CL 18:1/16:1,18:2/18:1	1428.0	DG 18:1/16:1	575.5
CL 18:2/18:1,18:1/16:1	1428.0	DG 18:2/18:1	601.5
CL 18:1/18:1,18:2/16:1	1428.0	DG 18:1/18:1	603.5
CL 18:2/18:3,18:2/18:2	1448.0	DG 18:2/18:3	597.5
CL 18:2/18:2,18:2/18:3	1448.0	DG 18:2/18:2	599.5
CL 18:2/18:2,18:2/18:2	1450.0	DG 18:2/18:2	599.5
CL 18:2/18:2,18:2/18:1	1452.0	DG 18:2/18:2	599.5
CL 18:2/18:1,18:2/18:2	1452.0	DG 18:2/18:1	601.5
CL 18:2/18:2,18:1/18:1	1454.0	DG 18:2/18:2	599.5
CL 18:2/18:1,18:2/18:1	1454.0	DG 18:2/18:1	601.5
CL 18:1/18:1,18:2/18:2	1454.0	DG 18:1/18:1	603.5
CL 18:2/18:1,18:1/18:1	1456.0	DG 18:2/18:1	601.5
CL 18:1/18:1,18:2/18:1	1456.0	DG 18:1/18:1	603.5
CL 18:2/16:1,18:2/22:6	1472.0	DG 18:2/16:1	573.5
CL 18:2/18:2,16:1/22:6	1472.0	DG 18:2/18:2	599.5
CL 16:1/22:6,18:2/18:2	1472.0	DG 16:1/22:6	621.5
CL 18:2/22:6,18:2/16:1	1472.0	DG 18:2/22:6	647.5
CL 18:2/18:2,18:2/20:4	1474.0	DG 18:2/18:2	599.5
CL 18:2/20:4,18:2/18 :2	1474.0	DG 18:2/20:4	623.5
CL 18:2/18:2,18:2/20:3	1476.0	DG 18:2/18:2	599.5
CL 18:2/20:3,18:2/18:2	1476.0	DG 18:2/20:3	625.5
CL 18:2/18:2,18:1/20:3	1478.0	DG 18:2/18:2	599.5
CL 18:2/18:1,18:2/20:3	1478.0	DG 18:2/18:1	601.5
CL 18:2/20:3,18:2/18:1	1478.0	DG 18:2/20:3	625.5
CL 18:1/20:3,18:2/18:2	1478.0	DG 18:1/20:3	627.5
CL 18:2/18:2,18:1/20:2	1480.0	DG 18:2/18:2	599.5
CL 18:2/18:1,18:2/20:2	1480.0	DG 18:2/18:1	601.5
CL 18:2/20:2,18:2/18:1	1480.0	DG 18:2/20:2	627.5
CL 18:1/20:2,18:2/18:2	1480.0	DG 18:1/20:2	629.5
CL 18:2/18:2,18:1/20:1	1482.0	DG 18:2/18:2	599.5
CL 18:2/18:1,18:2/20:1	1482.0	DG 18:2/18:1	601.5
CL 18:2/20:1,18:2/18:1	1482.0	DG 18:2/20:1	629.5
CL 18:1/20:1,18:2/18:2	1482.0	DG 18:1/20:1	631.5
CL 18:2/18:2,18:2/22:6	1498.0	DG 18:2/18:2	599.5

CL Species[a]	Q1 *m/z* $[M+H]^+$ parent ion	DG $[M+H]^+ -H_2O$ daughter ion	Q3 *m/z*
CL 18:2/22:6,18:2/18:2	1498.0	DG 18:2/22:6	647.5
CL 18:2/18:2,18:1/22:6	1500.0	DG 18:2/18:2	599.5
CL 18:2/18:1,18:2/22:6	1500.0	DG 18:2/18:1	601.5
CL 18:2/22:6,18:2/18:1	1500.0	DG 18:2/22:6	647.5
CL 18:1/22:6,18:2/18:2	1500.0	DG 18:1/22:6	649.5
CL 18:2/18:2,18:1/22:5	1502.0	DG 18:2/18:2	599.5
CL 18:2/18:1,18:2/22:5	1502.0	DG 18:2/18:1	601.5
CL 18:2/22:5,18:2/18:1	1502.0	DG 18:2/22:5	649.5
CL 18:1/22:5,18:2/18:2	1502.0	DG 18:1/22:5	651.5
CL 18:2/18:2,20:3/22:6	1524.0	DG 18:2/18:2	599.5
CL 18:2/20:3,18:2/22:6	1524.0	DG 18:2/20:3	625.5
CL 18:2/22:6,18:2/20:3	1524.0	DG 18:2/22:6	647.5
CL 20:3/22:6,18:2/18:2	1524.0	DG 20:3/22:6	673.5
CL 18:2/18:1,20:3/22:6	1526.0	DG 18:2/18:1	601.5
CL 18:2/20:3,18:1/22:6	1526.0	DG 18:2/20:3	625.5
CL 18:1/20:3,18:2/22:6	1526.0	DG 18:1/20:3	627.5
CL 18:2/22:6,18:1/20:3	1526.0	DG 18:2/22:6	647.5
CL 18:1/22:6,18:2/20:3	1526.0	DG 18:1/22:6	649.5
CL 20:3/22:6,18:2/18:1	1526.0	DG 20:3/22:6	673.5
CL 18:2/18:2,22:6/22:6	1546.0	DG 18:2/18:2	599.5
CL 18:2/22:6,18:2/22:6	1546.0	DG 18:2/22:6	647.5
CL 22:6/22:6,18:2/18:2	1546.0	DG 22:6/22:6	695.5

Liquid chromatography electrospray ionisation-tandem mass spectrometry and unscheduled multiple reaction monitoring experiments were performed in positive ion mode on a API 4000 Q/TRAP mass spectrometer using optimal voltages and default settings (Table 3.1). Dwell time: 15 msec

[a] This acquisition method was designed to capture all DG adduct daughter ions ($DG[M+H]^+ -H_2O$) generated from the 20 most abundant CL species in C57BL/6 wild-type mouse tissue extracts (heart, liver, skeletal muscle and adipose).

CL, cardiolipin; DG, diglyceride

induced dissociation (CID) of each CL$[M+H]^+$ parent ion. For example, CID of the CL 18:2/16:1,18:2/18:1$[M+H]^+$ parent ion (Q1 *m/z* 1426.00) generates four DG $[M+H]^+$ -H_2O daughter ions (DG 18:2/16:1$[M+H]^+$ -H_2O, DG 18:1/16:1$[M+H]^+$ -H_2O, DG 18:2/18:2$[M+H]^+$ -H_2O and DG 18:2/18:1$[M+H]^+$ -H_2O (Q3 *m/z* values 573.50, 575.50, 599.50 and 601.50 respectively). The simultaneous measurement of these four daughter ions revealed that the signal intensity of each paired Q3 DG $[M+H]^+$ -H_2O daughter ion was almost identical (i.e., DG 18:2/16:1$[M+H]^+$ -H_2O had the same signal intensity as DG 18:2/18:1$[M+H]^+$ -H_2O; and DG 18:1/16:1$[M+H]^+$ -H_2O had the same signal intensity as DG 18:2/18:2$[M+H]^+$ -H_2O) (data not shown). Therefore, each of the 20 CL species could be quantified by assigning one of the paired Q3 DG $[M+H]^+$ -H_2O daughter ions generated from each isomer within that CL species, and that the content of each CL species was equal to the sum of the contents of each isomer within that CL species.

Finally, an acquisition method containing scheduled MRM experiments and corresponding degeneracy factors designed to quantify these 20 CL species in mammalian tissues using LC ESI-MS/MS and optimal voltages for CL in positive ion mode is shown in Table 3.6. In cases where the CL$[M+H]^+$ parent or isomer ion (e.g. CL 18:2/18:1,18:2/18:1$[M+H]^+$) generates two identical DG $[M+H]^+$ -H_2O fragments (i.e., DG 18:2/18:1$[M+H]^+$ -H_2O), the signal intensity generated by this single MRM assignment must be divided by 2 to correct for the redundancy of the detected daughter ion.

Therefore, the developmental methods established in this chapter resulted in a total of 60 species [11 LPE, 5 PE, 14 PE(O), 10 PE(P) and 20 CL] being added to the list of ~270 lipid species that are routinely measured in our laboratory using LC ESI-MS/MS (Table 3.7).

3.4 DISCUSSION

Targeted lipid profiling using mass spectrometry techniques enables the comparative analysis of multiple lipid species in plasma, tissues, and cell culture samples, and offers the opportunity to examine the complex lipid abnormalities associated with specific disease states. Using this approach, a number of lipid species have been associated with obesity, IR and/or T2D, including FFA, the phospholipids PC and PE, the sphingolipids Cer and SM, and the glycerolipids DG and TG [9,25,28,29,65,66,67,68,69]. Recent evidence suggests that lipid species from other classes and subclasses may also contribute to the pathogenesis of T2D, including LPE [10,120], PE(O)

Table 3.6 Final acquisition method to quantify the 20 most abundant cardiolipin species in C57BL/6 wild-type mouse tissue.

CL species[a]	Q1 *m/z* of $[M+H]^+$ parent ion	$DG[M+H]^+-H_2O$ daughter ion	Q3 *m/z*	Retention time (min)	Degeneracy Factor
CL 14:0/14:0,14:0/14:0 (IS)	1242.0	DG 14:0/14:0	495.5	7.11	2
CL 18:2/16:1,18:2/18:2	1423.9	DG 18:2/16:1	573.5	7.46	1
CL 18:2/16:1,18:2/18:1	1426.0	DG 18:2/16:1	573.5	7.58	1
CL 18:1/16:1,18:2/18:2	1426.0	DG 18:1/16:1	575.5	7.58	1
CL 18:2/16:1,18:1/18:1	1428.0	DG 18:2/16:1	573.5	7.71	1
CL 18:1/16:1,18:2/18:1	1428.0	DG 18:1/16:1	575.5	7.71	1
CL 18:2/18:3,18:2/18:2	1448.0	DG 18:2/18:3	597.5	7.40	1
CL 18:2/18:2,18:2/18:2	1450.0	DG 18:2/18:2	599.5	7.51	2
CL 18:2/18:1,18:2/18:2	1452.0	DG 18:2/18:1	601.5	7.62	1
CL 18:2/18:1,18:2/18:1	1454.0	DG 18:2/18:1	601.5	7.74	2
CL 18:1/18:1,18:2/18:2	1454.0	DG 18:1/18:1	603.5	7.74	1
CL 18:1/18:1,18:2/18:1	1456.0	DG 18:1/18:1	603.5	7.86	1
CL 16:1/22:6,18:2/18:2	1472.0	DG 16:1/22:6	621.5	7.45	1
CL 18:2/22:6,18:2/16:1	1472.0	DG 18:2/22:6	647.5	7.45	1
CL 18:2/20:4,18:2/18:2	1474.0	DG 18:2/20:4	623.5	7.51	1
CL 18:2/20:3,18:2/18:2	1476.0	DG 18:2/20:3	625.5	7.56	1
CL 18:2/20:3,18:2/18:1	1478.0	DG 18:2/20:3	625.5	7.67	1
CL 18:1/20:3,18:2/18:2	1478.0	DG 18:1/20:3	627.5	7.67	1
CL 18:2/20:2,18:2/18:1	1480.0	DG 18:2/20:2	627.5	7.78	1
CL 18:1/20:2,18:2/18:2	1480.0	DG 18:1/20:2	629.5	7.78	1
CL 18:2/20:1,18:2/18:1	1482.0	DG 18:2/20:1	629.5	7.88	1
CL 18:1/20:1,18:2/18:2	1482.0	DG 18:1/20:1	631.5	7.88	1
CL 18:2/22:6,18:2/18:2	1498.0	DG 18:2/22:6	647.5	7.48	1
CL 18:2/22:6,18:2/18:1	1500.0	DG 18:2/22:6	647.5	7.58	1
CL 18:1/22:6,18:2/18:2	1500.0	DG 18:1/22:6	649.5	7.58	1
CL 18:2/22:5,18:2/18:1	1502.0	DG 18:2/22:5	649.5	7.71	1
CL 18:1/22:5,18:2/18:2	1502.0	DG 18:1/22:5	651.5	7.71	1
CL 18:2/20:3,18:2/22:6	1524.0	DG 18:2/20:3	625.5	7.52	1
CL 20:3/22:6,18:2/18:2	1524.0	DG 20:3/22:6	673.5	7.52	1
CL 18:2/18:1,20:3/22:6	1526.0	DG 18:2/18:1	601.5	7.64	1
CL 18:2/20:3,18:1/22:6	1526.0	DG 18:2/20:3	625.5	7.64	1
CL 18:2/22:6,18:1/20:3	1526.0	DG 18:2/22:6	647.5	7.64	1
CL 18:2/22:6,18:2/22:6	1546.0	DG 18:2/22:6	647.5	7.43	2
CL 22:6/22:6,18:2/18:2	1546.0	DG 22:6/22:6	695.5	7.43	1

[a] Liquid chromatography electrospray ionisation-tandem mass spectrometry and scheduled multiple reaction monitoring experiments were performed in C57BL/6 wild-type mouse tissue extracts (heart, liver, skeletal muscle and adipose) in positive ion mode on a API 4000 Q/TRAP mass spectrometer using optimal voltages and default settings (Table 3.1).
CL, cardiolipin; DG, diglyceride

Table 3.7 Targeted lipid profiling strategy for the measurement of lipid species using liquid chromatography electrospray ionisation tandem mass spectrometry in positive ion mode.

Lipid class or subclass[a]	No. of species	Internal Standard	Parent ion	Experiment[b]
Dihydroceramide	6	dhCer 8:0	$[M+H]^+$	PI, 284.3 *m/z*
Ceramide	6	Cer 17:0	$[M+H]^+$	PI, 264.3 *m/z*
Monohexosylceramide	6	MHC 16:0 d_3	$[M+H]^+$	PI, 264.3 *m/z*
Dihexosylceramide	6	DHC 16:0 d_3	$[M+H]^+$	PI, 264.3 *m/z*
Trihexosylceramide	6	THC 17:0	$[M+H]^+$	PI, 264.3 *m/z*
G_{M3} ganglioside	6	THC 17:0	$[M+H]^+$	PI, 264.3 *m/z*
Sphingomyelin	12	SM 12:0	$[M+H]^+$	PI, 184.1 *m/z*
Phosphatidylcholine	35	PC 13:0/13:0	$[M+H]^+$	PI, 184.1 *m/z*
Alkylphosphatidylcholine	16	PC 13:0/13:0	$[M+H]^+$	PI, 184.1 *m/z*
Alkenylphosphatidylcholine	13	PC 13:0/13:0	$[M+H]^+$	PI, 184.1 *m/z*
Lysophosphatidylcholine	19	LPC 13:0	$[M+H]^+$	PI, 184.1 *m/z*
Lysoalkylphosphatidylcholine	3	LPC 13:0	$[M+H]^+$	PI, 285.2 *m/z*
Phosphatidylethanolamine	20	PE 17:0/17:0	$[M+H]^+$	NL, 141 Da
Alkylphosphatidylethanolamine	14	PE 17:0/17:0	$[M+H]^+$	NL, 141 Da
Alkenylphosphatidylethanolamine	12	PE 17:0/17:0	$[M+H]^+$	NL, 141 Da
Lysophosphatidylethanolamine	8	LPE 14:0	$[M+H]^+$	NL, 141 Da
Phosphatidylinositol	17	PE 17:0/17:0	$[M+NH_4]^+$	PI, 184.1 *m/z*
Phosphatidylserine	7	PS 17:0/17:0	$[M+H]^+$	NL, 185 Da
Phosphatidylglycerol	4	PG 17:0/17:0	$[M+NH_4]^+$	NL, 189 Da
Bis(monoacylglycerol) phosphate	1	BMP 14:0/14:0	$[M+NH_4]^+$	PI, 339. *m/z*
Cardiolipin	20	CL 14:0/14:0/14:0/14:0	$[M+H]^+$	PI, DG$[M+H]^+$-H_2O
Cholesterol ester	31	CE 18:0 d_6	$[M+NH_4]^+$	PI, 369.3 *m/z*
Free cholesterol	1	COH d_7	$[M+NH_4]^+$	PI, 369.3 *m/z*
Diacylglycerol	27	DG 15:0/15:0	$[M+NH_4]^+$	NL, fatty acid
Triacylglycerol	44	TG 17:0/17:0/17:0	$[M+NH_4]^+$	NL, fatty acid

[a] Targeted lipid profiling methodology (multiple reaction monitoring experiments) was developed for 60 additional lipid species from the classes/subclasses highlighted in blue
[b] PI, precursor ion scan; NL, neutral loss scan; DG, diglyceride

[29,54], PE(P) [29,54,63,117] and CL [64,128,129,130,131]. As part of this PhD project, targeted lipid profiling methodology was developed to characterise PE, LPE, PE(O), PE(P) and CL species in both human and mouse models of obesity, IR and T2D.

3.4.1 Targeted lipid profiling of PE, PE(O), PE(P) and LPE species

This developmental methodology commenced with the optimisation of acquisition parameters and voltage settings for commercially available lipid standards (representing each class/subclass) on the API 4000 Q/TRAP triple quadrupole mass spectrometer using Q1 ion scans, product ion scans and precursor ion scans. Next, major lipid species in human plasma and mouse plasma and tissue extracts were identified using a combination of precursor ion scans, NL loss scans, unscheduled stepwise and scheduled MRM experiments in positive ion mode. In addition, full or partial fatty acid chain composition was determined in 36 of the 65 PE, PE(O) and PE(P) species identified in human plasma using unscheduled MRM experiments in negative ion mode. The fatty acid chain composition was unable to be determined in the other 29 species PE, PE(O) and PE(P) due to the high background and lower sensitivity encountered in negative ion mode, resulting in a higher limit of detection for these lipid product ions.

Although the neutral loss of 141.0 Da resulting from the CID of $[M+H]^+$ diacyl-PE and 1-O-alkyl-2-acyl-PE parent ions has been used as a diagnostic tool for the determination of PE and PE(O) species content in complex lipid mixtures [134], the signal intensity generated by the NL of 141.0 Da from $[M+H]^+$ 1-O-alk-1'-enyl-2-acyl-PE parent ions is far less than that generated from $[M+H]^+$ diacyl-PE parent ions (34). Using LC ESI-MS/MS in positive ion mode, Zemski Berry and Murphy showed that the CID of $[M+H]^+$ PE(P) parent ions in the phospholipid membranes of human neutrophils generated two prominent fragment ions [135]. Therefore, it was possible to detect all PE(P) species containing arachidonate (20:4) at the *sn*-2 position by a precursor ion scan of *m/z* 361, and all PE(P) species containing palmitate (16:0) at the *sn*-1 position by a precursor ion scan of *m/z* 364. Although a smaller neutral loss of 141.0 Da was observed, this was not the major fragment ion of PE(P) species [135]. Our identification of PE, PE(O), PE(P) or LPE species in human plasma was based on stepwise unscheduled MRM assignments constructed to detect fragment ions generated from the NL of mass 141.0. The NL of mass 141.0 had previously been found to generate the major fragment ion when MS acquisition parameters were optimised for the PE 17:0/17:0 standard [11], and we did not consider using precursor ion scans to detect the unique fragment ions generated from the CID of

the $[M+H]^+$ PE(P-18:0/18:1) parent ion in positive ion mode. Nonetheless, we were still able to perform comparative analysis of PE(P) species content from different subject groups, despite the lower signal generated by the NL of mass 141.0. However, the abundance of PE(P) species relative to other lipids within the same sample could not be considered without an appropriate correction.

3.4.2 Targeted lipid profiling of CL species in positive ion mode

Given that CL or diphosphatidylglycerols are complex anionic phospholipids with a dimeric structure containing two negative charges, most CL species were previously detected and identified in mammalian plasma and tissues using a variety of mass spectrometry methods in negative ion mode [64,121,123,128,129,130,131]. However, this was incompatible with the established methodology in our laboratory that routinely measures ~270 lipids in positive ion mode. One study, however, did employ multiple-stage ion-trap mass spectrometric methods for the structural characterization of CL isolated from *E. coli,* by detecting sodiated adduct ions [M −2H + 3Na]+ in positive ion mode [132]. This study reinforced the possibility that targeted profiling methodology could be developed using optimal LC ESI-MS/MS conditions in positive ion mode to detect, identify and compare relative levels of CL species obtained in mammalian plasma and/or tissue extracts from different population cohorts.

It was important to carefully design MRM experiments in positive ion mode to accurately quantify each CL species identified in mammalian plasma and/or tissues. An acquisition method consisting of unscheduled MRM experiments designed to capture all DG adduct daughter ions ($DG[M+H]^+ -H_2O$) generated from the 20 most abundant CL species in mouse tissue extracts (Table 3.5) revealed that each Q1 $CL[M+H]^+$ parent ion *m/z* value only needed to be assigned to one of the paired Q3 DG $[M+H]^+ -H_2O$ daughter ion fragments generated from each isomer within that CL species. For example, the parent ion CL 18:2/18:1,18:2/18:1$[M+H]^+$ with Q1 *m/z* 1454.0 theoretically exist as two isomers, namely CL 18:2/18:2,18:1/18:1$[M+H]^+$ and CL 18:2/18:1,18:2/18:1$[M+H]^+$. The signal intensity of the peak area generated by the daughter ions DG 18:2/18:2$[M+H]^+ -H_2O$ (Q3 *m/z* 599.5) and DG 18:1/18:1$[M+H]^+ -H_2O$ (Q3 *m/z* 603.5) from the first parent isomer CL 18:2/18:2,18:1/18:1$[M+H]^+$ was found to be equal, necessitating one MRM experiment only. However, the signal intensity of the peak area generated by the daughter ion DG 18:2/18:1$[M+H]^+ -H_2O$ (Q3 *m/z* value 601.5) from the second parent isomer CL 18:2/18:1,18:2/18:1$[M+H]^+$ has to be divided by 2 to correct for the redundancy of the detected

daughter ion (second MRM experiment). The total signal intensity obtained for the CL species, CL 18:2/18:1,18:2/18:1, was calculated by adding the signal intensity generated from the first parent isomer (first MRM experiment) to the redundancy-corrected signal intensity generated from the second parent isomer (second MRM experiment; Table 3.6). Redundancy factors also needed to be applied the internal standard CL 14:0/14:0,14:0/14:0, and the abundant CL species, CL 18:2/18:2,18:2/18:2 and CL 18:2/22:6,18:2/22:6 (Table 3.6).

It was also important to distinguish between low and high abundant isomers in each CL species so that only abundant isomers (with inclusion cut-off > 1.0 % of the major species detected) were measured in tissue extracts. For example, at Q1 *m/z* 1450.0, two parent isomers theoretically exist in positive ion mode, namely CL 18:2/18:2,18:2/18:2$[M+H]^+$ and CL18:2/18:1,18:2/18:3$[M+H]^+$. In mouse heart extract, the daughter ion DG 18:2/18:2$[M+H]^+$ -H_2O with Q3 *m/z* 599.5 yielded ~10^6counts/sec for peak area (with redundancy factor of 2), whereas the paired daughter ions DG 18:2/18:1$[M+H]^+$ -H_2O and DG 18:2/18:3$[M+H]^+$ -H_2O with Q3 *m/z* values 601.5 and 597.5 respectively both yielded ~6000 counts/sec for peak area. Therefore, the parent isomer CL 18:2/18:2,18:2/18:2 was ~83 times more abundant than CL 18:2/18:1,18:2/18:3, indicating that the low abundant CL parent isomer was below the inclusion cut-off. Likewise, at Q1 *m/z* 1452.0, two CL parent isomers theoretically exist in positive ion mode, namely CL 18:2/18:2,18:2/18:1$[M+H]^+$ and CL18:2/18:1,18:1/18:3$[M+H]^+$. In a mouse heart extract, the paired daughter ions DG 18:2/18:2$[M+H]^+$ -H_2O and DG 18:2/18:1$[M+H]^+$ -H_2O detected at Q3 *m/z* values 599.5 and 601.5 respectively both yielded ~45000 counts/sec for peak area, whereas the paired daughter ions DG 18:2/18:3 $[M+H]^+$-H_2O and DG 18:1/18:1$[M+H]^+$ -H_2O detected at Q3 *m/z* values 597.5 and 603.5 respectively both yielded ~500 counts/sec respectively. Therefore, the parent isomer CL 18:2/18:2,18:2/18:1 was ~90 times more abundant than CL 18:2/18:1,18:1/18:3, indicating that the low abundant CL parent isomer was below the inclusion cut-off.

3.4.3 Conclusion

In conclusion, 78 LPE, PE, PE-O and PE-P species were detected and identified in a 10 µl human plasma extract using an acquisition method in positive ion mode consisting of scheduled MRM experiments incorporating the NL of mass 141.0 Da. Fatty acid composition was determined in 36 of the 65 identified PE, PE-O and PE-P species using unscheduled acquisition methods in negative ion mode consisting of MRM experiments designed to detect negatively

charged fatty acid daughter ions. The fatty acid content of the 13 identified LPE species was evident from the positive ion analyses. Based on the abundance and biological significance of species identified in each of these classes/subclasses, a total of 40 species (11 LPE, 5 PE, 14 PE-O and 10 PE-P) were added to the list of ~270 lipid species routinely measured in our laboratory using optimal LC ESI-MS/MS conditions and established MRM experiments in positive ion mode.

Similarly, from the 31 CL species identified, the 20 most abundant CL species identified in 10 µl wild-type C57BL/6 mouse heart extracts (cut-off >1.5 % of the major species detected) were quantified in 10 µl wild-type C57BL/6 mouse heart extracts using scheduled MRM experiments in positive ion mode designed to detect specific DG daughter ion fragments. These 20 CL species were also tested in wild-type C57BL/6 mouse liver, skeletal muscle and adipose extracts, and added to the final list of lipid species routinely measured in positive ion mode in a single experiment. Simultaneously, MRM experiments were developed by other personnel in our laboratory to identify PC(P) species. Therefore, an enhanced targeted lipid profiling strategy containing a final list of 330 lipid species (Table 3.7) was employed to characterise lipid profiles in plasma and tissue samples obtained from the Obese/diabetic *db/db*mouse study (Chapter 4) and the Human insulin resistance and obesity study (Chapter 6).

CHAPTER 4 CHARACTERISATION OF PLASMA AND TISSUE LIPID PROFILES IN A MOUSE MODEL OF TYPE 2 DIABETES

4.1 INTRODUCTION

4.1.1 The *db/db* genetic mouse model

Leptin is a hormone secreted by adipocytes which acts as a feedback signal on the brain to suppress feeding and stimulate metabolism. Normally, leptin production increases in proportion to the size of body fat stores [136], and stimulation of a hypothalamic leptin receptor suppresses hunger and food intake [100]. Leptin also increases fatty acid oxidation rates in peripheral tissues by central and peripheral signaling via leptin receptors [137]. The *db* gene mutation (autosomal recessive point mutation on chromosome 4 with complete penetrance) occurred spontaneously in the C57BL/KsJ-*db/db* strain of mice from the Jackson Laboratory, (Bar Harbor, ME, USA). This mutation is a single nucleotide substitution which encodes for an amino acid substitution near the carboxyl terminus of a leptin receptor that has a long intracellular domain, the long-form leptin receptor (ObRb) [138]. This gene mutation results in a global deficiency in the protein expression of the leptin receptor [72], which leads to the development of type 2 diabetes (T2D) in homozygous (*db/db*) mice.

In the *db/db* mouse, peripheral leptin signalling via short-form leptin receptors is intact, but signal transduction via long-form leptin receptors is inhibited in the hypothalamus as well as in the periphery [138,139]. Leptin receptor deficiency results in weight gain (due to increased food intake), decreased energy expenditure, and insulin resistance (IR). The diabetic phenotype of *db/db* mice is determined by the genetic background on which the mutation is expressed [73]. Circulating leptin levels are elevated in *db/db* mice, reflecting severe leptin resistance [97,98]. Central or peripheral administration of recombinant leptin had no effect on food intake or body weight in C57BL/KsJ *db/db* mice [100].

4.1.2 Progression of disease in the homozygous C57BL/KsJ *db/db* mouse

The *db/db* mice with a C57BL/KsJ genetic background provides a good monogenic model of IR, obesity and T2D, which is characterised by early obesity, hyperinsulinaemia and IR, progressive

hyperglycaemia, hyperlipidaemia and hyperglucagonaemia, and a gradual loss of pancreatic function (insulin secretion) resulting in low insulin and extremely high glucose levels [73,85,140,141,142,143]. This model closely resembles disease progression to T2D in humans, in which the first stage is IR, followed by progressive hyperglycemia, and endocrine pancreatic secretory dysfunction [72,91].

The time-frame of disease progression in the homozygous C57BL/KsJ *db/db* mouse can be divided into three distinct phases. Firstly, at 4-6 weeks of age, the *db/db* mouse overeats (unrestricted standard chow diet), weighs significantly more than the *H/H* littermates, and has hyperinsulinaemia and IR (and normoglycaemia). By 7-9 weeks of age, the time-dependent increases in obesity and IR are accompanied by persisting hyperinsulinaemia, hyperlipidaemia (elevated plasma non-esterified fatty acids and triglyceride levels), hyperglucagonaemia, and hyperglycaemia (diabetes). However, by 14-16 weeks of age, both chronic hyperglycaemia and hyperlipidaemia lead to severely decreased insulin secretion in the presence of sustained hyperglucagonaemia and IR [85,141,142,143,144]. In contrast, the heterozygous male *db/h* mice develop a milder form of obesity and IR, and do not develop diabetes. The female mice are less obese and suffer less severe pathology than their equivalent male genotypes, likely as a result of cardio-protection by oestrogen, and survive longer [95,143]. The C57BL/KsJ *H/H* littermates act as appropriate controls.

4.1.3 Other metabolic abnormalities associated with the *db/db* mice

Homozygous *db/db* mice also suffer renal impairment from birth (kidney function declines rapidly with the onset of diabetes) and contractile cardiac dysfunction (i.e., an increased reliance on fatty acids as the preferred fuel for oxidative metabolism), which manifests at 8-10 weeks of age [93,145]. There is a significant decrease in respiratory exchange ratio, whole-body oxygen consumption rate, exercise capacity, and insulin-stimulated Akt and glycogen synthase kinase 3β phosphorylation in six week old *db/db* mice fed an unrestricted standard chow diet compared with age-matched *db/h* mice [76].

4.1.4 Lipidomic analysis of plasma and metabolic tissues in obesity, insulin resistance and type 2 diabetes

In humans, obesity, IR and T2D are associated with elevated circulating free fatty acids (FFA) and triglycerides [146,147], but the lipid classes and species associated with the onset and progression of disease have not been fully elucidated. While there have been a number of studies in human cohorts that have examined the plasma lipidome in obesity, IR, prediabetes and/or T2D [9,13,26,28,29,148], very few studies have performed comprehensive lipidomic analysis (by mass spectrometry) that has compared plasma and metabolic tissue lipid abnormalities in obesity, IR and/or T2D [70,149] or sequentially tracked the lipid abnormalities that occur with disease progression [65]. Most lipidomic studies to date have only collected one-off fasting blood samples from two groups of subjects (e.g. obese versus lean controls) to compare relative levels of lipid species from a small number of lipid groups.

The *db/db* genetic mouse model of leptin receptor deficiency (C57BL/KsJ background) closely resembles disease progression to T2D in humans [72,91] and offers an ideal model to investigate real time lipid abnormalities associated with the onset of obesity, IR and T2D. In the present study, comprehensive lipidomic analysis using liquid chromatography and tandem mass spectrometry (LC ESI-MS/MS) was used to investigate temporal (6, 10 and 16 weeks of age) and tissue-specific (plasma and liver, adipose, heart and skeletal muscle) changes in the levels of lipid classes, subclasses and species associated with the onset of obesity, IR and progression to T2D in male and female *db/h* and *db/db* mice compared with their corresponding *H/H* littermates (a total of 170 mice were classified into 18 groups containing 7-12 mice per group). As well as employing LC ESI-MS/MS and MRM experiments in positive ion mode to routinely quantify ~270 lipids from 19 lipid subclasses, targeted lipid profiling methodology was developed to characterise 60 additional lipid species (11 LPE, 5 PE, 14 PE-O, 10 PE-P and 20 CL) considered to be implicated in the pathogenesis of T2D (Chapter 3).

4.2 MATERIALS AND METHODS

4.2.1 Mouse genotypes

All animal experiments were approved by the Alfred Medical Research and Education Precinct (AMREP) Animal Ethics Committee. Both homozygous *db/db* and heterozygous *db/h* mice were

generated in the Jackson Laboratory by backcrossing onto a C57BL/KsJ background (*H/H*) for nine generations, with genotypes verified by PCR using primers previously reported [150]. Animals were housed in a temperature-controlled environment with a 12 h light-dark cycle in specific pathogen-free conditions, and the study was performed at Baker IDI Heart and Diabetes Institute, Melbourne, Australia, in accordance with guidelines from the AMREP Ethics Committee and the National Health and Medical Research Council of Australia.

4.2.2 Diet, health monitoring and metabolic tests

The experimental design employed for the *db/db* mouse study is summarised in Table 4.1A. Mice from six groups (male and female *H/H*, *db/h* and *db/db* mice with a C57BL/KsJ background) were placed on an unrestricted standard chow diet (14.0 MJ/kg, 8% energy as fat, 69% as carbohydrate, 23% as protein; Specialty Feeds, Perth, WA, Australia) with free access to water for either 6, 10 or 16 weeks (7-12 mice per group at each time-point). The calculated fatty acid composition of the chow diet (according to the manufacturer) is shown in Table 4.1B. Throughout the designated study period, body weight, blood and urinary glucose, and glycated haemoglobin (%) of each mouse were monitored weekly. Once the appearance of glucose in the urine was confirmed by consecutive measurements at 8-10 weeks of age (where applicable), the above mentioned clinical and biochemical parameters were measured three times weekly leading up to the final metabolic tests performed within one week of cull.

One week before the cull (i.e., at 5, 9 or 15 weeks of age), Intraperitoneal Glucose Tolerance Test (IPGTT; glucose injection = 1.0 g/kg lean body mass) and Intraperitoneal Insulin Tolerance Test (IPITT; insulin injection = 0.5 U/kg lean body mass) were performed in 6 h fasted mice on separate days, with blood samples taken from the tail tip at 0, 15, 30, 60 and 120 min for blood glucose measurements. Metabolic caging was performed in the Mouse Metabolic Phenotyping Facility to measure 24 h food and water intake, and urinary output, preceded by a 200 µl submandibular blood sample for measurement of creatinine clearance.

4.2.3 Collection of plasma and tissues from mice at time of cull

At the designated age (6, 10 or 16 weeks), each mouse in the *db*/*db* mouse study was fasted for 6 h, then weighed. A 50-100 ul blood sample was taken from the tail tip, with a drop used for glucose measurement (glucometer), and the remainder collected into an appropriate EDTA tube,

Table 4.1A Experimental design[a] for the *db/db* mouse study.

Genotypes	C57BL/KsJ male and female *H/H, db/h* and *db/db* mice
Sex	87 male and 83 female
Ages	6 weeks, 10 weeks and 16 weeks
Numbers	7-12 per group (18 groups: total 170 mice)
Diet	Unrestricted standard mouse chow (8% fat as energy)
Regular maintenance tests	Body weight, blood and urinary glucose, glycated haemoglobin %
Tests performed within one week of cull	Metabolic Caging: 24 h food and water intake; urinary output 2 h IPGTT[b], 2 h IPITT[c] (serial blood glucose measurements)
Cull samples following 6 h fast	Blood (cardiac puncture) and liver, skeletal muscle (gastrocnemius), left-ventricle, and adipose (omental) tissue for targeted lipid profiling/gene expression[d]

[a] Collaboration with Professor Josephine Forbes and Brooke Harcourt PhD, Glycation and Diabetes Laboratory, Baker IDIHeart & Diabetes Institute, Melbourne
[b] IPGTT, intraperitoneal glucose tolerance test
[c] IPITT, intraperitoneal insulin tolerance test
[d] The PhD candidate collected and processed blood and tissue samples, but did not perform maintenance or metabolic tests

Table 4.1B Calculated fatty acid composition of the chow diet fed ad libitum to the mice.

Fatty acid	Calculated fatty acid composition[e]
Myristic acid 14:0	0.03%
Palmitic acid 16:0	0.50%
Stearic acid 18:0	0.14%
Palmitoleic acid 16:1	0.01%
Oleic acid 18:1	1.90%
Gadoleic acid 20:1	0.03%
Linoleic acid 18:2 n6	1.30%
α-Linolenic acid 18:3 n3	0.30%
Arachidonic acid 20:4 n6	0.01%
EPA 20:5 n3[f]	0.02%
DHA 22:6 n3[g]	0.05%

[e] Reproduced in part from Specialty Feeds, Perth, WA, Australia ([redacted]
[f] EPA, eicosapentaenoic acid
[g] DHA, docosahexaenoic acid

placed on ice, centrifuged within 2 h (4,000 g, 15 min, 4°C), and the separated plasma frozen and stored at -80°C for subsequent lipid analysis. Each mouse was anaesthetised with an intraperitoneal injection of the barbiturate euthal (non-recovery; 100 mg/kg body mass). Mice were then exsanguinated by taking a blood sample via cardiac puncture (1 ml, 27G needle), followed by immediate removal of the heart (left-ventricle), liver, skeletal muscle (gastrocnemius) and adipose (omental) tissues. Tissues were weighed, placed separately into pre-labelled 2.0 ml DNase-free and RNase-free tubes, snap frozen in liquid nitrogen, and stored at -80°C (freezer). Of the 170 mice that completed the study, a total of 165 plasma, 167 liver, 166 skeletal muscle, 168 heart, and 162 adipose samples were collected.

4.2.4 Laboratory Analyses

Blood glucose was measured using a glucometer (AccuCheck II, Roche, Castle Hill, NSW, Australia) [151], serum insulin was measured using a standard ELISA kit [152] and plasma glycated haemoglobin (%) was measured by HPLC [153]. Homeostasis model assessment of insulin resistance (HOMA-IR) was calculated as fasting insulin (mU/l) × fasting glucose (mmol/l)/22.5. HOMA-IR has yet to be validated as a true measure of "insulin sensitivity" in mice, but is used as a comparative surrogate measure in different mouse groups alongside fasting plasma glucose and insulin levels. The total glucose area under the curve calculated during the IPGTT ($AUC_{IPGTT,}$ mmol/l) and IPITT ($AUC_{IPITT,}$ mmol/l) were used as measures of glucose tolerance and insulin tolerance respectively.

4.2.5 Lipid analysis of mouse tissues and plasma

Fasting mouse plasma and tissue (liver, skeletal muscle, left-ventricle and adipose) samples collected at the time of cull were prepared for lipid extraction and subsequent targeted lipid profiling using LC ESI-MS/MS and Analyst 1.5 MultiQuant data system (AB Sciex) as previously described (Chapter 2; sections 2.2, 2.3 and 2.5) [10]. A separate lipid extraction and LC ESI-MS/MS analysis was performed for each tissue or plasma sample set. Each analytic run containing approximately 170 samples also contained 12-14 evenly spaced quality control (QC) samples prepared specifically from a pool of at least eight mouse tissue or plasma samples being extracted. All lipids with the exception of the DG and TG species were analyzed in a single LC ESI-MS/MS experiment of 14 min, using gradient solvent conditions as described in Materials

and Methods, Chapter 2. The DG and TG species were analysed in a separate experiment of 6 min using isocratic conditions as described in Materials and Methods, Chapter 2.

4.2.6 Statistical analyses

Clinical characteristics and non-lipidomic laboratory data are presented as means ± SEM. Lipid levels are expressed as median ± lower and upper quartile values to accommodate for the non-normal (usually right-skewed) distribution of many lipids. Statistical comparisons of relative lipid levels in liver, skeletal muscle, left-ventricle, adipose and plasma between study groups was performed using Matlab R2013a (Mathworks Inc, Natick, MA, USA) as detailed below. Lipid names were matched to LIPID MAPs nomenclature [16,17] which places lipids into eight main categories, and is available online (website http://www.lipidmaps.org).

4.2.6.1 Principal component analysis of global lipid profiles

Principal component analysis (PCA) is a statistical dimension reduction method which converts large numbers of lipid species into a few linearly uncorrelated variables, known as principal components. These components are basically a linear combination of lipid species, but derived in such a way that first component accounts for as much of the variability in the data as possible. Each of the subsequent components is derived such that it not only explains the highest variance of the data, but is also uncorrelated with the previous components [154].

In the present study, PCA modelling was used to compare the internal structure of the lipid data from different groups. Samples from different groups (e.g. *H/H* vs. *db/h* vs. *db/db* mice) were plotted according to their first and second principal components, which were derived using lipid levels that were log-transformed to normalise their distribution. In this way, PCA modelling was employed to compare the independent effects of 1) gender; 2) age (6 vs. 10 vs. 16 weeks); and 3) genotype (*H/H* vs. *db/h* vs. *db/db*) on global liver lipid profiles in each of the tissues and plasma for all mice using Matlab R2013a statistical software package (Mathworks).

4.2.6.2 Relationship between gender and lipid levels

Statistical testing of the relationship between gender and lipid classes, subclasses and species in plasma and each of the tissues was determined for the three genotypes at each age by the non-

parametric Mann-Whitney *U* test (corrected for multiple comparisons using the Benjamini-Hochberg method [155]. A corrected *P*-value < 0.05 was considered significant. The following analyses were performed:

1) male *H/H* vs. female *H/H* mice at 6 weeks of age
2) male *H/H* vs. female *H/H* mice at 10 weeks of age
3) male *H/H* vs. female *H/H* mice at 16 weeks of age
4) male *db/h* vs. female *db/h* mice at 6 weeks of age
5) male *db/h* vs. female *db/h* mice at 10 weeks of age
6) male *db/h* vs. female *db/h* mice at 16 weeks of age
7) male *db/db* vs. female *db/db* mice at 6 weeks of age
8) male *db/db* vs. female *db/db* mice at 10 weeks of age
9) male *db/db* vs. female *db/db* mice at 16 weeks of age

4.2.6.3 Relationship between age and lipid levels

Having established that there were significant differences between gender and lipid levels in many of the study groups (see Results section 4.3.3.4), statistical testing of the relationship between age (6 vs. 10 vs. 16 weeks) and lipid classes, subclasses and species in plasma and each of the tissues was determined independently of gender and genotype. The non-parametric one-way Kruskal-Wallis test was employed to determine whether any lipid classes, subclasses and/or species were statistically different between the three age groups in female or male mice in the three genotypes (i.e., six statistical tests). The overall *P*-value obtained across the three age groups was corrected for multiple comparisons using the Benjamini-Hochberg method [155] (*P* < 0.05 was considered significant), and post-hoc analyses between groups were performed using the Mann Whitney *U* test with Dunn-Sidak correction for multiple group comparisons. The following analyses were performed:

10) female *H/H* mice at 6 weeks of age vs. 10 weeks of age vs. 16 weeks of age
11) female *db/h* mice at 6 weeks of age vs. 10 weeks of age vs. 16 weeks of age
12) female *db/db* mice at 6 weeks of age vs. 10 weeks of age vs. 16 weeks of age
13) male *H/H* mice at 6 weeks of age vs. 10 weeks of age vs. 16 weeks of age
14) male *db/h* mice at 6 weeks of age vs. 10 weeks of age vs. 16 weeks of age
15) male *db/db* mice at 6 weeks of age vs. 10 weeks of age vs. 16 weeks of age

4.2.6.4 Relationship between genotype and lipid levels

Statistical testing of the relationship between genotype (*H/H* vs. *db/h* vs. *db/db*) and lipid classes, subclasses and species in plasma and each of the tissues was determined independently of gender and age. The non-parametric one-way Kruskal-Wallis test was employed to determine whether any lipid species and/or lipid classes in each of the tissues were statistically different between the three genotype groups in female or male mice at each age (i.e., six statistical tests).

The overall *P*-value obtained across the three genotype groups was corrected for multiple comparisons using the Benjamini-Hochberg approach [155] ($P < 0.05$ was considered significant), and post-hoc analyses between groups were performed using the Mann Whitney *U* test with Dunn-Sidak correction for multiple group comparisons. The following analyses were performed:

16) female *H/H* vs. female *db/h* vs. female *db/db* mice (at 6 weeks of age)
17) female *H/H* vs. female *db/h* vs. female *db/db* mice (at 10 weeks of age)
18) female *H/H* vs. female *db/h* vs.female *db/db* mice (at 16 weeks of age)
19) male *H/H* vs. male *db/h* vs. male *db/db* mice (at 6 weeks of age)
20) male *H/H* vs. male *db/h* vs. male *db/db* mice (at 10 weeks of age)
21) male *H/H* vs. male *db/h* vs. male *db/db* mice (at 16 weeks of age)

4.3 RESULTS

4.3.1 Body composition, biochemical and metabolic characteristics in female mice

In the female mice, there was no significant difference in daily food consumption between the *H/H*, *db/h* and *db/db* genotypes at 6 and 10 weeks of age (range: 2.3 to 3.1 g/day). At 16 weeks of age, the female *db/db* mice ate 50% more chow than the female *db/h* mice (3.3 ± 0.2 vs. 2.2 ± 0.2 g/day; $P < 0.01$), and 38% more than their *H/H* counterparts (2.4 ± 0.3 g/day; *P* non-significant (NS)). Body weight was significantly higher in the female *db/h* and *db/db* mice compared with their *H/H* littermates at 10 weeks of age (but not six weeks), and strikingly higher in the female *db/db* mice compared with their *H/H* and *db/h* littermates at 16 weeks of age (Figure 4.1A). Body weight was significantly higher in all genotypes in female mice at 16 weeks compared with 10 weeks of age. In contrast to body weight, omental fat weight was

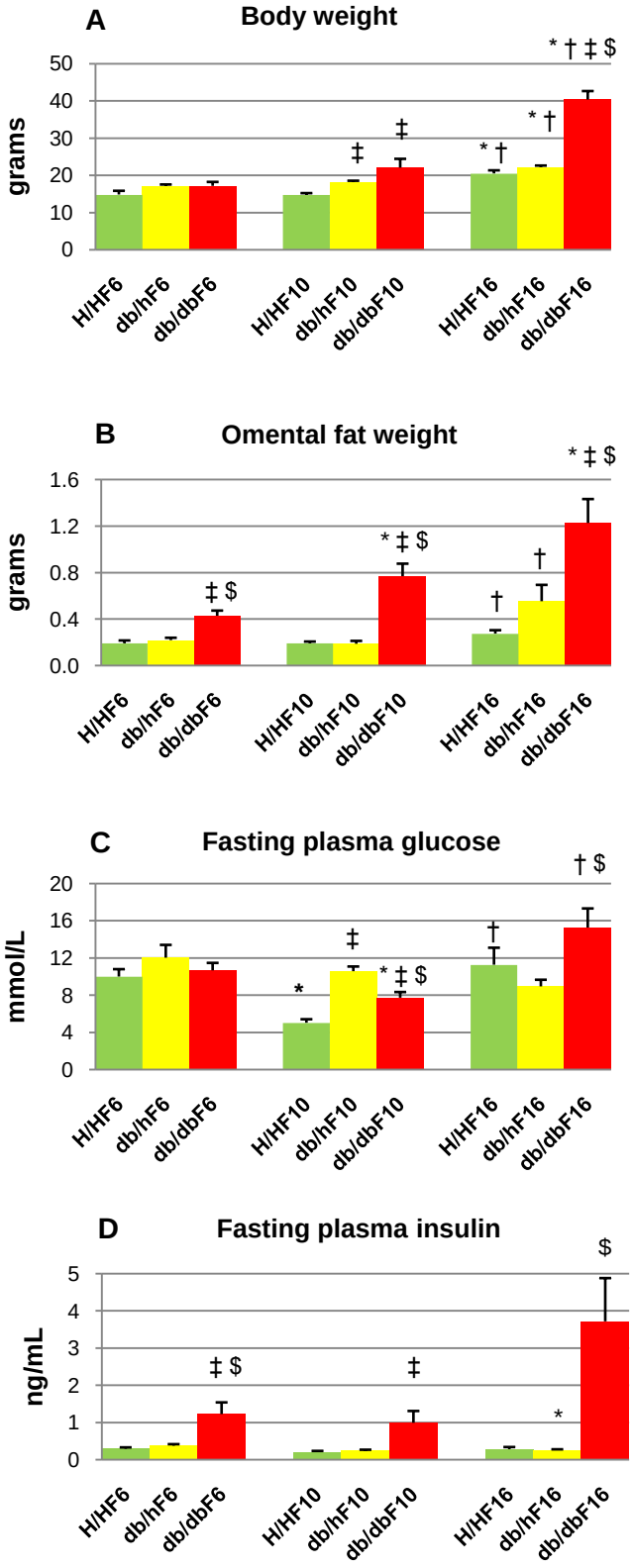

Figure 4.1 Body composition and biochemical measures in female mice. Body weight (A), omental fat weight (B), fasting plasma glucose (C) and fasting plasma insulin (D) in female (F) *H/H*, *db/h* and *db/db* mice on unrestricted chow diet at 6, 10 and 16 weeks of age. Values are expressed as mean ± SEM (7-12 mice per group).
* $P < 0.05$ vs. corresponding genotype at 6 weeks of age; † $P < 0.05$ vs. corresponding genotype at 10 weeks of age; ‡ $P < 0.05$ vs. *H/H* mice at same age; $ $P < 0.05$ vs. *db/h* mice at same age using Mann-Whitney *U* test.

already significantly elevated by ≥ 90% in female *db/db* mice compared with*H/H* and *db/h* mice at 6 weeks of age (Figure 4.1B). Omental fat weight rose significantly in female *db/db* mice, but not female *H/H* or *db/h* mice, at 10 weeks of age compared with 6 weeks of age. Although omental fat weight rose significantly in the *H/H* and *db/h* mice at 16 weeks of age compared with 10 weeks of age, omental fat weight remained significantly higher by ≥ 120% in the female *db/db* mice compared with their *H/H* and *db/h* counterparts at 16 weeks of age. There were no significant differences in fasting plasma glucose levels in female *H/H*, *db/h* and *db/db* mice at 6 weeks of age, and fasting glucose levels significantly dropped in female *H/H* and *db/db* mice at 10 weeks of age (Figure 4.1C). At 16 weeks of age, fasting glucose levels significantly increased in both female *H/H* and *db/db* mice compared with 10 weeks of age, and were now significantly higher by 70% in the female *db/db* mice compared with their *db/h* counterparts at 16 weeks of age. In addition, the female *db/db* mice had significantly higher glycated haemoglobin (%) than the female *db/h* mice at 16 weeks of age (7.4 ± 1.1 vs. 4.9 ± 0.1%; $P < 0.05$), but not their *H/H* counterparts (5.9 ± 0.9%; *P* NS). Similar to the results obtained for omental fat weight, fasting plasma insulin levels in the female *db/db* mice were significantly higher (by ≥ 3-fold) compared with both female *H/H* and *db/h* mice at 6 weeks of age. Fasting plasma insulin levels remained significantly elevated in female *db/db* mice compared with female *H/H* mice at 10 weeks of age, and compared with female *db/h* mice 16 weeks of age (Figure 4.1D).

Based mainly on the results obtained for fasting plasma insulin, HOMA-IR in the female *db/db* mice was significantly elevated compared with the *H/H* mice at 6 and 10 weeks of age, and significantly higher than the *db/h* mice at 16 weeks of age (Figure 4.2A). Of note, total glucose area under the curve during the 2 h IPGTT (AUC_{IPGTT}; measure of glucose tolerance) was significantly elevated in the female *db/h* mice compared with *H/H* mice at 6 weeks of age, and significantly higher (by 90%) in the female *db/db* mice compared with *H/H* mice at 10 weeks of age (Figure 4.2B). Glucose tolerance continued to worsen in female *db/db* mice, with AUC_{IPGTT} significantly higher in female *db/db* mice compared with both *H/H* and *db/h* mice at 16 weeks of age. Total glucose area under the curve during the 2 h IPITT (AUC_{IPITT}; measure of insulin tolerance) was significantly increased in female *db/db* mice compared with both *H/H* and *db/h* mice at 6, 10 and 16 weeks of age, but little change in AUC_{IPITT} was seen in female *db/h* mice with increasing age (Figure 4.2C). The phenotypic abnormalities in female *db/h* and *db/db* mice compared with their corresponding female *H/H* littermates at 6, 10 and 16 weeks of age are summarised in Table 4.2.

4.3.2 Body composition, biochemical and metabolic characteristics in male mice

In the male mice, there was no significant difference in daily food consumption between the *H/H*, *db/h* and *db/db* genotypes at 6 weeks of age (range: 2.8 to 3.6 g/day). However, food consumption was significantly lower by ≤ 20% in male *db/h* mice compared with their *H/H* counterparts at 10 and 16 weeks of age, while the male *db/db* mice showed a trend for greater chow consumption compared with the male *db/h* mice at 16 weeks of age (3.4 ± 0.8 vs. 2.1 ± 0.1 g/day; $P = 0.08$). Body weight was significantly elevated in the male *db/db* mice compared with both *H/H* and *db/h* mice at 6 weeks of age (Figure 4.3A). Body weight significantly increased in the three genotypes at 10 weeks of age, but was proportionally higher in the male *db/db* mice, followed by the *db/h* and *H/H* mice. Body weight continued to rise significantly in the male *db/db* and *db/h* mice at 16 weeks of age, but was 50% higher in the *db/db* mice relative to the *db/h* mice. Similar to body weight, omental fat weight was significantly higher in male *db/db* mice compared with both *H/H* and *db/h* mice at 6 weeks of age (Figure 4.3B). Omental fat weight continued to rise significantly in male *db/db* mice at 10 weeks of age, but not at 16 weeks of age. However, there was a significant 2.9-fold rise in omental fat weight in the *db/h* mice at 16 weeks of age compared with 10 weeks of age.

There were almost no significant differences in fasting plasma glucose levels in male *H/H*, *db/h* and *db/db* mice at 6, 10 or 16 weeks of age (Figure 4.3C). This was similar to the plasma glucose findings in female *db/db* mice, and indicates that the *db/db* mice in this study did not develop diabetes by 16 weeks of age (i.e., fasting plasma glucose was expected to reach 25-30 mmol/l). However, these *db/db* mice were pre-diabetic, and would have developed diabetes if they were allowed to age more.

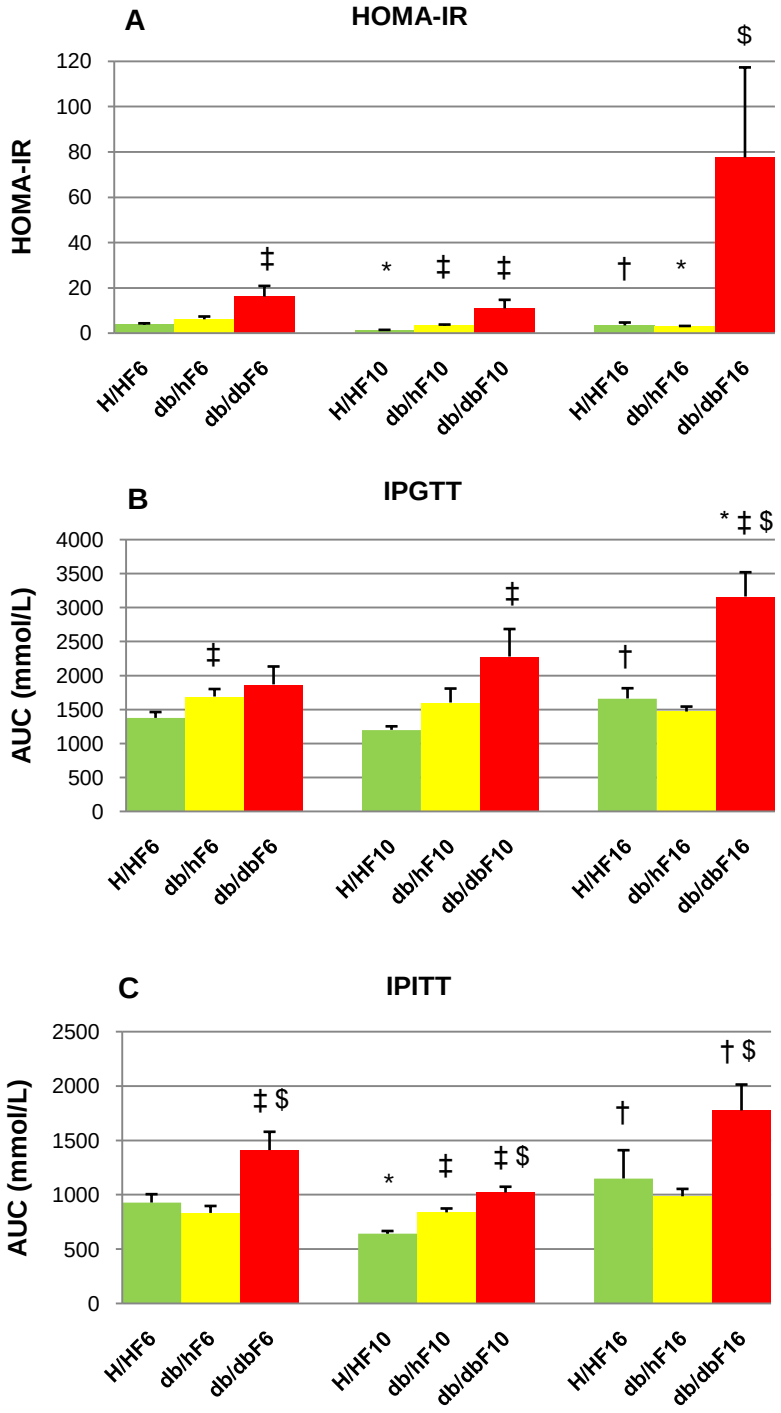

Figure 4.2 Metabolic measures in female mice. HOMA-IR, homeostasis model assessment of insulin resistance (A), AUC_{IPGTT}, total glucose area under the curve during intraperitoneal glucose tolerance test (B), and AUC_{IPITT}, total glucose area under the curve during intraperitoneal insulin tolerance test (C) in female (F) *H/H*, *db/h* and *db/db* mice on unrestricted chow diet at 6, 10 and 16 weeks of age. Values are expressed as mean ± SEM (7-12 mice per group). * $P < 0.05$ vs. corresponding genotype at 6 weeks of age; † $P < 0.05$ vs. corresponding genotype at 10 weeks of age; ‡ $P < 0.05$ vs. *H/H* mice at same age; $ $P < 0.05$ vs. *db/h* mice at same age using Mann-Whitney *U* test.

Table 4.2 Female and male *db/h* and *db/db* mice phenotypes compared with their corresponding *H/H* littermates.

Age (weeks)	*db/h* mice		*db/db* mice	
	Female	**Male**	**Female**	**Male**
6	Glucose intolerant	Not different to male *H/H* mice	Fasting hyperinsulinaemia and IR	Mildly obese and glucose intolerant, with trend for raised fasting insulin (*P* = 0.07)
10	Mildly obese with fasting hyperglycaemia and IR	Mildly obese and glucose intolerant	Mildly obese and glucose intolerant, with fasting hyperglycaemia and hyperinsulinaemia, and IR	Obese with fasting hyperinsulinaemia and IR
16	Not different to female *H/H* mice	Obese and glucose intolerant, with low fasting insulin and insulin sensitive	Obese and glucose intolerant	Severely obese and glucose intolerant, with trend for raised fasting insulin (*P* = 0.08)

IR, insulin resistant based on homeostasis model assessment of insulin resistance (HOMA-IR)

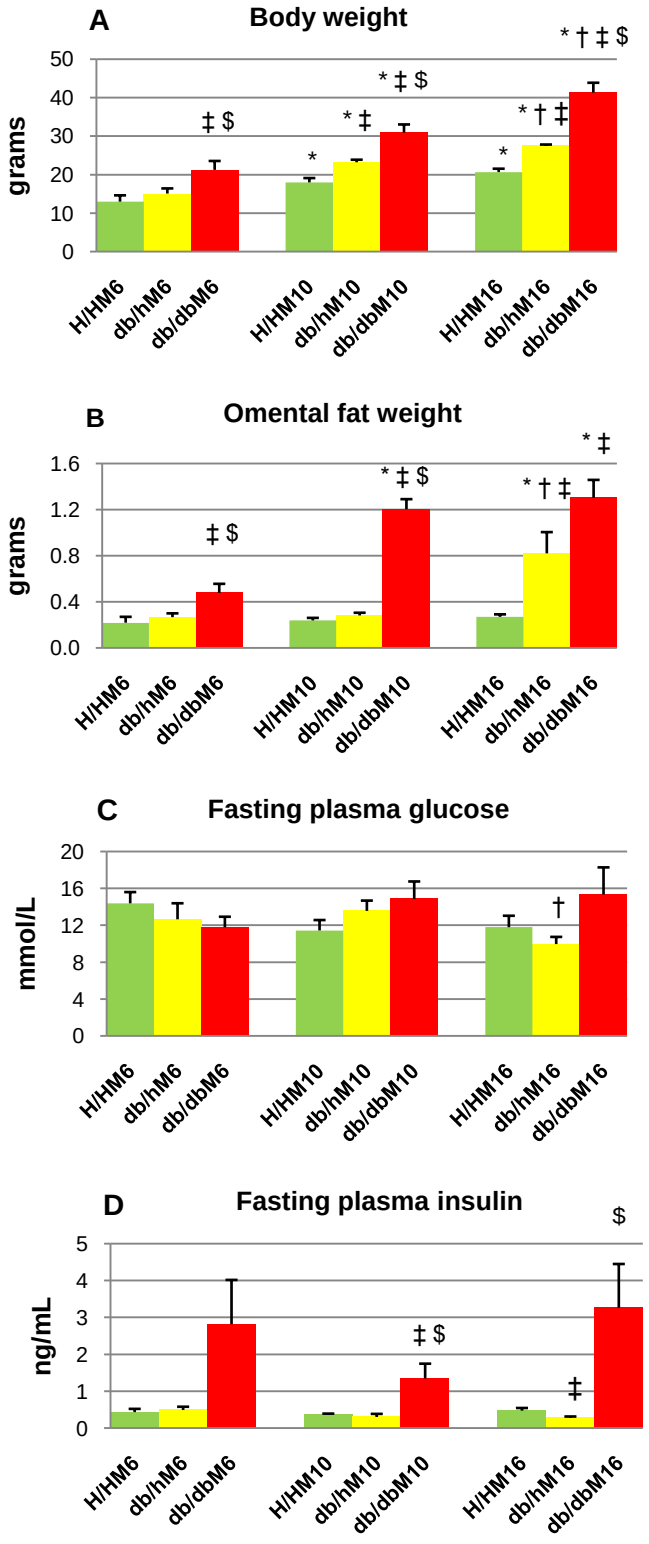

Figure 4.3 Body composition and biochemical measures in male mice. Body weight (A), omental fat weight (B), fasting plasma glucose (C) and fasting plasma insulin (D) in male (M) *H/H*, *db/h* and *db/db* mice on unrestricted chow diet at 6, 10 and 16 weeks of age. Values are expressed as mean ± SEM (7-12 mice per group).
* $P < 0.05$ vs. corresponding genotype at 6 weeks of age; † $P < 0.05$ vs. corresponding genotype at 10 weeks of age; ‡ $P < 0.05$ vs. *H/H* mice at same age; $ $P < 0.05$ vs. *db/h* mice at same age using Mann-Whitney *U* test.

However, the male *db/db* mice had significantly higher glycated haemoglobin (%) than the male *db/h* mice at 16 weeks of age (8.7 ± 1.1vs. 5.1 ± 0.1%; $P < 0.01$), but not their *H/H* counterparts (7.0 ± 1.7%; *P* NS). Although there appeared to be a substantial rise in fasting plasma insulin levels in male *db/db* mice compared with *H/H* and *db/h* mice at 6 and 10 weeks of age, this rise was only significant at 10 weeks of age (Figure 4.3D). Fasting plasma insulin remained significantly elevated in the male *db/db* compared with *db/h* mice at 16 weeks of age.

Although HOMA-IR appeared to be elevated in the male *db/db* mice compared with the *H/H* and *db/h* mice at all three age groups, this rise was only significant at 10 weeks of age (Figure 4.4A) due to the large variance in the *db/db* mice. Notably, AUC_{IPGTT} was significantly elevated in the male *db/db* compared with *H/H* and *db/h* mice at 6 weeks of age (Figure 4.4B). At 10 weeks of age, AUC_{IPGTT} rose significantly in the male *db/h* mice compared with *H/H* mice, but AUC_{IPGTT} remained significantly elevated in the male *db/db* compared with both *H/H* and *db/h* mice at 16 weeks of age. Similar to the pattern seen with fasting plasma insulin, AUC_{IPITT} was significantly increased in male *db/db* mice compared with *H/H* and *db/h* mice at 10 and 16 weeks of age, but not at 6 weeks of age (Figure 4.4C). However, there was a significant rise in AUC_{IPITT} in male *db/h* mice compared with *H/H* mice at 16 weeks of age. The phenotypic abnormalities in male *db/h* and *db/db* mice compared with their corresponding male *H/H* littermates at 6, 10 and 16 weeks of age are summarised in Table 4.2.

4.3.3. Assay performance of lipid measurements

The number of individual lipid species that were sufficiently abundant (i.e., detected in at least 93% of samples) in mouse tissue homogenates (liver, skeletal muscle, left-ventricle and adipose) and plasma for comparative statistical analyses between study groups is shown in Table 4.3. This number ranged from 227 lipid species in liver to 271 species in left-ventricle and plasma. Notably, plasma contained more ether- and vinyl ether-linked species (PC(O), PC(P), PE(O) and PE(P)) and lyso-species (LPC and LPE), but less DG and CL species than the tissues.

To assess the assay performance of our lipidomic profiling we determined the coefficient of variation (%CV) of each lipid species using the 12-14 specific QC samples spaced evenly throughout each tissue analysis. The median %CV in the plasma QCs was 9.6% (from 271 lipid species), while the median %CV in skeletal muscle homogenate QCs was 19.7% (from 238 lipid species) (Table 4.4). In plasma QCs, 90% of the lipid species had a CV less than 18.6%, and this

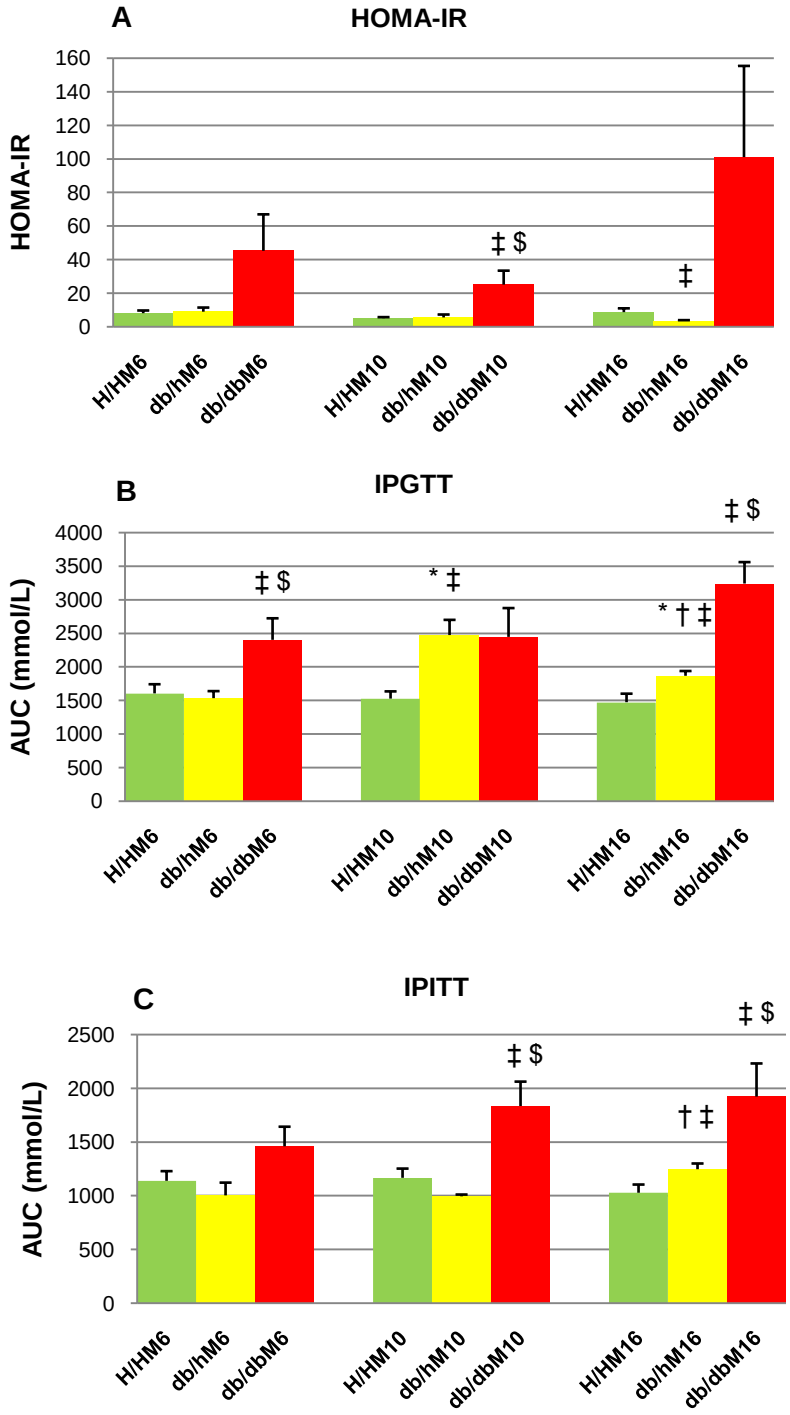

Figure 4.4 Metabolic measures in male mice. HOMA-IR, homeostasis model assessment of insulin resistance (A), AUC_{IPGTT}, total glucose area under the curve during intraperitoneal glucose tolerance test (B), and AUC_{IPITT}, total glucose area under the curve during intraperitoneal insulin tolerance test (C) in male (M) *H/H*, *db/h* and *db/db* mice on unrestricted chow diet at 6, 10 and 16 weeks of age. Values are expressed as mean ± SEM (7-12 mice per group). * $P < 0.05$ vs. corresponding genotype at 6 weeks of age; † $P < 0.05$ vs. corresponding genotype at 10 weeks of age; ‡ $P < 0.05$ vs. *H/H* mice at same age; $ $P < 0.05$ vs. *db/h* mice at same age using Mann-Whitney *U* test.

.**Table 4.3 Lipid species quantified in mouse tissues and plasma.**

	Number of lipid species				
Lipid class or subclass	**Liver**	**Skeletal muscle**	**Left-ventricle**	**Adipose**	**Plasma**
Sphingosine	0	0	1	1	1
Ceramide	6	5	6	6	6
Monohexosylceramide	5	5	3	4	6
Dihexosylceramide	1	0	2	0	0
Trihexosylceramide	0	0	1	0	0
GM3 ganglioside	0	1	5	0	0
Sphingomyelin	10	13	15	15	19
Phosphatidylcholine	42	45	43	45	48
Alkylphosphatidylcholine	12	10	17	17	20
Phosphatidylcholine plasmalogen	9	9	13	9	13
Lysophosphatidylcholine	7	8	15	13	22
Lysoalkylphosphatidylcholine	0	0	1	1	7
Phosphatidylethanolamine	20	18	18	19	13
Alkylphosphatidylethanolamine	5	7	11	9	11
Phosphatidylethanolamine plasmalogen	3	9	9	10	9
Lysophosphatidylethanolamine	5	4	8	6	6
Phosphatidylinositol	8	14	13	10	15
Lysophosphatidylinositol	0	0	0	0	3
Phosphatidylserine	7	7	7	7	2
Phosphatidylglycerol	5	5	5	4	0
Bis(monoacylglycerol) phosphate	1	0	2	1	0
Cardiolipin	11	13	17	5	0
Cholesteryl ester	10	5	7	14	18
Free cholesterol	1	1	1	1	1
Diacylglycerol	22	17	16	20	11
Triacylglycerol	37	42	35	41	40
Total	**227**	**238**	**271**	**258**	**271**

result was highest in liver homogenate QCs (32.2%). In plasma, only 1% of lipid species had a CV of greater than 30%, and this result was highest in liver homogenate QCs (11%). Those lipid species within QC samples that had a CV greater than 30% were primarily found in low abundance (< 50 pmol/mg protein in tissues or < 200 pmol/ml in plasma).

4.3.4 Early changes in plasma and tissue lipid profiles in *db/h* mice

Given that the *db/h* mouse is a good monogenic model of obesity, it was biologically important to determine which lipid abnormalities occurred in *db/h* mice before the onset of obesity, and whether these lipids were precursors (biomarkers) to the worsening lipid abnormalities that accompanied the onset of obesity and insulin resistance. As shown in Table 4.5, the earliest lipid abnormalities were detected in both male *db/h* mice (plasma only) and female *db/h* mice (plasma and all tissues) at 6 weeks of age, even though these mice were clinically and metabolically similar to the corresponding *H/H* mice (i.e., no significant differences were found in body weight, omental fat weight, fasting plasma glucose, fasting plasma insulin, HOMA-IR, AUC_{IPGTT} or AUC_{IPITT}; Figures 4.1 to 4.4).

Significantly elevated levels of five plasma lipid classes/subclasses (MHC, PC, PE, PI and CE) and 42 species were observed in male *db/h* compared with male *H/H* mice at 6 weeks of age. These included multiple species of sphingolipids (Cer, MHC and SM), major glycerophospholipids (PC and PE), plasmalogens (PE(P)), lysophospholipids (LPE), PI and CE (Table S4.5). Notably, this list did not include any DG or TG species. However, only 13 plasma lipid species were significantly different in female *db/h* mice compared with female *H/H* mice at 6 weeks of age, including significantly higher levels of three TG species (TG 14:0/16:1/18:1, TG 14:1/16:1/18:0 and TG 16:1/16:1/16:1) and significantly lower levels of multiple species of PC(O), PC(P) and PE(O) (Table S4.10).

Similar to the pattern seen in plasma, relatively few lipid abnormalities occurred in liver, skeletal muscle, left-ventricle and adipose tissue in female *db/h* mice compared with female *H/H* mice at 6 weeks of age (Table 4.5). There were 14 liver lipid species that were significantly increased in female *db/h* mice compared with female *H/H* mice at 6 weeks of age, including three CE species (CE 16:1, CE 18:0 and CE 18:1), two DG species (DG 16:1/18:0 and DG 16:1/18:1) and eight

Table 4.4 Assay performance of lipid measurements in mice tissue and plasma.

Assay performance[a]	Liver	Skeletal muscle	Left-ventricle	Adipose	Plasma
Total number of lipids measured	227	238	271	258	271
Median %CV[b] for lipid species	13.6	19.7	13.2	15.4	9.6
90% Percentile %CV	32.2	30.2	25.8	28.0	18.6
Number of lipid species with CV > 30%	26	24	20	17	3

[a] Based on 12-14 quality controls prepared specifically for each tissue or plasma extraction procedure, and evenly spaced throughout run
[b] %CV, percent coefficient of variation

Table 4.5 Early lipid abnormalities in male *db/h* mice (plasma only) and female *db/h* mice (plasma and tissues) at 6 weeks of age compared with corresponding *H/H* mice.

Male *db/h* mouse phenotype	**Early lipid abnormalities in male *db/h* mice**
Not different to male *H/H* mice	**Plasma:** five lipid classes/subclasses (MHC, PC, PE, PI and CE) and 42 species significantly elevated, including multiple species of Cer, MHC, SM (six species), PC (eight species containing only even-numbered carbon fatty acids), PE (all 13 species), PE(P), LPE, PI and CE
Female *db/h* mouse phenotype	**Early lipid abnormalities in female *db/h* mice**
Glucose intolerant	**Plasma:** three TG species significantly elevated (TG 14:0/16:1/18:1, TG 14:1/16:1/18:0 and TG 16:1/16:1/16:1); and ten lipids significantly lower, including two PC(O) species, two PC(P) species and three PE(O) species **Liver:** CE subclass and 14 lipids significantly elevated, including three CE species (CE 16:1, CE 18:0 and CE 18:1), two DG species (DG 16:1/18:0 and DG 16:1/18:1) and eight TG species **Skeletal muscle:** three PC species significantly elevated (PC 28:0, PC 32:1 and PC 34:4); and PC(O-38:4) significantly lower **Left-ventricle:** CL 18:2/18:2/18:2/16:1, DG 18:1/20:4 and TG 18:1/18:1/20:4 significantly elevated **Adipose:** eight lipids significantly elevated, including five PC(P) species, PE(O-36:5) and PE(P-36:4); and two lipids significantly lower

TG species (containing only even-numbered carbon fatty acids) (Table S4.6). Additionally, CL 18:2/18:2/18:2/16:1 was significantly elevated in left-ventricle, and there was a significant rise in five PC(P) species and PE(P-36:4) in adipose in female *db/h* mice at 6 weeks of age (Table S4.9).

4.3.5 Dominant effect of genotype, and not gender or age, on global lipid profiles

Initially, PCA modelling was employed to compare the independent effects of 1) gender; 2) age (6 vs. 10 vs. 16 weeks); and 3) genotype (*H/H* vs. *db/h* vs. *db/db*) on global liver lipid profiles (i.e., levels of all measured lipid species) in plasma and each of the tissues for all mice. In particular, PCA plots comparing global liver lipid profiles in the three genotypes revealed good right-shifted separation of the PC1 axis in *db/db* mice compared with both *H/H* and *db/h* mice (Figure 4.5A). In contrast, PCA plots comparing global liver lipid profiles in female and male mice (Figure 4.5B) and the three age groups (Figure 4.5C) revealed little separation between the groups. Therefore, PCA plots comparing the independent effect of genotype on global lipid profiles in skeletal muscle, left-ventricle, adipose and plasma are presented in Figure 4.6 (A to D). Good right-shifted separation of the PC1 lipid axis occurred in left-ventricle of *db/db* mice compared with both *H/H* and *db/h* mice (Figure 4.6B), and there was a tendency towards right-shifted separation of the PC1 lipid axis in skeletal muscle, adipose and plasma of *db/db* mice. In contrast, PCA plots comparing the independent effects of gender and age on global lipid profiles in skeletal muscle, left-ventricle, adipose and plasma revealed little separation between the groups (data not shown).

4.3.6 Relationship between gender and global lipid profiles

Using the non-parametric Mann-Whitney *U* test corrected for multiple comparisons with the Benjamini-Hochberg method [155], lipid species and classes/subclasses that were significantly different between male and female *H*/*H*, *db*/*h* and *db*/*db* mice at 6, 10 and 16 weeks of age were identified (Table 4.6). There were substantial differences between genders in the liver lipid profiles in *H/H* and *db*/*h* mice at 16 weeks of age, in the skeletal muscle lipid profile in *H*/*H* mice at 10 weeks of age, and in the left-ventricle lipid profile in *db*/*h* mice at 10 weeks of age. There were also very large differences between genders in the plasma lipid profiles in *H*/*H* mice at 10 and 16 weeks of age, and in *db*/*h* mice at 6, 10 and 16 weeks of age, whereby the number

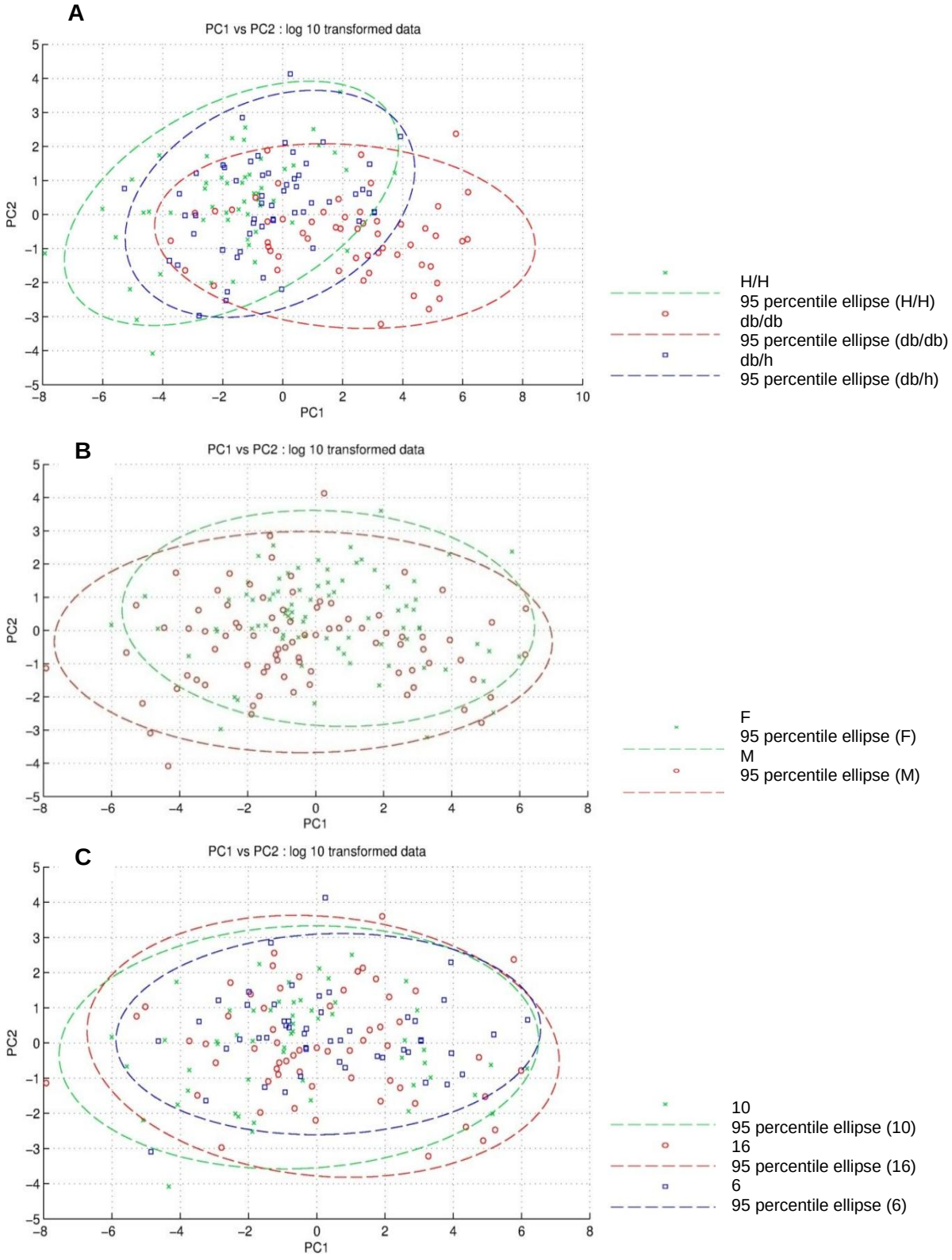

Figure 4.5 Principal component analysis (PCA) modellingof liver lipid profiles. The independent effects of genotype (*H/H* vs. *db/h* vs. *db/db*) (A), gender (B) and age (6 vs. 10 vs.16 weeks) (C) on liver lipid profiles (i.e., log-transformed lipid levels) were compared in mice fed an unrestricted chow diet. Each PCA plot shows the 95 percentile ellipse. F, female; M, male.

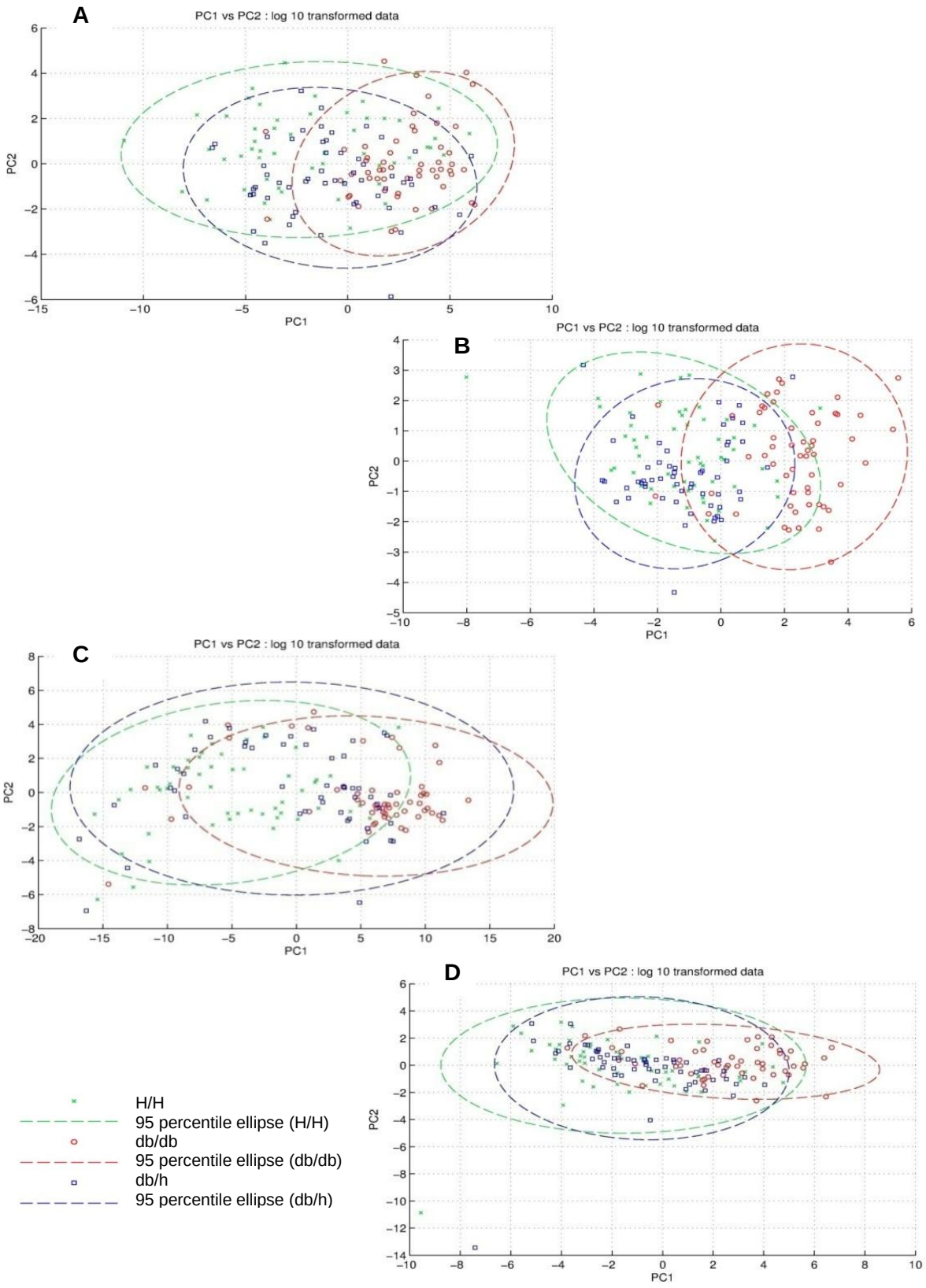

Figure 4.6 Principal component analysis (PCA) modelling of tissue and plasma lipid profiles. The independent effects of genotype (*H/H* vs. *db/h* vs. *db/db*) on lipid profiles (i.e., log-transformed lipid levels) in skeletal muscle (A), left-ventricle (B), adipose (C) and plasma (D) were compared in mice fed an unrestricted chow diet. Each PCA plot shows the 95 percentile ellipse.

Table 4.6 Relationship between gender and lipid species and classes/subclasses in tissues and plasma in *H/H*, *db*/*h* and *db*/*db* mice.

		Number of significant lipids[b]		
Tissue[a]	**Genotype**	**6 weeks**	**10 weeks**	**16 weeks**
Liver	*H/H*	0 (0)	4 (0)	44 (3)
227 (21)	*db*/*h*	0 (0)	0 (0)	80 (2)
	db/*db*	0 (0)	0 (0)	0 (0)
Skeletal muscle	*H/H*	0 (0)	84 (5)	0 (0)
238 (21)	*db*/*h*	0 (0)	0 (0)	0 (0)
	db/*db*	0 (0)	0 (0)	0 (0)
Left-ventricle	*H/H*	0 (0)	15 (0)	0 (0)
271 (25)	*db*/*h*	0 (0)	42 (2)	15 (0)
	db/*db*	0 (0)	0 (0)	0 (0)
Adipose	*H/H*	0 (0)	0 (0)	0 (0)
258 (22)	*db*/*h*	0 (0)	0 (0)	2 (1)
	db/*db*	0 (0)	0 (0)	0 (0)
Plasma	*H/H*	0 (0)	202 (12)	52 (0)
271 (20)	*db*/*h*	152 (13)	121 (5)	192 (16)
	db/*db*	0 (0)	0 (0)	0 (0)

[a] Tissue analysed and the total number of lipid species and (classes/subclasses) measured
[b] The number of lipid species and (classes/subclasses) found to be significantly different between male and female mice ($P < 0.05$ using Mann-Whitney U test with Benjamini-Hochberg correction for multiple lipid comparisons).

of lipid species and classes that were significantly different between male and female mice in these groups ranged from 121 to 202 lipid species and five to 16 classes/subclasses (Table 4.6). In contrast, there were almost no differences between genders in adipose lipid profiles in any of the groups, and more specifically, there was no difference between genders in any tissue or plasma lipid profiles in *db*/*db* mice (Table 4.6).

4.3.7 Relationship between age and global lipid profiles

Using the Kruskal-Wallis test across the three age groups (with the overall *P*-value corrected for multiple comparisons with the Benjamini-Hochberg method [155], and subsequent post-hoc analyses, we identified lipid species and classes/subclasses that were significantly different between the different ages in female and male mice within each genotype (Table 4.7). The effect of age on lipid profiles in each tissue is summarised as follows:

Liver: There was no difference in the liver lipid profiles at different ages in any genotypes in the female mice. However, there were significant differences between ages (overall) in 25 liver lipid species in male *db/db* mice, which were mainly attributable to significant differences in lipid levels at 16 weeks of age (Table 4.7).

Skeletal muscle: There were significant differences between ages (overall) in 45 skeletal muscle lipid species (and five classes/subclasses) in female *H*/*H* mice, but no differences in male *H*/*H* mice. In female *db*/*h* mice, there were significant differences between ages (overall) in 124 skeletal muscle lipid species (and 11 classes/subclasses), which were mainly due to differences in lipid levels at 6 weeks of age (Table 4.7). In contrast, the significant differences between ages (overall) in the skeletal muscle lipid profile in female *db*/*db* mice was mainly attributable to differences in lipid levels at 16 weeks of age. Notably, there were fewer significant differences between ages (overall) in skeletal muscle lipids in male *db*/*h* and *db*/*db* mice compared with the corresponding female genotypes.

Left-ventricle: There was no difference in the left-ventricle lipid profiles at different ages in female *H*/*H* mice. A small number of lipids (23) overall were affected in the female *db/h* mice, while a relatively large number of lipids overall were affected in the female *db/db* mice, which was mainly driven by differences at 16 weeks of age. In contrast, all male genotypes had a

Table 4.7 Relationship between age and lipid species and classes/subclasses in tissues and plasma in *H/H*, *db*/*h* and *db*/*db* mice.

		Female mice				Male mice			
		Number of significant lipids				Number of significant lipids			
Tissue[a]	Genotype	Overall[b]	10 vs. 6 weeks[c]	16 vs. 6 weeks[c]	16 vs. 10 weeks[c]	Overall[b]	10 vs. 6 weeks[c]	16 vs. 6 weeks[c]	16 vs. 10 weeks[c]
Liver	*H*/*H*	0(0)	0 (0)	0 (0)	0 (0)	0 (0)	0 (0)	0 (0)	0 (0)
227 (21)	*db*/*h*	0 (0)	0 (0)	0 (0)	0 (0)	0 (0)	0 (0)	0 (0)	0 (0)
	db/*db*	0 (0)	0 (0)	0 (0)	0 (0)	25 (0)	3 (0)	19 (0)	20 (0)
Skeletal muscle	*H*/*H*	45 (5)	15 (2)	33 (3)	26 (4)	0 (0)	0 (0)	0 (0)	0 (0)
238 (21)	*db*/*h*	124 (11)	101 (10)	86 (7)	26 (1)	48 (3)	27 (3)	48 (3)	11 (0)
	db/*db*	45 (1)	4 (0)	34 (1)	41 (1)	26 (0)	13 (0)	24 (0)	17 (0)
Left-ventricle	*H*/*H*	0 (0)	0 (0)	0 (0)	0 (0)	74 (10)	55 (8)	70 (9)	0 (0)
271 (25)	*db*/*h*	23 (0)	20 (0)	19 (0)	5 (0)	106 (13)	89 (12)	88 (12)	4 (0)
	db/*db*	100 (13)	0 (0)	89 (13)	82 (11)	100 (11)	37 (9)	81 (6)	44 (1)
Adipose	*H*/*H*	0 (0)	0 (0)	0 (0)	0 (0)	0 (0)	0 (0)	0 (0)	0 (0)
258 (22)	*db*/*h*	0 (0)	0 (0)	0 (0)	0 (0)	0 (0)	0 (0)	0 (0)	0 (0)
	db/*db*	0 (0)	0 (0)	0 (0)	0 (0)	0 (0)	0 (0)	0 (0)	0 (0)
Plasma	*H*/*H*	158 (12)	106 (10)	21 (1)	85 (7)	8 (1)	8 (1)	8 (1)	0 (0)
271 (20)	*db*/*h*	0 (0)	0 (0)	0 (0)	0 (0)	10 (0)	1 (0)	10 (0)	9 (0)
	db/*db*	0 (0)	0 (0)	0 (0)	0 (0)	0 (0)	0 (0)	0 (0)	0 (0)

[a] Tissue analysed and the total number of lipid species and (classes/subclasses) measured

[b] The number of lipid species and (classes/subclasses) found to be significantly different between ages for each genotype (overall) using the Kruskal Wallis test with Benjamini-Hochberg correction for multiple lipid comparisons. $P < 0.05$ was considered significant

[c] The number of lipid species and (classes/subclasses) found to be significantly different using post-hoc analysis by Mann Whitney *U* test with Dunn-Sidak correction for multiple group comparisons. $P < 0.05$ was considered significant.

relatively large number of left-ventricle lipids affected by age, which were primarily driven by differences at 6 weeks of age (Table 4.7).

Adipose: There was no difference in adipose lipid profiles at different ages in any genotypes in female or male mice (Table 4.7).

Plasma: There were many differences in plasma lipid profiles in female *H*/*H* mice at different ages (Table 4.7).

4.3.8 Relationship between genotype and global lipid profiles

From this point onwards, the term "effect of genotype" is regularly used to describe the differences in lipid profiles (i.e., lipid classes/subclasses and/or species) observed between genotype groups, independently of gender and age. We acknowledge that genotype was not adjusted for other independent variables (covariates) that may influence lipid profiles (e.g. diet, body weight, fasting plasma glucose, fasting plasma insulin), but prefer to use the term "effect of genotype" for convenience and simplicity.

Using the Kruskal-Wallis test across the three genotypes (with the overall *P*-value corrected for multiple comparisons with the Benjamini-Hochberg method [155]), and subsequent post-hoc analyses, we identified lipid species and classes/subclasses that were significantly different between the different genotypes in female and male mice at 6, 10 and 16 weeks of age (Table 4.8). Generally, the genotype effect was stronger than that seen for gender (Table 4.6) or age (Table 4.7). However, there was no effect of genotype on lipid profiles in liver, skeletal muscle and adipose in female mice at 16 weeks of age. In male mice, there was no effect of genotype on lipid profiles in liver, skeletal muscle, left-ventricle and adipose at 6 weeks of age, and only minimal effects on the plasma lipid profile at 16 weeks of age. The effect of genotype on lipid profiles in each tissue is summarised as follows:

Liver: A genotype effect was apparent for a substantial number of lipid species and classes overall in female mice both at 6 and 10 weeks of age, resulting primarily from differences in the *db/db* mice (Table 4.8). A similar genotype effect was seen in male mice both at 10 and 16 weeks of age.

Table 4.8 Relationship between genotype and lipid species and classes/subclasses in tissues and plasma in *H/H*, *db*/*h* and *db*/*db* mice.

		Female mice				Male mice			
		Number of significant lipids				Number of significant lipids			
Tissue[a]	Age (wks)	Overall[b]	*db*/*h* vs. *H/H*[c]	*db*/*db* vs. *H/H*[c]	*db*/*db* vs. *db*/*h*[c]	Overall[b]	*db*/*h* vs. *H/H*[c]	*db*/*db* vs. *H/H*[c]	*db*/*db* vs. *db*/*h*[c]
Liver	6	101 (5)	14 (1)	84(4)	70 (4)	0 (0)	0 (0)	0 (0)	0 (0)
227(21)	10	61 (3)	0 (0)	56 (3)	57 (2)	108 (6)	21 (2)	102 (5)	85 (4)
	16	0 (0)	0 (0)	0 (0)	0 (0)	107 (9)	6 (0)	100 (9)	85 (5)
Skeletal muscle	6	52 (3)	4 (0)	47 (3)	44 (3)	0 (0)	0 (0)	0 (0)	0 (0)
238 (21)	10	146 (14)	99 (13)	75 (3)	108 (8)	88 (4)	9 (0)	82 (3)	19 (1)
	16	0 (0)	0 (0)	0 (0)	0 (0)	116 (7)	34 (5)	80 (2)	82 (4)
Left-ventricle	6	117 (9)	3 (0)	108 (7)	97 (7)	0 (0)	0 (0)	0 (0)	0 (0)
271 (25)	10	161 (15)	19 (2)	136 (9)	142 (13)	155 (10)	36 (2)	116 (4)	114 (7)
	16	73 (2)	0 (0)	54 (1)	68 (2)	111 (5)	19 (2)	93 (4)	86 (2)
Adipose	6	165 (14)	10 (0)	144 (13)	147 (10)	0 (0)	0 (0)	0 (0)	0 (0)
258 (22)	10	156 (12)	7 (1)	145 (12)	60 (8)	137 (14)	17 (3)	130 (12)	19 (0)
	16	0 (0)	0 (0)	0 (0)	0 (0)	192 (16)	124 (10)	172 (15)	11 (0)
Plasma	6	151 (7)	13 (0)	97 (3)	136 (6)	105 (8)	42 (5)	85 (7)	40 (3)
271 (20)	10	99 (4)	21 (1)	97 (4)	61 (2)	46 (1)	1 (0)	43 (1)	40 (2)
	16	62 (2)	2 (0)	45 (1)	60 (2)	6 (0)	3 (0)	3 (0)	6 (0)

[a] Tissue analysed and the total number of lipid species and (classes/subclasses) measured.
[b] The number of lipid species and (classes/subclasses) found to be significantly different between genotypes at each age (overall) using the Kruskal Wallis test with Benjamini-Hochberg correction for multiple lipid comparisons. $P < 0.05$ was considered significant.
[c] The number of lipid species and (classes/subclasses) found to be significantly different using post-hoc analysis by Mann Whitney *U* test with Dunn-Sidak correction for multiple group comparisons. $P < 0.05$ was considered significant.

Skeletal muscle: A substantial number of lipids (52) overall were affected by genotype in female mice at 6 weeks of age, which was mainly attributable to differences in the *db/db* mice (Table 4.8). Impressively, 146 lipid species overall were affected by genotype in female mice at 10 weeks of age, with all three genotypes contributing to the differences in lipid species. A large number of lipids overall were affected by genotype in male mice both at 10 and 16 weeks of age, mainly driven by differences between *db/db* and *H/H* mice at 10 weeks of age, and by differences in *db/db* mice at 16 weeks of age.

Left-ventricle: A very large number of lipids overall were affected by genotype in female mice at 6, 10 and 16 weeks of age, which was mainly attributable to differences in *db*/*db* mice (Table 4.8). A similar genotype effect was seen in male mice both at 10 and 16 weeks of age.

Adipose: A very large number of lipids overall were affected by genotype in female mice at 6 and 10 weeks of age, mainly driven by differences in *db*/*db* mice (Table 4.8). A very large number of lipids overall were affected by genotype in male mice both at 10 and 16 weeks of age, primarily driven by differences between *db/db* and *H/H* mice at 10 weeks of age, and by differences in *db/db* and *db/h* mice compared with *H/H* mice at 16 weeks of age.

Plasma: The genotype effects on plasma lipid profiles overall in female mice at 6 and 10 weeks of age were similar to those seen in liver, left-ventricle and adipose, being mainly attributable to differences in the female *db/db* mice (Table 4.8). The genotype effect on the plasma lipid profile overall in female mice at 16 weeks of age was very similar to that seen in left-ventricle. A large number of plasma lipids overall were affected by genotype in male mice at 6 weeks of age, with all three genotypes contributing to the differences in lipid species. In contrast, the tissues exhibited no genotype effect on lipid profiles in male mice at 6 weeks of age. A substantial number of lipid species (46) overall were affected by genotype in male mice at 10 weeks of age, mainly driven by differences in *db/db* mice.

The results described in sections 4.3.6 to 4.3.8 above clearly show that the independent effect of genotype on global lipid profiles in tissues and plasma was consistently more substantial and ubiquitous than the independent effects of gender or age, which confirm the earlier findings using PCA modelling (section 4.3.5).

4.3.9 Comparison of lipid classes and species in *db/db* vs. *H/H* mice

The dominant effect of genotype was examined in greater detail by determining not only which lipid classes, subclasses and species in each of the tissues and plasma were significantly different between genotypes (*H*/*H*, *db*/*h* or *db*/*db*) in both male and female mice at 6, 10 and 16 weeks of age, but also the magnitude and direction of change. This information is highlighted in Tables 4.9 to 4.13 (relationship between genotype and lipid classes and subclasses) and Supplementary Tables S4.1 to S4.10 (relationship between genotype and lipid species).

Based on the results shown in Table 4.8 and section 4.3.8, it is clear that, in the majority of cases, the effects of genotype on the lipid profiles in tissues and plasma were mainly due to differences in lipid levels in the *db/db* mice relative to the *db/h* or *H/H* mice for both genders. In addition, the differences in lipid profiles seen in *db/db* versus *H/H* mice and *db/db* versus *db/h* mice in each tissue or plasma were generally very similar. However, the effects of genotype on lipid profiles in each tissue and plasma were quite different in male compared with female mice. Therefore, for clarity and convenience, the following results section summarizes the most important effects of genotype (based on the number, magnitude and direction of change of significantly different lipid classes, subclasses and species) in each tissue and plasma in male *db/db* mice compared with male *H/H* mice, and in female *db/db* mice compared with female *H/H* mice (at each age group).

For ease of comparison, the lipid classes and subclasses were divided into seven main lipid groups, namely 1) sphingolipids (Sph, Cer, MHC, DHC, THC, GM3 and SM); 2) the major glycerophospholipids (PC and PE); 3) ether- and vinyl ether-linked phospholipids (PC(O), PC(P), PE(O) and PE(P)); 4) lysophospholipids (LPC, LPC(O) and LPE); 5) other glycerophospholipids (PI, PS, PG and BMP); 6) cardiolipins (CL); and 7) cholesteryl esters and glycerolipids (CE, DG and TG).

4.3.9.1 Liver lipid profiles in male *db/db* vs. *H/H* mice

There were no differences in the liver lipid profiles in 6 week old male mice. Early liver lipid abnormalities in male *db/db* versus *H/H* mice (at 10 weeks of age) included significantly higher total levels of five lipid classes (LPE, BMP, CE, DG and TG) (Table 4.9A and Figure 4.7) and

Table 4.9A Relationship between genotype and liver lipid classes and subclasses in male mice.

	6 weeks				10 weeks				16 weeks			
Lipid class	*P*-value[a]	db/h vs. H/H[b]	db/db vs. H/H[b]	db/db vs. db/h[b]	*P*-value[a]	db/h vs. H/H[b]	db/db vs. H/H[b]	db/db vs. db/h[b]	*P*-value[a]	db/h vs. H/H[b]	db/db vs. H/H[b]	db/db vs. db/h[b]
Cer	0.823	0.0	0.0	0.1	0.686	0.0	-0.1	0.2	0.746	0.0	0.0	0.1
MHC	0.533	0.3	0.0	-0.2	0.991	0.0	0.0	0.0	0.378	0.0	-0.1	-0.4
DHC	0.719	-0.1	0.0	0.1	0.704	0.0	0.3	0.0	0.080	0.8	1.1	0.0
SM	0.362	0.2	0.0	-1.3	0.449	0.0	-0.1	-0.4	0.046	0.0	-1.4	-1.1
PC	0.953	0.0	0.0	0.0	0.628	0.1	0.2	0.0	0.265	-0.1	-0.5	-0.3
PC(O)	0.467	0.0	-0.8	-0.3	0.112	0.0	-1.0	-0.6	0.076	0.0	-1.5	-0.5
PC(P)	0.514	0.1	-0.1	-0.5	0.257	0.0	-0.7	-0.3	0.002	-0.7	-3.2	-2.1
LPC	0.459	0.7	0.4	0.0	0.041	0.4	1.0	1.3	0.024	0.1	1.7	1.2
PE	0.730	0.1	0.0	-0.1	0.733	-0.1	0.1	0.0	0.131	0.0	-1.0	-0.6
PE(O)	0.467	0.0	-0.1	-0.8	0.167	-0.1	-1.1	0.1	0.319	0.0	-0.5	-0.2
PE(P)	0.469	0.0	-0.1	-0.8	0.704	0.0	-0.1	0.0	0.013	0.0	-2.1	-1.5
LPE	0.398	1.1	0.5	0.0	0.005	1.8	3.3	0.2	0.006	1.2	2.5	0.5
PI	0.825	0.0	0.0	0.0	0.465	0.0	0.5	0.0	0.559	-0.1	-0.1	0.1
PS	0.613	0.0	0.0	-0.5	0.961	0.0	0.0	0.0	0.033	-0.1	-1.9	-0.7
PG	0.794	0.0	0.0	-0.1	0.909	0.0	0.0	0.0	0.075	0.0	-1.0	-1.0
BMP	0.516	0.0	0.1	0.5	0.021	0.0	2.4	0.8	0.378	0.2	0.4	0.0
CL	0.717	0.0	0.0	-0.2	0.827	0.0	0.0	0.0	0.148	-0.6	-0.8	0.0
CE	0.339	0.1	0.9	0.9	0.001	0.3	3.5	3.1	0.009	0.0	1.7	2.2
COH	0.448	0.2	0.0	-0.9	0.856	0.0	0.0	0.0	0.974	0.0	0.0	0.0
DG	0.516	0.3	0.3	0.0	0.005	0.1	2.6	2.1	0.013	0.0	1.9	1.8
TG	0.549	0.0	0.1	0.4	0.001	1.4	4.1	3.1	0.002	-0.1	3.1	3.0

Table 4.9B Relationship between genotype and liver lipid classes and subclasses in female mice.

	6 weeks				10 weeks				16 weeks			
Lipid class	*P*-value[a]	db/h vs. H/H[b]	db/db vs. H/H[b]	db/db vs. db/h[b]	*P*-value[a]	db/h vs. H/H[b]	db/db vs. H/H[b]	db/db vs. db/h[b]	*P*-value[a]	db/h vs. H/H[b]	db/db vs. H/H[b]	db/db vs. db/h[b]
Cer	0.016	-0.1	1.8	2.3	0.248	0.0	0.2	1.1	0.181	-0.6	0.0	1.3
MHC	0.087	0.0	-1.6	-0.3	0.004	-0.4	-3.3	-3.0	0.195	-0.1	-0.9	-0.7
DHC	0.395	-0.4	0.0	0.1	0.769	0.0	0.0	-0.2	0.332	-0.4	-0.6	0.0
SM	0.189	0.0	-0.8	-0.4	0.829	0.0	0.0	0.0	0.322	-0.6	-0.4	0.0
PC	0.179	0.0	-0.7	-0.5	0.853	0.0	0.0	0.0	0.474	-0.3	-0.3	0.0
PC(O)	0.018	-0.5	-2.3	-1.0	0.004	-0.2	-3.3	-3.9	0.192	-0.4	-1.1	-0.5
PC(P)	0.043	0.0	-1.5	-1.4	0.445	-0.1	-0.4	0.0	0.195	-0.6	-1.1	-0.2
LPC	0.477	0.0	0.3	0.1	0.424	0.3	0.3	0.0	0.918	0.0	0.0	0.0
PE	0.961	0.0	0.0	0.0	0.726	-0.1	0.0	0.0	0.322	-0.6	-0.4	0.0
PE(O)	0.063	-0.3	-1.6	-0.3	0.142	-0.1	-1.3	-0.4	0.181	-1.1	-1.0	-0.1
PE(P)	0.105	0.0	-1.1	-0.6	0.051	-0.6	-1.6	-0.8	0.162	-1.1	-1.9	-0.9
LPE	0.076	1.1	0.9	0.0	0.562	0.0	0.2	0.2	0.537	-0.1	0.0	0.2
PI	0.189	0.1	0.0	-1.4	0.993	0.0	0.0	0.0	0.301	-0.4	-0.6	-0.1
PS	0.116	0.0	-0.5	-1.1	0.039	-0.9	-2.4	0.1	0.352	-0.2	-0.6	-0.1
PG	0.660	-0.1	0.0	0.1	0.414	-0.1	0.0	0.5	0.322	-0.2	-0.9	0.0
BMP	0.009	-0.1	2.1	3.3	0.105	-0.1	0.4	1.7	0.162	-0.4	0.1	1.8
CL	0.738	0.0	0.0	-0.1	0.998	0.0	0.0	0.0	0.322	-0.7	-0.2	0.1
CE	0.048	1.3	0.0	-1.4	0.461	0.5	0.0	0.0	0.918	0.0	0.0	0.0
COH	0.305	-0.1	-0.8	0.0	0.981	0.0	0.0	0.0	0.368	-0.7	0.1	0.1
DG	0.149	0.7	0.6	0.0	0.321	0.6	0.4	0.0	0.918	0.0	0.0	0.0
TG	0.055	1.6	0.7	-0.1	0.375	0.7	0.0	0.0	0.294	0.0	0.6	0.6

[a] *P*-value for the comparison of levels of each lipid class or subclass between genotypes at each age using the Kruskal Wallis test with Benjamini-Hochberg correction for multiple comparisons. $P < 0.05$ was considered significant (highlighted in pink).

[b] Post-hoc analysis was performed using the Mann Whitney *U* test with Dunn-Sidak correction for multiple group comparisons. Values were derived from the formula: sign(difference in median levels)*-log10(post-hoc *P*-value). Colour-coded values 1.3 to 2.0 (light red, $P = 0.05$-0.01) and > 2.0 (dark red, $P < 0.01$) indicate a significant increase relative to the reference group. Colour-coded values -1.3 to -2.0 (light green, $P = 0.05$-0.01) and < -2.0 (dark green, $P < 0.01$) indicate a significant decrease relative to the reference group.

Table 4.10A Relationship between genotype and skeletal muscle lipid classes and subclasses in male mice.

	6 weeks				10 weeks				16 weeks			
Lipid class	*P*-value[a]	db/h vs. H/H[b]	db/db vs. H/H[b]	db/db vs. db/h[b]	*P*-value[a]	db/h vs. H/H[b]	db/db vs. H/H[b]	db/db vs. db/h[b]	*P*-value[a]	db/h vs. H/H[b]	db/db vs. H/H[b]	db/db vs. db/h[b]
Cer	0.284	-0.8	-0.2	0.1	0.296	-0.5	-0.4	0.0	0.058	-1.5	-0.2	0.5
MHC	0.354	-0.3	0.0	0.3	0.325	-0.2	0.0	0.6	0.802	0.0	0.0	0.0
GM3	0.293	-0.7	-0.3	0.0	0.033	-0.8	-1.8	-0.5	0.081	-1.1	-0.8	0.0
SM	0.284	-0.5	0.0	0.6	0.056	-0.9	0.0	1.5	0.022	-1.5	0.1	1.8
PC	0.257	-0.8	0.0	0.9	0.176	-0.8	0.0	0.5	0.043	-1.8	0.0	0.7
PC(O)	0.626	-0.2	0.0	0.0	0.519	-0.1	-0.2	0.0	0.636	-0.2	0.0	0.0
PC(P)	0.279	-0.6	-0.7	0.0	0.056	-0.6	-1.2	-0.7	0.221	-0.5	-0.5	0.0
LPC	0.593	0.0	0.0	0.2	0.344	-0.1	0.0	0.5	0.123	0.1	1.2	0.3
PE	0.279	-0.3	0.0	0.9	0.127	-1.1	-0.2	0.4	0.013	-2.5	-0.1	1.0
PE(O)	0.269	-0.2	0.0	1.3	0.084	-1.3	-0.2	0.5	0.464	-0.2	0.0	0.3
PE(P)	0.302	-0.4	0.0	0.4	0.192	-0.8	-0.2	0.2	0.240	-0.8	0.0	0.2
LPE	0.733	0.0	0.0	0.0	0.338	-0.3	0.0	0.4	0.212	0.0	0.4	0.7
PI	0.325	-0.5	0.0	0.2	0.251	-0.7	-0.1	0.1	0.043	-1.8	-0.2	0.4
PS	0.288	-0.6	0.0	0.4	0.288	-0.4	0.0	0.4	0.197	-0.7	0.0	0.5
PG	0.269	-0.4	0.0	0.9	0.050	-0.9	0.0	1.7	0.483	-0.2	0.0	0.2
CL	0.255	-0.8	0.0	1.5	0.101	-0.4	0.0	1.4	0.006	-2.5	0.0	2.7
CE	0.381	0.0	-0.1	-0.4	0.846	0.0	0.0	0.0	0.051	-0.3	1.0	1.2
COH	0.320	-0.5	0.0	0.2	0.350	-0.4	-0.1	0.1	0.182	-0.1	0.3	0.8
DG	0.269	0.1	0.8	0.4	0.024	0.1	3.3	0.5	0.009	0.1	2.5	1.5
TG	0.284	0.4	0.4	0.3	0.011	0.7	4.1	0.7	0.004	0.3	3.2	2.2

Table 4.10B Relationship between genotype and skeletal muscle lipid classes and subclasses in female mice.

	6 weeks				10 weeks				16 weeks			
Lipid class	*P*-value[a]	db/h vs. H/H[b]	db/db vs. H/H[b]	db/db vs. db/h[b]	*P*-value[a]	db/h vs. H/H[b]	db/db vs. H/H[b]	db/db vs. db/h[b]	*P*-value[a]	db/h vs. H/H[b]	db/db vs. H/H[b]	db/db vs. db/h[b]
Cer	0.026	0.1	-1.6	-2.1	0.035	-2.5	-0.9	0.2	0.404	0.0	-0.3	-0.5
MHC	0.241	0.4	0.8	0.0	0.304	-1.2	-0.1	0.5	0.993	0.0	0.0	0.0
GM3	0.015	0.2	-2.3	-2.3	0.035	-2.4	-0.4	0.9	0.649	-0.2	0.0	0.1
SM	0.697	0.1	0.1	0.0	0.006	-3.3	0.0	3.9	0.590	0.0	0.0	0.4
PC	0.208	0.2	-0.4	-0.8	0.008	-3.0	-0.8	2.4	0.844	-0.1	-0.1	0.0
PC(O)	0.076	0.0	-1.0	-1.6	0.012	-2.9	-2.0	0.1	0.328	-0.2	-0.7	-0.1
PC(P)	0.060	-0.1	-0.7	-2.3	0.034	-1.9	-2.2	0.0	0.343	0.0	-0.6	-0.3
LPC	0.103	0.0	-0.3	-2.5	0.028	-2.3	-0.1	1.7	0.948	0.0	0.0	0.0
PE	0.255	0.0	-0.7	-0.4	0.014	-2.9	-0.2	1.7	0.629	-0.2	0.0	0.1
PE(O)	0.294	0.2	-0.3	-0.4	0.107	-2.0	-0.1	0.6	0.919	0.0	0.0	0.0
PE(P)	0.103	0.3	-0.4	-1.5	0.089	-2.0	-0.9	0.0	0.404	0.0	-0.5	-0.4
LPE	0.156	0.5	-0.2	-1.0	0.096	-1.8	0.0	1.1	0.787	0.0	0.0	0.1
PI	0.035	0.1	-1.6	-1.8	0.019	-2.6	-0.3	1.5	0.971	0.0	0.0	0.0
PS	0.269	0.3	0.0	-0.8	0.017	-2.8	-0.7	1.0	0.707	-0.1	0.0	0.1
PG	0.091	1.2	0.9	-0.1	0.011	-2.2	0.1	3.6	0.894	-0.1	0.0	0.0
CL	0.523	0.3	0.0	-0.1	0.019	-2.3	0.0	2.4	0.317	-0.2	0.1	0.8
CE	0.717	0.0	0.0	-0.1	0.287	-1.4	-0.3	0.2	0.452	0.0	0.1	0.4
COH	0.376	0.4	0.0	-0.4	0.037	-2.3	-0.4	0.9	0.926	0.0	0.0	0.0
DG	0.536	0.0	0.1	0.3	0.192	0.0	1.0	1.6	0.216	0.0	0.5	1.0
TG	0.146	0.0	0.5	1.5	0.014	-0.1	2.2	3.9	0.190	0.0	0.6	1.5

[a] *P*-value for the comparison of levels of each lipid class or subclass between genotypes at each age using the Kruskal Wallis test with Benjamini-Hochberg correction for multiple comparisons. $P < 0.05$ was considered significant (highlighted in pink).

[b] Post-hoc analysis was performed using the Mann Whitney *U* test with Dunn-Sidak correction for multiple group comparisons. Values were derived from the formula: sign(difference in median levels)*-log10(post-hoc *P*-value). Colour-coded values 1.3 to 2.0 (light red, $P = 0.05$-0.01) and > 2.0 (dark red, $P < 0.01$) indicate a significant increase relative to the reference group. Colour-coded values -1.3 to -2.0 (light green, $P = 0.05$-0.01) and < -2.0 (dark green, $P < 0.01$) indicate a significant decrease relative to the reference group.

Table 4.11A Relationship between genotype and L-V lipid classes and subclasses in male mice.

Lipid class	6 weeks				10 weeks				16 weeks			
	P-value[a]	db/h vs. H/H[b]	db/db vs. H/H[b]	db/db vs. db/h[b]	*P*-value[a]	db/h vs. H/H[b]	db/db vs. H/H[b]	db/db vs. db/h[b]	*P*-value[a]	db/h vs. H/H[b]	db/db vs. H/H[b]	db/db vs. db/h[b]
Sph	0.236	0.3	0.0	-0.8	0.247	0.0	0.1	0.7	0.084	-1.6	0.0	0.5
Cer	0.236	-0.7	-0.2	0.2	0.013	-2.5	-0.8	0.7	0.041	-1.7	-0.1	0.8
MHC	0.328	0.2	-0.1	-0.5	0.123	-0.5	-0.9	0.0	0.006	-0.4	-3.1	-1.3
DHC	0.983	0.0	0.0	0.0	0.220	0.1	0.6	0.2	0.406	0.0	-0.2	-0.4
THC	0.473	0.0	0.2	0.3	0.460	0.0	0.0	0.3	0.343	-0.4	-0.4	0.0
GM3	0.345	0.0	-0.5	-0.3	0.468	0.0	-0.2	-0.2	0.783	0.0	0.0	0.1
SM	0.230	-0.2	-1.1	-0.1	0.049	-1.0	-1.4	0.0	0.007	-2.4	-2.2	0.0
PC	0.384	-0.4	0.0	0.1	0.182	-0.7	0.0	0.5	0.158	-0.8	0.0	0.7
PC(O)	0.124	-1.1	-1.4	0.0	0.086	-1.0	-0.9	0.0	0.212	-0.7	0.0	0.6
PC(P)	0.060	-1.3	-2.3	-0.1	0.036	-0.9	-1.3	-0.5	0.289	-0.1	0.1	0.7
LPC	0.877	0.0	0.0	0.0	0.018	-1.3	0.0	1.9	0.186	-1.0	0.0	0.3
LPC(O)	0.127	0.0	-1.5	-0.9	0.561	0.0	0.0	0.2	0.132	0.0	-0.7	-1.0
PE	0.124	-0.1	0.8	1.3	0.054	-0.5	0.2	1.4	0.118	-0.3	0.3	1.1
PE(O)	0.619	-0.1	0.1	0.1	0.213	-0.8	0.0	0.3	0.590	-0.1	0.0	0.2
PE(P)	0.457	-0.2	0.0	0.3	0.124	-1.1	-0.4	0.1	0.329	-0.6	0.0	0.2
LPE	0.874	0.0	0.0	0.0	0.025	-0.2	0.5	2.0	0.658	0.0	-0.2	0.0
PI	0.448	-0.2	0.0	0.3	0.093	-1.0	0.0	0.8	0.460	-0.2	0.0	0.3
PS	0.235	-0.5	-0.7	0.1	0.247	-0.7	-0.2	0.0	0.446	-0.3	0.0	0.3
PG	0.180	-0.3	0.6	0.8	0.010	-0.8	0.6	2.3	0.713	-0.2	0.0	0.0
BMP	0.230	0.2	0.7	0.3	0.053	0.1	1.4	0.7	0.097	-0.2	0.8	1.0
CL	0.302	-0.2	-0.1	0.6	0.007	-1.1	0.4	2.5	0.125	-0.1	0.3	1.3
CE	0.383	0.0	0.5	0.2	0.026	-1.1	0.1	1.6	0.883	0.0	0.0	0.0
COH	0.484	0.1	0.0	-0.4	0.355	-0.3	-0.3	0.0	0.658	-0.1	-0.1	0.0
DG	0.292	0.0	0.4	0.6	0.001	-0.8	2.3	2.8	0.008	0.1	2.5	1.9
TG	0.209	0.3	0.8	0.3	0.001	0.0	2.8	3.2	0.006	0.0	2.6	2.4

Table 4.11B Relationship between genotype and L-V lipid classes and subclasses in female mice.

Lipid class	6 weeks				10 weeks				16 weeks of age			
	P-value[a]	db/h vs. H/H[b]	db/db vs. H/H[b]	db/db vs. db/h[b]	*P*-value[a]	db/h vs. H/H[b]	db/db vs. H/H[b]	db/db vs. db/h[b]	*P*-value[a]	db/h vs. H/H[b]	db/db vs. H/H[b]	db/db vs. db/h[b]
Sph	0.419	-0.1	-0.4	-0.1	0.391	-0.3	-0.2	0.0	0.262	-0.1	0.1	1.0
Cer	0.072	-1.0	0.1	1.1	0.004	-2.2	0.4	1.9	0.578	-0.1	-0.2	0.0
MHC	0.020	-0.6	-1.9	-0.9	0.063	-0.3	-1.0	-0.8	0.045	0.0	-1.2	-2.0
DHC	0.201	-0.4	0.0	1.0	0.187	-0.2	0.3	0.6	0.514	0.2	0.0	-0.2
THC	0.749	-0.1	0.0	0.1	0.959	0.0	0.0	0.0	0.201	0.9	0.1	-0.4
GM3	0.004	0.0	-3.9	-2.8	0.003	-0.3	-3.0	-2.2	0.262	0.1	-0.2	-0.8
SM	0.421	-0.3	-0.3	0.0	0.122	-1.1	-0.4	0.0	0.091	0.0	-1.1	-1.2
PC	0.632	-0.1	0.0	0.2	0.021	-0.6	1.1	1.5	0.376	-0.1	-0.5	-0.1
PC(O)	0.955	0.0	0.0	0.0	0.286	-0.6	0.0	0.2	0.591	0.0	-0.3	0.0
PC(P)	0.559	0.0	-0.3	0.0	0.824	-0.1	0.0	0.0	0.220	-0.4	-0.7	-0.1
LPC	0.955	0.0	0.0	0.0	0.012	-2.2	-0.1	1.0	0.719	0.0	0.1	0.1
LPC(O)	0.016	0.2	-1.0	-2.8	0.005	-0.6	-3.0	-1.2	0.648	0.1	0.0	-0.1
PE	0.007	0.0	3.1	2.0	0.002	0.0	3.9	3.3	0.483	-0.5	0.0	0.0
PE(O)	0.510	0.0	0.3	0.2	0.038	0.0	1.2	1.5	0.902	0.0	0.0	0.0
PE(P)	0.510	0.0	0.2	0.2	0.038	0.0	0.9	1.9	0.227	-0.6	-0.6	-0.1
LPE	0.939	0.0	0.0	0.0	0.151	-1.1	-0.2	0.0	0.551	0.2	0.2	0.0
PI	0.018	0.0	2.3	1.5	0.004	-0.1	2.2	3.0	0.469	-0.4	-0.1	0.0
PS	0.393	-0.2	0.0	0.4	0.028	-0.7	0.4	1.7	0.190	-0.2	-0.9	-0.3
PG	0.022	-0.2	0.8	2.3	0.009	0.0	2.6	1.7	0.880	0.0	0.0	0.0
BMP	0.399	0.3	0.3	0.0	0.197	-0.6	0.1	0.4	0.514	0.0	0.3	0.2
CL	0.092	0.0	1.5	0.5	0.002	0.0	3.9	3.3	0.736	-0.1	0.0	0.0
CE	0.006	0.0	2.8	2.3	0.002	-0.2	2.6	3.9	0.144	-0.1	0.2	1.4
COH	0.593	0.2	0.0	0.1	0.196	-0.7	-0.1	0.3	0.269	0.0	-0.6	-0.5
DG	0.021	0.2	2.8	0.5	0.001	-0.7	3.9	3.9	0.082	0.0	0.8	1.6
TG	0.006	0.2	3.9	1.5	0.002	0.0	2.4	3.9	0.032	0.0	1.6	2.4

[a] *P*-value for the comparison of levels of each lipid class or subclass between genotypes at each age using the Kruskal Wallis test with Benjamini-Hochberg correction for multiple comparisons. $P < 0.05$ was considered significant (highlighted in pink).

[b] Post-hoc analysis was performed using the Mann Whitney *U* test with Dunn-Sidak correction for multiple group comparisons. Values were derived from the formula: sign(difference in median levels)*-log10(post-hoc *P*-value). Colour-coded values 1.3 to 2.0 (light red, $P = 0.05$-0.01) and > 2.0 (dark red, $P < 0.01$) indicate a significant increase relative to the reference group. Colour-coded values -1.3 to -2.0 (light green, $P = 0.05$-0.01) and < -2.0 (dark green, $P < 0.01$) indicate a significant decrease relative to the reference group. L-V, left-ventricle

Table 4.12A Relationship between genotype and adipose lipid classes and subclasses in male mice.

	6 weeks				10 weeks				16 weeks			
Lipid class	*P*-value[a]	db/h vs. H/H[b]	db/db vs. H/H[b]	db/db vs. db/h[b]	*P*-value[a]	db/h vs. H/H[b]	db/db vs. H/H[b]	db/db vs. db/h[b]	*P*-value[a]	db/h vs. H/H[b]	db/db vs. H/H[b]	db/db vs. db/h[b]
Sph	0.627	0.2	0.0	-0.1	0.517	0.0	0.4	0.0	0.671	0.0	0.0	-0.1
Cer	0.401	0.6	0.0	-0.3	0.049	-1.1	-1.4	0.0	0.006	-2.4	-1.2	0.4
MHC	0.366	0.6	-0.1	-1.2	0.046	0.0	-1.6	-0.9	0.018	-0.8	-2.1	0.0
SM	0.980	0.0	0.0	0.0	0.350	-0.2	0.0	0.4	0.062	-0.1	0.8	1.0
PC	0.368	0.0	-0.3	-0.7	0.045	-1.1	-1.6	0.0	0.002	-2.9	-2.0	0.0
PC(O)	0.407	0.0	-0.1	-0.6	0.095	0.0	-0.9	-0.7	0.012	-0.6	-2.1	-0.5
PC(P)	0.366	0.0	-0.5	-1.1	0.031	-1.1	-2.1	0.0	0.012	-1.6	-1.6	0.0
LPC	0.653	0.0	0.0	-0.3	0.042	-0.9	-2.0	0.0	0.004	-2.7	-1.6	0.0
LPC(O)	0.366	0.6	0.9	0.0	0.044	1.3	0.0	-1.2	0.635	0.0	0.0	-0.2
PE	0.366	0.0	-0.3	-0.9	0.193	-0.6	-0.4	0.1	0.001	-3.1	-2.8	0.0
PE(O)	0.366	0.0	-1.4	-1.1	0.043	0.0	-2.8	-0.2	0.048	-0.7	-1.4	0.0
PE(P)	0.366	0.0	-0.3	-0.8	0.043	-0.7	-2.1	0.0	0.023	-1.0	-1.7	0.0
LPE	0.951	0.0	0.0	0.0	0.045	-0.3	-1.3	-0.8	0.011	-2.0	-1.3	0.0
PI	0.401	0.0	-0.4	-0.3	0.040	-1.6	-1.0	0.1	0.009	-1.7	-1.8	0.0
PS	0.384	0.1	-0.1	-0.7	0.770	0.0	0.0	0.1	0.169	-0.7	-0.2	0.2
PG	0.366	0.0	-0.8	-0.7	0.295	-0.7	-0.2	0.0	0.002	-2.8	-2.4	0.0
BMP	0.366	1.6	0.8	-0.1	0.019	2.1	2.8	0.7	0.696	0.0	0.0	0.1
CL	0.366	0.0	-1.2	-1.8	0.167	-0.1	-0.8	-0.2	0.001	-3.6	-3.6	-0.4
CE	0.629	0.2	0.1	0.0	0.019	1.2	2.6	0.7	0.002	0.9	3.1	1.2
COH	0.401	0.6	0.0	-0.3	0.985	0.0	0.0	0.0	0.343	-0.2	0.0	0.3
DG	0.366	0.1	1.2	0.1	0.023	0.8	1.7	1.1	0.001	1.2	3.6	1.3
TG	0.378	0.0	0.4	0.6	0.019	0.6	2.8	0.9	0.001	2.5	2.9	1.0

Table 4.12B Relationship between genotype and adipose lipid classes and subclasses in female mice.

	6 weeks				10 weeks				16 weeks			
Lipid class	*P*-value[a]	db/h vs. H/H[b]	db/db vs. H/H[b]	db/db vs. db/h[b]	*P*-value[a]	db/h vs. H/H[b]	db/db vs. H/H[b]	db/db vs. db/h[b]	*P*-value[a]	db/h vs. H/H[b]	db/db vs. H/H[b]	db/db vs. db/h[b]
Sph	0.066	-0.2	0.4	1.3	0.151	0.9	0.3	0.0	0.692	-0.2	0.0	0.0
Cer	0.003	0.9	-3.9	-3.3	0.020	-0.4	-1.6	-1.8	0.926	0.0	0.0	0.0
MHC	0.035	0.1	-1.6	-0.7	0.018	0.0	-2.4	-2.4	0.120	-0.7	-1.6	-0.3
SM	0.199	-0.1	-0.8	-0.1	0.893	0.0	0.0	0.0	0.647	0.0	0.1	0.2
PC	0.003	0.2	-3.3	-3.3	0.019	-0.5	-2.4	-0.9	0.193	0.0	-0.8	-0.7
PC(O)	0.149	0.0	-0.9	-0.2	0.018	0.0	-2.2	-2.2	0.092	-0.1	-1.3	-1.5
PC(P)	0.003	0.9	-3.6	-3.3	0.027	-0.1	-1.8	-1.3	0.163	0.0	-0.5	-1.4
LPC	0.025	0.4	-0.8	-1.8	0.191	0.0	-0.6	-0.5	0.417	0.0	-0.2	-0.5
LPC(O)	0.622	-0.1	-0.1	0.0	0.263	0.4	0.0	-0.4	0.347	-0.3	-0.5	0.0
PE	0.003	0.0	-3.3	-3.0	0.053	-0.2	-1.5	-0.6	0.696	0.0	0.0	-0.2
PE(O)	0.004	0.0	-2.6	-3.0	0.018	0.0	-2.4	-2.2	0.176	-0.2	-0.6	-1.0
PE(P)	0.003	0.7	-3.6	-3.3	0.022	-0.2	-1.8	-1.6	0.199	0.0	-0.3	-1.2
LPE	0.055	0.4	-0.2	-1.5	0.165	0.0	-0.8	-0.5	0.856	0.0	0.0	-0.1
PI	0.192	0.1	-0.1	-0.9	0.398	-0.1	-0.6	0.0	0.351	0.1	-0.1	-0.6
PS	0.014	0.1	-2.6	-0.9	0.314	0.0	-0.2	-0.5	0.748	-0.1	0.0	0.0
PG	0.003	-0.1	-3.6	-2.4	0.018	0.0	-2.2	-2.2	0.155	-0.3	-1.1	-0.7
BMP	0.684	0.0	-0.1	0.0	0.791	0.1	0.0	0.0	0.930	0.0	0.0	0.0
CL	0.003	0.0	-3.9	-3.0	0.018	0.0	-3.4	-2.4	0.152	0.0	-0.5	-1.8
CE	0.825	0.0	0.0	0.0	0.022	1.4	1.8	0.0	0.081	1.0	2.2	0.3
COH	0.036	-0.1	-1.8	-0.5	0.688	0.1	0.0	-0.1	0.809	0.0	0.1	0.0
DG	0.036	0.0	1.4	1.2	0.020	1.0	2.1	0.4	0.067	0.5	2.4	1.4
TG	0.014	-0.1	2.1	1.6	0.022	0.8	1.8	0.8	0.160	0.0	1.4	0.6

[a] *P*-value for the comparison of levels of each lipid class or subclass between genotypes at each age using the Kruskal Wallis test with Benjamini-Hochberg correction for multiple comparisons. $P < 0.05$ was considered significant (highlighted in pink).

[b] Post-hoc analysis was performed using the Mann Whitney *U* test with Dunn-Sidak correction for multiple group comparisons. Values were derived from the formula: sign(difference in median levels)*-log10(post-hoc *P*-value). Colour-coded values 1.3 to 2.0 (light red, $P = 0.05$-0.01) and > 2.0 (dark red, $P < 0.01$) indicate a significant increase relative to the reference group. Colour-coded values -1.3 to -2.0 (light green, $P = 0.05$-0.01) and < -2.0 (dark green, $P < 0.01$) indicate a significant decrease relative to the reference group.

Table 4.13A Relationship between genotype and plasma lipid classes and subclasses in male mice.

	6 weeks				10 weeks				16 weeks			
Lipid class	*P*-value[a]	db/h vs. H/H[b]	db/db vs. H/H[b]	db/db vs. db/h[b]	*P*-value[a]	db/h vs. H/H[b]	db/db vs. H/H[b]	db/db vs. db/h[b]	*P*-value[a]	db/h vs. H/H[b]	db/db vs. H/H[b]	db/db vs. db/h[b]
Sph	0.151	0.0	-0.8	-0.6	0.909	0.0	0.0	0.0	0.631	0.0	0.2	0.0
Cer	0.044	0.9	1.4	0.6	0.654	0.0	0.0	0.5	0.307	0.5	0.5	0.0
MHC	0.031	2.0	1.6	0.0	0.742	0.0	0.0	0.2	0.141	1.1	-0.1	-0.9
SM	0.058	1.2	1.2	0.0	0.689	0.0	0.0	0.3	0.791	0.0	0.1	0.0
PC	0.024	1.3	1.8	1.8	0.193	0.0	0.8	0.7	0.083	0.6	1.8	0.2
PC(O)	0.085	1.0	0.8	0.0	0.935	0.0	0.0	0.0	0.658	0.0	-0.1	-0.1
PC(P)	0.096	0.8	0.9	0.0	0.617	-0.2	-0.3	0.0	0.434	0.0	-0.3	-0.3
LPC	0.047	0.4	1.4	1.0	0.089	0.2	1.1	1.1	0.223	0.0	0.7	0.7
LPC(O)	0.094	0.4	0.9	0.3	0.791	0.1	0.1	0.0	0.201	0.7	0.0	-0.8
PE	0.024	3.0	0.9	-0.6	0.778	0.0	-0.1	-0.1	0.594	0.2	0.1	0.0
PE(O)	0.051	0.6	1.2	0.8	0.426	0.0	0.2	0.6	0.338	0.1	0.6	0.2
PE(P)	0.062	0.7	1.1	0.5	0.742	-0.1	0.0	0.2	0.959	0.0	0.0	0.0
LPE	0.043	0.6	1.6	0.8	0.177	0.0	0.3	1.3	0.230	0.0	0.8	0.6
PI	0.024	1.4	2.0	1.6	0.181	0.2	0.8	0.6	0.201	0.2	1.0	0.2
LPI	0.495	0.0	0.0	0.3	0.079	0.0	1.0	1.5	0.352	0.0	0.3	0.6
PS	0.062	1.3	0.9	0.0	0.889	0.0	0.0	0.0	0.972	0.0	0.0	0.0
CE	0.024	1.7	2.0	1.6	0.040	0.1	1.8	1.4	0.141	0.1	1.3	0.6
COH	0.082	0.5	1.1	0.2	0.635	0.1	0.4	0.0	0.167	0.0	0.8	1.0
DG	0.128	0.1	0.6	0.7	0.936	0.0	0.0	0.0	0.141	0.5	1.0	0.6
TG	0.078	0.1	0.7	1.2	0.885	0.0	0.0	0.0	0.113	0.9	1.3	0.2

Table 4.13B Relationship between genotype and plasma lipid classes and subclasses in female mice.

	6 weeks				10 weeks				16 weeks			
Lipid class	*P*-value[a]	db/h vs. H/H[b]	db/db vs. H/H[b]	db/db vs. db/h[b]	*P*-value[a]	db/h vs. H/H[b]	db/db vs. H/H[b]	db/db vs. db/h[b]	*P*-value[a]	db/h vs. H/H[b]	db/db vs. H/H[b]	db/db vs. db/h[b]
Sph	0.659	0.0	0.0	-0.2	0.344	0.1	-0.1	-0.5	0.271	0.4	0.7	0.0
Cer	0.040	-1.0	0.1	1.5	0.283	0.1	0.6	0.3	0.125	-0.3	0.2	1.4
MHC	0.119	-0.9	0.1	0.6	0.844	0.0	0.0	0.0	0.524	0.0	-0.2	-0.2
SM	0.033	-0.8	0.1	2.0	0.300	0.3	0.4	0.1	0.478	0.0	0.0	0.7
PC	0.021	-0.3	1.0	2.0	0.048	0.9	1.4	0.4	0.109	0.0	0.8	1.4
PC(O)	0.135	-0.7	0.0	0.8	0.375	0.1	0.6	0.0	0.895	0.0	0.0	0.0
PC(P)	0.143	-0.9	-0.1	0.4	0.286	0.4	0.5	0.0	0.972	0.0	0.0	0.0
LPC	0.062	0.0	1.0	1.1	0.609	0.1	0.2	0.0	0.139	0.0	0.7	1.1
LPC(O)	0.370	-0.2	0.0	0.3	0.783	0.1	0.0	0.0	0.648	0.1	0.0	0.2
PE	0.135	-1.0	-0.2	0.2	0.003	1.5	3.5	2.2	0.627	0.0	0.2	0.1
PE(O)	0.127	-0.4	0.2	0.9	0.229	0.3	0.7	0.1	0.535	-0.1	0.1	0.2
PE(P)	0.561	-0.2	-0.1	0.0	0.299	0.4	0.5	0.0	0.972	0.0	0.0	0.0
LPE	0.012	-0.4	1.6	2.0	0.450	0.0	0.4	0.1	0.254	0.0	0.4	0.8
PI	0.008	-0.4	1.3	3.0	0.216	0.2	0.6	0.5	0.078	0.0	0.8	1.9
LPI	0.348	0.0	0.3	0.3	0.931	0.0	0.0	0.0	0.439	-0.1	0.1	0.4
PS	0.133	-0.5	-0.9	0.0	0.822	0.0	0.1	0.0	0.427	0.0	-0.4	-0.2
CE	0.055	0.0	0.7	1.6	0.422	0.1	0.4	0.1	0.035	-0.1	0.8	3.9
COH	0.085	-0.4	0.4	1.0	0.117	0.0	1.3	0.7	0.363	-0.1	0.1	0.6
DG	0.023	0.0	2.1	1.2	0.012	1.1	2.4	0.8	0.107	0.0	0.9	1.3
TG	0.004	0.5	2.8	3.0	0.008	0.6	2.9	1.7	0.035	0.0	2.1	2.4

[a] *P*-value for the comparison of levels of each lipid class or subclass between genotypes at each age using the Kruskal Wallis test with Benjamini-Hochberg correction for multiple comparisons. $P < 0.05$ was considered significant (highlighted in pink).

[b] Post-hoc analysis was performed using the Mann Whitney *U* test with Dunn-Sidak correction for multiple group comparisons. Values were derived from the formula: sign(difference in median levels)*-log10(post-hoc *P*-value). Colour-coded values 1.3 to 2.0 (light red, $P = 0.05$-0.01) and > 2.0 (dark red, $P < 0.01$) indicate a significant increase relative to the reference group. Colour-coded values -1.3 to -2.0 (light green, $P = 0.05$-0.01) and < -2.0 (dark green, $P < 0.01$) indicate a significant decrease relative to the reference group.

90 lipid species, including multiple species of PC containing only even-numbered carbon fatty acids (FA) (ten species), PE, LPC, LPE (five species), PI, CL (five species) CE (nine species), DG (11 species) and TG (37 species) (Table S4.1). In contrast, only 12 lipid species were significantly lower in male *db/db* mice, including multiple species of PC containing an odd-numbered carbon FA (five species), PC(O), PC(P) and the most abundant CL species, CL 18:2/18:2,18:2/18:2. Notably, three of the five liver CL species that were significantly increased in the male *db/db* mice at 10 weeks of age contained one ester-linked 16:1 FA chain, and the other two CL species contained a combination of 18:1 and 18:2 FA chains (Figure 4.8). Despite these findings, total CL was not significantly different between the study groups at 10 weeks of age because the magnitude of the significant decrease in CL 18:2/18:2,18:2/18:2 cancelled out the sum of the significant elevations in the other CL species.

At 16 weeks of age, total LPE, CE, DG and TG remained significantly increased (Figure 4.7), total LPC was now significantly increased, and total SM, PC(P), PE(P) and PS were now significantly decreased in the now pre-diabetic male *db/db* versus corresponding male *H/H* mice. The 56 liver lipid species that were now significantly increased in the male *db/db* mice included multiple species of LPC, LPE, CE (six species), DG (eight species) and TG (35 species) that remained significantly increased, and now some Cer species, but no longer any PC, PE, PI or CL species. The 44 liver lipid species that were now significantly decreased in male *db/db* mice at 16 weeks of age included a greater number of PC (14 species), PC(O) and PC(P) (six species), and now some SM (five species), PE (seven species), PE(O), PI and PS species. There were 59 liver lipid species that were significantly different in male *db/db* mice at both 10 and 16 weeks of age (Table S4.1).

4.3.9.2 Skeletal muscle lipid profiles in male *db/db* vs. *H/H* mice

There were no differences in the skeletal muscle lipid profiles in six week old male mice. By ten weeks of age, total DG and TG (Table 4.10, panel A) and 62 lipid species were elevated in male *db/db* versus *H/H* mice, including eight DG species, all 42 TG species, and multiple species of SM, PE, and PC species containing only even-numbered carbon FA (Table S4.2). Twenty lipid species were lower in the male *db/db* mice, including eight PC species (most containing an odd-numbered carbon FA), and multiple species of PC(P), PI and CL. At 16 weeks of age, total skeletal muscle DG and TG remained significantly higher, and 67 lipid species were elevated in the now pre-diabetic male *db/db* mice relative to the *H/H* mice, including multiple species of

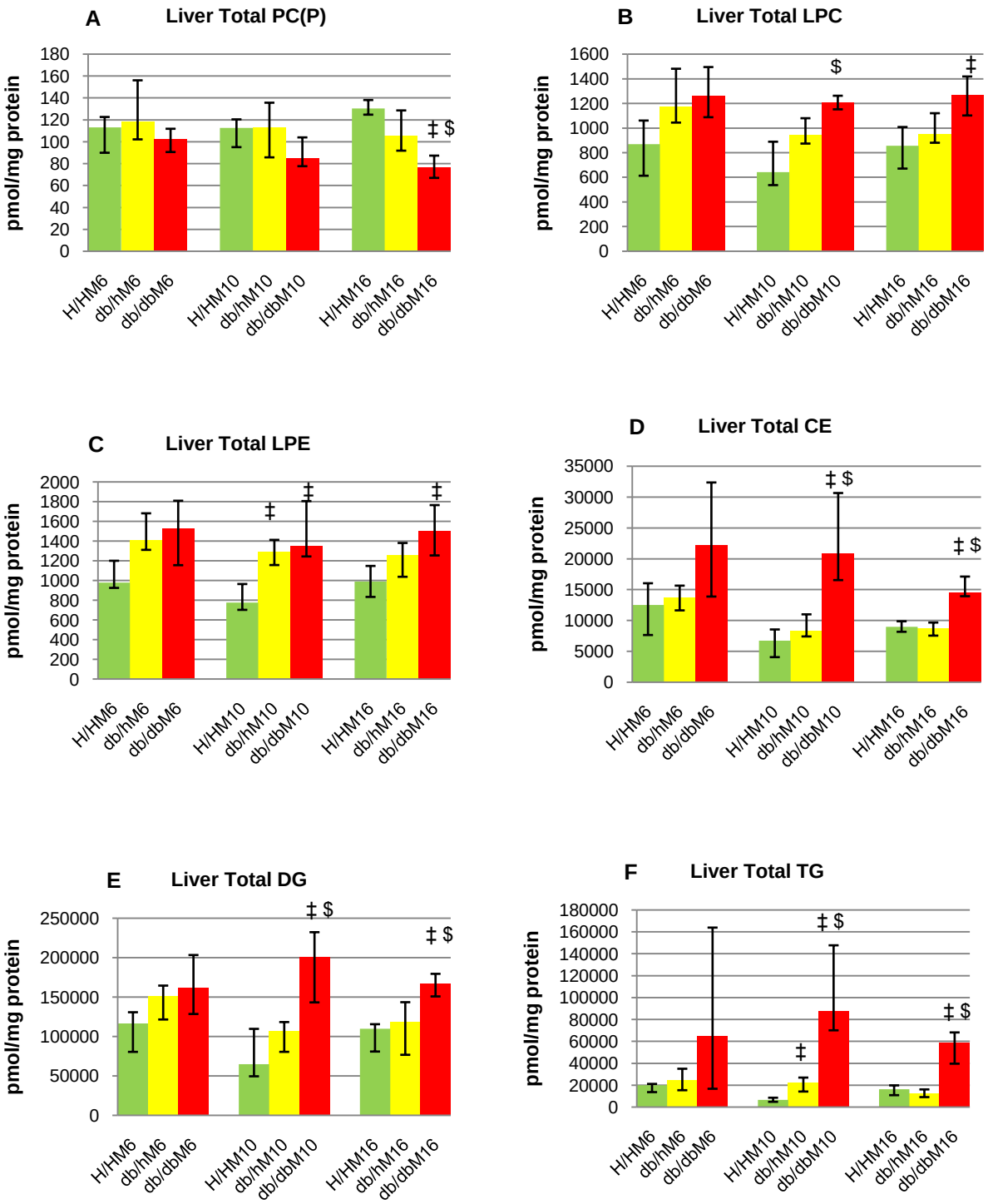

Figure 4.7 Relative liver lipid levels in male mice. Levels of lipid classes or subclasses in male (M) mice at 6, 10 and 16 weeks of age are expressed as median ± upper and lower quartile (7-12 mice per group). The *P*-value for the comparison of each lipid class or subclass between genotypes at each age was obtained using the Kruskal Wallis test with post-hoc analysis by Mann Whitney *U* test with Dunn-Sidak correction for multiple group comparisons. ‡ $P < 0.05$ vs. *H/H* mice at same age; $ $P < 0.05$ vs. *db/h* mice at same age.

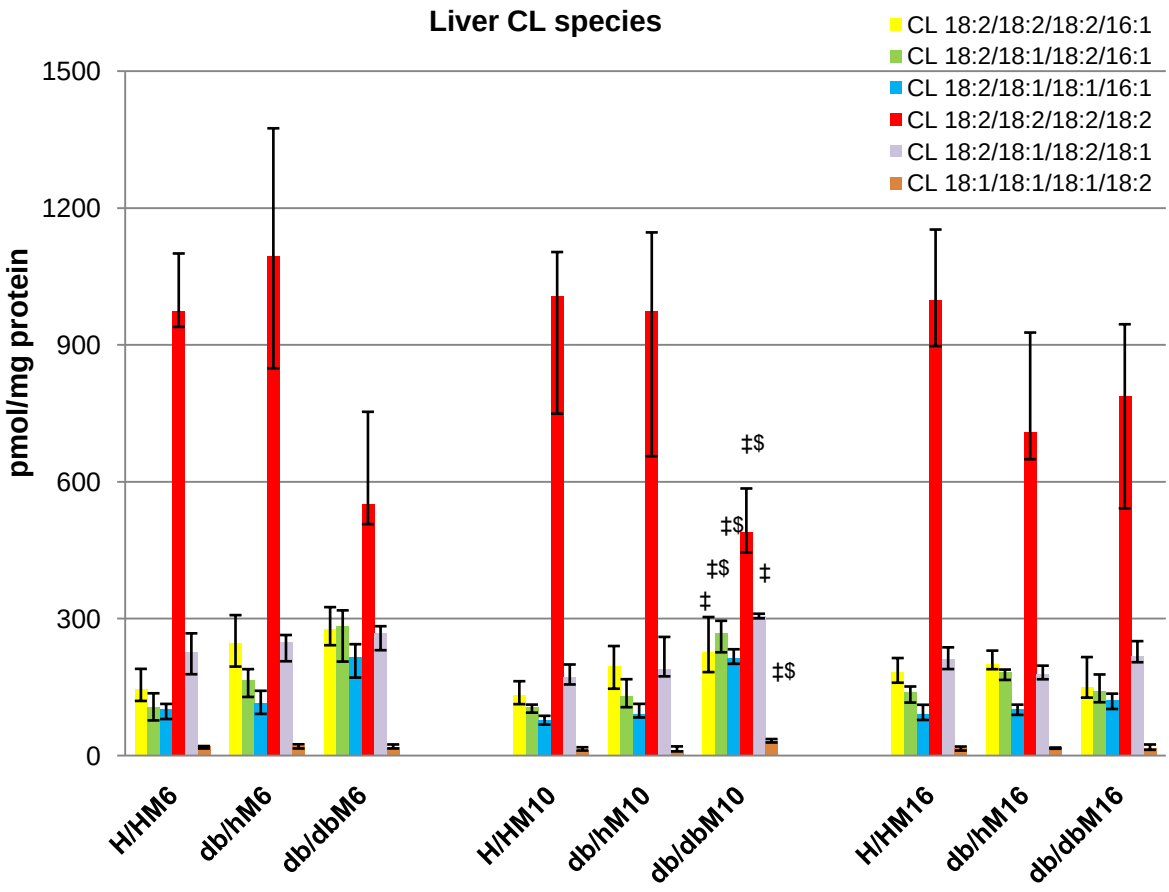

Figure 4.8 Relative liver cardiolipin (CL) levels in male mice. Levels of CL species in male (M) mice at 6, 10 and 16 weeks of age are expressed as median ± upper and lower quartile (7-12 mice per group). The *P*-value for the comparison of each lipid class or subclass between genotypes at each age was obtained using the Kruskal Wallis test with post-hoc analysis by Mann Whitney *U* test with Dunn-Sidak correction for multiple group comparisons. ‡ $P < 0.05$ vs. *H/H* mice at same age; $ $P < 0.05$ vs. *db/h* mice at same age.

DG, TG and SM, and additional species of LPC and CE. However, PC and PE species were no longer significantly higher in the *db/db* mice. The 13 lipid species that were now lower in the male *db/db* mice included multiple species of PC and CL, and some additional PE species, but no longer any PC(P) or PI species. There were 61 skeletal muscle lipid species that were significantly different in male *db/db* mice versus *H/H* mice at both 10 and 16 weeks of age (Table S4.2).

4.3.9.3 Left-ventricle lipid profiles in male *db/db* vs. *H/H* mice

There were no differences in the left-ventricle lipid profiles in six week old male mice. By 10 weeks of age, total DG and TG were elevated, but total SM and PC(P) were significantly lower in male *db/db* versus *H/H* mice (Table 4.11, panel A; and Figure 4.9). The 78 left-ventricle lipid species that were higher in the male *db/db* mice included nine DG species, 31 TG species, 12 PC species containing only even-numbered carbon FA, ten PE species, and multiple species of LPC, LPE, PI, PG, CL and CE. (Table S4.3). The 38 lipid species that were significantly lower in the male *db/db* mice included eight PC species (most containing an odd-numbered carbon FA), nine PC(O) species), five PC(P) species, and multiple species of SM and CL.

At 16 weeks of age, total left-ventricle DG and TG remained significantly higher, and total SM subclass remained lower in the now pre-diabetic male *db/db* relative to the *H/H* mice. The 64 lipid species that were higher in the male *db/db* mice included multiple species of DG, TG, PC containing only even-numbered carbon FA, PE, LPC, PI and CL, and some additional PC(O), PC(P) and PE(O) species, but no longer any LPE, PG or CE species. The 29 lipid species that were now lower in the male *db/db* mice included multiple species of PC (most containing an odd-numbered carbon FA), PC(O) and SM, and some additional PE(O) species, but no longer any PC(P) or CL species. There were 65 left-ventricle lipid species that were significantly different in male *db/db* mice versus *H/H* mice at both 10 and 16 weeks of age (Table S4.3).

The early onset and progression of left-ventricle CL remodelling in male *db/db* mice at 6 and 10 weeks of age is shown in Figure 4.10. Two 16:1 FA-containing CL species and two 16:1 FA-containing PC species (PC 32:1 and PC 32:2) were nearly significantly elevated (*P*-value 0.05-0.10), and two 22:6-containing CL species and two 22:6 FA-containing PC species (PC 38:6b

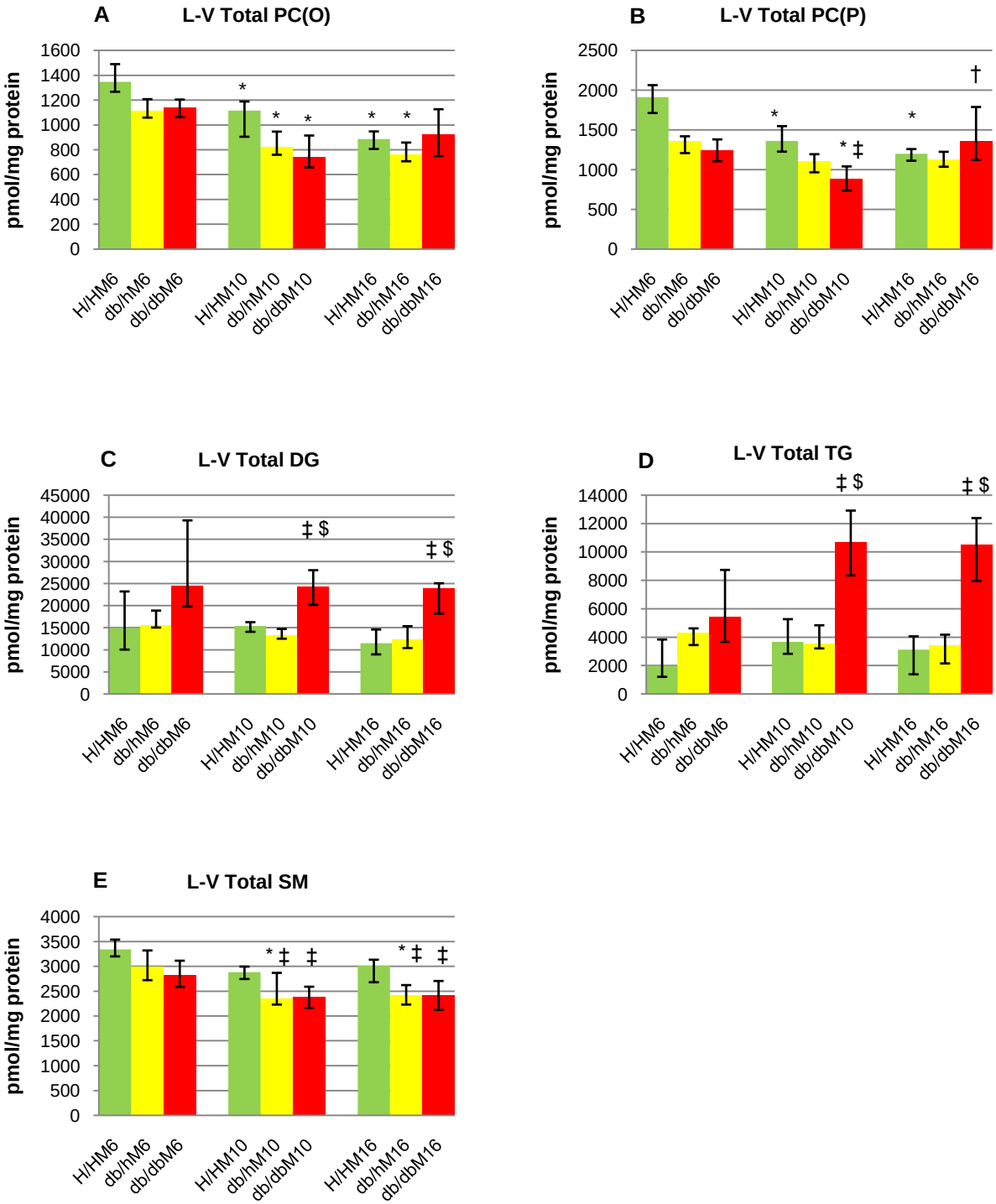

Figure 4.9 Relative left-ventricle (L-V) lipid levels in male mice. Levels of lipid classes or subclasses in male (M) mice at 6, 10 and 16 weeks of age are expressed as median ± upper and lower quartile (7-12 mice per group). The *P*-value for the comparison of each lipid class or subclass between genotypes at each age was obtained using the Kruskal Wallis test with post-hoc analysis by Mann Whitney *U* test with Dunn-Sidak correction for multiple group comparisons. * $P < 0.05$ vs. corresponding genotype at 6 weeks of age; † $P < 0.05$ vs. corresponding genotype at 10 weeks of age; ‡ $P < 0.05$ vs. *H/H* mice at same age; $ $P < 0.05$ vs. *db/h* mice at same age.

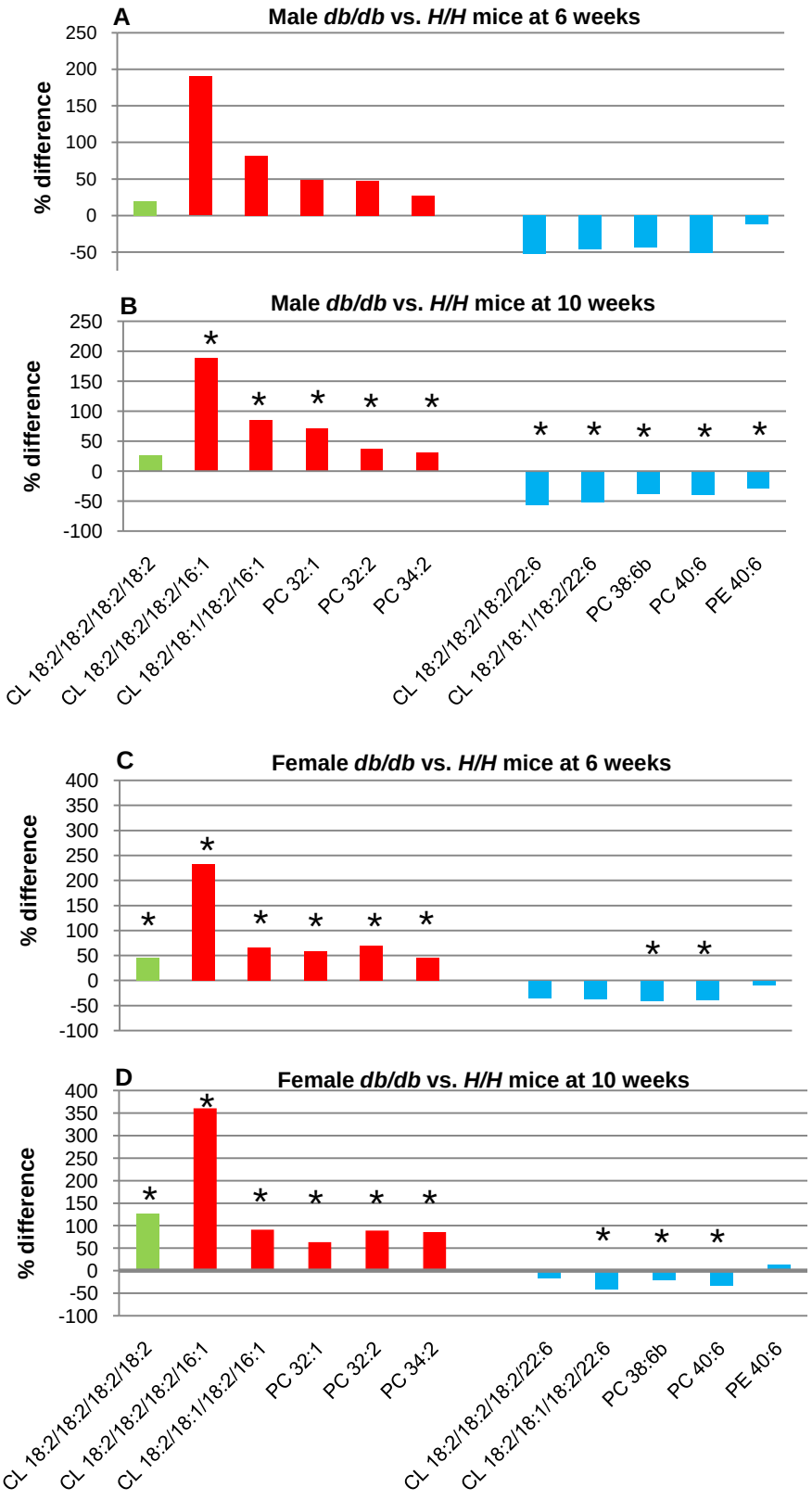

Figure 4.10 Left-ventricle cardiolipin (CL) remodelling in *db/db* mice. The percent (%) difference in median levels of CL 18:2/18:2/18:2/18:2 (shaded green), 16:1 fatty acid (FA)-containing CL and PC species (shaded red), and 22:6 FA-containing CL, PC and PE species (shaded blue) in male mice at 6 weeks (A) and 10 weeks of age (B), and in female mice at 6 weeks (C) and 10 weeks of age (D) compared with corresponding *H/H* mice (7-12 mice per group). * $P < 0.05$ vs. corresponding *H/H* mice using Mann Whitney *U* test.

the corresponding *H/H* mice (Figure 4.10, Panel A). These PC species are involved in the CL and PC 40:6) were nearly significantly lower in six week old male *db/db* mice compared with remodelling process, donating *sn*-2 acyl-16:1 or 22:6 FA chains to monolysocardiolipin (via transacylases) to yield mature CL species (41). By 10 weeks of age, the 16:1 FA-CL species and three donor 16:1 FA-containing PC species (including PC 34:2) were significantly elevated (% difference), and the 22:6 FA-containing CL species, donor 22:6 FA-containing PC species and donor 22:6 FA-containing PE 40:6 were significantly lower in male *db/db* mice compared with the corresponding *H/H* mice (Figure 4.10, Panel B).

4.3.9.4 Adipose lipid profiles in male *db/d* vs. *H/H* mice

There were no differences in the adipose lipid profiles in 6 week old male mice. Early adipose lipid abnormalities in male *db/db* versus *H/H* mice (at 10 weeks of age) were unique, involving significant increases in total CE, DG and TG, but significant decreases in eight classes (Cer, MHC, PC, PC(P), PE(O), PE(P), LPC and LPE) (Table 4.12, panel A; and Figures 4.11 and 4.12). The 71 lipid species that were significantly increased in the male *db/db* mice included (almost exclusively) ten of 14 CE species, 18 of 20 DG species, and all 41 TG species (Table S4.4). In contrast, the 59 lipid species that were significantly decreased in the male *db/db* mice included multiple species of MHC, PC (26 species), PC(O) (six species), PC(P) (eight of nine species), PE(O), PE(P), LPC (six species), LPE and CL 18:2/18:2,18:2/18:2.

At 16 weeks of age, total CE, DG and TG remained significantly increased, seven of eight classes remained significantly decreased (MHC, PC, PC(P), PE(O), PE(P), LPC and LPE), and now total PE, PC(O), PI, PG and CL were significantly decreased in the male *db/db* versus *H/H* mice. The 73 adipose lipid species that were now significantly increased in the male *db/db* mice included (almost exclusively) multiple species of CE (ten species), DG (20 species) and TG (39 species) that remained significantly increased, and now some SM species. The 99 adipose lipid species that were now significantly decreased in the male *db/db* mice at 16 weeks of age included multiple species of MHC, PC (35 species), PC(O) (11 species), PC(P) (seven species), PE(O), PE(P), LPC (six species) and LPE that remained significantly decreased, and now some Cer, PE (12 species), PI, PG, and CL (five species). There were 115 adipose lipid species that were significantly different in male *db/db* mice at both 10 and 16 weeks of age (Table S4.4).

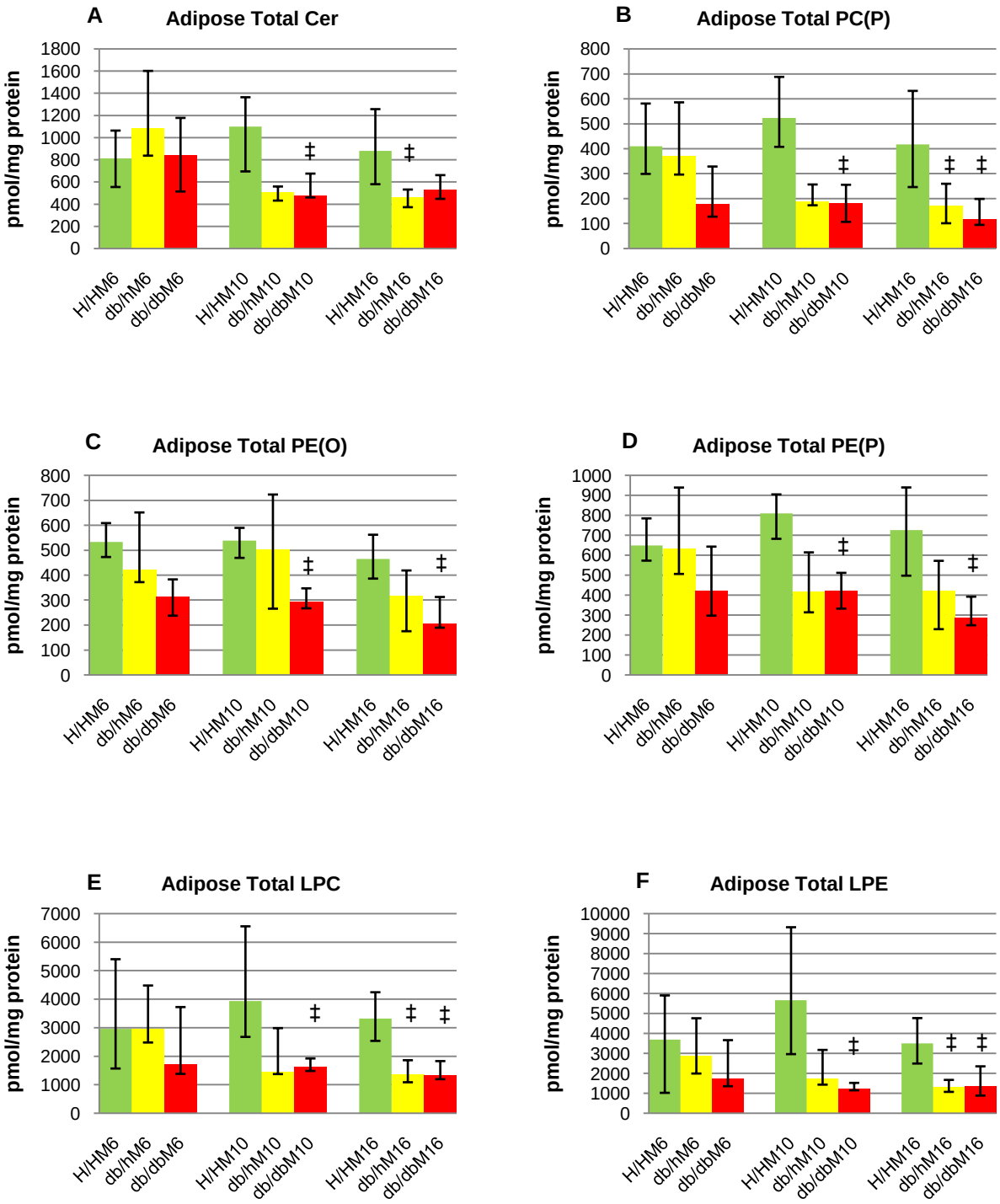

Figure 4.11 Relative adipose lipid levels in male mice. Levels of lipid classes or subclasses in male (M) mice at 6, 10 and 16 weeks of age are expressed as median ± upper and lower quartile (7-12mice per group). The *P*-value for the comparison of each lipid class or subclass between genotypes at each age was obtained using the Kruskal Wallis test with post-hoc analysis by Mann Whitney *U* test with Dunn-Sidak correction for multiple group comparisons.
‡ $P < 0.05$ vs. *H/H* mice at same age.

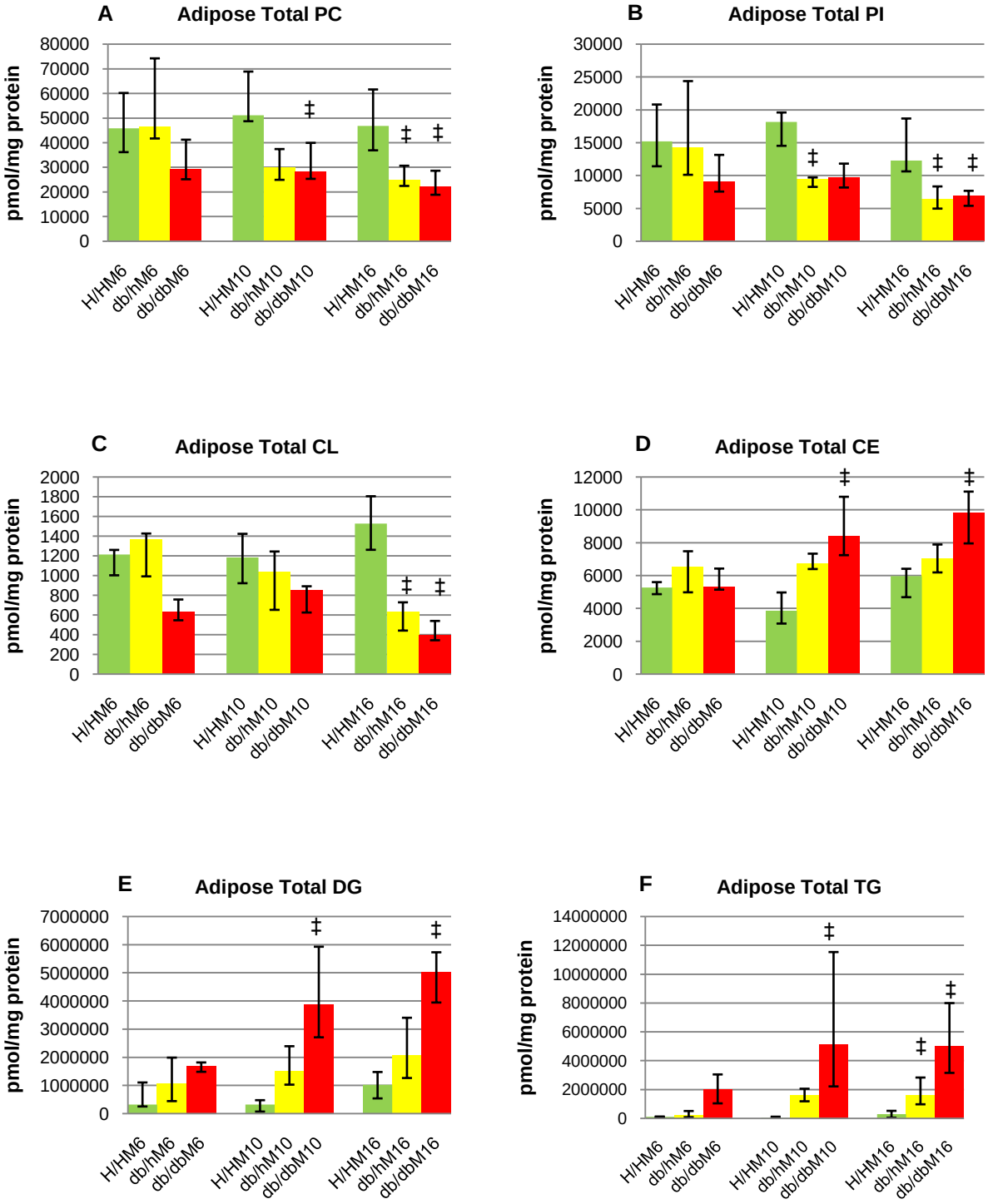

Figure 4.12 Relative adipose lipid levels in male mice. Levels of lipid classes or subclasses in male (M) mice at 6, 10 and 16 weeks of age are expressed as median ± upper and lower quartile (7-12 mice per group). The *P*-value for the comparison of each lipid class or subclass between genotypes at each age was obtained using the Kruskal Wallis test with post-hoc analysis by Mann Whitney *U* test with Dunn-Sidak correction for multiple group comparisons. ‡ $P < 0.05$ vs. *H/H* mice at same age.

4.3.9.5 Plasma lipid profiles in male *db/db* vs. *H/H* mice

Early plasma lipid abnormalities in male *db/db* versus *H/H* mice occurred at 6 weeks of age, and included significant increases in seven lipid classes (Cer, MHC, PC, LPC, LPE, PI and CE) (Table 4.13, panel A; and Figure 4.13). The 85 lipid species that were significantly increased in male *db/db* mice included multiple species of Cer, MHC, SM (seven species), PC (23 species), PE (five species), PC(O), PC(P), PE(P), LPC (ten species), LPE, PI (12 of 15 species), CE (seven species) and TG (Table S4.5). No plasma lipid species were significantly decreased in the male *db/db* mice at 6 weeks of age.

At 10 weeks of age, only total CE lipid remained significantly increased in the male *db/db* mice versus *H/H* mice. The 35 plasma lipid species that were now significantly increased in the male *db/db* mice included multiple species of SM, PC containing only even-numbered carbon FA (nine species), LPC (eight species), PI (five species), CE (five species) and TG that remained significantly increased, but no longer any Cer, MHC, PE, PC(O), PC(P), PE(P) or LPE species. The eight plasma lipid species that were now significantly decreased in the male *db/db* mice included some species of PC(P) and (surprisingly) TG. There were 31 plasma lipid species that were significantly different in male *db/db* mice at both 6 and 10 weeks of age (Table S4.5).

4.3.9.6 Liver lipid profiles in female *db/db* vs. *H/H* mice

Early liver lipid abnormalities in female *db/db* versus *H/H* mice (at 6 weeks of age) included significant increases in total Cer and BMP, and significant decreases in total PC(O) and PC(P) (Table 4.9, panel B; and Figure 4.14). The 49 liver lipid species that were significantly increased in the female *db/db* mice included multiple species of Cer, PC containing only even-numbered carbon FA (eight species), PE (eight species), LPC, PI, CL, DG (six species) and TG (12 species). (Table S4.6). The 35 lipid species that were significantly decreased in the female *db/db* mice at 6 weeks of age included multiple species of SM, PC (ten species), PE, PC(O) (five species), PC(P), PE(O), CL and DG.

At 10 weeks of age, total PC(O) remained highly significantly decreased, and total MHC and PS were now highly significantly decreased in the female *db/db* versus *H/H* mice. The 27 liver lipid species that were now significantly increased in the female *db/db* mice included multiple species of PC containing only even-numbered carbon FA (eight species), PE, CL, DG (five species) and

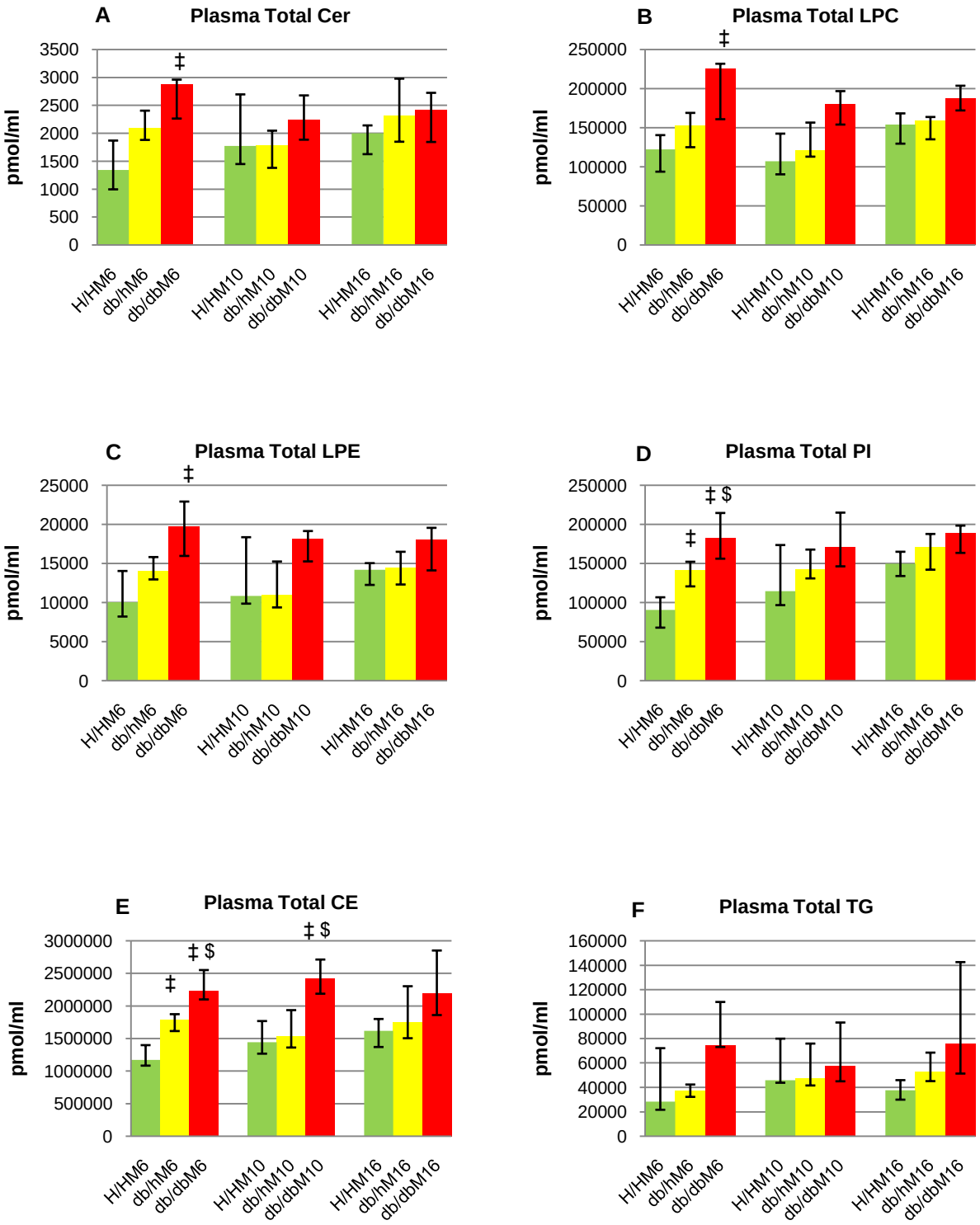

Figure 4.13 Relative plasma lipid levels in male mice. Levels of lipid classes or subclasses in male (M) mice at 6, 10 and 16 weeks of age are expressed as median ± upper and lower quartile (7-12 mice per group). The *P*-value for the comparison of each lipid class or subclass between genotypes at each age was obtained using the Kruskal Wallis test with post-hoc analysis by Mann Whitney *U* test with Dunn-Sidak correction for multiple group comparisons. ‡ $P < 0.05$ vs. *H/H* mice at same age; $ $P < 0.05$ vs. *db/h* mice at same age.

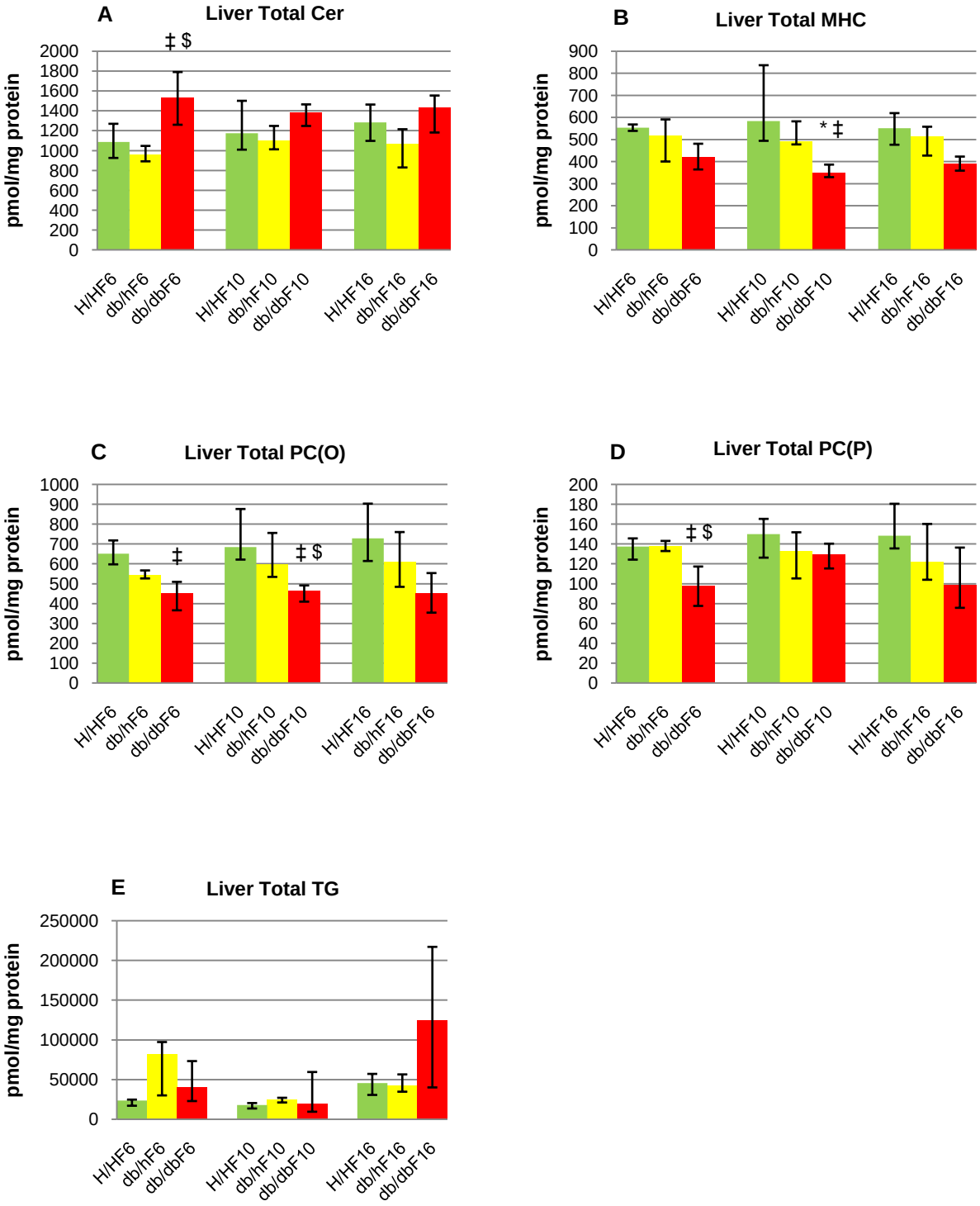

Figure 4.14 Relative liver lipid levels in female mice. Levels of lipid classes or subclasses in female (F) mice at 6, 10 and 16 weeks of age are expressed as median ± upper and lower quartile (7-12 mice per group). The *P*-value for the comparison of each lipid class or subclass between genotypes at each age was obtained using the Kruskal Wallis test with post-hoc analysis by Mann Whitney *U* test with Dunn-Sidak correction for multiple group comparisons. * $P < 0.05$ vs. corresponding genotype at 6 weeks of age; ‡ $P < 0.05$ vs. *H/H* mice at same age; $ $P < 0.05$ vs. *db/h* mice at same age.

TG that remained significantly increased, but no longer any Cer, LPC or PI species. The 29 liver lipid species that were now significantly decreased in the female *db/db* mice at 10 weeks of age included multiple species of PC (nine species), PC(O) (five species), PC(P), PE(O) and CL that remained significantly decreased, and now some MHC species, but no longer any PE or DG species. There were 48 liver lipid species that were significantly different in female *db/db* mice at both 6 and 10 weeks of age (Table S4.6). There were no differences in the liver lipid profiles in 16 week old female mice. Comparison of the earliest liver lipid abnormalities detected in the hyperinsulinaemic/IR female *db/db* mice (at 6 weeks of age) and obese/IR male *db/db* mice (at 10 weeks of age) indicated that the CE, DG and TG classes contributed 57 of the 90 species that were significantly elevated in male *db/db* mice (versus corresponding male *H/H* mice), but only contributed 19 of the 49 species that were significantly elevated in female *db/db* mice. However, there was a greater number of PC, PC(O), PC(P) and PE(O) species that were significantly decreased in the female *db/db* mice.

4.3.9.7 Skeletal muscle lipid profiles in female *db/db* vs. *H/H* mice

Early skeletal muscle lipid abnormalities in female *db/db* versus *H/H* mice at 6 weeks of age included significant decreases in total Cer, GM3 and PI (Table 4.10, panel B). The 23 lipid species that were significantly increased in the female *db/db* mice included multiple species of SM, PC containing only even-numbered carbon FA (eight species), PE and TG (ten species) (Table S4.7). The 24 lipid species that were significantly decreased in the female *db/db* mice included multiple species of PC (most containing an odd-numbered carbon FA) (ten species), PC(O) and PI.

At 10 weeks of age, total TG subclass was now significantly increased, and total PC(O) and PC(P) were now significantly decreased in the female *db/db* versus *H/H* mice. The 48 skeletal muscle lipid species that were now significantly increased in the female *db/db* mice included multiple species of PC (eight species, seven which contained only even-numbered carbon FA), PE and TG (31 species) that remained significantly increased, and now some DG species, but no longer any SM species. The 27 skeletal muscle lipid species that were now significantly decreased in the female *db/db* mice at 10 weeks of age included multiple species of PC (six species), PC(O) (five species) and PI that remained significantly decreased, and now some PE, PC(P) and PE(P) species. There were 37 skeletal muscle lipid species that were significantly

different in female *db/db* mice at both 6 and 10 weeks of age (Table S4.7). There were no differences in the skeletal muscle lipid profiles in 16 week old female mice.

Comparison of the earliest skeletal muscle lipid abnormalities detected in female *db/db* mice (at 6 weeks of age) and male *db/db* mice (at 10 weeks of age) indicated that the DG and TG classes contributed 50 of the 62 species that were significantly elevated in male *db/db* mice (versus corresponding male *H/H* mice), but only contributed 11 of the 23 species that were significantly elevated in female *db/db* mice. Otherwise, the profile of early skeletal muscle lipid abnormalities seen in male and female *db/db* mice was very similar.

4.3.9.8 Left-ventricle lipid profiles in female *db/db* vs. *H/H* mice

Early left-ventricle lipid abnormalities in female *db/db* versus *H/H* mice at 6 weeks of age included significant increases in five classes (PE, PI, CE, DG and TG), and significant decreases in total MHC and GM3 (Table 4.11, panel B; and Figure 4.15). The 97 lipid species that were significantly increased in the female *db/db* mice included multiple species of PC containing only even-numbered carbon FA (17 species), PE (nine species), PC(P), PE(O), PE(P), LPC, LPE, PI (six species), PS, PG, CL (four species), CE, DG (ten species) and TG (29 species) (Table S4.8). The 11 lipid species that were significantly decreased in the female *db/db* mice at 6 weeks of age included multiple species of GM3, SM, PC and PC(O).

At 10 weeks of age, total PE, PI, CE, DG and TG remained highly significantly increased, and total PG and CL were now highly significantly increased in the female *db/db* versus *H/H* mice. Furthermore, total GM3 remained significantly decreased, and total LPC(O) was now significantly decreased in the diabetic female *db/db* mice. The 115 left-ventricle lipid species that were now significantly increased in the female *db/db* mice included multiple species of PC containing only even-numbered carbon FA (20 species), PE (13 species), PC(P), PE(O), PE(P), LPC (five species), LPE, PI (seven species), PS, PG, CL (seven species), CE, DG (14 species) and TG (25 species) that remained significantly increased. The 21 left-ventricle lipid species that were now significantly decreased in the female *db/db* mice included multiple species of GM3, SM and PC (six species) that remained significantly decreased, and now some LPC and CL species, but no longer any PC(O) species. There were 92 left-ventricles lipid species that were significantly different in female *db/db* mice at both 6 and 10 weeks of age (Table S4.8).

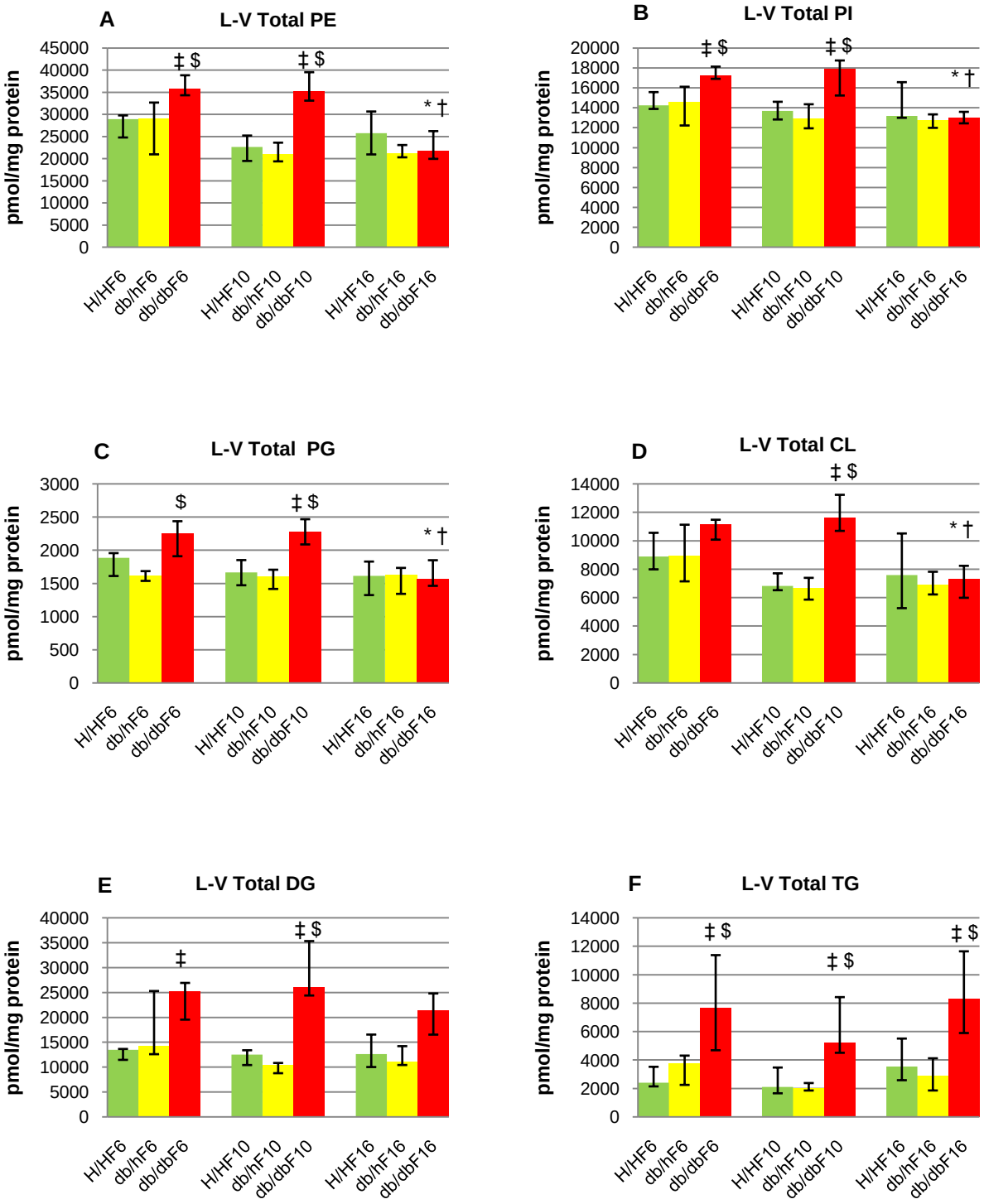

Figure 4.15 Relative left-ventricle (L-V) lipid levels in female mice. Levels of lipid classes or subclasses in female (F) mice at 6, 10 and 16 weeks of age are expressed as median ± upper and lower quartile (7-12 mice per group). The *P*-value for the comparison of each lipid class or subclass between genotypes at each age was obtained using the Kruskal Wallis test with post-hoc analysis by Mann Whitney *U* test with Dunn-Sidak correction for multiple group comparisons. ‡ $P < 0.05$ vs. *H/H* mice at same age; $ $P < 0.05$ vs. *db/h* mice at same age.

At 16 weeks of age, some lipid abnormalities persisted in the left-ventricle, but only total TG was significantly different (i.e., increased) in the now pre-diabetic female *db/db* mice versus *H/H* mice (Table 4.11, panel B). The 32 left-ventricle lipid species that were now significantly increased in the female *db/db* mice included a smaller number of CL and DG species, and 20 TG species that remained significantly increased (Table S4.8). The 22 left-ventricle lipid species that were now significantly lower in the female *db/db* mice at 16 weeks of age included multiple species of SM and PC (five species) that remained significantly lower, and now some PC(O) (eight species) and PC(P) species (Table S4.8).

The early onset and progression of left-ventricle CL remodelling in female *db/db* mice at 6 and 10 weeks of age is shown in Figure 4.10. There was already a significant elevation (% difference) in the most abundant CL species, CL 18:2/18:2,18:2/18:2, both 16:1 FA-containing CL species, and the three donor 16:1 FA-containing PC species (PC 32:1, PC 32:2 and PC 34:2) in the six week old female *db/db* mice compared with the corresponding *H/H* mice (Figure 4.10, Panel C). This was accompanied by a non-significant drop (*P*-value 0.05-0.10) in the 22:6 FA-containing CL species, CL 18:2/18:2,18:2/22:6, and a significant fall in the donor 22:6 FA-containing PC species, PC 38:6b and PC 40:6. At 10 weeks of age, this CL effect was sustained, but now there was a significant fall in CL 18:2/18:1,18:2/22:6 (Figure 4.10, Panel D). However, there was also a significant rise in the CL subclass and four other CL species in the ten week old female *db/db* mice (Table S4.8).

Comparison of the earliest left-ventricle lipid abnormalities detected in female *db/db* mice (at 6 weeks of age) and male *db/db* mice (at 10 weeks of age) indicated that there was a very similar and substantial contribution of CE, DG and TG subclasses to the total number of species that were significantly elevated in male and female *db/db* mice (versus corresponding male *H/H* mice). Otherwise, the profile of early left-ventricle lipid abnormalities seen in male and female *db/db* mice was very similar, except some PC(P), PE(O) and PE(P) species were (surprisingly) significantly increased in female *db/db* mice, but not in male *db/db* mice.

4.3.9.9 Adipose lipid profiles in female *db/db* vs. *H/H* mice

Early adipose lipid abnormalities in female *db/db* versus *H/H* mice at 6 weeks of age were unique, involving significant increases in total DG and TG, but significant decreases in 11 classes (Cer, MHC, PC, PE, PC(P), PE(O), PE(P), PS, PG, CL and COH) (Table 4.12, panel B;

and Figures 4.16 and 4.17). The 58 lipid species that were significantly increased in the female *db/db* mice included multiple species of SM, CE, DG (12 species) and TG (40 species) (Table S4.9). The 86 lipid species that were significantly decreased in the female *db/db* mice at 6 weeks of age included multiple species of Cer (all six species), SM, PC (30 species), PE (ten species), PC(P) (nine species), PE(O) (seven species), PE(P) (six species), LPC, PS, PG and CL.

At 10 weeks of age, total DG and TG remained significantly increased, and the CE class was now significantly increased in the female *db/db* versus *H/H* mice. Moreover, total Cer, MHC, PC, PC(P), PE(O), PE(P), PG and CL remained significantly decreased, and total PC(O) was now significantly decreased in the female *db/db* mice. The 75 adipose lipid species that were now significantly increased in the female *db/db* mice included multiple species of SM, CE (nine species), DG (19 species) and TG (all 41 species) that remained significantly increased, and now some PE species. The 70 adipose lipid species that were now significantly decreased in the female *db/db* mice at 10 weeks of age included multiple species of Cer (five species), PC (21 species), PE (seven species), PC(P) (six species), PE(O) (seven species), PE(P), LPC, PS, PG and CL that remained significantly decreased, and now some MHC and five PC(O) species, but no longer any SM species. There were 118 adipose lipid species that were significantly different in female *db/db* mice at both 6 and 10 weeks of age (Table S4.9). There were no differences in the adipose lipid profiles in 16 week old female mice.

Comparison of the earliest adipose lipid abnormalities detected in female *db/db* mice (at 6 weeks of age) and male *db/db* mice (at 10 weeks of age) indicated very similar profiles. Total CE, DG and TG contributed almost exclusively to the species that were significantly elevated in both male and female *db/db* mice (versus corresponding male *H/H* mice), and most of the other lipid groups, including lysophospholipids, contributed to the large number of species that were significantly decreased in *db/db* mice.

4.3.9.10 Plasma lipid profiles in female *db/db* vs. *H/H* mice

Early plasma lipid abnormalities in female *db/db* versus *H/H* mice (at 6 weeks of age) were also unique, involving significant increases in total LPE, DG and TG (Table 4.13, panel B; and Figure 4.18) and 91 lipid species, including multiple species of SM, PC containing only even-numbered carbon FA (14 species), LPC (seven species), LPE, PI (11 species), CE (seven species), DG (eight species) and TG (33 species) (Table S4.10). Only six lipid species were

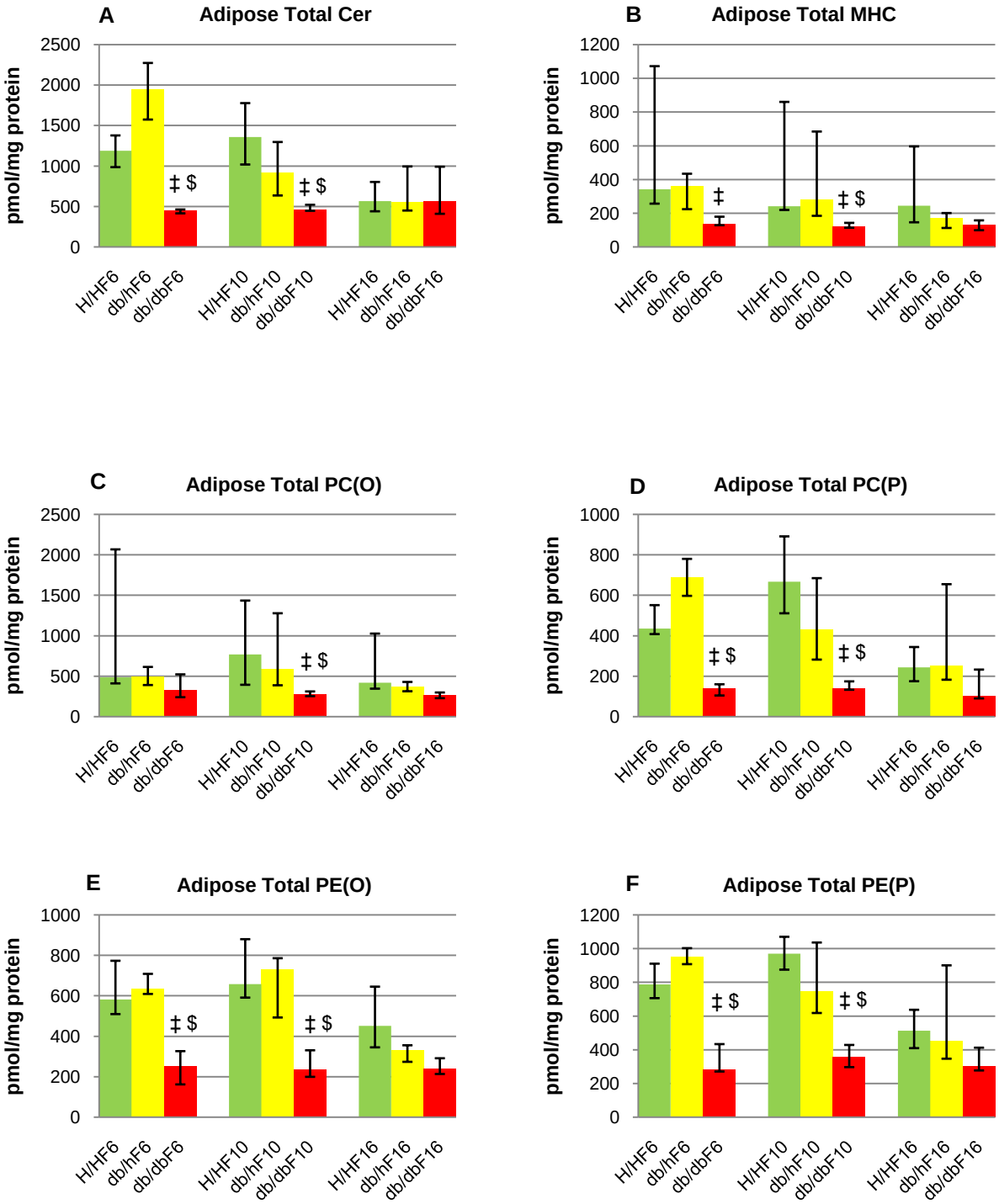

Figure 4.16 Relative adipose lipid levels in female mice. Levels of lipid classes or subclasses in female (F) mice at 6, 10 and 16 weeks of age are expressed as median ± upper and lower quartile (7-12 mice per group). The *P*-value for the comparison of each lipid class or subclass between genotypes at each age was obtained using the Kruskal Wallis test with post-hoc analysis by Mann Whitney *U* test with Dunn-Sidak correction for multiple group comparisons. ‡ $P < 0.05$ vs. *H/H* mice at same age; $ $P < 0.05$ vs. *db/h* mice at same age.

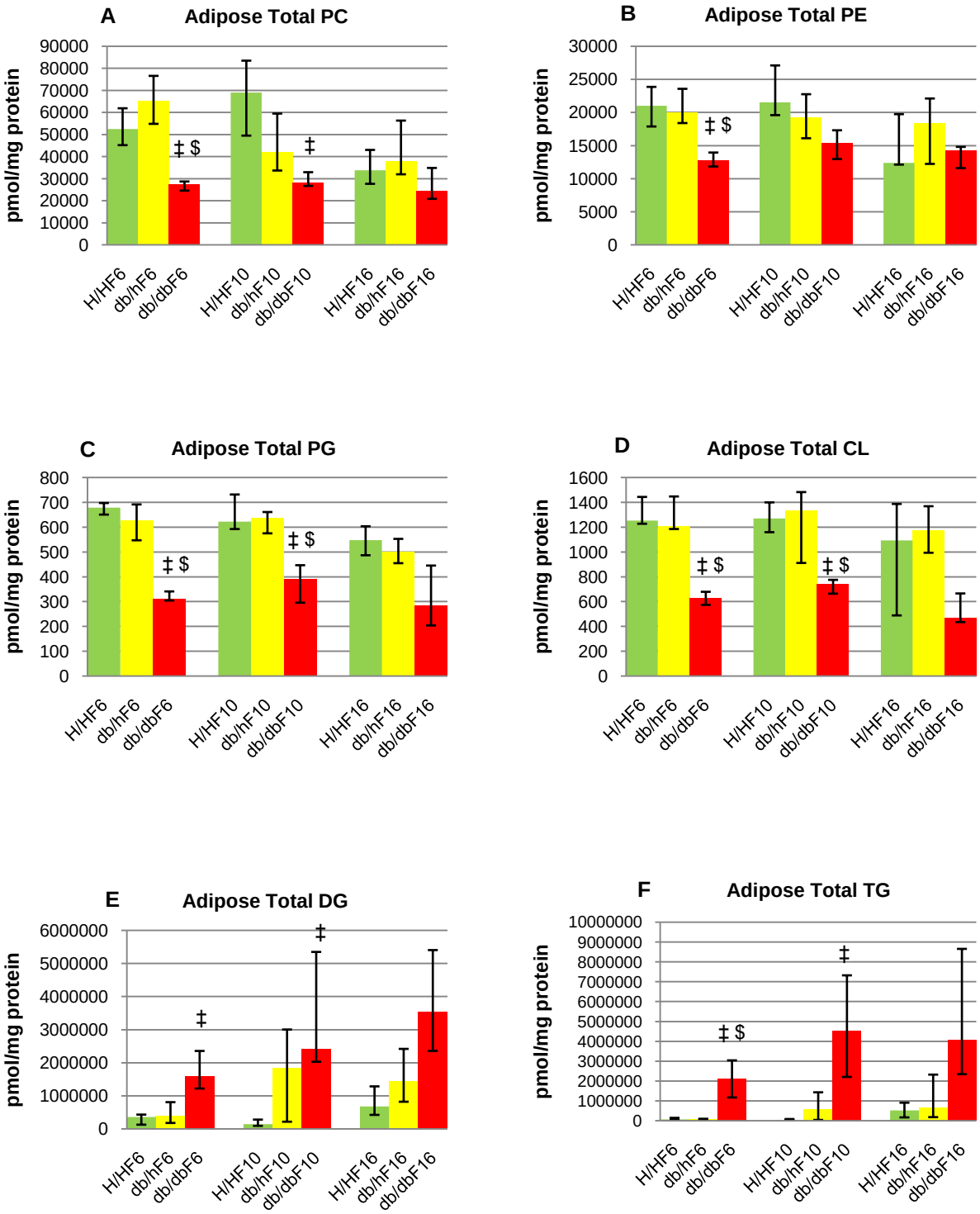

Figure 4.17 Relative adipose lipid levels in female mice. Levels of lipid classes or subclasses in female (F) mice at 6, 10 and 16 weeks of age are expressed as median ± upper and lower quartile (7-12 mice per group). The *P*-value for the comparison of each lipid class or subclass between genotypes at each age was obtained using the Kruskal Wallis test with post-hoc analysis by Mann Whitney *U* test with Dunn-Sidak correction for multiple group comparisons. ‡ $P < 0.05$ vs. *H/H* mice at same age; $ $P < 0.05$ vs. *db/h* mice at same age.

significantly decreased in the female *db/db* mice, including PC(O-34:0), PC(O-34:1) and PC(P-40:6).

At 10 weeks of age, total DG and TG remained significantly increased, and total PC and PE were now also significantly increased in the female *db/db* mice versus *H/H* mice. The 97 plasma lipid species that were now significantly increased in the female *db/db* mice included multiple species of SM (five species), PC (25 species) LPC, PI (six species), CE, DG (five species) and TG (28 species) that remained significantly increased, and now some PE (13 species), PC(O) (five species) and PC(P) species, but no longer any LPE species. No plasma lipid species were significantly decreased in the female *db/db* mice at 10 weeks of age. There were 61 plasma lipid species that were significantly different in female *db/db* mice at both 6 and 10 weeks of age (Table S4.10). At 16 weeks of age, some lipid abnormalities persisted in plasma, but only total TG was significantly different (i.e., increased) in the pre-diabetic female *db/db* mice versus *H/H* mice (Table 4.13, panel B). The 44 plasma lipid species that were now significantly increased in the female *db/db* mice included multiple species of SM, PI, CE and TG (28 species) that remained significantly increased, but no longer any PC, PE, PC(O), PC(P), LPC or DG species. (Table S4.10). Only one plasma lipid species (CE 20:5) was now significantly decreased in the female *db/db* mice at 16 weeks of age (Table S4.10).

The earliest plasma lipid abnormalities were detected in both male and female *db/db* mice at 6 weeks of age. Comparison of these early plasma lipid abnormalities indicated that the CE, DG and TG classes contributed only 10 of the 85 species that were significantly elevated in male *db/db* mice (versus corresponding male *H/H* mice), but contributed 48 of the 91 species that were significantly elevated in female *db/db* mice. In addition, some PC(O), PC(P) and PE(P) species were (surprisingly) significantly increased in male *db/db* mice, but not in female *db/db* mice.

4.3.10 Fatty acid composition of elevated triacylglycerol species in *db/db* mice

The fatty acid (FA) composition of individual TG species has been identified as a critical factor in the association of TG species with obesity, IR and risk of T2D [13,29,31,156,157]. To assess this relationship, the 40-odd TG species measured in plasma and each of the tissues were divided into “saturated” or “unsaturated” species according to the definition described in Table 4.14. This definition is similar to that employed by Barber *et al.* [26], and attempts to distinguish

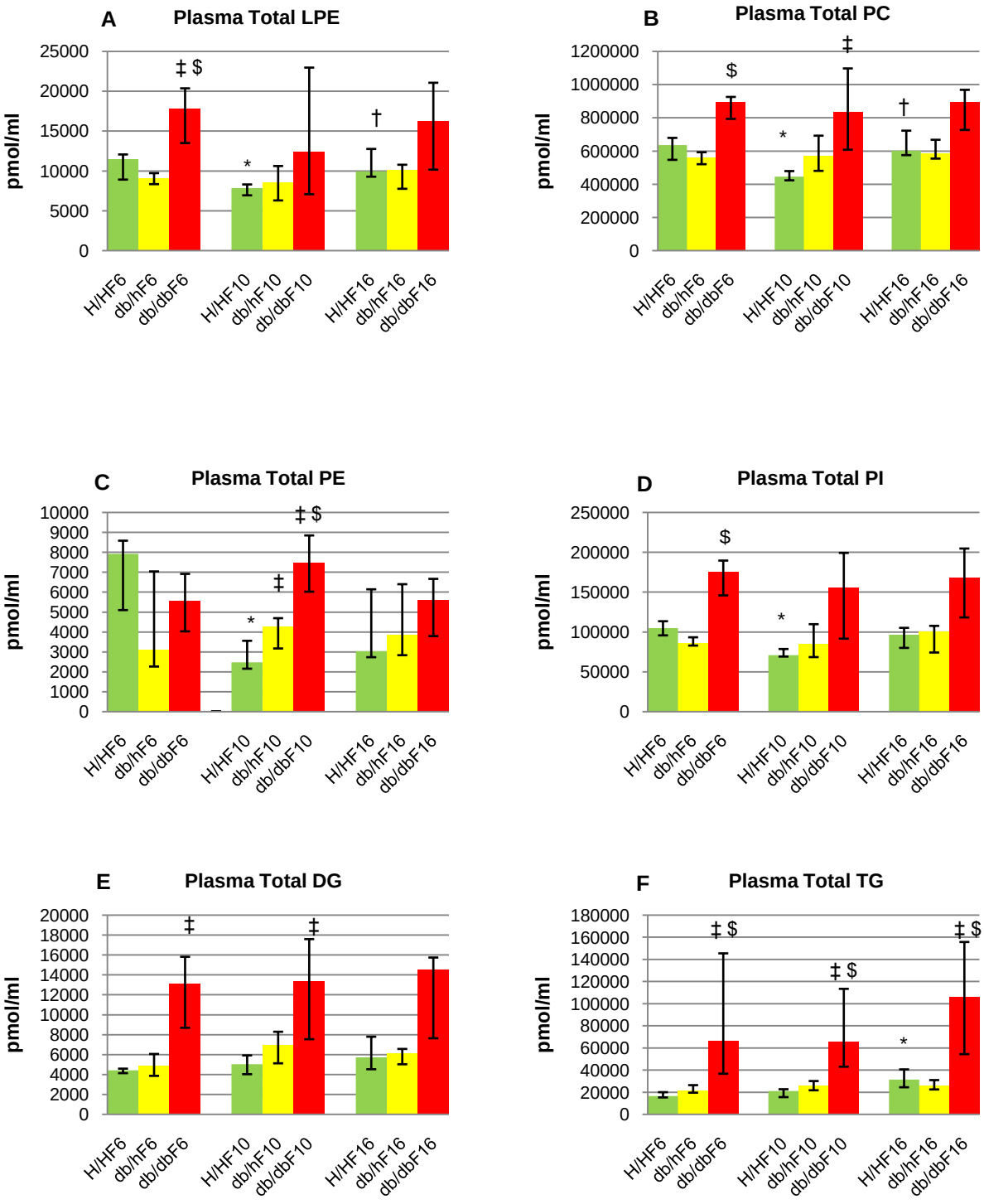

Figure 4.18 Relative plasma lipid levels in female mice. Levels of lipid classes or subclasses in female (F) mice at 6, 10 and 16 weeks of age are expressed as median ± upper and lower quartile (7-12 mice per group). The *P*-value for the comparison of each lipid class or subclass between genotypes at each age was obtained using the Kruskal Wallis test with post-hoc analysis by Mann Whitney *U* test with Dunn-Sidak correction for multiple group comparisons. * $P < 0.05$ vs. corresponding genotype at 6 weeks of age; ‡ $P < 0.05$ vs. *H/H* mice at same age; $ $P < 0.05$ vs. *db/h* mice at same age.

between TG species incorporating "saturated" FA derived from hepatic *de novo* lipogenesis (e.g. 16:0, 16:1, 18:0, 18:1) and those TG species incorporating "unsaturated" FA with two or more double bonds (e.g. 16:2, 18:2). The number of "saturated" and "unsaturated" TG species that were significantly elevated in plasma and tissues of male and female *db/db* mice at 6, 10 and 16 weeks of age compared with the corresponding *H/H* mice is shown in Table 4.14. There was no statistical difference in the number of "saturated" versus "unsaturated" TG species that were significantly elevated in male or female *db/db* mice in any of the treatment groups, regardless of age or the tissue-type.

4.3.11 Role of hepatic *de novo* lipogenesis in the supply of circulating fatty acids

Hepatic *de novo* lipogenesis is activated by high circulating levels of insulin and carbohydrate generated from a low-fat/high-carbohydrate diet [47,158], and repressed by high dietary fat [47]. The unrestricted standard chow diet fed to mice in our *db/db* mouse study was low in total fatty acid content (4.8% w/w; but 8.0% total energy as fat) and high in carbohydrate content (59.4% w/w). Notably, the diet contained virtually no palmitoleate (16:1) or arachidonic acid (20:4n-6), but 30% of the total fatty acid composition consisted of linoleic acid (18:2n-6) (Table 4.1B). In these circumstances, 16:1 is generated almost exclusively from hepatic *de novo* lipogenesis via delta-9 desaturase activity [47]. Long-chain fatty acids (16:0, 16:1, 18:0 and 18:1) derived from hepatic *de novo* lipogenesis are incorporated into hepatic DG and TG and released into the circulation as VLDL-bound triglyceride [50]. On the other hand, 18:2n-6 is an essential FA that must be provided in the diet. Thus, the ratio of total 16:1 acyl-FA to total 18:2 acyl-FA content in liver DG species (total 16:1/18:2 in DG) and liver TG species (total 16:1/18:2 in TG) was evaluated as a surrogate measure of hepatic *de novo* lipogenesis in the *db/db* mouse study.

4.3.11.1 Contribution of hepatic *de novo* lipogenesis to liver diacylglycerols and triacylglycerols

The mean ratio of liver total 16:1/18:2 in DG species was already markedly higher (by ~3.5-fold) in six week old male *db/db* mice compared with the corresponding *H/H* and *db/h* mice, and this strong effect was sustained at 10 weeks of age (Figure 4.19, Panel A). However, this ratio had significantly dropped (by ~50%) in the male *db/db* mice at 16 weeks of age compared with the value observed at 10 weeks of age, and was no longer significantly higher than the value obtained in the corresponding *db/h* mice. A very similar pattern was seen in the mean ratio of

Table 4.14 Number of significantly elevated "saturated" and "unsaturated" triacylglycerol species in plasma and tissues of male and female *db/db* mice compared with corresponding *H/H* mice.

Tissue	No. of TG species measured		Male *db/db* mice (6 weeks)		Male *db/db* mice (10 weeks)		Male *db/db* mice (16 weeks)	
	Sat[a]	Unsat[b]	No. of sat TG species	No. of unsat TG species	No. of sat TG species	No. of unsat TG species	No. of sat TG species	No.of unsat TG species
Plasma	20	20	1	2	1	2	NS	NS
Liver	19	18	NS	NS	19	18	17	18
SkM	22	20	NS	NS	22	20	22	20
L-V	17	18	NS	NS	15	16	15	16
Adip	23	18	NS	NS	23	18	21	18
	No. of TG species measured		Female *db/db* mice (6 weeks)		Female *db/db* mice (10 weeks)		Female *db/db* mice (16 weeks)	
Tissue	Sat[a]	Unsat	No. of sat TG species	No. of unsat TG species	No. of sat TG species	No. of unsat TG species	No. of sat TG species	No. of unsat TG species
Plasma	20	20	18	15	17	12	16	15
Liver	19	18	6	6	2	2	NS	NS
SkM	22	20	4	6	14	18	NS	NS
L-V	17	18	15	15	11	14	10	10
Adip	23	18	22	18	23	18	NS	NS

No., number; TG, triacylglycerol; Sat, saturated; Unsat, unsaturated; SkM, skeletal muscle; L-V, left-ventricle; Adip, adipose; NS, not significant.

[b] "Saturated" TG species were defined as having a total of two or less fatty acid-double bonds, and that each fatty acid within the TG species contained no more than one double bond (e.g. TG 14:0/16:1/18:1).

[c] "Unsaturated" TG species were defined as having a total of more than two fatty acid-double bonds, but also included TG species that contained a total of two fatty acid-double bonds when one fatty acid moiety contained two double bonds (e.g. TG 14:0/16:0/18:2, TG 14:0/16:1/18:2).

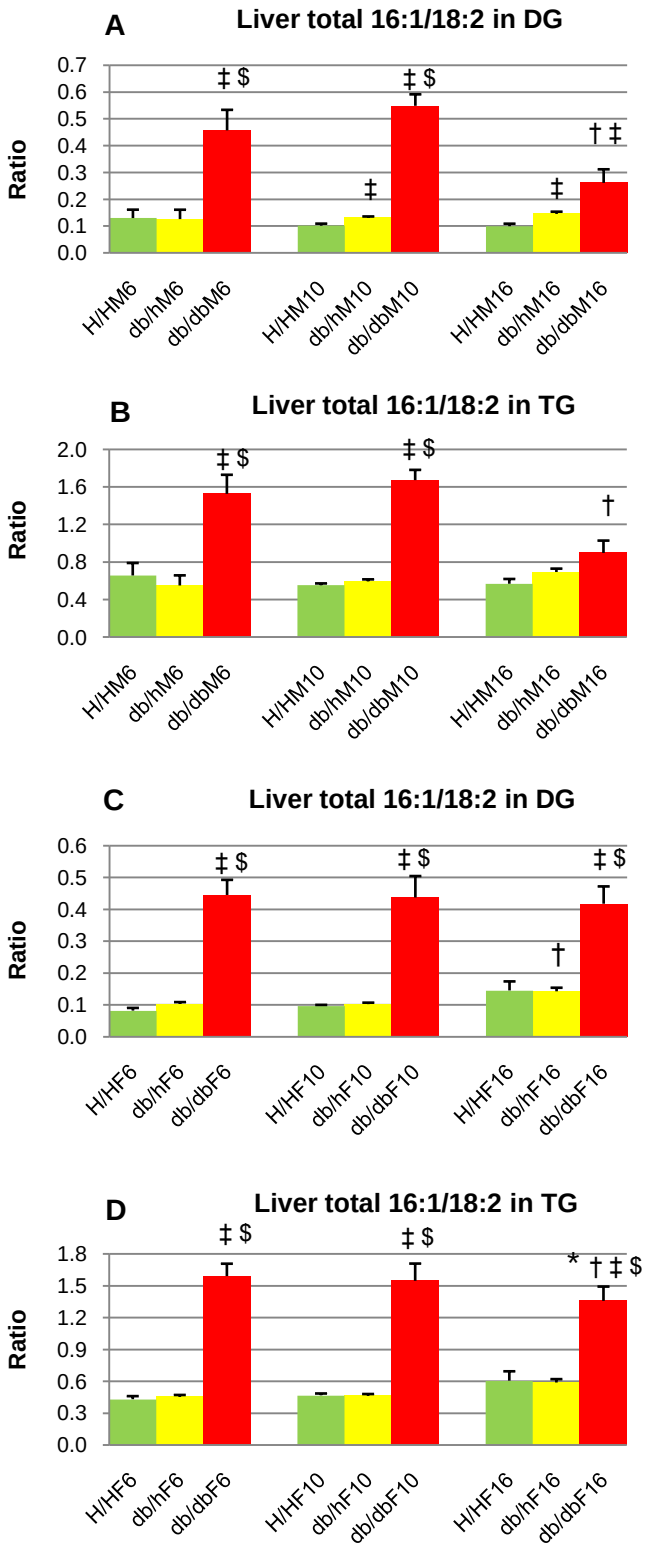

Figure 4.19 Surrogate measures of hepatic *de novo* lipogenesis in mice. Ratio of total 16:1to total 18:2 fatty acid content in liver diacylglyerol (DG) species and triacylglycerol (TG) species in male (M) mice (A and B respectively) and female (F) mice (C and D respectively) on unrestricted chow diet at 6, 10 and 16 weeks of age. Values are expressed as mean ± SEM (7-12 mice per group). * $P < 0.01$ vs. corresponding genotype at 6 weeks of age; † $P < 0.01$ vs. corresponding genotype at 10 weeks of age; ‡ $P < 0.01$ vs. *H/H* mice at same age; $ $P < 0.01$ vs. *db/h* mice at same age using Mann-Whitney *U* test.

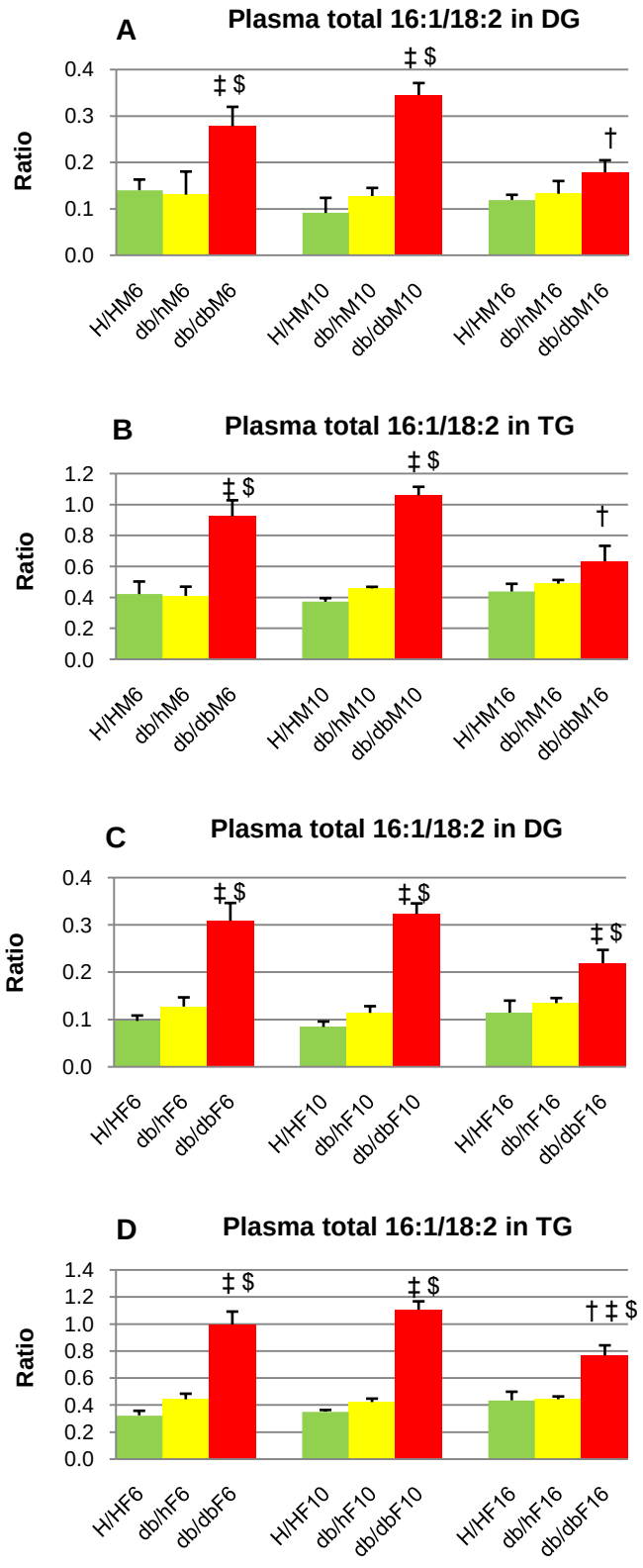

Figure 4.20 Surrogate measures of hepatic *de novo* lipogenesis in mice are reflected in plasma. Ratio of total 16:1 to total 18:2 fatty acid content in plasma diacylglyerol (DG) species and triacylglycerol (TG) species in male (M) mice (A and B respectively) and female (F) mice (C and D respectively) on unrestricted chow diet at 6, 10 and 16 weeks of age. Values are expressed as mean ± SEM (7-12 mice per group). † $P < 0.01$ vs. corresponding genotype at 10 weeks of age; ‡ $P < 0.01$ vs. *H/H* mice at same age; $ $P < 0.01$ vs. *db/h* mice at same age using Mann-Whitney *U* test.

liver total 16:1/18:2 in TG species in male *db/db* mice (Figure 4.19, Panel B). A similar pattern of marked elevations in the ratios of liver total 16:1/18:2 in DG species and TG species also occurred in female *db/db* mice at 6 and 10 weeks of age (Figure 4.19, Panels C and D). However, unlike the findings in male *db/db* mice, both measures remained significantly higher in female *db/db* mice at 16 weeks of age compared with the corresponding *H/H* and *db/h* mice, despite a small but significant drop (~15%) in the mean ratio of liver total 16:1/18:2 in TG species in female *db/db* mice at 16 weeks of age.

4.3.11.2 Contribution of hepatic *de novo* lipogenesis to plasma diacylglycerols and triacylglycerols

The same total 16:1/18:2 ratios were measured in plasma DG and TG species to establish whether these surrogate measures of hepatic *de novo* lipogenesis were reflected in plasma. Similar to the findings in liver, the mean ratios of plasma total 16:1/18:2 in DG and TG species were already significantly higher (by 2 to 2.5-fold) in six week old male *db/db* mice, and sustained at 10 weeks of age, but significantly attenuated (by ~50%) by 16 weeks of age, being no longer different to the values obtained in the corresponding *H/H* and *db/h* mice (Figure 4.20, Panels A and B). Also similar to the findings in liver, there were significant elevations in the mean ratios of plasma total 16:1/18:2 in DG and TG species in female *db/db* mice at 6 and 10 weeks of age, and both of these measures remained significantly higher in female *db/db* mice at 16 weeks of age compared with the corresponding *H/H* and *db/h* mice, despite being blunted by ~30% in female *db/db* mice (Figure 4.20, Panels C and D).

4.4 DISCUSSION

4.4.1 The *db/db* mouse represents a progressive model of type 2 diabetes

The leptin receptor-deficient *db/db* mouse model with a C57BL/KsJ background provides a good monogenic model of IR, obesity and T2D [73,85,140,141,142,143,144], and closely resembles disease progression to T2D in humans [72,91]. However, one must be conservative when comparing the key metabolic and lipidomic changes observed in any suitable mouse model and comparable human subjects, as inevitable inter-species differences occur. For example, the fatty acid composition of mouse tissues is different to humans, containing much more DHA (22:6), and leptin receptor deficiency is rare in humans, accounting for only 3 per cent of obesity.

It was anticipated that female *db/db* mice would become less obese and suffer less severe pathology than age-matched male *db/db* mice due to cardio-protection by oestrogen [95,143]. In the present study, the six week old female *db/db* mice were non-obese, but already had elevated omental fat weight, hyperinsulinaemia and IR (versus corresponding female *H/H* mice) (Table 4.2; Figures 4.1 and 4.2). Even though our six week old male *db/db* mice were mildly obese, with elevated omental fat weight and glucose intolerance, they were not statistically considered to be hyperinsulinaemic or IR, despite having mean fasting plasma insulin and HOMA-IR values that were 2-3 fold higher than the female *db/db* mice, and 5-6 fold higher than the corresponding male *H/H* mice (Figures 4.3 and 4.4). The failure to reach statistical significance may relate to the high inter-animal variance in these measurements, possibly due to the more unstable male *db/db* phenotype. If more mice had been studied, it is likely that fasting plasma insulin and HOMA-IR levels may have been significantly elevated in the six week old male *db/db* mice, which would better reflect the more severe pathology expected in male *db/db* mice compared with age-matched female *db/db* mice.

At 10 weeks of age, the female *db/db* mice were mildly obese, with sustained hyperinsulinaemia and IR, and glucose homeostatic abnormalities. By 16 weeks of age, the female *db/db* mice were severely obese, with modest hyperglycaemia, very high fasting insulin and IR levels, and sustained glucose and insulin intolerance. Similar phenotypic changes were observed in male *db/db* mice at 10 and 16 weeks of age, but obesity was more pronounced in the male *db/db* mice at 10 weeks of age, and glucose was not elevated at any age. Contrary to literature findings [73,85,140,141,142,143], the severe obesity in the *db/db* mice at 16 weeks of age was not accompanied by decreased insulin secretion and severe hyperglycaemia. Therefore, the *db/db* mice were not diabetic by 16 weeks of age, but may have developed diabetes later. Given that food intake was not significantly higher in the 16 week old *db/db* mice compared with their corresponding *db/h* and *H/H* littermates, the main effect of genotype in this batch of mice appears to be reduced energy expenditure due to the leptin receptor-deficient mutation.

4.4.2 Genotype, rather than gender or age, is the dominant effect on mouse lipid profiles

In the present study, targeted lipid profiling using LC ESI-MS/MS and subsequent comprehensive lipidomic analysis was employed to characterise temporal (6, 10 and 16 weeks of age) and tissue-specific (liver, skeletal muscle, left-ventricle, adipose and plasma) changes

among 25 lipid classes/subclasses and ~330 lipid species (Table 4.3) associated with the onset of obesity, IR and/or T2D in male and female intermediate (*db/h*) and more severe (*db/db*) mouse phenotypes compared with their corresponding *H/H* littermates. These lipid abnormalities were compared with those observed in studies investigating human obesity, IR and T2D (Chapter 6).

The independent effects of gender, age and mouse genotype on global lipid profiles in plasma and tissues were assessed using conventional statistical methods (Tables 4.6 to 4.8) and PCA modelling (Figures 4.5 and 4.6). Not surprisingly, the effect of the *db/db* genotype on plasma and tissue lipid abnormalities was clearly the dominant effect in the majority of cases. The following sections summarize and discuss the effect of the *db/db* genotype (versus corresponding *H/H* mice), and where appropriate, the effect of gender and age, on lipid abnormalities in the seven main lipid groups defined previously in Results section 4.3.9.

4.4.3 Higher inter-animal variance in lipid levels in male *db/db* mice prevents detection of early lipid abnormalities in tissues

Despite the expectation that cardio-protection by oestrogen in female *db/db* mice would result in less significant changes in lipid profiles than their age-matched male equivalent [28], we found substantial early plasma and tissue lipid abnormalities in our six week old non-obese, hyperinsulinaemic/IR female *db/db* mice (versus female *H/H* mice). In contrast, substantial early lipid abnormalities were observed in plasma, but not in any tissues, in our six week old mildly obese, glucose intolerant (almost hyperinsulinaemic) male *db/db* mice (versus male *H/H* mice).

The failure to reach statistical significance for any lipids in any tissues in the six week old male *db/db* mice may relate to the higher inter-animal variance in tissue lipid levels observed in the more unstable male *db/db* phenotype (e.g., sporadic dietary consumption), and the relatively smaller early changes observed in tissue lipids versus plasma lipids. These factors, combined with the superior assay performance of plasma lipid versus tissue lipid measurements (Table 4.4), low animal numbers (7-12 mice per group) and stringent statistical testing (Benjamini-Hochberg correction for multiple lipid comparisons) resulted in no tissue lipids, but 85 plasma lipids being significantly different in male *db/db* mice compared with male *H/H* mice at 6 weeks of age.

4.4.4 Metabolic pathway maps for plasma, liver and left-ventricle in male *db/db* mice

The remaining sections of this chapter discuss the lipidomic changes in plasma and the different tissues in *db/db* mice compared with *H/H* mice at each age, particularly focusing on the seven major lipid groups defined in section 4.3.9, and how these changes relate to the literature findings. For clarity and ease of comparison, and given the magnitude and contrasting nature of the lipid abnormalities associated with plasma, liver and left-ventricle of male *db/db* mice, three metabolic pathway maps were constructed to highlight the alterations in these lipid groups in plasma (Figure 4.21), liver (Figure 4.22) and left-ventricle (Figure 4.23) of male *db/db* mice with increasing severity of disease compared with the corresponding male *H/H* mice. These metabolic maps offer a visual representation of the temporal and tissue-specific lipid abnormalities associated with the progression to pre-diabetes, and will be referred to where appropriate.

4.4.5 Differential elevation of glycerolipids and cholesteryl esters in plasma and tissues of *db/db* mice

Given that elevated circulating CE, DG and TG lipid levels are established markers of obesity [26,27,28,29,51], pre-diabetes [9] and T2D [9,13], it was puzzling that total CE but very few plasma DG and TG species were significantly elevated in the male *db/db* mice at 6 and 10 weeks of age compared with *H/H* mice (Table 4.13A, Figure 4.13 and Table S4.5). In contrast, both plasma total DG and TG were markedly elevated in the six week old non-obese/IR female *db/db* mice, and this effect was sustained for both classes at 10 weeks of age, and for TG thereafter (Table 4.13B, Figure 4.18 and Table S4.10). The higher inter-animal variance and relatively smaller elevations in the levels of many plasma DG and TG species may explain the lack of DG and TG species that were significantly elevated in male *db/db* mice.

Paradoxically, there was an early trend for elevated liver total CE, DG and TG in the six week old male *db/db* mice (Figure 4.7), and all three classes were significantly elevated at 10 and 16 weeks of age with increasing severity of disease (Table S4.1). However, there was only a modest effect on liver DG and TG in female *db/db* mice at 6 weeks of age and beyond (Figure 4.14 and Table S4.6). The early elevations in plasma CE, DG and TG species (dyslipidaemia) in female *db/db* mice were of greater magnitude and/or appeared much earlier than changes in the liver, which precede fatty liver. Regardless, there is enough evidence to suggest that the *db/db* mouse phenotype was characterised by early elevations of CE, DG and TG lipids in plasma and/or

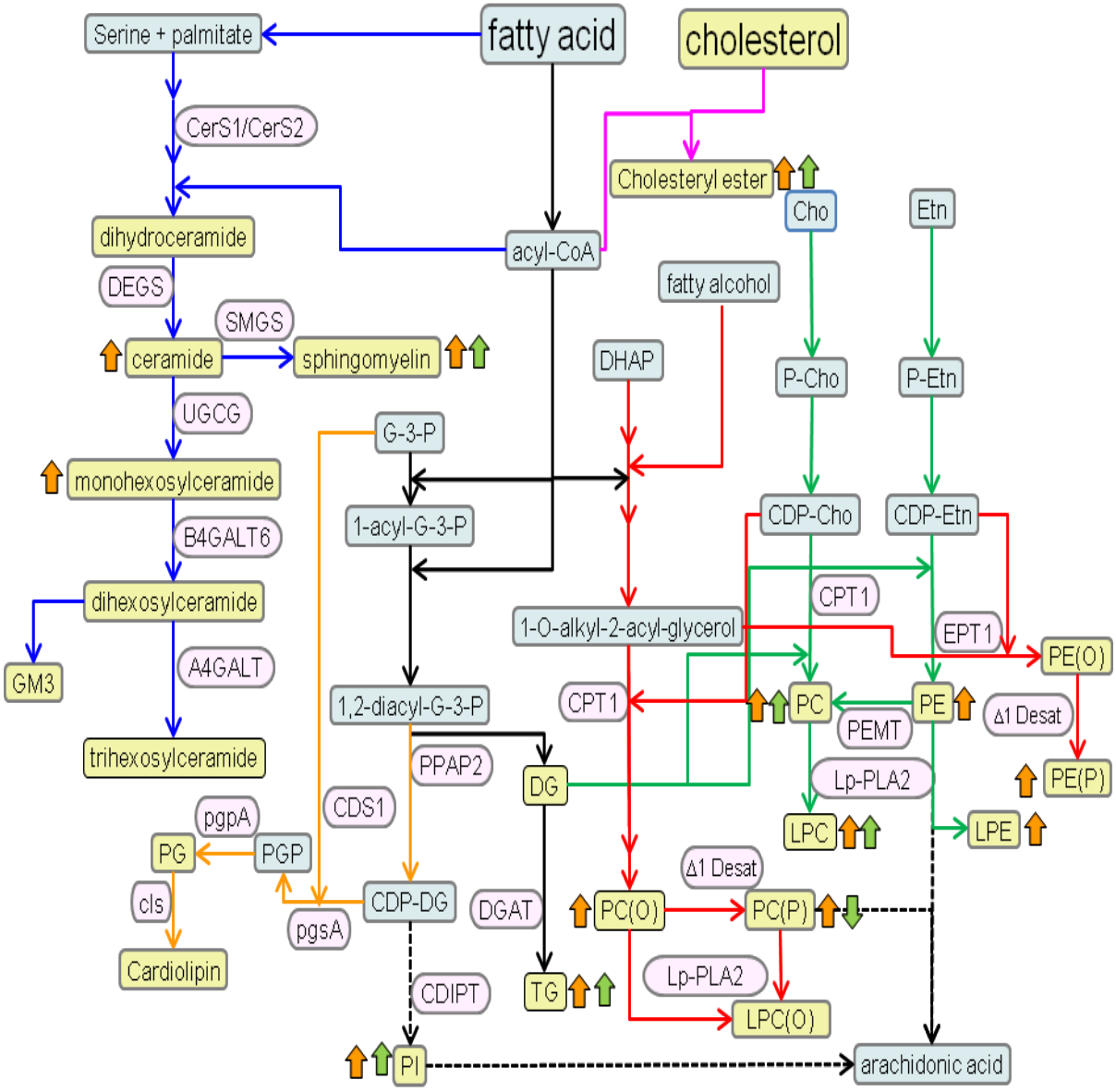

Figure 4.21 Metabolic pathways altered in plasma of male *db/db* mice with progression to type 2 diabetes. Partial lipid metabolic pathways showing the major lipids (blue and yellow boxes), the measured lipids (yellow boxes), and the enzymes involved (pink boxes). The sphingolipid (blue lines), cholesteryl ester (pink lines), cardiolipin (orange lines), glycerolipid (black lines), choline/ethanolamine phospholipids (green lines), plasmalogen (red lines) and arachidonic acid (dotted lines) biosynthetic pathways are shown. The direction of association between lipids in the plasma of male *db/db* mice compared with male *H/H* mice at 6 weeks of age (orange arrows) and 10 weeks of age (green arrows) is indicated.
Metabolite abbreviations: Cho, choline; CDP, cytidine diphosphate; DHAP, dihydroxyacetonephosphate; Etn, ethanolamine; G-3-P, glycerol-3-phosphate; PGP, phosphatidylglycerolphosphate. Abbreviations of measured lipids are shown in Table 7.1**. Enzyme abbreviations:** A4GALT, lactosylceramide 4-alphagalactosyltransferase; B4GALT6, beta-1,4-galactosyltransferase 6; CDIPT, CDP-diacylglycerol-inositol 3-phosphatidyltransferase; CDS1, phosphatidate cytididyltransferase; CerS, ceramide synthase; cls, cardiolipin synthase; CPT1, diacylglycerol cholinephosphotransferase; Δ1 Desat, delta-1 desaturase; DEGS, sphingolipid delta-4 desaturase; DGAT, diacylglycerol O-acyltransferase; EPT1, ethanolaminephosphotransferase; Lp-PLA2, lipoprotein phospholipase A2; PEMT, phosphatidylethanolamine N-methyltransferase; pgpA, phosphatidylglycerophosphatase A; pgsA, phosphatidylglycerosynthase A; PPAP2, phosphatidate phosphatase; SMGS, sphingomyelin synthase; UGCG, ceramide glucosyltransferase.

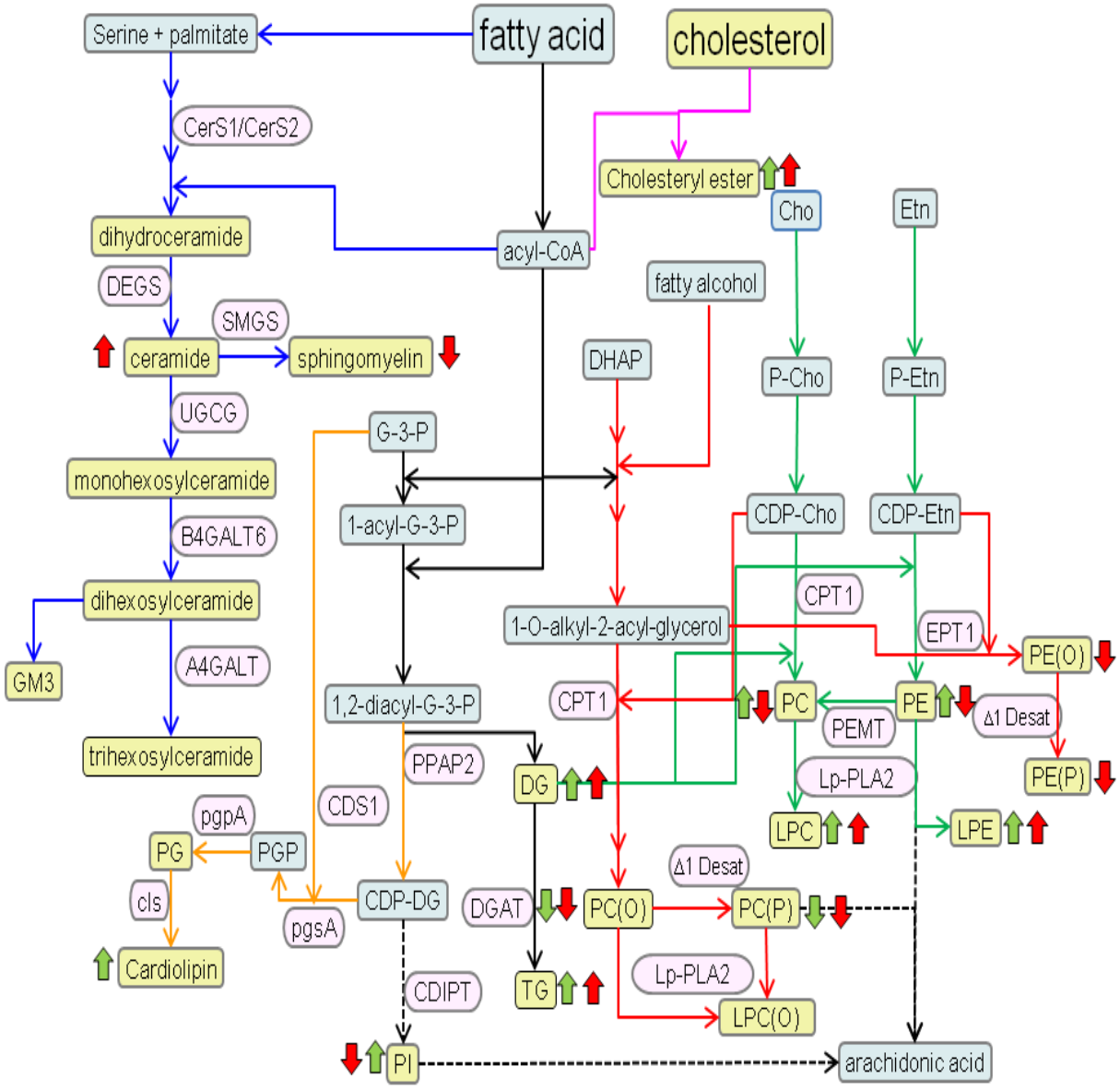

Figure 4.22 Metabolic pathways altered in liver of male *db/db* mice with progression to type 2 diabetes. Partial lipid metabolic pathways showing the major lipids (blue and yellow boxes), the measured lipids (yellow boxes), and the enzymes involved (pink boxes). The sphingolipid (blue lines), cholesteryl ester (pink lines), cardiolipin (orange lines), glycerolipid (black lines), choline/ethanolamine phospholipids (green lines), plasmalogen (red lines) and arachidonic acid (dotted lines) biosynthetic pathways are shown. The direction of association between lipids in the liver of male *db/db* mice compared with male *H/H* mice at 10 weeks of age (green arrows) and 16 weeks of age (red arrows) is indicated.
Metabolite abbreviations: Cho, choline; CDP, cytidine diphosphate; DHAP, dihydroxyacetonephosphate; Etn, ethanolamine; G-3-P, glycerol-3-phosphate; PGP, phosphatidylglycerolphosphate. Abbreviations of measured lipids are shown in Table 7.1**. Enzyme abbreviations:** A4GALT, lactosylceramide 4-alphagalactosyltransferase; B4GALT6, beta-1,4-galactosyltransferase 6; CDIPT, CDP-diacylglycerol-inositol 3-phosphatidyltransferase; CDS1, phosphatidate cytididyltransferase; CerS, ceramide synthase; cls, cardiolipin synthase; CPT1, diacylglycerol cholinephosphotransferase; Δ1 Desat, delta-1 desaturase; DEGS, sphingolipid delta-4 desaturase; DGAT, diacylglycerol O-acyltransferase; EPT1, ethanolaminephosphotransferase; Lp-PLA2, lipoprotein phospholipase A2; PEMT, phosphatidylethanolamine N-methyltransferase; pgpA, phosphatidylglycerophosphatase A; pgsA, phosphatidylglycerosynthase A; PPAP2, phosphatidate phosphatase; SMGS, sphingomyelin synthase; UGCG, ceramide glucosyltransferase.

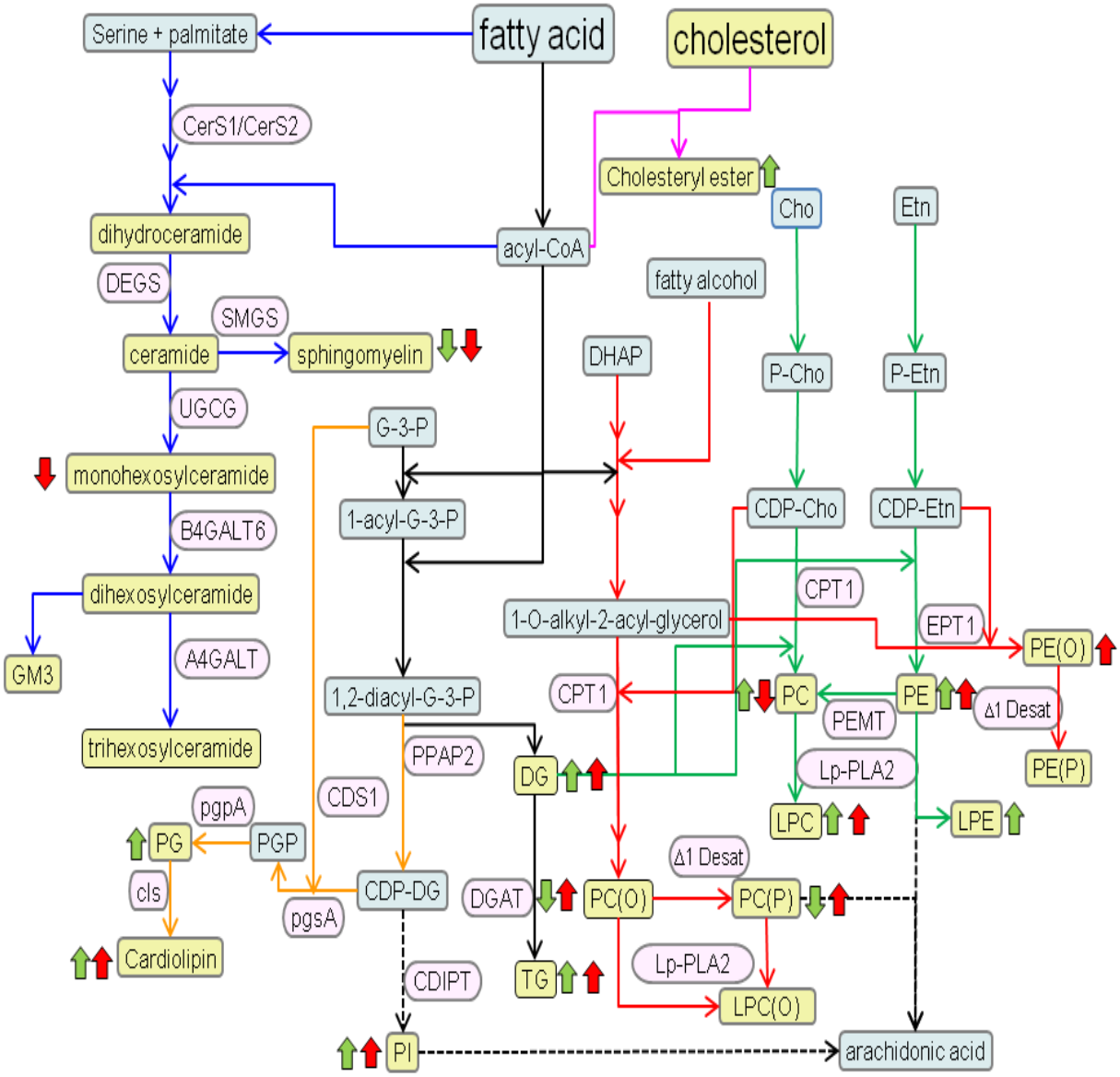

Figure 4.23 Metabolic pathways altered in left-ventricle of *db/db* mice with progression to type 2 diabetes. Partial lipid metabolic pathways showing the major lipids (blue and yellow boxes), the measured lipids (yellow boxes), and the enzymes involved (pink boxes). The sphingolipid (blue lines), cholesteryl ester (pink lines), cardiolipin (orange lines), glycerolipid (black lines), choline/ethanolamine phospholipids (green lines), plasmalogen (red lines) and arachidonic acid (dotted lines) biosynthetic pathways are shown. The direction of association between lipids in the left-ventricle of male *db/db* mice compared with male *H/H* mice at 10 weeks of age (green arrows) and 16 weeks of age (red arrows) is indicated.
Metabolite abbreviations: Cho, choline; CDP, cytidine diphosphate; DHAP, dihydroxyacetonephosphate; Etn, ethanolamine; G-3-P, glycerol-3-phosphate; PGP, phosphatidylglycerolphosphate. Abbreviations of measured lipids are shown in Table 7.1**. Enzyme abbreviations:** A4GALT, lactosylceramide 4-alphagalactosyltransferase; B4GALT6, beta-1,4-galactosyltransferase 6; CDIPT, CDP-diacylglycerol-inositol 3-phosphatidyltransferase; CDS1, phosphatidate cytididyltransferase; CerS, ceramide synthase; cls, cardiolipin synthase; CPT1, diacylglycerol cholinephosphotransferase; Δ1 Desat, delta-1 desaturase; DEGS, sphingolipid delta-4 desaturase; DGAT, diacylglycerol O-acyltransferase; EPT1, ethanolaminephosphotransferase; Lp-PLA2, lipoprotein phospholipase A2; PEMT, phosphatidylethanolamine N-methyltransferase; pgpA, phosphatidylglycerophosphatase A; pgsA, phosphatidylglycerosynthase A; PPAP2, phosphatidate phosphatase; SMGS, sphingomyelin synthase; UGCG, ceramide glucosyltransferase.

liver by six weeks of age. The early accumulation of fat in the liver of the six week old male *db/db* mice (hepatosteatosis) may be linked to the lack of leptin signaling in *db/db* mice [102], and the potential role of leptin-receptor deficiency (as opposed to the imbalance between energy intake and consumption) in mediating many of the genotype-dependent lipid abnormalities in *db/db* mice relative to *H/H* mice should not be underestimated. Similar to our findings in *db/db* mice, Graessler *et al*. reported that nearly all fasting plasma TG and DG species, and CE 16:0 and CE 16:1 were significantly elevated in obese men [28], and Meikle *et al.* found that nearly all 26 CE species, 22 DG species and 43 TG species measured in fasting plasma were positively associated with both pre-diabetes and T2D subjects, independent of obesity, in two large human cohort studies [9]. Moreover, chronic high-fat diet induced obesity in male C57BL/6J mice was associated with markedly elevated fasting plasma 16:0, 18:0 or 18:1 FA-containing TG and DG species [26].

In our mouse study, total CE subclass and seven CE species, including CE 16:1 and six essential polyunsaturated FA-containing CE species were significantly elevated in fasting plasma in the six week old mildly obese, almost hyperinsulinaemic male *db/db* mice, and this pattern was sustained at 10 weeks of age. Similarly, CE 14:0, CE 16:1 and five essential polyunsaturated FA-containing CE species (with CE 20:3, CE 20:5 and CE 22:5 being common to both male and female *db/db* mice) were significantly elevated in six week old non-obese/IR female *db/db* mice, and this pattern was sustained at 10 weeks of age. Therefore, fasting plasma CE 16:1 and specific polyunsaturated FA-containing CE species are precursors to obesity and IR in *db/db* mice. These findings compare to previous studies have shown that the proportions of 14:0, 16:0, 18:0 and 18:2 fatty acids (but not 18:1) in serum CEs reflect the amount of fatty acids in the diet [39], and that fasting serum CE species containing high proportions of 16:0, 16:1 and 18:0 fatty acids, and a low proportion of 18:2 fatty acid are related to obesity [40] and T2D [41,42,43].

4.4.5.1 Diet induced activation of hepatic *de novo* lipogenesis in *db/db* mice

Caution must be exercised when comparing plasma lipid profiles in *db/db* mice fed an unrestricted standard chow diet to high-fat fed models of rodent obesity, as dietary fat and carbohydrate composition can greatly influence hepatic *de novo* lipogenesis [47] and lipidomic profiles [26,48]. Hepatic *de novo* lipogenesis is activated by low-fat/high-carbohydrate diets, and high levels of insulin and carbohydrate [47]. Long-chain fatty acids (16:0, 16:1, 18:0 and 18:1) derived from increased hepatic *de novo* lipogenesis are released into the circulation as VLDL-

bound triglyceride [50] to maintain normal 16:1/16:0 and 18:1/18:0 ratios in metabolic tissues [47]. Conversely, high-fat diets provide plentiful long-chain saturated and monounsaturated fatty acids, thereby inhibiting hepatic *de novo* lipogenesis and delta-9 desaturase activity [47]. However, the development of obesity and IR may induce hepatic *de novo* lipogenesis in the presence of a high-fat diet [51,52].

The standard chow diet fed to our mice was also low in fatty acid content (8% total energy as fat) and high in carbohydrate content (69% total energy as carbohydrate), and likely to activate early hepatic *de novo* lipogenesis in our hyperinsulinaemic *db/db* mice before the onset of chronic obesity, IR or increased caloric uptake. Given the fatty acid composition of the diet, the ratio of liver total 16:1/18:2 in DG species and TG species were considered surrogate measures of hepatic *de novo* lipogenesis in our *db/db* mouse study (Figure 4.19). The same total 16:1/18:2 ratios were measured in plasma DG and TG species to confirm whether the surrogate measures of *de novo* hepatic lipogenesis were reflected in plasma (Figure 4.20).

The results indicated that hepatic *de novo* lipogenesis was significantly elevated by six weeks of age in male and female *db/db* mice, increasing the available pool of 16:1 FA for use by peripheral tissues to compensate for the lack of dietary 16:1 FA. Hepatic *de novo* lipogenesis and the circulating pool of 16:1 FA in DG and TG remained significantly elevated in male and female *db/db* mice at 10 weeks of age, but was significantly attenuated in male *db/db* mice by 16 weeks of age, suggesting that 16:1 FA stores were depleted in the now severely obese/pre-diabetic male *db/db* mice. This same pattern of results was observed for total 16:1/18:2 ratios in plasma DG and TG species, confirming that surrogate measures of *de novo* hepatic lipogenesis in *db/db* mice were reflected in plasma. Monounsaturated fatty acids are major components of membrane phospholipids, TG and CE, and are required for normal membrane fluidity and transmembrane receptor/enzyme activity [159]. Palmitoleate also acts as an endocrine signal, improving muscle insulin sensitivity and decreasing hepatosteatosis [160].

4.4.5.2 "Saturated" and "unsaturated" triacylglycerol species are equally predictive of pre-diabetes in *db/db* mice

The fatty acid composition is critical in determining whether a particular TG species is positively or negatively associated with obesity, IR and risk of T2D. Kotronen *et al.* reported that total fasting serum esterified 16:0, 16:1 *n*-7, and 18:1 *n*-9 fatty acids were positively correlated, and

18:2 *n*-6 was negatively correlated with HOMA-IR in non-diabetic individuals [31]. In the same study, serum saturated and monounsaturated TG species such as TG 16:0/16:0/18:1 and TG 16:0/18:1/18:0 were positively correlated, and polyunsaturated TG species containing essential fatty acids such as TG 18:1/18:2/18:2 were negatively correlated with HOMA-IR. Importantly, the same saturated and monounsaturated TG species contained in VLDL particles also positively correlated with HOMA-IR, which may reflect increased hepatic *de novo* lipogenesis [156,157]. Rhee *et al.* found that circulating TG species containing low total FA-carbon number (≤ 52) and low total FA double bond number (≤ 2) were associated with IR (by HOMA-IR) and increased risk of T2D, whereas TG species containing higher total FA-carbon number and higher total FA double bond number were associated with decreased risk of T2D, and were not correlated with IR [13]. Furthermore, diet-induced weight loss in obese individuals led to a reduction in circulating saturated and short-chain FA-containing TG species, which was associated with improved insulin sensitivity [30].

In our *db/db* mouse study, the number of "saturated" TG species (defined as having a total of two or less FA double bonds, as long as each FA within the TG species contained no more than one double bond) and "unsaturated" TG species (defined as having a total of more than two FA double bonds, but included TG species that contained a total of two FA double bonds when one FA moiety contained two double bonds) that were significantly elevated in plasma and each of the tissues in male and female *db/db* mice at each age compared with corresponding *H/H* mice was not statistically different (Table 4.14). Therefore, "saturated" and "unsaturated" TG species were equally predictive of obesity, IR and pre-diabetes in *db/db* mice, despite evidence of elevated hepatic *de novo* lipogenesis (Figures 4.19 and 4.20), which should result in higher levels of liver TG species containing "saturated" FAs (particularly 16:0 and 18:0) and monounsaturated FAs (particularly 16:1 and 18:1) for distribution to plasma and other metabolic tissues.

The inability to discriminate between "saturated" and "unsaturated" TG species as biomarkers of disease progression in our *db/db* mice may relate to the severity of disease, which often resulted in nearly all of the measured TG species being significantly elevated, particularly in male *db/db* mice (Table 4.14). However, even when 12 or less TG species were significantly elevated in *db/db* mice, as was seen in liver and skeletal muscle of six week old female *db/db* mice, the number of significantly elevated "saturated" and "unsaturated" TG species remained similar. Although the definition of "saturated" and "unsaturated" TG species was rationalised in section

4.3.10, a clearer definition and outcome may have been achieved if TG species were defined as "polyunsaturated" (i.e., TG species containing one or more fatty-acyl moieties with two or more double bonds) or "non-polyunsaturated" (i.e., TG species containing no fatty-acyl moieties with two or more double bonds).

4.4.5.3 Early elevation of glycerolipids and chlolesteryl esters in adipose of *db/db* mice

There was already a trend towards elevated adipose total DG and TG in our six week old mildly obese/glucose intolerant male *db/db* mice (Figure 4.10), and these lipid classes contributed almost exclusively to the adipose lipid species that were significantly elevated in non-obese/IR female *db/db* mice at 6 weeks of age (versus corresponding *H/H* mice) (Figure 4.15 and Table S4.9). By 10 weeks of age, the CE, DG and TG classes contributed almost exclusively to the adipose lipid species that were significantly elevated in both male and female *db/db* mice, and this strong effect was sustained in the male *db/db* mice at 16 weeks of age (Table S4.4).

Adipocyte cell size has been shown to correlate with obesity and T2D [161,162]. Large *et al*. found that mean fat cell volume was significantly higher (by ~77%) in morbidly obese adults (mean BMI 43.1 kg/m^2) than non-obese subjects (mean BMI 23.5 kg/m^2) [163]. The TGs stored within lipid droplets are surrounded by a phospholipid monolayer consisting mainly of PC lipids, a lesser amount of PE lipids [77], and some mitochondria for FA utilization. Theoretically, the greatly increased uptake and storage of TG in lipid droplets would also lead to an increase in adipocyte size in our obese *db/db* mice, resulting in a significantly higher volume to surface area, but little rise in overall protein content of the cell. Given these morphological changes, and the fact that lipid levels in our study are normalised to protein content, it is not surprising that TG and its putative lipolytic product, DG, were markedly elevated, but the relative levels of shingolipids (particularly Cer and MHC) and phospholipids, including PC(O), PC(P), LPC, PC, PE and CL, were significantly lower in adipose tissue in *db/db* mice compared with *H/H* mice. Similarly, most adipose TG species were found to be elevated in obese women with high fatty liver content compared with age- and BMI-matched women with low liver fat content [66]. However, adipose DG species content was not different in the two groups, despite the presence of higher serum insulin concentrations and infiltration of macrophages (inflammation) in the adipose tissue of obese women with high fatty liver content [66].

4.4.5.4 Early elevation of glycerolipids in left-ventricle and skeletal muscle in *db/db* mice

There was also an early trend towards elevated total DG and TG (but not CE) in left-ventricle and skeletal muscle in the six week old male *db/db* mice, leading to significant elevations of the DG and TG classes at 10 and 16 weeks of age (Figure 4.9; and Tables S4.2 and S4.3). Thus, DG and TG accumulation in left-ventricle and skeletal muscle preceded the development of whole-body hyperinsulinaemia and IR in male *db/db* mice. Similarly, total CE, DG and TG were already significantly elevated, and numerous TG species were elevated in the left-ventricle of six week old female *db/db* mice prior to the onset of obesity (Figure 4.15; and Tables S4.7 and S4.8). Therefore, early elevation of hepatic *de novo* lipogenesis in *db/db* mice resulted in increased circulation and ectopic deposition of excess fatty acids (particularly 16:1) as TG and DG in left-ventricle and skeletal muscle.

There are few published articles that have examined individual CE, DG and TG species in metabolic tissues in animal or human obesity, IR and/or T2D. DeMarco *et al.* found that total TG and DG levels were significantly elevated in the left-ventricles of 12- and 15-week old male *db/db* compared with age-matched *db*/wild-type mice [77]. In addition, the relative increase in TG species containing low acyl-chain double-bond number and low acyl-chain carbon number was higher in the *db/db* mice at 15 weeks compared with the corresponding *db*/wild-type mice, which was accompanied by increased capacity for myocardial mitochondrial FA oxidation, increased oxidative stress (generation of reactive oxygen species), and the development of diastolic dysfunction. In another study, only low abundant skeletal muscle DG species that contained an unsaturated FA on both positions (e.g. DG 16:1/18:1) were significantly elevated in obese-sedentary subjects compared with both normal weight-sedentary and normal weight-endurance trained athletes [36]. The authors concluded that even relatively small amounts of specific intramuscular DG species may be lipotoxic. Other studies have shown that elevated skeletal muscle DGs are associated with impaired insulin signaling and IR [38], and that skeletal muscle DGs induce IR associated with human obesity and T2D [164].

In our mouse study, both "saturated" and "unsaturated" DG species, as defined for TG species in Table 4.14, were equally predictive of obesity, IR and pre-diabetes in plasma and each of the tissues in male and female *db/db* mice compared with corresponding *H/H* mice at each age group (data not shown). The only exception to these findings occurred in the liver of male *db/db* mice at 10 weeks of age, in which all nine "saturated" DG species, but only two of 13

"unsaturated" DG species were significantly elevated in male *db/db* mice. This latter result suggests that hepatic "saturated" DG species were associated with increased hepatic *de novo* lipogenesis, which corresponded to the onset of IR in male *db/db* mice at 10 weeks of age.

4.4.6 Relationship between saturated fatty acids, inflammation, sphingolipid synthesis and insulin resistance

Circulating factors associated with obesity [e.g., increased saturated FAs such as palmitate (16:0) and stearate (18:0), and inflammatory cytokines such as TNF-α and IL-6] selectively induce enzymes that induce the synthesis of sphingolipids (e.g. ceramide and/or its derivatives GM3 gangliosides and sphingosine), which are associated with certain metabolic diseases, including IR (via inhibited activation of both Akt and glycogen synthase kinase3β early in the insulin signalling pathway) [165], pancreatic β-cell failure, cardiomyopathy, and vascular dysfunction [20]. On the other hand, unsaturated FAs [e.g., linoleate (18:2)] induce IR by ceramide-independent mechanisms involving, for example, DG-activated protein kinase C isoforms or phosphatidic acid 18:2/18:2 [22,166].

4.4.6.1 Sphingolipids are differentially regulated in plasma and liver in *db/db* mice

Fasting plasma total Cer, MHC and (almost) SM, along with the 16:1 FA-containing SM 32:2 and SM 34:2 were already significantly elevated in our six week old mildly obese/glucose intolerant (and hyperinsulinaemic) male *db/db* mice, prior to the onset of IR (Figure 4.12, Table S4.5 and Figure 4.21). In the six week old IR female *db/db* mice, four fasting plasma SM species (including the 16:1 FA-containing SM 32:1 and 32:2) were already significantly elevated prior to the onset of obesity, and this SM effect persisted with increasing severity of disease (Table S4.10). The early elevation of plasma 16:1 FA-containing SM species in our *db/db* mice may reflect the increased pool of 16:1 generated by hepatic *de novo* lipogenesis (Figures 4.19 and 4.20).

Similar to our findings in six week old male *db/db* mice, Haus *et al.* found that fasting plasma total Cer and Cer 18:0, Cer 20:0 and Cer 24:1 levels were significantly higher in obese/T2D subjects compared with lean healthy subjects [25]. Additionally, fasting plasma total Cer and several Cer species negatively correlated with insulin sensitivity (measured by clamp), and Cer 18:0 and Cer 18:1 positively correlated with fasting plasma TNF-α, an inflammatory cytokine.

Also in agreement with our findings, Barber *et al.* revealed that fasting plasma levels of several species of Cer, SM, MHC and DHC were significantly increased in male C57BL/6J mice fed a high-fat diet for 12 weeks compared with low fat-fed mice [26]. Furthermore, Eisinger *et al.* found that fasting serum levels of most SM species (but not polyunsaturated SM species) were significantly elevated in high fat-fed male C57BL/6 mice, but serum ceramides were not significantly different [27]. Although Meikle *et al.* found that both T2D and prediabetes were positively associated with fasting plasma total Cer and its precursor dhCer in two human cohorts, there was no association between T2D or prediabetes and other sphingolipid subclasses (i.e., total MHC, DHC, THC, GM3 ganglioside or SM) [9]. In a prospective large case-cohort study, Floegel *et al.* revealed that baseline serum SM 34:2 was independently associated with decreased risk of T2D [148], which opposes our finding of elevated SM 34:2 in six week old male *db/db* mice.

In liver, there was no effect of sphingolipids in our male *db/db* mice until 16 weeks of age, when Cer 16:0 and Cer 18:0 were significantly elevated, and the SM subclass and five SM species (mostly saturated) were significantly lower compared with the corresponding male *H/H* mice (Table 4.9A, Table S4.1 and Figure 4.22). In contrast, liver total Cer was already significantly elevated in the six week old female IR *db/db* mice prior to the onset of obesity, and the early trend for lower total MHC intensified by 10 weeks of age (Table 4.9B, Figure 4.13 and Table S4.6). To date, no studies have examined the association of individual sphingolipid species in liver with lipid oversupply, obesity and T2D. However, liver total Cer content was found to be increased in male C57BL/6J mice after 3 days of high-fat diet [61], unaltered in male Sprague-Dawley rats after 3 days high saturated- or high unsaturated-fat diet despite elevated hepatic DG, activated PKCε and impaired hepatic IRS-2 signalling [167], and unaltered in C57BL/6 mice after 12 weeks of high-fat diet, despite marked obesity and IR [76].

4.4.6.2 Sphingolipids are differentially regulated in adipose, left-ventricle and skeletal muscle in *db/db* mice

In contrast to our sphingolipid findings in plasma, adipose total Cer and MHC were significantly lower in the obese/IR male *db/db* mice at 10 weeks of age. This strong effect was sustained with increasing severity of disease (Figure 4.8 and Table 4.12A), and was accompanied by a significant elevation of three SM species (SM 34:0, SM 34:1 and SM 34:2) (Table S4.4). In female *db/db* mice, there was already a significantly lower adipose total Cer and all six Cer

species in six week old IR female *db/db* mice prior to the onset of obesity, which indicates a strong negative association between adipose Cer levels and IR (Figure 4.13 and Table S4.9). This effect was sustained in the mildly obese/IR female *db/db* mice at 10 weeks of age, and was accompanied by a significantly lower total MHC and all four MHC species.

Few studies have examined adipose sphingolipid species content in models of obesity. Samad *et al.* found contrasting effects of sphingolipids in plasma and adipose tissue of leptin-deficient genetically obese C57BL *ob/ob* mice at 14-16 weeks of age [70]. Fasting plasma levels of total Cer and four Cer species, and total SM and five SM species were significantly increased, but adipose levels of total Cer and three Cer species, and total SM and five SM species were significantly decreased in obese *ob/ob* mice compared with age-matched lean C57BL/6J mice, despite increased mRNA expression of all key enzymes involved in adipose ceramide metabolism. In the same study, similar adipose sphingolipid and enzyme mRNA expression results were found in obese *db/db* mice, but this data was not shown [70]. Adipose total ceramide content was also found to be significantly lower in both obese non-diabetic and obese/T2D subjects compared with lean subjects, which corresponded to elevated mRNA expression and increased activity of most key enzymes responsible for adipose ceramide metabolism [105]. In the same study, adipose total ceramide content positively correlated with plasma adiponectin concentration, and negatively correlated with HOMA-IR index. These results generally support our findings of significantly elevated fasting plasma Cer, MHC and SM species, and significantly lower adipose total Cer and MHC levels in *db/db* mice.

In our mouse study, total SM was significantly lower in the left-ventricle of male *db/db* mice at both 10 and 16 weeks of age (Figure 4.7, Table S4.3 and Figure 4.23). Total GM3 and some left-ventricle SM species were significantly lower in the female *db/db* mice at 6 and 10 weeks of age, and the SM effect was sustained at 16 weeks of age. These findings contrast with those of DeMarco *et al.*, who found that left-ventricle total SM levels were significantly higher in male obese/IR *db/db* mice at both 12- and 15-weeks of age, and Cer levels were elevated at 12 weeks of age compared with age-matched *db*/wild-type mice [77]. These differences may be partly attributable to the profoundly hyperglycaemic (diabetic) state observed in the *db/db* mice at both 12- and 15-weeks of age in the latter study compared to the pre-diabetic state of our *db/db* mice at similar ages.

There were only minor effects of skeletal muscle Cer and SM species in our male and female *db/db* mice compared with *H/H* mice. Ussher *et al.* also found that total Cer levels were unchanged in gastrocnemius muscle of six week old *db/db* mice compared with age-matched heterozygous *db/h* lean mice, but treatment with myriocin (a serine palmitoyl transferase-1 inhibitor) for four weeks was associated with an improvement in fasting glucose, glucose and insulin tolerance, insulin sensitivity and insulin signalling [76]. In other studies, total Cer and most Cer species were significantly elevated in soleus muscle of female diabetic fatty ZDF (*fa/fa*) rats fed a high saturated fat diet for eight weeks [90], and the content of 18:1 FA-containing DG species and saturated Cer species were significantly elevated in vastus lateralis muscle of obese and T2D subjects compared with lean subjects [37]. Furthermore, elevated total Cer content in soleus muscle of female Sprague-Dawley rats fed a high saturated fat diet for two weeks was associated with blunted insulin signalling [62]. Importantly, total Cer content was significantly elevated in soleus and red gastrocnemius muscle (but not white gastrocnemius) in male Wistar rats fed a high saturated fat diet for five weeks, but did not change in any muscle from rats fed a high polyunsaturated fat diet [23]. These findings indicate that the regulation of skeletal muscle Cer content depends on the composition of the diet and type of skeletal muscle, and support the lack of change in ceramide species observed in gastrocnemius muscle of our unrestricted low-fat chow fed *db/db* mice.

4.4.7 Differential regulation of the major glycerophospholipids in plasma and liver of *db/db* mice

In the mouse study, total PC along with 23 PC species and five PE species were already significantly elevated in fasting plasma in six week old mildly obese/glucose intolerant male *db/db* mice compared with *H/H* mice, but this rise in PC and PE lipids was attenuated by 10 weeks of age (Table 4.13A and Table S4.5). In the six week old non-obese/IR female *db/db* mice, 14 fasting plasma PC species were already significantly elevated, and by 10 weeks of age, total PC and PE, along with 25 PC species and all 13 PE species were significantly elevated (Figure 4.17 and Table S4.10). However, this effect had almost dissipated by 16 weeks of age.

In contrast to plasma, there was a dichotomous and delayed effect on PC species in liver of male *db/db* mice, with ten PC species (containing only even-numbered carbon FA) being significantly elevated, but five PC species (containing an odd-numbered carbon FA) being significantly lower at 10 weeks of age compared with the male *H/H* mice (Table S4.1). However, by 16 weeks of

age, 14 PC species and seven PE species were significantly lower in the now severely obese/pre-diabetic male *db/db* mice (Figure 4.22). There was also a dichotomous but early effect on liver PC and PE species in the six week old female *db/db* mice, which was sustained at 10 weeks of age (Table S4.6).

4.4.7.1 Specific phosphatidylcholine species are risk factors for type 2 diabetes in *db/db* mice and humans

The role of plasma PC and PE species as potential risk factors for obesity, IR and T2D has not been fully explored. In the same study that showed that fasting plasma TG species containing FA with a lower number of carbons and double bonds were associated with increased risk of T2D, fasting plasma PC 16:0/18:2 and PC 18:0/18:2 were independently associated with increased risk, and PC 18:1/20:5 and/or PC 18:2/20:4 with decreased risk of T2D [13]. In another prospective large case-cohort study, Floegel *et al.* revealed that four baseline serum diacyl-PC species (PC 32:1, PC 36:1, PC 38:3 and PC 40:5) were independently associated with increased risk of T2D [148]. Notably, the six PC species that were associated with increased risk of T2D in these two prospective human studies were already significantly elevated in plasma in six week old male and female *db/db* mice (except PC 34:2 in the female *db/db* mice). These findings indicate that the same plasma PC species that predict T2D risk in human studies were also positively associated with the early onset of obesity and IR in six week old *db/db* mice**.**

4.4.7.2 Even-chain and odd-chain phosphatidylcholine species are differentially regulated in *db/db* mice

In the mouse study, a very strong and consistent pattern emerged whereby the PC species that were significantly increased in liver, skeletal muscle and left-ventricle in male and female *db/db* mice compared with corresponding *H/H* mice contained only even-numbered carbon FAs. This pattern was also observed in plasma in six week old female *db/db* mice and ten week old male *db/db* mice. However, most of the PC species that were significantly decreased in liver, skeletal muscle and left-ventricle in male *db/db* mice (but not female *db/db* mice) contained an odd-numbered carbon FA. Given that approximately two-thirds of the 40-odd measured PC species contained only even-numbered carbon FAs and the other one-third contained an odd-numbered carbon FA, these results appear to confirm a negative association between tissue odd-chain PC species and obesity, IR and pre-diabetes in our male *db/db* mice. Odd-chain 15:0 and 17:0 FAs

derived from dietary fat in the standard chow diet may be used as an energy source, but any protective role for odd-chain PC species against T2D is speculative. Given that monounsaturated 16:1 and 18:1 FAs are critical components of lipids in membranes [159] and that hepatic *de novo* lipogenesis was elevated in the male *db/db* mice (Figures 4.19), the selective uptake of 16:1 and 18:1 FA-containing PC species into metabolic tissues may have resulted in the simultaneous removal of less favoured PC species containing odd-chain 15:0 and 17:0 FAs.

Meikle *et al.* showed that both T2D and prediabetes were positively associated with fasting plasma total PE and most PE species in two large human cohorts (vs. NGT subjects), and with total PC in one human cohort [9]. Paradoxically, however, there was a negative association of T2D with some fasting plasma PC species containing an odd-numbered carbon FA, specifically PC 33:2 and PC 35:2 [9]. In human diets, these odd-chain FAs (products of ruminant digestion) are derived primarily from dairy fats [168,169], and negative associations have been found between 15:0 and 17:0 FAs and incident T2D [170,171], which supports a protective role for dairy lipids against T2D. In another study, Meikle *et al.* also found that stable coronary artery disease was positively associated with total PE and most PE species, and negatively associated with PC 33:2 and PC 35:2 (vs. NGT subjects) [10]. Graessler *et al.* showed that some PC and PE species were significantly elevated in a group of obese men compared with leaner men [28].

In other human studies, Pietilainen *et al.* found that fasting plasma 22:6 FA-containing PC species (PC 16:0/22:6 and PC 18:0/22:6) were negatively correlated with fat depots, and PC 16:0/22:6 was positively correlated with insulin sensitivity, and negatively correlated with fasting serum insulin in young adult monozygotic obese co-twins [29]. These associations suggest that PC 16:0/22:6 may be positively linked with insulin signaling. DHA (22:6n-3) is an essential FA with known health benefits [172]. In our *db/db* mice, fasting plasma PC 40:7 was significantly elevated in six week old male *db/db* mice and in ten week old female *db/db* mice compared with the corresponding *H/H* mice, but there was no association of any other plasma 22:6 FA-containing PC species with *db/db* mice.

4.4.7.3 Alterations in phosphatidylcholine and phosphatidylethanolamine species in adipose, left-ventricle and skeletal muscle of *db/db* mice

To date, there are few studies that have performed lipidomic analysis (by mass spectrometry) in metabolic tissues to examine the role of individual PC and PE species in lipid oversupply,

obesity, IR and T2D. In contrast to the early elevation of plasma PC and species, there was an early trend for lower adipose total PC levels in six week old mildly obese/glucose intolerant male *db/db* mice (Figure 4.12). By 10 weeks of age, total PC and 26 PC species were significantly lower in male *db/db* mice, and by 16 weeks of age, total PC and PE, along with 35 PC species and 12 PE species were significantly lower in the now severely obese/pre-diabetic male *db/db* mice (Figure 4.12 and Table S4.4). Adipose total PC and PE were already markedly lower in six week old female *db/db* mice prior to the onset of obesity, and this strong outcome was sustained at 10 weeks of age (vs. *H/H* mice).

The pattern of lipid abnormalities found in fasting adipose and plasma in the *db/db* mice was similar to that observed in adipocyte-specific fatty acid transport protein 4 (*Fatp4)*-deficient knock-out mice fed a high saturated fat diet for 24 weeks [173]. Body weight, fat pad mass, adipocyte size and fasting subcutaneous adipose total TG content were significantly increased in *Fatp4*-deficient mice, but total SM, PC, LPC, PE, PS, PI and CE content were significantly decreased, and total Cer, PE(P) and PG content were unaltered compared with control mice fed the same diet. However, fasting serum total TG, Cer, PC, LPC and CE content were significantly elevated in the *Fatp4*-deficient mice [173]. These results reinforce our view that the relative elevation in adipose TG levels, but lower levels of adipose and phospholipids (including PC and PE) and some sphingolipids in our *db/db* mice may be explained by the increase in adipocyte size (storage of TG in lipid droplets).

In left-ventricle, there were no significant changes in total PC and PE levels in our male *db/db* mice at 10 or 16 weeks of age. However, there was a dichotomous effect on PC species and a significant elevation in ten PE species at 10 weeks of age, and a blunting of significantly elevated PC and PE species at 16 weeks of age (Table S4.3). In contrast, total PE along with 17 PC species (containing only even-numbered carbon FA) and nine PE species were already significantly elevated in the six week old female *db/db* mice, and these strong PE and PC outcomes were sustained in the female *db/db* mice at 10 weeks of age (Figure 4.12 and Table S4.8). Notably, the significant lowering of the 22:6 FA-containing PC 38:6 and PC 40:6 in left-ventricle were closely associated with the significantly lowering of 22:6 FA-containing CL species in both male and female *db/db* mice at 6 and 10 weeks of age (Figure 4.10). DeMarco *et al.* found that total PC and PE levels were significantly elevated at 12 weeks of age, and total PC content remained elevated at 15 weeks of age in male *db/db* mice compared with age-matched *db*/wild-type mice [77].

In skeletal muscle, we found that the 16:1 FA-containing PC species, PC 32:1, PC 32:2 and PC 32:3, were significantly elevated in skeletal muscle in male *db/db* mice at 10 weeks of age (Table S4.2), and in female *db/db* mice at 6 and 10 weeks of age (Table S4.7), but many polyunsaturated FA-containing PC species (most containing an odd-numbered carbon FA) were significantly lower compared with the corresponding *H/H* mice (e.g. PC 36:4, PC 37:4, PC 37:6, PC 38:6 and PC 39:7). The elevated 16:1 FA-containing PC species in skeletal muscle may reflect the increased hepatic *de novo* lipogenesis seen in the *db/db* mice at 6 and 10 weeks of age (Figures 4.19 and 4.20). Magnusson *et al.* also found that there was a a reduced relative abundance of polyunsaturated FA-containing DG and PC species, and an increased relative abundance of monounsaturated FA-containing DG and PC species in the gastrocnemius muscle of 10-week-old male obese *ob/ob* mice compared with lean wild-type C57/BL6 mice [174]. A reduction in polyunsaturated FA in skeletal muscle phospholipids can lead to changes in membrane fluidity [175], resulting in decreased insulin sensitivity [176].

4.4.7.4 The *db/db* phenotype is strongly associated with early elevations in fasting plasma phosphatidylinositol species

There was already an early significant increase in total PI and 12 of 15 measured PI species in fasting plasma in six week old male *db/db* mice compared with corresponding *H/H* mice, but this strong effect on PI was slightly attenuated by 10 weeks of age (Figure 4.13, Table S4.5 and Figure 4.21). A similar elevation of total PI was evident in female *db/db* mice at 6 and 10 weeks of age, but this effect had almost dissipated by 16 weeks of age (Figure 4.16 and Table S4.10).

In agreement with our findings, Meikle *et al.* found that T2D and prediabetes were positively associated with total PI and most PI species (including many 20:4 FA-containing PI species) in two large human cohort studies [9]. In another study, Meikle *et al.* found that stable coronary artery disease was positively associated with total PI and some PI species, including some 20:4 FA-containing PI species [10]. PE and PI species containing arachidonic acid (20:4) are primary substrates for the production of proinflammatory eicosinoids, including prostaglandins. Many of the significantly elevated plasma PI species in our *db/db* mice were also 20:4 FA-containing PI species. In male C57BL/6 mice fed a high-fat diet for 14 weeks, fasting serum total monounsaturated PI was significantly elevated compared with age-matched low fat-fed mice [27]. In addition, the low abundant PI 34:1 remained positively correlated with fasting serum

glucose and proinsulin after adjusting for body weight, suggesting that PI 34:1 may be a negative modulator of glucose homeostasis and/or insulin signalling. Therefore, the early elevation of plasma PI 34:1 in the six week old male and female *db/db* mice may serve as a biomarker for insulin resistance and/or glucose intolerance prior to the onset of obesity. PI and PI-phosphates are also a major source of DGs, which serve as negative modulators of insulin signalling [177].

4.4.7.5 Minor glycerophospholipids are differentially regulated in liver and left-ventricle in *db/db* mice

As yet, no studies have examined individual PI, PG and BMP species in metabolic tissues in models of lipid oversupply, obesity and/or T2D. In liver, four of eight PI species (including 20:4 FA-containing PI 38:2, PI 40:4 and PI 40:5) and BMP 18:1/18:1 were significantly elevated in male *db/db* mice at 10 weeks of age (Table S4.1 and Figure 4.22). Similarly, there was an early elevation of the same three liver PI species and BMP 18:1/18:1 in the six week old female *H/H* mice, but this effect had almost disappeared by 10 weeks of age (Table S4.6). These findings indicate that altered hepatic arachidonic acid metabolism may also contribute to the proinflammatory state in *db/db* mice.

In left-ventricle, three PI species, two PG species and BMP 18:1/18:1 were significantly elevated in the ten week old male *db/db* mice, but this effect was blunted by 16 weeks of age (Table S4.3). In contrast, total PI along with six PI species and three PG species (PG 34:2, PG 36:2 and PG 36:3) were already significantly elevated in left-ventricle in the six week old female *H/H* mice (Figure 4.12 and Table S4.8). This effect was sustained at 10 weeks of age, but had almost vanished by 16 weeks of age. PG is the biosynthetic precursor of mitochondrial-specific immature CL, leading to the generation of mature CL [124], and there was marked CL remodelling in left-ventricle in *db/db* mice at 6 and 10 weeks of age (Figure 4.23). The elevation of BMP 18:1/18:1 levels in liver, adipose and left-ventricle in male *db/db* mice at 10 weeks of age is also of interest, given that the plasma concentration of BMP 18:1/18:1 (located primarily within the endosomal/lysosomal membranes of cells) was significantly elevated in patients with lysosomal storage disorders involving storage in macrophages and/or with hepatomegaly compared with control plasmas [178].

4.4.8 Cardiolipin remodelling is associated with oxidative stress, obesity and diabetes

Cardiolipins (CL) are mitochondrial membrane phospholipids (diphosphatidylglycerols) found in metabolic tissues such as heart, liver and skeletal muscle that are required for oxidative phosphorylation and normal mitochondrial function, including the maintenance of the mitochondrial membrane proton gradient and activities of mitochondrial enzymes and proteins [179,180]. The biological function of CL is determined by the composition of its fatty acyl (FA)-chains. The predominant 18:2-rich FA composition within CL species is believed to be achieved by an acyl-chain remodelling process [124].

Obesity and diabetes are associated with systemic oxidative stress, a primary causative factor of IR, which is characterized by increased reactive oxygen species (ROS) production [181,182,183]. Elevated levels of ROS induce CL peroxidation and pathological remodelling of CL, resulting in a loss of the predominant CL species, CL 18:2/18:2,18:2/18:2, and replacement of linoleic acid (18:2n-6) with polyunsaturated FAs, mainly DHA (22:6n-3) [64,184]. The increased DHA content in CL stimulates mitochondrial membrane potential and proton leakage, and renders CL highly sensitive to oxidative damage, leading to increased cell oxidant production [185,186], further lipid peroxidation, mitochondrial dysfunction, and metabolic complications associated with diabetes.

4.4.8.1 Left-ventricle cardiolipin remodelling in *db/db* mice is associated with obesity, insulin resistance and diabetes

There was an early trend towards elevation of two left-ventricle 16:1 FA-containing CL species and reduction of two 22:6 FA-containing CL species in the six week old mildly obese/glucose intolerant male *db/db* mice (Table S4.3). These CL remodelling effects were consolidated at 10 weeks of age, but attenuated by 16 weeks of age, with only CL 18:2/18:1,18:2/16:1 remaining significantly higher in the now severely obese/diabetic male *db/db* mice. The three left-ventricle 16:1 FA-containing CL species and, surprisingly, CL 18:2/18:2,18:2/18:2 were already significantly elevated in the six week old IR female *db/db* mice prior to the onset of obesity (Table S4.8). By 10 weeks of age, this CL remodelling effect had intensified, with the CL subclass, along with seven CL species being significantly elevated, but CL 18:2/18:1,18:2/22:6 and CL 18:2/22:6,18:2/20:3 being significantly lower in the now mildly obese/IR female *db/db*

mice (Figure 4.15 and Table 4.11B). However, by 16 weeks of age, only two 16:1 FA-containing CL species remained significantly higher in the female *db/db* mice.

Our findings of elevations of 16:1 FA-containing CL species in left-ventricle in six and ten week old male and female *db/db* mice (Tables S4.3 and S4.8) were similar to those observed in the myocardium of male *ob/ob* mice at two months of age (the onset of IR), in which the content of CL 18:2/18:2,18:2/16:1 was significantly elevated compared with age-matched wild-type C57BL/6 mice [64]. However, our findings of reductions in left-ventricle 22:6 FA-containing CL species in *db/db* mice, and elevation in left-ventricle CL 18:2/18:2,18:2/18:2 in female *db/db* mice contrast with those of Han *et al*., who found a progressive redistribution from the abundant 18:2 FA-containing CL species (including CL 18:2/18:2,18:2/16:1) to 22:6 FA-containing CL species in the myocardium of genetically obese male *ob/ob* mice at two to four months of age (onset of hyperglycaemia) [64]. In another study, treatment of male obese/diabetic (NZO x NON) mice with rosiglatazone, an insulin-sensitising drug, caused substantial remodelling of heart CL, resulting in a significant elevation of 18:2n-6 content, but a significant reduction in 22:6n-3 content in CL [184]. ALCAT1, an acyltransferase that catalyzes the reacylation of lyso-CL species to mature CL species using acyl-FA chains donated by acyl CoA [124], has been shown to be involved in the pathological remodelling of CL in response to early oxidative stress associated with mitochondrial dysfunction, obesity and diabetes [187].

4.4.8.2 Left-ventricle cardiolipin remodelling in *db/db* mice is associated with increased hepatic *de novo* lipogenesis

The early onset of left-ventricle CL remodelling in our *db/db* mice (i.e., elevation of 16:1 FA-containing CL species, and reduction in 22:6 FA-containing CL species) emphasises the susceptibility of CL species to the early oxidative stress (ROS production) and peroxidation that accompanies mild obesity and IR, but also reflects the increased 16:1 FA pool (from the diet-induced increase in hepatic lipogenesis; Figures 4.19 and 4.20) and decreased 22:6 FA pool (induced by the type of diet, obesity and IR) in *db/db* mice. The elevated levels of 16:1 FA-containing CL species in male and female *db/db* mice at 6 and 10 weeks of age corresponded to elevated levels of the donor *sn*-2 acyl-16:1 FA-containing PC species (PC 32:1, PC 32:2 and PC 34:2), and the lower levels of 22:6 FA-containing CL species corresponded to lower levels of donor *sn*-2 acyl-22:6 FA-containing species (PC 38:6b, PC 40:6 and PE 40:6) (Figure 4.10).

However, left-ventricle CL remodelling was severely attenuated in both male and female *db/db* mice by 16 weeks of age (Tables S4.3 and S4.8), which corresponded to a blunting in surrogate measures of hepatic lipogenesis both in liver (Figure 4.19) and plasma (Figure 4.20). This indicates that increased caloric intake by the progressively more obese and IR *db/db* mice may repress hepatic *de novo* lipogenesis [50], thereby reducing the availability of FAs for CL remodelling at 16 weeks of age. There is also an increased reliance of the heart on fatty acid oxidation with increasing severity of disease in *db/db* mice [77], which leads to increased generation of ROS, and further lipid peroxidation [181,188].

4.4.8.3 Cardiolipins undergo remodelling in liver and skeletal muscle of *db/db* mice

Substantial CL remodelling also occurred in other tissues (liver and skeletal muscle) in the *db/db* mice, indicating early oxidative stress and mitochondrial dysfunction. Similar to the CL findings in left-ventricle, there were elevations in 16:1 FA-containing CL species in liver (Figure 4.8 and Table S4.1) and skeletal muscle (Table S4.2), and reductions in 22:6 FA-containing CL species in skeletal muscle of male *db/db* mice. Notably, there was a lowering of CL 18:2/18:2,18:2/18:2 in the liver of both male and female *db/db* mice, which was similar to the findings in the myocardium of male *ob/ob* mice at three and four months of age (with the onset of hyperglycaemia) [64]. There was also a significant age effect on some liver CL species in male *db/db* mice at 16 versus 10 weeks of age, which may have negated the significant genotype effect (*db/db* vs. *H/H*) seen in these CL species at 10 weeks of age (Table S4.1).

4.4.9 Ether- and vinyl ether-linked phospholipids are differentially regulated in plasma and tissues of *db/db* mice

There is no published literature that has examined ether-linked and/or ether vinyl-linked phospholipids in *db/db* mice or other animal models of obesity/diabetes. Therefore, our findings of elevated plasma PC(O), PC(P) and PE(P) lipids (Figure 4.21), lower liver PC(O), PC(P) and PE(O) lipids (Figure 4.22), marked lowering of adipose PC(O), PC(P), PE(O) and PE(P) lipids, gradual lowering of PC(O), PC(P) and PE(P) lipids in skeletal muscle of *db/db* mice, and mixture of elevated and reduced PC(O), PC(P), PE(O) and PE(P) lipids in left ventricle (Figure 4.23) relative to *H/H* mice are unique.

The early trend for elevated plasma ether-linked (PC(O) and PE(O)) and vinyl-ether linked (PC(P) and PE(P)) phospholipids in the six week old mildly obese/glucose intolerant male *db/db* mice (Table 4.13A) was accompanied by significantly elevated total PC levels, probably resulting from the over-production of hepatic VLDL induced by *de novo* lipogenesis (Table S4.5; Figures 4.19 and 4.20). In contrast, there was a delayed elevation of five plasma PC(O) and two PC(P) species (most containing 16:1 FA) in the mildly obese/IR female *db/db* mice at 10 weeks of age, which was accompanied by significant elevations in total PC and PE levels (Table 4.13B and Table S4.10).

In contrast to plasma levels, there was a delayed trend for lower liver total PC(O) and PC(P) levels in the 10 week old obese/IR male *db/db* mice (Figure 4.7). By 16 weeks of age, total PC(P) and PE(P), along with four PC(O) species and six of nine PC(P) species were significantly lower in the now severely obese/pre-diabetic male *db/db* mice (Table S4.1), which was accompanied by the significant lowering of 14 liver PC and 7 PE species (most containing 16:1 FA), and a significant blunting of hepatic lipogenesis in male *db/db* mice (Figure 4.19). In contrast, liver PC(O) and PC(P) subclasses were already significantly lower in the six week old non-obese/IR female *db/db* mice, and this effect was sustained at 10 weeks of age (Figure 4.14; Table 4.9B and Table S4.6). Despite timing differences relating to the onset of abnormalities in male versus female *db/db* mice, it is clear that ether-linked phospholipids and vinyl ether-linked plasmalogens were elevated in plasma, and reduced in liver relative to *H/H* mice.

Similar to our findings, Graessler *et al.* found that two PE(P) plasmalogen species were significantly elevated in fasting plasma in obese men compared with leaner men [28]. Moreover, Donovan *et al.* found that five PC(O) species (including the arachidonic acid containing PC(O-18:0/20:4) and PE(P-18:0/20:4)) were elevated in morbidly obese subjects (mean BMI 49.9 kg/m^2) compared with lean subjects (mean BMI 25.8 kg/m^2), and that treatment of human coronary artery endothelial cells with the plasmalogen PE(P-18:0/20:4) induced expression of cell adhesion molecules, indicative of endothelial cell activation and atherogenesis [63]. Recently, Heilbronn *et al.* observed elevations in fasting plasma PE(P) and PE(O) subclasses in response to 28 days overfeeding by 1250 kcal/day (45% total energy as fat) in healthy adults [54]. In these studies, plasmalogens may function as free radical scavengers, being preferentially synthesized as an antioxidant in response to increasing oxidative stress associated with obesity and short term overfeeding [189].

Conversely, young adult monozygotic obese co-twins had decreased levels of fasting serum ether-linked phospholipids compared with non-obese co-twins [29], and both prediabetes and T2D were negatively associated with fasting plasma PC(O) and PC(P) subclasses [9]. Furthermore, Floegel *et al.* revealed that five baseline serum polyunsaturated acyl-alkyl-PC(O) species (PC(O-34:3), PC(O-40:6), PC(O-42:5), PC(O-44:4) and PC(O-44:5)) were independently associated with decreased risk of T2D [148]. In these studies, decreased plasmalogen levels in obesity, prediabetes and T2D were considered indicators of oxidative stress. It is likely that the severity of disease and milieu in each individual may explain the large discrepancies seen in relative abundance, pattern of change, and effects induced by ether-linked PC(O) and PE(O) and plasmalogen PC(P) and PE(P) species in different human cohorts [63].

Given that the vinyl ether linkage of the PC(P) and PE(P) plasmalogens is particularly susceptible to oxidation by reactive oxygen species [119], and obesity and IR are linked to oxidative stress, our finding of significantly lower plasmalogen levels in liver, adipose and skeletal muscle (but not plasma) of *db/db* mice at 10 and 16 weeks of age may be due to increased free radical attack of the vinyl-ether bond by ROS. Although the ether linkage of the ether phospholipids PC(O) and PE(O) is not susceptible to oxidation, species containing polyunsaturated fatty acids are susceptible to oxidative modification [9]. We found that many polyunsaturated FA-containing PC(O), PC(P) and PE(P) species were significantly lower in skeletal muscle of our female *db/db* mice. The lower levels of PC(O), PC(P) and PE(P) species observed in the tissues of our *db/db* mice may also relate to decreased biosynthesis [189].

4.4.10 Early elevation of lysophospholipids in plasma of *db/db* mice

In our mouse study, both plasma total LPC and LPE, along with ten LPC species (including LPC 16:0, LPC 16:1, LPC 18:0, LPC 18:1 and LPC 20:5), LPE 16:0 and LPE 18:0 were already significantly elevated in six week old mildly obese/glucose intolerant male *db/db* mice compared with corresponding *H/H* mice, and the strong LPC outcome was sustained at 10 weeks of age (Table 4.13A; Figure 4.13 and Table S4.5). Total LPE (and almost total LPC), along with LPC 16:1, LPC 18:1 and LPC 20:5 were also already significantly elevated in six week old non-obese/IR female *db/db* mice at 6 weeks of age but this effect had almost dissipated by 10 weeks of age, although LPC 16:1 remained significantly elevated (Table 4.13B; Figure 4.18 and Table S4.10).

Similar to our findings in fasting plasma of male *db/db* mice, Pietilainen *et al.* found that young adult monozygotic obese co-twins had increased levels of five fasting serum LPC species compared with non-obese co-twins (including LPC 16:0, LPC 18:0 and LPC 18:1), and that LPC 16:0 and LPC 20:4 were negatively correlated with insulin sensitivity, independent of genetic factors [29]. Kim *et al.* showed that overweight/obese IR men had elevated fasting plasma LPC 14:0 and LPC 18:0, and lower LPC 18:1 levels compared with lean men, and concluded that the amount of saturated fat in the diet may influence the degree of saturation of the acyl-linked FA on plasma LPC [48]. Furthermore, Meikle *et al.* showed that several LPC species (mostly saturated and monounsaturated LPC species) were significantly elevated in subjects with prediabetes compared with NGT subjects [9]. Another study showed that elevated LPC levels in young pigs with early obesity were associated with endothelial dysfunction and oxidative stress [57]. The early elevation of plasma LPC 16:0, LPC 16:1, LPC 18:0 and LPC 18:1 in our mildly obese (almost hyperinsulinaemic) male *db/db* mice may reflect the increased hepatic *de novo* lipogenesis (Figures 4.19 and 4.20), as lysophospholipids are derived from the oxidation of polyunsaturated (particularly 20:4 and 22:6)-containing vinyl ether-linked plasmalogens, PC(P) and PE(P), but are also products of PC and PE hydrolysis by secretory phospholipases [54,63]. In particular, LPCs can induce endothelial cell expression of cell adhesion molecules [59] and inhibit hepatic fatty acid oxidation in mitochondria [60].

In contrast to our findings in *db/db* mice, Barber *et al.* showed a significant reduction in many fasting plasma LPC species in obese/insulin sensitive and obese/T2D subjects compared with lean healthy subjects, and found that fasting circulating LPCs were negatively associated with both BMI and plasma insulin levels [26]. Circulating LPC levels were also found to be decreased in glucose intolerant individuals [53], and Floegel *et al.* revealed that baseline serum LPC 18:2 was independently associated with decreased risk of T2D [148]. Moreover, Barber *et al.* found a significant reduction in eight LPC species (including LPC 16:0, LPC 16:1 and LPC 18:1), but a significant rise in LPC 18:0 and LPC 20:4 in fasting plasma in male C57BL/6J mice fed a high-fat diet for 12 weeks (versus mice fed a low-fat diet) [26]. Barber *et al.* concluded that diet was more important than IR and adiposity in determining circulating LPC levels in high-fat fed mice. In another study, circulating LPC levels were decreased in mice with non-alcoholic steatohepatitis [190].

Unlike the low fat/high-carbohydrate diet fed to our *db/db* mice, which activates hepatic *de novo* lipogenesis to compensate for the lack of dietary 16:1 FA, high-fat diets repress hepatic *de novo*

lipogenesis [47]. Therefore, the diet, and probably the genotype of the animal, is critical in determining the types of changes in plasma LPC levels in rodent models of obesity. The early elevation of plasma and liver LPC 16:1 in our *db/db* mice may serve as a biomarker of increased hepatic *de novo* lipogenesis.

4.4.10.1 Lysophospholipids are differentially regulated in liver, adipose and skeletal muscle in *db/db* mice

In the mouse study, there was little elevation of LPC and LPE levels in the liver of six week old male *db/db* mice (Figure 4.7). However, by 10 weeks of age, liver total LPE subclass (and almost total LPC), including LPC 16:1, LPC 18:1, LPC 18:2 and all five LPE species were significantly elevated, and these LPC and LPE outcomes were sustained in the now severely obese/pre-diabetic male *db/db* mice at 16 weeks of age (Table 4.9A; Figure 4.7 and Table S4.1). Although liver LPC 16:1 and LPC 18:2 were significantly elevated in six week old female *db/db* mice, only LPC 16:1 remained significantly elevated at 10 weeks of age (Table S4.6). Therefore, the delayed elevations in liver LPC and LPE subclasses were associated with the more severe pathology seen in the male *db/db* mice. We also found a significant lowering of total LPC and LPE levels in adipose, and a significant elevation of some LPC species in skeletal muscle (but not left-ventricle) in male *db/db* mice.

Similar to our findings in *db/db* mice, Han *et al.* showed that liver and skeletal muscle LPC levels were elevated in *db/db* mice, and lowering tissue LPCs ameliorated IR and diabetes in these mice [191]. LPC has also been shown to inhibit the insulin signaling pathway in rat vascular smooth muscle by impairing IRS-1 tyrosine phosphorylation [192]. Our decisive findings of elevated total LPC and LPE in liver and lowering of total LPC and LPE in adipose of male *db/db* mice differ from those of Barber *et al.* who showed that very few LPC species were significantly altered in liver, skeletal muscle and adipose tissue in C57BL/6J mice fed a high-fat diet for 12 weeks [26]. Given that dietary FAs influence the lipidomic profile by activating specific transcription factors that regulate inflammatory and metabolic genes [49], and that the *db/db* mice were fed an unrestricted standard chow diet and are genetically predisposed to obesity and diabetes, it is not surprising that our LPC results in plasma and tissues differ from those observed in high-fat induced obese rodents.

4.4.11 Conclusion

In the present study, targeted lipid profiling using LC ESI-MS/MS and MRM experiments in positive-ion mode was employed to characterise temporal (6, 10 and 16 weeks of age) and tissue-specific (plasma, liver, skeletal muscle, left-ventricle and adipose) changes among 25 lipid classes/subclasses representing ~330 species in male and female *H/H*, *db/h* and *db/db* mice (C57BL/KsJ background), an established genetic model of IR, obesity and T2D. This included the development of methodology to characterise a further 60 lipid species from the PE, LPE, PE(O), PE(P) and CL classes implicated in the pathogenesis of T2D (Chapter 3).

Overall, the phenotype associated with progression to diabetes was similar in male and female *db/db* mice, but obesity occurred earlier in male *db/db* mice. The failure of elevated fasting plasma insulin and HOMA-IR levels to reach statistical significance in the six week old male *db/db* mice was related to the high inter-animal variance in these measurements, possibly due to the more unstable male *db/db* phenotype. The severe obesity observed in the *db/db* mice at 16 weeks of age was not accompanied by the expected lack of insulin secretion or severe hyperglycaemia, indicating that these mice were pre-diabetic, with an increased risk of developing diabetes.

The independent effect of the *db/db* genotype on plasma and tissue lipid abnormalities was clearly superior to the independent effects of gender or age in the majority of cases. Therefore, the lipid abnormalities in seven main lipid groups (as defined in section 4.3.8) were examined in greater detail in male and female *db/db* mice (versus corresponding *H/H* mice). The *db/db* mouse phenotype was characterised by early elevations of CE, DG and TG lipids in fasting plasma and/or liver by six weeks of age. This was accompanied by the early elevation of hepatic *de novo* lipogenesis in *db/db* mice (measured by elevated ratios of total 16:1/18:2 in DG and TG species in liver and plasma) to compensate for the lack of dietary 16:1 FA, resulting in ectopic deposition of excess fatty acids as TG and DG in left-ventricle and skeletal muscle. However, hepatic *de novo* lipogenesis was significantly attenuated in male *db/db* mice by 16 weeks of age, resulting in a depleted circulating pool of 16:1 FA, and compromised membrane fluidity and transmembrane receptor/enzyme activity [159].

The elevation in fasting plasma total Cer, MHC and (almost) SM in our six week old mildly obese/glucose intolerant male *db/db* mice occurred prior to the onset of IR. There was also a

strong elevation of the PC subclass in fasting plasma of six week old male and female *db/db* mice. Importantly, the same PC species that predicted T2D risk in human studies were positively associated with the early onset of obesity and IR in our *db/db* mice. However, most of the PC species that were significantly decreased in liver, skeletal muscle and left-ventricle in male *db/db* mice contained an odd-numbered carbon FA (15:0 or 17:0). There was also an early elevation in the total PI subclass and most PI species in fasting plasma in six week old *db/db* mice. In this regard, PI species containing arachidonic acid (20:4) are primary substrates for the production of proinflammatory eicosinoids, including prostaglandins. The elevation of BMP 18:1/18:1 levels in liver, adipose and left-ventricle in male *db/db* mice may reflect abnormalities in the repackaging and storage of lipid nutrients in endosomal/lysosomal membranes of cells.

The early onset of left-ventricle CL remodelling in our *db/db* mice (i.e., elevated levels of 16:1 FA-containing CL species and lower levels of 22:6 FA-containing CL species) mirrored the changes seen in specific donor *sn*-2 16:1 FA-containing PC species (PC 32:1, PC 32:2 and PC 34:2), and *sn*-2 22:6 FA-containing species (PC 38:6b, PC 40:6 and PE 40:6), and was associated with elevations in specific precursor PG species, hepatic *de novo* lipogenesis, and the TG subclass. Early CL remodelling also occurred in liver and skeletal muscle in our *db/db* mice, highlighting the susceptibility of CL species to the early oxidative stress (production of reactive oxygen species) and peroxidation associated with mild obesity and IR.

Ether-linked phospholipids and vinyl ether-linked plasmalogens were found to be elevated in fasting plasma, and reduced in liver, adipose and skeletal muscle of *db/db* mice relative to *H/H* mice, which mirrored the changes seen in PC and PE species. These changes indicate an increased susceptibility of these lipids to oxidative modification (or decreased biosynthesis) in tissues with increasing severity of disease. Furthermore, the early elevation of plasma LPC 16:0, LPC 16:1, LPC 18:0 and LPC 18:1 in our mildly obese (almost hyperinsulinaemic) male *db/db* mice may reflect the low-fat diet induced increase in hepatic *de novo* lipogenesis, as lysophospholipids are derived from the oxidation of ether-linked and ester-linked phospholipids. In addition, the delayed elevations of total LPC and LPE in liver, and elevation of some LPC species in skeletal muscle in the male *db/db* mice supports a role for LPCs in proatherogenesis and IR.

The biological and physiological important and novel findings related to the tissue-specific and temporal lipid abnormalities associated with the development of obesity, IR and pre-diabetes in

C57BL/KsJ male *db/db* mice fed an unrestricted standard chow diet can be summarised as follows. Initially, the early trend for the elevation of liver total CE, DG and TG (steatosis) at six weeks of age was due to diet-induced elevation of hepatic *de novo* lipogenesis in the presence of leptin receptor deficiency, reduced energy expenditure, mild obesity, hyperinsulinaemia, oxidative stress and increased adipose fat mass (hyperplasia). This increased lipogenesis was reflected by the increased availability of circulating 16:1 FA, and resulted in ectopic deposition of excess fatty acids as TG, and its putative product DG, in peripheral tissues (left-ventricle and skeletal muscle), and early CL left-ventricle remodelling, compromising mitochondrial membrane integrity. Elevated hepatic lipogenesis also contributed to a significant elevation of fasting total Cer and MHC, total PC (with six elevated PC species known to be predictive of T2D in human studies), total PI plasma (including the elevation of many 20:4 FA-containing PI species that act as primary substrates for the production of proinflammatory eicosinoids), and elevated hepatic "saturated" DG species (negative modulators of insulin signalling) that corresponded to the onset of IR at 10 weeks of age. Additionally, plasma total LPC and LPE (including many saturated and monosaturated species) were already elevated in male *db/db* mice at six weeks of age, suggesting early oxidative stress and inflammation. Specifically, elevated plasma and liver LPC 16:1 may serve as a biomarker for increased hepatic *de novo* lipogenesis.

With increasing severity of disease (severe obesity, hyperinsulinaemia and IR), there was a significant blunting of hepatic lipogenesis in male *db/db* mice, which resulted in a significant lowering of liver PC and PE species (most containing 16:1 FA), a significant lowering of ether- and vinyl-ether linked phospholipids levels in liver (mainly due to increased free radical attack by ROS), and reduced CL remodelling in tissues due to peroxidation and reduced availability of acyl-FA from donor PC and PE species. This pattern of CL remodelling illustrated that the male *db/db* mice were in a dynamic phase of lipid metabolism and disease development at six and ten weeks of age, but were blunted by reduced substrate availability at 16 weeks of age. The morphological changes in adipose (omental fat) tissue with obesity (increased cell size and number of lipid droplets) and normalisation of lipid measurements to protein content are most likely to explain the significant elevation of TG and DG, and significant lowering of sphingolipid and phospholipid classes/subclasses in *db/db* mice relative to *H/H* mice.

As the *db/db* genetic mouse model closely resembles disease progression to T2D in humans, the myriad of temporal and tissue-specific lipid abnormalities described in this chapter should be translatable to the lipid abnormalities associated with human obesity, IR and T2D. These

lipidomic studies provide an invaluable insight into the differential regulation of lipid metabolic pathways in plasma and metabolic tissues with increasing severity of disease, and provide the opportunity to identify new therapeutic targets for early detection and prevention of disease progression. Importantly, many of the 60 lipid species of PE, LPE, PE(O), PE(P) and CL classes that were included for measurement in the *db/db* mouse study based on method development (Chapter 3) were shown to contribute to disease progression, and provide vital links to the advancement of knowledge in this field.

CHAPTER 5 RELATIONSHIP BETWEEN GLOBAL GENE EXPRESSION AND LIPID PROFILES IN A MOUSE MODEL OF TYPE 2 DIABETES

5.1 INTRODUCTION

5.1.1 The genetic *db/db* mouse model resembles human type 2 diabetes

The Australian population and indeed most of the developed world are facing an obesity epidemic, which is associated with a dramatic increase in the incidence and prevalence of type 2 diabetes (T2D) [1,2]. Therefore, there is an urgency to discover the underlying mechanisms and metabolic pathways involved in the pathogenesis of T2D so that better preventative and therapeutic options can be tested and implemented to arrest this burgeoning health problem. The monogenic leptin receptor-deficient *db/db* mouse (C57BL/KsJ background) is a suitable model to study the pathogenesis of T2D [73], as it closely resembles disease progression to T2D in humans, which is mainly characterised by insulin resistance (IR) (increased hepatic glucose production and decreased peripheral glucose utilization), obesity and hyperglycaemia [74,75]. Disease progression in the *db/db* mouse includes early hyperinsulinaemia and IR by 5 weeks of age, followed by progressive obesity, hyperglycaemia, hyperlipidaemia (elevated plasma non-esterified fatty acids and triglyceride levels), and a gradual loss of pancreatic function (insulin secretion) resulting in low circulating insulin and high glucose levels by 16 weeks of age [81,85,140,141,142,143,144].

5.1.2 Identification of genes associated with lipid abnormalities in *db/db* mice

In this chapter, we aimed to employ global gene expression profiling (using DNA microarray) to identify transcriptional differences at the gene and metabolic pathway/diabetes-specific disease states level that may explain the mechanisms for the lipidomic abnormalities observed in tissues and plasma in the C57BL/KsJ *db/db* mouse model of obesity, IR and pre-diabetes (Chapter 4).

Comprehensive statistical analyses of targeted lipid profiling revealed that the independent effect of the *db/db* mouse genotype in tissues and plasma was clearly more dominant than the independent effects of gender or age on global lipid profiles (Chapter 4, Table 4.8). More specifically, five lipid classes/subclasses were significantly elevated, and 102 species were

statistically different in livers of obese/IR male *db/db* compared with male *H/H* mice at 10 weeks of age (Chapter 4, Table 4.9A and Table S4.1). In addition, nine lipid classes/subclasses and 100 species were statistically different in livers of severely obese/diabetic male *db/db* compared with male *H/H* mice at 16 weeks of age. Therefore, approximately 45% of the 227 lipid species quantified in liver were statistically different in male *db/db* mice at 10 and/or 16 weeks of age, which reflects the pre-diabetic phenotype.

Furthermore, surrogate measures of hepatic *de novo* lipogenesis (i.e., total 16:1/18:2 ratios in liver DG and TG species) were found to be markedly elevated in the male *db/db* mice compared with the corresponding male *H/H* mice at both 6 and 10 weeks of age, but were attenuated by 16 weeks of age (Chapter 4, Figure 4.19). Hepatic *de novo* lipogenesis has been shown to be a significant source of fatty acids that accumulate in liver triacylglcerols (TG) and TG-rich very low density lipoprotein (VLDL) in non-alcoholic fatty liver disease patients (NAFLD) [193]. Given that high rates of hepatic *de novo* lipogenesis are induced by low-fat/high-carbohydrate diets, hyperinsulinemia and hyperglycemia [47,158], the male *db/db* mice represent an ideal model to track the relationships between liver global gene expression profiles and lipid abnormalities associated with progressive obesity, IR and pre-diabetes.

5.1.3 Role of the liver in the pathogenesis of type 2 diabetes

The liver plays a key role in glucose metabolism and homeostasis. Impaired hepatic glucose metabolism, including an increased rate of hepatic gluconeogenesis, contributes to the development of T2D [74,75,106]. Metabolic defects associated with the liver in the *db/db* mouse include increased expression of hepatic gluconeogenic enzyme genes [80], increased hepatic glycogenolytic and gluconeogenic enzyme activities [81], early defects in hepatic insulin signalling [78], inhibition of signal-transducer and activator of transcription 3 (STAT3)-dependent suppression of hepatic gluconeogenic enzymes [79], and hepatic steatosis associated with elevated stearoyl-CoA desaturase 1 (SCD1) gene expression [194]. Impaired hepatic fatty acid metabolism is also involved in the development of T2D [107,108,109], but overt T2D only becomes manifest with pancreatic β-cell insulin secretory defects.

5.1.4 Gene expression profiling tracks hepatic metabolic defects in type 2 diabetes

Gene expression profiling is a powerful tool for examining hepatic defects in specific metabolic pathways and the mechanism of action of drugs that treat T2D. Metformin, a widely used hypoglycaemic agent for the treatment of T2D, induces fatty acid oxidation, and inhibits lipogenesis and hepatic gluconeogenesis [195]. Using DNA microarray analysis to study the effects of single-dose metformin treatment on global gene expression in the livers of 8 week old obese diabetic male C57BL/KsJ-*db/db* mice, Heishi *et al.* found a reduction in hepatic glucose-6-phosphatase gene expression and enzyme activity (a key rate-limiting enzyme in gluconeogenesis), which closely correlated with reduced blood glucose levels [111]. Moreover, metformin treatment significantly altered the gene expression profiles of ten metabolic pathways, including those involved in glycolysis/gluconeogenesis, the citrate cycle, fatty acid and glycerolipid metabolism, and amino acid metabolism. Recently, Zhang *et al.* compared gene expression profiling in the livers of 9 week old male wild-type C57BL/6 and male diabetic *db/db* mice, and found that the upregulated genes were mainly enriched in lipid and fatty acid metabolic processes, and the downregulated genes were mainly enriched in immune-related processes [110]. More detailed pathway network analyses revealed that the fatty acid oxidation and storage pathways (but not fatty acid synthesis) along with glycolysis, gluconeogenesis and glycogenolysis were enhanced, and that the hepatic local immune response, liver cancer and hepatitis were most likely associated with diabetes in the diabetic *db/db* mice [110].

5.1.5 Tracking of gene expression and lipid profiling abnormalities in *db/db* mice

These studies in *db/db* mice provide valuable insights into how particular drug treatments and disease states influence hepatic gene expression profiling and specific metabolic pathways. It would also be highly beneficial to sequentially track the gene expression profiles and simultaneous lipid abnormalities associated with the onset of obesity, IR and progression to T2D in obese/diabetic *db/db* mice to define the underlying changes in gene expression and metabolic pathways associated with the pathogenesis of T2D.

In the present study, we tested the hypothesis that transcriptional gene regulation results in lipidomic abnormalities observed in liver in the C57BL/KsJ *db/db* mouse model of obesity, IR and pre-diabetes (Chapter 4). DNA microarrays were used to compare mouse whole-genome gene expression profiles from livers of male *db/db* mice (C57BL/KsJ background) and their corresponding male *H/H* littermates at 6, 10, and 16 weeks of age. The gene expression

abnormalities identified in male *db/db* mice were compared with lipid abnormalities identified in the same liver sample by targeted lipid profiling (LC ESI-MS/MS) to identify lipid metabolic pathways and diabetes-specific genes associated with disease progression. This strategy may identify specific gene candidates or lipid classes/species as potential therapeutic targets for early prevention or treatment of human obesity, IR and T2D.

5.2 MATERIALS AND METHODS

5.2.1 Global gene expression profiling in mouse liver using DNA microarrays

For DNA microarray analysis, we wanted to maximise the statistical power achieved for each group comparison. Based on the strength of the lipid metabolic dysfunction seen in the liver of male *db/db* mice, coupled with the level of technical noise, data quality, expression variance and statistical robustness associated with mouse whole-genome gene expression BeadChips comprising 45281 probes, a total of 36 liver samples, consisting of six liver samples from each of six groups (male *db/db* versus male *H/H* mice at 6, 10 and 16 weeks of age) were selected for DNA microarray analysis. This strategy may identify candidate genes associated with progression to T2D which are translatable to comparable human disease cohorts.

5.2.2 Preparation of mouse liver samples for total RNA extraction

The collection of liver samples from 6 h fasted anaesthetized mice at the time of cull has been described previously (Chapter 4, section 4.2.3). The cryomilling of frozen mouse liver (0.4-1.8 g wet weight) into a fine homogenous powder for subsequent targeted lipid profiling and gene expression profiling has been described previously (Chapter 2, section 2.2.1).

Total RNA was extracted from ~30-50 mg frozen liver powder with 1 ml ice-cold TRIzol® reagent (Invitrogen™, Life Technologies, Thermo Fisher Scientific Inc. MA, USA). The powder was resuspended by rigorously vortexing at room temperature for 3 min, incubated at room temperature for 3 min to permit complete dissociation of the nucleoprotein complex, and centrifuged at 14,000 g for 5 min at 4^{o}C. Chloroform (0.2 ml) was added to the supernatant, and the mixture was vortexed for 45 sec, incubated at room temperature for 4 min, and centrifuged (14,000 g, 15 min, 4^{o}C). The top clear aqueous layer containing the RNA was decanted, and an equal volume of 70% (v/v) aqueous ethanol was added to the supernatant, with gentle mixing.

The RNA was further purified using the RNeasy® Mini-column Qiagen Kit (QiagenPty. Ltd., Melbourne, Australia) using a series of binding, spin and wash steps according to the manufacturer's RNA Cleanup protocol instructions. The purified liver RNA sample was eluted with 30 µl RNase-free sterile water, and the quantity and quality of RNA was initially determined using a Nano-drop Bioanalyser 2100 (Agilent Technologies, CA, USA). The sample was deemed acceptable for further processing if the purity of RNA (ratio of absorbances at 260 nm versus 280 nm) exceeded 1.8, and the concentration exceeded 150 ng/µl.

To more accurately measure the purity and quality of total RNA, the purified liver RNA extracts were diluted to a calculated concentration of 70 ng/µl with RNase-free sterile water. A 2 µl aliquot was prepared for quantification (RNA HS assay) and measured at 560 nm on a Qubit fluorometer (Agilent Technologies, CA, USA). Another 3 µl aliquot was prepared and assessed for quality using a MultiNA electrophoresis Bioanalyser (Shimadzu, Columbia MD, USA). The RNA quality was deemed acceptable for microarray preparation if the ratio of the areas of the 28S strand and 18S strand exceeded 1.4, and there was little fragmentation of RNA (Figure 5.1).

5.2.3 Mouse whole-genome gene expression direct hybridization assay

5.2.3.1 First and second strand cDNA synthesis

For microarray analysis, the starting amount of purified liver total RNA used for cRNA synthesis was 300 ng, which was initially diluted to 11 µl with nuclease-free water. The Reverse Transcription Master Mix was prepared according to the Illumina® Totalprep RNA Amplification Kit instructions (Ambion®, Life Technologies, Thermo Fisher Scientific Inc. MA, USA). After gentle mixing and centrifugation, 9 µl ice-cold Reverse Transcription Master Mix was added to 11 µl purified liver RNA sample. The PCR reaction tubes were mixed, centrifuged briefly, and placed in a thermal cycler at 42°C for 2 h.

The Second Strand Master Mix was prepared on ice according to the manufacturer's protocol. After gentle mixing and centrifugation, 80 µl ice-cold Second Strand Master Mix was added to the 20 µl first strand cDNA samples generated above. The PCR reaction tubes were mixed, centrifuged briefly, and placed in a thermal cycler at 16°C for 2 h.

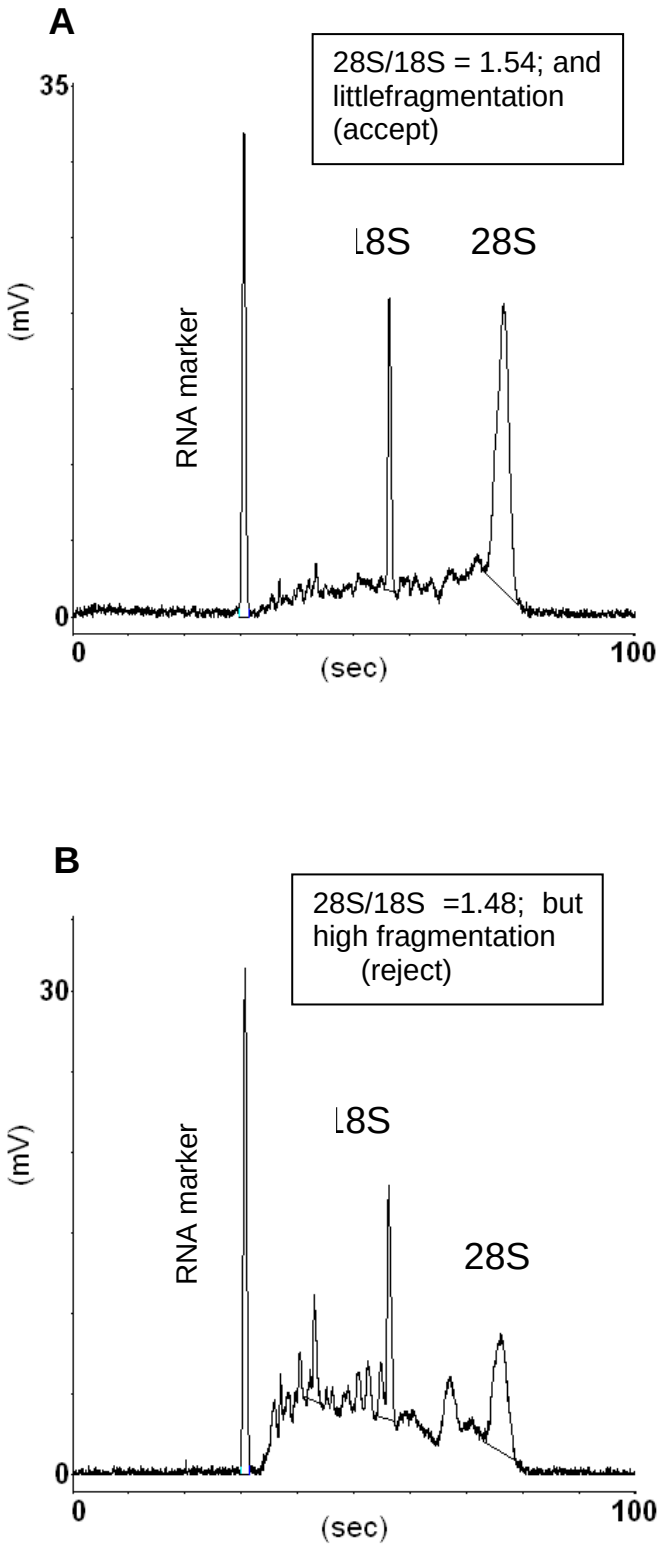

Figure 5.1 MultiNA electrophoresis Bioanalyser chromatograms of liver total RNA. Extracted and purified liver total RNA samples are accepted (A) or rejected (B) for subsequent microarray preparation if the ratio of 28S to 18S strand area > 1.4, and there is little fragmentation of the total RNA.

5.2.3.2 Double-stranded cDNA purification and synthesis of cRNA

Each 100 µl double-stranded cDNA sample generated above was transferred to a 1.5 ml microcentifuge tube containing 250 µl cDNA binding buffer, mixed well, and centrifuged briefly. This mixture was added to a cDNA filter cartridge, and centrifuged (10,000 g, 1 min, room temperature). After two wash and spin steps were performed according to the manufacturer's instructions, the double-stranded cDNA was eluted with 20 µl nuclease-free water (pre-heated to 55°C), and the entire ~17.5 µl purified cDNA sample was placed on ice. The In Vitro Transcription Master Mix was prepared at room temperature according to the manufacturer's protocol. After gentle mixing and centrifugation, 7.5 µl In Vitro Transcription Master Mix was added to the ~17.5 µl purified cDNA sample above. The PCR reaction tubes were mixed, centrifuged briefly, and placed in a thermal cycler at 37°C for 16 h. The reaction was stopped by adding 75 µl Nuclease-free water to the cRNA sample, and after mixing, the 100 µl cRNA sample was transferred to a sterile 1.5 ml eppendorf tube.

5.2.3.3 cRNA purification

Purification of cRNA was required to remove enzymes, salts and unincorporated nucleotides from the sample. Firstly, 350 µl cRNA binding buffer was added to the 100 µl cRNA sample, and 250 µl reagent grade 100% ethanol was quickly added, with gentle mixing. The 700 µl mixture was immediately added to a cRNA filter cartridge, and centrifuged (10,000 g, 1 min, room temperature). After two wash and spin steps were performed according to manufacturer's instructions, 100 µl Nuclease-free water (pre-heated to 55°C) was added to the cRNA filter cartridge. The sample was incubated at 55°C for 10 min, centrifuged (10,000 g, 2 min, room temperature), and the eluate containing the purified cRNA was collected.

5.2.3.4 Determination of cRNA purity and quantity

The purified cRNA samples were measured for both purity and quantity using a Nano-drop 2100 Bioanalyser. The minimum concentration of cRNA required for the mouse whole-genome gene expression direct hybridization assay was 150 ng/µl. When the concentration was less than 150 ng/µl, a vacuum concentrator was used to evaporate these samples at room temperature until the concentration of cRNA exceeded 150 ng/µl. Prior to hybridization, the quality of the purified

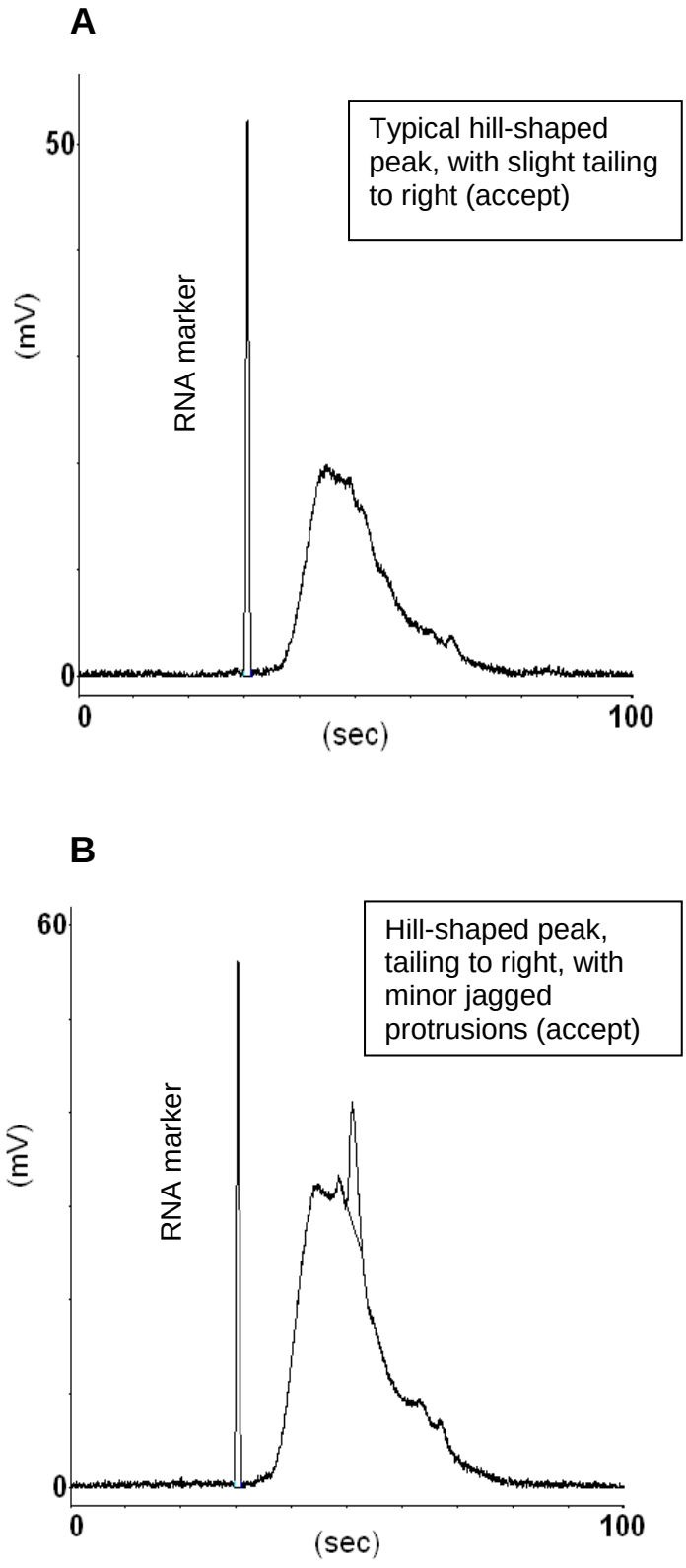

Figure 5.2 MultiNA electrophoresis Bioanalyser chromatograms of liver cRNA samples. Purified liver cRNA samples accepted for hybridization and subsequent microarray analysis. A typically shaped peak (Panel A), and a peak with minor jagged protrusions (still acceptable) is shown in Panel B.

cRNA samples was assessed using the MultiNA electrophoresis Bioanalyser. The integrity of the purified cRNA sample was achieved if the hill- shaped peak was reasonably smooth (minor jagged protrusions were allowed), with slight tailing to the right side of the peak (Figure 5.2). The integrity of all 36 purified cRNA samples on the chromatograms generated by MultiNA were deemed acceptable.

5.2.3.5 Hybridization of cRNA to whole-genome gene expression BeadChips

Six mouse whole-genome gene expression BeadChips (WG-6 version 2.0; 45,281 probes; Illumina Inc., San Diego, CA, USA) were let stand at room temperature for at least 30 min, and the barcode data from each BeadChip was downloaded onto a microarray platform (*i*Scan; Illumina Inc., San Diego, CA, USA). Prior to hybridization, exactly 1,500 ng purified cRNA was added to fresh PCR tubes. The volume was made up to 10 µl with Nuclease-free water, and 20 µl Hybridization buffer (pre-heated to 58°C for 10 min, then cooled to room temperature, and thoroughly mixed) was added. The hybridization tubes were heated in a thermal cycler at 65°C for 5 min, gently mixed, centrifuged briefly, and allowed to cool to room temperature.

The BeadChip hybridization chamber (maximum of six BeadChips) was assembled by adding 200 µl Hybridization chamber buffer to each of the reservoirs, and each BeadChip was unpacked, and placed in a gasket in the chamber. The entire 30 µl of each hybridization sample was carefully added to one allocated array of a Beadchip (six arrays per Beadchip) using a capillary motion, and the hybridization chamber was incubated in an oven at 58°C with gentle rocking for 16 h.

5.2.3.6 Washing, staining, and scanning of gene expression BeadChips

Following hybridization**,** each BeadChip was removed from the chamber, placed in 400 ml E1BC Wash buffer, and the cover-seal removed. The BeadChips were washed successively with E1BC Wash buffer, High-Temperature (55°C) Wash buffer, 100% ethanol, and Block E1 buffer according to the manufacturer's instructions. The BeadChips were incubated in 2 ml strepavidin-Cy3 staining solution (rocking at 20 rpm, 10 min, 20°C), then washed with 200 ml E1BC Wash buffer (orbital shaker at 100 rpm, 5 min, 20°C), centrifuged (275 g, 4 min, 20°C) and scanned immediately on the microarray platform, *i*Scan.

5.2.4 Liver gene expression profiling and data analysis

Each Illumina BeadChip has 6 independent arrays, each comprising a randomised mix of microscopic beads manufactured with one of 45,281 50-mer oligonucleotide probes attached. The manufacturer guarantees that each type of bead is present at least 14 times on each array and each chip is supplied with a compact disk containing files giving the coordinates of each bead containing each specific oligonucleotide probe. After hybridisation and imaging, raw data files are generated using BeadStudio software supplied by Illumina which reads each array image and summarises the expression from each of the multiple beads for each oligonucleotide and their variability. Identification and descriptive data relating to the 45,281 probes in the mouse whole-genome WG-6 version 2.0 BeadChips is found in the accompanying Excel annotated files, 'MouseWG-6_V2_0_R2_11278593_A'.xlsx and 'MouseWG-6_V2_0_R3_11278593_A'.xlsx, available from the Illumina website.

Non-differential pre-processing steps were performed ignoring the status of each sample to avoid bias. Raw expression intensities were normalised between arrays using quantile normalisation after background correction and log2 transformation in the *lumi* Bioconductor package (version 2.10.0) [196] to minimise technical sources of variation. Normalised data quality was assessed using the arrayQualityMetrics Bioconductor package (version 3.14.0) [197], which showed that all of the arrays were technically acceptable for the analyses described below. Examination of the normalised data using *lumi* suggested that 31,696 probes (about 70% of all probes) showed detectable expression at a probability of 0.01 in at least half of the arrays. Probes with expression levels below this threshold were removed from further analysis since they are likely to be uninformative. Differential expression was tested using a Bayesean moderated t-test implemented in the *limma* Bioconductor package (version 3.14.4) to compare expression levels and expression variance in the two groups at each time point [198]. Genes were considered significantly differentially expressed if the *P*-value from the moderated t-test, adjusted for multiple testing using the Benjamini-Hochberg method [155], was lower than 0.05. All Bioconductor software packages are available from the Bioconductor project at www.bioconductor.org

.

5.2.5 Strategy linking liver gene expression and lipid profiling abnormalities

To determine any associations that exist between whole-genome liver gene expression and targeted lipid profiling abnormalities in the male *db/db* mice compared with male *H/H* mice at 6, 10, and 16 weeks of age, an initial list of 1,017 mouse genes known to be associated with lipid metabolism, carbohydrate metabolism, energy metabolism and endocrine/metabolic disease pathways [using The Kyoto Encyclopaedia of Genes and Genomes (KEGG) Pathway Maps; http://www.genome.jp/kegg/] or diabetes-specific disease states such as T2D, obesity and dyslipidemias [using DisGeNET, a database of gene-disease associations; http://ibi.imim.es/DisGeNET/web/] was compiled. The DisGeNET is a database for human genes, but the matching homologous mouse genes were located using the Jackson Laboratory database website (www.informatics.jax.org/marker/MGI). However, 22 of the selected human genes from DisGeNET did not have a homologous mouse gene, and another 76 selected mouse genes were not recognised by any probe on the mouse whole-genome gene expression WG-6 version 2.0 BeadChips. Therefore, liver genes that were differentially expressed in male *db/db* mice compared with male *H/H* mice were screened against a final list of 919 mouse genes representing 20 lipid pathway/diabetes-specific disease states (Table 5.1).

5.3 RESULTS

5.3.1 Differential liver gene expression in all male *db/db* versus male *H/H* mice

To examine the effect of mouse genotype on liver gene expression profiles, we compared liver genome-wide gene expression profiles of all male *db/db* mice (n = 18) and all male *H/H* mice (n = 18), with ages combined. From a total of 31,696 detected probes, a total of 1,178 genes appeared to be significantly differentially expressed [adjusted (adj.) *P*-value < 0.05]. However, when the same gene expression was detected by more than one probe, the probe that generated the largest differential expression of that gene (i.e., smallest *P*-value) was considered. Removal of redundant probes resulted in the significant differential expression of 1,032 liver genes, of which 524 genes were significantly underexpressed, and 508 genes were significantly overexpressed in male *db/db* mice compared with male *H/H* mice (Table 5.2, Box A).

The top 24 ranked differentially expressed liver genes in all male *db/db* mice (in order of increasing adj. *P*-values) generated adj. *P*-values < 1.0E-07. Among the top 24 ranked genes

Table 5.1 919 mouse genes were compiled from the Kyoto Encyclopaedia of Genes and Genomes (KEGG) pathway maps and DisGeNET gene-disease associations databases.

Genes sourced from KEGG Pathway Maps[a] (groups 1-17):
Group 1. Genes in Fatty acid biosynthesis (4)[b]
Group 2. Genes in Fatty acid elongation (8)
Group 3. Genes in Fatty acid metabolism (29)
Group 4. Steroid biosynthesis (13)
Group 5. Genes in Steroid Hormone Biosynthesis (35)
Group 6. Genes in Glycerolipid Metabolism (27)
Group 7. Genes in Glycerophospholipid Metabolism (33)
Group 8. Genes in Ether Lipid Metabolism (34)
Group 9. Genes in Sphingolipid Metabolism (30)
Group 10. Genes in Arachidonic Acid Metabolism (28)
Group 11. Genes in Linoleic Acid Metabolism (8)
Group 12. Genes in Biosynthesis of Unsaturated Fatty Acids (8)
Group 13. Genes in Glycolysis/Gluconeogenesis (41)
Group 14. Genes in citrate Cycle (TCA Cycle) (20)
Group 15. Genes in Inositol Phosphate Metabolism (36)
Group 16. Genes in Oxidative Phosphorylation (75)
Group 17. Genes in Type II Diabetes Mellitus (25)
Genes sourced from DisGeNET gene-disease associations[c] (groups 18-20):
Group 18. Genes in Diabetes Mellitus, Type 2 (200)
Group 19. Genes in Obesity (197)
Group 20. Genes in Dyslipidemias (68)

[a] KEGG Pathway Maps genes were compiled from lipid metabolism pathways (groups 1-12), carbohydrate metabolism pathways (groups 13-15), an energy metabolism pathway (group 16), and an endocrine and metabolic disease pathway (group 17).
[b] Numbers in parentheses indicate number of genes selected in each group.
[c] DisGeNET genes were compiled from diabetes-specific disease states (groups 18-20). The DisGeNET is a database for human genes, but the matching homologous mouse genes were located using the Jackson Laboratory database website (www.informatics.jax.org/marker/MGI).

Table 5.2 Total number of differentially expressed liver genes, and the number of differentially expressed genes from 919 selected genes linked to lipid pathway/diabetes-specific disease states in male *db/db* versus male *H/H* mice.

Group comparisons at different ages
A) All male *db/db* (n=18) vs All male *H/H* mice (n=16):
Total number of differentially expressed liver genes: 1032
Number of liver genes underexpressed in male *db/db* mice: **524**
Number of liver genes overexpressed in male *db/db* mice: **508**
From selected list of 919 lipid pathway/diabetes-specific disease state genes:
Number of liver genes underexpressed in male *db/db* mice: **23**
Number of liver genes overexpressed in male *db/db* mice: **45**
B) Male *db/db* (n=5) vs. male *H/H* mice (n=5) at 6 weeks of age:
Total number of differentially expressed liver genes: 8
Number of liver genes underexpressed in male *db/db* mice: **1**
Number of liver genes overexpressed in male *db/db* mice: **7**
From selected list of 919 lipid pathway/diabetes-specific disease state genes:
Number of liver genes underexpressed in male *db/db* mice: **1**
Number of liver genes overexpressed in male *db/db* mice: **0**
C) Male *db/db* (n=6) vs. male *H/H* mice (n=6) at 10 weeks of age:
Total number of differentially expressed liver genes: 284
Number of liver genes underexpressed in male *db/db* mice: **118**
Number of liver genes overexpressed in male *db/db* mice: **166**
From selected list of 919 lipid pathway/diabetes-specific disease state genes:
Number of liver genes underexpressed in male *db/db* mice: **6**
Number of liver genes overexpressed in male *db/db* mice: **27**
D) Male *db/db* (n=7) vs. male *H/H* mice (n=5) at 16 weeks of age:
Total number of differentially expressed liver genes: 223
Number of liver genes underexpressed in male *db/db* mice: **96**
Number of liver genes overexpressed in male *db/db* mice: **127**
From selected list of 919 lipid pathway/ diabetes-specific disease state genes:
Number of liver genes underexpressed in male *db/db* mice: **11**
Number of liver genes overexpressed in male *db/db* mice: **20**

were the underexpressed genes *Igfbp2* (encodes insulin-like growth factor binding protein 2), *Socs2* (encodes suppressor of cytokine signalling 2; and is associated with obesity) and *Hsd3b5* (encodes a hydroxysteroid dehydrogenase, which regulate glucocorticoids, mediators of obesity and IR). Among the top 24 ranked genes were the overexpressed genes were *Fitm1* (encodes fat storage-inducing transmembrane protein 1, and plays a key role in lipid droplet accumulation) and Pparg (encodes peroxisome proliferator activated receptor (PPAR)-γ; controls the peroxisomal β-oxidation pathway of fatty acids, and is associated with obesity).

5.3.2 Differential liver gene expression in male *db/db* mice at each age

Genome-wide differential liver gene expression was then determined in male *db/db* mice compared with male *H/H* mice at each age group. There was only one liver gene that was underexpressed (*Irs2*; encodesinsulin receptor substrate 2), and seven genes that were overexpressed (including *Fitm1*) in male *db/db* mice compared with male *H/H* mice at 6 weeks of age (Table 5.2, Box B). This finding was similar to the targeted liver lipid profiling results, in that none of the 227 measured liver lipid species were statistically different in the two groups at 6 weeks of age (Chapter 4, Table 4.8).

In contrast, there were 284 differentially expressed liver genes in male *db/db* mice compared with male *H/H* mice at 10 weeks of age, of which 118 genes were underexpressed and 166 genes were overexpressed (Table 5.2, Box C). The top 24 ranked differentially expressed genes in 10 week old male *db/db* mice generated adj. *P*-values < 5.0E-07. Among the top 24 ranked genes were the underexpressed genes *Hsd3b5, Cyp7b1* (encodes a monooxygenase; and is part of the steroid hormone biosynthesis pathway) and *Egfr* (encodes epidermal growth factor receptor). Among the top 24 ranked genes were the overexpressed genes *Acot3 (*encodes acyl-CoA thioesterase 3; and is part of the biosynthesis of unsaturated fatty acids pathway), *Cyp17a1* (encodes a monooxygenase; and is associated with diabetes mellitus, type 2), and *Apoa4* (encodes apolipoprotein A-IV, the major protein component of HDL, is a potent activator of lecithin-cholesterol acyltransferase; and is associated with dyslipidemias). This finding compares with the targeted liver lipid profiling results, in which 102 liver lipid species were statistically different in the two groups, with 90 lipid species being significantly elevated in the 10 week old male *db/db* mice (Chapter 4, section 4.3.9.1 and Table S4.1).

At 16 weeks of age, there were 223 differentially expressed liver genes in male *db/db* mice compared with male *H/H* mice, of which 96 genes were underexpressed and 127 genes were overexpressed (Table 5.2, Box D). The top 24 ranked differentially expressed genes in 16 week old male *db/db* mice generated adj. *P*-values < 4.0E-08. Among the top 24 ranked genes were the underexpressed genes *Hsd3b5*, *Cyp7b1* and *Igfbp2*. Among the top 24 ranked genes were the overexpressed genes *Apoa4*, *Gal3st1* (encodes galactose-3-O-sulfotransferase 1; and is part of the sphingolipid metabolism pathway) and *Cyp17a1*. This finding compares with the targeted liver lipid profiling results, in which 100 liver lipid species were statistically different in the two groups, with 56 lipid species being significantly elevated in the 16 week old male *db/db* mice (Chapter 4, section 4.3.9.1 and Table S4.1).

5.3.3 Effect of ageing on differential liver gene expression in male *db/db* and male H/H mice

We next examined the effect of increasing age on liver gene expression profiles. In male *H/H* mice, there were 37 differentially expressed liver genes at 10 weeks compared with 6 weeks of age, of which 18 genes were underexpressed and 19 genes were overexpressed (data not shown). However, targeted liver lipid profiling revealed that none of the 227 measured liver lipid species were statistically different between the two groups (Chapter 4, Table 4.7). There were 39 differentially expressed liver genes in male *H/H* mice at 16 weeks compared with 6 weeks of age, of which 17 genes were underexpressed and 22 genes were overexpressed (data not shown). Again, targeted liver lipid profiling revealed that no liver lipid species were statistically different in the two groups (Chapter 4, Table 4.7). There was no differential liver gene expression in male *H/H* mice at 16 weeks compared with 10 weeks of age, which mirrored the targeted liver lipid profiling results.

In male *db/db* mice, there was no differential liver gene expression at any of the age groups. This finding contrasted slightly with the targeted liver lipid profiling results, which showed that 19 lipid species in male *db/db* mice were significantly different at 16 weeks compared with 6 weeks of age, and 20 lipid species were significantly different at 16 weeks compared with 10 weeks of age (Chapter 4, Table 4.7). Overall, these results highlight the dominant effect of the *db/db* genotype on both differential liver gene expression and targeted lipid profiling compared with the effect of age.

Table 5.3 Identity of 68 differentially expressed liver genes from 919 selected genes linked to lipid pathway/diabetes-specific disease states in all male *db/db* versus all male *H/H* mice.

Mouse gene symbol[a]	log-fold change (FC)[b]	adj. *P*-value[c]	Lipid pathway/diabetes-specific disease states[d]
Aldh3a2	0.889	1.07E-05	Group 3. Fatty acid metabolism
Acadm	0.623	3.21E-04	
Cyp4a31	1.369	2.49E-03	
Acat1	0.644	2.52E-03	
Cpt2	0.438	3.22E-02	
Soat2	-0.549	7.23E-03	Group 4. Steroid Biosynthesis
Cyp7b1	-2.11	1.88E-04	Group 5. Steroid Hormone Biosynthesis
Hsd17b6	-0.678	1.76E-02	
Dak	0.683	8.72E-03	Group 6. Glycerolipid Metabolism
Agpat9	1.016	1.04E-02	
Agpat6	0.489	2.97E-02	
Mgll	0.55	3.57E-02	
Agpat2	1.038	6.68E-04	Group 7. Glycerophospholipid Metabolism
Pla2g15	0.464	2.29E-02	
Chpt1	1.45	1.42E-05	Group 8. Ether Lipid Metabolism
Pla2g4f	0.613	2.95E-03	
Enpp2	-0.378	3.07E-02	
Gal3st1	1.228	5.37E-05	Group 9. Sphingolipid Metabolism
Arsa	0.63	3.11E-03	
Smpd3	0.812	4.75E-03	
Gba	-0.436	6.72E-03	
Ugcg	-0.404	3.57E-02	
Ptgis	-0.723	2.33E-05	Group 10. Arachidonic Acid Metabolism
Cyp2b10	2.258	1.66E-04	
Cyp4f13	-0.508	3.07E-03	
Cyp2c39	0.896	2.74E-03	Group 11. Linoleic Acid Metabolism
Cyp1a2	-0.714	6.25E-03	
Acot4	1.03	9.56E-03	Group 12. Biosynthesis of Unsaturated Fatty Acids
Acot3	1.849	2.45E-02	
Gapdh	0.467	5.01E-04	Group 13. Glycolysis/Gluconeogenesis
Eno1	0.584	3.40E-03	
Gm5506	0.558	6.78E-03	
G6pc	0.825	9.97E-03	
Pgam1	0.473	1.31E-02	
Suclg2	0.402	2.89E-02	Group 14. citrate Cycle (TCA Cycle)
Dlst	0.341	3.91E-02	
Pcx	0.424	4.56E-02	

Mouse gene symbol[a]	log-fold change (FC)[b]	adj. *P*-value[c]	Lipid pathway/diabetes-specific disease states[d]
Pip4k2a	-0.421	3.97E-02	Group 15. Inositol Phosphate Metabolism
Pik3cd	-0.433	4.88E-02	Group 17. Type II Diabetes Mellitus
Vldlr	1.333	3.57E-05	Group 18. Diabetes Mellitus, Type 2
Nqo1	0.763	3.53E-04	
Cyp17a1	1.81	4.25E-04	
Maob	0.584	7.07E-04	
Ttc39b	-0.553	1.17E-03	
Pltp	0.795	1.07E-02	
Mlxipl	-0.582	2.98E-02	
Tsc22d1	0.941	3.07E-02	
Nrf1	-0.462	3.64E-02	
Prkcb	-0.457	3.97E-02	
Socs2	-1.886	9.40E-08	Group 19. Obesity
Pparg	1.144	1.83E-07	
Ntrk2	1.031	3.57E-05	
Sort1	-1.2	3.79E-05	
Irs2	1.123	1.24E-04	
Gpd1	0.85	2.19E-04	
Nat1	0.649	1.97E-03	
Btc	0.496	1.40E-02	
Cyp2c55	0.884	1.60E-02	
Rxrg	0.37	3.42E-02	
Pcsk9	-0.668	3.71E-02	
Apoa4	1.843	2.63E-05	Group 20. Dyslipidemias
Hhex	-0.862	5.79E-05	
Insig2	2.117	1.27E-04	
Prkcz	-0.65	2.66E-03	
Ube2e2	0.42	5.14E-03	
Pklr	0.904	6.44E-03	
Abcg8	-0.521	3.84E-02	
Aif1	-0.574	4.69E-02	

[a] Yellow-shaded genes were also differentially expressed in male *db/db* mice at 10 and 16 weeks of age versus corresponding male *H/H* mice (and in the same direction of change).
[b] Positive (black font) and negative (red font) indicate that genes were overexpressed or underexpressed respectively in the male *db/db* mice.
[c] Adj. *P* -value is derived from the original *P* value, corrected for multiple testing using the Benjamini-Hochberg method. Adj. *P*-value < 0.05 was considered significant.
[d] Sorted by ascending order of group number, then descending order of adj. *P*-value within each group.

5.3.4 Liver genes associated with lipid pathway/diabetes-specific disease states in all male *db/db* mice

To determine any associations that exist between liver gene expression and targeted lipid profiling abnormalities, the 1,032 liver genes that were differentially expressed in male *db/db* mice compared to male *H/H* mice (ages combined) were screened against a selected list of 919 mouse genes linked to lipid pathway/diabetes-specific disease states. There were 68 differentially expressed liver genes found on this selected list, of which 23 were underexpressed and 45 were overexpressed in male *db/db* mice compared with male *H/H* mice (Table 5.3). Notably, the seven genes associated with fatty acid β-oxidation (groups 3 and 12), the four genes linked to glycerolipid metabolism (group 6), the five genes linked to glycolysis/gluconeogenesis (group 13) and the three genes linked to citrate cycle (group 14) were overexpressed in male *db/db* mice. In contrast, the three genes linked to steroid biosynthesis or steroid hormone biosynthesis (groups 4 and 5) were underexpressed in male *db/db* mice (Table 5.3). In addition, multiple genes linked to ether lipid metabolism (group 8), sphingolipid metabolism (group 9), arachidonic acid metabolism (group 10), diabetes mellitus, type 2 (group 18), obesity (group 19) and dyslipidemias (group 20) were differentially expressed in male *db/db* mice (all ages combined).

5.3.5 Liver genes associated with lipid pathway/diabetes-specific disease states in male *db/db* mice at 10 and/or 16 weeks of age

Of the 284 liver genes that were differentially expressed in male *db/db* mice compared with male *H/H* mice at 10 weeks of age, 33 genes were from the selected list of 919 mouse genes linked to lipid pathway/diabetes-specific disease states, of which six were underexpressed and 27 were overexpressed in male *db/db* mice (Table 5.4). The eight genes associated with fatty acid β-oxidation (groups 3 and 12), the two genes linked to sphingolipid metabolism (group 9), the five genes linked to diabetes mellitus, type 2 (group 18) and the three genes linked to dyslipidemias (group 20) were overexpressed in male *db/db* mice (Table 5.4). In addition, multiple genes linked to steroid hormone biosynthesis (group 5) and obesity (group 19) were differentially expressed in male *db/db* mice at 10 weeks of age. Among the underexpressed obesity genes was *Lpl*, which encodes the lipoprotein lipase precursor that catalyzes the hydrolysis of triglycerides. Notably, none of the KEGG-derived glucose or energy metabolism pathways were represented.

Table 5.4 Identity of 33 differentially expressed liver genes from 919 selected genes linked to lipid pathway/diabetes-specific disease states in male *db/db* mice versus male *H/H* mice at 10 weeks of age.

Mouse gene symbol	log-fold change (FC)[a]	adj. *P*-value[b]	Lipid pathway/diabetes-specific disease states[c]
Aldh3a2	1.318	2.18E-04	Group 3. Fatty acid metabolism
Ehhadh	1.588	4.57E-04	
Cyp4a31	1.758	1.83E-03	
Acadm	0.969	1.14E-02	
Acsl5	1.009	2.74E-02	
Acadl	1.527	3.24E-02	
Cyp7b1	-3.064	1.11E-07	Group 5. Steroid Hormone Biosynthesis
Ugt1a2	1.805	6.74E-04	
Ugt1a5	1.919	9.20E-04	
Cyp7a1	-1.567	9.90E-03	
Agpat9	1.692	1.05E-05	Group 6. Glycerolipid Metabolism
Agpat2	1.313	4.95E-02	Group 7. Glycerophospholipid Metabolism
Chpt1	2.124	2.34E-05	Group 8. Ether Lipid Metabolism
Gal3st1	1.268	1.04E-02	Group 9. Sphingolipid Metabolism
Smpd3	0.985	4.85E-02	
Cyp2b10	2.95	4.12E-05	Group 10. Arachidonic Acid Metabolism
Ptgis	-0.929	2.03E-02	
Cyp2c39	1.373	5.86E-04	Group 11. Linoleic Acid Metabolism
Acot3	3.636	2.45E-10	Group 12. Biosynthesis of Unsaturated Fatty Acids
Acot4	1.655	4.39E-04	
Cyp17a1	2.925	3.08E-08	Group 18. Diabetes Mellitus, Type 2
Vldlr	1.945	1.05E-05	
Pltp	1.61	2.38E-04	
Scd1	1.018	7.90E-03	
Maob	0.943	2.33E-02	
Socs2	-2.424	1.84E-06	Group 19. Obesity
Pparg	1.55	3.67E-05	
Sort1	-1.701	5.53E-05	
Lpl	-1.584	5.89E-04	
Ntrk2	1.136	2.81E-02	
Apoa4	2.58	1.62E-07	Group 20. Dyslipidemias
Insig2	2.723	1.23E-04	
Pklr	1.516	2.61E-03	

[a] Positive (black font) and negative (red font) indicate that genes were overexpressed or underexpressed respectively in the male *db/db* mice.
[b] Adj. *P* –value is derived from the original *P* value, corrected for multiple testing using the Benjamini-Hochberg method. Adj. *P*-value < 0.05 was considered significant.
[c] Sorted by ascending order of group number, then descending order of adj. *P*-value within each group.

Table 5.5 Identity of 31 differentially expressed liver genes from 919 selected genes linked to lipid pathway/diabetes-specific disease states in male *db/db* mice versus male *H/H* mice at 16 weeks of age.

Mouse gene symbol	log-fold change (FC)[a]	adj. *P*-value[b]	Lipid pathway/diabetes-specific disease states[c]
Cyp4a31	1.785	1.65E-03	Group 3. Fatty acid metabolism
Aldh3a2	0.93	2.62E-02	
Cyp7b1	-2.547	1.62E-06	Group 5. Steroid Hormone Biosynthesis
Agpat9	1.052	3.70E-02	Group 6. Glycerolipid Metabolism
Agpat2	1.299	9.97E-03	Group 7. Glycerophospholipid Metabolism
Pla2g15	0.926	2.98E-02	
Chpt1	1.296	2.05E-02	Group 8. Ether Lipid Metabolism
Enpp2	-0.952	3.87E-02	
Gal3st1	1.955	1.28E-05	Group 9. Sphingolipid Metabolism
Smpd3	1.319	4.52E-03	
Cyp2b10	2.208	1.69E-03	Group 10. Arachidonic Acid Metabolism
Ptgis	-0.878	3.14E-02	
Cyp2c39	1.334	6.12E-04	Group 11. Linoleic Acid Metabolism
Cyp1a2	-1.072	4.26E-02	
Acot3	1.974	8.71E-03	Group 12. Biosynthesis of Unsaturated Fatty Acids
Acot4	1.024	2.89E-02	
Cyp17a1	2.079	3.34E-05	Group 18. Diabetes Mellitus, Type 2
Vldlr	1.258	1.01E-03	
Dbp	-1.153	1.01E-02	
Nqo1	0.956	3.66E-02	
Socs2	-1.619	3.57E-04	Group 19. Obesity
Ntrk2	1.263	1.45E-03	
Pparg	1.192	1.65E-03	
Sort1	-1.283	3.54E-03	
Irs2	-1.251	8.24E-03	
Ppargc1b	-0.984	1.52E-02	
Ttc39b	-0.771	4.55E-02	
Apoa4	2.319	4.19E-06	Group 20. Dyslipidemias
Insig2	2.367	1.28E-04	
Cidea	1.832	2.08E-02	
Lpin1	-1.345	2.71E-02	

[a] Positive (black font) and negative (red font) indicate that genes were overexpressed or underexpressed respectively in the male *db/db* mice.
[b] Adj. *P* –value is derived from the original *P* value, corrected for multiple testing using the Benjamini-Hochberg method. Adj. *P*-value < 0.05 was considered significant.
[c] Sorted by ascending order of group number, then descending order of adj. *P*-value within each group.

Likewise, of the 223 liver genes that were differentially expressed in male *db/db* mice compared with male *H/H* mice at 16 weeks of age, 31 genes were from the selected list of 919 mouse genes linked to lipid pathway/diabetes-specific disease states, of which 11 were underexpressed and 20 were overexpressed in male *db/db* mice (Table 5.5). The four genes associated with fatty acid β-oxidation (groups 3 and 12), the two genes linked to glycerophospholipid metabolism (group 7) and the two genes linked to sphingolipid metabolism (group 9) were overexpressed in the male *db/db* mice. In addition, multiple genes linked to diabetes mellitus, type 2 (group 18), obesity (group 19) and dyslipidemias (group 20) were differentially expressed in male *db/db* at mice at 16 weeks of age. Notably, none of the KEGG-derived glucose or energy metabolism pathways were represented.

5.3.6 Twenty-one liver genes are associated with lipid pathway/diabetes-specific disease states in male *db/db* mice at both 10 and 16 weeks of age

There were 21 liver genes from the selected list of lipid pathway/diabetes-specific genes that were differentially expressed in the male *db/db* mice at both 10 and 16 weeks of age compared with the corresponding male *H/H* mice (Table 5.6). The same four genes were underexpressed and the same 17 genes were overexpressed in the male *db/db* mice at both ages. In addition, the same 21 genes were differentially expressed (and in the same direction of change) in male *db/db* mice compared with male *H/H* mice when the three age groups were combined (Table 5.3), suggesting that these genes contributed robustly to the progressively worsening phenotype of the obese/diabetic male *db/db* mice.

More specifically, 13 of the 21 genes dysregulated at both 10 and 16 weeks of age represented nine of the 12 KEGG-derived lipid pathway groups, indicating a wide distribution of gene abnormalities in the lipid pathway network. The other eight genes dysregulated at both 10 and 16 weeks of age represented the DisGeNET-derived diabetes-specific T2D, obesity or dyslipidemia groups. Six of these eight genes were overexpressed in male *db/db* mice, including *Vldlr* (encodes the VLDL receptor, binds VLDL and transports it into cells by endocytosis, but also transports TG from the liver to adipose tissue), *Pparg*, *Apoa4* and *Insig2* (insulin-induced gene 2, encodes a protein that blocks the processing of sterol regulatory element binding proteins that stimulate hepatic lipogenesis). The two DisGeNet-derived genes that were underexpressed in male *db/db* mice were *Socs2* and *Sort1* (encodes sortilin 1, a sorting receptor in the Golgi compartment).

Table 5.6 Identity of 21 liver genes from the selected list of 919 selected genes linked to lipid pathway/diabetes-specific disease states that were differentially expressed in male *db/db* mice versus male *H/H* mice at both 10 and 16 weeks of age.

Mouse gene symbol[a]	Lipid pathway/diabetes-specific disease states
Aldh3a2, Cyp4a31	Group 3. Fatty acid metabolism
Cyp7b1	Group 5. Steroid Hormone Biosynthesis
Agpat9	Group 6. Glycerolipid Metabolism
Agpat2	Group 7. Glycerophospholipid Metabolism
Chpt1	Group 8. Ether Lipid Metabolism
Gal3st1, Smpd3	Group 9. Sphingolipid Metabolism
Cyp2b10, Ptgis	Group 10. Arachidonic Acid Metabolism
Cyp2c39	Group 11. Linoleic Acid Metabolism
Acot3, Acot4	Group 12. Biosynthesis of Unsaturated Fatty Acids
Cyp17a1, Vldlr	Group 18. Diabetes Mellitus, Type 2
Socs2, Pparg, Sort1, Ntrk2	Group 19. Obesity
Apoa4, Insig2	Group 20. Dyslipidemias

[a] Positive (black font) and negative (red font) indicate that genes were overexpressed or underexpressed respectively in the male *db/db* miceat both 10 and 16 weeks of age.

5.3.7 Correlation of lipid classes/subclasses with differentially expressed genes linked to lipid pathway/diabetes-specific disease states in male *db/db* mice

It was also important to determine whether there was any association between the liver lipid classes (measured by targeted lipid profiling) and the differentially expressed liver genes in male *db/db* mice. Therefore, non-parametric Spearman rank correlation analyses were performed on the content of 21 liver lipid classes/subclasses (pmol/mg tissue) against log-2 expression values for the 68 differentially expressed liver genes in male *db/db* mice that were linked to lipid pathway/diabetes-specific disease states (Table 5.3). The correlation analyses included liver lipid and gene data from the 18 male *db/db* mice and their 18 male H/H littermates. The *P*-values obtained for each of the 1428 correlations were corrected for multiple gene and lipid comparisons using the Bonferroni approach, with $P < 0.05$ considered significant. This resulted in 21 significantly negative correlations and 44 significantly positive correlations generated from 30 different genes representing 12 lipid pathway/diabetes-specific disease states, but only five different lipid classes/subclasses, namely TG, DG, CE, LPE and LPC (Table 5.7).

The TG class was positively correlated with 18 genes and negatively correlated with six genes across 11 different groups, including 14 of the 21 genes that were differentially expressed in male *db/db* mice versus male *H/H* mice at both 10 and 16 weeks of age (Table 5.6). Notably, the TG class was negatively correlated with four genes associated with obesity and/or dyslipidemias, namely *Socs2*, *Sort1*, *Pcsk9* (plays a role in cholesterol homeostasis, and is downregulated following a high cholesterol diet) and *Hhex* (encodes a member of the homeobox family of transcription factors, and may play a role in hematopoietic differentiation). Although the DG and CE classes were only significantly correlated with ten and seven genes respectively, all of these genes (except *Prkcz*, which was negatively correlated with DG) were also strongly correlated with the TG class (Table 5.7). In particular, TG, DG and CE were positively correlated with *Agpat9* (glycerolipid biosynthesis) and *Vldlr* (binds VLDL and initiates endocytosis, but also transports TG from liver to adipose).

Strikingly, the LPE subclass was positively correlated with 14 genes and negatively correlated with six genes across eight different groups, including 11 of the 21 genes that were differentially expressed in male *db/db* mice at both 10 and 16 weeks of age (Table 5.6). Like the TG class, the LPE subclass was positively correlated with *Vldlr* and *Pparg* (stimulates peroxisomal fatty acid β-oxidation) and negatively correlated with *Socs2*, *Sort1*, *Pcsk9* and *Hhex*, but also showed a

Table 5.7 Significant correlations obtained from the analyses of 21 liver lipid classes/subclasses versus 68 differentially expressed liver genes linked to lipid pathway/diabetes-specific disease states in male *db/db* versus male *H/H* mice.

Lipid pathway/diabetes-specific disease states[a]	Mouse gene symbol[b]	Lipid class/subclass[c]									
		TG		DG		CE		LPE		LPC	
		r value[d]	*P*-value[e]	*r* value[d]	*P*-value[e]	*r* value[d]	*P*-value[e]	*r* value[d]	*P*-value[e]	*r* value[d]	*P*-value[e]
Group 3. Fatty acid metabolism	**Aldh3a2**	0.83	1.9E-06					0.77	1.2E-04	0.70	7.1E-03
	Acadm	0.80	2.5E-05					0.70	7.3E-03		
	Cyp4a31	0.75	4.9E-04								
	Cpt2	0.72	2.4E-03								
Group 5. Steroid Hormone Biosynthesis	**Cyp7b1**	-0.67	2.3E-02	-0.69	1.0E-02	-0.70	5.0E-03				
Group 6. Glycerolipid Metabolism	**Agpat9**	0.74	6.7E-04	0.69	9.0E-03	0.65	3.8E-02				
	Mgll	0.68	1.1E-02	0.66	2.7E-02						
Group 8. Ether Lipid Metabolism	**Chpt1**	0.75	5.3E-04					0.65	4.4E-02		
	Pla2g4f	0.65	4.7E-02								
Group 9. Sphingolipid Metabolism	**Smpd3**							0.67	2.2E-02		
Group 10. Arachidonic Acid Metabolism	**Ptgis**							-0.68	1.6E-02		
	Cyp2b10	0.75	5.5E-04	0.68	1.6E-02	0.67	2.0E-02	0.73	1.7E-03		
	Cyp4f13	-0.72	2.7E-03					-0.71	3.9E-03		
Group 12. Biosynthesis of Unsaturated Fatty Acids	**Acot4**	0.67	1.8E-02								
Group 13. Glycolysis/Gluconeogenesis	**Gapdh**	0.69	7.5E-03	0.67	2.2E-02			0.74	7.4E-04	0.74	6.3E-04
Group 14. citrate Cycle (TCA Cycle)	**Suclg2**	0.66	2.5E-02								
Group 18. Diabetes Mellitus, Type 2	**Vldlr**	0.79	4.1E-05			0.65	4.2E-02	0.72	2.7E-03		
	Cyp17a1	0.75	5.0E-04								
	Maob	0.73	1.5E-03					0.71	3.7E-03		

Lipid pathway/diabetes-specific disease states[a]	Mouse gene symbol[b]	Lipid class/subclass[c]									
		TG		DG		CE		LPE		LPC	
		r value[d]	*P*-value[e]	*r* value[d]	*P*-value[e]	*r* value[d]	*P*-value[e]	*r* value[d]	*P*-value[e]	*r* value[d]	*P*-value[e]
Group 19. Obesity	**Socs2**	-0.70	6.2E-03					-0.72	2.8E-03	-0.69	1.0E-02
	Pparg	0.70	5.4E-03					0.66	3.7E-02		
	Ntrk2							0.71	3.3E-03		
	Sort1	-0.75	4.1E-04	-0.72	1.9E-03	-0.67	2.1E-02	-0.65	4.1E-02		
	Nat1							0.67	1.9E-02		
	Pcsk9	-0.73	1.7E-03					-0.67	1.9E-02		
Group 20. Dyslipidemias	**Apoa4**	0.83	1.9E-06	0.79	4.1E-05	0.69	8.1E-03	0.74	7.3E-04		
	Hhex	-0.66	2.7E-02	-0.68	1.3E-02	-0.69	1.0E-02	-0.70	6.1E-03	-0.66	2.6E-02
	Insig2	0.85	4.5E-07	0.68	1.5E-02			0.70	5.3E-03		
	Prkcz			-0.67	2.4E-02						
	Ube2e2							0.66	2.9E-02		

[a] The 68 differentially expressed liver genes in male *db/db* versus male *H/H* mice were derived from 919 selected genes linked to 20 lipid pathway/diabetes-specific disease states [using the gene KEGG Pathway Maps and DisGeNET gene search websites (section 5.2.5 and Table 5.3)].
[b] Gene expression intensities were log2-transformed. Positive (black font) and negative (red font) indicate that genes were overexpressed or underexpressed respectively in the male *db/db* mice.
[c] The content ofeach lipid class/subclass is the sum of the content (pmol/mg protein) of each measured species within that class/subclass.
[d] Spearman rank correlation coefficient (*r* value) with [e] *P*-value corrected for multiple comparisons using Bonferroni approach
TG, triacylglycerol; DG, diacylglycerol, CE, cholesteryl ester; LPE, lysophosphatidylethanolamine; LPC, lysophosphatidylcholine.

negative correlation with the *Ptgis* gene (involved in anti-inflammatory actions). Although the LPC subclass was only significantly correlated with four genes (*Socs2*, *Aldh3a2*, *Hhex* and *Gapdh*), these genes were also strongly correlated with the LPE subclass (Table 5.7). Notably, the *Hhex* gene was significantly negatively correlated with all five lipid classes/subclasses, indicating that it had a global effect on the progressive dyslipidemia observed in the livers of *db/db* mice.

5.4 DISCUSSION

5.4.1 Biomarker genes associated with metabolic defects in male *db/db* mice at 6 weeks of age

In the present study, whole-genome gene expression and targeted lipid profiling abnormalities (at the lipid class and species level) associated with the pathogenesis of T2D were sequentially tracked in the livers of male *db/db* mice (C57BL/KsJ background) at 6, 10, and 16 weeks of age (versus corresponding male *H/H* littermates). By 6 weeks of age, the male *db/db* mice were already mildly obese and glucose intolerant, with significantly elevated omental fat weight, and a trend towards raised fasting plasma insulin levels and IR (by HOMA-IR) compared with the corresponding male *H/H* mice. However, targeted liver lipid profiling revealed that none of the 227 measured liver lipid species were statistically different in the two groups, and only eight liver genes were differentially expressed in six week old male *db/db* mice. Crucially, expression of the *Irs2* gene, which encodes insulin receptor substrate 2, was decreased, suggesting early compromise of the insulin signaling pathway. In addition, gene expression of *Fitm1*, which encodes fat storage-inducing transmembrane protein 1 (i.e, plays an important role in lipid droplet accumulation) was increased in the livers of six week old male *db/db* mice, indicating an early increased flow of free fatty acids from inflamed adipose tissue to the liver, resulting in increased fatty acid uptake and accumulation in the liver [199]. In addition, surrogate measures of hepatic *de novo* lipogenesis (total 16:1/18:2 ratios in liver DG and TG species) and the circulating pool of fatty acid 16:1 in DG and TG were already markedly elevated in our six week old male *db/db* mice. Thus, there appears to be an increased flux through the glycerolipid synthesis pathway in six week old male *db/db* mice without any increase in the gene expression of the enzyme protein levels.

5.4.2 Upregulation of hepatic fatty acid oxidation, lipogenesis, glycerolipid and glycerophospholipid synthesis in male *db/db* mice at 10 weeks of age

By 10 weeks of age, our male *db/db* mice were obese and IR, with markedly elevated omental fat weight compared with the corresponding male *H/H* mice. This increased severity of disease phenotype corresponded to a significant elevation of total LPE, BMP, CE, DG and 90 lipid species, and a significant lowering of 12 lipid species, including multiple species of PC(O) and PC(P), in livers of male *db/db* mice. These liver lipid abnormalities corresponded to 284 genes that were differentially expressed in the livers of male *db/db* mice at 10 weeks of age, including 33 genes (6 underexpressed and 27 overexpressed genes) from 919 selected mouse genes linked to lipid pathway/diabetes-specific disease states using the KEGG and DisGeNET databases (Table 5.4).

No liver genes associated with fatty acid biosynthesis (KEGG group 1) were differentially expressed in male *db/db* mice at 10 weeks of age. However, eight liver genes associated with fatty acid β-oxidation (KEGG groups 3 and 12) were overexpressed in male *db/db* mice at 10 weeks of age, which indicates that fatty acids were the preferred fuel source for these mice with increasing severity of disease. In addition, stearoyl-CoA desaturase 1 encoding gene, *Scd1* (DisGeNET group 18), was overexpressed in male *db/db* mice, which is consistent with our findings of elevated surrogate measures of hepatic *de novo* lipogenesis (i.e., total 16:1/18:2 ratios in liver DG and TG species). Likewise, the *Agpat9* gene (KEGG group 6), which encodes the enzyme that transfers the acyl-group from acyl-CoA to the *sn*-1 position of glycerol-3-phosphate to form lysophosphatidic acid (an essential step in glycerolipid biosynthesis) was overexpressed, which corresponded to the elevated liver DG and TG classes observed in our male *db/db* mice at 10 weeks of age. The increased fatty acid uptake in the liver directly or indirectly (via PPAR-γ signalling) stimulates mitochondrial fatty acid β-oxidation, and also stimulates fatty acid desaturation and esterification (storage) [110]. At the same time, the upregulation of fatty acid β-oxidation inhibits fatty acid synthesis.

Similar to our findings, Zhang *et al.* revealed that mRNA expression of five genes associated with enzymes in the fatty acid β-oxidation and storage pathways (long-chain fatty acid elongation, desaturation and esterification to DG and TG), but not the fatty acid synthesis pathway, were enhanced in the livers of 9 week old male diabetic *db/db* mice compared with male wild-type C57BL/6 mice [110]. However, Zhang *et al.* used high-throughput RNA

sequencing technology and 12 mice per group, and defined differentially expressed genes as having an absolute fold change ≥ 1.5 and a false discovery rate < 0.001, but did not correct the *P*-values for multiple testing [110]. According to this criteria, Zhang *et al.* found that 2627 genes were differentially expressed between normal and diabetic *db/db* mouse liver samples, whereas our microarray analysis found that 1032 liver genes were differentially expressed in male *db/db* mice versus male *H/H* mice (ages combined; 18 mice per group), with the *P*-values adjusted for multiple gene comparisons using the Benjamini-Hochberg method [155]. Unfortunately, Zhang *et al.* made no mention of the phenotypic characteristics of the experimental mice. However, *db/db* mice with a C57BL/6J background exhibit a less severe diabetic phenotype (and pancreatic hyperplasia) compared with *db/db* mice with a C57BL/KsJ background (and islet degeneration) [73]. In another study, the expression of genes involved in fatty acid β-oxidation were also increased in *ob/ob* mice compared with lean wild-type mice [112,200], indicating common links between gene expression and lipid abnormalities in the two genetically obese mouse models.

Within the glycerophospholipid metabolism pathway (KEGG group 7), the *Agpat2* gene, which encodes the enzyme that converts lysophosphatidic acid to phosphatidic acid, the second step in *de novo* phospholipid biosynthesis (and part of the glycerolipid pathway) was overexpressed in male *db/db* mice at 10 weeks of age. This corresponded to significant elevations in many glycerophospholipids, including multiple species of PC, PE, LPC, LPE, PI and CL. Within the arachidonic acid metabolism pathway (KEGG group 10), the *Ptgis* gene, which encodes a monooxygenase that converts prostaglandin H2 to prostacyclin, a potent vasodilator and inhibitor of platelet aggregation, was underexpressed in male *db/db* mice at 10 weeks of age.

There were also 13 diabetes-specific genes from the DisGeNET groups 18-20 that were differentially expressed in male *db/db* mice at 10 weeks of age. Overexpressed diabetes-specific genes of interest included *Vldlr and Pparg* (activates peroxisomal β-oxidation pathway of fatty acids), and underexpressed genes of interest included *Socs2* (suppressor of cytokine signalling) and *Lpl*. Vldlr expression has been shown to be regulated by PPAR-γ. Pioglitazone, an agonist of PPAR-γ, increased VLDLR mRNA expression and protein levels in experiments using mouse fibroblasts, and pioglitazone-treated mice exhibited a higher conversion rate of plasma triglycerides into epididymal fats [201]. Although *Vldlr* is

expressed at very low levels in liver under basal conditions [202], it is induced in liver during endoplasmic reticulum stress, and is thought to contribute to hepatic steatosis [203].

5.4.3 Upregulation of hepatic fatty acid oxidation/storage is linked to impaired insulin signalling and inflammation in male *db/db* mice at 16 weeks of age

By 16 weeks of age, our male *db/db* mice had severe obesity, glucose intolerance, hyperinsulinaemia and markedly elevated omental fat, which corresponded to a significant difference in the levels of nine lipid classes/subclasses [sustained elevations of LPE, LPC, CE, DG and TG; and now reductions of SM, PC(P), PE(P) and PS] and 100 lipid species (56 elevated and 44 reduced species) in livers of severely obese/diabetic male *db/db* compared with male *H/H* mice at 16 weeks of age. In addition, 223 liver genes were differentially expressed in livers of male *db/db* mice at 16 weeks of age, including 31 genes (11 underexpressed and 20 overexpressed genes) from the selected list of 919 mouse genes linked to lipid pathway/diabetes-specific disease states (Table 5.5).

As 21 liver genes from the selected list of lipid pathway/diabetes-specific genes were differentially expressed in the male *db/db* mice at both 10 and 16 weeks of age (Table 5.6), only ten 'other' genes were exclusively differentially expressed in livers of male *db/db* mice at 16 weeks of age. Among these were the overexpressed *Pla2g15* gene (KEGG group 7), which encodes a lysosomal enzyme with both phospholipase A2 and transacylase activities, resulting in the release of lysophospholipids. This corresponded to significant elevations in many LPC and LPE species at this time-point. In contrast, the *Irs2* gene (DisGeNET group 19), which encodes the insulin receptor substrate 2, was underexpressed, although this result in itself does not prove that the insulin signalling pathway is impaired. Also, the overexpressed gene *Cidea* (DisGeNET group 20) encodes an effector that binds to lipid droplets and regulates their enlargement, thereby restricting lipolysis and favouring TG storage (highly expressed in brown adipose tissue). However, overexpressed *Cidea* also induces apoptosis. These detrimental effects in the 16 week old male *db/db* mice corresponded to an attenuation of surrogate measures of hepatic *de novo* lipogenesis (total 16:1/18:2 ratios in liver DG and TG species), which was accompanied by a reduced circulating pool of fatty acid 16:1 in DG and TG, and may indicate decreased liver function in this advanced stage of the disease.

5.4.4 Upregulation of fatty acid and glucose metabolic pathways is associated with stimulation of glucocorticoids in male *db/db* mice

There were 68 differentially expressed liver genes in all male *db/db* versus all male *H/H* mice from the selected list of 919 mouse genes linked to lipid pathway/diabetes-specific disease states (Table 5.3). As well as including the 21 genes from the selected list of lipid pathway/diabetes-specific genes that were differentially expressed in the male *db/db* mice at both 10 and 16 weeks of age (Table 5.6), this expanded gene list generally included the same KEGG lipid pathways as those represented in the 10 and 16 weeks age groups, but more differentially expressed genes appeared in the diabetes-specific gene groups (DisGeNET groups 18-20). Strikingly though, five genes in the glycolysis/gluconeogenesis pathway (KEGG group 13) were overexpressed in male *db/db* mice compared with male *H/H* mice (ages combined), including the *G6pc* gene (encodes the key gluconeogenic enzyme glucose-6-phosphatase, which hydrolyzes glucose-6-phosphate to glucose) and *Pgam1* (encodes phosphoglycerate mutase 1, which catalyzes the interconversion of 3- and 2-phosphoglycerate). In addition, the *Pklr* gene (DisGeNET group 20), which encodes pyruvate kinase that converts phosphoenolpyruvate to pyruvate and ATP (rate-limiting step of glycolysis), was overexpressed in male *db/db* mice (ages combined and at 10 weeks of age). Furthermore, three genes in the citrate cycle pathway (KEGG group 14) were also overexpressed in male *db/db* mice (ages combined). Together, these findings point to increased rates of gluconeogenesis and glycolysis in our male *db/db* mice.

Similarly, Zhang *et al.* revealed that mRNA expression of genes associated with glycolysis, gluconeogenesis and glycogenolysis were enhanced in the livers of 9 week old male diabetic *db/db* mice compared withmale wild-type C57BL/6 mice [110]. About 90% of the increase in hepatic glucose production in type 2 diabetic subjects is accounted for by accelerated gluconeogenesis [204]. Also, increased hepatic fatty acid oxidation (induced by PPAR-γ signalling, which is activated by the increased uptake of fatty acids) can enhance gluconeogenesis, and stimulate hepatic glucose production [110,205]. The over-expression of genes that encode pyruvate kinase and citrate cycle enzymes, combined with upregulated fatty acid oxidation and gluconeogenesis indicate an upregulation of fatty acid and glucose metabolic pathways in our male *db/db* mice. Sustained hepatic gluconeogenesis particularly leads to chronic hyperglycaemia and the development of T2D.

Some genes from the steroid hormone biosynthesis pathway (e.g. *Hsd3b5, Hsd17b6* and *Cyp7b1*) were underexpressed in our male *db/db* mice. It has been shown that 11β-hydroxysteroid dehydrogenase type 1 (11 β-HSD1) regulates glucocorticoids, which are mediators of obesity and IR [101]. Moreover, impaired hepatic 11 β-HSD1 expression corresponded to increased levels of circulating corticosterone and weight gain in *ob*/*ob* mice, and contributed to the pathogenesis of obesity [60]. Similarly, Zhang *et al.* found that the *Hsd3b5* gene had the second greatest fold-change of any downregulated gene in the livers of 9 week old male diabetic *db/db* mice compared with male wild-type C57BL/6 mice [110].

5.4.5 Correlations between liver lipid classes/subclasses and differentially expressed genes associated with lipid pathways in male *db/db* mice

One of the advantages of this study design was the ability to directly compare the lipid abnormalities with differentially expressed genes associated with lipid pathway/diabetes-specific disease states in the livers of male *db/db* mice using the same samples. The lipid and gene expression datasets were generated independently of each other. The content of 21 liver lipid classes/subclasses were correlated against the expression levels of the 68 liver genes that were differentially expressed in male *db/db* mice compared with male *H/H* mice (n = 36 mice), with the 65 significant correlations shown in Table 5.7. The five lipid classes/subclasses that were significantly elevated in the male *db/db* mice at 10 and 16 weeks of age (TG, DG, CE, LPE and LPC) were found to be significantly correlated with 30 different genes representing 12 lipid pathway/diabetes-specific disease states, with no other lipid classes/subclasses reaching significance. The TG class and LPE subclass were particularly prominent, being significantly correlated with 24 and 20 genes respectively, with 15 genes common to both including; *Socs2*, *Sort1*, *Pcsk9*, *Hhex*, *Vldlr*, *Pparg*, *Apoa4*,*Aldh3a2*, *Acadm* and *Chpt1*. Notably, the TG, DG and CE were positively correlated with *Agpat9* (glycerolipid biosynthesis), and the LPE subclass was negatively correlated with *Ptgis* (anti-inflammatory actions). These findings highlight the advantage of combining a targeted lipidomic approach with gene expression profiling to determine which genes are connected to lipid dysregulation and associated disease processes.

5.4.6 Differentially expressed mouse genes in male *db/db* mice are candidate genes for human obesity and type 2 diabetes

Also of interest in this study was whether the genes that were differentially expressed in the monogenic leptin receptor-deficient *db/db* mouse model of obesity, IR and T2D were linked to candidate genes that were associated with human obesity and T2D. In a study that examined seven independent modelling methods used to select the most likely candidate genes for human obesity and T2D from data obtained from genome-wide linkage analysis and association studies, nine genes were selected as potential primary candidate genes for obesity, T2D, or both, by six of the seven methods [113]. Seven of the nine primary candidate genes identified for human T2D alone were involved in the processing of metabolites in the glycolytic and mitochondrial oxidative phosphorylation pathways. Among these genes was PGM1, mouse equivalent *Pgam1* (glycolysis/gluconeogenesis; which was found to be overexpressed in our male *db/db* mice) and *Lpl* (hydrolysis of triglycerides; which was found to be underexpressed in the male *db/db* mice at 10 weeks of age). In addition, *Vldlr* was only one of three primary candidate genes identified for human obesity, and was found to be overexpressed in the male *db/db* mice (a good model of endoplasmic reticulum stress), indicating that the uptake of VLDL-bound TG, DG and CE into the liver is increased (lipotoxicity). Given that only 12 primary candidates were selected for human obesity and/or T2D from 9556 starting genes [113], our discovery of three common genes from a selected list of 919 mouse genes representing lipid pathway/diabetes-specific disease states supports the use of the leptin receptor-deficient *db/db* mouse (C57BL/KsJ background) as a suitable model to study the pathogenesis of T2D.

In another study, a core set of 213 candidate genes for T2D were determined across multiple tissues in human and mouse using meta-analysis of existing data sources such as DNA microarraysand qualitative data [206]. Among the top 30 ranked T2D candidate genes were *scd1* (desaturation of saturated fatty acids; and was found to be overexpressed in our 10 week old *db/db* mice), *Hsd11b1* (regulates glucocorticoids; and was matched by the under-expression of *Hsd3b5*, *Hsd17b6* and *Cyp7b1* in the *db/db* mice), *Acadl* (fatty acid oxidation; and was found to be overexpressed in the 10 week old *db/db* mice), *Socs2* (suppressor of cytokine signalling 2; and was found to be overexpressed in the *db/db* mice) and *Lpin1* (plays a role in triglyceride metabolism; and was found to be underexpressed in the 16 week old *db/db* mice). Other genome-wide association studies have identified *Pparg (*controls β-fatty

acid oxidation, and was positively correlated with both total TG and LPE in the *db/db* mice, and *Hhex* (involved with transcription factors, and was negatively correlated with total TG, DG, CE, LPE and LPC in the *db/db* mice) as candidate genes for human T2D [207,208]. Together, these findings support our notion that the *db/db* mouse model closely resembles human obesity and T2D, and provides gene candidates that are linked to specific lipid abnormalities. Similar to our findings in *db/db* mice, Han *et al.* showed that liver LPC levels were elevated in *db/db* mice, and lowering tissue LPCs ameliorated IR and diabetes in these mice [191]. Although liver LPE has yet to be measured in animal models of obesity, Meikle *et al.* found elevated LPE 20:4 and LPE 22:6 in fasting plasma of subjects with stable coronary artery disease compared with control subjects, most likely due to degradation of PE(P) plasmalogens by ROS [10].

5.4.7 Conclusion

In conclusion, the tracking of gene expression and simultaneous targeted lipid profiling abnormalities associated with the onset of obesity, IR and progression to T2D in the livers of male *db/db* mice (C57BL/KsJ background) at 6, 10 and 16 weeks of age (versus corresponding male *H/H* mice) identified genes linked to lipid metabolic pathway/diabetes-specific disease states. In particular, differential gene expression indicated that hepatic fatty acid oxidation, *de novo* lipogenesis, glycerolipid and glycerophospholipid biosynthesis, as well as glycolysis, gluconeogenesis and citrate cycle metabolic pathways were upregulated in male *db/db* mice. Disease progression was also associated with impaired insulin signalling, inflammation and downregulation of steroid hormone biosynthesis, which induces the activation of glucocorticoids, mediators of obesity and IR. Strikingly, the same 21 genes (including *Pparg,Vldlr*, *Apoa4*, *Socs2* and *Ptgis*) were differentially expressed (and in the same direction of change) in male *db/db* mice compared with male *H/H* mice at 10 and 16 weeks of age, and when the three age groups were combined (Table 5.6), indicating that these genes are strongly associated with the pathogenesis of T2D.

Initially, targeted lipid profiling revealed that total TG, DG, CE and LPE were significantly elevated in the male *db/db* mice at both 10 and 16 weeks of age, and total LPC was significantly elevated at 16 weeks of age (and almost 10 weeks of age). Correlation analyses of the 21 liver lipid classes/subclasses against the 68 liver genes associated with lipid pathway/diabetes-specific disease states in male *db/db* mice showed that these five lipid

classes/subclasses were significantly correlated with 30 different genes (totalling 65 significant correlations) representing 12 lipid pathway/diabetes-specific disease states. Total TG and LPE were significantly correlated with 24 and 20 genes respectively, with 15 genes common to both (including *Socs2*, *Sort1*, *Pcsk9*, *Hhex*, *Vldlr*, *Pparg*, *Apoa4*, *Aldh3a2*, *Acadm* and *Chpt1*), which suggests a strong link between increased phospholipase A2 activity and the overproduction of lysophospholipids as a substrate for liver TG and VLDL-bound TG in the setting of obesity, IR and inflammation (increased cytokine signalling). These correlation analyses confirm the close link between liver lipid abnormalities (by targeted lipid profiling) and differentially expressed genes associated with lipid pathway/diabetes-specific expression (by microarray) in *db/db* mice.

Finally, many of the differentially expressed liver genes that were linked to lipid pathway/diabetes-specific disease states in the *db/db* mice (*Acadl*, *Scd1*, *Pparg*, *Socs2*, *Vldlr*, *Hhex*, *Pgam1*, *Lpl* and *Lpin1*) have been determined as candidate genes for human T2D. Therefore, the *db/db* mice (C57BL/KsJ background) mouse model of obesity, IR and T2D is suitable for identifying specific gene candidates or lipid classes/species as potential therapeutic targets for early prevention or treatment of comparable human disease cohorts.

CHAPTER 6 CHARACTERISATION OF PLASMA AND SKELETAL MUSCLE LIPID PROFILES IN HUMAN INSULIN RESISTANCE AND OBESITY

6.1 INTRODUCTION

6.1.1 Insulin resistance, obesity and lipid abnormalities contribute to type 2 diabetes

A major challenge for researchers studying the pathogenesis of type 2 diabetes (T2D) is the multiple metabolic perturbations associated with the disease, and the difficulty in measuring the separate contributions of these defects to the onset and progression of overt diabetes. The primary (diagnostic) defect that characterises T2D is hyperglycaemia (due to increased hepatic glucose output), but T2D is also associated with insulin resistance (IR), obesity, dyslipidaemia, insulin secretory dysfunction, and chronic low-grade inflammation.

In particular, dyslipidaemia [traditionally characterised by increased plasma free fatty acids (FFA) and triglycerides, and decreased HDL-cholesterol] plays a pivotal role in the development of IR and β-cell dysfunction in obesity and T2D [26,146,147,209]. The recent introduction of high throughput targeted "lipid profiling" using mass spectrometry (MS) techniques has made it possible to perform comprehensive lipidomic analysis of "non-classical" individual lipid species in plasma, tissues and cell culture extracts in human and animal models of IR and obesity. Using this approach, a number of lipid species have been implicated in the pathogenesis of T2D, including FFA, the phospholipids phosphatidylcholine (PC) and phosphatidylethanolamine (PE), the sphingolipids ceramide (Cer) and sphingomyelin (SM), and the glycerolipids diacylglycerol (DG) and triacylglycerol (TG) [9,13,26,28,29,48].

6.1.2 Early metabolic defects in the pathogenesis of type 2 diabetes

It has been shown that defects in insulin action occur early in individuals at high risk for developing T2D, prior to the onset of obesity [3,210,211,212,213]. For instance, healthy lean offspring of Mexican American parents with T2D (i.e., the earliest stage in the natural history of T2D) had impaired glucose uptake during a euglycaemic-hyperinsulinaemic clamp (which primarily reflects skeletal muscle insulin sensitivity), which was mostly accounted for by

reduced skeletal muscle glycogen synthesis [211]. Other early metabolic defects reported in lean NGT individuals with a strong family history of T2D included decreased basal and insulin-stimulated skeletal muscle insulin receptor substrate-1 (IRS-1) tyrosine phosphorylation and phosphatidylinositol (PI) 3-kinase activity (required for the activation of glucose transport and glycogen synthesis) [212], increased intramyocellular lipid content [214], and a connection between mitochondrial dysfunction (including decreased fatty acid oxidation), increased intramuscular triglyceride levels, and IR [215]. Collectively, these findings indicate that IR in skeletal muscle is the earliest metabolic defect in the pathogenesis of T2D. However, lean normal glucose tolerant offspring of two Mexican American parents with T2D also had a normal rate of basal hepatic glucose production in the presence of fasting hyperinsulinemia and elevated fasting plasma FFA, which indicates early hepatic IR [211]. In addition, the same individuals had increased plasma FFA during the euglycemic-hyperinsulinaemic clamp, which indicates early adipocyte resistance to insulin mediated suppression of lipolysis [211]. Regardless of which organ is primarily responsible for IR in lean individuals susceptible to T2D, these studies indicate that it may be possible to identify lipid abnormalities associated with IR (independently of obesity) and obesity (independently of IR) as early metabolic defects in the development of combined obesity and IR, and eventually T2D in humans. It is also important to gain an understanding of how these lipid abnormalities and associated metabolic pathways contribute to the etiology of T2D.

6.1.3 Plasma lipid abnormalities associated with insulin resistance, obesity and type 2 diabetes

To date, few studies have examined associations between the fasting plasma lipidome and IR, obesity and T2D in humans using MS techniques [9,25,26,28,29,48]. Two studies have examined the independent effect of obesity on lipid abnormalities in human plasma. Graessler *et al.* found that nearly all fasting plasma TG and DG species, some cholesterol ester (CE), PC, PE, ether-linked PE (PE(O)) species, and the lysophospatidylcholine (LPC) species LPC 16:0 were elevated in obese men (BMI > 27.5 kg/m^2) compared with a group of leaner men (BMI < 27.5 kg/m^2) [28]. Pietilainen *et al.* found that the fasting serum levels of some LPC species were elevated, and some ether-linked phospholipid species were decreased in healthy young obese adults when compared with their monozygotic non-obese twin (10 to 25 kg weight difference) [29]. Moreover, some LPC species and TG species containing ≥ 54 FA-carbons were negatively

correlated with insulin sensitivity, and some 22:6 FA-containing PC species and ether-linked phospholipid species were positively correlated with insulin sensitivity.

The study by Graessler *et al.* also examined the independent effect of IR on lipid abnormalities in the same male human cohort, and found that only one fasting plasma lipid species (PE 38:2) was significantly different in IR men [homeostasis model assessment of insulin resistance (HOMA-IR) > 3.5] compared with insulin sensitive men (HOMA-IR ≤ 3.5), despite trends towards lower levels of LPC, PC, ether-linked PC (PC(O)), PE and SM, and higher levels of PE(O) species [28]. The authors concluded that any changes in the lipidome induced by moderate IR were minor compared with the effects of obesity.

Other studies have employed a variety of MS techniques to investigate the combined effects of obesity, IR and/or T2D on levels of fasting plasma lipid classes and species in humans. For instance, total Cer and several Cer species are elevated in obese/T2D subjects, and negatively correlated with insulin sensitivity [25], and higher dietary saturated fat intake resulted in a higher proportion of FA 18:0 and a lower proportion of FA 18:1 in fasting serum phospholipids in overweight/obese IR men [48]. Furthermore, both T2D and prediabetes were positively associated with fasting plasma Cer, dihydroceramide (dhCer), DG, TG, CE, PE, phosphatidylglycerol (PG) and phosphatidylinositol (PI), and negatively associated with ether-linked PC(O) and vinyl ether-linked PC(P) subclasses [9].

Although these studies give an insight into the different associations that exist between the plasma lipid abnormalities that are associated with combined obesity, IR, prediabetes and/or T2D, no single study has examined the association of lipid abnormalities (at both the lipid class and species level) with obesity (independently of IR), IR (independently of obesity), and ultimately, how progressive lipid metabolic defects contribute to the etiology of T2D in humans.

6.1.4 The Human insulin resistance and obesity study

The Human insulin resistance and obesity study was designed and undertaken by Dorit Samocha-Bonet, Katherine Tonks, and Jerry Greenfield, Diabetes and Obesity Research Program, at the Garvan Institute of Medical Research, Sydney. This study included 80 adult participants, classified into one of four groups according to BMI, HOMA-IR, and diabetic status (see Methods, section 6.2.1). The team led by Jerry Greenfield collected paired fasting (baseline)

and steady-state (SS) euglycaemic-hyperinsulinaemic clamp plasma and skeletal muscle biopsy samples from study participants, primarily to examine the relative contributions of obesity versus IR to perturbations in the phosphoinositide 3-kinase/Akt insulin signalling pathway within vastus lateralis muscle. In collaboration with these researchers from the Garvan Institute, we had the opportunity to perform targeted lipid profiling on plasma and skeletal muscle samples obtained from this cohort using reverse phase high performance liquid chromatography combined with electrospray ionisation tandem mass spectrometry (LC ESI-MS/MS). This enabled us to examine the association of plasma and skeletal muscle lipid abnormalities with obesity, IR, combined obesity/IR and T2D.

We hypothesised that different lipid abnormalities would be associated with obesity (independently of IR) and IR (independently of obesity), and that lipid abnormalities associated with combined obesity/IR would ultimately contribute to the development of T2D. It would be highly valuable to predict early an individual's risk of developing diabetes, based for example, on their plasma lipid profile, so that those at greatest risk can undergo lifestyle intervention and/or therapeutic measures to prevent the onset of obesity, IR and T2D.

6.2 MATERIALS AND METHODS

The following sections 6.2.1 to 6.2.5 related to the recruitment of participants and clinical measures of IR and obesity were undertaken by the above mentioned Garvan group team as part of the collaborative study. A full description of the methods used in this study has been published elsewhere [216]. However, for completeness, the sections that are relevant to lipidomic analyses have been summarised in this chapter.

6.2.1 Classification of study participants

Based on screening tests and exclusion criteria characteristics, a total of 81 participants were included in the study [216]. The study protocol was approved by the Human Research and Ethics Committee at St Vincent's Hospital, Sydney. Informed written consent was obtained from all participants. One of the female participants in the original study [216] did not complete the euglycaemic-hyperinsulinaemic clamp procedure, and so was excluded from subsequent lipidomic analysis. Participants were classified into the following four groups according to BMI, HOMA-IR [calculated as fasting insulin (mU/l) × fasting glucose (mmol/l)/22.5] and diabetic

status, with individuals without known diabetes assessed by a 75g oral glucose tolerance test (OGTT):

1) Lean insulin-sensitive controls (Lean/IS): BMI ≤ 25 kg/m^2, HOMA-IR < 2.0, and normal glucose tolerance (NGT; *n* = 23);
2) Overweight-to-obese, insulin-sensitive individuals (Ov-ob/IS): BMI > 25 kg/m^2, HOMA-IR < 2.0 (*n* = 16);
3) Overweight-to-obese, insulin-resistant individuals (Ov-ob/IR): BMI > 25 kg/m^2, HOMA-IR > 3.0 (*n* = 20); or
4) Overweight-to-obese individuals with T2D (T2D): BMI > 25 kg/m^2, fasting blood glucose ≥ 7.0 mmol/l and/or 2 h post-challenge blood glucose ≥ 11.1 mmol/l (*n* = 21)

Two individuals in the Ov-ob/IS group had impaired glucose tolerance (2 h post-challenge blood glucose level 7.8-11.0 mmol/l), and in the Ov-ob/IR group, six individuals had impaired glucose tolerance, two had impaired fasting glucose (fasting blood glucose level 6.0-6.9 mmol/l), and one had both [216]. In the T2D group, the individuals were well-controlled (HbA_{1c} < 9%, diagnosed with diabetes within the last 5 years, with no clinical evidence of diabetes-related complications, and not taking medication for diabetes other than metformin or a sulfonylurea). However, metformin (known to affect insulin sensitivity) was ceased 2 weeks prior to the metabolic study, and was replaced with a sulfonylurea if fasting blood glucose levels consistently exceeded 7.0 mmol/l, but ceased on the day before the metabolic study. Other exclusion criteria characteristics for the study participants are described by Tonks *et al*. [216]. A total of 19 participants were taking statin medication (three from the Ov-ob/IS group, four from the Ov-ob/IR group, and 12 from the T2D group), but there was no difference in clamp-derived insulin sensitivity between statin users and non-users in these groups. Menstruating women (*n* = 9) were studied in the follicular phase of their menstrual cycle [216].

6.2.2 Anthropometric, body composition and insulin clamp measurements

On the metabolic study day, participants underwent dual energy X-ray absorptiometry scanning (DEXA, Lunar DPX-Lunar Radiation, Madison WI) to determine total body fat, fat-free mass (FFM) and central (abdominal) fat, and computed tomography scanning (Phillips Gemini GXL) to determine visceral and subcutaneous fat areas between the second and third lumbar vertebrae discs (L2/L3), and fourth and fifth discs (L4/L5) [10,216].

Participants were instructed not to exercise or consume alcohol for 48 h prior to the study [216]. Participants attended the Clinical Research Facility at 8 am for the metabolic study after a 12-hour fast, and had weight, height, waist, hip and blood pressure measurements taken. Infusion solutions were administered via a catheter (Intracath, Becton Dickinson Co., Sandy, UT), placed in an antecubital vein, and blood samples were drawn from a catheter (Angioset, Parke-Davis Co., Sandy, UT) inserted in a contralateral antecubital vein. After a supine rest period of at least 30 min, fasting (baseline) blood samples were drawn, and participants underwent a 150 min hyperinsulinaemic (80 mU/m^2/min)-euglycaemic (5.0 mmol/l)-clamp, as previously described [216,217]. The mean steady-state (SS) glucose infusion rate (GIR) was determined during the last 30 min of the clamp. Insulin sensitivity was calculated by dividing GIR by the fat-free mass (FFM).

Although GIR/FFM obtained from the hyperinsulinaemic-euglycaemic clamp procedure is considered the gold standard measure of insulin sensitivity, GIR/FFM values were not used to categorize the study groups because the Ov-Ob subjects had to be classified as either IS or IR before the clamp was performed (metabolic study day). The Ov-Ob subjects were strictly classified according to their screening visit HOMA-IR value (HOMA-IR < 2.0 for IS group, and > 3.0 for IR group), which ensured that differences in lipid profiles between the Ov-Ob/IR and Ov-Ob/IS groups were attributable to IR.

6.2.3 Blood collection and muscle biopsies

Fasting and SS clamp blood collected for lipid analysis was placed into EDTA tubes, placed on ice, centrifuged within 2 h (4,000g, 4°C for 15 min; Heraeus multifuge 1S-R, Thermo Electron Corporation), and the separated plasma stored at -80°C. Percutaneous needle biopsies (Bërgstrom) of vastus lateralis muscle were performed just prior to commencing the clamp (baseline), and at 145 min (SS clamp period). Biopsies were performed through separate incisions 5 cm apart, and unwanted blood, fat and connective tissue was rapidly removed from the excised muscle samples in ice-cold saline before snap-freezing the samples in liquid nitrogen [216]. Initially, only 77 fasting (baseline) and 67 SS clamp muscle samples were collected for lipidomic analysis (out of 80 participants). In addition, two other muscle samples were excluded from statistical analysis [one baseline sample from the Lean/IS group exhibited extremely high (outlier) total DG and TG contents, and another SS clamp sample from the Ov-ob/IS group

exhibited extremely high (outlier) total TG content]. Therefore, comparative lipidomic statistical analysis was performed on 76 baseline muscle samples (21 Lean/IS, 16 Ov-ob/IS, 19 Ov-ob/IR, and 20 T2D) and 66 SS clamp muscle samples (18 Lean/IS, 13 Ov-ob/IS, 18 Ov-ob/IR, and 17 T2D). The percentage difference in lipid content between the SS clamp and baseline muscle samples was only measured in those individuals with paired muscle samples.

6.2.4 Biochemical analysis

Plasma glucose was analysed using a glucose oxidase electrode (YSI Life Sciences, Yellow Springs, OH, USA). Screening day serum insulin levels were measured using the Advia Centaur immunoassay (Walpole, MA, USA), and metabolic study day serum insulin levels were measured using radioimmunoassay (Linco Research, St Charles, MO, USA). Plasma non-esterified fatty acid (NEFA) concentrations were measured using an enzymatic calorimetric assay (Wako, Osaka, Japan), and serum total adiponectin levels were measured using a Sandwich ELISA [216].

6.2.5 Plasma and skeletal muscle lipid analysis

Paired fasting and SS hyperinsulinaemic-euglycaemic clamp plasma and skeletal muscle biopsy samples were prepared for lipid extraction and subsequent targeted lipid profiling using LC ESI-MS/MS; on a 4000 Q/TRAP mass spectrometer) and multiple reaction monitoring (MRM) experiments as previously described (Chapter 2; sections 2.1 to 2.4). Lipid peak integration, and calculation of relative amounts of lipid classes/subclasses and species (pmol/ml of plasma or pmol/mg protein in tissues) was performed as previously described (Chapter 2, section 2.4). The number of lipid species identified in each lipid class or subclass from plasma and skeletal muscle extracts for subsequent statistical analyses is shown in Table 6.1.

6.2.6 Statistical analyses

Non-parametric Mann-Whitney *U* tests were used to compare the anthropometric, body composition, and both fasting and SS clamp blood biochemistry results between groups. Data are presented as means ± SEM. $P < 0.05$ was considered significant. Prior to logistic and linear regression analysis, lipid species were standardised to the interquartile range (IQR) to allow comparison of lipid species that differ greatly in concentration. Binary logistic regression

Table 6.1 Number of lipid species identified in each lipid class or subclass from plasma and skeletal muscle extracts.

		Number of species	
Lipid class or subclass[a]	**Abbreviation**	**Plasma**	**Skeletal muscle**
Dihydroceramide	dhCer	6	0
Ceramide	Cer	6	6
Monohexosylceramide	MHC	6	0
Dihexosylceramide	DHC	6	5
Trihexosylceramide	THC	6	5
GM3 ganglioside	GM3	6	4
Sphingomyelin	SM	18	17
Phosphatidylcholine	PC	46	45
Alkylphosphatidylcholine	PC(O)	18	19
Alkenylphosphatidylcholine	PC(P)	10	13
Lysophosphatidylcholine	LPC	21	12
Lysoalkylphosphatidylcholine	LPC(O)	9	0
Phosphatidylethanolamine	PE	20	20
Alkylphosphatidylethanolamine	PE(O)	14	13
Alkenylphosphatidylethanolamine	PE(P)	12	11
Lysophosphatidylethanolamine	LPE	8	4
Phosphatidylinositol	PI	16	14
Phosphatidylserine	PS	7	7
Phosphatidylglycerol	PG	0	4
Bis(monoacylglycerol) phosphate	BMP	0	2
Cardiolipin	CL	0	13
Free cholesterol	COH	1	0
Cholesterol ester	CE	25	8
Diacylglycerol	DG	25	15
Triacylglycerol	TG	44	42
Total		**330**	**279**

[a] Sum of the individual lipid species within that class or subclass.

analysis was performed to identify associations of lipid species and lipid classes/subclasses with obesity, adjusted for the covariates age, sex, systolic blood pressure, and fasting plasma glucose and insulin levels. The IQR odds ratio obtained for each lipid or lipid class/subclass represents the number of times an individual with a lipid measurement in the 75th percentile is more likely to have obesity than an individual with a lipid measurement in the 25th percentile. The *P*-values for logistic regression were corrected for multiple comparisons using the Benjamini-Hochberg method, with $P < 0.05$ considered significant [155].

Analysis of covariance (ANCOVA) was used to identify significant differences in classes/subclasses and species between groups. ANCOVA analyses were adjusted for covariates as indicated and corrected for multiple comparisons using the Benjamini-Hochberg method ($P < 0.05$ was considered significant) [155]. Post-hoc testing was performed using logistic regression analysis with the same covariates.

To further define the association of obesity, IR and T2D with lipid species and classes in fasting plasma and skeletal muscle across the study groups, linear regression was performed with selected independent variables (outcomes), including BMI (a measure of obesity), HOMA-IR and GIR/FFM (measures of insulin sensitivity), and fasting plasma glucose and 2 h-post challenge glucose levels (measures of glycemia). The β-coefficient describes the slope of the regression line and represents the change in outcome measure associated with an IQR increase in the lipid measurement. Linear regression outcomes were adjusted for covariates as indicated. All *P*-values obtained for linear regression were adjusted for multiple comparisons using the Benjamini-Hochberg method ($P < 0.05$ was considered significant).

To assess the effect of the hyperinsulinaemic-euglycaemic clampon plasma lipids, the paired Student's t-test of log10-transformed data (corrected for multiple comparisons) was used to identify significant percentage (%) differences in plasma lipid classes/subclasses during the SS clamp compared with fasting concentrations in each study group ($P < 0.05$ was considered significant).

6.3 RESULTS

6.3.1 Subject characteristics at baseline and during steady-state insulin clamp

The female-to-male subject ratio was significantly different in the Ov-ob/IR group compared with the Ov-ob/IS group (Table 6.2). As expected, measures of adiposity (waist circumference, BMI, % total body fat, and % central fat) were significantly higher in the three overweight/obese groups compared with the Lean/IS group, but waist circumference, BMI, and % central fat were also significantly higher in the Ov-ob/IR group compared with the Ov-ob/IS group. These results indicate that any differences in metabolic or lipidomic measurements observed between the Ov-ob/IR and Ov-ob/IS groups are due to the combined effects of IR and central (visceral) obesity, and not IR alone. Therefore, all analyses comparing these two groups were adjusted for appropriate covariates, including BMI. Systolic blood pressure was significantly increased by ~15 mm Hg in the Ov-ob/IR and T2D groups compared with the Lean/IS group, and diastolic blood pressure was significantly elevated by ~10-12 mm Hg in all three overweight/obese groups compared with the Lean/IS group. Fasting plasma glucose and insulin levels were significantly higher in the Ov-ob/IR and T2D groups compared with both the Ov-ob/IS and Lean/IS groups, but fasting plasma NEFA levels were not different in any of the groups. Fasting plasma adiponectin levels were significantly lower in both the Ov-ob/IR and T2D groups compared with the Lean/IS group.

During the hyperinsulinaemic-euglycaemic clamp, SS plasma glucose and insulin levels were not different in any of the groups, with SS insulin levels increasing to approximately 300 mU/l during the 150 min clamp. The SS plasma NEFA levels were totally suppressed in all groups by the selected insulin infusion rate (80 mU/m^2/min), but plasma adiponectin levels were virtually unchanged by the insulin clamp, although there was a significant 13% drop in SS plasma adiponectin levels compared with fasting levels in the Lean/IS group. Insulin sensitivity (GIR/FFM) during the hyperinsulinaemic-euglycaemic clamp was significantly reduced by ~50% in the T2D group compared with both the Ov-ob/IS and Lean/IS groups, and significantly reduced by ~35% in the Ov-ob/IR group compared with the Lean/IS group. Although GIR/FFM was reduced by 29% in the Ov-ob/IR group compared with the Ov-ob/IS group, and was 26% higher in the Ov-ob/IR group compared with the T2D group, these values did not reach statistical significance.

Table 6.2 Baseline and steady-state hyperinsulinaemic-euglycaemic clamp characteristics of study subjects.

Subject characteristics	Lean/IS	Ov-ob/IS	Ov-ob/IR	T2D
Sex (F/M)	14F/9M	11F/5M	**7F/13M**†	12F/9M
Age (years)	54.7 ± 1.7	58.5 ± 2.3	56.3 ± 1.9	60.7 ± 1.7
Waist circumference (cm)	80.5 ± 1.8	**99.8 ± 3.1***	**111.2 ± 2.3**$^{* \dagger}$	**102.8 ± 2.6***
BMI (kg/m^2)	21.9 ± 0.4	29.0 ± 0.9*	**34.3 ± 1.5**$^{* \dagger}$	**30.2 ± 0.8***
FFM (kg)	45.8 ± 1.7	47.6 ± 2.7	**59.9 ± 2.5**$^{* \dagger}$	51.1 ± 2.8
Total body fat (%)	27.3 ± 1.7	**40.4 ± 2.0***	**40.8 ± 2.2***	**40.1 ± 1.6***
Central fat (%)	23.6 ± 1.6	**38.5 ± 2.3***	**43.5 ± 1.4**$^{* \dagger}$	**42.4 ± 1.4***
Systolic blood pressure (mm Hg)	120 ± 3	131 ± 4	**135 ± 4***	**136 ± 4***
Diastolic blood pressure (mm Hg)	73 ± 2	**84 ± 3***	**85 ± 2***	**82 ± 2***
Fasting glucose (mmol/l)	4.5 ± 0.1	4.8 ± 0.1	**5.3 ± 0.1**$^{* \dagger}$	**6.3 ± 0.3**$^{* \dagger}$
2 h post-load glucose (mmol/l)	5.2 ± 0.2	6.3 ± 0.3	**7.1 ± 0.3***	**11.0 ± 0.4**$^{* \dagger \ddagger}$
Fasting insulin (mU/l)	11.8 ± 2.6	11.7 ± 1.0	**23.9 ± 1.9**$^{* \dagger}$	**23.7 ± 2.4**$^{* \dagger}$
Fasting NEFA (mmol/l)	0.37 ± 0.03	0.38 ± 0.04	0.32 ± 0.03	0.37 ± 0.03
Fasting adiponectin (mg/l)	25.5 ± 2.7	22.2 ± 2.6	**13.8 ± 1.7***	**14.7 ± 2.0***
HOMA-IR	1.08 ± 0.08	1.19 ± 0.08	**4.28 ± 0.24**$^{* \dagger}$	NM
SS glucose (mmol/l)	5.0 ± 0.1	5.0 ± 0.1	5.0 ± 0.1	5.1 ± 0.1
SS insulin (mU/l)	272 ± 10	323 ± 26	334 ± 22	358 ± 27
SS NEFA (mmol/l))	0.02 ± 0.00	0.01 ± 0.00	0.02 ± 0.01	0.01 ± 0.00
SS adiponectin (mg/l)	22.3 ± 2.7	21.0 ± 2.9	**12.6 ± 1.5***	**14.0 ± 2.0***
SS GIR/FFM (µmol.min^{-1}/kg^{-1})	92.3 ± 4.9	85.6 ± 9.3	**60.9 ± 5.4***	**44.8 ± 3.0**$^{* \dagger}$

Values expressed as mean ± SEM. IS, insulin sensitive; Ov-ob, overweight-to-obese; IR, insulin resistant; T2D, type 2 diabetic; F, female; M, male; BMI, body mass index; FFM, fat-free mass; NEFA, non-esterified fatty acids; HOMA-IR, homeostatic model assessment of insulin resistance; NM, not measured; SS, steady-state (clamp); GIR/FFM, exogenous glucose infusion rate/fat-free mass.
$^{*}P < 0.05$ vs. Lean/IS group; $^{\dagger}P < 0.05$ vs. Ov-ob/IS group; $^{\ddagger}P < 0.05$ vs. Ov-ob/IR group by Mann-Whitney *U* test for paired group comparisons.

6.3.2 Assay performance of lipid measurements

To assess the assay performance of our lipidomic profiling we determined the %CV of each lipid species using the 12-14 specific QC samples spaced evenly throughout the lipid extraction procedure. For plasma extracts, the median %CV of the 330 lipid species in the plasma QCsamples was 10.4%, with 90% of lipid species having a %CV below 20.1%. For skeletal muscle extracts, the median %CV of the 279 lipid species in the THP-1 (monocyte) QC samples was 16.3%, with 90% of lipid species having a %CV below 35.1%. Those lipid species that had a CV greater than 30% (n = 3 and n = 43 in plasma and THP-1 QC samples respectively) were primarily low abundant and/or had poor chromatography resolution.

6.3.3 Lipids associated with obesity, insulin resistance and type 2 diabetes

To investigate the relationship between fasting plasma lipids with obesity and IR, ANCOVA analysis of fasting plasma lipids in the four study groups (adjusted for age, sex and systolic blood pressure) was performed. This analysis revealed that 11 lipid classes/subclasses (TG, LPC, LPC(O), PC(O), THC, PC(P), GM3, PS, DHC, DG and CE) and 84 species (including 19 TG, 15 LPC, eight LPC(O), eight PC, six PC(O), five THC and four PC(P) species) were significantly different across the four groups (overall Benjamini-Hochberg corrected *P*-values < 0.05) (Tables 6.3 and S6.1). Post-hoc analysis revealed that two lipid classes (TG and PS) and 11 species were significantly different in the Ov-ob/IS group compared with the Lean/IS group, including a reduction in multiple species of THC and PC(O) (obesity-induced effects). Moreover, the CE lipid class and 20 species were significantly different in the Ov-ob/IR group compared with the Ov-ob/IS group, including a reduction in nine LPC species, and elevation in multiple species of CE, DG and TG (IR-induced effects).

Post-hoc analysis also revealed that three lipid classes/subclasses (LPC, LPC(O) and PS) and 22 species were significantly different in the T2D group compared with the Ov-ob/IS group, including a reduction in multiple species of PC, PC(P), LPC and LPC(O) (combined IR- and T2D-induced effects). Strikingly, eight lipid classes/subclasses and 65 species were significantly different in the Ov-ob/IR group compared with the Lean/IS group (combined IR- and obesity-induced effects), and seven lipid classes/subclasses and 68 lipid species were significantly different in the T2D group compared with the Lean/IS group (combined IR-, obesity- and T2D-induced effects) (Tables 6.3 and S6.1). Notably, 55 of these lipid species were significantly

Table 6.3 Significance levels obtained for comparisons of fasting plasma lipid classes and subclasses between the four study groups.

Lipid class or subclass[a]	ANCOVA[b]	Ov-ob/IS vs. Lean/IS	Ov-ob/IR vs. Lean/IS	T2D vs. Lean/IS	Ov-ob/IR vs. Ov-ob/IS	T2D vs. Ov-ob/IS	T2D vs. Ov-ob/IR
	Corrected *P*-value[c]	Post-hoc *P*-value[d]	Post-hoc *P*-value[d]	Post-hoc *P*-value[d]	Post-hoc *P*-value[d]	Post-hoc *P*-value[d]	Post-hoc *P*-value[d]
dhCer	1.84E-01	3.73E-01 (+)	4.77E-01 (+)	1.16E-01 (+)	1.00E+00	9.97E-01(+)	9.81E-01 (+)
Cer	6.37E-01	9.24E-01 (+)	5.90E-01 (+)	9.26E-01 (+)	9.96E-01 (+)	1.00E+00	9.92E-01 (-)
MHC	7.25E-02	6.41E-01 (-)	9.60E-02 (-)	5.42E-02 (-)	9.16E-01 (-)	8.07E-01 (-)	1.00E+00
DHC	**3.22E-02**	2.18E-01 (-)	**8.27E-03 (-)**	1.04E-01 (-)	8.16E-01 (-)	1.00E+00	9.05E-01 (+)
THC	**2.75E-04**	**2.02E-02 (-)**	**2.33E-04 (-)**	**3.17E-05 (-)**	7.49E-01 (-)	3.85E-01 (-)	9.98E-01 (-)
GM3	**6.68E-03**	6.34E-01 (-)	**9.30E-04 (-)**	**3.44E-02 (-)**	9.75E-02 (-)	7.05E-01 (-)	7.65E-01 (+)
SM	4.17E-01	9.98E-01 (-)	9.35E-01 (-)	3.40E-01 (-)	9.99E-01 (-)	7.01E-01 (-)	9.20E-01 (-)
PC	4.44E-01	1.00E+00	1.00E+00	5.40E-01 (-)	1.00E+00	5.75E-01 (-)	7.08E-01 (-)
PC(O)	**2.89E-02**	1.19E-01 (-)	5.87E-02 (-)	**6.78E-03 (-)**	1.00E+00	9.22E-01 (-)	9.79E-01 (-)
PC(P)	**2.89E-02**	8.53E-01 (-)	9.36E-02 (-)	**8.35E-03 (-)**	7.39E-01 (-)	1.90E-01 (-)	9.55E-01 (-)
LPC	**1.21E-03**	8.79E-01 (-)	**2.10E-03 (-)**	**9.07E-04 (-)**	6.80E-02 (-)	**3.12E-02 (-)**	1.00E+00
LPC(O)	**2.75E-04**	5.66E-01 (-)	**6.77E-04 (-)**	**2.76E-05 (-)**	9.80E-02 (-)	**8.01E-03 (-)**	9.58E-01 (-)
PE	3.45E-01	8.82E-01 (+)	5.04E-01 (+)	2.77E-01 (+)	9.95E-01 (+)	9.44E-01 (+)	1.00E+00
PE(O)	8.33E-01	9.75E-01 (-)	1.00E+00	9.92E-01 (-)	9.38E-01 (+)	1.00E+00	9.64E-01 (-)
PE(P)	8.33E-01	9.98E-01 (+)	9.56E-01 (+)	1.00E+00	1.00E+00	9.89E-01 (-)	8.93E-01 (-)
LPE	5.99E-02	7.78E-01 (-)	**4.55E-02 (-)**	8.08E-02 (-)	6.36E-01 (-)	7.78E-01 (-)	1.00E+00
PI	9.57E-01	1.00E+00	1.00E+00	9.99E-01 (-)	1.00E+00	1.00E+00	9.96E-01 (-)
PS	**2.89E-02**	**1.41E-02 (+)**	9.98E-01 (+)	1.00E+00	6.49E-02 (-)	**3.06E-02 (-)**	1.00E+00
COH	8.33E-01	9.66E-01 (+)	1.00E+00	1.00E+00	9.27E-01 (-)	9.33E-01 (-)	1.00E+00
CE	**5.00E-02**	9.54E-01 (-)	1.92E-01 (+)	1.00E+00	**3.13E-02 (+)**	9.95E-01 (+)	7.76E-02 (-)
DG	**5.00E-02**	1.00E+00	**4.12E-02 (+)**	9.98E-01 (+)	7.92E-02 (+)	1.00E+00	1.01E-01 (-)
TG	**3.37E-02**	7.08E-01 (+)	**2.12E-02 (+)**	**3.88E-02 (+)**	5.17E-01 (+)	6.62E-01 (+)	1.00E+00

Ov-ob, overweight-to-obese; IS, insulin sensitive; IR, insulin resistant; T2D, type 2 diabetic

[a] Sum of the individual species within that class or subclass.

[b] Analysis of covariance of each lipid class or subclass in the four groups, adjusted for age, sex, and systolic blood pressure, with [c] *P*-value corrected for multiple comparisons using Benjamini-Hochberg method.

[d] Post-hoc analysis was performed using the Mann Whitney *U* test with Dunn-Sidak correction for multiple group comparisons.

Bold type indicates $P < 0.05$, with positive or negative sign in brackets indicating direction of change of lipid class or subclass relative to latter group.

altered (and in the same direction) in both group comparisons (Table 6.6). Consistent with these findings, there was very little difference in lipid profiles between the T2D and Ov-ob/IR groups, with only four lipid species (PE(O-42:7), SM 38:1, PC 31:1 and CE 18:2) found to be significantly different (T2D-induced effects). ANCOVA analysis of fasting skeletal muscle lipids in the four study groups (adjusted for age, sex and systolic blood pressure) identified 16 lipid species (including multiple species of PC(P), LPC, PE(O), PI and TG) with overall uncorrected *P*-values < 0.05. However, after Benjamini-Hochberg correction for multiple comparisons, no lipid species remained significantly different across the four groups (data not shown). Despite this lack of significance, the mean total TG levels in fasting skeletal muscle in the Ov-Ob/IR group [21751 ± 2569 (SEM) pmol/mg protein] and T2D group (29794 ± 7545 pmol/mg protein) were elevated by 47% and 102% respectively compared with the Lean/IS group (14785 ± 3607 pmol/mg protein). To lessen the variability of lipid contents, fasting skeletal muscle lipid levels were normalised to total PC content, which are stable and abundant membrane lipids. Using this normalised data, ANCOVA analysis of the four study groups now identified 22 lipid species (including multiple species of Cer, PC(P), LPC, PE(O), PI, CL and TG species) with overall uncorrected *P*-values < 0.05. However, only PE(P-36:2) remained significantly different across the four groups after Benjamini-Hochberg correction for multiple comparisons (data not shown). In addition, the insulin clamp did not significantly alter the levels of any skeletal muscle lipid classes/subclasses compared with their corresponding fasting levels in any of the groups.

6.3.4 Lipids associated with measures of insulin sensitivity

Linear regression of fasting plasma lipids against HOMA-IR (a measure of IR) in the three non-diabetic groups only (HOMA-IR was not measured in 18 previously diagnosed T2D subjects), adjusted for age, sex, BMI and systolic blood pressure, identified two lipid classes (DG and CE) and 34 species (including 15 DG, 15 TG, three CE species, and LPC 22:6) that remained significantly associated with HOMA-IR after Benjamini-Hochberg correction for multiple comparisons ($P < 0.05$) (Tables 6.4 and S6.2). Notably, all DG, TG and CE species were positively associated with HOMA-IR. Linear regression of SS clamp plasma against HOMA-IR identified three lipid classes (DG, TG and CE) and 71 lipid species (including 26 TG, 24 DG, 15 CE and three PE species) that remained significantly associated with HOMA-IR after Benjamini-Hochberg correction for multiple comparisons (Tables 6.4 and S6.2). Notably, all

Table 6.4 Linear regression of lipid classes and subclasses with HOMA-IR in fasting plasma and steady-state clamp plasma.

Lipid class[a] or subclass	HOMA-IR[b] (fasting plasma)			HOMA-IR[b] (steady-state clamp plasma)		
	β-Coefficient (95% CI)[c]	Uncorrected *P*-value	Corrected *P*-value[d]	β-Coefficient (95% CI)[c]	Uncorrected *P*-value	Corrected *P*-value[d]
dhCer	0.11 (-0.28 - 0.49)	5.88E-01	7.57E-01	0.19 (-0.18 - 0.55)	3.26E-01	5.09E-01
Cer	0.31 (-0.16 - 0.77)	2.05E-01	5.51E-01	0.31 (-0.05 - 0.67)	9.69E-02	2.69E-01
MHC	-0.07 (-0.48 - 0.34)	7.51E-01	8.23E-01	-0.05 (-0.47 - 0.38)	8.27E-01	8.61E-01
DHC	-0.20 (-0.55 - 0.15)	2.62E-01	5.51E-01	-0.40 (-0.83 - 0.04)	8.36E-02	2.69E-01
THC	-0.05 (-0.57 - 0.46)	8.37E-01	8.72E-01	-0.17 (-0.72 - 0.38)	5.50E-01	6.55E-01
GM3	-0.32 (-0.84 - 0.21)	2.43E-01	5.51E-01	-0.25 (-0.71 - 0.22)	3.02E-01	5.07E-01
SM	0.12 (-0.28 - 0.52)	5.48E-01	7.57E-01	0.01 (-0.36 - 0.38)	9.70E-01	9.70E-01
PC	0.19 (-0.19 - 0.58)	3.25E-01	5.51E-01	0.15 (-0.22 - 0.52)	4.38E-01	5.62E-01
PC(O)	0.08 (-0.32 - 0.48)	6.93E-01	8.23E-01	0.19 (-0.30 - 0.68)	4.46E-01	5.62E-01
PC(P)	-0.07 (-0.54 - 0.39)	7.57E-01	8.23E-01	-0.13 (-0.59 - 0.34)	6.03E-01	6.85E-01
LPC	-0.31 (-0.75 - 0.13)	1.74E-01	5.51E-01	-0.27 (-0.78 - 0.23)	2.99E-01	5.07E-01
LPC(O)	-0.39 (-0.98 - 0.20)	2.00E-01	5.51E-01	-0.22 (-0.78 - 0.34)	4.50E-01	5.62E-01
PE	0.20 (-0.13 - 0.53)	2.42E-01	5.51E-01	0.39 (0.08 - 0.70)	**1.82E-02**	1.14E-01
PE(O)	0.22 (-0.25 - 0.69)	3.67E-01	5.73E-01	0.28 (-0.13 - 0.69)	1.85E-01	4.22E-01
PE(P)	0.12 (-0.32 - 0.56)	6.05E-01	7.57E-01	0.27 (-0.22 - 0.76)	2.88E-01	5.07E-01
LPE	-0.30 (-0.91 - 0.30)	3.31E-01	5.51E-01	0.22 (-0.19 - 0.63)	3.04E-01	5.07E-01
PI	0.22 (-0.18 - 0.63)	2.82E-01	5.51E-01	0.25 (-0.01 - 0.51)	6.90E-02	2.69E-01
PS	-0.46 (-0.94 - 0.01)	6.35E-02	3.97E-01	0.09 (-0.34 - 0.51)	6.92E-01	7.52E-01
COH	0.00 (-0.45 - 0.45)	9.99E-01	9.99E-01	0.18 (-0.24 - 0.60)	4.00E-01	5.62E-01
CE	0.68 (0.32 - 1.03)	**4.60E-04**	**1.15E-02**	0.61 (0.37 - 0.85)	**7.03E-06**	**1.76E-04**
DG	0.43 (0.18 - 0.68)	**1.33E-03**	**1.66E-02**	0.29 (0.15 - 0.44)	**3.16E-04**	**3.95E-03**
TG	0.34 (0.09 - 0.58)	**9.32E-03**	7.77E-02	0.71 (0.33 - 1.10)	**5.93E-04**	**4.94E-03**

HOMA-IR, homeostasis model assessment of insulin resistance

[a] Sum of the individual species within that class or subclass.

[b] Linear regression of HOMA-IR versus each lipid class or subclass in the three non-diabetic groups, adjusted for age, sex, BMI and systolic blood pressure.

[c] Beta-coefficient (95% confidence intervals) based on an interquartile range increase in predictor lipid class or subclass measurement.

[d] *P*-value corrected for multiple comparisons using Benjamini-Hochberg method. Bold type indicates $P < 0.05$.

TG, DG, CE and PE species were positively associated with HOMA-IR. Furthermore, all 33 DG, TG and CE species in fasting plasma that were positively associated with HOMA-IR were also positively associated with HOMA-IR in SS clamp plasma. Therefore, the hyperinsulinaemic-euglycaemic clamp conditions further strengthened the positive association that existed between plasma DG, TG and CE species and HOMA-IR. Linear regression of fasting plasma lipids against GIR/FFM (clamp measure of insulin sensitivity) in the four study groups, adjusted for age, sex, BMI and systolic blood pressure, identified five lipid classes/subclasses (dhCer, LPC, LPC(O), PE and TG) and 55 species (including 20 TG species, and multiple species of dhCer, PC(P), LPC, LPC(O), PE, CE and DG) that remained significantly associated with GIR/FFM after Benjamini-Hochberg correction for multiple comparisons (data not shown). Notably, all dhCer, PE, DG and TG species were negatively associated with GIR/FFM, and all PC(P), LPC and LPC(O) species were positively associated with GIR/FFM. However, only 11 fasting plasma lipid species (nine "saturated" TG species, DG 16:0/20:3 and DG 16:1/18:0) were significantly associated with both HOMA-IR and GIR/FFM.

Linear regression of SS clamp plasma against GIR/FFM identified the TG lipid class and 46 species (including 22 TG species, and multiple species of PC(P), LPC, PE, CE and DG) that remained significantly associated with HOMA-IR after Benjamini-Hochberg correction for multiple comparisons (data not shown). Notably, all PE, DG and TG species were negatively associated with GIR/FFM, and all PC(P) and LPC species were positively associated with GIR/FFM. Furthermore, 39 of the 55 lipid species in fasting plasma that were significantly associated with GIR/FFM were also associated with GIR/FFM in SS clamp plasma, and confirmed the consistent associations that existed between plasma PE, DG, TG, PC(P) and LPC species and GIR/FFM.

6.3.5 Lipids associated with body mass index and measures of glycaemia

Linear regression of fasting plasma and skeletal muscle lipids was also tested against BMI in the four study groups (adjusted for age, sex, systolic blood pressure, and fasting plasma glucose and insulin levels), against fasting plasma glucose in the four study groups (adjusted for age, sex, BMI and systolic blood pressure), and against 2 h-post load glucose in the three non-diabetic groups only (2 h-post load glucose was not measured in 14 previously diagnosed T2D subjects). Although linear regression resulted in numerous fasting plasma and skeletal muscle lipid classes/subclasses and species being associated with each of the outcomes, generating

uncorrected *P*-values < 0.05, none of these lipid classes/subclasses or species remained significantly associated with the specified outcome after Benjamini-Hochberg correction for multiple comparisons (data not shown). For example, linear regression of fasting plasma lipids against BMI identified five lipid classes/subclasses (THC, GM3, LPC, LPC(O), and LPE) and 34 species (including 13 LPC species, and multiple species of GM3, PC(P) and LPC(O)) with uncorrected *P*-values < 0.05. However, no lipid classes/subclasses or species remained significantly associated with BMI after correction for multiple comparisons. These findings indicate that some of these lipid classes/subclasses and species may have been significantly associated with fasting plasma glucose if more individuals had participated in the study.

6.3.6 Comparison of steady-state clamp and fasting plasma lipids

The effect of the hyperinsulinaemic-euglycaemic clamp on plasma lipids was assessed in each study group. Any changes in lipid levels during the clamp are induced by the acute effects of non-physiological and sustained circulating insulin levels. The SS clamp induced a significant percentage drop in 17 of the 21 plasma lipid classes/subclasses compared with fasting plasma in the Lean/IS group (Table 6.5). The SS clamp also resulted in a significant percentage drop in 14 of the 21 plasma lipid classes compared with fasting plasma in the Ov-Ob/IS group. Plasma lipid total PC(O), LPC, LPC(O) and COH were not significantly altered by the insulin clamp in either the Lean/IS or Ov-Ob/IS groups, and plasma total PC, PC(P) and CE were also not significantly altered by the insulin clamp in the Ov-Ob/IS group. In contrast, the SS clamp induced a significant percentage drop in only 6 of the 21 plasma lipid classes/subclasses compared with fasting plasma in the Ov-Ob/IR group, namely total dhCer, Cer, SM, PE(O), PE(P) and DG (Table 6.5). In the T2D group, the SS clamp induced a significant percentage drop in 15 of the 21 plasma lipid classes/subclasses compared with fasting plasma, which was almost identical to the pattern seen in the Ov-Ob/IS group.

6.4 DISCUSSION

6.4.1 Different lipid abnormalities are associated with obesity and insulin resistance

In the present human study, 80 adult participants were classified into one of four groups according to BMI, HOMA-IR, and diabetic status. Targeted lipid profiling was performed using LC ESI-MS/MS to identify plasma and skeletal muscle lipid abnormalities (at the class/subclass

Table 6.5 Fasting plasma levels and percentage differences (steady-state clamp vs. fasting) in lipid classes/subclasses in the four groups.

Lipid class or subclass[a]	Lean/IS		Ov-ob/IS		Ov-ob/IR		T2D	
	Fasting (pmol/ml)	% difference SS vs. fasting	Fasting (pmol/ml)	% difference SS vs. fasting	Fasting (pmol/ml)	% difference SS vs. fasting	Fasting (pmol/ml)	% difference SS vs. fasting
dhCer	606 ± 33	**-21.8 ± 2.6***	718 ± 65	**-18.1 ± 3.5***	721 ± 36	**-16.7 ± 2.8***	752 ± 49	**-18.2 ± 2.2***
Cer	4821 ± 170	**-14.8 ± 1.3***	5405 ± 356	**-13.9 ± 1.9***	5758 ± 433	**-9.5 ± 1.6***	5490 ± 281	**-13.2 ± 1.2***
MHC	9723 ± 438	**-14.0 ± 3.0***	8465 ± 724	**-12.9 ± 1.8***	8025 ± 421	-6.5 ± 2.5	7578 ± 651	**-10.0 ± 2.0***
DHC	5987 ± 249	**-12.2 ± 2.0***	5115 ± 259	**-13.3 ± 3.1***	4700 ± 192	-7.8 ± 2.5	5031 ± 317	**-10.3 ± 2.3***
THC	1850 ± 77	**-15.5 ± 2.3***	1540 ± 88	**-12.4 ± 2.4***	1353 ± 73	-8.4 ± 2.8	1366 ± 74	**-12.3 ± 2.4***
GM3	3145 ± 128	**-13.2 ± 2.2***	2938 ± 116	**-13.8 ± 2.0***	2513 ± 152	-6.9 ± 2.9	2740 ± 130	**-13.2 ± 1.7***
SM	350610 ± 10838	**-11.9 ± 1.5***	352344 ± 12830	**-9.0 ± 2.0***	341013 ± 12307	**-8.7 ± 1.5***	333627 ± 13711	**-9.1 ± 1.1***
PC	1388696 ± 34780	**-7.4 ± 1.8***	1393237 ± 33851	-1.2 ± 2.6	1391880 ± 42796	-2.7 ± 2.3	1312095 ± 35382	0.1 ± 2.1
PC(O)	46905 ± 1695	-4.3 ± 1.5	40715 ± 1595	-0.5 ± 2.5	40211 ± 1816	0.5 ± 2.2	39417 ± 1630	-1.0 ± 2.0
PC(P)	26070 ± 1216	**-5.2 ± 1.4***	24594 ± 1154	-1.9 ± 2.3	21740 ± 1232	-2.9 ± 1.9	21545 ± 867	-2.6 ± 1.8
LPC	151616 ± 6929	-8.1 ± 2.7	138458 ± 5616	-5.3 ± 2.5	121594 ± 8677	2.4 ± 2.6	115632 ± 5680	-1.2 ± 2.9
LPC(O)	449 ± 20	-0.9 ± 2.0	389 ± 23	2.7 ± 3.3	340 ± 18	7.5 ± 2.6	315 ± 18	**9.3 ± 2.2***
PE	23954 ± 1912	**-21.0 ± 2.8***	26378 ± 2199	**-16.8 ± 3.5***	28692 ± 2557	-3.5 ± 4.9	29243 ± 2257	**-16.6 ± 2.5***
PE(O)	4124 ± 258	**-15.3 ± 1.4***	3949 ± 259	**-15.2 ± 2.6***	4212 ± 312	**-13.4 ± 1.7***	4019 ± 242	**-18.3 ± 1.4***
PE(P)	32466 ± 1798	**-17.7 ± 2.0***	33942 ± 2330	**-16.1 ± 3.3***	34635 ± 2521	**-14.8 ± 2.4***	33289 ± 2199	**-18.7 ± 2.0***
LPE	2452 ± 126	**-24.5 ± 3.3***	2172 ± 118	**-20.3 ± 2.5***	1995 ± 115	-2.4 ± 4.0	2016 ± 96	**-18.0 ± 3.0***
PI	82067 ± 3864	**-14.8 ± 2.3***	81036 ± 3919	**-10.3 ± 2.7***	83914 ± 5283	-8.1 ± 2.8	80703 ± 4838	**-8.6 ± 1.9***
COH	719880 ± 40778	-0.5 ± 6.4	797069 ± 45401	-13.3 ± 6.0	736382 ± 56629	6.6 ± 7.0	763121 ± 77512	-8.8 ± 5.1
CE	4871222 ± 244917	**-12.2 ± 2.9***	4522363 ± 248715	-7.6 ± 4.0	6226779 ± 443481	-2.7 ± 7.0	4952933 ± 334876	-5.5 ± 6.0
DG	32117 ± 3201	**-31.3 ± 3.6***	33407 ± 5423	**-26.2 ± 3.4***	65370 ± 10315	**-19.9 ± 4.0***	39387 ± 4003	**-23.9 ± 2.5***
TG	318145 ± 29665	**-24.5 ± 4.1***	425322 ± 53883	**-25.5 ± 3.2***	667095 ± 102619	-7.5 ± 7.6	582380 ± 65464	**-21.5 ± 3.3***

Values expressed as mean ± SEM. IS, insulin sensitive; Ov-ob, overweight-to-obese; IR, insulin resistant; T2D, type 2 diabetic; SS, steady-state (clamp)

[a] Sum of the individual species within that class or subclass.

*P < 0.05 vs. corresponding fasting value by paired Student's t-test of log10-transformed data, corrected for multiple comparisons.

and species level) associated with obesity (independently of IR), IR (independently of obesity), combined obesity and IR, and T2D both in the fasting state and at the completion of a 150 min hyperinsulinaemic-euglycaemic clamp. This analysis was made possible by the inclusion of the Ov-ob/IS group, which enabled lipid abnormalities associated with obesity to be identified by comparing the Ov-ob/IS and Lean/IS groups, and lipid abnormalities associated with IR to be identified by comparing the Ov-ob/IR and Ov-ob/IS groups.

6.4.2 Lipid abnormalities associated with obesity

When ANCOVA post-hoc analysis was applied to identify fasting plasma lipids associated with obesity, 11 lipid species were significantly altered in the Ov-ob/IS group compared with the Lean/IS group. These differences included significantly lower levels of the THC subclass, along with THC 16:0, THC 20:0, PC(O-32:0), PC(O-34:1), PC(O-36:2), PC(P-32:0) and LPC(O-24:2) in the Ov-ob/IS group (Tables 6.3 and S6.1). In agreement with our findings, Pietilainen *et al.* found that young adult monozygotic obese twins (median BMI 30.4 kg/m^2) had decreased levels of some ether phospholipids in fasting plasma, including PC(O-34:1), compared with their non-obese twins (median BMI 25.4 kg/m^2) [29]. Additionally, several PC(O) species negatively correlated with subcutaneous fat mass, but PC(O-16:0/18:1) and PC(O-16:1/18:2) positively correlated with insulin sensitivity [29]. In contrast, Donovan *et al.* found that five PC(O) species, including the arachidonic acid containing PC(O-18:0/20:4) and PE(P-18:0/20:4), were elevated in morbidly obese subjects (mean BMI 49.9 kg/m^2) compared with lean subjects (mean BMI 25.8 kg/m^2) [63]. In addition, the treatment of human coronary artery endothelial cells with the plasmalogen PE(P-18:0/20:4) induced expression of cell adhesion molecules, indicative of endothelial cell activation and atherogenesis [63]. Recently, Heilbronn *et al.* observed elevations in fasting plasma PE(P) and PE(O) subclasses in response to 28 days overfeeding by 1250 kcal/day (45% total energy as fat) in healthy adults [54]. Furthermore, Graessler *et al.* found that two polyunsaturated PE(P) plasmalogens were significantly elevated in fasting plasma in obese men (BMI > 27.5 kg/m^2) compared with a group of leaner men (BMI ≤ 27.5 kg/m^2), but 13 other ether phospholipid species were unchanged by obesity [28].

It has been reported that the severity of disease in each individual and heterogenous populations may account for the large discrepancy in relative abundance, pattern of change, and effects induced by individual ether-linked PC(O) and PE(O) and plasmalogen PC(P) and PE(P) species indifferent human cohorts [63]. Presently, there is no consensus as to whether ether-linked

phospholipids are antioxidants and/or anti-inflammatory. Although vinyl ether-linked plasmalogens are more susceptible to free radical oxidation than ester-linked phospholipids [218,219], plasmalogens may function as free radical scavengers, being preferentially synthesized as an antioxidant in response to increasing oxidative stress with obesity or overfeeding [54,189]. Conversely, decreased plasmalogen levels in obesity [28] and in LDL from patients with the metabolic syndrome and diabetes were considered indicators of oxidative stress [220]. The decreased levels of three PC(O) species and PC(P-32:0) observed in our Ov-ob/IS group compared with the Lean/IS group may also relate to decreased biosynthesis [189].

6.4.3 Lipid abnormalities associated with insulin resistance

When ANCOVA post-hoc analysis was applied to identify fasting plasma lipids associated with IR, 20 lipid species were significantly altered in the Ov-ob/IR group compared with the Ov-ob/IS group. Strikingly, nine LPC species (including LPC 22:6) were significantly decreased in the Ov-ob/IR group, along with GM3 24:1, PE(P-40:4) and LPC(O-24:2), and two species each from the CE, DG, and TG lipid classes were significantly elevated in the Ov-ob/IR group (Table S6.1).

Decreased fasting plasma LPC levels have also been found in glucose intolerant and insulin resistant individuals [13,53], and the elevation in IR observed in healthy adults in response to 28 days overfeeding was accompanied by reductions in many fasting plasma LPC species, and in particular, LPC 22:6 was positively correlated with insulin sensitivity [54]. Recent evidence suggests that LPC may be a novel insulin-independent signal that regulates blood glucose levels [56]. Therefore, the decreased circulating LPC species in our Ov-ob/IR group may contribute to the defects in glucose homeostasis observed in IR and obesity. Barber *et al.* also showed a reduction in the level of many fasting plasma LPC species in obese/IS and obese/T2D subjects (matched for body mass and BMI) compared with lean healthy subjects, but since there were no differences in LPC levels between the obese/IS and obese/T2D subjects, obesity was considered more important than IR and T2D in determining LPC levels [26].

In contrast, Pietilainen *et al.* found that the fasting serum levels of some LPC species were elevated in healthy young adult monozygotic obese twins compared with their non-obese co-twins [29]. The lysophospholipids, LPC and LPE, are derived from the oxidation of polyunsaturated (particularly 20:4 and 22:6)-containing vinyl ether-linked plasmalogens, PC(P)

and PE(P), but are also products of PC and PE hydrolysis by secretory phospholipases [54,63]. However, LPCs can independently increase plasminogen activator inhibitor-1, a potent prothrombotic and proatherogenic protein [58], and induce endothelial cell expression of cell adhesion molecules [59]. Another study found that dietary fatty acid composition influenced the relative abundances of LPC species in overweight/obese IR men (with a higher fat intake) compared with age-matched lean healthy men [48]. In our study, the significant reduction in nine LPC species in the Ov-ob/IR group compared with the Ov-ob/IS group appeared to be closely linked to the severity of IR (in the setting of obesity), although the increased BMI in the Ov-ob/IR group (Table 6.2) may be a confounding factor.

Linear regression analysis of fasting plasma lipids against HOMA-IR in the three non-diabetic groups revealed that two lipid classes (DG and CE) and three CE, 15 DG and 15 TG species were positively associated with HOMA-IR, and only one lipid species (LPC 22:6) was negatively associated with HOMA-IR (Tables 6.4 and S6.2). This result compares with ANCOVA post-hoc analysis of the Ov-ob/IR versus Ov-ob/IS groups (i.e., IR effect), which revealed that nine LPC species were significantly reduced in the Ov-ob/IR group. It is likely that any linear association of LPC species with HOMA-IR was dissipated by the finding of no significant differences in any LPC species between the Ov-ob/IS and Lean/IS groups. Nonetheless, seven species (CE 18:2, CE 20:3, DG 16:0/18:0, DG 18:0/18:1, TG 18:0/18:0/18:1, TG 18:0/18:1/18:1 and LPC 22:6) showed a significant association with both testing methods.

6.4.4 Lipid abnormalities associated with combined obesity and insulin resistance

When ANCOVA post-hoc analysis was applied to identify fasting plasma lipids associated with combined obesity and IR, eight lipid classes/subclasses (DHC, THC GM3, LPC, LPC(O), LPE, DG and TG) and 65 species were significantly altered in the Ov-ob/IR group compared with the Lean/IS group (Table 6.3 and S6.1). While obesity was associated with significant decreases in some THC and PC(O) species, and IR was associated with significant decreases in many LPC species, combined obesity and IR was also associated with significant decreases in some DHC, GM3, LPC(O) and LPE species, and significant increases in many DG and TG species. Therefore, the complex lipid abnormalities associated with the combined setting of obesity and IR far outweighed the sum of the lipid abnormalities associated with obesity or IR alone.

The lower levels of the THC subclass and five of the six measured THC species in the Ov-ob/IR group compared with the Lean/IS group may be due to down regulation of the galactosyltransferases that convert ceramide to DHC and THC. Supporting these findings, Meikle *et al.* showed a negative association between the DHC and THC subclasses and 2 h-post load glucose levels (a measure of T2D) in the San Antonio Family Heart Study cohort [9]. LPC(O) lipids, also known as lysoplatelet activating factors, are derived from the cleavage of ether-linked phospholipids, PC(O) and PC(P), by lipoprotein phospholipase A2 (Lp-PLA2), but are also formed by the catabolic action of Lp-PLA2 on platelet activating factor, a potent proinflammatory signalling lipid [63]. LPC(O) opposes the actions of platelet activating factor, and has anti-inflammatory actions which include inhibiting the activation and aggregation of neutrophils and platelets [221]. In our study, seven fasting plasma LPC(O) species were significantly decreased in the Ov-ob/IR group compared with the Lean/IS group, including LPC(O-22:0), LPC(O-24:1) and LPC(O-24:2), which were also found to be negatively associated with T2D [9]. Similarly, Heilbronn *et al.* found that the LPC(O) subclass was significantly lower in fasting plasma of healthy adults after 28 days overfeeding, and that LPC(O-16:0) and LPC(O-22:1) negatively correlated with the inflammatory marker C-reactive protein at baseline [54]. Recently, Nestel *et al.*found that LPC(O-20:0) and LPC(O-22:1) from full-fat dairy diets were positively associated with insulin sensitivity and inversely associated with IR [55]. Paradoxically, Lp-PLA2 was found to be elevated in T2D [222,223], but lower in polycystic ovary syndrome patients, which was associated with IR [224].

We also found that three ganglioside species (GM3 16:0, GM3 18:0 and GM3 24:1) were significantly decreased in fasting plasma in the Ov-ob/IR group compared with the Lean/IS group. This finding is contrary to expectations, given that gangliosides have been implicated in IR, with GM3 synthase-deficient mice showing increased insulin sensitivity and enhanced insulin receptor phosphorylation in skeletal muscle [225]. Furthermore, both chronic high-fat/high sucrose diet-induced obese C57BL/6J mice and genetic severely obese KKAy mice exhibited significantly elevated GM3 species with shorter chain acyl (16:0 and 18:0) moieties in adipose tissue compared with each control group [71]. Our findings of lower levels of some GM3 species in subjects with combined obesity and IR may relate to measuring GM3 levels in plasma rather than tissues, where the metabolism of gangliosides may be different. However, in agreement with our findings, both fasting plasma GM3 18:0 and GM3 24:1 were significantly decreased in healthy subjects with 28 days overfeeding [54], which indicates that specific circulating GM3 species may be downregulated in response to IR. The significant increases in

many fasting plasma DG and TG species in the Ov-ob/IR is in agreement with other studies that have shown that elevated circulating CE, DG and TG lipids are established markers of obesity [26,28,29,30], prediabetes [9] and T2D [9,13], and are the primary source of fatty acids utilized in energy production [54].

6.4.5 Lipid abnormalities associated with type 2 diabetes

An ANCOVA post-hoc analysis was applied to identify fasting plasma lipids associated with T2D, only four species were significantly altered in the T2D group compared with the Ov-ob/IR group (Table S6.1). This indicated that the accumulated plasma lipid abnormalities associated with combined obesity/IR were very similar to those associated with T2D.

This result was able to be verified by comparing the fasting plasma lipid abnormalities that occurred in the Ov-ob/IR group versus Lean/IS group with those that occurred in the T2D group versus Lean/IS group. Similar to the eight lipid classes/subclasses and 65 species that were significantly altered in the Ov-ob/IR group compared with the Lean/IS group, seven lipid classes/subclasses (THC, GM3, PC(O), PC(P), LPC, LPC(O) and TG) and 68 species were significantly altered in the T2D group compared with the Lean/IS group (Table 6.3 and S6.1). Notably, 55 of the 65 lipid species that were significantly altered in the Ov-ob/IR group compared with the Lean/IS group were also significantly altered (and in the same direction) in the T2D group compared with the Lean/IS group (Table 6.6). These common lipid abnormalities included significant decreases in multiple species of THC, GM3, PC(P), PC(O), LPC and LPC(O), and significant increases in 18 TG species. This comparison confirms that ~85% of the fasting plasma lipid abnormalities in T2D subjects were present in the Ov-ob/IR group prior to the onset of T2D.

In a recent study, Meikle *et al.* showed that the fasting plasma lipid abnormalities associated with T2D were strikingly similar to those associated with prediabetes (relative to NGT subjects) in 351 individuals from the Australian Diabetes, Obesity and Lifestyle Study cohort [9]. Additionally, ~90% of the significant associations in the AusDiab cohort were subsequently validated in 1076 individuals from the San Antonio Family Heart Study. Using logistic regression analysis, Meikle *et al.* found that both prediabetes and T2D were positively associated with DG, TG, CE, Cer, dhCer, PE, PI and PG, and negatively associated with the ether-linked phospholipids PC(O) and PC(P) [9]. Although the pattern of fasting plasma lipid abnormalities

Table 6.6 Comparison of fasting plasma lipid classes/subclasses and species significantly altered in the Ov-Ob/IR versus Lean/IS group, and in the T2D versus Lean/IS group.

Ov-ob/IR vs. Lean/IS[a]		T2D vs. Lean/IS[a]		Lipid abnormalities common to both group comparisons	
Significantly increased[b]	**Significantly decreased[c]**	**Significantly increased[b]**	**Significantly decreased[c]**	**Significantly increased**	**Significantly decreased**
CE 20:3	DHC (C)	Cer 18:0	THC 18:0	**PE 36:1**	**THC (C)**
DG (C)	DHC 16:0	PE 32:1	SM 38:1	**TG (C)**	**THC 16:0**
DG 16:0/18:0	GM3 24:1	PE(O-42:7)	PC 34:2	**TG 14:0/16:0/18:1**	**THC 20:0**
DG 18:0/18:1	DHC 24:1		PC 35:2	**TG 14:0/17:0/18:1**	**THC 22:0**
TG 18:0/18:0/18:1	PC(P-32:1)		PC 36:4a	**TG 14:0/18:0/18:1**	**THC 24:0**
	LPC 22:1		PC(O) (C)	**TG 14:1/18:0/18:2**	**THC 24:1**
	LPC 22:6		PC(O-34:2)	**TG 15:0/16:0/18:1**	**GM3 (C)**
	LPE (C)		PC(P) (C)	**TG 16:0/16:0/16:0**	**GM3 16:0**
			LPC 17:1	**TG 16:0/16:0/18:0**	**GM3 18:0**
			LPC 18:0	**TG 16:0/16:0/18:1**	**PC 32:0**
			LPC 24:0	**TG 16:0/16:1/17:0**	**PC 40:7**
			LPC(O-18:0)	**TG 16:0/17:0/18:0**	**PC(O-32:0)**
				TG 16:0/17:0/18:1	**PC(O-34:1)**
				TG 16:0/17:0/18:2	**PC(O-36:2)**
				TG 16:0/18:0/18:1	**PC(O-38:5)**
				TG 16:0/18:1/18:1	**PC(O-40:7)**
				TG 16:1/16:1/18:0	**PC(P-32:0)**
				TG 16:1/17:0/18:1	**PC(P-34:1)**
				TG 17:0/18:1/18:1	**PC(P-34:2)**
				TG 18:0/18:1/18:1	**PC(P-36:2)**
					LPC (C)
					LPC 16:0
					LPC 17:0
					LPC 18:1
					LPC 18:2
					LPC 20:0
					LPC 20:1
					LPC 20:2
					LPC 22:5
					LPC 26:0
					LPC(O) (C)
					LPC(O-16:0)
					LPC(O-18:1)
					LPC(O-20:0)
					LPC(O-22:0)
					LPC(O-22:1)
					LPC(O-24:1)
					LPC(O-24:2)
					LPE 16:0
					CE 20:1

Ov-ob, overweight-to-obese; IR, insulin resistant; IS, insulin sensitive; T2D, type 2 diabetic; C, lipid class/subclass

[a] Derived from analysis of covariance of each lipid class or subclass in the four groups, adjusted for age, sex, and systolic blood pressure. Post-hoc analysis was performed using the Mann Whitney *U* test with Dunn-Sidak correction for multiple group comparisons. $P < 0.05$ was considered significant.

[b] Lipid class/subclass or species was significantly increased or [c] significantly decreased relative to latter group.

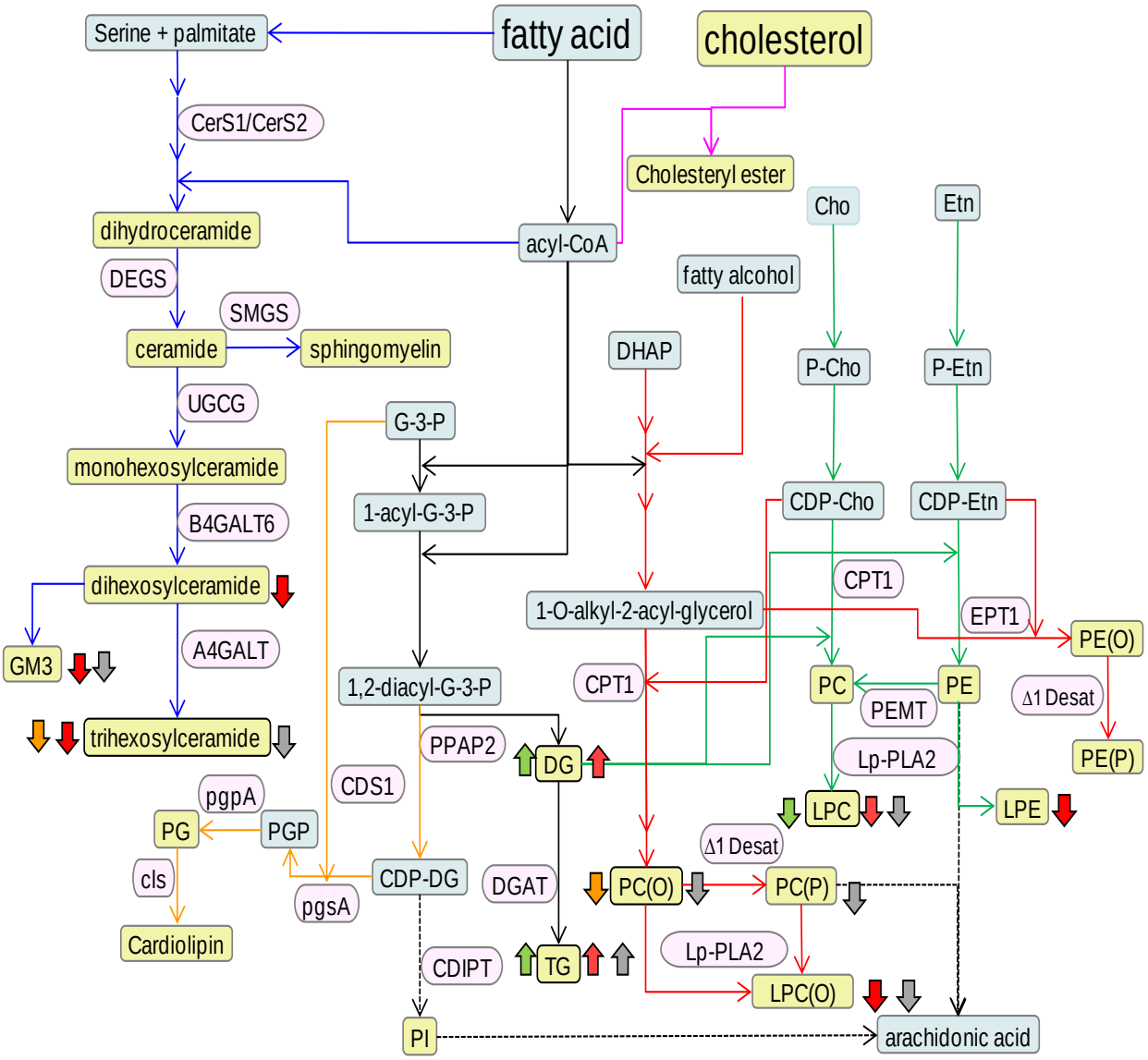

Figure 6.1. Metabolic pathways altered in progression to type 2 diabetes. Partial lipid metabolic pathways showing the major lipids (blue and yellow boxes), the measured lipids (yellow boxes), and the enzymes involved (pink boxes). The sphingolipid (blue lines), cholesteryl ester (pink lines), cardiolipin (orange lines), glycerolipid (black lines), choline/ethanolamine phospholipids (green lines), plasmalogen (red lines) and arachidonic acid (dotted lines) biosynthetic pathways are shown. The direction of association between lipids and obesity (orange arrows), IR (green arrows), combined obesity/IR (red arrows) and T2D (grey arrows) is indicated.
Metabolite abbreviations: Cho, choline; CDP, cytidine diphosphate; DHAP, dihydroxyacetonephosphate; Etn, ethanolamine; G-3-P, glycerol-3-phosphate; PGP, phosphatidylglycerolphosphate. Abbreviations of measured lipids are shown in Table 7.1**. Enzyme abbreviations:** A4GALT, lactosylceramide 4-alphagalactosyltransferase; B4GALT6, beta-1,4-galactosyltransferase 6; CDIPT, CDP-diacylglycerol-inositol 3-phosphatidyltransferase; CDS1, phosphatidate cytididyltransferase; CerS, ceramide synthase; cls, cardiolipin synthase; CPT1, diacylglycerol cholinephosphotransferase; Δ1 Desat, delta-1 desaturase; DEGS, sphingolipid delta-4 desaturase; DGAT, diacylglycerol O-acyltransferase; EPT1, ethanolaminephosphotransferase; Lp-PLA2, lipoprotein phospholipase A2; PEMT, phosphatidylethanolamine N-methyltransferase; pgpA, phosphatidylglycerophosphatase A; pgsA, phosphatidylglycerosynthase A; PPAP2, phosphatidate phosphatase; SMGS, sphingomyelin synthase; UGCG, ceramide glucosyltransferase.

in the prediabetes group in the Meikle *et al.* study and Ov-ob/IR group in our study are slightly different, they both closely resemble the lipid abnormalities observed in the corresponding T2D groups. It appears that T2D only becomes fully manifest when this plethora of fasting plasma lipid abnormalities is accompanied by progressive β-cell failure [226,227]. A schematic diagram showing the lipid metabolic pathways altered in the progression from obesity to IR to combined obesity/IR to T2D is shown in Figure 6.1.

6.4.6 Obesity-induced lipid abnormalities drive insulin resistance and type 2 diabetes

In the Australian Diabetes, Obesity and Lifestyle Study cohort, 55% of obese subjects were normal glucose tolerant (NGT) [228]. However, the inability of insulin secretion to compensate for a decrease in insulin action in susceptible individuals distinguishes those who progress to impaired glucose tolerance and diabetes to those who remain NGT. In a study in Pima Indians, a population with a high incidence of T2D, the obese NGT subjects who did not progress to impaired glucose tolerance or diabetes over a 5 year period retained a normal disposition index (the product of insulin sensitivity and insulin secretory function) owing to a compensatory increase in acute insulin secretion to compensate for a gradually decreasing insulin sensitivity [3]. Therefore, insulin secretion is already compromised (i.e., upregulated) early in the setting of obesity to maintain NGT in the presence of attenuated insulin sensitivity.

In our study, "healthy" obesity in the Ov-ob/IS group (a snapshot of health status) was associated with a significant lowering of some fasting plasma THC and PC(O) species, and unchanged fasting plasma glucose, insulin, FFA, adiponectin, glucose tolerance and insulin sensitivity (versus Lean/IS group) (Table 6.2). At face value, these "healthy" obese/IS individuals would be unlikely to progress to T2D based on these lipid abnormalities alone. On the other hand, IR was not only associated with significant decreases in many LPC species in the Ov-ob/IR compared with Ov-ob/IS group, but the DG and TG lipid classes were positively associated with HOMA-IR. However, this cluster of lipid abnormalities cannot be entirely attributed to IR, as the Ov-ob/IR and Ov-ob/IS groups were already influenced by the setting of obesity. The "true" association of lipid abnormalities with IR (independently of obesity) would only be achieved if a group of Lean/IR individuals were compared with the Lean/IS group, but recruiting sufficient numbers of suitable Lean/IR individuals is problematic due to low numbers in this category.

Although the lipid abnormalities associated with either obesity or IR in our study cannot assign causality, our results indicate that "healthy" obesity in insulin sensitive individuals is accompanied by relatively minor lipid abnormalities that are tolerated. However, persistent obesity in susceptible individuals may be associated with a gradual increase in the severity of lipid abnormalities, and eventually a state of obesity and IR which is accompanied by a cascade of other lipid abnormalities and metabolic defects that are similar to those observed in T2D. Notably, obesity/IR was associated with biochemical and metabolic defects including increased fasting plasma glucose and insulin, but decreased adiponectin levels, increased systolic and diastolic blood pressure, impaired glucose tolerance, and decreased GIR/FFM (insulin sensitivity).

6.4.7 Plasma triacylglycerol species are predictive of insulin resistance

As the FA composition is critical in determining whether a particular TG species is positively or negatively associated with obesity, IR and risk of T2D [13,26,29,30,31], we assessed whether the degree of FA saturation in TG species was an important risk factor for the development of IR. In our study, "saturated" TG species were defined as having a total of two or less FA-double bonds, and that each FA moiety within the TG species contained no more than one double bond (e.g. TG 14:0/16:1/18:1). "Unsaturated" TG species were defined as having a total of more than two FA-double bonds, but also included TG species that contained a total of two FA-double bonds when a single FA moiety contained two double bonds (e.g. TG 14:0/16:0/18:2, TG 14:0/16:1/18:2). We found that 14 of the 15 TG species from the three non-diabetic groups that were positively associated with HOMA-IR (by linear regression) were "saturated", and only one species was "unsaturated" (TG 16:0/16:0/18:2) (Table S6.2). The probability of 14 "saturated" TG species (out of 23 measured "saturated" TG species) and only one "unsaturated" TG species (out of 21 measured "unsaturated" TG species) being positively associated with HOMA-IR was statistically significant by unpaired Student's t-test ($P < 0.01$).

Odd-chain FAs are associated with dairy intake [168,169], and C15:0 and C17:0 have been shown to be negatively associated with incident T2D [170,171], which supports a protective role for dairy against T2D. Meikle *et al.* also showed a negative association of some PC and SM species containing C15:0 and C17:0 with prediabetes and T2D [9]. However, in the same study, most TG species containing an odd-chain FA were positively associated with prediabetes and T2D (versus NGT) [9]. In the present study, we assessed whether TG species containing an odd-

numbered carbon FA were predictive of IR. Of the 15 fasting plasma TG species that were positively associated with HOMA-IR (by linear regression), seven TG species contained an odd-numbered carbon FA (either C15:0 or C17:0) and eight TG species contained only even-numbered carbon FAs (Table S7.2). The probability of seven TG species containing an odd-numbered carbon FA (out of nine measured TG species that contained an odd-numbered carbon FA) and eight TG species containing only even-numbered carbon FAs (out of 35 measured TG species that contained only even-numbered carbon FAs) being positively associated with HOMA-IR was statistically significant by unpaired Student's t-test ($P < 0.05$). Therefore, fasting plasma TG species that were "saturated" and/or contained an odd-numbered carbon FA were highly predictive of IR in the three non-diabetic groups.

Some studies have found that total FA-carbon number is also critical in determining whether a particular TG species is positively or negatively associated with obesity, IR and T2D [13,29,30]. One retrospective human cohort study revealed that TG species with lower FA double-bond content and lower FA carbon number (TG 44:1, TG 46:1, TG 48:0, TG 48:1, TG 50:0 and TG 52:1) were associated with an increased risk of diabetes (and correlated with IR), whereas TG species with higher FA double-bond content and higher FA carbon number (TG 56:9, TG 58:10 and TG 60:12) were associated with a decreased risk of diabetes [13]. Moreover, Schwab *et al.* found that diet-induced weight loss in obese individuals corresponded to a reduction in circulating saturated and short-chain fatty acid-containing TG species, which was associated with improved insulin sensitivity [30]. However, Pietilainen *et al.* found that TG species containing ≥ 54 FA-carbons were negatively correlated with insulin sensitivity in young adult monozygotic obese twins compared with their non-obese twins [29].

Of the 15 fasting plasma TG species that were positively associated with HOMA-IR (by linear regression) in the present study, 13 TG species contained < 54 total FA-carbons and two TG species contained ≥ 54 total FA-carbons (Table S6.2). The probability of 13 TG species containing < 54 total FA-carbons (out of 33 measured TG species that contained < 54 total FA-carbons) and two TG species containing ≥ 54 total FA-carbons (out of 11 measured TG species that contained ≥ 54 total FA-carbons) being positively associated with HOMA-IR was not statistically significant by unpaired Student's t-test ($P > 0.05$). Therefore, total FA-carbon number in fasting plasma TG species was not predictive of IR in the three non-diabetic groups.

6.4.8 Plasma triacylglycerol species are predictive of combined obesity/insulin resistance and type 2 diabetes

ANCOVA post-hoc analysis of fasting plasma lipids in the four study groups revealed that the same 18 TG species were significantly increased in both compared with the Lean/IS group (Table 6.6). We found that 16 of these 18 TG species were "saturated" ($P < 0.01$ vs. "unsaturated" TG species), eight TG species contained an odd-numbered carbon FA ($P < 0.06$ vs. TG species that contained only even-numbered carbon FAs), and 17 TG species contained < 54 total FA-carbons ($P = 0.08$ vs.TG species containing ≥ 54 total FA-carbons). Therefore, fasting plasma "saturated" TG species were highly predictive of combined obesity/IR and T2D, and may reflect an increased circulating pool of saturated (16:0 and 18:0) and monounsaturated (16:1 and 18:1) fatty acids arising from elevated hepatic *de novo* lipogenesis in both the Ov-ob/IR and T2D groups. It is known that the development of obesity and IR may override the repressive effect of high-fat diets on hepatic *de novo* lipogenesis [51,52].

6.4.9 Steady-state clamp plasma glycerolipids and cholesteryl esters are associated with insulin resistance

Linear regression analysis of SS clamp plasma against HOMA-IR in the three non-diabetic groups revealed that three lipid classes (CE, DG and TG) and 3 PE, 15 CE, 24 DG and 26 TG species were positively associated with HOMA-IR, and only two lipid species (LPC 22:6 and PE(O-42:7)) were negatively associated with HOMA-IR (Tables 6.4 and S6.2). Notably, all 33 CE, DG and TG species lipid species that were positively associated with HOMA-IR in fasting plasma remained positively associated with HOMA-IR in SS clamp plasma, but another 32 CE, DG and TG species became positively associated with HOMA-IR in SS clamp plasma. These findings highlight the strength of the association of fasting plasma DG, TG and CE species with HOMA-IR under different physiological states (fasting versus severe hyperinsulinaemia/euglycaemia). In addition, ANCOVA post-hoc analysis of SS plasma lipid levels revealed that the CE, DG and TG classes were significantly elevated in the Ov-ob/IR group compared with both the Lean/IS and Ov-ob/IS groups (data not shown), confirming that these lipid classes were highly resistant to the antilipolytic effects of insulin during the clamp in the "high risk" Ov-ob/IR group.

6.4.10 Insulin clamp-induced suppression of plasma lipid classes/subclasses differs in obesity, insulin resistance and type 2 diabetes

In the majority of cases, the 150 min hyperinsulinaemic (80 mU/m^2/min)-euglycaemic (5.0 mmol/l) clamp in the four groups induced either no significant change or a drop in plasma lipid classes/subclasses by up to 30% compared with fasting levels (Table 6.5), despite complete suppression of circulating NEFA concentrations in all groups (Table 6.2). Although 17 of the 21 plasma lipid classes in the Lean/IS group decreased significantly during the clamp, the closely related PC(O), LPC and LPC(O) subclasses were resistant to the high SS clamp insulin levels (~300 mU/l). Notably, these same plasma lipid subclasses were resistant to the suppressive effects of the clamp in the Ov-Ob/IS group, but now the PC, PC(P) and CE classes/subclasses were also resistant. These findings suggest that some lipid classes/subclasses in the Ov-Ob/IS group may be associated with subtle resistance to the effects of insulin. However, the tissue responsible for this subtle IR in the Ov-Ob/IS group was not obvious, given the complete suppression of NEFA (indicating normal adipocyte insulin sensitivity), unchanged HOMA-IR (predominantly a reflection of hepatic insulin sensitivity) and unchanged GIR/FFM (a measure of skeletal muscle insulin sensitivity) compared with the Lean/IS group.

Strikingly, all but six of the 21 plasma lipid classes/subclasses were resistant to the antilipolytic effects of insulin in the Ov-Ob/IR group, which closely paralleled the magnitude and pattern of lipid abnormalities observed in the Ov-ob/IR group compared with the Lean/IS group (Table 6.3 and S6.1). Counter-intuitively, the SS clamp induced a significant decrease in 15 of the 21 plasma lipid classes/subclasses compared with fasting plasma in the T2D group, which was almost identical to the pattern seen in the Ov-Ob/IS group, despite a large reduction (by ~50%) in GIR/FFM whole-body insulin sensitivity.The favourable lipidomic findings in the SS clamp plasma of T2D subjects (but not in fasting plasma; Table 6.6) compared with the Ov-ob/IR group may partly relate to their well-controlled diabetic status (HbA_{1c} 6.1 ± 0.6%), and use of statins and/or anti-hypertensive medications to normalise cholesterol and blood pressure respectively. However, even though 12 of the 21 T2D subjects were taking statins, a previous study in the same subjects found that there was no difference in clamp-derived insulin sensitivity between statin users and non-users [217]. Another study found that very few non-cholesterol lipid species showed a significant association with statin use in stable coronary artery disease subjects, and statin was not a significant confounder in the comparative lipidomic analysis of stable coronary artery disease versus healthy controls [10].

Regardless of medication use in T2D subjects, one must also be mindful that the interpretation of this SS clamp lipidomics data is based on comparisons of the "number of lipid classes/subclasses" that are significantly suppressed by the insulin clamp in each group, and does not delve into the potency of individual lipid species or the complex interconnecting network of lipid metabolic pathways that ultimately determine the severity of lipid abnormalities associated with obesity/IR and T2D.

6.4.11 Conclusion

The experimental design employed in this study made it possible to determine lipid abnormalities in fasting and SS clamp plasma and skeletal muscle samples associated with obesity (independently of IR), IR (independently of obesity), combined obesity/IR, and ultimately, T2D in humans. In summary, obesity (independent of IR) occurred in the absence of elevated circulating FFA or any other biochemical or metabolic defects (Table 6.2), and was associated with a modest change in the sphingolipid metabolism pathway (lower THC) but, more particularly, decreased levels of ether-phospholipids, likely due to early oxidative stress (orange arrows, Figure 6.1). IR (independent of obesity) was associated with a significant reduction in nine LPC species (potentially a novel insulin-independent signal), likely due to the hydrolysis of oxidized PC(P) lipids by secretory phospholipases, and elevated "saturated" TG species (predictive of T2D) and DG species (associated with impaired insulin signalling) (green arrows, Figure 6.1). In addition to the previously manifested lipid abnormalities observed with obesity or IR, combined obesity/IR was also associated with significant decreases in some DHC, GM3, LPC(O) and LPE species (red arrows, Figure 6.1). The lower DHC, THC and GM3 levels suggest that enzymes downstream from *de novo* ceramide synthesis have been downregulated, even though GM3 gangliosides have previously been shown to be implicated in IR. The reduction in seven fasting plasma LPC(O) species is not surprising, given that LPC(O) opposes the proinflammatory actions of platelet activating factor, and is associated with insulin sensitivity. Similar to LPC, the reduction in LPE species was likely due to the hydrolysis of oxidized PC(P) lipids by secretory phospholipases, and may indicate increasing oxidative stress. Finally, ~85% of the lipid abnormalities associated with combined obesity/IR lipid species were also associated with T2D (grey arrows, Figure 6.1). However, the antioxidant PC(P) plasmalogen subclass was now significantly reduced in the T2D group compared with the Lean/IS group.

Fasting plasma TG species that were “saturated” and/or contained an odd-numbered carbon FA were highly predictive of IR (by HOMA-IR) in the three non-diabetic groups. In addition, fasting plasma “saturated” TG species were highly predictive, and odd-chain TG species were almost predictive (P = 0.06) of combined obesity/IR and T2D, which may reflect an increased circulating pool of saturated (16:0 and 18:0) and monounsaturated (16:1 and 18:1) fatty acids arising from elevated hepatic *de novo* lipogenesis in both the Ov-ob/IR and T2D groups. However, there was no indication that TG species were predictive of obesity, either by direct comparison of the Ov-ob/IS and Lean/IS groups, or by linear regression analysis of fasting plasma lipids against BMI in the four study groups.

The degree of suppression of plasma lipid classes/subclasses by the insulin clamp varied considerably in the four groups, but was an indicator of the lipid classes/subclasses that were resistant to the antilipolytic effects of insulin. Notably, the closely related PC(O), LPC and LPC(O) subclasses were resistant to the high SS clamp insulin levels in all groups. Strikingly, all but six of the 21 plasma lipid classes/subclasses were resistant to the antilipolytic effects of insulin in the “untreated” Ov-Ob/IR group, which closely paralelled the magnitude and pattern of lipid abnormalities observed in the Ov-ob/IR group compared with the Lean/IS group. The insulin clamp did not significantly alter the content of any skeletal muscle lipid classes/subclasses compared with fasting skeletal muscle in any of the groups, although the analysis of whole muscle rather than subcellular fractions (e.g. membrane-bound or mitochondrial) may reduce the capacity to find differences.

Unfortunately, comparative statistical analyses of large numbers of lipid species in four study groups comprising a relatively small number of participants resulted in a lack of statistical power, and limited the ability to detect differences in lipid classes/subclasses and species once the *P*-values were corrected for multiple comparisons. This problem could be resolved by increasing the number of participants in future study groups and/or reducing the number of lipid species that are statistically compared. In addition, knowledge of the dietary fatty acid composition and daily energy expenditure of participants would assist in determining the influence of hepatic *de novo* lipogenesis on the circulating pool of saturated and monosaturated fatty acids, and how the lipid abnormalities relate to metabolic pathways associated with disease progression.

Despite these experimental limitations, this human IR and obesity study provided invaluable insights into the separate associations of lipid abnormalities with obesity, IR, combined obesity/IR and T2D, and the contribution of novel lipid classes and species to obesity (e.g. reduction in PC(O) species), IR (reduction in LPC species), combined obesity/IR (reduction in LPE species) and T2D (reduction in PC(P) species). The design of this study provides the opportunity to identify specific lipid biomarkers for the early detection and intervention at any of the defined stages of disease.

CHAPTER 7 GENERAL DISCUSSION

7.1 DISCUSSION

7.1.1 Identification and characterisation of altered lipid metabolism in type 2 diabetes using a systems biology approach

The 'Omics' design employed to examine the association of global lipid profiles with the progression to pre-diabetes and/or type 2 diabetes (T2D) and gene expression profiling in the Obese/diabetic *db/db* mouse study (Chapters 4 and 5 respectively) and the Human insulin resistance (IR) and obesity study (Chapter 6) was predominantly a hypothesis-generating approach [229]. This design provides a solid platform to develop hypotheses to further investigate the complex relationship between changing lipid levels, lipid metabolic pathways and the pathogenesis of T2D. In particular, the relationship of lipids with body composition, biochemical and metabolic markers of glucose homeostasis, inflammatory and oxidative stress, and metabolic and gene expression pathways provide the opportunity to identify 1) lipid biomarkers associated with increased risk of developing pre-diabetes and/or T2D in a clinical setting, and 2) new therapeutic targets for the development of suitable preventative and/or therapeutic treatments associated with pre-diabetes and/or T2D. This thesis represents the first step in this process with the identification of classes, subclasses and multiple lipid species associated with the onset and progression of pre-diabetes and/or T2D in both mouse and human studies, combined with gene analysis to further characterise some of the relevant metabolic and signalling pathways.

7.1.2 Global lipid profiles and gene expression are associated with different stages of obesity insulin resistance and type 2 diabetes

The monogenic leptin receptor-deficient genetic *db/db* mouse model (C57BL/KsJ background) closely resembles disease progression to T2D in humans [72,91] and is an appropriate model for investigating real time lipid abnormalities associated with the onset of obesity, IR and T2D [73,85,140,141,142,143,144]. While there have been a number of studies in human cohorts that have examined the plasma lipidome in obesity, IR, prediabetes and/or T2D [9,13,28,29,148], most studies have collected one-off fasting blood samples to compare relative levels of lipids

from a limited number of classes in two groups of subjects (e.g. obese versus lean controls). Also, very few studies have employed comprehensive lipidomic analysis (by mass spectrometry) to compare lipid abnormalities in plasma and different tissues in obesity, IR, pre-diabetes and/or T2D [26,70,149,230] or sequentially tracked the lipid abnormalities that occur with disease progression [26,65]. It is possible to achieve more consistency and less variation in lipidomic and gene expression profiling measurements using a genetic mouse model of progressive obesity/diabetes (i.e., *db/db* with C57BL/KsJ background) with known time-frame and metabolic consequences, and controlled for genetic background and environmental factors (especially diet, medication and lifestyle), which cannot be achieved with heterogenous obese and T2D human populations.

The temporal and tissue-specific design of our *db/db* mouse study experiments enabled us to compare the timing, distribution and severity of lipid abnormalities (at the class and species level) in plasma and metabolic tissues (liver, skeletal muscle, left-ventricle and adipose) in the intermediate (*db/h*) and more severe (*db/db*) mouse phenotypes compared with their *H/H* littermates at 6, 10 and 16 weeks of age using LC ESI-MS/MS and MRM experiments in positive ion mode. The independent effects of gender, age and genotype on global lipid profiles were assessed (Chapter 4, Tables 4.6 to 4.8). The effect of the *db/db* genotype on lipid abnormalities in tissues and plasma was clearly the dominant effect in the majority of cases, although there was a large effect of age on left-ventricle lipid profiles in *db/db* mice.

A major advantage of the mouse model was the ability to perform gene expression profiling in the liver at different time points which could then be related back to the lipid profiles obtained in the same tissues. Importantly, by performing the same analyses on human cohorts we were able to compare and contrast the lipid metabolic changes observed in the mouse model with those observed in humans to identify common lipid metabolic alterations associated with obesity, insulin resistance and type to diabetes.

7.1.3 Early elevation of hepatic *de novo* lipogenesis in *db/db* mice and humans

Hepatic *de novo* lipogenesis (the metabolic pathway leading to the conversion of dietary sugars into fatty acids (FA), which are ultimately esterified with glycerol-3-phosphate to form liver triglycerides) is regulated by dietary composition at the transcriptional level [47,158]. High rates of hepatic *de novo* lipogenesis are induced by low-fat/high-carbohydrate diets, hyperinsulinemia

and hyperglycemia [47,158], similar to the conditions seen in our standard chow fed *db/db* mice. The transcription levels of genes encoding for enzymes involved in hepatic *de novo* lipogenesis and corresponding activities of lipogenic enzymes involved in hepatic palmitoyl-CoA elongation and stearoyl-CoA desaturation were markedly higher in male Wistar rats fed a low-fat/high-carbohydrate diet compared with rats fed either a high-fat/high-carbohydrate "Western" diet or high-fat diet [47]. Long-chain FAs (16:0, 16:1, 18:0 and 18:1) derived from elevated rates of hepatic *de novo* lipogenesis are incorporated into liver triglycerides, and released as VLDL-bound TG [157], resulting in increased circulating TG levels [47].

In the *db/db* mouse study, surrogate measures of hepatic *de novo* lipogenesis (i.e., total 16:1/18:2 ratios in liver DG and TG species) were markedly elevated in male and female *db/db* mice at six and ten weeks of age compared with the corresponding *H/H* and *db/h* mice (Chapter 4, Figure 4.19) in response to a higher calorie intake and marked IR. In this regard, hepatic lipogenesis acts like a sink for the excess carbohydrates that can no longer be metabolised or stored as glycogen (limited capacities), and therefore, has to be converted to fat. However, both surrogate measures of hepatic *de novo* lipogenesis were significantly attenuated in male *db/db* mice (but not female *db/db* mice) by 16 weeks of age, indicating that liver function was compromised in the more severely diabetic male *db/db* mice. An almost identical pattern was observed in male and female *db/db* mice when total 16:1/18:2 in plasma DG and TG species were measured (Chapter 4, Figure 4.20). Collectively, these results indicated that the elevated 16:1 FA generated from hepatic *de novo* lipogenesis via delta-9 desaturase activity [47] in male and female *db/db* mice at six and ten weeks of age was accompanied by an increased circulating pool of 16:1 FA in DG and TG species.

The depleted hepatic and circulating pool of 16:1 FA in DG and TG-containing VLDL in the 16 week old male *db/db* mice at 16 weeks of age is likely to have severe health consequences. Monounsaturated fatty acids are essential components of membrane phospholipids, TG and CE, and are required for normal membrane fluidity and transmembrane receptor/enzyme activity [159]. However, the ability of 16:1 FA to continue acting as an endocrine signal and improve muscle insulinsensitivity and decreasing hepatosteatosis [160] is impeded by the chronic setting of high calorie intake, IR and elevated TG and DG lipids.

The relative contribution of hepatic *de novo* lipogenesis as a source of FA for hepatic TG and plasma VLDL-bound TGs depends on dietary fat and carbohydrate composition, as well as the

health status of individuals. Donnelly *et al*. quantified the FA sources of hepatic TG and plasma VLDL-bound TGs in obese, hyperinsulinemic and triglyceridemic nonalcoholic fatty liver disease patients after 5 days of labelling with orally fed stable isotopes [193]. In the fasting state, 59% of fatty acids in liver TG (contained in lipid droplets) originated from FAs stored in adipose tissue that flowed to the liver (i.e. plasma nonesterified FA pool), 26% were derived from the hepatic *de novo* lipogenesis pathway, and 15% were derived from the diet (consisting of 30% dietary fat by energy). A similar proportion of FAs derived from the three sources were found in plasma VLDL-bound TGs secreted from the liver [193]. Another study showed that 10% of FAs in fasting plasma VLDL-bound TGs were derived from hepatic *de novo* lipogenesis in obese, hyperinsulinaemic subjects fed a moderately high-fat diet [51], but less than 5% of FAs in plasma VLDL-bound TGs were derived from hepatic *de novo* lipogenesis in fasting healthy subjects who consumed a similar diet [231,232]. However, fasting hepatic *de novo* lipogenesis rates tripled in fasting healthy subjects fed a high-carbohydrate diet for five days, but did not increase further in hyperinsulinaemic and IR subjects fed the same diet [51].

As the increased circulating pool of 16:1 FA in DG and TG species was found to closely reflect 16:1 FA levels generated from elevated hepatic *de novo* lipogenesis in our *db/db* mice, we employed the same surrogate measures (i.e., total 16:1/18:2 in plasma DG and TG species) to determine whether the circulating pool of 16:1 FA was altered in any of the obese groups fed a Western diet in our Human insulin resistance and obesity study (Chapter 6). The mean total 16:1/18:2 in plasma DG species was (Lean/insulin sensitive (IS): mean 0.20 ± 0.02 (SEM); Ov-ob/IS: 0.28 ± 0.02; Ov-ob/IR: 0.25 ± 0.02; and T2D: 0.32 ± 0.03 respectively), with significant elevations observed in the Ov-ob/IS and T2D groups compared with the lean/IS group (both $P < 0.05$). Likewise, the mean total 16:1/18:2 in plasma TG species was (Lean/IS: 0.79 ± 0.06; Ov-ob/IS: 0.98 ± 0.06; Ov-ob/IR: 0.92 ± 0.06; and T2D: 1.02 ± 0.08 respectively), with significant elevations again observed in the Ov-ob/IS and T2D groups compared with the lean/IS group (both $P < 0.05$). These results suggest that there was an increased synthesis of 16:1 FA in the Ov-ob/IS and T2D groups.

The total 16:1/16:0 FA ratio in fasting serum CEs (an estimation of stearoyl-CoA-desaturase activity) and 16:1 FA content in both fasting serum CEs and phospholipids were found to be biomarkers of the high saturated FA content of Western diets (consisting of 35% total energy as fats, with 57% of total fat content consisting of saturated fats) [233]. However, in our human study, and in most studies involving human subjects, the dietary fat and carbohydrate

composition of participants was not accurately recorded, making it difficult to determine the influence of dietary fats on fasting plasma FA composition and estimates of hepatic *de novo* lipogenesis.

Taken together, these data support an increase in lipogenesis associated with a high calorie diet in mice and humans, and that this is associated with obesity, IR and T2D. The total 16:1/18:2 in DG and TG species are sensitive markers for this. Interestingly, although the mice appear to show a difference in these surrogate measures at different ages (stages of disease), there does not appear to be a difference between the Ov-ob/IS, Ov-ob/IR and the T2D groups. This may be owing to a lack of statistical power given the small sample size of the human cohort and the variation within the cohort. Alternatively, different diets (proportion of fat and carbohydrate) in the different groups may mask any differences in lipogenesis rates between groups. The major difference between the mice and human studies is that the mice consumed identical diets (albeit in different amounts) whereas the human diets were not strictly recorded.

7.1.4 Triacylglycerol species are potential risk factors for obesity, insulin resistance and type 2 diabetes

The fatty acid composition is critical in determining whether a particular TG species is positively or negatively associated with obesity, IR and T2D [13,26,29,30,31]. Generally, circulating TG species containing low total FA-carbon number (≤ 52) and low total FA-double bond number (≤ 2) are associated with IR and increased risk of T2D, whereas TG species containing higher total FA-carbon number and higher total FA-double bond number are associated with decreased risk of T2D, and are not correlated with IR. Moreover, the accumulation of TG species containing lower total FA-carbon number and lower total FA-double bond number was more pronounced in hearts of 15 week old male obese, hyperglycaemic and IR *db/db* mice *db/db* mice compared with corresponding male wild-type mice [77].

In contrast, from the 40 TG species measured in our *db/db* mouse study (Chapter 4), we found that there was no statistical difference in the number of "saturated" and "unsaturated" (or low total FA-carbon number versus higher total FA-carbon number) TG species that were significantly elevated in plasma or any metabolic tissues (liver, skeletal muscle, left-ventricle and adipose) in male or female *db/db* mice at 6, 10 and 16 weeks of age compared with the corresponding *H/H* mice. We concluded that both "saturated" and "unsaturated" TG species

were equally predictive of obesity, IR and T2D in our *db/db* mice, and that the inability to discriminate between "saturated" and "unsaturated" TG speciesas biomarkers of disease progression in the *db/db* mice may relate to the severity of disease, which often resulted in nearly all of the TG species being significantly elevated, particularly in male *db/db* mice (Ch 4 Table 4.14). However, the inability to distinguish between "saturated" and "unsaturated" TG effects may also relate to the definition applied to these TG groups.

Conversely, in our Human insulin resistance and obesity study (Chapter 6), linear regression analysis revealed that fasting plasma TG species that were "saturated" and/or contained an odd-numbered carbon FA were highly predictive of IR (by HOMA-IR) in the three non-diabetic groups (Lean/IS, Ov-ob/IS and Ov-ob/IR). In addition, ANCOVA post-hoc analysis revealed that fasting plasma "saturated" TG species were highly predictive, and odd-chain TG species were almost predictive (P = 0.06) of combined obesity/IR and T2D. However, there was no indication that TG species were predictive of obesity, either by direct comparison of the Ov-ob/IS and Lean/IS groups, or by linear regression analysis of fasting plasma lipids against BMI in the four study groups.

Odd-chain fatty acids are thought to be derived totally from dietary sources (primarily from products of ruminant digestion in dairy animals), as they cannot be synthesised by mammals. Therefore, they represent a sensitive marker of dairy fat intake. A Western diet in humans may contain a relatively large amount of dairy fats, which are incorporated into TG species. Thus a high dietary fat content in humans is associated with IR and T2D, whereas the elevated hepatic lipogenesis induced by the low-fat/high-carbohydrate diet) in *db/db* mice is associated with IR and T2D. Therefore, humans that consume a high dairy and/or high saturated fat diet appear to be at higher risk of T2D than individuals eating a high carbohydrate diet, but the problem associated with increased hepatic lipogenesis in *db/db* mice is potentially more damaging.

7.1.5 Phosphatidylcholine species are potential risk factors for obesity, insulin resistance and type 2 diabetes in *db/db* mice

The role of plasma PC and PE species as potential risk factors for obesity, IR and T2D has not been fully explored. Notably, the six fasting plasma diacyl-PC species that were associated with increased risk of T2D in two prospective human cohort studies [13,148], namely PC 32:1, PC 34:2, PC 36:1, PC36:2, PC 38:3 and PC 40:5, were also significantly elevated in our six week

old male and female *db/db* mice (except PC 34:2 in the female *db/db* mice). These findings indicate that the same PC species that predict T2D risk in human studies are positively associated with early onset of obesity and IR in six week old *db/db* mice**.** Conversely, most of the PC species that were significantly decreased in liver, skeletal muscle and left-ventricle in male *db/db* mice (but not female *db/db* mice) contained an odd-numbered carbon FA. These latter findings are compelling, given that approximately two-thirds of the 40-odd measured PC species contain only even-numbered carbon FAs, and the other one-third contain an odd-numbered carbon FA. These results suggest a protective role for liver, skeletal muscle and left-ventricle odd-chain PC species against obesity, IR and T2D in our male *db/db* mice. Supporting our findings, Meikle *et al.* found that T2D and stable coronary artery disease were negatively associated with PC 33:2 and PC 35:2 (vs. NGT subjects) [9,10], and odd-chain 15:0 and 17:0 fatty acids were found to be negatively associated with incident T2D [170,171]. In mice, as in humans, odd-chain fatty acids are thought to be derived primarily from dairy fats), and suggests a protective role for liver, skeletal muscle and left-ventricle odd-chain PC species against obesity, IR and T2D in our male *db/db* mice [168,169].

An alternative explanation may involve the dilution of the dietary derived odd-chain fatty acids by the elevated pool of even-chain saturated (16:0 and 18:0) and monounsaturated (16:1 and 18:1) fatty acids derived from increased hepatic *de novo* lipogenesis in our male *db/db* mice (Figures 4.19 and 4.20). The relative amounts of odd-chain fatty acids being incorporated into PC species (by competitive competition) diminishes with a greater synthesis of even-chain saturated (16:0 and 18:0) and monounsaturated (16:1 and 18:1) fatty acids. This may contribute to the significant lowering of odd-chain PC species in liver, skeletal muscle and left-ventricle compared with the corresponding *H/H* mice. Harmancey *et al.* found that male Wistar rats fed a low-fat/high-carbohydrate diet had strikingly higher hepatic *de novo* lipogenic rate, delta-9 desaturase expression/activity and plasma 16:1-to-16:0 ratio than rats fed either a high-fat/high-carbohydrate "Western" diet or high-fat diet [47]. This increase in hepatic *de novo* lipogenesis was required to supply the heart with a normal amount of 16:1, and to maintain a normal cardiac 16:1-to-16:0 ratio, as monounsaturated fatty acids are critical components of lipids in membranes [159].

7.1.6 Early pathological cardiolipin remodelling and possible drug intervention strategies

Obesity and diabetes are associated with systemic oxidative stress, a primary causative factor of IR, which is characterised by increased ROS production [181,182,183]. Elevated levels of ROS induce CL peroxidation and pathological remodelling of CL, resulting in a loss of the predominant CL species, CL 18:2/18:2,18:2/18:2, and replacement of the 18:2n-6 FA with polyunsaturated fatty acids, mainly DHA, 22:6n-3 [64,184]. The increased 22:6n-3 content in CL stimulates mitochondrial membrane potential and proton leakage, and renders CL highly sensitive to oxidative damage, leading to increased cell oxidant production [185,186], further lipid peroxidation, mitochondrial dysfunction, and metabolic complications.

ALCAT1, an acyltransferase that catalyzes the reacylation of lyso-CL species to mature CL species using acyl-FA chains donated by acyl CoA [124], has already been targeted for drug intervention strategies to prevent obesity, IR, diabetes and heart failure. ALCAT1 is involved in the pathological remodelling of CL in response to oxidative stress that precedes and accompanies diabetes, obesity, and cardiomyopathy, generating CL species that are highly sensitive to oxidative damage [187,234,235].

Li *et al.* showed that stable over-expression of ALCAT1 in C2C12 mouse myoblasts decreased total fatty acyl-content in CL by 40% (versus empty vector), which included significant decreases in C16:0, C16:1, C18:1 and C18:2 content in CL, and significant increases in C20:1, C 20:3, C20:4 and C22:6 content in CL. This destructive CL remodelling was associated with increased ROS production and mitochondrial dysfunction [187]. Secondly, ALCAT1 deficiency in ALCAT$^{-/-}$ knock-out mice resulted in significant increases in heart CL 18:2/18:2/18:2/18:2 and liver PG, protection from high-fat diet-induced obesity and IR, and improved mitochondrial complex I activity, lipid oxidation and insulin signalling (insulin-simulated Akt phosphorylation). Thirdly, ALCAT1 mRNA expression was upregulated in heart, liver and skeletal muscle in high-fat diet-induced obese C56BL/6 mice, and both mRNA expression and enzyme activity were upregulated with the onset of T2D in *db/db* mice. Finally, ALCAT1 was found to have a causative role in mitochondrial dysfunction in response to oxidative stress in isolated primary cardiomyocytes from B56BL/6 mice [187]. The development of inhibitors of ALCAT1 may provide novel treatments for cardiac hypertrophy and other heart diseases [234].

In our *db/db* mice, early onset left-ventricle CL remodelling (i.e., elevated levels of 16:1 FA-containing CL species and lower levels of 22:6 FA-containing CL species) mirrored the changes seen in specific donor *sn*-2 16:1 FA-containing PC species (PC 32:1, PC 32:2 and PC 34:2) and *sn*-2 22:6 FA-containing species (PC 38:6b, PC 40:6 and PE 40:6) respectively (Chapter 4, Figure 4.10). Similar to the scenario observed with the decrease in odd-chain PC species in liver, skeletal muscle and left-ventricle of male *db/db* mice, the increased hepatic lipogenesis (increased 16:1 and 18:1) may have diluted out the dietary 18:2 and 22:6 fatty acids. This highlights the important balance that exists between different fatty acid species in maintaining lipid homeostasis in different lipid classes. Therefore, similar to the work done with ALCAT1 [187], a series of experiments could be designed to determine whether specific transacylases (enzymes that catalyze the reacylation of lyso-CL species to mature CL species using the *sn*-2 acyl FA-chain donated by abundant PC and PE species) [124] are directly involved in the pathological remodelling of CL species and mitochondrial dysfunction in response to oxidative stress. Eventually, specific transacylases in the CL remodelling pathway may be targeted for drug intervention strategies (e.g. inhibitors) designed to prevent obesity, IR, diabetes and heart failure.

7.1.7 Comparison of lipid abnormalities associated with obesity in humans and *db/db* mice

In our Human insulin resistance and obesity study, the PC(O) species (PC(O-32:0), PC(O-34:1) and PC(O-36:2)) and PC(P-32:0) were significantly lower in fasting plasma in the Ov-ob/IS versus Lean/IS group (i.e., obesity-induced effects) (Table S6.1). In agreement with these findings, Pietilainen *et al.* observed that some serum ether-linked phospholipids were significantly decreased in young adult monozygotic obese co-twins compared with non-obese co-twins, independent of genetic factors [29]. Moreover, a large prospective human case-cohort study revealed that five baseline serum acyl-alkyl-PC(O) species (PC(O-34:3), PC(O-40:6), PC(O-42:5), PC(O-44:4) and PC(O-44:5)) were independently associated with decreased risk of T2D [148], and Meikle *et al.* reported that prediabetes and T2D were negatively associated with fasting plasma PC(O) and PC(P) subclasses [9].

In contrast, there were significant elevations in some fasting plasma PC(O), PC(P) and PE(P) species in our six week old mildly obese/glucose intolerant male *db/db* mice (Table S4.5), and in PC(O) and PC(P) species in mildly obese/IR female *db/db* mice at 10 weeks of age (Table S4.10). In support of these findings, Graessler *et al.* found that PE(O-36:5) and PE(O-38:7) were

significantly elevated in fasting plasma in men with BMI > 27.5 kg/m^2 compared with leaner men [28]. The increase in plasmalogens early in the disease process both in *db/db* mice and obese men may be in response to increased oxidative stress, which is subsequently overwhelmed as the disease progresses with increasing oxidative stress. The contrasting results for ether-phospholipids in human and mouse studies may be attributable to the severity of disease in each individual, combined with differences in gender, age, genetic background, environmental factors (especially diet), species-type, and the robustness of the statistical tests. The use of large population based cohorts, coupled with appropriate statistical tests (e.g. linear and logistic regression) and covariates, provides the statistical power to identify significant but subtle independent associations between lipid species and classes/subclasses (e.g. PC(P) and PE(P) plasmalogens and LPC) and lifestyle measures (e.g. obesity and smoking) [11]. Further work is required to fully define the role of these ether-linked lipids in T2D.

7.1.8 Comparison of lipid abnormalities associated with insulin resistance in humans and *db/db* mice

In our Human insulin resistance and obesity study, ANCOVA analysis revealed that nine fasting plasma LPC species were significantly lower in the Ov-ob/IR group compared with the Ov-ob/IS group, and the CE class along with two CE, two DG and two TG species were significantly elevated in the Ov-ob/IR group (i.e., IR-induced effects) (Tables 6.3 and S6.1). The total LPC subclass and seven LPC species were also found to be significantly lower in fasting plasma of healthy sedentary adults after 28 days overfeeding (by 1250 kcal/day), which corresponded to decreased insulin sensitivity [54]. Notably, LPC 22:6 was also positively correlated with insulin sensitivity in this study, flagging this lipid as a sensitive biomarker of early IR.

In our *db/db* mouse study, fasting plasma LPC and LPE subclasses (mostly saturated and monounsaturated short-chain FA-containing LPC species) were already elevated in the mildly obese/hyperinsulinaemic ($P < 0.07$) male *db/db* mice and non-obese/hyperinsulinaemic and IR female *db/db* mice at 6 weeks of age (Table S5 and Table S10). These elevations in circulating LPC and LPE species occurred in the presence of hyperinsulinaemia before the onset of chronic obesity, and suggest a link between lysophospholipids and early inflammation and IR in *db/db* mice.

It is also likely that the early elevation of plasma LPC 16:0, LPC 16:1, LPC 18:0 and LPC 18:1 in our six week old *db/db* mice reflects the increased hepatic *de novo* lipogenesis (Figures 4.17 and 4.18), as hepatic *de novo* lipogenesis is activated by low-fat/high-carbohydrate diets, hyperinsulinaemia and hyperglycaemia [47]. Other studies have noted that the dietary fat composition is important in determining the FA composition and levels of circulating LPC species [26,48]. Therefore, the dietary FA composition and probably the genotype of the animal, is critical in determining the types of changes in LPC levels in rodent models of obesity/IR. The early elevation of plasma and liver LPC 16:1 in our *db/db* mice may serve as a biomarker of increased hepatic *de novo* lipogenesis.

Our LPC findings in *db/db* mice are in agreement with some, but not other, animal and human studies that have examined LPC in obesity, IR, prediabetes and T2D. In agreement with our findings, fasting plasma LPC species (mostly saturated and monounsaturated short-chain FA-containing LPC species) were found to be significantly elevated in adult monozygotic obese co-twins [29], overweight/obese IR men (with a higher saturated fat intake) [48], adults with prediabetes [9], and young pigs with early obesity, endothelial dysfunction and oxidative stress [57]. In contrast, fasting plasma LPC species were found to be significantly decreased in glucose intolerant and insulin resistant individuals [13,53], obese-insulin sensitive and obese-T2D subjects [26] and male C57BL/6J mice fed a high-fat diet for 12 weeks (vs. mice fed a low-fat diet) [26]. Similar to the variable results obtained with ether phospholipids, the independent association of LPC and lifestyle measures (e.g. obesity) can be better teased out using large population based cohorts, the appropriate statistical tests, covariates and correction of *P*-values for multiple comparisons [9, 11]. It is also highly important to design experiments that control for confounding influences and optimise the statistical power achieved within the datasets.

7.1.9 Liver genes linked to lipid metabolic pathway/diabetes-specific disease states in male *db/db* mice

It was also important to examine the relationship between lipid abnormalities and gene expression profiling in *db/db* mice to identify genes that were associated with specific metabolic pathways and lipid classes/subclasses affected by disease progression. This line of investigation offers the opportunity to identify specific gene candidates or lipid biomarkers as potential therapeutic targets for the development of suitable preventative and/or therapeutic treatments associated with human obesity, IR and T2D.

Correlation analyses of the 21 liver lipid classes/subclasses (using targeted lipid profiling) against the 68 differentially expressed genes (using DNA microarray of the mouse whole-genome) linked to lipid pathway/diabetes-specific disease states (compiled from KEGG Pathway Maps and DisGenet Gene-disease associations databases) showed that the elevated TG, DG, CE, LPE and LPC lipid classes/subclasses in male *db/db* mice at 10 and 16 weeks of age were significantly correlated with 30 different genes (totalling 65 significant correlations) representing 12 lipid pathway/diabetes-specific disease states. The TG class and LPE subclass were very prominent, showing significant correlations with 24 and 20 genes respectively, with 15 genes common to both (including *Aldh3a2*, *Acadm, Socs2*, *Pcsk9, Hhex, Vldlr* and *Pparg*).

These correlation analyses confirmed the close link between liver lipid abnormalities (by targeted lipid profiling) and differentially expressed genes associated with lipid pathway/diabetes-specific expression (by microarray) in *db/db* mice. It is a powerful tool for detecting not only the relationships between specific genes and lipid classes (and probably species), but also informing on the directional change and magnitude of metabolic perturbations associated with increasing severity of disease in the livers of male *db/db* mice. This approach could also be used to identify potentially important pathways for validation in suitable animal or human studies.

Finally, many of the differentially expressed liver genes that were linked to lipid pathway/diabetes-specific disease states in the *db/db* mice (*Acadl*, *Scd1*, *Pparg, Socs2*, *Vldlr, Hhex, Pgam1, Lpl* and *Lpin1*) have been determined as candidate genes for human T2D [113,206,207,208]. Therefore, the *db/db* mice (C57BL/KsJ background) mouse model of obesity, IR and T2D is suitable for identifying specific gene candidates or lipid classes/species as potential therapeutic targets for early prevention or treatment of comparable human disease cohorts.

7.1.10 Final thesis synopsis

The diabetic *db/db* mouse and human obesity and IR studies saw the development of surrogate markers that identified an important role for hepatic *de novo* lipogenesis in the pathogenesis of T2D. The early CL remodelling in the left-ventricle of *db/db* mice is associated with oxidative stress, and may be targeted to prevent the onset of mitochondrial dysfunction and disease

progression. The development of targeted lipid profiling methodology successfully characterised lipids (e.g.ether-phospholipids and lysophospolipids) that were implicated in the development of pre-diabetes. The combination of gene expression and targeted lipid profiling in the livers of male *db/db* mice identified specific lipid classes, metabolic pathways and genes as potential candidates for pre-diabetes and T2D. The comparison of lipid abnormalities associated with mouse and human obesity, IR, pre-diabetes and T2D defined lipids that were associated with obesity (independently of IR), IR (independent of obesity), and the deterioration of lipid profiles associated with combined obesity/IR and T2D.

In this regard, the 'Omics' design implemented in this thesis project provides a solid platform to develop hypotheses and more targeted experiments to further investigate the complex relationship between changing lipid levels, lipid metabolic pathways, gene expression and the pathogenesis of T2D. For example, one could test the following hypotheses generated from the findings of the mouse and human studies: 1) Early metabolic events in chow-fed *db/db* mice, including the elevation of hepatic lipogenesis, CL remodelling in the left-ventricle, hepatic steatosis (accumulation of TG), elevations in proinflammatory/proatherogenic species of the lysophospolipids LPE and LPC and/or decreases in anti-oxidant species of the plasmalogens PC(P) and PE(P) lead to the development of obesity, IR, prediabetes and T2D, and are associated with decreased energy expenditure, blocked leptin receptor signalling and/or oxidative stress; 2) Progression of disease in *db/db* mice is associated with more hepatosteatotis and oxidative stress, which corresponds to the generation of more reactive oxygen species, more peroxidation damage to susceptible CL, polyunsaturated and/or plasmalogen lipid species, and a decrease in the rate of hepatic *de novo* lipogenesis, reducing the availability of phospholipids (PC, PE, PI, CL) for membrane structure, energy metabolism and mitochondrial function; and 3) Transcriptional regulation at the gene and metabolic pathway level are responsible for the lipid abnormalities associated with obesity, IR, prediabetes and T2D.

These hypotheses could be tested using carefully designed experiments in appropriate models of murine obesity, IR and diabetes and similar human cohorts by simultaneously measuring markers of oxidative stress, the oxidation of specific lipid species, mitochondrial function, metabolite tracer studies designed to quantitate the uptake, metabolism and distribution of specific lipids/metabolites in plasma and different tissues, and the association of specific genes and lipids with progression of disease using microarrays and targeted lipid profiling respectively.

REFERENCES

1. Shaw JE, Sicree RA, Zimmet PZ (2010) Global estimates of the prevalence of diabetes for 2010 and 2030. Diabetes Res Clin Pract 87: 4-14.
2. Magliano DJ, Shaw JE, Shortreed SM, Nusselder WJ, Liew D, Barr EL, Zimmet PZ, Peeters A (2008) Lifetime risk and projected population prevalence of diabetes. Diabetologia 51: 2179-2186.
3. Weyer C, Bogardus C, Mott DM, Pratley RE (1999) The natural history of insulin secretory dysfunction and insulin resistance in the pathogenesis of type 2 diabetes mellitus. J Clin Invest 104: 787-794.
4. Civitarese AE, Smith SR, Ravussin E (2007) Diet, energy metabolism and mitochondrial biogenesis. Curr Opin Clin Nutr Metab Care 10: 679-687.
5. Shi H, Kokoeva MV, Inouye K, Tzameli I, Yin H, Flier JS (2006) TLR4 links innate immunity and fatty acid-induced insulin resistance. J Clin Invest 116: 3015-3025.
6. Watson AD (2006) Thematic review series: systems biology approaches to metabolic and cardiovascular disorders. Lipidomics: a global approach to lipid analysis in biological systems. J Lipid Res 47: 2101-2111.
7. Dennis EA, Deems RA, Harkewicz R, Quehenberger O, Brown HA, Milne SB, Myers DS, Glass CK, Hardiman G, Reichart D, Merrill AH, Jr., Sullards MC, Wang E, Murphy RC, Raetz CR, Garrett TA, Guan Z, Ryan AC, Russell DW, McDonald JG, Thompson BM, Shaw WA, Sud M, Zhao Y, Gupta S, Maurya MR, Fahy E, Subramaniam S (2010) A mouse macrophage lipidome. J Biol Chem 285: 39976-39985.
8. Quehenberger O, Armando AM, Brown AH, Milne SB, Myers DS, Merrill AH, Bandyopadhyay S, Jones KN, Kelly S, Shaner RL, Sullards CM, Wang E, Murphy RC, Barkley RM, Leiker TJ, Raetz CR, Guan Z, Laird GM, Six DA, Russell DW, McDonald JG, Subramaniam S, Fahy E, Dennis EA (2010) Lipidomics reveals a remarkable diversity of lipids in human plasma. J Lipid Res 51: 3299-3305.
9. Meikle PJ, Wong G, Barlow CK, Weir JM, Greeve MA, MacIntosh GL, Almasy L, Comuzzie AG, Mahaney MC, Kowalczyk A, Haviv I, Grantham N, Magliano DJ, Jowett JB, Zimmet P, Curran JE, Blangero J, Shaw J (2013) Plasma lipid profiling shows similar associations with prediabetes and type 2 diabetes. PLoS One 8: e74341.
10. Meikle PJ, Wong G, Tsorotes D, Barlow CK, Weir JM, Christopher MJ, MacIntosh GL, Goudey B, Stern L, Kowalczyk A, Haviv I, White AJ, Dart AM, Duffy SJ, Jennings GL, Kingwell BA (2011) Plasma lipidomic analysis of stable and unstable coronary artery disease. Arterioscler Thromb Vasc Biol 31: 2723-2732.
11. Weir JM, Wong G, Barlow CK, Greeve MA, Kowalczyk A, Almasy L, Comuzzie AG, Mahaney MC, Jowett JB, Shaw J, Curran JE, Blangero J, Meikle PJ (2013) Plasma lipid profiling in a large population-based cohort. J Lipid Res 54: 2898-2908.
12. Mitchell TW, Pham H, Thomas MC, Blanksby SJ (2009) Identification of double bond position in lipids: from GC to OzID. J Chromatogr B Analyt Technol Biomed Life Sci 877: 2722-2735.
13. Rhee EP, Cheng S, Larson MG, Walford GA, Lewis GD, McCabe E, Yang E, Farrell L, Fox CS, O'Donnell CJ, Carr SA, Vasan RS, Florez JC, Clish CB, Wang TJ, Gerszten RE (2011) Lipid profiling identifies a triacylglycerol signature of insulin resistance and improves diabetes prediction in humans. J Clin Invest 121: 1402-1411.
14. Kitabchi AE, Temprosa M, Knowler WC, Kahn SE, Fowler SE, Haffner SM, Andres R, Saudek C, Edelstein SL, Arakaki R, Murphy MB, Shamoon H, Diabetes Prevention Program Research G (2005) Role of insulin secretion and sensitivity in the evolution of type 2 diabetes in the diabetes prevention program: effects of lifestyle intervention and metformin. Diabetes 54: 2404-2414.
15. Knowler WC, Barrett-Connor E, Fowler SE, Hamman RF, Lachin JM, Walker EA, Nathan DM, Diabetes Prevention Program Research G (2002) Reduction in the incidence of type 2 diabetes with lifestyle intervention or metformin. N Engl J Med 346: 393-403.

16. Fahy E, Subramaniam S, Brown HA, Glass CK, Merrill AH, Jr., Murphy RC, Raetz CR, Russell DW, Seyama Y, Shaw W, Shimizu T, Spener F, van Meer G, VanNieuwenhze MS, White SH, Witztum JL, Dennis EA (2005) A comprehensive classification system for lipids. J Lipid Res 46: 839-861.
17. Fahy E, Subramaniam S, Murphy RC, Nishijima M, Raetz CR, Shimizu T, Spener F, van Meer G, Wakelam MJ, Dennis EA (2009) Update of the LIPID MAPS comprehensive classification system for lipids. J Lipid Res 50 Suppl: S9-14.
18. Summers SA (2006) Ceramides in insulin resistance and lipotoxicity. Prog Lipid Res 45: 42-72.
19. Holland WL, Brozinick JT, Wang LP, Hawkins ED, Sargent KM, Liu Y, Narra K, Hoehn KL, Knotts TA, Siesky A, Nelson DH, Karathanasis SK, Fontenot GK, Birnbaum MJ, Summers SA (2007) Inhibition of ceramide synthesis ameliorates glucocorticoid-, saturated-fat-, and obesity-induced insulin resistance. Cell Metab 5: 167-179.
20. Holland WL, Summers SA (2008) Sphingolipids, insulin resistance, and metabolic disease: new insights from in vivo manipulation of sphingolipid metabolism. Endocr Rev 29: 381-402.
21. Stratford S, Hoehn KL, Liu F, Summers SA (2004) Regulation of insulin action by ceramide: dual mechanisms linking ceramide accumulation to the inhibition of Akt/protein kinase B. J Biol Chem 279: 36608-36615.
22. Schmitz-Peiffer C (2010) Targeting ceramide synthesis to reverse insulin resistance. Diabetes 59: 2351-2353.
23. Blachnio-Zabielska A, Baranowski M, Zabielski P, Gorski J (2010) Effect of high fat diet enriched with unsaturated and diet rich in saturated fatty acids on sphingolipid metabolism in rat skeletal muscle. J Cell Physiol 225: 786-791.
24. Straczkowski M, Kowalska I, Nikolajuk A, Dzienis-Straczkowska S, Kinalska I, Baranowski M, Zendzian-Piotrowska M, Brzezinska Z, Gorski J (2004) Relationship between insulin sensitivity and sphingomyelin signaling pathway in human skeletal muscle. Diabetes 53: 1215-1221.
25. Haus JM, Kashyap SR, Kasumov T, Zhang R, Kelly KR, Defronzo RA, Kirwan JP (2009) Plasma ceramides are elevated in obese subjects with type 2 diabetes and correlate with the severity of insulin resistance. Diabetes 58: 337-343.
26. Barber MN, Risis S, Yang C, Meikle PJ, Staples M, Febbraio MA, Bruce CR (2012) Plasma lysophosphatidylcholine levels are reduced in obesity and type 2 diabetes. PLoS One 7: e41456.
27. Eisinger K, Liebisch G, Schmitz G, Aslanidis C, Krautbauer S, Buechler C (2014) Lipidomic analysis of serum from high fat diet induced obese mice. Int J Mol Sci 15: 2991-3002.
28. Graessler J, Schwudke D, Schwarz PE, Herzog R, Shevchenko A, Bornstein SR (2009) Top-down lipidomics reveals ether lipid deficiency in blood plasma of hypertensive patients. PLoS One 4: e6261.
29. Pietilainen KH, Sysi-Aho M, Rissanen A, Seppanen-Laakso T, Yki-Jarvinen H, Kaprio J, Oresic M (2007) Acquired obesity is associated with changes in the serum lipidomic profile independent of genetic effects--a monozygotic twin study. PLoS One 2: e218.
30. Schwab U, Seppanen-Laakso T, Yetukuri L, Agren J, Kolehmainen M, Laaksonen DE, Ruskeepaa AL, Gylling H, Uusitupa M, Oresic M (2008) Triacylglycerol fatty acid composition in diet-induced weight loss in subjects with abnormal glucose metabolism--the GENOBIN study. PLoS One 3: e2630.
31. Kotronen A, Velagapudi VR, Yetukuri L, Westerbacka J, Bergholm R, Ekroos K, Makkonen J, Taskinen MR, Oresic M, Yki-Jarvinen H (2009) Serum saturated fatty acids containing triacylglycerols are better markers of insulin resistance than total serum triacylglycerol concentrations. Diabetologia 52: 684-690.
32. Leskinen T, Rinnankoski-Tuikka R, Rintala M, Seppanen-Laakso T, Pollanen E, Alen M, Sipila S, Kaprio J, Kovanen V, Rahkila P, Oresic M, Kainulainen H, Kujala UM (2010) Differences in muscle and adipose tissue gene expression and cardio-metabolic risk factors in the members of physical activity discordant twin pairs. PLoS One 5.

33. Ellis BA, Poynten A, Lowy AJ, Furler SM, Chisholm DJ, Kraegen EW, Cooney GJ (2000) Long-chain acyl-CoA esters as indicators of lipid metabolism and insulin sensitivity in rat and human muscle. Am J Physiol Endocrinol Metab 279: E554-560.
34. Houmard JA, Tanner CJ, Yu C, Cunningham PG, Pories WJ, MacDonald KG, Shulman GI (2002) Effect of weight loss on insulin sensitivity and intramuscular long-chain fatty acyl-CoAs in morbidly obese subjects. Diabetes 51: 2959-2963.
35. Russell AP, Gastaldi G, Bobbioni-Harsch E, Arboit P, Gobelet C, Deriaz O, Golay A, Witztum JL, Giacobino JP (2003) Lipid peroxidation in skeletal muscle of obese as compared to endurance-trained humans: a case of good vs. bad lipids? FEBS Lett 551: 104-106.
36. Amati F, Dube JJ, Alvarez-Carnero E, Edreira MM, Chomentowski P, Coen PM, Switzer GE, Bickel PE, Stefanovic-Racic M, Toledo FG, Goodpaster BH (2011) Skeletal muscle triglycerides, diacylglycerols, and ceramides in insulin resistance: another paradox in endurance-trained athletes? Diabetes 60: 2588-2597.
37. Moro C, Galgani JE, Luu L, Pasarica M, Mairal A, Bajpeyi S, Schmitz G, Langin D, Liebisch G, Smith SR (2009) Influence of gender, obesity, and muscle lipase activity on intramyocellular lipids in sedentary individuals. J Clin Endocrinol Metab 94: 3440-3447.
38. Itani SI, Ruderman NB, Schmieder F, Boden G (2002) Lipid-induced insulin resistance in human muscle is associated with changes in diacylglycerol, protein kinase C, and IkappaB-alpha. Diabetes 51: 2005-2011.
39. Zock PL, Mensink RP, Harryvan J, de Vries JH, Katan MB (1997) Fatty acids in serum cholesteryl esters as quantitative biomarkers of dietary intake in humans. Am J Epidemiol 145: 1114-1122.
40. Warensjo E, Ohrvall M, Vessby B (2006) Fatty acid composition and estimated desaturase activities are associated with obesity and lifestyle variables in men and women. Nutr Metab Cardiovasc Dis 16: 128-136.
41. Laaksonen DE, Lakka TA, Lakka HM, Nyyssonen K, Rissanen T, Niskanen LK, Salonen JT (2002) Serum fatty acid composition predicts development of impaired fasting glycaemia and diabetes in middle-aged men. Diabet Med 19: 456-464.
42. Vessby B, Aro A, Skarfors E, Berglund L, Salminen I, Lithell H (1994) The risk to develop NIDDM is related to the fatty acid composition of the serum cholesterol esters. Diabetes 43: 1353-1357.
43. Wang L, Folsom AR, Zheng ZJ, Pankow JS, Eckfeldt JH (2003) Plasma fatty acid composition and incidence of diabetes in middle-aged adults: the Atherosclerosis Risk in Communities (ARIC) Study. Am J Clin Nutr 78: 91-98.
44. Liu G (2010) Recent advances in stearoyl-CoA desaturase 1 inhibitors for dyslipidemia and obesity. Curr Top Med Chem 10: 419-433.
45. Cohen P, Ntambi JM, Friedman JM (2003) Stearoyl-CoA desaturase-1 and the metabolic syndrome. Curr Drug Targets Immune Endocr Metabol Disord 3: 271-280.
46. Brown JM, Chung S, Sawyer JK, Degirolamo C, Alger HM, Nguyen T, Zhu X, Duong MN, Wibley AL, Shah R, Davis MA, Kelley K, Wilson MD, Kent C, Parks JS, Rudel LL (2008) Inhibition of stearoyl-coenzyme A desaturase 1 dissociates insulin resistance and obesity from atherosclerosis. Circulation 118: 1467-1475.
47. Harmancey R, Wilson CR, Wright NR, Taegtmeyer H (2010) Western diet changes cardiac acyl-CoA composition in obese rats: a potential role for hepatic lipogenesis. J Lipid Res 51: 1380-1393.
48. Kim JY, Park JY, Kim OY, Ham BM, Kim HJ, Kwon DY, Jang Y, Lee JH (2010) Metabolic profiling of plasma in overweight/obese and lean men using ultra performance liquid chromatography and Q-TOF mass spectrometry (UPLC-Q-TOF MS). J Proteome Res 9: 4368-4375.
49. Masi LN, Rodrigues AC, Curi R (2013) Fatty acids regulation of inflammatory and metabolic genes. Curr Opin Clin Nutr Metab Care 16: 418-424.
50. Sul HS, and Smith, S. (2008) Fatty acid synthesis in eukaryotes. In: Vance DE, and Vance, J.E., editor. Biochemistry of Lipids, Lipoproteins and Membranes. 5th ed. Amsterdam, The Netherlands: Elsevier. pp. 155-190.

51. Schwarz JM, Linfoot P, Dare D, Aghajanian K (2003) Hepatic de novo lipogenesis in normoinsulinemic and hyperinsulinemic subjects consuming high-fat, low-carbohydrate and low-fat, high-carbohydrate isoenergetic diets. Am J Clin Nutr 77: 43-50.
52. Stanhope KL, Schwarz JM, Keim NL, Griffen SC, Bremer AA, Graham JL, Hatcher B, Cox CL, Dyachenko A, Zhang W, McGahan JP, Seibert A, Krauss RM, Chiu S, Schaefer EJ, Ai M, Otokozawa S, Nakajima K, Nakano T, Beysen C, Hellerstein MK, Berglund L, Havel PJ (2009) Consuming fructose-sweetened, not glucose-sweetened, beverages increases visceral adiposity and lipids and decreases insulin sensitivity in overweight/obese humans. J Clin Invest 119: 1322-1334.
53. Zhao X, Fritsche J, Wang J, Chen J, Rittig K, Schmitt-Kopplin P, Fritsche A, Haring HU, Schleicher ED, Xu G, Lehmann R (2010) Metabonomic fingerprints of fasting plasma and spot urine reveal human pre-diabetic metabolic traits. Metabolomics 6: 362-374.
54. Heilbronn LK, Coster AC, Campbell LV, Greenfield JR, Lange K, Christopher MJ, Meikle PJ, Samocha-Bonet D (2013) The effect of short-term overfeeding on serum lipids in healthy humans. Obesity (Silver Spring) 21: E649-659.
55. Nestel PJ, Straznicky N, Mellett NA, Wong G, De Souza DP, Tull DL, Barlow CK, Grima MT, Meikle PJ (2014) Specific plasma lipid classes and phospholipid fatty acids indicative of dairy food consumption associate with insulin sensitivity. Am J Clin Nutr 99: 46-53.
56. Yea K, Kim J, Yoon JH, Kwon T, Kim JH, Lee BD, Lee HJ, Lee SJ, Kim JI, Lee TG, Baek MC, Park HS, Park KS, Ohba M, Suh PG, Ryu SH (2009) Lysophosphatidylcholine activates adipocyte glucose uptake and lowers blood glucose levels in murine models of diabetes. J Biol Chem 284: 33833-33840.
57. Galili O, Versari D, Sattler KJ, Olson ML, Mannheim D, McConnell JP, Chade AR, Lerman LO, Lerman A (2007) Early experimental obesity is associated with coronary endothelial dysfunction and oxidative stress. Am J Physiol Heart Circ Physiol 292: H904-911.
58. Kuniyasu A, Tokunaga M, Yamamoto T, Inoue S, Obama K, Kawahara K, Nakayama H (2011) Oxidized LDL and lysophosphatidylcholine stimulate plasminogen activator inhibitor-1 expression through reactive oxygen species generation and ERK1/2 activation in 3T3-L1 adipocytes. Biochim Biophys Acta 1811: 153-162.
59. Lee H, Lin CI, Liao JJ, Lee YW, Yang HY, Lee CY, Hsu HY, Wu HL (2004) Lysophospholipids increase ICAM-1 expression in HUVEC through a Gi- and NF-kappaB-dependent mechanism. Am J Physiol Cell Physiol 287: C1657-1666.
60. Hollie NI, Hui DY (2011) Group 1B phospholipase A(2) deficiency protects against diet-induced hyperlipidemia in mice. J Lipid Res 52: 2005-2011.
61. Lee YS, Li P, Huh JY, Hwang IJ, Lu M, Kim JI, Ham M, Talukdar S, Chen A, Lu WJ, Bandyopadhyay GK, Schwendener R, Olefsky J, Kim JB (2011) Inflammation is necessary for long-term but not short-term high-fat diet-induced insulin resistance. Diabetes 60: 2474-2483.
62. Mullen KL, Pritchard J, Ritchie I, Snook LA, Chabowski A, Bonen A, Wright D, Dyck DJ (2009) Adiponectin resistance precedes the accumulation of skeletal muscle lipids and insulin resistance in high-fat-fed rats. Am J Physiol Regul Integr Comp Physiol 296: R243-251.
63. Donovan EL, Pettine SM, Hickey MS, Hamilton KL, Miller BF (2013) Lipidomic analysis of human plasma reveals ether-linked lipids that are elevated in morbidly obese humans compared to lean. Diabetol Metab Syndr 5: 24.
64. Han X, Yang J, Yang K, Zhao Z, Abendschein DR, Gross RW (2007) Alterations in myocardial cardiolipin content and composition occur at the very earliest stages of diabetes: a shotgun lipidomics study. Biochemistry 46: 6417-6428.
65. Hsu FF, Bohrer A, Wohltmann M, Ramanadham S, Ma Z, Yarasheski K, Turk J (2000) Electrospray ionization mass spectrometric analyses of changes in tissue phospholipid molecular species during the evolution of hyperlipidemia and hyperglycemia in Zucker diabetic fatty rats. Lipids 35: 839-854.

66. Kolak M, Westerbacka J, Velagapudi VR, Wagsater D, Yetukuri L, Makkonen J, Rissanen A, Hakkinen AM, Lindell M, Bergholm R, Hamsten A, Eriksson P, Fisher RM, Oresic M, Yki-Jarvinen H (2007) Adipose tissue inflammation and increased ceramide content characterize subjects with high liver fat content independent of obesity. Diabetes 56: 1960-1968.
67. Wang C, Kong H, Guan Y, Yang J, Gu J, Yang S, Xu G (2005) Plasma phospholipid metabolic profiling and biomarkers of type 2 diabetes mellitus based on high-performance liquid chromatography/electrospray mass spectrometry and multivariate statistical analysis. Anal Chem 77: 4108-4116.
68. Yi L, He J, Liang Y, Yuan D, Gao H, Zhou H (2007) Simultaneously quantitative measurement of comprehensive profiles of esterified and non-esterified fatty acid in plasma of type 2 diabetic patients. Chem Phys Lipids 150: 204-216.
69. Yi LZ, He J, Liang YZ, Yuan DL, Chau FT (2006) Plasma fatty acid metabolic profiling and biomarkers of type 2 diabetes mellitus based on GC/MS and PLS-LDA. FEBS Lett 580: 6837-6845.
70. Samad F, Hester KD, Yang G, Hannun YA, Bielawski J (2006) Altered adipose and plasma sphingolipid metabolism in obesity: a potential mechanism for cardiovascular and metabolic risk. Diabetes 55: 2579-2587.
71. Tanabe A, Matsuda M, Fukuhara A, Miyata Y, Komuro R, Shimomura I, Tojo H (2009) Obesity causes a shift in metabolic flow of gangliosides in adipose tissues. Biochem Biophys Res Commun 379: 547-552.
72. Hummel KP, Dickie MM, Coleman DL (1966) Diabetes, a new mutation in the mouse. Science 153: 1127-1128.
73. Hummel KP, Coleman DL, Lane PW (1972) The influence of genetic background on expression of mutations at the diabetes locus in the mouse. I. C57BL-KsJ and C57BL-6J strains. Biochem Genet 7: 1-13.
74. Bouche C, Serdy S, Kahn CR, Goldfine AB (2004) The cellular fate of glucose and its relevance in type 2 diabetes. Endocr Rev 25: 807-830.
75. DeFronzo RA (2004) Pathogenesis of type 2 diabetes mellitus. Med Clin North Am 88: 787-835, ix.
76. Ussher JR, Koves TR, Cadete VJ, Zhang L, Jaswal JS, Swyrd SJ, Lopaschuk DG, Proctor SD, Keung W, Muoio DM, Lopaschuk GD (2010) Inhibition of de novo ceramide synthesis reverses diet-induced insulin resistance and enhances whole-body oxygen consumption. Diabetes 59: 2453-2464.
77. Demarco VG, Ford DA, Henriksen EJ, Aroor AR, Johnson MS, Habibi J, Ma L, Yang M, Albert CJ, Lally JW, Ford CA, Prasannarong M, Hayden MR, Whaley-Connell AT, Sowers JR (2013) Obesity-related alterations in cardiac lipid profile and nondipping blood pressure pattern during transition to diastolic dysfunction in male db/db mice. Endocrinology 154: 159-171.
78. Davis RC, Castellani LW, Hosseini M, Ben-Zeev O, Mao HZ, Weinstein MM, Jung DY, Jun JY, Kim JK, Lusis AJ, Peterfy M (2010) Early hepatic insulin resistance precedes the onset of diabetes in obese C57BLKS-db/db mice. Diabetes 59: 1616-1625.
79. Kimura K, Yamada T, Matsumoto M, Kido Y, Hosooka T, Asahara S, Matsuda T, Ota T, Watanabe H, Sai Y, Miyamoto K, Kaneko S, Kasuga M, Inoue H (2012) Endoplasmic reticulum stress inhibits STAT3-dependent suppression of hepatic gluconeogenesis via dephosphorylation and deacetylation. Diabetes 61: 61-73.
80. Dentin R, Hedrick S, Xie J, Yates J, 3rd, Montminy M (2008) Hepatic glucose sensing via the CREB coactivator CRTC2. Science 319: 1402-1405.
81. Chang AY, Schneider DI (1970) Abnormalities in hepatic enzyme activities during development of diabetes in db mice. Diabetologia 6: 274-278.
82. Fujita H, Fujishima H, Koshimura J, Hosoba M, Yoshioka N, Shimotomai T, Morii T, Narita T, Kakei M, Ito S (2005) Effects of antidiabetic treatment with metformin and insulin on serum and adipose tissue adiponectin levels in db/db mice. Endocr J 52: 427-433.

83. Kim WS, Lee YS, Cha SH, Jeong HW, Choe SS, Lee MR, Oh GT, Park HS, Lee KU, Lane MD, Kim JB (2009) Berberine improves lipid dysregulation in obesity by controlling central and peripheral AMPK activity. Am J Physiol Endocrinol Metab 296: E812-819.
84. Yajima K, Hirose H, Fujita H, Seto Y, Ukeda K, Miyashita K, Kawai T, Yamamoto Y, Ogawa T, Yamada T, Saruta T (2003) Combination therapy with PPARgamma and PPARalpha agonists increases glucose-stimulated insulin secretion in db/db mice. Am J Physiol Endocrinol Metab 284: E966-971.
85. Kjorholt C, Akerfeldt MC, Biden TJ, Laybutt DR (2005) Chronic hyperglycemia, independent of plasma lipid levels, is sufficient for the loss of beta-cell differentiation and secretory function in the db/db mouse model of diabetes. Diabetes 54: 2755-2763.
86. Del Guerra S, Lupi R, Marselli L, Masini M, Bugliani M, Sbrana S, Torri S, Pollera M, Boggi U, Mosca F, Del Prato S, Marchetti P (2005) Functional and molecular defects of pancreatic islets in human type 2 diabetes. Diabetes 54: 727-735.
87. Hellmann J, Tang Y, Kosuri M, Bhatnagar A, Spite M (2011) Resolvin D1 decreases adipose tissue macrophage accumulation and improves insulin sensitivity in obese-diabetic mice. FASEB J 25: 2399-2407.
88. Choi WS, Lee JJ, Kim Y, Kim IS, Zhang WY, Myung CS (2011) Synergistic improvement in insulin resistance with a combination of fenofibrate and rosiglitazone in obese type 2 diabetic mice. Arch Pharm Res 34: 615-624.
89. Motawi TM, Hashem RM, Rashed LA, El-Razek SM (2009) Comparative study between the effect of the peroxisome proliferator activated receptor-alpha ligands fenofibrate and n-3 polyunsaturated fatty acids on activation of 5'-AMP-activated protein kinase-alpha1 in high-fat fed rats. J Pharm Pharmacol 61: 1339-1346.
90. Smith AC, Mullen KL, Junkin KA, Nickerson J, Chabowski A, Bonen A, Dyck DJ (2007) Metformin and exercise reduce muscle FAT/CD36 and lipid accumulation and blunt the progression of high-fat diet-induced hyperglycemia. Am J Physiol Endocrinol Metab 293: E172-181.
91. Coleman DL (1978) Obese and diabetes: two mutant genes causing diabetes-obesity syndromes in mice. Diabetologia 14: 141-148.
92. Meister B, Arvidsson U (1996) [The hormone leptin reduces body weight. A mutant gene makes the mouse obese]. Lakartidningen 93: 247-251.
93. Buchanan J, Mazumder PK, Hu P, Chakrabarti G, Roberts MW, Yun UJ, Cooksey RC, Litwin SE, Abel ED (2005) Reduced cardiac efficiency and altered substrate metabolism precedes the onset of hyperglycemia and contractile dysfunction in two mouse models of insulin resistance and obesity. Endocrinology 146: 5341-5349.
94. Mazumder PK, O'Neill BT, Roberts MW, Buchanan J, Yun UJ, Cooksey RC, Boudina S, Abel ED (2004) Impaired cardiac efficiency and increased fatty acid oxidation in insulin-resistant ob/ob mouse hearts. Diabetes 53: 2366-2374.
95. Chen D, Wang MW (2005) Development and application of rodent models for type 2 diabetes. Diabetes Obes Metab 7: 307-317.
96. Wiegman CH, Bandsma RH, Ouwens M, van der Sluijs FH, Havinga R, Boer T, Reijngoud DJ, Romijn JA, Kuipers F (2003) Hepatic VLDL production in ob/ob mice is not stimulated by massive de novo lipogenesis but is less sensitive to the suppressive effects of insulin. Diabetes 52: 1081-1089.
97. Palmer G, Aurrand-Lions M, Contassot E, Talabot-Ayer D, Ducrest-Gay D, Vesin C, Chobaz-Peclat V, Busso N, Gabay C (2006) Indirect effects of leptin receptor deficiency on lymphocyte populations and immune response in db/db mice. J Immunol 177: 2899-2907.
98. Sloan C, Tuinei J, Nemetz K, Frandsen J, Soto J, Wride N, Sempokuya T, Alegria L, Bugger H, Abel ED (2011) Central leptin signaling is required to normalize myocardial fatty acid oxidation rates in caloric-restricted ob/ob mice. Diabetes 60: 1424-1434.
99. Ghilardi N, Ziegler S, Wiestner A, Stoffel R, Heim MH, Skoda RC (1996) Defective STAT signaling by the leptin receptor in diabetic mice. Proc Natl Acad Sci U S A 93: 6231-6235.

100. Halaas JL, Gajiwala KS, Maffei M, Cohen SL, Chait BT, Rabinowitz D, Lallone RL, Burley SK, Friedman JM (1995) Weight-reducing effects of the plasma protein encoded by the obese gene. Science 269: 543-546.
101. Liu Y, Nakagawa Y, Wang Y, Li R, Li X, Ohzeki T, Friedman TC (2003) Leptin activation of corticosterone production in hepatocytes may contribute to the reversal of obesity and hyperglycemia in leptin-deficient ob/ob mice. Diabetes 52: 1409-1416.
102. Huynh FK, Neumann UH, Wang Y, Rodrigues B, Kieffer TJ, Covey SD (2013) A role for hepatic leptin signaling in lipid metabolism via altered very low density lipoprotein composition and liver lipase activity in mice. Hepatology 57: 543-554.
103. Minokoshi Y, Toda C, Okamoto S (2012) Regulatory role of leptin in glucose and lipid metabolism in skeletal muscle. Indian J Endocrinol Metab 16: S562-568.
104. Anstee QM, McPherson S, Day CP (2011) How big a problem is non-alcoholic fatty liver disease? BMJ 343: d3897.
105. Blachnio-Zabielska AU, Pulka M, Baranowski M, Nikolajuk A, Zabielski P, Gorska M, Gorski J (2012) Ceramide metabolism is affected by obesity and diabetes in human adipose tissue. J Cell Physiol 227: 550-557.
106. Samuel VT, Shulman GI (2012) Mechanisms for insulin resistance: common threads and missing links. Cell 148: 852-871.
107. Lewis GF, Carpentier A, Adeli K, Giacca A (2002) Disordered fat storage and mobilization in the pathogenesis of insulin resistance and type 2 diabetes. Endocr Rev 23: 201-229.
108. McGarry JD (2002) Banting lecture 2001: dysregulation of fatty acid metabolism in the etiology of type 2 diabetes. Diabetes 51: 7-18.
109. Postic C, Girard J (2008) Contribution of de novo fatty acid synthesis to hepatic steatosis and insulin resistance: lessons from genetically engineered mice. J Clin Invest 118: 829-838.
110. Zhang F, Xu X, Zhang Y, Zhou B, He Z, Zhai Q (2013) Gene expression profile analysis of type 2 diabetic mouse liver. PLoS One 8: e57766.
111. Heishi M, Ichihara J, Teramoto R, Itakura Y, Hayashi K, Ishikawa H, Gomi H, Sakai J, Kanaoka M, Taiji M, Kimura T (2006) Global gene expression analysis in liver of obese diabetic db/db mice treated with metformin. Diabetologia 49: 1647-1655.
112. Bijl N, Sokolovic M, Vrins C, Langeveld M, Moerland PD, Ottenhoff R, van Roomen CP, Claessen N, Boot RG, Aten J, Groen AK, Aerts JM, van Eijk M (2009) Modulation of glycosphingolipid metabolism significantly improves hepatic insulin sensitivity and reverses hepatic steatosis in mice. Hepatology 50: 1431-1441.
113. Tiffin N, Adie E, Turner F, Brunner HG, van Driel MA, Oti M, Lopez-Bigas N, Ouzounis C, Perez-Iratxeta C, Andrade-Navarro MA, Adeyemo A, Patti ME, Semple CA, Hide W (2006) Computational disease gene identification: a concert of methods prioritizes type 2 diabetes and obesity candidate genes. Nucleic Acids Res 34: 3067-3081.
114. Smith PK, Krohn RI, Hermanson GT, Mallia AK, Gartner FH, Provenzano MD, Fujimoto EK, Goeke NM, Olson BJ, Klenk DC (1985) Measurement of protein using bicinchoninic acid. Anal Biochem 150: 76-85.
115. Folch J, Lees M, Sloane Stanley GH (1957) A simple method for the isolation and purification of total lipides from animal tissues. J Biol Chem 226: 497-509.
116. Munn NJ, Arnio E, Liu D, Zoeller RA, Liscum L (2003) Deficiency in ethanolamine plasmalogen leads to altered cholesterol transport. J Lipid Res 44: 182-192.
117. Goodenowe DB, Cook LL, Liu J, Lu Y, Jayasinghe DA, Ahiahonu PW, Heath D, Yamazaki Y, Flax J, Krenitsky KF, Sparks DL, Lerner A, Friedland RP, Kudo T, Kamino K, Morihara T, Takeda M, Wood PL (2007) Peripheral ethanolamine plasmalogen deficiency: a logical causative factor in Alzheimer's disease and dementia. J Lipid Res 48: 2485-2498.
118. Ford DA (2010) Lipid oxidation by hypochlorous acid: chlorinated lipids in atherosclerosis and myocardial ischemia. Clin Lipidol 5: 835-852.

119. Skaff O, Pattison DI, Davies MJ (2008) The vinyl ether linkages of plasmalogens are favored targets for myeloperoxidase-derived oxidants: a kinetic study. Biochemistry 47: 8237-8245.
120. Lankinen M, Schwab U, Erkkila A, Seppanen-Laakso T, Hannila ML, Mussalo H, Lehto S, Uusitupa M, Gylling H, Oresic M (2009) Fatty fish intake decreases lipids related to inflammation and insulin signaling--a lipidomics approach. PLoS One 4: e5258.
121. Valianpour F, Wanders RJ, Barth PG, Overmars H, van Gennip AH (2002) Quantitative and compositional study of cardiolipin in platelets by electrospray ionization mass spectrometry: application for the identification of Barth syndrome patients. Clin Chem 48: 1390-1397.
122. Schlame M, Ren M, Xu Y, Greenberg ML, Haller I (2005) Molecular symmetry in mitochondrial cardiolipins. Chem Phys Lipids 138: 38-49.
123. Han X, Yang K, Yang J, Cheng H, Gross RW (2006) Shotgun lipidomics of cardiolipin molecular species in lipid extracts of biological samples. J Lipid Res 47: 864-879.
124. Kiebish MA, Bell R, Yang K, Phan T, Zhao Z, Ames W, Seyfried TN, Gross RW, Chuang JH, Han X (2010) Dynamic simulation of cardiolipin remodeling: greasing the wheels for an interpretative approach to lipidomics. J Lipid Res 51: 2153-2170.
125. Pfeiffer K, Gohil V, Stuart RA, Hunte C, Brandt U, Greenberg ML, Schagger H (2003) Cardiolipin stabilizes respiratory chain supercomplexes. J Biol Chem 278: 52873-52880.
126. Schlame M, Rua D, Greenberg ML (2000) The biosynthesis and functional role of cardiolipin. Prog Lipid Res 39: 257-288.
127. Chicco AJ, Sparagna GC (2007) Role of cardiolipin alterations in mitochondrial dysfunction and disease. Am J Physiol Cell Physiol 292: C33-44.
128. Sparagna GC, Chicco AJ, Murphy RC, Bristow MR, Johnson CA, Rees ML, Maxey ML, McCune SA, Moore RL (2007) Loss of cardiac tetralinoleoyl cardiolipin in human and experimental heart failure. J Lipid Res 48: 1559-1570.
129. Petrosillo G, Portincasa P, Grattagliano I, Casanova G, Matera M, Ruggiero FM, Ferri D, Paradies G (2007) Mitochondrial dysfunction in rat with nonalcoholic fatty liver Involvement of complex I, reactive oxygen species and cardiolipin. Biochim Biophys Acta 1767: 1260-1267.
130. Pope S, Land JM, Heales SJ (2008) Oxidative stress and mitochondrial dysfunction in neurodegeneration; cardiolipin a critical target? Biochim Biophys Acta 1777: 794-799.
131. Sparagna GC, Johnson CA, McCune SA, Moore RL, Murphy RC (2005) Quantitation of cardiolipin molecular species in spontaneously hypertensive heart failure rats using electrospray ionization mass spectrometry. J Lipid Res 46: 1196-1204.
132. Hsu FF, Turk J (2006) Characterization of cardiolipin as the sodiated ions by positive-ion electrospray ionization with multiple stage quadrupole ion-trap mass spectrometry. J Am Soc Mass Spectrom 17: 1146-1157.
133. Liebisch G, Vizcaino JA, Kofeler H, Trotzmuller M, Griffiths WJ, Schmitz G, Spener F, Wakelam MJ (2013) Shorthand notation for lipid structures derived from mass spectrometry. J Lipid Res 54: 1523-1530.
134. Cole MJ, Enke CG (1991) Direct determination of phospholipid structures in microorganisms by fast atom bombardment triple quadrupole mass spectrometry. Anal Chem 63: 1032-1038.
135. Zemski Berry KA, Murphy RC (2004) Electrospray ionization tandem mass spectrometry of glycerophosphoethanolamine plasmalogen phospholipids. J Am Soc Mass Spectrom 15: 1499-1508.
136. Considine RV, Sinha MK, Heiman ML, Kriauciunas A, Stephens TW, Nyce MR, Ohannesian JP, Marco CC, McKee LJ, Bauer TL, et al. (1996) Serum immunoreactive-leptin concentrations in normal-weight and obese humans. N Engl J Med 334: 292-295.
137. Atkinson LL, Fischer MA, Lopaschuk GD (2002) Leptin activates cardiac fatty acid oxidation independent of changes in the AMP-activated protein kinase-acetyl-CoA carboxylase-malonyl-CoA axis. J Biol Chem 277: 29424-29430.
138. Chen H, Charlat O, Tartaglia LA, Woolf EA, Weng X, Ellis SJ, Lakey ND, Culpepper J, Moore KJ, Breitbart RE, Duyk GM, Tepper RI, Morgenstern JP (1996) Evidence that the diabetes gene

encodes the leptin receptor: identification of a mutation in the leptin receptor gene in db/db mice. Cell 84: 491-495.
139. Lee GH, Proenca R, Montez JM, Carroll KM, Darvishzadeh JG, Lee JI, Friedman JM (1996) Abnormal splicing of the leptin receptor in diabetic mice. Nature 379: 632-635.
140. Chan TM, Young KM, Hutson NJ, Brumley FT, Exton JH (1975) Hepatic metabolism of genetically diabetic (db/db) mice. I. Carbohydrate metabolism. Am J Physiol 229: 1702-1712.
141. Kodama H, Fujita M, Yamaguchi I (1994) Development of hyperglycaemia and insulin resistance in conscious genetically diabetic (C57BL/KsJ-db/db) mice. Diabetologia 37: 739-744.
142. Kodama H, Fujita M, Yamazaki M, Yamaguchi I (1994) The possible role of age-related increase in the plasma glucagon/insulin ratio in the enhanced hepatic gluconeogenesis and hyperglycemia in genetically diabetic (C57BL/KsJ-db/db) mice. Jpn J Pharmacol 66: 281-287.
143. Senador D, Kanakamedala K, Irigoyen MC, Morris M, Elased KM (2009) Cardiovascular and autonomic phenotype of db/db diabetic mice. Exp Physiol 94: 648-658.
144. Do OH, Low JT, Gaisano HY, Thorn P (2014) The secretory deficit in islets from db/db mice is mainly due to a loss of responding beta cells. Diabetologia 57: 1400-1409.
145. Belke DD, Severson DL (2012) Diabetes in mice with monogenic obesity: the db/db mouse and its use in the study of cardiac consequences. Methods Mol Biol 933: 47-57.
146. Bernstein RM, Davis BM, Olefsky JM, Reaven GM (1978) Hepatic insulin responsiveness in patients with endogenous hypertriglyceridaemia. Diabetologia 14: 249-253.
147. Reaven GM, Hollenbeck C, Jeng CY, Wu MS, Chen YD (1988) Measurement of plasma glucose, free fatty acid, lactate, and insulin for 24 h in patients with NIDDM. Diabetes 37: 1020-1024.
148. Floegel A, Stefan N, Yu Z, Muhlenbruch K, Drogan D, Joost HG, Fritsche A, Haring HU, Hrabe de Angelis M, Peters A, Roden M, Prehn C, Wang-Sattler R, Illig T, Schulze MB, Adamski J, Boeing H, Pischon T (2013) Identification of serum metabolites associated with risk of type 2 diabetes using a targeted metabolomic approach. Diabetes 62: 639-648.
149. Kim HJ, Kim JH, Noh S, Hur HJ, Sung MJ, Hwang JT, Park JH, Yang HJ, Kim MS, Kwon DY, Yoon SH (2011) Metabolomic analysis of livers and serum from high-fat diet induced obese mice. J Proteome Res 10: 722-731.
150. Petkov PM, Cassell MA, Sargent EE, Donnelly CJ, Robinson P, Crew V, Asquith S, Haar RV, Wiles MV (2004) Development of a SNP genotyping panel for genetic monitoring of the laboratory mouse. Genomics 83: 902-911.
151. Matthews VB, Allen TL, Risis S, Chan MH, Henstridge DC, Watson N, Zaffino LA, Babb JR, Boon J, Meikle PJ, Jowett JB, Watt MJ, Jansson JO, Bruce CR, Febbraio MA (2010) Interleukin-6-deficient mice develop hepatic inflammation and systemic insulin resistance. Diabetologia 53: 2431-2441.
152. Chung J, Nguyen AK, Henstridge DC, Holmes AG, Chan MH, Mesa JL, Lancaster GI, Southgate RJ, Bruce CR, Duffy SJ, Horvath I, Mestril R, Watt MJ, Hooper PL, Kingwell BA, Vigh L, Hevener A, Febbraio MA (2008) HSP72 protects against obesity-induced insulin resistance. Proc Natl Acad Sci U S A 105: 1739-1744.
153. Cefalu WT, Wang ZQ, Bell-Farrow A, Kiger FD, Izlar C (1994) Glycohemoglobin measured by automated affinity HPLC correlates with both short-term and long-term antecedent glycemia. Clin Chem 40: 1317-1321.
154. Shlens J (2003) Tutorial on Principal Component Analysis. University of California, San Diego. pp. 1-16.
155. Benjamini Y, Drai D, Elmer G, Kafkafi N, Golani I (2001) Controlling the false discovery rate in behavior genetics research. Behav Brain Res 125: 279-284.
156. Aarsland A, Wolfe RR (1998) Hepatic secretion of VLDL fatty acids during stimulated lipogenesis in men. J Lipid Res 39: 1280-1286.
157. Adiels M, Taskinen MR, Packard C, Caslake MJ, Soro-Paavonen A, Westerbacka J, Vehkavaara S, Hakkinen A, Olofsson SO, Yki-Jarvinen H, Boren J (2006) Overproduction of large VLDL particles is driven by increased liver fat content in man. Diabetologia 49: 755-765.

158. Postic C, Girard J (2008) The role of the lipogenic pathway in the development of hepatic steatosis. Diabetes Metab 34: 643-648.
159. Dowhan W, Bogdanov M (2009) Lipid-dependent membrane protein topogenesis. Annu Rev Biochem 78: 515-540.
160. Cao H, Gerhold K, Mayers JR, Wiest MM, Watkins SM, Hotamisligil GS (2008) Identification of a lipokine, a lipid hormone linking adipose tissue to systemic metabolism. Cell 134: 933-944.
161. Avram MM, Avram AS, James WD (2005) Subcutaneous fat in normal and diseased states: 1. Introduction. J Am Acad Dermatol 53: 663-670.
162. Dubois SG, Heilbronn LK, Smith SR, Albu JB, Kelley DE, Ravussin E (2006) Decreased expression of adipogenic genes in obese subjects with type 2 diabetes. Obesity (Silver Spring) 14: 1543-1552.
163. Large V, Reynisdottir S, Langin D, Fredby K, Klannemark M, Holm C, Arner P (1999) Decreased expression and function of adipocyte hormone-sensitive lipase in subcutaneous fat cells of obese subjects. J Lipid Res 40: 2059-2066.
164. Erion DM, Shulman GI (2010) Diacylglycerol-mediated insulin resistance. Nat Med 16: 400-402.
165. Chavez JA, Knotts TA, Wang LP, Li G, Dobrowsky RT, Florant GL, Summers SA (2003) A role for ceramide, but not diacylglycerol, in the antagonism of insulin signal transduction by saturated fatty acids. J Biol Chem 278: 10297-10303.
166. Cazzolli R, Mitchell TW, Burchfield JG, Pedersen DJ, Turner N, Biden TJ, Schmitz-Peiffer C (2007) Dilinoleoyl-phosphatidic acid mediates reduced IRS-1 tyrosine phosphorylation in rat skeletal muscle cells and mouse muscle. Diabetologia 50: 1732-1742.
167. Galbo T, Perry RJ, Jurczak MJ, Camporez JP, Alves TC, Kahn M, Guigni BA, Serr J, Zhang D, Bhanot S, Samuel VT, Shulman GI (2013) Saturated and unsaturated fat induce hepatic insulin resistance independently of TLR-4 signaling and ceramide synthesis in vivo. Proc Natl Acad Sci U S A 110: 12780-12785.
168. Hodge AM, Simpson JA, Gibson RA, Sinclair AJ, Makrides M, O'Dea K, English DR, Giles GG (2007) Plasma phospholipid fatty acid composition as a biomarker of habitual dietary fat intake in an ethnically diverse cohort. Nutr Metab Cardiovasc Dis 17: 415-426.
169. Wolk A, Furuheim M, Vessby B (2001) Fatty acid composition of adipose tissue and serum lipids are valid biological markers of dairy fat intake in men. J Nutr 131: 828-833.
170. Kroger J, Zietemann V, Enzenbach C, Weikert C, Jansen EH, Doring F, Joost HG, Boeing H, Schulze MB (2011) Erythrocyte membrane phospholipid fatty acids, desaturase activity, and dietary fatty acids in relation to risk of type 2 diabetes in the European Prospective Investigation into Cancer and Nutrition (EPIC)-Potsdam Study. Am J Clin Nutr 93: 127-142.
171. Patel PS, Sharp SJ, Jansen E, Luben RN, Khaw KT, Wareham NJ, Forouhi NG (2010) Fatty acids measured in plasma and erythrocyte-membrane phospholipids and derived by food-frequency questionnaire and the risk of new-onset type 2 diabetes: a pilot study in the European Prospective Investigation into Cancer and Nutrition (EPIC)-Norfolk cohort. Am J Clin Nutr 92: 1214-1222.
172. Horrocks LA, Yeo YK (1999) Health benefits of docosahexaenoic acid (DHA). Pharmacol Res 40: 211-225.
173. Lenz LS, Marx J, Chamulitrat W, Kaiser I, Grone HJ, Liebisch G, Schmitz G, Elsing C, Straub BK, Fullekrug J, Stremmel W, Herrmann T (2011) Adipocyte-specific inactivation of Acyl-CoA synthetase fatty acid transport protein 4 (Fatp4) in mice causes adipose hypertrophy and alterations in metabolism of complex lipids under high fat diet. J Biol Chem 286: 35578-35587.
174. Magnusson YK, Friberg P, Sjovall P, Malm J, Chen Y (2008) TOF-SIMS analysis of lipid accumulation in the skeletal muscle of ob/ob mice. Obesity (Silver Spring) 16: 2745-2753.
175. Tepperman HM, Tepperman J (1985) Membranes and the response to insulin. Proc Nutr Soc 44: 211-220.

176. Borkman M, Storlien LH, Pan DA, Jenkins AB, Chisholm DJ, Campbell LV (1993) The relation between insulin sensitivity and the fatty-acid composition of skeletal-muscle phospholipids. N Engl J Med 328: 238-244.
177. Skwarek LC, Boulianne GL (2009) Great expectations for PIP: phosphoinositides as regulators of signaling during development and disease. Dev Cell 16: 12-20.
178. Meikle PJ, Duplock S, Blacklock D, Whitfield PD, Macintosh G, Hopwood JJ, Fuller M (2008) Effect of lysosomal storage on bis(monoacylglycero)phosphate. Biochem J 411: 71-78.
179. Claypool SM, Koehler CM (2012) The complexity of cardiolipin in health and disease. Trends Biochem Sci 37: 32-41.
180. Schlame M (2008) Cardiolipin synthesis for the assembly of bacterial and mitochondrial membranes. J Lipid Res 49: 1607-1620.
181. Bonnard C, Durand A, Peyrol S, Chanseaume E, Chauvin MA, Morio B, Vidal H, Rieusset J (2008) Mitochondrial dysfunction results from oxidative stress in the skeletal muscle of diet-induced insulin-resistant mice. J Clin Invest 118: 789-800.
182. Furukawa S, Fujita T, Shimabukuro M, Iwaki M, Yamada Y, Nakajima Y, Nakayama O, Makishima M, Matsuda M, Shimomura I (2004) Increased oxidative stress in obesity and its impact on metabolic syndrome. J Clin Invest 114: 1752-1761.
183. Houstis N, Rosen ED, Lander ES (2006) Reactive oxygen species have a causal role in multiple forms of insulin resistance. Nature 440: 944-948.
184. Watkins SM, Reifsnyder PR, Pan HJ, German JB, Leiter EH (2002) Lipid metabolome-wide effects of the PPARgamma agonist rosiglitazone. J Lipid Res 43: 1809-1817.
185. Ng Y, Barhoumi R, Tjalkens RB, Fan YY, Kolar S, Wang N, Lupton JR, Chapkin RS (2005) The role of docosahexaenoic acid in mediating mitochondrial membrane lipid oxidation and apoptosis in colonocytes. Carcinogenesis 26: 1914-1921.
186. Watkins SM, Carter LC, German JB (1998) Docosahexaenoic acid accumulates in cardiolipin and enhances HT-29 cell oxidant production. J Lipid Res 39: 1583-1588.
187. Li J, Romestaing C, Han X, Li Y, Hao X, Wu Y, Sun C, Liu X, Jefferson LS, Xiong J, Lanoue KF, Chang Z, Lynch CJ, Wang H, Shi Y (2010) Cardiolipin remodeling by ALCAT1 links oxidative stress and mitochondrial dysfunction to obesity. Cell Metab 12: 154-165.
188. Boudina S, Sena S, Theobald H, Sheng X, Wright JJ, Hu XX, Aziz S, Johnson JI, Bugger H, Zaha VG, Abel ED (2007) Mitochondrial energetics in the heart in obesity-related diabetes: direct evidence for increased uncoupled respiration and activation of uncoupling proteins. Diabetes 56: 2457-2466.
189. Wallner S, Schmitz G (2011) Plasmalogens the neglected regulatory and scavenging lipid species. Chem Phys Lipids 164: 573-589.
190. Tanaka N, Matsubara T, Krausz KW, Patterson AD, Gonzalez FJ (2012) Disruption of phospholipid and bile acid homeostasis in mice with nonalcoholic steatohepatitis. Hepatology 56: 118-129.
191. Han MS, Lim YM, Quan W, Kim JR, Chung KW, Kang M, Kim S, Park SY, Han JS, Cheon HG, Dal Rhee S, Park TS, Lee MS (2011) Lysophosphatidylcholine as an effector of fatty acid-induced insulin resistance. J Lipid Res 52: 1234-1246.
192. Motley ED, Kabir SM, Gardner CD, Eguchi K, Frank GD, Kuroki T, Ohba M, Yamakawa T, Eguchi S (2002) Lysophosphatidylcholine inhibits insulin-induced Akt activation through protein kinase C-alpha in vascular smooth muscle cells. Hypertension 39: 508-512.
193. Donnelly KL, Smith CI, Schwarzenberg SJ, Jessurun J, Boldt MD, Parks EJ (2005) Sources of fatty acids stored in liver and secreted via lipoproteins in patients with nonalcoholic fatty liver disease. J Clin Invest 115: 1343-1351.
194. Sleeman MW, Garcia K, Liu R, Murray JD, Malinova L, Moncrieffe M, Yancopoulos GD, Wiegand SJ (2003) Ciliary neurotrophic factor improves diabetic parameters and hepatic steatosis and increases basal metabolic rate in db/db mice. Proc Natl Acad Sci U S A 100: 14297-14302.

195. Zhou G, Myers R, Li Y, Chen Y, Shen X, Fenyk-Melody J, Wu M, Ventre J, Doebber T, Fujii N, Musi N, Hirshman MF, Goodyear LJ, Moller DE (2001) Role of AMP-activated protein kinase in mechanism of metformin action. J Clin Invest 108: 1167-1174.
196. Du P, Kibbe WA, Lin SM (2008) lumi: a pipeline for processing Illumina microarray. Bioinformatics 24: 1547-1548.
197. Kauffmann A, Gentleman R, Huber W (2009) arrayQualityMetrics--a bioconductor package for quality assessment of microarray data. Bioinformatics 25: 415-416.
198. Smyth GK (2005) Limma: linear models for microarray data. . In: R. Gentleman VC, S. Dudoit, R. Irizarry, W. Huber editor. In: Bioinformatics and Computational Biology Solutions using R and Bioconductor. New York: Springer. pp. 397-420.
199. Brown MS, Goldstein JL (2008) Selective versus total insulin resistance: a pathogenic paradox. Cell Metab 7: 95-96.
200. Garcia-Ruiz I, Rodriguez-Juan C, Diaz-Sanjuan T, del Hoyo P, Colina F, Munoz-Yague T, Solis-Herruzo JA (2006) Uric acid and anti-TNF antibody improve mitochondrial dysfunction in ob/ob mice. Hepatology 44: 581-591.
201. Go GW, Mani A (2012) Low-density lipoprotein receptor (LDLR) family orchestrates cholesterol homeostasis. Yale J Biol Med 85: 19-28.
202. Oka K, Ishimura-Oka K, Chu MJ, Sullivan M, Krushkal J, Li WH, Chan L (1994) Mouse very-low-density-lipoprotein receptor (VLDLR) cDNA cloning, tissue-specific expression and evolutionary relationship with the low-density-lipoprotein receptor. Eur J Biochem 224: 975-982.
203. Jo H, Choe SS, Shin KC, Jang H, Lee JH, Seong JK, Back SH, Kim JB (2013) Endoplasmic reticulum stress induces hepatic steatosis via increased expression of the hepatic very low-density lipoprotein receptor. Hepatology 57: 1366-1377.
204. DeFronzo RA, Bonadonna RC, Ferrannini E (1992) Pathogenesis of NIDDM. A balanced overview. Diabetes Care 15: 318-368.
205. Foley JE (1992) Rationale and application of fatty acid oxidation inhibitors in treatment of diabetes mellitus. Diabetes Care 15: 773-784.
206. Rasche A, Al-Hasani H, Herwig R (2008) Meta-analysis approach identifies candidate genes and associated molecular networks for type-2 diabetes mellitus. BMC Genomics 9: 310.
207. Scott LJ, Mohlke KL, Bonnycastle LL, Willer CJ, Li Y, Duren WL, Erdos MR, Stringham HM, Chines PS, Jackson AU, Prokunina-Olsson L, Ding CJ, Swift AJ, Narisu N, Hu T, Pruim R, Xiao R, Li XY, Conneely KN, Riebow NL, Sprau AG, Tong M, White PP, Hetrick KN, Barnhart MW, Bark CW, Goldstein JL, Watkins L, Xiang F, Saramies J, Buchanan TA, Watanabe RM, Valle TT, Kinnunen L, Abecasis GR, Pugh EW, Doheny KF, Bergman RN, Tuomilehto J, Collins FS, Boehnke M (2007) A genome-wide association study of type 2 diabetes in Finns detects multiple susceptibility variants. Science 316: 1341-1345.
208. Sladek R, Rocheleau G, Rung J, Dina C, Shen L, Serre D, Boutin P, Vincent D, Belisle A, Hadjadj S, Balkau B, Heude B, Charpentier G, Hudson TJ, Montpetit A, Pshezhetsky AV, Prentki M, Posner BI, Balding DJ, Meyre D, Polychronakos C, Froguel P (2007) A genome-wide association study identifies novel risk loci for type 2 diabetes. Nature 445: 881-885.
209. Boden G, Shulman GI (2002) Free fatty acids in obesity and type 2 diabetes: defining their role in the development of insulin resistance and beta-cell dysfunction. Eur J Clin Invest 32 Suppl 3: 14-23.
210. Kashyap SR, Belfort R, Berria R, Suraamornkul S, Pratipranawatr T, Finlayson J, Barrentine A, Bajaj M, Mandarino L, DeFronzo R, Cusi K (2004) Discordant effects of a chronic physiological increase in plasma FFA on insulin signaling in healthy subjects with or without a family history of type 2 diabetes. Am J Physiol Endocrinol Metab 287: E537-546.
211. Gulli G, Ferrannini E, Stern M, Haffner S, DeFronzo RA (1992) The metabolic profile of NIDDM is fully established in glucose-tolerant offspring of two Mexican-American NIDDM parents. Diabetes 41: 1575-1586.

212. Pratipanawatr W, Pratipanawatr T, Cusi K, Berria R, Adams JM, Jenkinson CP, Maezono K, DeFronzo RA, Mandarino LJ (2001) Skeletal muscle insulin resistance in normoglycemic subjects with a strong family history of type 2 diabetes is associated with decreased insulin-stimulated insulin receptor substrate-1 tyrosine phosphorylation. Diabetes 50: 2572-2578.
213. Weyer C, Tataranni PA, Bogardus C, Pratley RE (2001) Insulin resistance and insulin secretory dysfunction are independent predictors of worsening of glucose tolerance during each stage of type 2 diabetes development. Diabetes Care 24: 89-94.
214. Petersen KF, Dufour S, Shulman GI (2005) Decreased insulin-stimulated ATP synthesis and phosphate transport in muscle of insulin-resistant offspring of type 2 diabetic parents. PLoS Med 2: e233.
215. Petersen KF, Dufour S, Befroy D, Garcia R, Shulman GI (2004) Impaired mitochondrial activity in the insulin-resistant offspring of patients with type 2 diabetes. N Engl J Med 350: 664-671.
216. Tonks KT, Ng Y, Miller S, Coster AC, Samocha-Bonet D, Iseli TJ, Xu A, Patrick E, Yang JY, Junutula JR, Modrusan Z, Kolumam G, Stockli J, Chisholm DJ, James DE, Greenfield JR (2013) Impaired Akt phosphorylation in insulin-resistant human muscle is accompanied by selective and heterogeneous downstream defects. Diabetologia 56: 875-885.
217. Samocha-Bonet D, Campbell LV, Viardot A, Freund J, Tam CS, Greenfield JR, Heilbronn LK (2010) A family history of type 2 diabetes increases risk factors associated with overfeeding. Diabetologia 53: 1700-1708.
218. Khaselev N, Murphy RC (1999) Susceptibility of plasmenyl glycerophosphoethanolamine lipids containing arachidonate to oxidative degradation. Free Radic Biol Med 26: 275-284.
219. Lessig J, Fuchs B (2010) HOCl-mediated glycerophosphocholine and glycerophosphoethanolamine generation from plasmalogens in phospholipid mixtures. Lipids 45: 37-51.
220. Colas R, Sassolas A, Guichardant M, Cugnet-Anceau C, Moret M, Moulin P, Lagarde M, Calzada C (2011) LDL from obese patients with the metabolic syndrome show increased lipid peroxidation and activate platelets. Diabetologia 54: 2931-2940.
221. Welch EJ, Naikawadi RP, Li Z, Lin P, Ishii S, Shimizu T, Tiruppathi C, Du X, Subbaiah PV, Ye RD (2009) Opposing effects of platelet-activating factor and lyso-platelet-activating factor on neutrophil and platelet activation. Mol Pharmacol 75: 227-234.
222. Nelson TL, Biggs ML, Kizer JR, Cushman M, Hokanson JE, Furberg CD, Mukamal KJ (2012) Lipoprotein-associated phospholipase A2 (Lp-PLA2) and future risk of type 2 diabetes: results from the Cardiovascular Health Study. J Clin Endocrinol Metab 97: 1695-1701.
223. Serban M, Tanaseanu C, Kosaka T, Vidulescu C, Stoian I, Marta DS, Tanaseanu S, Moldoveanu E (2002) Significance of platelet-activating factor acetylhydrolase in patients with non-insulin-dependent (type 2) diabetes mellitus. J Cell Mol Med 6: 643-647.
224. Fan P, Liu H, Wang Y, Zhang F, Bai H (2012) Apolipoprotein E-containing HDL-associated platelet-activating factor acetylhydrolase activities and malondialdehyde concentrations in patients with PCOS. Reprod Biomed Online 24: 197-205.
225. Yamashita T, Hashiramoto A, Haluzik M, Mizukami H, Beck S, Norton A, Kono M, Tsuji S, Daniotti JL, Werth N, Sandhoff R, Sandhoff K, Proia RL (2003) Enhanced insulin sensitivity in mice lacking ganglioside GM3. Proc Natl Acad Sci U S A 100: 3445-3449.
226. Abdul-Ghani MA, Tripathy D, DeFronzo RA (2006) Contributions of beta-cell dysfunction and insulin resistance to the pathogenesis of impaired glucose tolerance and impaired fasting glucose. Diabetes Care 29: 1130-1139.
227. Gastaldelli A, Ferrannini E, Miyazaki Y, Matsuda M, DeFronzo RA (2004) Beta-cell dysfunction and glucose intolerance: results from the San Antonio metabolism (SAM) study. Diabetologia 47: 31-39.
228. Dunstan DW, Zimmet PZ, Welborn TA, De Courten MP, Cameron AJ, Sicree RA, Dwyer T, Colagiuri S, Jolley D, Knuiman M, Atkins R, Shaw JE (2002) The rising prevalence of diabetes and

impaired glucose tolerance: the Australian Diabetes, Obesity and Lifestyle Study. Diabetes Care 25: 829-834.
229. Meikle PJ, Christopher MJ (2011) Lipidomics is providing new insight into the metabolic syndrome and its sequelae. Curr Opin Lipidol 22: 210-215.
230. Kotronen A, Seppanen-Laakso T, Westerbacka J, Kiviluoto T, Arola J, Ruskeepaa AL, Yki-Jarvinen H, Oresic M (2010) Comparison of lipid and fatty acid composition of the liver, subcutaneous and intra-abdominal adipose tissue, and serum. Obesity (Silver Spring) 18: 937-944.
231. Hudgins LC, Hellerstein MK, Seidman CE, Neese RA, Tremaroli JD, Hirsch J (2000) Relationship between carbohydrate-induced hypertriglyceridemia and fatty acid synthesis in lean and obese subjects. J Lipid Res 41: 595-604.
232. Parks EJ (2002) Dietary carbohydrate's effects on lipogenesis and the relationship of lipogenesis to blood insulin and glucose concentrations. Br J Nutr 87 Suppl 2: S247-253.
233. Warensjo E, Riserus U, Gustafsson IB, Mohsen R, Cederholm T, Vessby B (2008) Effects of saturated and unsaturated fatty acids on estimated desaturase activities during a controlled dietary intervention. Nutr Metab Cardiovasc Dis 18: 683-690.
234. Cao J, Liu Y, Lockwood J, Burn P, Shi Y (2004) A novel cardiolipin-remodeling pathway revealed by a gene encoding an endoplasmic reticulum-associated acyl-CoA:lysocardiolipin acyltransferase (ALCAT1) in mouse. J Biol Chem 279: 31727-31734.
235. Cao J, Shen W, Chang Z, Shi Y (2009) ALCAT1 is a polyglycerophospholipid acyltransferase potently regulated by adenine nucleotide and thyroid status. Am J Physiol Endocrinol Metab 296: E647-653.

APPENDICES

Table S4.1 Relationship between genotype and liver lipid species in male mice.

Lipid species	6 weeks				10 weeks				16 weeks			
	P-value[a]	db/h vs. H/H[b]	db/db vs. H/H[b]	db/db vs. db/h[b]	*P*-value[a]	db/h vs. H/H[b]	db/db vs. H/H[b]	db/db vs. db/h[b]	*P*-value[a]	db/h vs. H/H[b]	db/db vs. H/H[b]	db/db vs. db/h[b]
Cer 16:0	0.825	-0.1	0.0	0.0	0.196	0.0	0.4	0.8	0.007	0.0	2.6	1.7
Cer 18:0	0.717	-0.1	-0.2	0.0	0.058	0.0	1.3	0.9	0.006	-0.3	2.1	2.0
Cer 20:0	0.648	0.3	0.1	0.0	0.396	0.0	0.5	0.1	0.071	0.0	1.1	1.0
Cer 22:0	0.601	0.3	0.1	-0.1	0.733	0.0	0.0	0.1	0.861	0.0	0.0	0.0
Cer 24:0	0.755	0.1	0.1	0.0	0.852	0.0	0.0	0.0	0.148	0.0	-0.9	-0.6
Cer 24:1	0.755	0.0	0.0	0.1	0.464	0.0	0.2	0.3	0.890	0.0	0.0	0.0
MHC 16:0	0.794	0.0	0.0	-0.1	0.663	0.0	-0.1	-0.1	0.467	0.1	-0.1	-0.3
MHC 20:0	0.449	0.1	-0.3	-0.6	0.250	0.0	0.7	0.3	0.254	0.2	0.6	0.2
MHC 22:0	0.467	0.7	0.1	-0.1	0.628	0.1	0.2	0.0	0.479	0.3	0.0	-0.1
MHC 24:0	0.575	0.3	0.0	-0.1	0.659	0.0	-0.1	-0.1	0.070	0.0	-1.2	-0.9
MHC 24:1	0.776	0.0	0.0	-0.1	0.896	0.0	0.0	0.0	0.289	0.0	-0.4	-0.5
DHC 24:1	0.719	-0.1	0.0	0.1	0.704	0.0	0.3	0.0	0.080	0.8	1.1	0.0
SM 31:1	0.649	-0.1	-0.3	0.0	0.549	0.0	-0.1	-0.2	0.528	0.0	-0.1	-0.2
SM 34:1	0.660	0.0	-0.4	0.0	0.920	0.0	0.0	0.0	0.816	0.0	0.0	0.0
SM 35:1	0.093	0.0	-2.7	-4.1	0.325	0.0	-0.6	-0.2	0.895	0.0	0.0	0.0
SM 36:1	0.962	0.0	0.0	0.0	0.099	0.0	2.0	0.1	0.140	-1.1	-0.4	0.0
SM 38:1	0.264	0.5	0.0	-2.0	0.236	0.3	-0.2	-0.6	0.036	0.0	-1.5	-1.2
SM 38:2	0.700	0.1	0.1	0.0	0.375	0.3	0.4	0.0	0.061	0.5	-0.2	-1.5
SM 39:1	0.469	0.3	0.0	-0.5	0.070	0.0	-0.8	-1.3	0.025	0.1	-1.5	-1.5
SM 41:1	0.448	0.0	-0.6	-0.6	0.909	0.0	0.0	0.0	0.014	0.0	-1.9	-1.7
SM 41:2	0.948	0.0	0.0	0.0	0.479	0.0	0.0	-0.6	0.035	0.0	-1.5	-1.3
SM 42:1	0.591	0.2	0.0	-0.3	0.628	0.0	-0.2	-0.1	0.004	0.0	-2.4	-2.5
PC 30:0	0.700	0.0	0.0	0.2	0.909	0.0	0.0	0.0	0.018	0.0	-1.8	-1.6
PC 31:0	0.467	0.0	-0.5	-0.4	0.015	0.0	-1.8	-1.8	0.003	0.0	-2.9	-2.2
PC 31:1	0.624	0.0	0.3	0.1	0.832	0.0	0.0	0.0	0.633	0.0	-0.1	-0.1
PC 32:0	0.226	0.0	-1.9	-1.7	0.024	0.0	-1.0	-2.1	0.003	-0.4	-2.7	-2.4
PC 32:1	0.237	0.2	1.2	1.6	0.009	0.8	2.6	0.6	0.148	0.0	-0.4	-1.0
PC 32:2	0.249	0.3	1.2	1.3	0.010	0.8	2.3	0.9	0.100	0.6	-0.1	-1.1
PC 32:3	0.459	0.8	0.3	0.0	0.575	0.0	0.4	0.0	0.472	0.0	-0.1	-0.4
PC 33:0	0.362	0.0	-1.1	-0.8	0.029	0.0	-1.6	-1.2	0.002	-0.1	-3.0	-2.8
PC 33:1	0.873	0.0	0.0	0.1	0.740	0.0	-0.1	-0.1	0.002	0.0	-2.4	-3.3
PC 33:2	0.279	0.3	0.0	-1.8	0.005	0.0	-2.4	-2.2	0.009	0.0	-1.8	-2.2
PC 34:0	0.473	0.0	0.4	0.4	0.111	0.2	1.3	0.1	0.005	-0.2	-2.2	-2.3
PC 34:1	0.549	0.0	0.3	0.2	0.449	0.1	0.4	0.0	0.005	-0.7	-2.2	-1.9
PC 34:2	0.219	0.8	-0.4	-3.3	0.024	0.8	-0.3	-2.1	0.031	0.0	-1.6	-1.3
PC 34:3	0.649	0.2	0.1	0.0	0.513	0.3	0.0	-0.2	0.142	0.0	-0.6	-1.0
PC 34:4	0.603	0.1	0.3	0.0	0.628	0.1	0.2	0.0	0.210	0.0	-0.5	-0.6
PC 34:5	0.293	0.0	0.9	1.2	0.006	0.0	2.1	2.4	0.090	0.7	1.0	0.2
PC 35:0	0.509	-0.3	-0.5	0.0	0.738	0.1	0.0	0.0	0.413	0.2	0.2	-0.1
PC 35:1	0.823	0.0	0.1	0.0	0.704	0.0	0.0	0.2	0.191	0.0	-0.8	-0.5
PC 35:2	0.874	0.0	-0.1	0.0	0.250	-0.3	-0.5	-0.2	0.847	0.0	0.0	-0.1
PC 35:3	0.738	0.0	0.0	-0.1	0.055	0.1	-0.6	-1.6	0.006	0.5	-1.5	-2.4
PC 36:1	0.660	0.0	0.2	0.1	0.001	-0.1	3.5	3.4	0.947	0.0	0.0	0.0
PC 36:2	0.823	0.0	0.0	0.1	0.041	0.0	1.2	1.3	0.482	0.0	0.3	0.2
PC 36:3	0.459	0.0	0.6	0.4	0.006	0.1	3.5	1.1	0.960	0.0	0.0	0.0
PC 36:4a	0.717	0.1	0.2	0.0	0.662	0.1	0.2	0.0	0.771	0.0	0.0	0.0
PC 36:4b	0.226	0.2	-1.1	-2.6	0.006	0.7	-0.9	-3.1	0.005	-0.1	-2.6	-1.8
PC 36:5	0.253	0.0	1.2	1.4	0.001	0.0	4.1	3.7	0.479	0.1	0.3	0.0

Lipid species	6 weeks				10 weeks				16 weeks			
	P-value[a]	db/h vs. H/H[b]	db/db vs. H/H[b]	db/db vs. db/h[b]	*P*-value[a]	db/h vs. H/H[b]	db/db vs. H/H[b]	db/db vs. db/h[b]	*P*-value[a]	db/h vs. H/H[b]	db/db vs. H/H[b]	db/db vs. db/h[b]
PC 36:6	0.264	0.0	1.4	1.2	0.002	0.1	3.5	2.6	0.910	0.0	0.0	0.0
PC 37:4	0.459	0.0	-0.6	-0.4	0.024	0.0	-1.4	-1.6	0.381	0.0	-0.4	-0.2
PC 37:5	0.794	0.0	0.0	0.1	0.808	0.0	0.0	0.0	0.384	-0.1	-0.2	-0.3
PC 37:6	0.365	0.0	-0.4	-1.1	0.008	0.0	-2.1	-2.1	0.005	0.0	-2.6	-2.0
PC 38:2	0.459	0.1	0.4	0.5	0.160	0.3	0.9	0.1	0.017	0.1	-1.5	-1.9
PC 38:3	0.487	0.0	0.1	0.6	0.001	0.0	4.1	3.4	0.072	0.0	1.2	0.9
PC 38:4	0.459	0.0	-0.6	-0.4	0.721	0.1	0.0	-0.1	0.571	-0.2	0.0	0.0
PC 38:5	0.516	0.0	0.3	0.4	0.099	0.0	1.7	0.2	0.771	-0.1	0.0	0.0
PC 38:6a	0.875	0.0	0.0	0.0	0.832	0.0	0.0	0.0	0.099	-0.4	-1.1	-0.2
PC 38:6b	0.398	0.0	-0.4	-1.0	0.341	0.0	-0.3	-0.5	0.007	-1.2	-2.4	-0.5
PC 38:7	0.313	0.1	0.9	1.0	0.018	0.3	2.4	0.6	0.608	0.2	0.0	0.0
PC 39:6	0.516	0.0	-0.5	-0.1	0.413	-0.2	-0.5	0.0	0.357	-0.7	0.0	0.0
PC 39:7	0.934	0.0	0.0	0.0	0.259	0.0	-0.4	-0.6	0.025	0.0	-1.1	-2.1
PC 40:5	0.700	0.0	0.1	0.1	0.005	0.0	3.0	1.9	0.029	0.0	1.5	1.5
PC 40:6	0.911	0.0	0.0	0.0	0.302	0.0	0.5	0.3	0.060	-0.7	0.4	1.2
PC 40:7	0.825	0.0	0.0	0.0	0.196	0.0	0.8	0.3	0.384	-0.4	-0.2	0.0
PC(O-32:1)	0.846	0.0	0.1	0.0	0.817	0.0	0.0	0.0	0.409	0.1	-0.2	-0.3
PC(O-34:1)	0.514	0.0	-0.6	-0.3	0.185	0.0	-0.6	-0.6	0.061	0.0	-1.0	-1.2
PC(O-34:2)	0.710	0.0	-0.1	-0.2	0.245	0.0	-0.4	-0.7	0.051	0.0	-1.6	-0.9
PC(O-35:4)	0.459	0.2	0.6	0.1	0.853	0.0	0.0	0.0	0.141	0.4	-0.1	-1.0
PC(O-36:0)	0.516	0.0	0.0	-0.7	0.155	0.0	-0.8	-0.6	0.002	0.0	-2.9	-2.9
PC(O-36:2)	0.487	0.0	-0.1	-0.7	0.004	0.0	-3.8	-1.6	0.559	0.0	-0.1	-0.2
PC(O-36:3)	0.742	0.0	0.0	-0.2	0.018	-0.1	-1.6	-1.8	0.283	0.0	-0.5	-0.4
PC(O-36:4)	0.613	0.0	-0.3	-0.2	0.013	-0.2	-2.1	-1.3	0.021	0.0	-2.1	-1.1
PC(O-36:5)	0.516	0.0	-0.1	-0.5	0.843	0.0	0.0	-0.1	0.130	0.0	-0.9	-0.7
PC(O-38:5)	0.375	0.0	-1.2	-0.5	0.194	0.0	-0.7	-0.5	0.009	0.0	-1.8	-2.2
PC(O-40:6)	0.549	0.0	-0.3	-0.2	0.271	-0.2	-0.7	-0.1	0.357	-0.7	-0.1	0.0
PC(O-40:7)	0.226	0.0	-1.6	-1.8	0.117	0.2	-0.2	-1.2	0.042	0.0	-1.6	-1.0
PC(P-32:0)	0.648	0.0	-0.1	-0.3	0.567	0.0	0.0	-0.3	0.526	-0.3	-0.1	0.0
PC(P-34:1)	0.673	0.1	0.0	-0.2	0.035	0.0	-1.3	-1.3	0.007	0.0	-2.4	-1.9
PC(P-36:2)	0.875	0.0	0.0	0.0	0.130	-0.1	-0.8	-0.7	0.007	-0.1	-2.5	-1.6
PC(P-36:4)	0.730	0.0	0.0	-0.1	0.846	0.0	0.0	-0.1	0.099	0.0	-1.0	-0.7
PC(P-38:4)	0.448	0.8	0.1	-0.3	0.575	0.0	-0.2	-0.1	0.025	-0.1	-2.0	-0.8
PC(P-38:5)	0.533	0.0	-0.3	-0.4	0.745	0.0	-0.1	0.0	0.061	-0.4	-1.4	-0.2
PC(P-38:6)	0.362	0.0	-0.5	-1.1	0.069	0.0	-1.4	-0.6	0.002	-0.8	-3.3	-3.3
PC(P-40:5)	0.467	0.0	-1.2	-0.1	0.051	-0.5	-1.7	-0.2	0.008	-0.8	-2.3	-1.0
PC(P-40:6)	0.362	0.2	-0.4	-1.0	0.024	0.0	-1.4	-1.6	0.002	-1.4	-3.1	-1.0
LPC 16:0	0.449	0.8	0.4	0.0	0.131	0.4	0.8	0.3	0.090	0.1	1.2	0.6
LPC 16:1	0.226	0.2	1.6	1.4	0.001	1.4	4.1	3.7	0.002	2.5	3.0	0.5
LPC 18:0	0.816	0.0	0.1	0.0	0.051	0.0	0.8	1.5	0.153	0.0	0.7	0.8
LPC 18:1	0.448	0.2	0.8	0.3	0.016	0.2	1.7	1.6	0.559	0.1	0.2	0.0
LPC 18:2	0.449	0.3	0.9	0.0	0.021	0.7	1.3	1.5	0.045	0.4	1.5	0.6
LPC 20:4	0.738	0.1	0.1	0.0	0.069	0.8	1.2	0.1	0.275	0.0	0.7	0.2
LPC 22:6	0.710	0.1	0.1	0.0	0.022	0.7	2.0	0.5	0.055	0.0	1.3	1.0
PE 32:0	0.794	0.0	-0.1	0.0	0.628	0.0	-0.2	-0.1	0.016	-0.2	-1.9	-1.4
PE 32:1	0.253	0.0	1.1	1.6	0.001	2.0	3.8	1.3	0.061	0.9	0.0	-1.3
PE 34:1	0.459	0.0	0.3	0.7	0.099	0.2	1.2	-0.3	0.002	0.0	-2.7	-2.9
PE 34:2	0.833	0.1	0.0	0.0	0.521	0.3	0.0	-0.1	0.004	0.0	-2.3	-2.8
PE 34:3	0.375	0.3	0.6	0.6	0.099	0.8	1.0	0.0	0.015	0.2	-1.3	-2.0
PE 35:1	0.375	-0.7	0.0	0.8	0.289	0.0	0.1	0.7	0.148	0.1	-0.8	-0.6
PE 35:2	0.833	0.0	0.0	0.0	0.130	-0.3	-0.8	-0.6	0.340	0.0	-0.5	-0.2
PE 36:0	0.533	-0.1	0.1	0.4	0.249	0.0	0.8	0.2	0.378	0.0	-0.4	-0.2
PE 36:1	0.459	0.0	0.4	0.6	0.004	0.0	2.8	2.2	0.248	-0.2	-0.6	-0.2
PE 36:2	0.911	0.0	0.0	0.0	0.575	0.0	0.1	0.2	0.771	-0.1	0.0	0.0

Lipid species	6 weeks				10 weeks				16 weeks			
	P-value[a]	db/h vs. H/H[b]	db/db vs. H/H[b]	db/db vs. db/h[b]	*P*-value[a]	db/h vs. H/H[b]	db/db vs. H/H[b]	db/db vs. db/h[b]	*P*-value[a]	db/h vs. H/H[b]	db/db vs. H/H[b]	db/db vs. db/h[b]
PE 36:3	0.660	0.0	0.2	0.1	0.282	0.0	0.6	0.2	0.190	0.0	-0.7	-0.6
PE 36:4	0.982	0.0	0.0	0.0	0.284	0.3	0.7	0.0	0.023	0.0	-1.4	-1.8
PE 36:5	0.264	0.0	1.1	1.4	0.001	0.6	4.1	3.1	0.299	0.7	0.0	-0.1
PE 38:3	0.660	0.2	0.0	-0.1	0.733	-0.1	0.1	0.0	0.524	0.0	-0.1	-0.3
PE 38:4	0.448	0.1	0.0	-0.9	0.431	0.1	-0.1	-0.3	0.264	0.0	-0.5	-0.4
PE 38:5	0.755	0.0	0.1	0.1	0.142	0.2	1.3	0.0	0.816	0.0	-0.1	0.0
PE 38:6	0.516	0.0	0.0	-0.6	0.733	-0.1	0.0	-0.1	0.018	-0.5	-2.0	-0.7
PE 40:5	0.751	0.1	0.0	0.0	0.063	0.0	1.4	0.6	0.559	0.0	0.1	0.2
PE 40:6	0.515	0.1	0.0	-0.5	0.909	0.0	0.0	0.0	0.444	-0.4	0.0	0.1
PE 40:7	0.549	0.1	0.0	-0.4	0.704	0.2	0.0	-0.1	0.024	-0.5	-2.0	-0.4
PE(O-36:2)	0.833	0.0	0.0	0.0	0.130	-0.3	-0.8	-0.6	0.340	0.0	-0.5	-0.2
PE(O-36:5)	0.601	0.0	-0.1	-0.3	0.375	0.0	-0.5	-0.2	0.025	0.0	-2.0	-1.0
PE(O-38:4)	0.448	0.0	-0.3	-0.8	0.099	-0.1	-1.3	-0.3	0.004	0.1	-2.5	-2.4
PE(O-38:5)	0.953	0.0	0.0	0.0	0.932	0.0	0.0	0.0	0.095	-0.1	-1.2	-0.6
PE(O-40:6)	0.437	0.0	-0.4	-0.9	0.247	-0.2	-0.8	0.0	0.742	-0.1	0.0	0.1
PE(P-36:4)	0.575	0.0	-0.1	-0.4	0.403	0.0	-0.4	-0.2	0.025	0.0	-2.0	-1.0
PE(P-38:4)	0.398	0.0	-0.6	-0.8	0.784	0.0	0.0	-0.2	0.102	0.0	-1.6	-0.2
PE(P-38:5)	0.755	0.1	0.0	-0.1	0.879	0.0	0.0	0.0	0.059	0.0	-1.4	-0.8
LPE 16:0	0.533	0.3	0.3	0.0	0.042	0.8	1.7	0.1	0.277	0.5	0.4	0.0
LPE 18:0	0.449	0.9	0.3	0.0	0.012	1.8	2.3	0.0	0.003	1.6	2.6	1.3
LPE 18:1	0.375	0.4	0.9	0.3	0.004	0.9	3.0	1.2	0.005	1.6	2.3	0.6
LPE 20:4	0.467	0.6	0.4	0.0	0.017	0.8	2.6	0.1	0.357	0.2	0.4	0.0
LPE 22:6	0.467	0.8	0.1	0.0	0.049	0.7	1.8	0.0	0.314	0.3	0.4	0.1
PI 36:1	0.717	0.0	0.1	0.1	0.012	-0.1	1.2	2.4	0.581	-0.1	0.0	0.2
PI 36:2	0.873	0.0	0.0	0.0	0.607	0.0	-0.1	-0.2	0.032	-0.1	-1.3	-1.5
PI 38:2	0.264	0.0	1.1	1.4	0.001	-0.1	4.1	3.7	0.655	0.1	0.1	0.0
PI 38:3	0.249	0.0	1.2	1.6	0.001	-0.1	4.1	3.4	0.587	0.1	0.2	0.0
PI 38:4	0.603	0.0	0.0	-0.4	0.713	0.0	0.2	0.0	0.357	-0.5	0.0	0.2
PI 40:4	0.516	0.1	0.4	0.2	0.002	0.3	3.8	2.1	0.033	0.6	-0.7	-1.5
PI 40:5	0.467	0.0	0.5	0.5	0.003	0.0	2.8	2.6	0.771	0.0	0.1	0.0
PI 40:6	0.516	0.1	0.0	-0.5	0.607	0.0	-0.3	0.0	0.002	0.1	-3.6	-3.3
PS 36:1	0.533	0.0	-0.1	-0.4	0.856	0.0	0.0	0.0	0.025	-0.1	-1.7	-1.1
PS 36:2	0.825	0.0	0.0	0.0	0.740	-0.1	-0.1	0.0	0.210	-0.1	-0.8	-0.2
PS 38:3	0.872	0.0	0.0	0.0	0.254	0.0	0.7	0.3	0.465	0.0	-0.2	-0.2
PS 38:4	0.398	0.0	-0.2	-1.3	0.536	0.0	-0.3	-0.1	0.134	0.0	-0.8	-0.8
PS 38:5	0.467	0.0	0.5	0.4	0.008	0.0	2.0	2.2	0.442	0.0	-0.1	-0.4
PS 40:5	0.923	0.0	0.0	0.0	0.218	-0.1	0.3	0.7	0.076	-0.4	-1.4	-0.1
PS 40:6	0.575	0.0	-0.1	-0.4	0.721	-0.1	0.0	0.0	0.005	-1.0	-2.5	-1.1
PG 34:1	0.660	0.3	0.0	0.0	0.334	0.1	0.7	0.0	0.046	0.0	-1.0	-1.7
PG 34:2	0.601	0.0	-0.3	-0.1	0.005	0.0	-2.4	-2.2	0.006	-0.5	-2.5	-1.4
PG 36:1	0.533	0.2	0.0	-0.4	0.686	-0.1	-0.1	0.1	0.865	0.0	0.0	0.0
PG 36:2	0.362	0.0	-0.6	-1.1	0.250	0.0	-0.8	-0.2	0.378	-0.8	0.0	0.0
PG 36:3	0.873	0.0	0.0	0.0	0.532	0.0	0.0	0.5	0.628	0.0	0.1	0.1
BMP 18:1/18:1	0.516	0.0	0.1	0.5	0.021	0.0	2.4	0.8	0.378	0.2	0.4	0.0
CL 18:2/18:2/18:2/16:1	0.313	0.6	0.9	0.5	0.022	0.8	2.1	0.2	0.270	0.1	-0.2	-0.6
CL 18:2/18:1/18:2/16:1	0.279	0.3	0.8	1.1	0.001	0.4	4.1	3.4	0.153	1.1	0.0	-0.3
CL 18:2/18:1/18:1/16:1	0.267	0.1	0.8	1.6	0.001	0.5	4.1	3.4	0.209	0.1	0.7	0.4
CL 18:2/18:2/18:2/18:3	0.803	0.0	-0.1	0.0	0.816	0.0	0.0	0.0	0.283	0.0	-0.7	-0.2
CL 18:2/18:2/18:2/18:2	0.226	0.0	-2.1	-2.3	0.005	0.0	-2.4	-2.4	0.055	-1.4	-0.9	0.0
CL 18:2/18:2/18:2/18:1	0.717	0.0	0.0	-0.2	0.532	0.0	0.4	0.0	0.559	-0.2	-0.1	0.0
CL 18:2/18:1/18:2/18:1	0.673	0.0	0.1	0.1	0.005	0.2	3.8	1.1	0.051	-0.6	0.1	1.8
CL 18:1/18:1/18:1/18:2	0.948	0.0	0.0	0.0	0.005	0.0	3.5	1.6	0.949	0.0	0.0	0.0
CL 18:2/18:2/18:2/20:3	0.973	0.0	0.0	0.0	0.056	0.0	1.8	0.6	0.421	-0.2	0.0	0.3
CL 18:2/18:1/18:2/20:3	0.449	0.0	-0.5	-0.6	0.863	0.0	0.0	0.0	0.254	-0.4	-0.6	0.0

Lipid species	6 weeks				10 weeks				16 weeks			
	P-value[a]	db/h vs. H/H[b]	db/db vs. H/H[b]	db/db vs. db/h[b]	*P*-value[a]	db/h vs. H/H[b]	db/db vs. H/H[b]	db/db vs. db/h[b]	*P*-value[a]	db/h vs. H/H[b]	db/db vs. H/H[b]	db/db vs. db/h[b]
CL 18:2/18:1/18:2/20:2	0.365	0.1	-0.3	-1.2	0.846	0.0	0.0	0.0	0.509	-0.4	0.0	0.0
CE 16:0	0.730	0.0	0.1	0.1	0.020	0.1	1.7	1.5	0.040	-1.9	0.0	0.7
CE 16:1	0.226	0.1	1.2	2.1	0.001	1.1	4.1	3.7	0.007	0.2	2.2	1.9
CE 17:1	0.226	0.0	1.1	2.4	0.002	0.0	3.3	2.9	0.032	0.1	1.7	1.0
CE 18:0	0.546	0.0	0.1	0.5	0.041	0.0	1.7	0.9	0.004	-2.4	0.0	2.4
CE 18:1	0.459	0.0	0.5	0.5	0.006	0.4	2.4	1.6	0.191	-0.1	0.4	0.8
CE 18:2	0.473	0.7	0.1	0.0	0.013	0.0	1.6	2.2	0.016	-0.1	1.6	1.8
CE 18:3	0.613	0.0	0.3	0.1	0.004	0.0	2.6	2.4	0.002	-0.3	3.0	3.3
CE 20:3	0.279	0.0	0.9	1.3	0.004	0.0	2.0	3.4	0.075	0.0	0.9	1.2
CE 20:4	0.549	0.3	0.3	0.0	0.043	0.1	1.0	1.5	0.003	0.0	2.6	2.8
CE 22:5	0.279	0.1	1.2	1.0	0.001	0.0	3.3	3.7	0.002	0.0	2.9	2.8
COH	0.448	0.2	0.0	-0.9	0.856	0.0	0.0	0.0	0.974	0.0	0.0	0.0
DG 14:0/16:0	0.249	0.4	1.2	1.1	0.004	0.2	2.6	2.4	0.357	0.0	0.6	0.1
DG 14:0/18:1	0.226	0.5	1.2	1.4	0.001	0.1	4.1	3.7	0.061	0.1	1.3	0.7
DG 14:0/18:2	0.459	0.6	0.5	0.0	0.041	0.2	1.3	1.0	0.215	0.0	1.0	0.2
DG 16:0/16:0	0.362	0.7	0.8	0.4	0.009	0.5	2.6	0.9	0.485	0.0	0.4	0.0
DG 16:0/18:0	0.437	0.3	0.9	0.2	0.001	0.2	3.3	3.1	0.061	0.0	1.4	0.8
DG 16:0/18:1	0.448	0.3	0.8	0.1	0.001	0.2	3.5	3.1	0.044	0.1	1.6	0.7
DG 16:0/18:2	0.516	0.3	0.0	-0.4	0.263	0.3	0.7	0.0	0.191	0.0	0.8	0.5
DG 16:0/20:3	0.467	0.3	0.6	0.0	0.057	0.3	1.6	0.3	0.974	0.0	0.0	0.0
DG 16:0/20:4	0.516	0.2	0.0	-0.5	0.371	0.4	0.3	0.0	0.717	0.0	0.1	0.1
DG 16:0/22:5	0.738	0.1	0.1	0.0	0.010	0.1	2.1	1.8	0.002	0.0	2.8	3.0
DG 16:0/22:6	0.699	0.0	0.0	-0.2	0.054	0.3	1.6	0.4	0.018	-0.5	0.9	2.0
DG 16:1/18:0	0.237	0.4	1.2	1.3	0.001	0.1	4.1	3.7	0.004	0.1	2.7	2.1
DG 16:1/18:1	0.226	0.3	1.2	1.7	0.001	0.5	4.1	3.7	0.007	0.2	2.5	1.5
DG 18:0/18:1	0.448	0.1	0.8	0.3	0.002	0.0	3.0	2.6	0.005	0.0	2.5	2.1
DG 18:0/18:2	0.573	0.2	0.0	-0.3	0.302	0.0	0.5	0.3	0.024	0.0	1.4	1.8
DG 18:0/20:4	0.279	1.4	0.0	-0.8	0.740	0.0	0.0	-0.1	0.309	0.4	0.0	-0.4
DG 18:1/18:1	0.398	0.3	0.8	0.4	0.001	0.1	3.5	2.9	0.010	0.0	1.9	2.0
DG 18:1/18:2	0.469	0.3	0.0	-0.5	0.299	0.0	0.5	0.2	0.096	0.0	1.0	0.8
DG 18:1/18:3	0.624	0.3	0.0	-0.1	0.131	0.0	0.8	0.7	0.018	0.0	1.6	1.8
DG 18:1/20:3	0.700	0.2	0.0	0.0	0.402	0.0	0.5	0.1	0.482	0.0	0.3	0.1
DG 18:1/20:4	0.448	0.3	0.0	-0.8	0.470	0.1	0.4	0.0	0.252	0.0	0.4	0.7
DG 18:2/18:2	0.362	0.4	-0.1	-1.1	0.628	0.1	0.0	-0.2	0.551	0.0	0.0	0.3
TG 14:0/16:0/18:1	0.448	0.0	0.5	0.7	0.001	1.2	4.1	3.7	0.003	-0.3	2.2	2.6
TG 14:0/16:0/18:2	0.448	0.1	0.3	0.8	0.001	1.6	4.1	3.7	0.004	0.0	2.4	2.5
TG 14:0/16:1/18:1	0.398	0.0	0.5	0.9	0.001	1.2	4.1	3.7	0.004	0.0	2.6	2.4
TG 14:0/16:1/18:2	0.601	0.1	0.2	0.1	0.001	1.8	4.1	2.9	0.004	0.0	2.5	2.5
TG 14:0/17:0/18:1	0.575	0.0	0.1	0.4	0.001	0.7	4.1	3.7	0.002	-0.1	2.6	3.0
TG 14:1/16:0/18:1	0.533	0.0	0.2	0.4	0.001	1.4	4.1	3.7	0.008	0.0	1.9	2.2
TG 14:1/16:1/18:0	0.288	0.0	0.6	1.4	0.001	1.8	4.1	3.7	0.005	0.0	2.5	2.1
TG 14:1/18:1/18:1	0.448	0.0	0.4	0.7	0.001	1.6	4.1	3.7	0.002	0.0	3.3	3.3
TG 15:0/16:0/18:1	0.467	0.1	0.3	0.4	0.001	0.9	4.1	3.7	0.002	-0.3	2.6	3.1
TG 15:0/18:1/18:1	0.606	0.0	0.1	0.2	0.001	1.2	3.8	2.4	0.003	0.0	2.6	2.6
TG 16:0/16:0/16:0	0.447	0.0	0.5	0.8	0.001	1.6	4.1	3.7	0.010	-0.7	1.0	2.2
TG 16:0/16:0/18:0	0.459	0.0	0.5	0.5	0.001	1.2	4.1	3.7	0.004	-1.0	1.3	2.5
TG 16:0/16:0/18:1	0.549	0.0	0.2	0.4	0.001	1.4	4.1	3.7	0.002	-0.3	2.5	2.9
TG 16:0/16:0/18:2	0.823	0.0	0.0	0.0	0.001	1.4	3.8	2.2	0.002	-0.4	2.4	2.9
TG 16:0/16:1/17:0	0.487	0.0	0.3	0.4	0.001	0.9	4.1	3.7	0.002	-0.1	2.5	3.0
TG 16:0/16:1/18:1	0.448	0.1	0.4	0.8	0.001	1.4	4.1	3.7	0.002	0.0	3.1	2.8
TG 16:0/17:0/18:1	0.609	0.0	0.1	0.3	0.001	0.8	3.8	3.4	0.002	-0.4	3.1	3.3
TG 16:0/17:0/18:2	0.516	0.1	0.3	0.3	0.001	1.1	4.1	3.4	0.003	0.0	2.7	2.8
TG 16:0/18:0/18:1	0.601	0.0	0.1	0.3	0.001	0.8	4.1	3.4	0.002	-0.7	2.3	2.8
TG 16:0/18:1/18:1	0.549	0.0	0.1	0.4	0.001	1.2	3.8	3.1	0.002	-0.1	2.7	2.8

Lipid species	6 weeks				10 weeks				16 weeks			
	P-value[a]	db/h vs. H/H[b]	db/db vs. H/H[b]	db/db vs. db/h[b]	*P*-value[a]	db/h vs. H/H[b]	db/db vs. H/H[b]	db/db vs. db/h[b]	*P*-value[a]	db/h vs. H/H[b]	db/db vs. H/H[b]	db/db vs. db/h[b]
TG 16:0/18:1/18:2	0.794	0.1	0.1	0.0	0.001	1.4	3.5	1.9	0.004	-0.1	2.1	2.5
TG 16:0/18:2/18:2	0.808	0.1	0.0	0.0	0.006	1.6	2.8	0.4	0.010	-0.2	1.6	2.1
TG 16:1/16:1/16:1	0.288	0.0	0.6	1.4	0.001	1.4	4.1	3.7	0.003	0.1	2.8	2.5
TG 16:1/16:1/18:1	0.448	0.1	0.3	0.8	0.001	1.6	4.1	3.4	0.002	0.0	3.3	3.0
TG 16:1/17:0/18:1	0.514	0.0	0.3	0.4	0.001	1.1	3.8	3.1	0.002	0.0	2.9	2.9
TG 16:1/18:1/18:1	0.449	0.0	0.3	0.8	0.001	1.6	4.1	3.1	0.002	0.1	3.6	3.3
TG 16:1/18:1/18:2	0.699	0.1	0.1	0.1	0.001	1.6	3.8	2.2	0.002	0.0	3.3	3.1
TG 17:0/18:1/18:1	0.579	0.0	0.1	0.3	0.001	1.1	3.8	3.1	0.002	-0.1	3.1	3.0
TG 18:0/18:0/18:1	0.514	0.2	0.3	0.3	0.001	0.7	3.5	2.2	0.055	0.0	1.2	1.2
TG 18:0/18:1/18:1	0.648	0.0	0.1	0.2	0.001	0.8	3.8	2.9	0.002	-0.8	3.1	3.1
TG 18:0/18:2/18:2	0.875	0.0	0.0	0.0	0.010	1.1	2.4	0.6	0.005	-0.1	2.0	2.4
TG 18:1/18:1/18:1	0.533	0.0	0.3	0.4	0.001	1.1	3.8	2.6	0.002	0.0	3.6	3.3
TG 18:1/18:1/18:2	0.823	0.1	0.0	0.0	0.003	1.4	2.8	1.6	0.002	0.0	3.0	3.0
TG 18:1/18:1/20:4	0.660	0.0	0.0	-0.4	0.021	1.8	1.8	0.0	0.003	-0.2	2.4	2.6
TG 18:1/18:1/22:6	0.730	0.0	0.0	-0.2	0.028	1.2	2.0	0.0	0.013	-0.1	1.6	2.0
TG 18:1/18:2/18:2	0.865	0.0	0.0	0.0	0.006	1.4	2.8	0.6	0.002	-0.1	2.6	2.9
TG 18:2/18:2/18:2	0.573	0.0	0.0	-0.4	0.032	1.2	1.7	0.0	0.005	-0.2	2.0	2.5

[a] *P*-value for the comparison of levels of each lipid species between genotypes at each age using the Kruskal Wallis test with Benjamini-Hochberg correction for multiple comparisons. $P < 0.05$ was considered significant (highlighted in pink).

[b] Post-hoc analysis was performed using the Mann Whitney *U* test with Dunn-Sidak correction for multiple group comparisons. Values were derived from the formula: sign(difference in median levels)*-log10(post-hoc *P*-value). Colour-coded values 1.3 to 2.0 (light red, $P = 0.05$-0.01) and > 2.0 (dark red, $P < 0.01$) indicate a significant increase relative to the reference group. Colour-coded values -1.3 to -2.0 (light green, $P = 0.05$-0.01) and < -2.0 (dark green, $P < 0.01$) indicate a significant decrease relative to the reference group.

Table S4.2 Relationship between genotype and skeletal muscle lipid species in male mice.

Lipid species	6 weeks of age				10 weeks				16 weeks			
	P-value[a]	db/h vs. H/H[b]	db/db vs. H/H[b]	db/db vs. db/h[b]	*P*-value[a]	db/h vs. H/H[b]	db/db vs. H/H[b]	db/db vs. db/h	*P*-value[a]	db/h vs. H/H[b]	db/db vs. H/H[b]	db/db vs. db/h[b]
Cer 16:0	0.382	-0.3	-0.3	0.0	0.296	0.0	0.5	0.2	0.025	-1.0	0.6	1.6
Cer 18:0	0.288	-0.6	-0.6	0.0	0.038	-0.6	-2.1	-0.3	0.038	-1.2	-1.3	0.0
Cer 22:0	0.241	-1.3	0.0	1.8	0.251	-0.3	0.1	0.6	0.013	-0.8	0.8	2.4
Cer 24:0	0.255	-0.3	0.0	2.0	0.135	-0.2	0.2	1.1	0.027	-1.2	0.1	1.8
Cer 24:1	0.269	-0.8	-0.1	0.4	0.846	0.0	0.0	0.0	0.161	-0.8	0.0	0.6
MHC 18:0	0.354	-0.4	0.0	0.2	0.285	-0.2	0.0	0.7	0.549	0.0	0.2	0.1
MHC 20:0	0.434	-0.3	0.0	0.1	0.244	-0.4	-0.1	0.5	0.860	0.0	0.0	0.0
MHC 22:0	0.426	-0.2	0.0	0.2	0.316	-0.3	-0.1	0.4	0.882	0.0	0.0	0.0
MHC 24:0	0.354	-0.3	0.0	0.3	0.361	-0.1	0.0	0.5	0.789	0.0	0.0	0.0
MHC 24:1	0.330	-0.3	0.0	0.4	0.344	-0.2	0.0	0.5	0.661	0.0	-0.1	0.1
GM3 18:0	0.293	-0.7	-0.3	0.0	0.033	-0.8	-1.8	-0.5	0.081	-1.1	-0.8	0.0
SM 32:1	0.354	-0.2	0.0	0.5	0.029	0.0	1.4	1.6	0.084	-0.3	0.7	1.0
SM 33:1	0.485	0.0	-0.2	-0.1	0.325	0.0	-0.6	-0.1	0.856	0.0	0.0	0.1
SM 34:1	0.371	0.0	0.0	0.7	0.183	0.0	0.5	0.7	0.012	-0.1	2.1	1.6
SM 34:2	0.391	-0.2	0.0	0.4	0.025	-0.2	2.1	1.3	0.008	-0.4	1.9	2.4
SM 35:1	0.444	-0.4	-0.1	0.0	0.074	-0.5	-1.3	-0.3	0.332	-0.5	-0.2	0.0
SM 36:1	0.327	-0.5	-0.1	0.1	0.176	-0.7	-0.8	0.0	0.019	-1.8	-1.1	0.3
SM 36:2	0.311	-0.1	0.0	0.8	0.074	-0.8	0.0	1.4	0.021	-1.1	0.8	1.6
SM 38:1	0.288	-0.5	0.0	0.5	0.080	-1.0	-0.1	1.0	0.022	-1.6	0.0	1.8
SM 38:2	0.180	-0.8	0.3	2.7	0.010	-0.3	2.1	2.7	0.021	-0.4	1.3	1.6
SM 39:1	0.335	-0.6	-0.1	0.0	0.136	-0.9	-0.5	0.2	0.224	-0.7	0.0	0.4
SM 41:1	0.452	-0.1	0.0	0.4	0.284	0.0	0.5	0.4	0.008	0.0	2.7	1.9
SM 41:2	0.567	-0.1	0.0	0.1	0.636	-0.1	0.0	0.1	0.106	-0.4	0.4	1.0
SM 42:1	0.340	-0.3	0.0	0.4	0.398	-0.1	0.0	0.4	0.335	0.0	0.4	0.3
PC 24:0	0.788	0.0	0.0	0.0	0.176	0.0	0.1	1.2	0.090	-0.6	0.0	1.4
PC 28:0	0.255	-0.6	0.1	2.0	0.038	-0.1	0.4	2.3	0.277	0.0	-0.5	-0.4
PC 29:0	0.241	-1.8	-0.7	0.7	0.382	-0.4	-0.1	0.0	0.285	0.0	-0.4	-0.5
PC 30:0	0.269	-0.6	0.0	0.8	0.351	-0.1	0.0	0.6	0.128	0.0	-1.0	-0.6
PC 31:0	0.269	-1.0	-0.6	0.0	0.024	-1.2	-2.3	-0.2	0.010	-0.3	-2.3	-1.4
PC 31:1	0.255	-1.3	-0.7	0.1	0.202	-0.7	-0.5	0.0	0.292	0.0	-0.6	-0.2
PC 32:0	0.293	-0.6	-0.4	0.0	0.192	0.0	-0.8	-0.3	0.083	-0.1	-1.2	-0.6
PC 32:1	0.255	-0.7	0.3	1.8	0.015	0.0	2.0	2.1	0.530	0.0	0.3	0.1
PC 32:2	0.180	-1.0	0.6	2.0	0.010	-0.1	2.8	2.6	0.404	0.0	0.4	0.2
PC 32:3	0.180	-1.4	0.4	2.4	0.039	0.0	2.1	0.9	0.798	0.0	-0.1	0.0
PC 33:0	0.255	-1.3	-0.8	0.0	0.056	-1.3	-1.3	0.0	0.135	-0.3	-0.9	-0.2
PC 33:1	0.279	-0.7	-0.4	0.1	0.102	-0.5	-1.2	-0.1	0.098	0.0	-1.0	-0.9
PC 33:2	0.371	-0.4	-0.2	0.0	0.051	-1.5	-0.3	0.9	0.303	-0.5	0.0	0.3
PC 34:0	0.293	-0.6	-0.1	0.2	0.641	-0.1	0.0	0.1	0.325	-0.7	-0.1	0.0
PC 34:1	0.255	-1.3	-0.1	0.7	0.062	-0.5	0.0	1.7	0.111	-0.7	0.1	0.9
PC 34:2	0.269	-0.6	0.0	0.7	0.082	-1.0	-0.1	1.0	0.021	-1.5	0.0	2.0
PC 34:3	0.180	-1.6	0.3	2.4	0.010	-0.1	2.1	2.7	0.031	-0.2	1.3	1.4
PC 34:4	0.255	-1.1	0.0	1.8	0.799	0.0	0.0	0.0	0.022	-1.1	-1.8	-0.2
PC 35:0	0.284	-0.7	-0.6	0.0	0.364	0.0	-0.4	0.2	0.292	0.0	-0.5	-0.3
PC 35:1	0.255	-1.6	-0.7	0.2	0.160	-0.9	-0.7	0.0	0.730	-0.1	-0.1	0.0
PC 35:2	0.257	-1.1	-0.2	0.4	0.183	-0.7	-0.4	0.2	0.147	-0.9	0.0	0.6
PC 35:3	0.255	-1.6	-0.3	0.1	0.115	-0.9	-1.0	0.0	0.647	-0.1	0.0	0.1
PC 35:4	0.255	-1.0	-1.0	0.0	0.051	-0.2	-1.7	-0.7	0.026	-0.7	-1.9	-0.2
PC 36:1	0.312	-0.2	0.0	0.6	0.082	-0.3	0.1	1.5	0.022	-0.6	0.7	2.0
PC 36:2	0.255	-0.3	0.0	1.8	0.053	-0.1	0.6	1.6	0.011	-0.8	1.2	2.2
PC 36:3	0.257	-1.1	0.0	0.6	0.507	-0.1	0.0	0.2	0.030	-1.9	0.0	1.1
PC 36:4a	0.255	-0.1	0.3	1.8	0.051	-0.6	-0.1	1.7	0.058	-0.4	0.5	1.4
PC 36:4b	0.311	-0.5	-0.3	0.0	0.026	-0.2	-2.0	-1.2	0.007	-1.6	-2.6	-0.3

Lipid species	6 weeks of age				10 weeks				16 weeks			
	P-value[a]	db/h vs. H/H[b]	db/db vs. H/H[b]	db/db vs. db/h[b]	*P*-value[a]	db/h vs. H/H[b]	db/db vs. H/H[b]	db/db vs. db/h	*P*-value[a]	db/h vs. H/H[b]	db/db vs. H/H[b]	db/db vs. db/h[b]
PC 36:5	0.180	-1.1	0.2	2.2	0.023	0.0	0.8	2.5	0.158	-0.6	0.1	0.7
PC 36:6	0.180	-1.8	-0.1	1.6	0.317	-0.4	-0.4	0.0	0.160	-0.1	-0.9	-0.3
PC 37:4	0.257	-1.1	-0.7	-0.1	0.038	-0.2	-2.0	-0.7	0.010	-0.9	-2.4	-0.5
PC 37:5	0.269	-1.0	-0.6	0.0	0.024	-0.4	-2.4	-0.7	0.036	-0.1	-1.9	-0.5
PC 37:6	0.269	-0.8	-0.7	0.0	0.023	-0.4	-2.4	-0.7	0.227	0.0	-0.6	-0.5
PC 38:2	0.279	-0.6	0.0	0.6	0.551	-0.1	-0.1	0.0	0.259	-0.1	0.4	0.4
PC 38:3	0.255	-0.4	0.0	1.8	0.051	-0.6	0.0	1.8	0.007	-2.1	0.1	2.9
PC 38:4	0.275	-1.0	-0.3	0.0	0.507	-0.2	0.0	0.2	0.014	-2.2	-0.8	0.5
PC 38:5	0.255	-0.8	-0.2	0.9	0.361	-0.4	-0.1	-0.1	0.304	-0.4	0.0	0.5
PC 38:6a	0.180	-2.3	-0.1	1.6	0.181	0.0	0.1	1.2	0.063	-0.6	0.3	1.4
PC 38:6b	0.312	-0.5	-0.3	0.0	0.022	-0.6	-2.4	-0.7	0.413	-0.2	-0.4	0.0
PC 38:7	0.180	-1.6	-0.1	2.7	0.200	-0.1	0.1	0.9	0.418	0.0	0.3	0.2
PC 39:6	0.269	-0.4	-1.0	-0.2	0.015	-1.2	-2.8	-0.5	0.317	0.0	-0.5	-0.2
PC 39:7	0.255	-0.5	-1.2	-0.4	0.016	-0.4	-2.4	-1.4	0.057	0.0	-1.4	-0.9
PC 40:5	0.269	-1.0	-0.2	0.2	0.119	-0.9	0.0	0.9	0.123	-0.4	0.2	1.0
PC 40:6	0.302	-0.5	-0.4	0.0	0.192	-0.7	-0.5	0.1	0.123	-0.3	0.1	1.3
PC 40:7	0.284	-0.7	-0.6	0.0	0.288	-0.5	-0.4	0.0	0.325	0.0	0.1	0.6
PC(O-32:0)	0.298	0.0	-0.3	-0.6	0.202	0.0	-0.9	-0.2	0.205	-0.1	-0.9	-0.1
PC(O-32:1)	0.542	0.0	0.1	0.1	0.416	0.0	0.2	0.3	0.647	0.0	0.1	0.1
PC(O-34:1)	0.567	-0.2	0.0	0.0	0.552	-0.2	-0.1	0.0	0.545	-0.3	0.0	0.0
PC(O-34:2)	0.800	0.0	0.0	0.0	0.206	-0.5	-0.7	0.0	0.772	-0.1	0.0	0.0
PC(O-36:2)	0.538	-0.3	0.0	0.0	0.426	-0.3	-0.2	0.0	0.418	-0.5	0.0	0.0
PC(O-36:4)	0.269	-0.2	-0.8	-0.5	0.176	-0.2	-1.0	0.1	0.168	-0.5	-0.8	0.0
PC(O-38:4)	0.407	-0.1	-0.3	-0.1	0.043	-0.1	-2.1	-0.7	0.089	-1.1	-0.7	0.0
PC(O-38:5)	0.284	-0.4	-0.6	-0.2	0.498	-0.2	-0.2	0.0	0.184	-0.3	0.1	0.9
PC(O-40:6)	0.444	-0.3	-0.2	0.0	0.520	-0.2	-0.1	0.0	0.992	0.0	0.0	0.0
PC(O-40:7)	0.255	-1.0	-1.2	0.0	0.176	-0.2	-0.8	-0.3	0.305	-0.1	0.1	0.6
PC(P-32:0)	0.311	-0.3	-0.7	0.0	0.071	0.0	-1.0	-1.1	0.074	-0.5	-1.2	-0.2
PC(P-32:1)	0.542	0.0	0.0	-0.2	0.422	0.0	0.3	0.2	0.798	0.0	0.0	0.0
PC(P-34:1)	0.754	0.0	0.0	0.0	0.071	-0.4	-0.8	-1.0	0.527	0.1	0.0	-0.2
PC(P-34:2)	0.269	-1.1	-0.6	0.0	0.116	-0.9	-0.8	-0.1	0.404	-0.6	0.0	0.0
PC(P-36:4)	0.255	-0.8	-1.0	-0.2	0.050	-0.3	-1.3	-1.0	0.123	-0.7	-0.8	0.0
PC(P-38:5)	0.298	-0.8	-0.2	0.0	0.176	-0.7	-0.8	0.0	0.634	-0.2	0.0	0.0
PC(P-38:6)	0.284	-0.3	-0.8	0.0	0.024	-0.4	-1.8	-1.3	0.052	-0.4	-1.4	-0.4
PC(P-40:5)	0.255	-0.8	-1.2	0.0	0.082	-1.2	-1.0	0.0	0.433	-0.1	-0.4	0.0
PC(P-40:6)	0.355	-0.4	-0.3	0.0	0.015	-1.1	-2.4	-0.9	0.259	-0.2	-0.7	0.0
LPC 14:0	0.396	0.0	0.0	0.5	0.442	-0.2	0.0	0.2	0.439	0.4	0.0	0.0
LPC 16:0	0.917	0.0	0.0	0.0	0.817	0.0	0.0	0.0	0.317	0.2	0.4	0.0
LPC 16:1	0.264	0.0	0.8	0.9	0.014	0.1	2.8	1.6	0.012	0.6	2.3	0.7
LPC 18:0	0.590	0.0	0.1	0.1	0.093	-0.1	0.6	1.1	0.006	0.0	2.8	2.2
LPC 18:1	0.981	0.0	0.0	0.0	0.202	0.0	0.9	0.3	0.022	1.1	1.8	0.1
LPC 18:2	0.284	0.0	0.3	0.9	0.133	-0.4	0.1	1.0	0.006	-0.5	1.9	2.9
LPC 20:4	0.354	-0.6	0.0	0.0	0.551	-0.1	0.0	0.2	0.043	-1.5	0.0	1.2
LPC 22:6	0.366	-0.4	0.0	0.1	0.220	-0.7	-0.3	0.1	0.204	-0.4	0.2	0.6
PE 32:0	0.311	-0.5	-0.3	0.0	0.920	0.0	0.0	0.0	0.302	-0.5	-0.3	0.0
PE 32:1	0.255	0.0	0.7	1.5	0.013	-0.3	1.7	2.4	0.621	0.0	0.0	0.2
PE 34:1	0.300	-0.2	0.1	0.5	0.031	-0.4	0.2	2.3	0.192	0.1	0.5	0.6
PE 34:2	0.307	-0.1	0.0	0.7	0.176	-0.4	0.0	0.9	0.026	-1.1	0.3	1.8
PE 34:3	0.298	0.0	0.4	0.5	0.036	0.0	2.0	1.0	0.160	-0.1	0.5	0.7
PE 35:2	0.311	-0.1	0.3	0.4	0.723	0.0	0.0	0.1	0.383	-0.2	0.0	0.3
PE 36:1	0.311	-0.3	0.0	0.5	0.190	-0.7	0.0	0.6	0.227	-0.1	0.2	0.7
PE 36:2	0.255	-0.1	0.2	1.6	0.019	-0.7	0.4	2.5	0.007	-1.7	0.8	2.7
PE 36:3	0.261	0.0	0.3	1.3	0.116	0.0	0.5	1.1	0.010	-0.9	1.2	2.2
PE 36:4	0.325	-0.4	0.0	0.3	0.419	-0.3	-0.3	0.0	0.036	-1.7	-0.6	0.2

Lipid species	6 weeks of age				10 weeks				16 weeks			
	P-value[a]	db/h vs. H/H[b]	db/db vs. H/H[b]	db/db vs. db/h[b]	*P*-value[a]	db/h vs. H/H[b]	db/db vs. H/H[b]	db/db vs. db/h	*P*-value[a]	db/h vs. H/H[b]	db/db vs. H/H[b]	db/db vs. db/h[b]
PE 36:5	0.255	0.0	1.0	1.6	0.010	-0.3	2.0	3.0	0.169	-0.6	0.0	0.7
PE 38:3	0.269	0.0	0.4	0.9	0.387	-0.2	0.0	0.3	0.037	-1.4	0.0	1.4
PE 38:4	0.269	-0.5	0.0	0.9	0.553	-0.2	0.0	0.1	0.014	-2.2	-0.2	1.1
PE 38:5	0.255	-0.3	0.0	1.8	0.202	-0.3	0.0	0.9	0.027	-2.0	-0.1	0.8
PE 38:6	0.472	-0.2	-0.3	0.0	0.056	-1.1	-1.6	0.0	0.007	-2.8	-1.6	0.1
PE 40:5	0.636	-0.1	0.0	0.0	0.200	-0.2	-0.9	-0.1	0.008	-1.8	-2.0	-0.3
PE 40:6	0.548	-0.2	0.0	0.0	0.061	-1.5	-0.8	0.2	0.030	-2.0	-0.1	0.7
PE 40:7	0.312	-0.3	0.0	0.5	0.361	-0.3	0.0	0.4	0.022	-1.7	0.1	1.5
PE(O-34:1)	0.270	-0.1	0.2	1.0	0.533	-0.2	-0.1	-0.1	0.473	-0.3	-0.1	0.0
PE(O-36:2)	0.393	0.0	0.1	0.4	0.220	-0.5	0.0	0.5	0.778	0.0	0.0	0.1
PE(O-38:5)	0.255	-1.0	0.0	1.6	0.183	-0.4	0.1	0.8	0.147	-0.8	0.1	0.6
PE(O-40:5)	0.390	-0.1	0.0	0.4	0.344	-0.3	0.0	0.4	0.314	0.0	0.2	0.6
PE(O-40:6)	0.662	-0.1	0.0	0.0	0.116	-1.2	-0.7	0.0	0.464	-0.3	0.0	0.1
PE(O-40:7)	0.288	-0.5	0.0	0.5	0.322	-0.6	0.0	0.2	0.452	0.0	-0.1	0.3
PE(O-42:7)	0.464	0.0	0.3	0.1	0.877	0.0	0.0	0.0	0.549	0.0	0.2	0.1
PE(P-34:1)	0.291	0.0	0.1	0.8	0.135	-0.6	0.0	1.0	0.413	-0.1	-0.1	0.3
PE(P-36:1)	0.391	0.0	0.3	0.3	0.426	-0.3	0.0	0.1	0.684	0.0	0.1	0.1
PE(P-36:2)	0.320	-0.3	0.0	0.4	0.251	-0.4	0.0	0.5	0.600	0.0	0.1	0.2
PE(P-36:4)	0.382	-0.3	0.0	0.2	0.943	0.0	0.0	0.0	0.021	-1.8	0.0	1.6
PE(P-38:4)	0.644	0.0	0.0	0.2	0.233	0.0	-0.4	-0.6	0.488	-0.3	-0.1	0.0
PE(P-38:5)	0.269	-0.7	0.0	0.8	0.183	-1.0	0.0	0.4	0.111	-1.2	-0.2	0.2
PE(P-38:6)	0.307	-0.3	-0.4	-0.1	0.176	-0.4	-0.8	-0.2	0.065	-1.3	-0.8	0.0
PE(P-40:5)	0.269	-1.0	0.0	0.4	0.055	-1.3	-0.4	0.8	0.023	-2.3	-0.4	0.3
PE(P-40:6)	0.288	-0.7	-0.3	0.1	0.033	-1.5	-1.8	0.0	0.022	-1.7	-1.2	0.1
LPE 16:0	0.865	0.0	0.0	0.0	0.741	0.0	-0.1	0.0	0.424	0.3	0.1	0.0
LPE 18:0	0.973	0.0	0.0	0.0	0.281	-0.2	0.1	0.5	0.022	0.1	1.6	1.5
LPE 18:1	0.527	-0.1	0.0	0.2	0.225	-0.1	0.3	0.6	0.227	0.0	0.7	0.3
LPE 22:6	0.464	-0.1	-0.3	0.0	0.213	-0.9	-0.4	0.0	0.142	-0.9	-0.5	0.0
PI 32:0	0.888	0.0	0.0	0.0	0.416	-0.4	0.0	0.1	0.224	-0.3	-0.6	-0.1
PI 34:0	0.255	0.3	1.4	0.4	0.690	0.0	0.0	0.1	0.182	-0.8	-0.4	0.0
PI 34:1	0.371	0.0	0.3	0.4	0.570	0.0	0.1	0.1	0.580	-0.1	-0.1	0.0
PI 36:1	0.354	-0.3	0.0	0.3	0.176	-0.4	0.0	0.9	0.109	-0.6	0.1	1.0
PI 36:2	0.255	-0.3	0.0	1.6	0.063	-1.1	0.0	1.3	0.036	-1.2	0.1	1.5
PI 36:4	0.799	0.0	0.0	0.0	0.335	-0.1	-0.5	-0.1	0.035	-1.5	-1.1	0.0
PI 38:2	0.287	-0.3	0.1	0.7	0.273	-0.3	0.0	0.6	0.052	0.0	1.2	1.3
PI 38:3	0.907	0.0	0.0	0.0	0.329	-0.4	-0.1	0.2	0.128	-0.1	0.5	0.9
PI 38:4	0.284	-0.7	-0.3	0.1	0.277	-0.7	-0.3	0.0	0.027	-2.0	-0.7	0.1
PI 38:5	0.288	-0.4	0.0	0.6	0.476	-0.2	0.0	0.2	0.040	-1.6	0.0	1.1
PI 38:6	0.255	-0.4	-0.8	-0.8	0.044	-0.5	-1.4	-0.8	0.208	-0.5	-0.5	0.0
PI 40:4	0.447	-0.2	-0.3	0.0	0.296	-0.3	-0.5	0.0	0.008	-1.7	-2.3	0.0
PI 40:5	0.261	-0.7	0.0	0.9	0.102	-1.2	-0.1	0.6	0.025	-1.5	0.1	1.6
PI 40:6	0.284	-0.3	-0.6	-0.2	0.017	-1.0	-2.6	-0.7	0.036	-1.7	-0.8	0.0
PS 36:1	0.312	-0.4	0.0	0.4	0.251	-0.3	0.0	0.7	0.715	0.0	0.0	0.1
PS 36:2	0.288	-0.7	0.0	0.4	0.325	-0.3	0.0	0.5	0.136	-0.2	0.4	0.9
PS 38:3	0.820	0.0	0.0	0.1	0.202	0.0	0.7	0.5	0.108	-0.6	0.0	1.2
PS 38:4	0.302	-0.3	-0.1	0.4	0.516	0.0	0.1	0.2	0.056	-0.3	0.8	1.3
PS 38:5	0.257	-0.3	0.0	1.6	0.183	-0.7	0.0	0.7	0.730	-0.1	0.0	0.0
PS 40:5	0.255	-0.7	0.0	1.2	0.056	-0.4	0.1	1.7	0.019	-2.1	0.0	1.4
PS 40:6	0.255	-1.3	-1.4	0.0	0.117	-1.1	-0.8	0.0	0.013	-2.5	-0.8	0.2
PG 32:0	0.293	-0.6	-0.2	0.1	0.173	-0.6	-0.8	0.0	0.008	-0.4	-2.6	-1.1
PG 34:1	0.269	-0.3	0.0	1.2	0.066	-0.3	0.0	1.8	0.088	-1.3	-0.1	0.5
PG 34:2	0.288	-0.1	0.1	0.8	0.056	-0.9	0.0	1.5	0.285	-0.6	0.0	0.3
PG 36:1	0.302	-0.4	0.0	0.4	0.208	-0.4	0.0	0.7	0.602	0.0	0.1	0.1
PG 36:2	0.381	-0.2	-0.4	0.0	0.084	-0.4	0.0	1.5	0.141	-1.0	-0.1	0.3

Lipid species	6 weeks of age				10 weeks				16 weeks			
	P-value[a]	db/h vs. H/H[b]	db/db vs. H/H[b]	db/db vs. db/h[b]	*P*-value[a]	db/h vs. H/H[b]	db/db vs. H/H[b]	db/db vs. db/h	*P*-value[a]	db/h vs. H/H[b]	db/db vs. H/H[b]	db/db vs. db/h[b]
CL 18:2/18:2/18:2/16:1	0.255	-0.2	0.3	2.0	0.010	0.0	3.8	2.8	0.004	-0.9	2.2	3.3
CL 18:2/18:1/18:2/16:1	0.269	-0.2	0.3	0.9	0.073	0.0	0.9	1.2	0.206	-0.1	0.5	0.5
CL 18:2/18:1/18:1/16:1	0.714	0.0	0.1	0.0	0.136	0.0	0.8	0.7	0.782	-0.1	0.0	0.0
CL 18:2/18:2/18:2/18:2	0.255	-0.8	0.0	1.3	0.029	-0.8	0.1	2.1	0.005	-2.3	0.2	3.9
CL 18:2/18:2/18:2/18:1	0.374	-0.2	0.0	0.4	0.150	-1.0	-0.2	0.4	0.010	-2.2	0.0	2.0
CL 18:2/18:1/18:2/18:1	0.590	-0.2	0.0	0.0	0.514	-0.1	-0.2	0.0	0.058	-1.8	-0.2	0.2
CL 18:1/18:1/18:1/18:2	0.403	-0.2	-0.3	0.0	0.192	-0.8	-0.5	0.0	0.644	0.0	0.1	0.1
CL 18:2/18:2/18:2/20:3	0.284	-0.3	0.0	0.8	0.176	-0.3	0.0	0.9	0.008	-1.7	0.2	2.7
CL 18:2/18:1/18:2/20:3	0.288	-0.5	0.0	0.4	0.183	-0.4	-0.8	-0.1	0.025	-1.5	-1.4	0.0
CL 18:2/18:1/18:2/20:2	0.260	-0.7	-1.0	-0.1	0.022	-0.4	-2.1	-1.1	0.004	-1.8	-3.0	-0.6
CL 18:2/18:2/18:2/20:4	0.551	0.0	0.0	0.3	0.033	-2.3	-0.6	0.4	0.160	-1.1	0.0	0.4
CL 18:2/18:2/18:2/22:6	0.291	-0.4	-0.6	0.0	0.027	-2.1	-1.6	0.0	0.051	-1.3	0.0	1.2
CL 18:2/18:1/18:2/22:6	0.335	-0.5	-0.1	0.0	0.037	-1.2	-1.7	-0.2	0.267	-0.6	-0.3	0.0
CE 18:0	0.288	0.3	0.0	-0.7	0.982	0.0	0.0	0.0	0.632	-0.1	0.0	0.1
CE 18:1	0.288	0.0	-0.6	-0.6	0.192	0.0	-1.3	0.0	0.299	-0.5	0.1	0.3
CE 18:2	0.626	0.2	0.0	0.0	0.854	0.0	0.0	0.0	0.066	-0.3	0.7	1.2
CE 20:4	0.447	0.1	0.0	-0.3	0.622	0.0	0.1	0.0	0.035	-0.1	1.5	1.2
CE 22:6	0.527	0.0	0.0	-0.2	0.240	0.0	0.8	0.2	0.044	-0.1	1.3	1.1
COH	0.320	-0.5	0.0	0.2	0.350	-0.4	-0.1	0.1	0.182	-0.1	0.3	0.8
DG 14:0/16:0	0.418	0.0	0.2	0.3	0.248	0.0	0.7	0.3	0.141	-0.4	0.2	0.8
DG 14:0/18:1	0.260	0.2	0.8	0.7	0.021	-0.1	4.1	0.5	0.011	0.0	2.3	1.5
DG 16:0/16:0	0.291	-0.7	0.0	0.2	0.744	-0.1	0.0	0.0	0.206	-0.2	0.2	0.7
DG 16:0/18:1	0.275	0.1	0.7	0.5	0.024	0.1	3.5	0.5	0.009	0.0	2.6	1.6
DG 16:0/18:2	0.269	0.6	0.8	0.1	0.029	0.2	3.0	0.4	0.013	0.0	2.1	1.6
DG 16:0/20:4	0.447	-0.3	0.0	0.1	0.523	0.0	0.2	0.1	0.427	-0.3	0.1	0.2
DG 16:0/22:5	0.255	-0.3	0.0	1.6	0.051	-0.1	0.9	1.4	0.005	-0.1	2.8	3.1
DG 16:0/22:6	0.295	-0.2	0.0	0.8	0.053	-0.4	0.6	1.4	0.102	-0.7	0.1	1.0
DG 16:1/18:1	0.255	0.4	0.7	1.0	0.010	1.6	4.1	0.5	0.004	0.9	3.1	1.6
DG 18:0/18:1	0.327	0.0	0.6	0.2	0.037	0.0	3.0	0.5	0.008	0.0	2.6	1.9
DG 18:0/18:2	0.374	0.0	0.6	0.1	0.059	0.0	2.3	0.4	0.011	0.0	2.2	1.8
DG 18:0/20:4	0.626	-0.1	0.0	-0.1	0.489	-0.1	0.0	0.2	0.864	0.0	0.0	0.0
DG 18:1/18:1	0.284	0.2	0.7	0.3	0.023	0.2	3.5	0.5	0.005	0.4	3.1	1.6
DG 18:1/18:2	0.269	0.8	0.7	0.1	0.052	0.2	2.3	0.3	0.008	0.5	2.3	1.5
DG 18:1/18:3	0.255	0.5	1.0	0.6	0.015	0.3	4.1	0.5	0.007	0.5	2.5	1.6
DG 18:1/20:4	0.320	0.0	0.1	0.6	0.041	0.0	2.4	0.7	0.016	0.0	2.3	1.2
DG 18:2/18:2	0.255	0.8	1.0	0.1	0.111	0.3	1.6	0.1	0.011	0.5	2.3	0.9
TG 14:0/16:0/18:1	0.270	0.3	0.4	0.6	0.010	0.6	4.1	1.0	0.009	0.0	2.3	2.0
TG 14:0/16:0/18:2	0.261	0.3	0.6	0.9	0.010	1.2	4.1	1.4	0.005	0.4	2.9	1.8
TG 14:0/16:1/18:1	0.269	0.5	0.4	0.8	0.010	1.3	4.1	0.8	0.004	0.7	3.6	2.4
TG 14:0/16:1/18:2	0.269	0.5	0.6	0.5	0.010	1.2	4.1	0.6	0.005	0.7	3.2	1.4
TG 14:0/17:0/18:1	0.288	0.5	0.4	0.1	0.021	0.2	3.5	0.5	0.009	0.1	2.4	1.6
TG 14:0/18:0/18:1	0.390	0.1	0.3	0.2	0.020	0.0	3.0	1.0	0.009	-0.1	2.0	2.2
TG 14:0/18:2/18:2	0.284	0.5	0.4	0.2	0.013	0.7	4.1	0.6	0.008	0.2	2.6	1.4
TG 14:1/16:0/18:1	0.269	0.3	0.4	0.9	0.010	1.0	4.1	1.2	0.004	0.5	3.2	1.9
TG 14:1/16:1/18:0	0.260	0.3	0.4	1.2	0.007	2.3	4.1	2.5	0.004	0.9	3.5	1.6
TG 14:1/18:0/18:2	0.255	0.7	0.7	0.8	0.010	0.8	4.1	0.8	0.004	0.7	3.3	1.8
TG 14:1/18:1/18:1	0.261	0.5	0.6	0.7	0.010	1.3	4.1	1.0	0.004	0.7	3.6	1.8
TG 15:0/16:0/18:1	0.298	0.4	0.4	0.1	0.023	0.3	3.3	0.5	0.008	0.0	2.5	1.9
TG 15:0/18:1/18:1	0.291	0.6	0.4	0.0	0.024	0.5	2.8	0.4	0.008	0.2	2.6	1.6
TG 16:0/16:0/16:0	0.279	0.3	0.6	0.4	0.010	0.4	4.1	1.2	0.009	-0.2	2.0	2.2
TG 16:0/16:0/18:0	0.327	0.0	0.6	0.2	0.023	0.0	2.6	1.2	0.007	-0.4	2.0	2.5
TG 16:0/16:0/18:1	0.279	0.4	0.4	0.4	0.010	0.5	4.1	1.0	0.005	0.0	2.9	2.5
TG 16:0/16:0/18:2	0.288	0.5	0.4	0.1	0.015	0.4	3.5	0.7	0.007	0.0	2.6	2.4
TG 16:0/16:1/17:0	0.269	0.6	0.6	0.2	0.014	0.3	4.1	0.8	0.008	0.0	2.5	1.8

Lipid species	6 weeks of age				10 weeks				16 weeks			
	P-value[a]	db/h vs. H/H[b]	db/db vs. H/H[b]	db/db vs. db/h[b]	*P*-value[a]	db/h vs. H/H[b]	db/db vs. H/H[b]	db/db vs. db/h	*P*-value[a]	db/h vs. H/H[b]	db/db vs. H/H[b]	db/db vs. db/h[b]
TG 16:0/16:1/18:1	0.269	0.3	0.4	0.7	0.010	1.1	4.1	1.1	0.004	0.7	3.6	2.5
TG 16:0/17:0/18:0	0.298	0.3	0.6	0.0	0.029	0.1	3.0	0.5	0.009	0.0	2.5	1.8
TG 16:0/17:0/18:1	0.302	0.3	0.6	0.1	0.022	0.1	3.5	0.7	0.008	0.0	2.6	2.0
TG 16:0/17:0/18:2	0.295	0.4	0.4	0.1	0.016	0.4	3.5	0.7	0.007	0.2	2.6	1.8
TG 16:0/18:0/18:1	0.382	0.0	0.4	0.1	0.015	0.0	3.5	1.2	0.006	-0.2	2.3	2.7
TG 16:0/18:1/18:1	0.302	0.3	0.4	0.1	0.015	0.4	3.5	0.7	0.004	0.1	3.3	2.5
TG 16:0/18:1/18:2	0.291	0.5	0.4	0.1	0.015	0.8	3.5	0.5	0.005	0.3	3.0	2.0
TG 16:0/18:2/18:2	0.284	0.5	0.6	0.1	0.014	0.7	4.1	0.5	0.005	0.3	2.8	2.0
TG 16:1/16:1/16:1	0.255	0.3	0.7	1.2	0.010	2.3	4.1	1.5	0.004	1.5	3.2	1.0
TG 16:1/16:1/18:0	0.269	0.3	0.4	0.7	0.010	0.4	4.1	1.4	0.011	0.0	1.8	2.4
TG 16:1/16:1/18:1	0.265	0.3	0.6	0.8	0.010	2.0	4.1	1.1	0.004	0.9	3.6	2.0
TG 16:1/17:0/18:1	0.288	0.4	0.6	0.1	0.014	0.7	4.1	0.5	0.005	0.6	2.9	1.8
TG 16:1/18:1/18:1	0.284	0.4	0.4	0.4	0.010	1.2	4.1	0.8	0.004	0.7	3.6	2.4
TG 16:1/18:1/18:2	0.270	0.5	0.6	0.3	0.010	1.1	4.1	0.6	0.004	0.7	3.6	1.8
TG 17:0/18:1/18:1	0.295	0.4	0.6	0.0	0.023	0.4	3.3	0.3	0.008	0.1	2.5	2.0
TG 18:0/18:0/18:1	0.593	0.0	0.2	0.0	0.033	0.0	2.1	1.0	0.009	-0.1	2.1	2.0
TG 18:0/18:1/18:1	0.407	0.1	0.3	0.1	0.015	0.1	3.3	1.1	0.005	0.0	2.8	2.7
TG 18:0/18:2/18:2	0.311	0.3	0.4	0.0	0.021	0.3	3.3	0.5	0.006	0.2	2.6	2.2
TG 18:1/18:1/18:1	0.304	0.4	0.4	0.0	0.017	0.7	3.5	0.3	0.005	0.4	3.1	1.8
TG 18:1/18:1/18:2	0.295	0.4	0.6	0.0	0.021	0.8	3.3	0.2	0.005	0.5	2.8	1.8
TG 18:1/18:1/20:4	0.311	0.3	0.3	0.1	0.010	1.1	4.1	0.7	0.004	0.5	3.6	2.2
TG 18:1/18:2/18:2	0.291	0.4	0.6	0.0	0.015	1.0	3.5	0.3	0.005	0.6	2.8	1.6
TG 18:2/18:2/18:2	0.291	0.4	0.6	0.0	0.018	0.8	3.5	0.2	0.008	0.5	2.3	1.6
TG 18:2/18:2/20:4	0.291	0.4	0.4	0.1	0.017	0.6	3.8	0.3	0.008	0.5	2.4	1.4

[a] *P*-value for the comparison of levels of each lipid species between genotypes at each age using the Kruskal Wallis test with Benjamini-Hochberg correction for multiple comparisons. $P < 0.05$ was considered significant (highlighted in pink).

[b] Post-hoc analysis was performed using the Mann Whitney *U* test with Dunn-Sidak correction for multiple group comparisons. Values were derived from the formula: sign(difference in median levels)*-log10(post-hoc *P*-value). Colour-coded values 1.3 to 2.0 (light red, $P = 0.05$-0.01) and > 2.0 (dark red, $P < 0.01$) indicate a significant increase relative to the reference group. Colour-coded values -1.3 to -2.0 (light green, $P = 0.05$-0.01) and < -2.0 (dark green, $P < 0.01$) indicate a significant decrease relative to the reference group.

Table S4.3 Relationship between genotype and left-ventricle lipid species in male mice.

Lipid species	6 weeks				10 weeks				16 weeks			
	P-value[a]	db/h vs. H/H[b]	db/db vs. H/H[b]	db/db vs. db/h[b]	*P*-value[a]	db/h vs. H/H[b]	db/db vs. H/H[b]	db/db vs. db/h[b]	*P*-value[a]	db/h vs. H/H[b]	db/db vs. H/H[b]	db/db vs. db/h[b]
Sph 18:1	0.236	0.3	0.0	-0.8	0.247	0.0	0.1	0.7	0.084	-1.6	0.0	0.5
Cer 16:0	0.516	-0.2	-0.2	0.0	0.038	-1.2	-0.9	0.5	0.118	-0.8	0.0	1.0
Cer 18:0	0.230	-0.8	0.0	0.4	0.018	-2.0	0.0	1.5	0.007	-2.9	0.0	1.9
Cer 20:0	0.100	-0.7	0.2	1.6	0.065	-2.0	0.0	0.5	0.161	-1.1	-0.1	0.1
Cer 22:0	0.236	-0.6	-0.4	0.1	0.004	-3.3	-2.0	0.3	0.056	-1.9	-0.2	0.2
Cer 24:0	0.543	-0.1	-0.4	0.0	0.043	-1.8	-0.6	0.2	0.014	-2.5	-0.5	0.4
Cer 24:1	0.272	-0.5	-0.5	0.0	0.062	-1.3	-0.5	0.3	0.185	-1.0	0.0	0.3
MHC 22:0	0.677	0.0	0.0	-0.1	0.952	0.0	0.0	0.0	0.030	-0.4	-1.7	-0.8
MHC 24:0	0.566	0.0	-0.1	-0.2	0.050	-0.7	-1.4	-0.2	0.093	-0.1	-1.4	-0.4
MHC 24:1	0.448	0.4	0.1	-0.1	0.060	-0.8	-1.4	0.0	0.073	0.0	-1.6	-0.5
DHC 20:0	0.677	0.0	-0.1	-0.1	0.214	0.6	0.5	0.0	0.910	0.0	0.0	0.0
DHC 22:0	0.801	0.0	0.1	0.0	0.249	0.0	0.3	0.6	0.228	0.0	-0.5	-0.6
THC 18:0	0.473	0.0	0.2	0.3	0.460	0.0	0.0	0.3	0.343	-0.4	-0.4	0.0
GM3 18:0	0.733	-0.1	0.0	0.0	0.087	-1.2	0.0	0.7	0.228	-1.0	0.0	0.1
GM3 20:0	0.209	0.0	-1.0	-0.6	0.460	0.1	-0.1	-0.2	0.843	0.0	0.0	0.0
GM3 22:0	0.443	0.0	-0.3	-0.3	0.373	0.0	-0.2	-0.3	0.661	-0.2	0.0	0.0
GM3 24:0	0.877	0.0	0.0	0.0	0.680	0.0	0.1	0.0	0.878	0.0	0.0	0.0
GM3 24:1	0.352	0.1	-0.2	-0.4	0.612	-0.1	-0.1	0.0	0.592	0.0	-0.2	-0.1
SM 31:1	0.230	0.0	-1.0	-0.4	0.297	-0.4	-0.3	0.0	0.567	0.0	-0.2	-0.1
SM 32:1	0.302	-0.1	0.3	0.5	0.310	-0.3	0.0	0.4	0.013	-2.3	0.0	1.5
SM 33:1	0.568	0.0	-0.1	-0.3	0.045	-0.5	-1.6	-0.3	0.011	-1.9	-1.9	0.0
SM 34:0	0.124	-0.9	0.0	1.3	0.018	-2.3	-1.4	0.0	0.046	-1.9	0.1	0.5
SM 34:1	0.223	-0.3	-1.0	-0.1	0.059	-0.8	-1.6	0.0	0.012	-2.7	-1.0	0.1
SM 34:2	0.484	0.2	0.0	-0.2	0.036	0.0	-1.6	-0.9	0.093	-1.7	-0.2	0.0
SM 35:1	0.141	-0.2	-1.5	-0.4	0.035	-2.0	-1.1	0.0	0.012	-2.6	-1.2	0.0
SM 36:1	0.230	-0.8	-0.5	0.0	0.083	-1.2	-0.3	0.4	0.009	-3.3	-0.7	0.1
SM 36:2	0.343	-0.5	-0.3	0.0	0.077	-1.0	-0.5	0.4	0.006	-3.0	0.0	2.2
SM 38:1	0.328	-0.3	-0.6	0.0	0.409	-0.1	-0.3	0.0	0.014	-1.0	-2.2	-0.3
SM 38:2	0.381	0.0	-0.6	-0.1	0.446	0.0	-0.2	-0.2	0.012	-1.6	-2.0	-0.1
SM 39:1	0.056	0.1	-3.0	-1.7	0.010	-0.1	-1.8	-1.8	0.002	0.0	-3.6	-3.3
SM 41:1	0.083	0.0	-1.7	-1.5	0.021	-0.3	-1.7	-1.1	0.011	-1.9	-1.9	-0.1
SM 41:2	0.124	0.1	-0.6	-1.6	0.538	-0.2	0.0	0.1	0.141	-0.7	-0.9	0.0
SM 42:1	0.249	0.0	-0.7	-0.4	0.061	-0.1	-1.1	-0.8	0.014	-2.0	-1.6	0.0
PC 24:0	0.457	0.1	-0.1	-0.3	0.285	0.4	0.4	0.0	0.843	0.0	0.0	0.0
PC 30:0	0.066	-0.4	1.7	1.5	0.011	-1.2	0.9	1.7	0.358	-0.5	-0.2	0.0
PC 31:0	0.066	-0.7	-1.7	-0.9	0.023	-0.9	-1.6	-0.7	0.003	0.0	-3.5	-2.6
PC 31:1	0.292	-0.6	-0.4	0.0	0.028	-2.1	-1.0	0.0	0.132	-0.9	-0.7	0.0
PC 32:0	0.065	0.0	-2.1	-1.5	0.234	0.0	-0.6	-0.2	0.011	-1.0	-1.7	-1.5
PC 32:1	0.083	0.0	1.5	1.6	0.002	-0.1	3.3	2.7	0.485	-0.6	0.0	0.0
PC 32:2	0.056	-0.9	1.7	1.7	0.003	-0.9	1.7	2.5	0.167	-0.9	0.0	0.6
PC 33:0	0.102	-0.1	-1.5	-1.0	0.017	-1.1	-1.8	-0.7	0.005	-0.2	-2.9	-2.2
PC 33:1	0.567	-0.1	-0.2	0.0	0.318	-0.5	-0.1	0.1	0.007	0.1	-2.3	-2.3
PC 33:2	0.236	-0.2	0.1	0.8	0.112	-1.5	-0.3	0.0	0.547	0.0	-0.3	-0.1
PC 34:0	0.056	-0.1	-2.7	-1.5	0.149	-0.4	-0.9	0.0	0.022	-1.1	-1.9	-0.1
PC 34:1	0.224	0.0	0.6	0.7	0.002	0.2	3.8	2.3	0.615	-0.1	-0.1	0.0
PC 34:2	0.108	-0.1	1.2	1.3	0.007	0.1	2.3	1.8	0.598	-0.1	0.0	0.1
PC 34:3	0.056	-0.1	2.3	2.0	0.001	-1.2	3.3	3.2	0.011	0.0	2.2	1.8
PC 34:4	0.060	-0.3	1.7	1.9	0.003	-2.0	0.4	2.7	0.510	0.0	0.2	0.2
PC 35:0	0.144	-0.9	-1.1	-0.1	0.049	-0.1	-1.7	-0.5	0.006	0.0	-3.0	-2.0
PC 35:1	0.209	0.0	-1.1	-0.4	0.364	-0.2	-0.4	0.0	0.003	0.0	-3.2	-2.9
PC 35:2	0.124	-0.1	0.5	1.6	0.365	-0.4	0.0	0.2	0.415	0.0	-0.4	-0.2
PC 35:3	0.084	-0.1	0.8	2.0	0.021	-0.4	0.5	1.9	0.510	0.2	0.0	-0.2

Lipid species	6 weeks				10 weeks				16 weeks			
	P-value[a]	db/h vs. H/H[b]	db/db vs. H/H[b]	db/db vs. db/h[b]	*P*-value[a]	db/h vs. H/H[b]	db/db vs. H/H[b]	db/db vs. db/h[b]	*P*-value[a]	db/h vs. H/H[b]	db/db vs. H/H[b]	db/db vs. db/h[b]
PC 35:4	0.470	-0.4	-0.1	0.0	0.070	-1.3	-0.8	0.0	0.289	0.0	0.2	0.7
PC 36:0	0.188	-0.6	-1.2	0.0	0.317	0.5	0.1	-0.1	0.289	-0.6	-0.3	0.0
PC 36:1	0.186	0.0	0.5	1.0	0.002	0.0	3.8	2.3	0.088	-1.0	-1.0	0.1
PC 36:2	0.122	0.0	1.4	1.1	0.001	0.0	3.3	2.8	0.112	-0.7	-0.1	1.0
PC 36:3	0.073	0.0	1.9	1.5	0.001	-0.1	4.1	3.2	0.088	-0.1	0.8	1.0
PC 36:4a	0.121	-0.1	1.2	1.2	0.003	-0.7	1.7	2.6	0.063	0.0	0.8	1.6
PC 36:4b	0.659	0.0	0.0	0.1	0.210	-0.1	0.1	0.8	0.028	-1.0	0.5	1.6
PC 36:5	0.063	-0.2	1.7	1.7	0.001	-1.6	3.0	3.2	0.016	0.0	1.8	1.8
PC 36:6	0.060	-2.2	-0.2	1.1	0.025	-1.8	-0.3	1.0	0.567	-0.1	0.0	0.2
PC 37:4	0.230	-0.3	-1.1	0.0	0.448	-0.4	0.0	0.0	0.460	0.0	0.2	0.2
PC 37:5	0.624	-0.1	0.0	0.1	0.143	-1.3	-0.3	0.0	0.069	0.0	0.8	1.5
PC 37:6	0.056	-2.0	-1.9	-0.3	0.005	-1.1	-2.8	-1.1	0.547	0.3	0.1	0.0
PC 38:2	0.689	-0.1	-0.1	0.0	0.289	-0.4	-0.4	0.0	0.191	0.0	-0.8	-0.4
PC 38:3	0.062	0.6	1.7	1.3	0.025	0.0	1.3	1.5	0.658	-0.1	0.0	-0.1
PC 38:4	0.352	-0.1	0.1	0.4	0.294	-0.2	0.0	0.5	0.093	-0.5	0.3	1.1
PC 38:5	0.367	-0.2	0.0	0.5	0.025	-1.0	0.0	1.8	0.011	0.0	1.7	2.3
PC 38:6a	0.209	0.0	0.8	0.6	0.002	-1.2	1.4	3.0	0.007	0.0	2.3	2.5
PC 38:6b	0.059	-1.0	-1.9	-1.0	0.014	-0.5	-2.0	-1.1	0.771	-0.1	0.0	0.0
PC 38:7	0.093	-0.9	0.0	1.9	0.017	-1.5	0.0	1.9	0.058	0.0	1.2	1.3
PC 39:6	0.056	-0.8	-2.1	-1.3	0.009	-1.0	-2.4	-0.7	0.726	0.0	-0.2	0.0
PC 39:7	0.124	-1.2	-1.2	0.0	0.025	-1.6	-1.6	0.0	0.910	0.0	0.0	0.0
PC 40:5	0.083	-1.6	-1.5	0.0	0.098	-1.3	-0.5	0.0	0.013	-0.5	1.2	2.1
PC 40:6	0.066	-1.2	-1.2	-1.0	0.005	-1.0	-2.6	-1.3	0.116	-0.7	-1.0	0.0
PC 40:7	0.114	-0.6	-1.7	-0.2	0.052	-1.6	-0.9	0.0	0.193	0.0	0.3	1.0
PC(O-30:0)	0.617	0.0	-0.1	-0.1	0.099	-0.3	-1.2	-0.2	0.009	-0.7	-2.3	-1.4
PC(O-32:0)	0.083	0.0	-1.5	-1.6	0.005	-0.2	-2.6	-1.8	0.002	-0.5	-3.2	-2.9
PC(O-32:1)	0.376	-0.1	0.0	0.5	0.198	0.0	-0.8	-0.3	0.036	0.0	-1.6	-1.1
PC(O-34:0)	0.185	-0.6	-1.0	-0.1	0.006	-0.8	-2.4	-1.3	0.004	-1.8	-2.5	-1.7
PC(O-34:1)	0.056	0.0	-2.1	-2.0	0.005	-1.1	-2.3	-1.5	0.002	-1.0	-3.2	-2.4
PC(O-34:2)	0.161	-0.4	-1.1	-0.4	0.014	-0.7	-2.3	-0.7	0.012	-0.1	-2.0	-1.8
PC(O-34:3)	0.260	-0.6	-0.3	0.1	0.207	-0.1	-0.6	-0.3	0.071	0.0	-1.3	-1.0
PC(O-36:0)	0.415	-0.1	-0.4	0.0	0.013	-0.5	-2.6	-0.7	0.008	-0.8	-2.2	-1.7
PC(O-36:1)	0.230	-0.6	-0.6	0.0	0.039	-0.1	-1.7	-0.7	0.008	-1.7	-2.2	-0.5
PC(O-36:2)	0.100	-1.0	-1.5	-0.2	0.021	-0.4	-2.0	-0.8	0.010	-0.5	-2.3	-1.3
PC(O-36:3)	0.132	-0.2	-1.7	-0.4	0.013	-1.6	-2.0	-0.4	0.093	-1.0	-1.0	0.0
PC(O-36:4)	0.230	-0.7	-0.3	0.2	0.098	-1.1	-0.8	0.0	0.210	-0.9	0.0	0.3
PC(O-36:5)	0.384	-0.3	0.0	0.3	0.182	-0.3	0.0	0.9	0.006	-0.4	1.7	2.9
PC(O-38:4)	0.056	-1.9	-1.9	-0.4	0.087	-0.6	-1.1	-0.1	0.076	-0.3	-1.6	-0.2
PC(O-38:5)	0.308	-0.4	-0.5	0.0	0.249	-0.8	0.0	0.2	0.002	-0.5	2.8	3.3
PC(O-40:6)	0.056	-2.6	-3.0	-1.2	0.015	-0.4	-2.0	-1.1	0.555	-0.2	-0.2	0.0
PC(O-40:7)	0.056	-1.1	-2.7	-0.3	0.094	-1.2	-0.7	0.0	0.093	0.0	1.0	1.0
PC(P-32:0)	0.097	-1.2	-1.4	-0.2	0.035	-0.7	-1.7	-0.3	0.009	-1.8	-2.0	-0.4
PC(P-32:1)	0.451	0.1	0.3	0.1	0.118	0.0	0.9	0.6	0.460	-0.4	0.0	0.1
PC(P-34:1)	0.723	0.0	-0.1	0.0	0.886	0.0	0.0	0.0	0.638	0.0	0.2	0.0
PC(P-34:2)	0.191	-0.5	-1.1	0.0	0.085	0.2	-0.6	-0.9	0.560	-0.2	-0.1	0.0
PC(P-34:3)	0.521	0.0	-0.1	-0.3	0.240	0.0	-0.5	-0.4	0.185	-0.7	-0.6	0.0
PC(P-36:2)	0.236	-0.4	-0.6	-0.1	0.021	0.0	-1.6	-1.5	0.883	0.0	0.0	0.0
PC(P-36:4)	0.364	-0.4	0.0	0.3	0.213	-0.3	0.0	0.7	0.004	-1.1	1.6	2.9
PC(P-36:5)	0.248	0.0	0.3	0.8	0.031	-0.4	0.4	1.7	0.024	-0.2	1.5	1.6
PC(P-38:4)	0.179	-0.9	-0.8	0.0	0.699	-0.1	0.0	0.0	0.191	-0.2	0.2	0.9
PC(P-38:5)	0.056	-1.6	-2.7	-0.1	0.059	-1.0	-0.9	-0.4	0.054	-0.1	0.7	1.8
PC(P-38:6)	0.056	-1.3	-3.0	-0.9	0.009	-0.9	-1.8	-1.4	0.636	-0.2	0.0	0.0
PC(P-40:5)	0.056	-2.0	-2.7	-1.6	0.019	-0.4	-1.7	-1.2	0.454	-0.2	-0.3	0.0
PC(P-40:6)	0.056	-2.4	-2.5	-1.0	0.001	-1.6	-3.5	-1.7	0.445	0.0	-0.4	-0.1

Lipid species	6 weeks				10 weeks				16 weeks			
	P-value[a]	db/h vs. H/H[b]	db/db vs. H/H[b]	db/db vs. db/h[b]	*P*-value[a]	db/h vs. H/H[b]	db/db vs. H/H[b]	db/db vs. db/h[b]	*P*-value[a]	db/h vs. H/H[b]	db/db vs. H/H[b]	db/db vs. db/h[b]
LPC 14:0	0.550	0.0	0.3	0.1	0.005	-1.1	0.5	2.6	0.800	-0.1	0.0	0.0
LPC 15:0	0.308	0.0	-0.4	-0.5	0.283	-0.2	-0.4	-0.2	0.328	0.0	-0.4	-0.4
LPC 16:0	0.357	0.3	0.0	-0.4	0.365	-0.2	0.0	0.4	0.155	-0.4	-0.8	-0.3
LPC 16:1	0.146	0.2	1.1	0.7	0.001	0.0	3.5	3.0	0.242	0.0	0.7	0.3
LPC 17:0	0.280	-0.1	-0.5	-0.4	0.400	-0.2	-0.3	0.0	0.118	0.0	-1.0	-0.7
LPC 17:1	0.699	0.1	0.0	-0.1	0.506	-0.3	0.0	0.0	0.355	-0.1	-0.4	-0.2
LPC 18:0	0.908	0.0	0.0	0.0	0.059	-0.8	0.0	1.4	0.193	-0.7	-0.6	0.0
LPC 18:1	0.342	0.1	0.5	0.2	0.003	0.0	2.3	2.7	0.023	-1.5	0.1	1.7
LPC 18:2	0.186	0.1	0.8	0.7	0.002	-1.2	1.1	3.1	0.041	-1.2	0.2	1.3
LPC 20:1	0.516	0.1	0.0	-0.2	0.740	0.0	0.0	-0.1	0.118	0.0	-0.8	-1.0
LPC 20:3	0.161	0.0	0.7	1.1	0.001	-3.6	0.7	3.2	0.006	-0.9	1.0	3.0
LPC 20:4	0.449	0.0	0.3	0.2	0.002	-2.5	0.2	2.8	0.007	-1.4	0.8	2.6
LPC 22:4	0.384	-0.1	0.0	0.5	0.213	0.0	0.1	0.9	0.009	-0.2	2.2	2.0
LPC 22:5	0.484	-0.2	0.0	0.2	0.004	-2.5	0.2	2.4	0.004	-0.1	2.6	3.1
LPC 22:6	0.056	-2.2	-1.9	-0.2	0.004	-3.3	-2.6	0.0	0.155	-0.4	0.0	1.0
LPC(O-16:0)	0.127	0.0	-1.5	-0.9	0.561	0.0	0.0	0.2	0.132	0.0	-0.7	-1.0
PE 32:0	0.249	0.7	0.4	0.0	0.247	-0.2	0.0	0.7	0.467	-0.2	-0.3	0.0
PE 34:1	0.154	0.2	1.4	0.4	0.003	0.0	3.3	2.1	0.883	0.0	0.0	0.0
PE 34:2	0.065	0.2	2.3	1.1	0.002	0.0	2.6	2.6	0.663	-0.1	0.0	0.1
PE 34:3	0.056	0.0	2.7	1.7	0.001	0.0	3.5	2.7	0.029	0.0	1.5	1.6
PE 35:1	0.292	-0.2	0.0	0.7	0.538	0.0	0.1	0.2	0.088	0.0	-1.0	-1.0
PE 35:2	0.174	0.1	1.0	0.6	0.211	0.0	0.5	0.5	0.528	0.2	0.0	-0.2
PE 36:1	0.550	0.0	0.4	0.0	0.182	-0.2	0.1	0.9	0.082	-0.2	-1.2	-0.6
PE 36:2	0.065	0.3	2.3	1.0	0.001	0.0	3.8	2.7	0.168	-0.9	-0.1	0.4
PE 36:3	0.060	0.1	2.3	1.3	0.001	0.0	3.5	3.2	0.144	-0.2	0.4	1.0
PE 36:4	0.056	0.0	2.7	1.7	0.001	0.0	4.1	3.2	0.009	0.0	2.3	2.1
PE 36:5	0.056	0.0	2.1	2.0	0.001	-1.3	3.8	3.2	0.006	0.0	2.2	2.8
PE 38:3	0.267	0.0	0.6	0.4	0.007	0.0	2.1	2.0	0.069	0.2	1.5	0.5
PE 38:4	0.056	0.0	2.7	2.0	0.001	0.0	4.1	2.8	0.005	-0.1	2.4	2.9
PE 38:5	0.056	-0.1	2.7	2.0	0.001	-0.8	2.4	3.1	0.004	-0.4	2.1	3.1
PE 38:6	0.467	-0.4	-0.1	0.0	0.094	-0.8	-1.0	0.0	0.415	0.1	0.1	0.4
PE 40:5	0.800	-0.1	0.0	0.0	0.226	0.0	-0.7	-0.2	0.007	-1.5	-2.4	-0.7
PE 40:6	0.308	-0.5	-0.4	0.0	0.036	-1.0	-1.6	-0.2	0.257	-0.6	-0.4	0.0
PE 40:7	0.287	-0.6	-0.2	0.1	0.112	-1.2	-0.1	0.3	0.205	0.0	0.3	1.0
PE(O-34:1)	0.779	0.0	0.0	0.0	0.346	-0.1	-0.5	0.0	0.034	-1.2	-1.4	-0.2
PE(O-36:2)	0.602	0.0	0.1	0.2	0.037	-0.3	-1.6	-0.7	0.046	0.0	-1.5	-1.1
PE(O-36:3)	0.942	0.0	0.0	0.0	0.846	0.1	0.0	0.0	0.074	-0.7	-1.4	0.0
PE(O-36:4)	0.185	0.0	1.0	0.7	0.886	0.0	0.0	0.0	0.074	-0.6	0.1	1.5
PE(O-36:5)	0.555	0.2	0.0	-0.1	0.123	-0.1	0.4	0.9	0.909	0.0	0.0	0.0
PE(O-38:4)	0.328	-0.5	0.0	0.3	0.216	-0.3	-0.6	-0.1	0.514	-0.2	-0.2	0.0
PE(O-38:5)	0.124	0.0	1.7	0.8	0.005	-0.1	1.4	2.6	0.007	-0.5	2.0	2.3
PE(O-40:4)	0.521	0.0	0.2	0.2	0.886	0.0	0.0	0.0	0.118	0.0	-1.5	-0.4
PE(O-40:5)	0.659	-0.1	0.0	0.1	0.099	-0.9	-0.1	0.7	0.679	0.0	0.1	0.1
PE(O-40:6)	0.186	-0.6	-1.0	0.0	0.030	-1.8	-1.2	0.0	0.807	-0.1	0.0	0.0
PE(O-40:7)	0.144	-0.8	-1.4	0.0	0.198	-0.6	-0.1	0.4	0.004	-0.1	2.3	3.3
PE(P-34:2)	0.146	0.0	1.2	0.9	0.867	0.0	0.0	0.0	0.561	-0.4	0.0	0.0
PE(P-36:2)	0.846	0.0	0.0	0.0	0.800	0.0	0.0	0.0	0.014	-0.5	-2.7	-0.3
PE(P-36:4)	0.141	0.0	0.8	1.3	0.045	-0.1	0.5	1.6	0.369	-0.2	0.0	0.5
PE(P-38:4)	0.144	-0.6	0.2	1.2	0.036	-1.0	0.0	1.6	0.210	-0.5	0.0	0.7
PE(P-38:5)	0.230	-0.1	0.4	0.7	0.044	-1.0	0.0	1.4	0.030	-0.7	0.5	1.8
PE(P-38:6)	0.461	-0.4	-0.1	0.0	0.090	-1.1	-0.8	0.0	0.289	-0.4	0.0	0.5
PE(P-40:4)	0.855	0.0	0.0	0.0	0.895	0.0	0.0	0.0	0.651	0.0	0.0	0.2
PE(P-40:5)	0.652	-0.2	0.0	0.0	0.113	-0.7	-0.9	0.0	0.738	-0.1	0.0	0.0
PE(P-40:6)	0.083	-0.7	-1.9	-0.4	0.022	-1.3	-1.8	-0.1	0.467	-0.2	-0.3	0.0

Lipid species	6 weeks				10 weeks				16 weeks			
	P-value[a]	db/h vs. H/H[b]	db/db vs. H/H[b]	db/db vs. db/h[b]	*P*-value[a]	db/h vs. H/H[b]	db/db vs. H/H[b]	db/db vs. db/h[b]	*P*-value[a]	db/h vs. H/H[b]	db/db vs. H/H[b]	db/db vs. db/h[b]
LPE 16:0	0.659	0.0	0.0	-0.2	0.346	0.0	0.1	0.5	0.242	0.0	-0.5	-0.6
LPE 18:0	0.827	0.0	0.0	-0.1	0.118	0.0	0.6	0.9	0.257	0.0	-0.5	-0.6
LPE 18:1	0.545	0.1	0.0	-0.3	0.112	0.3	1.0	0.2	0.180	0.0	-0.8	-0.6
LPE 18:2	0.230	0.1	1.1	0.1	0.031	0.0	1.0	1.6	0.258	-0.1	-0.7	-0.1
LPE 20:4	0.157	0.0	1.1	0.9	0.001	-1.6	4.1	3.2	0.015	-0.7	1.0	1.9
LPE 22:5	0.230	0.1	0.6	0.6	0.001	-0.1	4.1	3.2	0.002	0.0	3.6	3.3
LPE 22:4	0.776	0.0	0.0	-0.1	0.005	-0.2	1.3	2.6	0.791	-0.1	0.0	0.0
LPE 22:6	0.146	-0.8	-1.2	0.0	0.005	-3.6	-2.0	0.0	0.186	-1.0	-0.1	0.2
PI 34:1	0.154	0.2	1.5	0.3	0.001	0.0	4.1	3.0	0.897	0.0	0.0	0.0
PI 36:1	0.360	0.8	0.1	0.0	0.017	-0.2	0.8	2.1	0.344	-0.1	0.1	0.6
PI 36:2	0.934	0.0	0.0	0.0	0.460	-0.4	-0.1	0.0	0.074	-0.4	-1.4	-0.3
PI 36:3	0.099	0.1	1.7	1.0	0.001	-0.6	3.5	3.2	0.097	0.3	1.3	0.2
PI 36:4	0.189	0.0	0.5	1.0	0.198	-0.5	0.0	0.6	0.272	-0.7	-0.3	0.0
PI 38:2	0.179	0.0	0.3	1.5	0.903	0.0	0.0	0.0	0.760	0.0	0.0	-0.1
PI 38:3	0.522	0.0	0.1	0.2	0.188	-0.4	0.1	0.6	0.987	0.0	0.0	0.0
PI 38:4	0.406	-0.3	-0.2	0.1	0.109	-1.1	-0.5	0.0	0.186	-0.6	0.0	0.7
PI 38:5	0.097	0.0	1.7	1.2	0.001	-1.3	2.4	3.2	0.014	0.0	1.6	2.1
PI 38:6	0.108	-1.9	-0.4	0.2	0.021	-2.0	-1.4	0.1	0.754	-0.1	0.0	0.1
PI 40:4	0.580	-0.1	-0.2	0.0	0.038	-1.5	-1.0	0.2	0.897	0.0	0.0	0.0
PI 40:5	0.124	-0.8	0.0	1.3	0.030	-1.0	0.5	1.4	0.002	0.0	3.6	3.0
PI 40:6	0.059	-0.3	-2.5	-1.1	0.072	-0.2	-1.3	-0.4	0.574	-0.1	0.0	0.2
PS 36:1	0.272	0.0	-0.5	-0.5	0.560	-0.2	-0.1	0.0	0.202	-0.1	-0.7	-0.4
PS 36:2	0.877	0.0	0.0	0.0	0.249	-0.8	0.0	0.2	0.567	-0.2	0.0	0.1
PS 38:3	0.894	0.0	0.0	0.0	0.295	-0.4	-0.1	-0.1	0.630	-0.2	0.0	0.1
PS 38:4	0.285	-0.6	-0.4	0.0	0.134	-0.8	-0.5	0.1	0.411	-0.2	0.0	0.4
PS 38:5	0.383	-0.3	0.0	0.4	0.011	-1.3	0.2	2.1	0.283	0.0	0.7	0.2
PS 40:5	0.448	-0.2	0.0	0.3	0.090	-0.7	0.0	1.1	0.685	-0.1	0.0	0.1
PS 40:6	0.230	-0.4	-1.0	0.0	0.346	-0.5	-0.2	0.0	0.460	-0.4	0.0	0.1
PG 34:1	0.186	-0.5	0.3	0.8	0.029	-0.3	0.5	1.7	0.845	0.0	0.0	0.0
PG 34:2	0.093	-0.1	1.5	1.3	0.002	-0.3	2.3	2.6	0.941	0.0	0.0	0.0
PG 36:1	0.463	-0.2	-0.3	0.0	0.124	-0.6	-0.9	0.0	0.180	-0.9	-0.4	0.0
PG 36:2	0.163	-0.1	0.8	0.9	0.018	-1.6	0.0	1.7	0.344	-0.4	-0.2	0.0
PG 36:3	0.056	-0.7	1.0	2.4	0.005	0.0	2.3	2.3	0.791	0.0	0.0	0.1
BMP 16:0/18:1	0.230	0.0	0.7	0.6	0.506	0.0	0.2	0.1	0.754	0.0	0.0	0.1
BMP 18:1/18:1	0.393	0.5	0.2	0.0	0.018	0.0	2.0	1.4	0.123	0.0	0.7	1.0
CL 18:2/18:2/18:2/16:1	0.087	0.1	1.5	1.3	0.001	0.0	4.1	3.2	0.077	0.2	1.2	0.7
CL 18:2/18:1/18:2/16:1	0.097	0.0	1.4	1.5	0.001	0.0	3.5	3.1	0.025	0.0	1.8	1.4
CL 18:2/18:1/18:1/16:1	0.328	0.0	0.4	0.4	0.029	-0.1	0.5	1.9	0.159	0.0	0.9	0.6
CL 18:2/18:2/18:2/18:3	0.348	-0.4	-0.3	0.0	0.010	-0.6	0.1	2.8	0.386	-0.2	0.0	0.5
CL 18:2/18:2/18:2/18:2	0.203	-0.1	0.6	0.8	0.003	-1.1	1.2	2.7	0.574	0.0	0.1	0.2
CL 18:2/18:2/18:2/18:1	0.457	-0.3	-0.1	0.1	0.207	-0.5	0.0	0.5	0.196	-0.1	0.1	1.1
CL 18:2/18:1/18:2/18:1	0.152	-0.8	-1.0	-0.2	0.150	-1.1	-0.4	0.0	0.094	-0.5	0.2	1.2
CL 18:1/18:1/18:1/18:2	0.146	-1.5	-0.5	0.0	0.926	0.0	0.0	0.0	0.012	-1.0	0.6	2.3
CL 18:2/18:2/18:2/20:3	0.139	-0.3	0.4	1.3	0.055	-0.3	0.2	1.5	0.050	0.0	1.3	1.3
CL 18:2/18:1/18:2/20:3	0.230	-0.7	-0.5	0.0	0.047	-1.8	-0.9	0.0	0.411	-0.2	0.0	0.4
CL 18:2/18:1/18:2/20:2	0.161	-0.7	-1.2	0.0	0.023	-0.9	-1.7	-0.6	0.211	-1.0	-0.2	0.0
CL 18:2/18:2/18:2/20:4	0.169	-0.5	0.1	1.1	0.165	-0.5	-0.1	0.7	0.228	0.0	0.3	0.9
CL 18:2/18:1/18:2/20:1	0.979	0.0	0.0	0.0	0.458	-0.3	0.0	0.1	0.843	0.0	0.0	0.0
CL 18:2/18:2/18:2/22:6	0.056	-1.2	-2.3	-0.5	0.005	-2.5	-2.6	-0.2	0.446	0.0	0.2	0.4
CL 18:2/18:1/18:2/22:6	0.056	-2.6	-2.3	0.0	0.015	-1.0	-2.3	-0.4	0.567	0.0	0.0	0.3
CL 18:2/18:1/18:2/22:5	0.066	-2.4	-0.7	0.2	0.129	-1.0	0.0	0.5	0.878	0.0	0.0	0.0
CL 18:2/22:6/18:2/20:3	0.330	-0.3	-0.5	-0.1	0.300	0.0	-0.5	-0.2	0.293	0.0	0.4	0.6
CE 18:1	0.934	0.0	0.0	0.0	0.109	-0.7	0.1	0.8	0.514	0.0	-0.3	-0.1
CE 18:2	0.230	0.0	0.5	0.8	0.015	-0.8	0.2	2.3	0.865	0.0	0.0	0.0

Lipid species	6 weeks				10 weeks				16 weeks			
	P-value[a]	db/h vs. H/H[b]	db/db vs. H/H[b]	db/db vs. db/h[b]	*P*-value[a]	db/h vs. H/H[b]	db/db vs. H/H[b]	db/db vs. db/h[b]	*P*-value[a]	db/h vs. H/H[b]	db/db vs. H/H[b]	db/db vs. db/h[b]
CE 18:3	0.293	0.0	0.5	0.4	0.022	-1.6	0.0	1.5	0.510	0.0	0.2	0.2
CE 20:3	0.097	0.5	1.7	0.6	0.004	-0.4	2.1	2.3	0.463	0.0	0.3	0.2
CE 20:4	0.372	0.0	0.5	0.1	0.060	-1.1	0.0	1.1	0.117	0.0	1.0	0.8
CE 20:5	0.060	0.0	1.7	2.0	0.001	-0.4	3.3	3.2	0.028	0.4	1.7	0.8
CE 22:6	0.617	0.0	0.2	0.0	0.025	-1.8	0.0	1.4	0.161	0.1	0.8	0.5
COH	0.484	0.1	0.0	-0.4	0.355	-0.3	-0.3	0.0	0.658	-0.1	-0.1	0.0
DG 16:0/16:0	0.209	0.0	0.5	0.9	0.001	-1.6	1.8	3.1	0.009	0.0	1.9	2.3
DG 16:0/18:1	0.239	0.0	0.5	0.7	0.001	-1.0	3.0	3.2	0.007	0.0	2.4	2.3
DG 16:0/18:2	0.415	0.0	0.2	0.4	0.002	-1.5	1.4	2.7	0.009	0.1	2.3	1.9
DG 16:0/20:4	0.202	-0.1	0.2	1.2	0.112	-0.3	0.2	0.9	0.247	0.3	0.6	0.1
DG 16:0/22:5	0.146	-0.3	0.4	1.2	0.003	-2.0	1.6	2.0	0.004	0.2	3.0	2.4
DG 16:0/22:6	0.249	-0.8	-0.2	0.1	0.066	-1.5	-0.2	0.5	0.210	0.0	0.4	0.8
DG 16:1/18:1	0.182	0.0	0.6	1.1	0.001	-0.4	2.0	3.2	0.027	0.1	1.6	1.5
DG 18:0/18:1	0.228	0.0	0.3	1.0	0.001	-2.0	1.8	3.1	0.014	0.0	1.6	2.1
DG 18:0/18:2	0.503	0.0	0.1	0.3	0.007	-2.3	0.0	2.1	0.056	-0.3	0.6	1.6
DG 18:0/20:4	0.669	0.0	-0.1	0.0	0.046	-0.6	-1.6	-0.2	0.037	-1.3	-1.3	-0.1
DG 18:1/18:1	0.246	0.0	0.5	0.6	0.002	0.0	2.8	3.0	0.008	0.1	2.4	2.0
DG 18:1/18:2	0.341	0.0	0.5	0.3	0.008	-0.1	1.8	2.0	0.006	0.5	3.0	1.5
DG 18:1/18:3	0.203	0.0	0.5	1.1	0.004	-0.8	1.4	2.4	0.007	0.2	2.6	1.8
DG 18:1/20:3	0.227	0.0	0.3	1.1	0.052	0.0	1.1	1.1	0.168	0.1	0.9	0.4
DG 18:1/20:4	0.249	0.0	0.2	1.0	0.044	-0.8	0.2	1.4	0.059	0.3	1.5	0.6
DG 18:2/18:2	0.554	0.1	0.2	0.1	0.547	0.0	0.0	0.2	0.011	1.1	2.3	0.6
TG 14:0/16:0/18:1	0.161	0.1	0.5	1.3	0.001	-0.1	3.0	3.2	0.025	0.0	1.3	2.0
TG 14:0/16:0/18:2	0.224	0.1	0.5	0.7	0.002	-0.3	1.7	3.0	0.059	0.0	1.1	1.4
TG 14:0/16:1/18:1	0.182	0.1	0.7	0.8	0.003	0.0	1.7	3.2	0.037	0.0	1.4	1.5
TG 14:0/16:1/18:2	0.209	0.2	0.7	0.5	0.002	-0.1	2.0	3.2	0.013	0.0	1.9	1.9
TG 14:0/17:0/18:1	0.302	0.1	0.5	0.4	0.002	-0.4	1.6	3.0	0.008	0.0	2.1	2.5
TG 14:1/16:0/18:1	0.174	0.2	0.8	0.8	0.001	-0.1	2.6	3.1	0.012	0.0	1.9	2.1
TG 14:1/16:1/18:0	0.154	0.2	0.8	0.9	0.002	0.0	1.7	3.2	0.076	0.0	1.2	1.0
TG 14:1/18:1/18:1	0.191	0.3	0.5	0.8	0.001	-0.1	2.6	3.2	0.009	0.0	2.2	2.1
TG 16:0/16:0/16:0	0.249	0.0	0.5	0.6	0.001	-1.0	2.8	3.2	0.027	0.0	1.2	2.0
TG 16:0/16:0/18:0	0.249	0.0	0.5	0.6	0.001	-1.2	2.3	3.2	0.012	-0.1	1.6	2.2
TG 16:0/16:0/18:1	0.230	0.3	0.5	0.4	0.001	0.0	3.8	3.2	0.011	0.0	1.9	2.2
TG 16:0/16:0/18:2	0.330	0.1	0.5	0.2	0.001	-0.3	3.0	3.1	0.010	0.1	1.9	2.2
TG 16:0/16:1/18:1	0.122	0.2	1.1	1.1	0.001	0.0	2.6	3.2	0.010	0.0	2.1	2.1
TG 16:0/17:0/18:1	0.209	0.1	0.6	0.9	0.001	-0.1	3.0	3.2	0.009	0.0	1.9	2.4
TG 16:0/17:0/18:2	0.448	0.1	0.3	0.2	0.002	-0.3	2.0	2.8	0.011	0.1	2.0	2.0
TG 16:0/18:0/18:1	0.235	0.1	0.5	0.6	0.001	-0.2	2.3	3.2	0.013	-0.1	1.6	2.2
TG 16:0/18:1/18:1	0.209	0.4	0.8	0.1	0.001	0.0	3.0	3.0	0.006	0.1	2.7	2.4
TG 16:0/18:1/18:2	0.231	0.6	0.5	0.0	0.001	0.0	3.5	3.0	0.004	0.2	2.8	2.5
TG 16:0/18:2/18:2	0.146	1.2	0.8	0.0	0.005	0.0	2.1	2.4	0.002	0.2	3.3	2.9
TG 16:1/16:1/16:1	0.220	0.2	0.7	0.4	0.003	-0.1	1.4	3.2	0.059	0.0	1.2	1.2
TG 16:1/16:1/18:0	0.209	0.0	0.3	1.2	0.008	-0.1	1.0	2.6	0.029	0.0	1.3	1.8
TG 16:1/16:1/18:1	0.124	0.3	1.0	1.1	0.002	0.0	1.8	3.2	0.016	0.0	1.8	1.8
TG 16:1/17:0/18:1	0.292	0.2	0.6	0.1	0.001	0.0	2.8	3.1	0.006	0.0	2.5	2.4
TG 16:1/18:1/18:1	0.116	0.4	1.2	0.8	0.001	0.0	2.6	3.2	0.009	0.1	2.3	1.9
TG 16:1/18:1/18:2	0.144	0.7	1.0	0.4	0.001	0.0	2.8	3.2	0.006	0.2	2.6	2.2
TG 17:0/18:1/18:1	0.470	0.0	0.2	0.3	0.018	-0.1	1.1	1.8	0.017	0.1	1.8	1.6
TG 18:0/18:0/18:1	0.186	0.0	0.6	1.0	0.001	-0.4	2.0	3.2	0.008	-0.1	1.9	2.5
TG 18:0/18:1/18:1	0.330	0.2	0.5	0.1	0.002	0.0	2.1	3.1	0.009	0.0	1.8	2.4
TG 18:1/18:1/18:1	0.209	0.7	0.6	0.1	0.002	0.2	2.8	2.5	0.004	0.0	3.0	2.6
TG 18:1/18:1/18:2	0.209	1.1	0.4	0.0	0.004	0.1	2.6	2.0	0.003	0.0	3.2	2.8
TG 18:1/18:1/20:4	0.248	0.6	0.6	0.0	0.005	0.8	2.3	1.5	0.002	0.4	3.3	2.9
TG 18:1/18:1/22:6	0.384	0.6	0.1	0.0	0.025	0.0	1.7	1.3	0.004	0.8	2.8	2.0

Lipid species	6 weeks				10 weeks				16 weeks			
	P-value[a]	db/h vs. H/H[b]	db/db vs. H/H[b]	db/db vs. db/h[b]	*P*-value[a]	db/h vs. H/H[b]	db/db vs. H/H[b]	db/db vs. db/h[b]	*P*-value[a]	db/h vs. H/H[b]	db/db vs. H/H[b]	db/db vs. db/h[b]
TG 18:1/18:2/18:2	0.185	1.3	0.4	0.0	0.007	0.2	2.4	1.6	0.002	0.2	3.6	2.8
TG 18:2/18:2/18:2	0.209	0.9	0.2	-0.3	0.240	0.1	0.8	0.1	0.002	0.7	3.5	2.9
TG 18:2/18:2/20:4	0.059	2.4	0.7	-0.6	0.092	0.0	0.8	0.9	0.011	0.0	1.9	2.2

[a] *P*-value for the comparison of levels of each lipid species between genotypes at each age using the Kruskal Wallis test with Benjamini-Hochberg correction for multiple comparisons. $P < 0.05$ was considered significant (highlighted in pink).

[b] Post-hoc analysis was performed using the Mann Whitney *U* test with Dunn-Sidak correction for multiple group comparisons. Values were derived from the formula: sign(difference in median levels)*-log10(post-hoc *P*-value). Colour-coded values 1.3 to 2.0 (light red, $P = 0.05$-0.01) and > 2.0 (dark red, $P < 0.01$) indicate a significant increase relative to the reference group. Colour-coded values -1.3 to -2.0 (light green, $P = 0.05$-0.01) and < -2.0 (dark green, $P < 0.01$) indicate a significant decrease relative to the reference group.

Table S4.4 Relationship between genotype and adipose lipid species in male mice.

Lipid species	6 weeks				10 weeks				16 weeks			
	P-value[a]	db/h vs. H/H[b]	db/db vs. H/H[b]	db/db vs. db/h[b]	*P*-value[a]	db/h vs. H/H[b]	db/db vs. H/H[b]	db/db vs. db/h[b]	*P*-value[a]	db/h vs. H/H[b]	db/db vs. H/H[b]	db/db vs. db/h[b]
Sph 18:1	0.627	0.2	0.0	-0.1	0.517	0.0	0.4	0.0	0.671	0.0	0.0	-0.1
Cer 16:0	0.589	0.2	0.0	-0.2	0.177	-0.6	-0.5	0.0	0.085	-0.8	0.0	0.8
Cer 18:0	0.638	0.1	0.2	0.0	0.050	-1.2	0.0	1.2	0.054	-1.3	-0.1	0.6
Cer 20:0	0.384	0.4	0.0	-0.5	0.045	-1.2	-1.1	0.2	0.011	-1.8	-1.5	0.0
Cer 22:0	0.619	0.3	0.0	-0.1	0.122	-0.9	-0.7	0.0	0.001	-3.0	-2.4	0.1
Cer 24:0	0.726	0.0	0.0	-0.2	0.053	-0.9	-1.6	0.0	0.004	-2.4	-1.5	0.6
Cer 24:1	0.565	0.3	0.0	-0.1	0.048	-0.9	-1.6	0.0	0.002	-2.3	-2.7	0.0
MHC 16:0	0.366	0.7	0.0	-0.8	0.979	0.0	0.0	0.0	0.150	-0.6	-0.5	0.0
MHC 22:0	0.366	0.6	-0.1	-1.2	0.075	0.0	-0.9	-0.9	0.009	-0.8	-2.5	-0.2
MHC 24:0	0.366	0.4	-0.3	-0.9	0.044	0.0	-2.0	-0.7	0.009	-1.1	-2.3	-0.2
MHC 24:1	0.366	0.2	-0.1	-0.8	0.032	0.0	-2.6	-0.7	0.052	-0.5	-1.6	0.0
SM 32:1	0.384	0.1	0.8	0.0	0.095	-0.1	0.6	0.9	0.085	0.0	1.0	0.7
SM 33:1	0.580	0.0	-0.1	-0.2	0.068	-0.3	-1.3	-0.3	0.816	-0.1	0.0	0.0
SM 34:0	0.739	0.0	0.1	0.0	0.126	0.0	0.6	0.8	0.009	0.0	2.3	1.4
SM 34:1	0.886	0.0	0.0	0.0	0.531	-0.3	0.0	0.1	0.013	-0.1	1.8	1.4
SM 34:2	0.793	0.0	0.1	0.0	0.140	0.0	0.5	0.8	0.011	-0.1	2.0	1.4
SM 35:1	0.827	0.0	0.0	0.0	0.675	-0.1	0.0	0.0	0.473	0.1	0.2	0.0
SM 35:2	0.577	0.1	0.3	0.0	0.177	0.0	0.4	0.7	0.511	0.0	0.3	0.1
SM 36:1	0.996	0.0	0.0	0.0	0.252	0.0	0.1	0.7	0.489	0.0	0.0	0.4
SM 36:2	0.954	0.0	0.0	0.0	0.151	0.0	0.5	0.8	0.458	0.0	0.0	0.4
SM 38:1	0.366	0.0	-0.6	-0.5	0.064	-1.2	-1.0	0.0	0.188	-0.7	-0.2	0.1
SM 38:2	0.896	0.0	0.0	0.0	0.294	-0.2	0.0	0.6	0.700	0.0	-0.1	0.0
SM 39:1	0.822	0.0	0.0	0.1	0.396	0.2	0.0	-0.3	0.056	0.3	-0.2	-1.6
SM 41:1	0.455	0.0	0.5	0.0	0.052	0.6	1.3	0.4	0.099	0.0	1.0	0.4
SM 41:2	0.384	0.3	0.6	0.0	0.055	0.4	1.2	0.5	0.054	0.5	1.2	0.2
SM 42:1	0.366	0.0	-0.3	-1.1	0.126	-0.8	-0.8	0.0	0.014	-1.8	-0.7	0.6
PC 24:0	0.684	-0.1	-0.1	0.0	0.252	-0.3	-0.6	0.0	0.022	-0.8	-1.7	-0.1
PC 28:0	0.980	0.0	0.0	0.0	0.979	0.0	0.0	0.0	0.979	0.0	0.0	0.0
PC 30:0	0.384	0.0	-0.5	-0.4	0.042	-0.1	-2.8	-0.1	0.010	-0.9	-2.3	-0.2
PC 31:0	0.366	0.0	-0.9	-0.8	0.031	-0.1	-3.3	-0.3	0.009	-0.9	-2.4	-0.2
PC 31:1	0.886	0.0	0.0	0.0	0.299	0.0	-0.4	-0.2	0.827	0.0	0.0	0.0
PC 32:0	0.366	0.0	-0.8	-1.1	0.027	-0.1	-2.6	-0.7	0.005	-1.3	-2.6	-0.2
PC 32:1	0.758	0.0	-0.1	-0.1	0.368	-0.4	0.0	0.2	0.035	-1.0	-1.4	0.0
PC 32:2	0.950	0.0	0.0	0.0	0.051	-0.3	0.4	1.4	0.732	-0.1	0.0	0.0
PC 32:3	0.977	0.0	0.0	0.0	0.568	0.0	0.2	0.0	0.343	0.2	0.4	0.0
PC 33:0	0.366	-0.1	-0.8	-0.9	0.027	-0.1	-3.5	-0.3	0.013	-0.8	-2.0	-0.3
PC 33:1	0.511	0.0	-0.2	-0.3	0.021	-1.0	-3.3	0.0	0.002	-1.4	-2.9	-1.0
PC 33:2	0.407	0.0	-0.4	-0.3	0.019	-1.0	-3.0	-0.3	0.009	-1.1	-1.8	-0.8
PC 34:0	0.366	0.0	-0.8	-1.1	0.025	-0.2	-2.8	-0.6	0.002	-1.8	-3.0	-0.1
PC 34:1	0.407	0.0	-0.3	-0.4	0.038	-1.2	-1.7	0.0	0.003	-2.5	-2.0	0.0
PC 34:2	0.366	0.0	-0.5	-0.7	0.031	-1.0	-2.3	0.0	0.008	-2.3	-1.5	0.0
PC 34:3	0.401	0.0	-0.2	-0.6	0.038	-1.2	-1.7	0.0	0.010	-1.8	-1.6	0.0
PC 34:4	0.366	0.0	-0.9	-0.3	0.052	-0.8	-1.7	0.0	0.019	-1.1	-1.7	0.0
PC 35:0	0.401	0.0	-0.6	-0.1	0.024	-0.7	-2.1	-0.7	0.003	0.0	-2.7	-2.2
PC 35:1	0.679	0.0	-0.1	-0.2	0.045	-1.3	-1.2	-0.1	0.001	-2.7	-3.6	-1.3
PC 35:2	0.401	0.0	-0.2	-0.5	0.032	-0.8	-2.1	-0.2	0.046	-0.9	-1.1	-0.1
PC 35:3	0.366	0.2	-0.4	-0.8	0.020	-1.1	-2.8	-0.1	0.002	-2.5	-2.1	-0.6
PC 35:4	0.366	0.0	-0.4	-0.7	0.021	-0.7	-3.0	-0.2	0.012	-1.1	-1.9	-0.2
PC 35:5	0.366	0.0	-0.4	-0.9	0.032	-1.1	-2.1	0.0	0.070	-1.1	-0.4	0.2
PC 36:0	0.912	0.0	0.0	0.0	0.740	0.0	-0.1	0.0	0.031	0.0	-1.5	-1.0
PC 36:1	0.749	0.0	0.1	0.0	0.207	-0.2	0.0	0.7	0.049	-1.2	-0.7	0.1
PC 36:2	0.736	0.1	0.0	0.0	0.592	-0.2	0.0	-0.1	0.003	-2.9	-1.6	0.1

Lipid species	6 weeks				10 weeks				16 weeks			
	P-value[a]	db/h vs. H/H[b]	db/db vs. H/H[b]	db/db vs. db/h[b]	*P*-value[a]	db/h vs. H/H[b]	db/db vs. H/H[b]	db/db vs. db/h[b]	*P*-value[a]	db/h vs. H/H[b]	db/db vs. H/H[b]	db/db vs. db/h[b]
PC 36:3	0.366	0.0	-0.4	-0.8	0.027	-1.1	-2.3	-0.1	0.003	-2.8	-1.8	-0.1
PC 36:4a	0.366	0.1	-0.3	-0.7	0.019	-1.5	-2.3	-0.8	0.002	-3.0	-1.8	-0.6
PC 36:4b	0.366	0.0	-0.4	-0.8	0.031	-0.9	-2.3	-0.1	0.010	-1.5	-1.8	-0.1
PC 36:5	0.398	0.0	-0.3	-0.5	0.034	-1.1	-2.0	0.1	0.013	-1.5	-1.6	0.0
PC 36:6	0.436	0.0	-0.3	-0.3	0.025	-1.6	-1.8	0.2	0.051	-1.2	-0.8	0.0
PC 37:4	0.366	0.0	-0.3	-0.8	0.044	-0.5	-2.1	0.0	0.011	-1.2	-1.8	-0.2
PC 37:5	0.511	0.0	-0.3	-0.2	0.024	-1.0	-2.6	-0.1	0.018	-1.0	-1.7	-0.1
PC 38:2	0.790	-0.1	0.0	0.0	0.168	-0.5	-0.8	0.0	0.009	-0.6	-2.5	-0.5
PC 38:3	0.980	0.0	0.0	0.0	0.101	-1.2	-0.1	0.4	0.001	-3.0	-3.5	0.0
PC 38:4	0.529	0.0	-0.1	-0.3	0.052	-0.9	-1.4	-0.1	0.001	-2.7	-2.6	-0.1
PC 38:5	0.384	0.0	-0.4	-0.5	0.040	-0.8	-2.1	0.0	0.009	-1.5	-2.0	0.0
PC 38:6a	0.366	0.0	-0.5	-0.8	0.030	-0.5	-2.1	-0.5	0.009	-1.9	-1.6	-0.2
PC 38:6b	0.393	0.0	-0.4	-0.4	0.038	-1.3	-1.6	0.0	0.008	-1.7	-1.9	-0.1
PC 38:7	0.433	0.0	-0.4	-0.2	0.027	-1.5	-2.0	0.1	0.029	-1.4	-1.1	0.0
PC 39:6	0.401	0.0	-0.2	-0.6	0.093	-0.3	-1.6	0.0	0.011	-0.5	-2.2	-0.6
PC 39:7	0.422	0.0	-0.2	-0.4	0.586	0.0	-0.2	-0.1	0.252	-0.2	-0.6	0.0
PC 40:5	0.954	0.0	0.0	0.0	0.406	-0.3	-0.3	0.0	0.011	-1.1	-1.9	-0.3
PC 40:6	0.674	-0.1	-0.1	0.0	0.106	-1.1	-0.7	0.0	0.008	-1.3	-2.1	-0.3
PC 40:7	0.401	0.0	-0.5	-0.2	0.056	-0.7	-1.6	0.0	0.010	-1.5	-1.8	-0.1
PC(O-30:0)	0.629	0.0	0.0	-0.2	0.322	0.0	-0.4	-0.3	0.013	-0.3	-2.0	-0.9
PC(O-32:0)	0.366	0.3	-0.1	-1.2	0.019	0.1	-2.1	-2.0	0.008	-0.3	-2.3	-1.2
PC(O-32:1)	0.790	0.0	0.1	0.0	0.453	0.1	0.0	-0.4	0.272	0.0	-0.2	-0.5
PC(O-34:0)	0.726	0.0	-0.1	-0.1	0.038	-0.1	-1.0	-1.4	0.015	-0.1	-1.7	-1.3
PC(O-34:1)	0.589	0.0	-0.1	-0.2	0.321	0.2	0.0	-0.5	0.146	-0.1	-0.9	-0.2
PC(O-34:2)	0.684	0.0	0.0	-0.2	0.026	0.1	-1.6	-1.5	0.010	0.0	-2.0	-1.6
PC(O-34:4)	0.726	0.2	0.0	0.0	0.674	0.0	-0.1	0.0	0.862	0.0	0.0	0.0
PC(O-36:0)	0.934	0.0	0.0	0.0	0.026	0.0	-1.4	-1.6	0.034	-0.2	-1.3	-0.9
PC(O-36:1)	0.781	0.0	-0.1	0.0	0.098	0.0	-0.8	-0.9	0.032	0.0	-1.6	-0.9
PC(O-36:2)	0.977	0.0	0.0	0.0	0.137	0.3	-0.2	-0.9	0.054	0.0	-1.4	-0.6
PC(O-36:3)	0.401	0.3	0.0	-0.5	0.271	0.0	-0.4	-0.4	0.016	-0.4	-2.0	-0.5
PC(O-36:4)	0.366	0.4	-0.3	-1.2	0.038	0.0	-2.3	-0.7	0.013	-0.8	-1.8	-0.5
PC(O-36:5)	0.731	0.0	0.0	-0.1	0.158	-0.1	-1.2	0.0	0.048	-0.7	-1.4	0.0
PC(O-38:4)	0.401	0.0	-0.1	-0.6	0.027	0.1	-1.4	-1.5	0.008	-0.3	-2.6	-0.7
PC(O-38:5)	0.401	0.1	0.0	-0.7	0.714	0.0	0.0	-0.1	0.093	-0.7	-0.9	0.0
PC(O-40:6)	0.911	0.0	0.0	0.0	0.038	0.0	-1.7	-1.0	0.043	-0.1	-1.6	-0.4
PC(O-40:7)	0.583	0.0	-0.1	-0.3	0.586	0.0	-0.2	-0.1	0.343	-0.1	-0.4	0.0
PC(P-32:0)	0.366	0.2	-0.2	-0.8	0.022	-1.1	-2.8	0.0	0.006	-2.1	-1.9	0.0
PC(P-34:1)	0.366	0.3	-0.3	-1.2	0.038	-0.6	-2.3	0.0	0.005	-2.0	-2.0	-0.3
PC(P-34:2)	0.401	0.0	-0.4	-0.3	0.024	-1.2	-2.6	0.0	0.009	-1.9	-1.5	0.1
PC(P-34:3)	0.366	0.3	-0.8	-1.6	0.019	0.0	-3.0	-1.2	0.010	-0.9	-2.5	0.0
PC(P-36:2)	0.368	0.0	-0.1	-0.9	0.020	-0.8	-3.3	-0.2	0.021	-1.6	-1.1	-0.2
PC(P-36:4)	0.366	0.0	-0.4	-0.7	0.031	-1.2	-2.1	0.0	0.016	-1.6	-1.4	0.0
PC(P-38:4)	0.401	0.0	-0.3	-0.4	0.034	-1.2	-1.8	0.0	0.015	-0.8	-2.1	-0.1
PC(P-38:5)	0.436	0.0	-0.3	-0.3	0.056	-0.5	-1.7	-0.1	0.033	-1.0	-1.3	0.0
PC(P-38:6)	0.378	0.0	-0.6	-0.3	0.031	-1.3	-2.0	0.0	0.023	-1.4	-1.2	0.0
LPC 14:0	0.977	0.0	0.0	0.0	0.108	-0.4	-1.1	0.0	0.137	-0.8	-0.5	0.0
LPC 16:0	0.392	0.0	-0.3	-0.6	0.047	-0.4	-1.7	-0.3	0.004	-2.6	-1.7	0.0
LPC 16:1	0.684	0.0	0.2	0.0	0.269	-0.5	-0.2	0.1	0.022	-1.5	-1.2	0.0
LPC 17:0	0.653	-0.3	-0.1	0.0	0.118	-0.2	-1.4	0.0	0.274	-0.4	-0.3	0.0
LPC 18:0	0.401	0.1	0.6	0.0	0.992	0.0	0.0	0.0	0.118	-0.8	-0.1	0.4
LPC 18:1	0.798	0.0	0.0	-0.1	0.049	-0.8	-1.8	0.0	0.003	-2.7	-1.8	-0.1
LPC 18:2	0.508	0.0	0.0	-0.5	0.064	-0.8	-1.4	0.0	0.010	-2.2	-1.3	0.0
LPC 20:1	0.790	0.0	0.0	0.0	0.032	0.1	-0.7	-1.8	0.002	-0.3	-3.1	-1.5
LPC 20:3	0.577	0.0	0.0	-0.5	0.032	-1.0	-2.3	0.0	0.009	-2.1	-1.5	0.0

Lipid species	6 weeks				10 weeks				16 weeks			
	P-value[a]	db/h vs. H/H[b]	db/db vs. H/H[b]	db/db vs. db/h[b]	*P*-value[a]	db/h vs. H/H[b]	db/db vs. H/H[b]	db/db vs. db/h[b]	*P*-value[a]	db/h vs. H/H[b]	db/db vs. H/H[b]	db/db vs. db/h[b]
LPC 20:4	0.401	0.0	-0.1	-0.6	0.028	-0.9	-2.8	0.0	0.020	-1.6	-1.2	0.0
LPC 22:4	0.366	0.0	-0.6	-0.8	0.028	-0.9	-2.3	-0.2	0.010	-2.1	-1.2	0.1
LPC 22:5	0.759	0.0	0.0	-0.2	0.064	-1.0	-1.2	0.0	0.060	-1.3	-0.5	0.0
LPC 22:6	0.401	0.0	-0.3	-0.4	0.019	-1.5	-3.5	0.0	0.012	-1.8	-1.4	0.0
LPC(O-16:0)	0.366	0.6	0.9	0.0	0.044	1.3	0.0	-1.2	0.635	0.0	0.0	-0.2
PE 32:0	0.583	0.0	-0.1	-0.2	0.064	-0.1	-1.7	-0.3	0.220	0.0	-0.7	-0.1
PE 32:1	0.977	0.0	0.0	0.0	0.059	0.1	0.8	1.2	0.553	0.0	-0.2	0.0
PE 34:1	0.580	0.1	0.0	-0.3	0.100	-1.1	-0.4	0.2	0.009	-1.7	-1.8	0.0
PE 34:2	0.384	0.2	0.0	-0.7	0.322	-0.5	0.0	0.1	0.016	-1.9	-0.3	0.7
PE 34:3	0.466	0.3	0.2	-0.1	0.239	0.0	0.7	0.2	0.741	-0.1	0.0	0.0
PE 35:1	0.401	0.2	0.0	-0.6	0.184	-0.8	-0.3	0.1	0.130	-0.8	-0.4	0.1
PE 35:2	0.407	0.2	0.0	-0.5	0.960	0.0	0.0	0.0	0.486	-0.1	0.0	0.3
PE 36:1	0.407	0.1	-0.1	-0.4	0.247	-0.4	-0.3	0.1	0.004	-2.1	-2.3	0.0
PE 36:2	0.401	0.2	0.0	-0.6	0.347	-0.3	0.0	0.3	0.006	-2.4	-0.4	1.4
PE 36:3	0.366	0.1	-0.1	-0.9	0.597	0.0	-0.1	0.0	0.003	-2.8	-1.5	0.4
PE 36:4	0.366	0.0	-0.3	-0.8	0.056	-0.6	-1.8	0.0	0.012	-1.6	-1.6	0.0
PE 36:5	0.384	0.0	-0.3	-0.7	0.239	0.0	0.4	0.5	0.003	-2.1	-2.4	0.0
PE 38:3	0.401	0.0	-0.1	-0.6	0.150	-0.4	-0.9	0.0	0.002	-2.1	-3.0	-0.1
PE 38:4	0.366	0.0	-1.9	-1.1	0.394	-0.5	0.0	0.0	0.001	-3.2	-3.5	-0.1
PE 38:5	0.366	0.1	-1.1	-1.6	0.071	-1.1	-1.0	0.0	0.001	-3.1	-2.4	0.0
PE 38:6	0.402	0.0	-0.5	-0.2	0.032	-1.2	-2.0	0.0	0.005	-1.9	-2.3	0.0
PE 40:5	0.583	0.0	-0.1	-0.3	0.318	-0.2	-0.5	0.0	0.001	-2.2	-3.1	-0.7
PE 40:6	0.726	0.0	-0.1	0.0	0.396	-0.2	0.0	0.4	0.001	-1.7	-3.2	-0.4
PE 40:7	0.366	0.0	-0.4	-1.2	0.064	-1.0	-1.2	0.0	0.003	-2.6	-1.8	-0.4
PE(O-34:1)	0.407	0.0	-0.4	-0.3	0.094	0.0	-1.8	-0.2	0.037	-0.5	-1.6	-0.2
PE(O-36:4)	0.366	0.0	-1.1	-0.9	0.027	-0.3	-3.5	0.1	0.012	-1.4	-1.8	0.0
PE(O-36:5)	0.366	0.0	-1.1	-0.7	0.163	-0.1	-1.2	0.0	0.504	0.0	-0.4	0.0
PE(O-38:4)	0.384	0.0	-0.6	-0.2	0.020	0.0	-2.3	-1.5	0.011	-0.5	-2.2	-0.5
PE(O-38:5)	0.378	0.0	-0.5	-0.5	0.161	0.0	-1.4	-0.1	0.080	-0.9	-0.8	0.0
PE(O-40:4)	0.630	0.0	0.0	-0.3	0.383	0.0	-0.3	-0.3	0.069	-0.2	-1.3	-0.2
PE(O-40:5)	0.388	0.4	0.0	-0.5	0.197	0.0	-0.8	-0.3	0.240	-0.2	-0.7	0.0
PE(O-40:6)	0.674	0.0	0.0	-0.2	0.946	0.0	0.0	0.0	0.125	-0.2	-1.0	-0.1
PE(O-40:7)	0.366	-0.1	-0.9	-0.4	0.507	0.0	-0.4	0.0	0.090	-0.8	-0.7	0.1
PE(P-34:1)	0.454	0.3	0.0	-0.3	0.214	-0.4	-0.5	0.0	0.112	-0.9	-0.4	0.1
PE(P-36:1)	0.739	0.1	0.0	0.0	0.346	-0.1	-0.4	-0.1	0.084	-0.2	-1.3	-0.1
PE(P-36:4)	0.366	0.0	-0.5	-0.9	0.069	-0.6	-1.6	0.0	0.038	-0.8	-1.5	0.0
PE(P-37:4)	0.366	0.0	0.9	0.6	0.714	0.0	-0.1	-0.1	0.159	-0.4	0.0	0.7
PE(P-38:4)	0.392	0.0	-0.2	-0.6	0.042	-0.7	-2.1	0.0	0.010	-1.6	-1.8	0.0
PE(P-38:5)	0.366	0.0	-0.4	-0.7	0.038	-1.0	-2.0	0.0	0.031	-1.2	-1.2	0.0
PE(P-38:6)	0.407	0.0	-0.3	-0.3	0.038	-1.0	-2.0	0.1	0.015	-1.3	-1.7	0.0
PE(P-40:4)	0.954	0.0	0.0	0.0	0.986	0.0	0.0	0.0	0.489	-0.2	0.0	0.2
PE(P-40:5)	0.401	0.0	-0.3	-0.4	0.249	0.0	-0.6	-0.2	0.057	-0.4	-1.4	-0.1
PE(P-40:6)	0.580	0.0	-0.2	-0.2	0.049	-1.6	-0.9	-0.2	0.009	-1.4	-2.1	-0.1
LPE 16:0	0.980	0.0	0.0	0.0	0.163	-0.1	-0.7	-0.4	0.162	-0.7	-0.2	0.2
LPE 18:0	0.911	0.0	0.0	0.0	0.610	0.0	-0.1	-0.1	0.130	-0.8	-0.4	0.1
LPE 18:1	0.980	0.0	0.0	0.0	0.173	0.0	-0.6	-0.5	0.026	-1.6	-1.0	0.0
LPE 18:2	0.726	0.0	0.0	-0.3	0.098	-0.5	-1.0	-0.1	0.019	-1.8	-1.0	0.0
LPE 20:4	0.393	0.0	-0.3	-0.6	0.020	-1.2	-2.8	0.1	0.007	-2.0	-1.7	-0.2
LPE 22:6	0.424	0.0	-0.3	-0.3	0.019	-1.3	-2.8	-0.2	0.009	-1.8	-1.6	-0.2
PI 34:1	0.384	0.0	-0.1	-0.8	0.089	-1.0	-0.9	0.0	0.048	-1.1	-1.0	0.0
PI 36:1	0.407	0.1	0.0	-0.7	0.031	-1.6	-1.7	0.0	0.031	-1.3	-1.1	0.0
PI 36:2	0.510	0.0	0.0	-0.5	0.088	-0.9	-0.9	0.1	0.022	-1.5	-0.3	1.0
PI 36:3	0.798	0.0	-0.1	0.0	0.031	-1.3	-0.6	1.2	0.054	-0.9	0.0	1.2
PI 36:4	0.455	-0.2	-0.4	0.0	0.053	-1.3	-0.6	0.4	0.016	-1.3	-1.6	0.0

Lipid species	6 weeks				10 weeks				16 weeks			
	P-value[a]	db/h vs. H/H[b]	db/db vs. H/H[b]	db/db vs. db/h[b]	*P*-value[a]	db/h vs. H/H[b]	db/db vs. H/H[b]	db/db vs. db/h[b]	*P*-value[a]	db/h vs. H/H[b]	db/db vs. H/H[b]	db/db vs. db/h[b]
PI 38:3	0.411	0.0	-0.2	-0.4	0.163	-0.5	-0.3	0.4	0.005	-1.6	-2.3	-0.2
PI 38:4	0.407	0.0	-0.4	-0.3	0.058	-1.6	-0.8	0.0	0.009	-1.7	-1.9	0.0
PI 38:5	0.774	0.0	-0.1	0.0	0.065	-0.8	0.0	1.3	0.029	-1.2	-1.2	0.0
PI 40:4	0.655	0.0	-0.1	-0.2	0.160	-0.3	-0.8	-0.2	0.015	-1.2	-1.8	0.0
PI 40:5	0.562	0.0	-0.3	-0.1	0.093	-1.2	-0.7	0.0	0.175	-0.3	-0.8	0.0
PS 36:1	0.366	0.0	-1.1	-1.6	0.431	-0.2	-0.3	0.0	0.003	-2.7	-1.9	0.0
PS 36:2	0.366	0.3	-0.1	-1.8	0.152	-0.1	-0.9	-0.2	0.015	-1.9	-0.2	0.9
PS 38:3	0.366	0.2	-0.3	-1.2	0.622	0.0	0.1	-0.1	0.255	-0.4	-0.4	0.0
PS 38:4	0.366	0.1	-0.3	-1.2	0.334	0.0	0.5	0.2	0.086	-0.5	0.1	1.0
PS 38:5	0.933	0.0	0.0	0.0	0.045	0.0	1.8	0.7	0.003	0.0	2.9	2.1
PS 40:5	0.888	0.0	0.0	0.0	0.207	0.0	0.4	0.7	0.630	-0.1	-0.1	0.0
PS 40:6	0.858	0.0	0.0	0.0	0.192	0.0	0.5	0.6	0.850	-0.1	0.0	0.0
PG 34:1	0.440	0.0	-0.3	-0.3	0.081	-1.0	-0.9	0.0	0.002	-2.1	-2.8	0.0
PG 34:2	0.684	0.0	-0.1	-0.1	0.943	0.0	0.0	0.0	0.009	-1.2	-2.1	-0.3
PG 36:1	0.366	0.0	-0.8	-0.7	0.642	0.0	-0.2	0.0	0.024	-1.6	-0.8	-0.1
PG 36:2	0.843	0.0	0.0	0.0	0.531	0.0	0.0	0.2	0.005	-1.8	-2.3	0.0
BMP 18:1/18:1	0.366	1.6	0.8	-0.1	0.019	2.1	2.8	0.7	0.696	0.0	0.0	0.1
CL 18:2/18:2/18:2/16:1	0.401	0.6	0.1	-0.2	0.507	0.3	0.0	-0.1	0.007	-1.4	-1.9	-0.7
CL 18:2/18:1/18:2/16:1	0.977	0.0	0.0	0.0	0.989	0.0	0.0	0.0	0.005	-1.0	-2.1	-1.4
CL 18:2/18:2/18:2/18:2	0.366	0.0	-1.1	-1.6	0.036	-0.5	-2.0	-0.3	0.001	-3.2	-3.3	0.0
CL 18:2/18:2/18:2/18:1	0.366	0.0	-1.4	-2.0	0.091	-0.3	-0.9	-0.5	0.001	-3.6	-3.6	-0.4
CL 18:2/18:1/18:2/18:1	0.366	0.0	-1.2	-1.1	0.271	-0.2	-0.5	0.0	0.001	-3.6	-3.6	-0.5
CE 14:0	0.416	0.0	0.8	0.0	0.020	1.0	2.1	0.8	0.006	1.0	2.3	0.7
CE 16:0	0.476	0.3	0.0	-0.2	0.071	0.9	1.2	0.0	0.937	0.0	0.0	0.0
CE 16:1	0.575	0.1	0.3	0.0	0.019	0.4	2.4	1.3	0.001	1.3	3.1	1.3
CE 18:0	0.511	0.4	0.1	0.0	0.106	1.1	0.7	0.0	0.343	0.1	0.3	0.1
CE 18:1	0.366	0.1	-0.4	-0.6	0.568	0.1	0.2	0.0	0.085	0.0	0.8	0.9
CE 18:2	0.977	0.0	0.0	0.0	0.025	1.2	2.3	0.1	0.083	0.2	1.4	0.1
CE 18:3	0.977	0.0	0.0	0.0	0.019	1.3	3.0	0.5	0.001	1.7	3.2	1.0
CE 20:3	0.798	0.0	0.1	0.0	0.019	0.7	3.5	2.3	0.049	0.4	1.6	0.0
CE 20:4	0.932	0.0	0.0	0.0	0.019	1.2	3.0	0.2	0.021	0.8	1.8	0.1
CE 20:5	0.401	0.0	0.5	0.3	0.019	0.8	3.5	2.1	0.002	1.9	2.4	0.9
CE 22:0	0.366	0.0	0.9	0.9	0.122	0.9	0.7	0.0	0.001	2.4	2.9	1.0
CE 22:5	0.888	0.0	0.0	0.0	0.019	1.5	3.5	0.9	0.020	1.0	1.6	0.1
CE 22:6	0.540	0.2	0.3	0.0	0.019	1.3	3.0	0.5	0.004	1.6	2.3	0.5
CE 24:0	0.366	0.0	0.6	0.9	0.019	1.0	2.8	1.2	0.001	2.4	3.0	1.2
COH	0.401	0.6	0.0	-0.3	0.985	0.0	0.0	0.0	0.343	-0.2	0.0	0.3
DG 14:0/16:0	0.401	0.3	0.6	0.0	0.031	0.8	1.6	0.7	0.047	0.2	1.6	0.2
DG 14:0/18:1	0.366	0.0	1.1	0.2	0.023	0.8	1.7	1.1	0.001	1.2	3.6	0.8
DG 14:0/18:2	0.392	0.0	0.6	0.2	0.030	0.8	1.8	0.5	0.001	2.5	3.6	0.6
DG 16:0/16:0	0.378	0.7	0.3	0.0	0.052	0.4	1.3	0.5	0.048	0.0	1.6	0.5
DG 16:0/18:0	0.366	0.7	0.4	0.0	0.030	0.7	1.4	1.0	0.008	0.0	2.8	1.0
DG 16:0/18:1	0.378	0.1	0.8	0.2	0.021	0.8	1.8	1.1	0.001	1.4	3.6	1.6
DG 16:0/18:2	0.384	0.0	0.8	0.2	0.031	0.8	1.8	0.4	0.001	2.6	3.6	1.1
DG 16:0/20:4	0.466	0.0	0.3	0.2	0.053	0.6	1.3	0.3	0.002	1.2	2.8	1.2
DG 16:1/18:0	0.366	0.0	1.1	0.4	0.019	0.9	1.8	1.4	0.001	0.6	3.6	1.3
DG 16:1/18:1	0.366	0.1	1.1	0.1	0.020	0.9	1.7	1.4	0.001	1.0	3.6	1.2
DG 18:0/18:1	0.366	0.1	1.2	0.1	0.020	0.8	1.8	1.4	0.002	0.4	3.6	1.2
DG 18:0/18:2	0.401	0.1	0.8	0.0	0.024	0.8	1.8	0.9	0.001	1.2	3.6	1.1
DG 18:0/20:4	0.366	0.1	0.5	0.5	0.024	1.3	2.4	0.0	0.001	2.1	2.8	0.8
DG 18:1/18:1	0.366	0.0	1.2	0.1	0.021	0.8	1.7	1.3	0.001	0.7	3.6	1.2
DG 18:1/18:2	0.504	0.0	0.4	0.0	0.031	0.8	1.7	0.5	0.001	1.2	3.6	1.2
DG 18:1/18:3	0.407	0.0	0.6	0.1	0.034	0.8	1.6	0.5	0.001	1.2	3.6	1.2
DG 18:1/20:0	0.401	0.2	0.6	0.0	0.038	0.9	1.7	0.2	0.001	2.3	3.6	0.1

Lipid species	6 weeks				10 weeks				16 weeks			
	P-value[a]	db/h vs. H/H[b]	db/db vs. H/H[b]	db/db vs. db/h[b]	*P*-value[a]	db/h vs. H/H[b]	db/db vs. H/H[b]	db/db vs. db/h[b]	*P*-value[a]	db/h vs. H/H[b]	db/db vs. H/H[b]	db/db vs. db/h[b]
DG 18:1/20:3	0.511	0.1	0.4	0.0	0.019	1.0	1.7	1.5	0.001	1.5	3.6	1.0
DG 18:1/20:4	0.684	0.0	0.1	0.0	0.043	0.3	1.4	0.7	0.016	0.1	2.1	0.7
DG 18:2/18:2	0.621	0.0	0.3	0.0	0.042	0.8	1.6	0.3	0.001	1.6	3.6	1.0
TG 14:0/16:0/18:1	0.366	0.0	0.4	0.7	0.020	0.7	2.4	0.9	0.007	1.7	1.8	0.3
TG 14:0/16:0/18:2	0.378	0.0	0.3	0.7	0.019	0.7	2.4	1.2	0.003	2.3	2.1	0.4
TG 14:0/16:1/18:1	0.366	0.0	0.4	0.8	0.019	0.9	2.6	1.3	0.001	2.7	2.8	0.6
TG 14:0/16:1/18:2	0.366	0.0	0.4	0.8	0.019	0.9	2.6	0.9	0.001	3.2	2.9	0.6
TG 14:0/17:0/18:1	0.366	0.0	0.4	0.7	0.021	0.7	2.4	0.6	0.003	2.4	2.0	0.4
TG 14:0/18:0/18:1	0.366	0.0	0.4	0.7	0.019	0.7	2.4	1.0	0.012	1.1	1.8	0.3
TG 14:0/18:2/18:2	0.366	0.0	0.4	0.8	0.020	0.9	2.6	0.6	0.001	3.2	2.7	0.4
TG 14:1/16:0/18:1	0.366	0.0	0.3	0.8	0.019	0.7	2.4	1.2	0.002	2.5	2.3	0.6
TG 14:1/16:1/18:0	0.378	0.0	0.3	0.7	0.019	0.9	2.6	1.5	0.001	2.6	2.6	0.6
TG 14:1/18:1/18:1	0.366	0.0	0.5	0.6	0.019	0.9	2.6	1.4	0.001	3.1	3.1	0.7
TG 15:0/16:0/18:1	0.366	0.0	0.4	0.8	0.020	0.7	2.4	0.7	0.006	1.9	1.9	0.3
TG 15:0/18:1/18:1	0.366	0.0	0.4	0.8	0.019	0.8	2.6	0.7	0.001	3.1	2.8	0.9
TG 16:0/16:0/16:0	0.366	0.0	0.9	0.4	0.021	0.7	2.1	0.9	0.120	0.6	0.7	0.0
TG 16:0/16:0/18:0	0.366	0.0	0.9	0.5	0.019	0.4	2.6	1.3	0.085	0.0	1.0	0.6
TG 16:0/16:0/18:1	0.384	0.0	0.4	0.5	0.022	0.6	2.3	0.7	0.006	1.6	1.9	0.6
TG 16:0/16:0/18:2	0.384	0.0	0.3	0.7	0.025	0.7	2.3	0.5	0.006	1.6	2.0	0.4
TG 16:0/16:1/17:0	0.366	0.0	0.4	0.7	0.020	0.7	2.4	0.7	0.004	2.0	2.0	0.4
TG 16:0/16:1/18:1	0.378	0.0	0.3	0.7	0.019	0.8	2.8	1.3	0.001	2.5	2.8	0.7
TG 16:0/17:0/18:0	0.366	0.2	0.9	0.6	0.031	0.5	2.3	0.3	0.004	2.4	1.9	0.0
TG 16:0/17:0/18:1	0.366	0.0	0.4	0.7	0.020	0.5	2.4	0.9	0.003	2.3	2.1	0.6
TG 16:0/17:0/18:2	0.366	0.0	0.3	0.8	0.019	0.9	2.6	0.8	0.002	2.7	2.2	0.5
TG 16:0/18:0/18:1	0.392	0.0	0.3	0.5	0.019	0.5	2.6	1.0	0.009	1.0	2.0	0.6
TG 16:0/18:1/18:1	0.366	0.0	0.4	0.8	0.019	0.8	2.8	0.9	0.001	2.5	2.6	1.0
TG 16:0/18:1/18:2	0.366	0.0	0.3	0.8	0.019	1.0	2.6	0.6	0.001	2.9	2.6	0.7
TG 16:0/18:2/18:2	0.378	0.0	0.3	0.8	0.020	0.9	2.6	0.4	0.001	2.9	2.3	0.6
TG 16:1/16:1/16:1	0.366	0.0	0.4	0.8	0.019	0.9	2.6	1.5	0.001	3.0	3.1	0.5
TG 16:1/16:1/18:0	0.384	0.0	0.3	0.7	0.019	0.9	2.6	1.5	0.006	1.7	1.9	0.4
TG 16:1/16:1/18:1	0.366	0.0	0.4	0.8	0.019	0.9	2.6	1.3	0.001	2.9	3.1	0.7
TG 16:1/17:0/18:1	0.366	0.0	0.4	0.8	0.019	0.9	2.6	0.9	0.001	3.1	2.8	0.7
TG 16:1/18:1/18:1	0.366	0.0	0.6	0.7	0.019	0.9	2.8	1.4	0.001	2.9	3.2	1.0
TG 16:1/18:1/18:2	0.366	0.0	0.6	0.8	0.019	0.9	2.6	1.0	0.001	3.2	3.2	1.1
TG 17:0/18:1/18:1	0.366	0.0	0.3	0.8	0.019	0.7	2.8	1.0	0.001	2.6	2.6	0.9
TG 18:0/18:0/18:0	0.384	0.2	0.6	0.1	0.019	0.4	2.6	1.7	0.009	0.0	1.8	1.9
TG 18:0/18:0/18:1	0.401	0.0	0.3	0.4	0.019	0.5	2.6	1.0	0.009	1.0	1.9	0.9
TG 18:0/18:1/18:1	0.378	0.0	0.3	0.7	0.019	0.8	3.0	1.2	0.002	1.6	2.6	1.1
TG 18:0/18:2/18:2	0.366	0.0	0.4	0.8	0.019	1.1	2.8	0.5	0.001	2.9	2.5	0.9
TG 18:1/18:1/18:1	0.366	0.1	0.6	0.6	0.019	0.8	2.8	0.8	0.001	3.1	3.3	1.2
TG 18:1/18:1/18:2	0.366	0.0	0.6	0.7	0.019	0.8	2.6	0.7	0.001	3.2	3.5	1.0
TG 18:1/18:1/20:4	0.366	0.1	0.9	0.8	0.020	0.8	2.3	0.9	0.001	3.2	3.5	1.0
TG 18:1/18:2/18:2	0.366	0.0	0.5	0.8	0.020	0.9	2.6	0.6	0.001	3.2	3.3	1.1
TG 18:2/18:2/18:2	0.366	0.0	0.3	0.9	0.021	1.0	2.4	0.4	0.001	3.2	3.3	0.7

[a] *P*-value for the comparison of levels of each lipid species between genotypes at each age using the Kruskal Wallis test with Benjamini-Hochberg correction for multiple comparisons. $P < 0.05$ was considered significant (highlighted in pink).

[b] Post-hoc analysis was performed using the Mann Whitney *U* test with Dunn-Sidak correction for multiple group comparisons. Values were derived from the formula: sign(difference in median levels)*-log10(post-hoc *P*-value). Colour-coded values 1.3 to 2.0 (light red, $P = 0.05$-0.01) and > 2.0 (dark red, $P < 0.01$) indicate a significant increase relative to the reference group. Colour-coded values -1.3 to -2.0 (light green, $P = 0.05$-0.01) and < -2.0 (dark green, $P < 0.01$) indicate a significant decrease relative to the reference group.

Table S4.5 Relationship between genotype and plasma lipid species in male mice.

Lipid species	6 weeks				10 weeks				16 weeks			
	P-value[a]	db/h vs. H/H[b]	db/db vs. H/H[b]	db/db vs. db/h[b]	*P*-value[a]	db/h vs. H/H[b]	db/db vs. H/H[b]	db/db vs. db/h[b]	*P*-value[a]	db/h vs. H/H[b]	db/db vs. H/H[b]	db/db vs. db/h[b]
Sph 18:1	0.151	0.0	-0.8	-0.6	0.909	0.0	0.0	0.0	0.631	0.0	0.2	0.0
Cer 16:0	0.031	0.8	2.0	0.7	0.136	-0.2	0.5	1.2	0.021	0.2	3.2	1.9
Cer 18:0	0.830	0.0	0.0	0.0	0.081	0.0	1.1	1.4	0.065	-0.1	1.5	1.6
Cer 20:0	0.035	1.8	1.4	0.2	0.645	0.0	0.3	0.1	0.076	0.0	1.5	1.4
Cer 22:0	0.043	1.7	1.2	0.1	0.954	0.0	0.0	0.0	0.484	0.3	0.2	0.0
Cer 24:0	0.039	1.1	1.2	0.8	0.778	0.0	0.0	0.2	0.352	0.6	0.0	-0.3
Cer 24:1	0.061	0.5	1.2	0.6	0.173	0.0	0.7	0.9	0.407	0.5	0.1	-0.1
MHC 16:0	0.139	0.4	0.9	0.0	0.542	-0.1	0.0	0.5	0.316	0.7	0.0	-0.2
MHC 18:0	0.981	0.0	0.0	0.0	0.079	-0.5	0.4	1.6	0.603	0.0	0.2	0.1
MHC 20:0	0.067	1.1	1.1	0.0	0.235	0.0	0.8	0.5	0.167	0.0	1.0	0.8
MHC 22:0	0.031	2.0	1.8	0.0	0.843	0.0	0.1	0.0	0.305	0.8	0.0	-0.2
MHC 24:0	0.043	1.2	1.6	0.2	0.808	0.0	0.0	0.2	0.113	0.6	-0.3	-1.4
MHC 24:1	0.039	1.6	1.6	0.0	0.760	0.0	0.1	0.2	0.095	0.9	-0.3	-1.4
SM 31:1	0.103	0.1	1.1	0.6	0.136	0.1	0.9	0.9	0.352	0.0	0.5	0.4
SM 32:1	0.059	0.3	1.6	0.6	0.059	0.0	0.8	1.9	0.062	-0.3	1.3	1.9
SM 32:2	0.024	1.2	2.2	1.1	0.017	0.0	2.1	2.3	0.113	0.6	1.3	0.4
SM 33:1	0.072	0.5	1.2	0.3	0.429	0.0	0.1	0.7	0.279	0.0	0.5	0.6
SM 34:1	0.187	0.4	0.6	0.0	0.284	-0.1	0.1	0.9	0.113	0.0	0.9	1.5
SM 34:2	0.036	1.8	1.6	0.0	0.990	0.0	0.0	0.0	0.400	0.5	0.2	0.0
SM 34:3	0.024	2.0	3.0	1.3	0.040	0.3	1.6	1.5	0.073	0.2	2.2	0.4
SM 35:1	0.574	0.1	0.2	0.0	0.428	-0.4	0.0	0.5	0.192	-0.1	0.5	1.0
SM 35:2	0.295	0.3	0.4	0.0	0.791	0.0	0.0	0.2	0.451	0.0	0.2	0.4
SM 36:1	0.384	0.0	0.0	-0.4	0.719	0.0	0.0	0.2	0.306	-0.6	0.0	0.4
SM 36:2	0.217	0.5	0.4	0.0	0.617	0.0	0.1	0.4	0.246	0.0	0.5	0.7
SM 36:3	0.024	2.0	2.4	0.2	0.077	0.0	0.9	1.7	0.021	-0.1	2.5	2.8
SM 37:2	0.045	1.1	2.0	0.0	0.742	-0.2	0.0	0.0	0.262	0.6	0.0	-0.6
SM 38:1	0.041	1.6	1.6	0.0	0.679	0.0	0.1	0.2	0.623	0.1	0.1	0.0
SM 38:2	0.052	1.4	1.2	0.0	0.791	0.0	0.0	0.1	0.927	0.0	0.0	0.0
SM 39:1	0.061	1.4	0.8	0.0	0.854	0.0	0.0	0.0	0.443	0.0	-0.2	-0.4
SM 41:1	0.024	1.8	2.4	0.1	0.742	0.0	0.0	0.2	0.477	0.4	0.0	-0.1
SM 41:2	0.043	1.7	1.2	0.0	0.882	0.0	0.0	0.0	0.256	0.2	-0.3	-0.6
SM 42:1	0.051	1.6	1.1	0.0	0.975	0.0	0.0	0.0	0.502	0.0	-0.1	-0.3
PC 24:0	0.223	0.0	0.7	0.3	0.920	0.0	0.0	0.0	0.509	0.0	0.3	0.2
PC 28:0	0.228	0.0	0.5	0.4	0.607	-0.4	0.0	0.2	0.429	0.1	0.5	0.0
PC 29:0	0.130	0.0	0.7	0.7	0.889	0.0	0.0	0.0	0.361	0.3	0.4	0.0
PC 30:0	0.024	0.7	2.0	1.6	0.677	0.0	0.1	0.2	0.636	0.1	0.0	-0.1
PC 31:0	0.107	0.8	0.3	-0.5	0.295	0.0	-0.4	-0.7	0.140	0.2	-0.8	-1.0
PC 31:1	0.152	0.2	0.9	0.2	0.459	-0.1	0.1	0.5	0.569	0.1	0.2	0.0
PC 32:0	0.049	1.6	0.9	-0.1	0.742	0.0	0.0	-0.2	0.274	0.0	-0.5	-0.6
PC 32:1	0.024	1.1	2.0	1.6	0.021	0.5	2.4	1.4	0.349	0.6	0.2	0.0
PC 32:2	0.062	0.7	1.2	0.3	0.150	0.0	0.8	0.9	0.167	0.9	0.9	0.0
PC 32:3	0.024	1.8	2.7	0.4	0.136	0.0	0.8	1.2	0.079	0.2	1.9	0.6
PC 33:0	0.281	0.4	0.3	0.0	0.771	0.0	-0.1	0.0	0.073	0.3	-0.8	-1.9
PC 33:1	0.031	0.9	1.6	1.0	0.692	0.2	0.2	0.0	0.056	1.5	-0.4	-1.9
PC 33:2	0.083	0.8	1.1	0.0	0.157	0.0	-0.9	-0.9	0.167	1.0	0.0	-0.7
PC 33:3	0.068	0.4	1.4	0.3	0.635	0.2	0.0	-0.2	0.474	0.1	0.4	0.0
PC 34:0	0.062	0.8	1.2	0.2	0.559	0.0	0.2	0.4	0.893	0.0	0.0	0.0
PC 34:1	0.025	1.3	2.2	0.6	0.125	0.1	1.1	0.9	0.569	0.4	0.0	-0.1
PC 34:2	0.026	1.7	1.6	0.7	0.920	0.0	0.0	0.0	0.106	0.5	1.6	0.2
PC 34:3	0.024	1.4	2.2	0.8	0.458	0.0	0.5	0.2	0.073	1.3	1.5	-0.2
PC 34:4	0.025	0.8	1.6	1.9	0.177	0.1	1.0	0.5	0.167	0.8	0.8	-0.1
PC 34:5	0.024	0.2	2.4	1.8	0.010	0.1	2.6	2.4	0.389	0.0	0.5	0.2

Lipid species	6 weeks				10 weeks				16 weeks			
	P-value[a]	db/h vs. H/H[b]	db/db vs. H/H[b]	db/db vs. db/h[b]	*P*-value[a]	db/h vs. H/H[b]	db/db vs. H/H[b]	db/db vs. db/h[b]	*P*-value[a]	db/h vs. H/H[b]	db/db vs. H/H[b]	db/db vs. db/h[b]
PC 35:0	0.060	0.0	1.2	1.2	0.811	-0.1	0.0	0.0	0.073	1.1	-0.1	-1.8
PC 35:1	0.050	0.1	1.4	1.2	0.640	0.0	0.1	0.4	0.275	0.8	0.0	-0.3
PC 35:2	0.072	0.0	0.8	1.3	0.679	-0.1	0.0	0.2	0.079	0.8	1.6	0.3
PC 35:3	0.061	0.5	1.4	0.4	0.791	0.0	-0.1	0.0	0.073	1.9	0.5	-0.4
PC 35:4	0.094	0.8	0.4	-0.4	0.089	0.0	-0.9	-1.4	0.861	0.0	0.0	0.0
PC 36:0	0.056	0.3	1.4	0.9	0.089	0.0	0.8	1.5	0.255	0.1	0.7	0.4
PC 36:1	0.024	1.0	2.4	0.9	0.008	0.0	2.6	2.8	0.150	0.4	1.0	0.6
PC 36:2	0.029	0.3	1.8	1.9	0.050	0.0	0.8	2.3	0.045	0.8	2.2	1.9
PC 36:3	0.025	0.2	2.0	2.1	0.040	0.0	1.8	1.6	0.065	0.6	1.9	0.8
PC 36:4a	0.037	0.3	1.8	1.3	0.268	0.0	0.1	1.1	0.054	1.9	1.8	1.0
PC 36:4b	0.049	1.6	0.4	-0.6	0.222	0.7	0.0	-0.8	0.501	0.2	0.0	-0.2
PC 36:5	0.024	0.7	2.4	1.5	0.003	0.0	4.1	3.0	0.092	0.4	1.7	0.4
PC 36:6	0.024	0.4	2.4	1.6	0.006	0.4	3.3	2.5	0.189	1.0	0.6	0.0
PC 37:4	0.228	0.3	0.0	-0.6	0.019	0.0	-2.4	-1.8	0.763	0.0	0.1	0.1
PC 37:5	0.104	0.0	0.6	1.1	0.860	0.0	0.0	0.0	0.476	0.3	0.0	-0.2
PC 37:6	0.128	0.7	0.0	-0.6	0.079	0.0	-1.6	-1.1	0.021	2.4	-0.5	-2.9
PC 38:2	0.030	0.5	1.8	1.5	0.245	0.0	0.7	0.7	0.218	1.0	0.0	-0.4
PC 38:3	0.024	0.5	2.4	1.9	0.010	0.0	2.8	2.3	0.087	0.5	1.3	1.0
PC 38:4	0.060	1.8	0.3	-0.1	0.889	0.0	0.0	0.0	0.307	0.1	0.6	0.1
PC 38:5	0.024	0.6	2.4	2.4	0.059	0.1	2.0	0.9	0.129	0.6	1.4	0.1
PC 38:6a	0.024	0.2	2.0	2.4	0.086	0.4	1.7	0.5	0.140	0.4	1.3	0.2
PC 38:6b	0.062	1.7	0.4	-0.1	0.256	0.4	0.0	-0.9	0.622	0.2	0.0	-0.1
PC 38:7	0.024	1.4	3.0	1.6	0.021	0.8	2.3	1.4	0.118	1.3	1.0	0.0
PC 39:6	0.278	0.4	0.3	0.0	0.428	-0.1	-0.5	-0.1	0.246	0.3	0.6	0.3
PC 39:7	0.148	0.5	0.7	0.0	0.285	0.0	-0.4	-0.8	0.057	2.7	0.1	-0.7
PC 40:5	0.036	0.6	1.8	1.0	0.017	0.0	2.1	2.3	0.065	0.3	1.7	1.3
PC 40:6	0.127	0.9	0.5	0.0	0.194	0.0	0.5	1.0	0.136	0.5	1.1	0.5
PC 40:7	0.024	2.1	2.7	1.2	0.136	0.2	1.3	0.4	0.167	1.0	0.8	0.0
PC(O-30:0)	0.024	1.2	2.4	0.8	0.944	0.0	0.0	0.0	0.092	0.1	-0.6	-1.9
PC(O-32:0)	0.041	1.6	0.3	-1.0	0.117	0.0	-0.9	-1.2	0.056	0.0	-1.4	-2.3
PC(O-32:1)	0.050	0.0	1.2	1.6	0.730	-0.2	0.0	0.1	0.407	0.5	0.1	0.0
PC(O-32:1)	0.027	1.0	2.0	0.9	0.329	0.2	0.7	0.2	0.256	0.7	0.0	-0.6
PC(O-34:0)	0.217	0.4	0.0	-0.6	0.066	-0.1	-2.0	-0.8	0.087	0.0	-1.3	-1.5
PC(O-34:1)	0.151	0.8	0.3	0.0	0.552	0.0	-0.4	-0.2	0.065	0.1	-0.9	-2.3
PC(O-34:2)	0.080	0.4	1.2	0.3	0.674	-0.3	-0.1	0.0	0.167	0.0	-0.4	-1.4
PC(O-34:3)	0.105	0.0	1.4	0.5	0.065	-1.6	-1.6	0.0	0.289	0.0	-0.1	-1.0
PC(O-34:4)	0.026	1.0	2.2	0.8	0.216	0.0	0.4	0.9	0.256	0.0	0.5	0.7
PC(O-35:4)	0.255	0.1	0.4	0.3	0.997	0.0	0.0	0.0	0.784	0.0	0.1	0.0
PC(O-36:0)	0.887	0.0	0.0	0.0	0.265	-0.4	-1.0	0.0	0.223	-0.1	-0.8	-0.5
PC(O-36:1)	0.804	0.0	0.0	0.0	0.617	-0.6	0.0	0.0	0.076	0.0	-1.2	-1.8
PC(O-36:2)	0.072	0.3	1.4	0.5	0.676	-0.3	-0.1	0.0	0.305	0.0	-0.4	-0.7
PC(O-36:3)	0.098	0.4	0.9	0.3	0.796	0.0	0.0	0.1	0.978	0.0	0.0	0.0
PC(O-36:4)	0.062	1.1	1.2	0.0	0.981	0.0	0.0	0.0	0.940	0.0	0.0	0.0
PC(O-36:5)	0.049	0.1	1.6	1.2	0.023	-0.1	1.3	2.4	0.169	0.0	0.9	0.8
PC(O-38:4)	0.068	1.0	1.2	0.0	0.400	-0.1	-0.7	0.1	0.279	0.0	-0.3	-0.9
PC(O-38:5)	0.269	0.5	0.3	0.0	0.782	0.1	0.0	-0.1	0.451	0.0	0.2	0.4
PC(O-40:6)	0.083	0.5	0.9	0.4	0.649	0.0	-0.5	0.0	0.056	0.0	1.8	2.1
PC(O-40:7)	0.073	1.1	0.3	-0.5	0.216	0.5	0.0	-0.9	0.672	0.0	0.0	0.1
PC(P-32:0)	0.078	1.2	0.0	-0.6	0.125	0.0	-0.6	-1.4	0.073	-0.1	-1.3	-1.6
PC(P-32:1)	0.349	0.1	0.4	0.0	0.786	0.0	0.0	0.2	0.264	0.0	-0.4	-0.8
PC(P-34:0)	0.123	0.9	0.4	0.0	0.015	-0.3	-4.1	-0.9	0.192	-0.2	-0.9	-0.4
PC(P-34:1)	0.180	0.7	0.4	0.0	0.635	0.2	0.0	-0.2	0.065	0.0	-1.3	-1.9
PC(P-34:2)	0.039	0.5	1.6	1.1	0.635	-0.1	0.0	0.4	0.167	0.3	-0.1	-1.3
PC(P-34:3)	0.043	0.6	1.8	0.6	0.550	-0.3	0.0	0.3	0.509	0.0	-0.2	-0.2

Lipid species	6 weeks				10 weeks				16 weeks			
	P-value[a]	db/h vs. H/H[b]	db/db vs. H/H[b]	db/db vs. db/h[b]	*P*-value[a]	db/h vs. H/H[b]	db/db vs. H/H[b]	db/db vs. db/h[b]	*P*-value[a]	db/h vs. H/H[b]	db/db vs. H/H[b]	db/db vs. db/h[b]
PC(P-36:2)	0.037	0.6	2.0	0.7	0.536	-0.6	0.0	0.1	0.167	0.2	-0.2	-1.4
PC(P-36:4)	0.205	0.6	0.3	0.0	0.269	-0.6	-0.3	0.4	0.429	-0.1	0.1	0.3
PC(P-36:5)	0.039	0.0	2.0	1.5	0.007	-0.1	2.6	2.8	0.113	0.0	0.9	1.6
PC(P-38:4)	0.408	0.2	0.3	0.0	0.784	-0.1	0.0	0.1	0.940	0.0	0.0	0.0
PC(P-38:5)	0.077	1.2	0.7	0.0	0.808	0.0	0.0	-0.1	0.564	0.0	-0.2	-0.2
PC(P-40:5)	0.269	0.5	0.2	0.0	0.333	0.0	-0.8	-0.2	0.065	0.1	-1.0	-2.2
PC(P-40:6)	0.180	0.8	0.1	-0.2	0.040	-0.3	-2.4	-0.9	0.056	0.0	-1.5	-2.3
LPC 14:0	0.024	0.4	2.2	1.9	0.019	0.4	2.0	2.0	0.940	0.0	0.0	0.0
LPC 15:0	0.335	0.1	0.3	0.1	0.491	0.2	0.0	-0.5	0.256	0.6	0.0	-0.6
LPC 16:0	0.036	0.8	2.0	0.6	0.172	0.4	0.8	0.5	0.672	0.1	0.1	0.0
LPC 16:1	0.024	0.7	2.2	1.6	0.003	1.3	3.5	2.5	0.218	0.9	0.5	0.0
LPC 17:0	0.073	0.0	1.1	1.0	0.678	0.0	0.3	0.1	0.167	0.5	1.0	0.2
LPC 17:1	0.037	0.3	1.8	1.2	0.089	0.4	1.3	0.8	0.192	1.0	0.0	-0.4
LPC 18:0	0.027	0.8	2.0	1.1	0.040	0.0	1.6	1.7	0.056	0.3	1.7	1.8
LPC 18:1	0.031	0.5	1.8	1.5	0.010	0.2	3.0	2.3	0.484	0.0	0.3	0.2
LPC 18:2	0.062	0.0	1.1	1.2	0.089	0.0	1.1	1.3	0.167	0.0	0.8	1.0
LPC 18:3	0.062	0.3	1.6	0.6	0.079	0.0	1.1	1.4	0.414	0.1	0.4	0.1
LPC 20:0	0.057	1.1	1.4	0.0	0.371	0.2	0.0	-0.8	0.021	2.2	-0.6	-2.9
LPC 20:1	0.025	0.7	2.4	1.1	0.065	0.4	2.1	0.5	0.065	2.2	0.0	-1.1
LPC 20:2	0.046	0.0	1.4	1.6	0.010	0.3	3.0	1.9	0.509	0.4	0.1	0.0
LPC 20:3	0.067	0.0	1.1	1.2	0.011	0.2	2.8	2.0	0.442	0.0	0.3	0.2
LPC 20:4	0.802	0.0	0.0	0.0	0.679	0.3	0.1	0.0	0.965	0.0	0.0	0.0
LPC 20:5	0.043	-0.2	1.4	1.5	0.003	0.0	3.8	3.2	0.113	0.0	1.4	1.0
LPC 22:0	0.037	0.8	1.6	0.8	0.932	0.0	0.0	0.0	0.202	0.5	-0.1	-0.8
LPC 22:1	0.081	0.5	1.2	0.2	0.719	0.1	0.0	-0.2	0.021	2.4	-0.6	-3.0
LPC 22:4	0.139	0.1	0.8	0.4	0.154	0.1	1.3	0.4	0.901	0.0	0.0	0.0
LPC 22:5	0.082	0.1	1.1	0.8	0.025	0.0	1.7	2.1	0.284	0.0	0.6	0.5
LPC 22:6	0.568	0.0	0.3	0.0	0.736	0.1	0.1	0.0	0.949	0.0	0.0	0.0
LPC 24:0	0.078	0.6	1.1	0.2	0.931	0.0	0.0	0.0	0.416	0.1	-0.2	-0.3
LPC(O-16:0)	0.061	0.8	1.1	0.4	0.654	0.3	0.1	0.0	0.284	0.4	0.0	-0.7
LPC(O-18:0)	0.205	0.3	0.4	0.3	0.757	0.0	-0.2	0.0	0.056	0.4	-1.0	-2.3
LPC(O-18:1)	0.278	0.0	0.5	0.2	0.736	0.1	0.1	0.0	0.307	0.8	0.0	-0.2
LPC(O-20:0)	0.159	0.1	0.6	0.5	0.936	0.0	0.0	0.0	0.407	0.1	-0.1	-0.4
LPC(O-22:0)	0.488	0.0	0.3	0.1	0.508	0.0	0.5	0.2	0.167	1.3	0.0	-0.5
LPC(O-22:1)	0.228	0.1	0.4	0.4	0.954	0.0	0.0	0.0	0.337	0.6	0.0	-0.3
LPC(O-24:1)	0.127	0.8	0.6	0.0	0.969	0.0	0.0	0.0	0.167	0.0	-0.8	-1.1
PE 34:1	0.044	1.4	1.6	0.0	0.889	0.0	0.0	0.0	0.719	0.1	0.0	-0.1
PE 34:2	0.041	1.8	1.1	-0.1	0.846	0.0	0.0	-0.1	0.504	0.2	0.2	0.0
PE 36:1	0.024	2.6	2.4	0.0	0.702	-0.1	0.0	0.2	0.768	0.0	0.1	0.0
PE 36:2	0.037	2.0	1.2	0.0	0.776	-0.1	0.0	0.1	0.307	0.1	0.8	0.1
PE 36:3	0.024	2.6	1.6	-0.2	0.962	0.0	0.0	0.0	0.472	0.2	0.3	0.0
PE 36:4	0.024	2.8	0.8	-0.6	0.649	0.0	-0.1	-0.3	0.407	0.5	0.1	0.0
PE 38:3	0.024	3.5	1.2	-0.2	0.776	0.0	0.0	-0.2	0.594	0.2	0.1	0.0
PE 38:4	0.024	3.5	0.7	-0.6	0.450	0.0	-0.5	-0.3	0.569	0.0	0.3	0.0
PE 38:5	0.024	3.5	1.4	-0.3	0.689	0.1	0.0	-0.2	0.474	0.1	0.4	0.0
PE 38:6	0.024	3.0	0.5	-0.7	0.036	0.0	-1.7	-1.8	0.575	0.2	0.0	-0.1
PE 40:5	0.031	2.0	1.6	0.0	0.839	0.1	0.0	0.0	0.564	0.0	0.3	0.1
PE 40:6	0.024	4.1	0.7	-1.1	0.245	0.0	-0.5	-0.8	0.706	0.0	0.1	0.0
PE 40:7	0.036	2.1	0.4	-0.6	0.143	0.0	-0.6	-1.2	0.692	0.1	0.1	0.0
PE(O-34:1)	0.060	0.3	1.2	0.9	0.677	0.0	0.2	0.2	0.141	0.6	-0.1	-1.3
PE(O-34:2)	0.179	0.4	0.5	-0.2	0.679	0.0	-0.2	-0.1	0.054	1.1	-1.0	-2.4
PE(O-36:2)	0.062	0.4	1.2	0.7	0.520	-0.1	0.0	0.5	0.744	0.1	0.0	0.0
PE(O-36:3)	0.124	0.2	0.9	0.3	0.782	0.0	0.0	0.1	0.476	0.0	-0.2	-0.3
PE(O-36:4)	0.061	1.0	1.1	0.2	0.889	0.0	0.0	0.0	0.895	0.0	0.0	-0.1

Lipid species	6 weeks				10 weeks				16 weeks			
	P-value[a]	db/h vs. H/H[b]	db/db vs. H/H[b]	db/db vs. db/h[b]	*P*-value[a]	db/h vs. H/H[b]	db/db vs. H/H[b]	db/db vs. db/h[b]	*P*-value[a]	db/h vs. H/H[b]	db/db vs. H/H[b]	db/db vs. db/h[b]
PE(O-38:4)	0.054	0.7	1.4	0.5	0.679	0.0	0.0	0.3	0.122	-0.1	0.9	1.2
PE(O-38:5)	0.043	0.2	1.8	1.1	0.089	-0.1	0.7	1.4	0.305	0.5	0.5	0.0
PE(O-40:4)	0.145	0.4	0.8	0.1	0.443	0.0	0.1	0.7	0.122	0.0	0.8	1.6
PE(O-40:5)	0.054	0.1	1.4	1.1	0.147	0.0	0.8	1.0	0.134	0.1	1.2	0.8
PE(O-40:7)	0.072	0.4	1.4	0.3	0.579	0.3	0.3	0.0	0.628	-0.1	0.0	0.2
PE(O-42:7)	0.193	0.3	0.6	0.2	0.635	0.1	0.3	0.1	0.722	0.0	0.2	0.0
PE(P-36:1)	0.062	0.4	1.2	0.7	0.520	-0.1	0.0	0.5	0.744	0.1	0.0	0.0
PE(P-36:2)	0.044	0.4	1.4	1.1	0.654	0.0	0.1	0.3	0.845	0.0	0.0	0.0
PE(P-36:4)	0.026	2.3	1.8	0.0	0.782	0.0	-0.1	0.0	0.735	-0.1	0.0	-0.1
PE(P-38:4)	0.115	0.8	0.8	0.0	0.733	-0.1	0.0	0.2	0.964	0.0	0.0	0.0
PE(P-38:5)	0.104	0.9	0.7	0.0	0.936	0.0	0.0	0.0	0.355	0.0	-0.2	-0.6
PE(P-38:6)	0.031	2.6	0.9	0.0	0.605	-0.1	-0.4	0.0	0.715	-0.1	0.1	0.0
PE(P-40:4)	0.058	0.4	1.1	1.0	0.137	0.0	0.6	1.3	0.092	-0.2	0.7	1.7
PE(P-40:5)	0.096	0.3	0.8	0.6	0.782	0.0	0.0	0.2	0.843	0.0	0.0	0.1
PE(P-40:6)	0.276	0.5	0.2	0.0	0.875	-0.1	0.0	0.0	0.407	0.1	-0.1	-0.4
LPE 16:0	0.024	1.8	2.0	0.5	0.379	0.0	0.5	0.4	0.768	0.0	0.0	-0.1
LPE 18:0	0.031	1.3	1.6	0.6	0.080	0.0	0.8	1.7	0.192	0.0	1.0	0.6
LPE 18:1	0.051	0.2	1.6	1.0	0.040	-0.1	1.0	2.0	0.171	0.0	1.0	0.7
LPE 18:2	0.068	0.1	1.2	0.8	0.157	-0.1	0.1	1.4	0.138	0.1	1.3	0.6
LPE 20:4	0.067	0.4	1.1	0.7	0.177	0.0	0.8	0.9	0.407	0.0	0.6	0.1
LPE 22:6	0.061	1.2	0.6	-0.4	0.889	-0.1	0.0	0.0	0.893	0.0	0.0	0.0
PI 32:0	0.134	0.7	0.6	0.1	0.866	-0.1	0.0	0.0	0.416	-0.1	0.1	0.4
PI 32:1	0.024	0.5	2.0	2.1	0.050	0.3	1.8	1.0	0.256	0.8	0.1	-0.3
PI 34:1	0.031	0.2	1.8	1.8	0.679	0.0	0.1	0.2	0.451	0.0	0.1	0.6
PI 36:1	0.061	0.0	1.4	1.1	0.333	-0.2	0.1	0.7	0.314	0.0	0.3	0.7
PI 36:2	0.037	0.5	1.4	1.3	0.771	0.0	0.0	0.2	0.352	0.1	0.5	0.2
PI 36:3	0.024	0.8	2.0	1.6	0.118	0.1	1.4	0.6	0.398	0.5	0.1	-0.1
PI 36:4	0.024	1.2	1.8	1.3	0.177	0.5	1.0	0.1	0.264	0.8	0.0	-0.4
PI 38:2	0.046	0.0	1.4	1.6	0.003	0.1	4.1	3.1	0.927	0.0	0.0	0.0
PI 38:3	0.030	0.5	2.2	1.1	0.010	0.2	3.3	1.9	0.201	0.5	0.6	0.4
PI 38:4	0.029	1.4	2.0	0.4	0.273	0.3	0.7	0.2	0.140	0.0	1.2	0.9
PI 38:5	0.024	1.1	2.7	2.2	0.037	0.2	2.1	1.3	0.164	1.0	0.8	0.0
PI 38:6	0.024	0.8	1.6	1.9	0.733	0.0	0.1	0.1	0.151	1.0	0.0	-1.0
PI 40:4	0.030	0.5	2.4	1.0	0.014	0.8	3.3	1.1	0.167	1.3	0.2	-0.2
PI 40:5	0.024	1.0	2.7	3.7	0.003	0.4	3.8	2.8	0.217	0.8	0.5	0.2
PI 40:6	0.039	1.4	1.2	0.4	0.899	0.0	0.0	0.0	0.256	0.5	0.0	-0.7
LPI 18:1	0.085	0.0	0.7	1.1	0.040	0.0	1.2	2.0	0.192	-0.1	0.3	1.2
LPI 18:2	0.217	-0.1	0.2	0.6	0.172	-0.3	0.4	1.0	0.564	0.0	0.2	0.2
LPI 20:4	0.400	0.0	0.1	0.4	0.089	0.0	1.1	1.3	0.400	0.0	0.3	0.4
PS 38:4	0.138	0.7	0.7	0.0	0.784	0.2	0.0	0.0	0.959	0.0	0.0	0.0
PS 40:6	0.031	2.3	1.1	-0.1	0.791	0.0	-0.1	0.0	0.631	0.0	-0.1	-0.1
CE 14:0	0.510	0.1	0.2	0.0	0.050	0.0	1.3	1.7	0.258	0.4	0.7	0.0
CE 15:0	0.616	0.1	0.2	0.0	0.112	0.0	0.7	1.4	0.942	0.0	0.0	0.0
CE 16:0	0.528	0.1	0.2	0.0	0.089	0.0	1.2	1.2	0.722	0.0	0.0	-0.2
CE 16:1	0.031	0.8	1.6	1.2	0.003	0.6	4.1	3.1	0.178	0.9	0.7	0.1
CE 16:2	0.152	0.3	0.7	0.2	0.125	0.0	0.5	1.4	0.146	0.1	1.3	0.4
CE 17:0	0.836	0.0	0.0	0.0	0.112	-1.0	-1.4	0.0	0.614	0.0	-0.2	-0.1
CE 17:1	0.499	0.2	0.2	0.0	0.054	0.0	1.4	1.5	0.589	0.1	0.0	-0.2
CE 18:1	0.125	0.5	1.1	0.0	0.079	0.0	0.8	1.6	0.857	0.0	0.0	0.0
CE 18:2	0.024	1.8	1.6	2.1	0.163	0.0	1.2	0.6	0.138	0.0	1.6	0.4
CE 18:3	0.083	0.5	0.9	0.4	0.041	-0.1	0.9	2.0	0.217	0.1	1.1	0.1
CE 20:3	0.024	0.7	2.2	1.6	0.003	0.6	4.1	3.2	0.256	0.4	0.5	0.3
CE 20:4	0.031	1.7	1.6	0.3	0.253	0.3	0.8	0.2	0.122	0.0	1.5	0.7
CE 20:5	0.274	-0.3	-0.5	0.0	0.400	-0.2	-0.5	-0.1	0.614	-0.2	-0.1	0.0

Lipid species	6 weeks				10 weeks				16 weeks			
	P-value[a]	db/h vs. H/H[b]	db/db vs. H/H[b]	db/db vs. db/h[b]	*P*-value[a]	db/h vs. H/H[b]	db/db vs. H/H[b]	db/db vs. db/h[b]	*P*-value[a]	db/h vs. H/H[b]	db/db vs. H/H[b]	db/db vs. db/h[b]
CE 20:5	0.024	0.5	2.7	2.4	0.003	0.1	4.1	3.2	0.073	0.2	1.6	1.1
CE 22:4	0.062	0.9	0.3	-1.0	0.040	0.1	2.1	1.2	0.569	0.2	0.1	0.0
CE 22:5	0.024	0.7	2.4	2.2	0.003	0.1	4.1	3.2	0.056	0.1	2.2	1.9
CE 22:6	0.031	2.0	1.6	0.1	0.349	0.1	0.6	0.3	0.246	0.2	0.9	0.1
CE 24:6	0.116	0.3	0.8	0.4	0.405	0.0	0.1	0.8	0.458	0.0	-0.3	-0.2
COH	0.082	0.5	1.1	0.2	0.635	0.1	0.4	0.0	0.167	0.0	0.8	1.0
DG 16:0/16:0	0.065	0.0	0.7	1.6	0.918	0.0	0.0	0.0	0.171	0.0	0.9	0.8
DG 16:0/18:0	0.152	0.0	0.4	0.8	0.719	0.0	0.0	0.3	0.395	0.0	0.2	0.6
DG 16:0/18:1	0.097	0.1	0.9	0.7	0.981	0.0	0.0	0.0	0.167	0.7	0.7	0.4
DG 16:0/18:2	0.391	0.1	0.2	0.2	0.245	0.0	-0.5	-0.8	0.297	0.6	0.4	0.1
DG 16:1/18:1	0.053	0.0	1.2	1.5	0.025	0.5	2.4	1.2	0.056	1.8	1.2	1.2
DG 18:0/18:0	0.830	0.0	0.0	0.0	0.405	-0.1	0.1	0.6	0.172	0.0	0.6	1.0
DG 18:0/18:1	0.078	0.0	0.8	1.2	0.679	-0.1	0.0	0.3	0.138	0.5	0.8	1.0
DG 18:1/18:1	0.109	0.0	0.8	0.8	0.786	0.0	0.0	0.1	0.167	0.2	0.9	0.7
DG 18:1/18:2	0.425	0.0	0.2	0.2	0.305	0.0	-0.6	-0.5	0.307	0.4	0.4	0.1
DG 18:1/20:4	0.326	0.3	0.0	-0.3	0.010	0.0	-2.8	-2.4	0.817	0.0	0.0	0.0
DG 18:2/18:2	0.767	0.0	0.0	-0.1	0.136	0.0	-0.8	-1.1	0.657	0.0	0.2	0.0
TG 14:0/16:0/18:1	0.066	0.1	1.1	1.1	0.472	0.0	0.3	0.4	0.070	0.1	1.4	1.7
TG 14:0/16:0/18:2	0.056	0.2	1.2	1.1	0.089	0.3	1.7	0.4	0.065	0.8	1.6	1.1
TG 14:0/16:1/18:1	0.061	0.1	1.1	1.2	0.089	0.3	1.1	1.0	0.056	0.8	1.7	1.6
TG 14:0/16:1/18:2	0.060	0.2	1.1	1.2	0.784	0.1	0.1	0.0	0.065	0.5	1.8	1.0
TG 14:0/17:0/18:1	0.062	-0.1	0.9	1.3	0.791	0.0	0.0	0.1	0.398	0.1	0.3	0.2
TG 14:0/18:2/18:2	0.148	0.0	0.4	0.9	0.890	0.0	0.0	0.0	0.309	0.4	0.5	0.0
TG 14:1/16:0/18:1	0.061	0.5	1.1	0.8	0.205	0.0	0.8	0.6	0.073	0.2	1.9	0.7
TG 14:1/16:1/18:0	0.037	0.4	1.4	1.6	0.025	0.7	1.8	1.6	0.073	1.0	1.3	0.6
TG 14:1/18:1/18:1	0.062	0.1	0.9	1.2	0.113	0.1	1.1	0.9	0.056	1.3	1.6	1.7
TG 15:0/16:0/18:1	0.072	0.0	0.9	1.2	0.782	0.0	0.0	0.1	0.316	0.0	0.6	0.3
TG 15:0/18:1/18:1	0.103	0.0	0.6	1.1	0.742	-0.2	-0.1	0.0	0.290	0.6	0.5	0.0
TG 16:0/16:0/16:0	0.124	0.0	0.3	1.2	0.782	0.0	0.0	0.2	0.065	0.0	1.9	1.5
TG 16:0/16:0/18:0	0.084	0.0	0.6	1.3	0.760	-0.1	0.0	0.1	0.167	0.0	0.9	0.9
TG 16:0/16:0/18:1	0.096	0.1	0.6	1.1	0.742	0.0	0.0	0.2	0.146	0.1	1.1	0.7
TG 16:0/16:0/18:2	0.218	0.0	0.2	0.9	0.701	0.0	-0.2	-0.1	0.352	0.1	0.5	0.1
TG 16:0/16:1/17:0	0.072	0.0	0.7	1.5	0.936	0.0	0.0	0.0	0.223	0.6	0.6	0.1
TG 16:0/16:1/18:1	0.061	0.2	1.1	1.1	0.079	0.0	1.6	1.0	0.070	0.9	1.4	0.9
TG 16:0/17:0/18:1	0.049	0.0	1.2	1.6	0.542	-0.1	0.0	0.5	0.245	0.4	0.6	0.2
TG 16:0/17:0/18:2	0.091	0.0	0.7	1.1	0.901	0.0	0.0	0.0	0.136	1.0	1.0	0.0
TG 16:0/18:0/18:1	0.072	0.0	1.1	1.1	0.177	-0.4	0.0	1.2	0.136	0.0	1.0	1.2
TG 16:0/18:1/18:1	0.081	0.1	0.7	1.2	0.635	0.0	0.2	0.3	0.198	0.6	0.7	0.2
TG 16:0/18:1/18:2	0.391	0.1	0.1	0.3	0.348	0.0	-0.4	-0.7	0.474	0.4	0.1	0.0
TG 16:0/18:2/18:2	0.589	0.1	0.1	0.0	0.079	0.0	-0.9	-1.6	0.484	0.5	0.1	0.0
TG 16:1/16:1/16:1	0.039	0.3	1.4	1.5	0.037	0.5	1.7	1.4	0.056	1.1	1.7	1.1
TG 16:1/16:1/18:1	0.056	0.3	1.1	1.2	0.177	0.3	1.0	0.3	0.056	1.3	1.6	1.0
TG 16:1/17:0/18:1	0.079	0.0	0.7	1.3	0.901	0.0	0.0	0.0	0.167	1.1	0.7	0.0
TG 16:1/18:1/18:1	0.043	0.1	1.6	1.3	0.030	0.0	2.1	1.6	0.056	1.3	1.5	1.3
TG 16:1/18:1/18:2	0.093	0.1	0.5	1.2	0.944	0.0	0.0	0.0	0.079	1.2	1.4	0.1
TG 17:0/18:1/18:1	0.093	0.0	0.7	1.1	0.615	0.0	0.1	0.4	0.216	0.4	0.8	0.2
TG 18:0/18:0/18:0	0.277	0.0	0.2	0.6	0.742	0.0	0.0	0.2	0.138	0.0	0.8	1.4
TG 18:0/18:0/18:1	0.048	0.2	0.9	1.8	0.796	-0.1	0.0	0.1	0.323	0.6	0.3	0.1
TG 18:0/18:1/18:1	0.086	0.0	0.8	1.0	0.143	-0.4	0.0	1.4	0.070	0.1	1.5	1.5
TG 18:0/18:2/18:2	0.295	0.0	0.2	0.6	0.936	0.0	0.0	0.0	0.178	0.5	1.0	0.1
TG 18:1/18:1/18:1	0.062	0.0	1.1	1.3	0.333	0.0	0.3	0.7	0.056	1.0	1.6	1.3
TG 18:1/18:1/18:2	0.139	0.0	0.5	0.9	0.828	0.0	0.0	0.0	0.118	0.9	1.3	0.1
TG 18:1/18:1/20:4	0.078	0.8	0.0	-1.0	0.010	0.0	-2.6	-2.6	0.601	0.3	0.0	-0.1
TG 18:1/18:1/22:6	0.067	0.8	0.0	-1.3	0.015	0.0	-2.4	-2.1	0.452	0.5	0.0	-0.1

Lipid species	6 weeks				10 weeks				16 weeks			
	P-value[a]	db/h vs. H/H[b]	db/db vs. H/H[b]	db/db vs. db/h[b]	*P*-value[a]	db/h vs. H/H[b]	db/db vs. H/H[b]	db/db vs. db/h[b]	*P*-value[a]	db/h vs. H/H[b]	db/db vs. H/H[b]	db/db vs. db/h[b]
TG 18:1/18:2/18:2	0.228	0.1	0.4	0.4	0.679	0.0	-0.2	-0.2	0.225	0.6	0.7	0.1
TG 18:2/18:2/18:2	0.528	0.1	0.2	0.0	0.405	0.0	-0.4	-0.4	0.284	0.4	0.6	0.1
TG 18:2/18:2/20:4	0.094	0.7	0.0	-0.9	0.003	0.0	-4.1	-3.2	0.681	0.1	0.0	-0.1

[a] *P*-value for the comparison of levels of each lipid species between genotypes at each age using the Kruskal Wallis test with Benjamini-Hochberg correction for multiple comparisons. $P < 0.05$ was considered significant (highlighted in pink).

[b] Post-hoc analysis was performed using the Mann Whitney *U* test with Dunn-Sidak correction for multiple group comparisons. Values were derived from the formula: sign(difference in median levels)*-log10(post-hoc *P*-value). Colour-coded values 1.3 to 2.0 (light red, $P = 0.05$-0.01) and > 2.0 (dark red, $P < 0.01$) indicate a significant increase relative to the reference group. Colour-coded values -1.3 to -2.0 (light green, $P = 0.05$-0.01) and < -2.0 (dark green, $P < 0.01$) indicate a significant decrease relative to the reference group.

Table S4.6 Relationship between genotype and liver lipid species in female mice.

Lipid species	6 weeks				10 weeks				16 weeks			
	P-value[a]	db/h vs. H/H[b]	db/db vs. H/H[b]	db/db vs. db/h[b]	*P*-value[a]	db/h vs. H/H[b]	db/db vs. H/H[b]	db/db vs. db/h[b]	*P*-value[a]	db/h vs. H/H[b]	db/db vs. H/H[b]	db/db vs. db/h[b]
Cer 16:0	0.022	-0.2	1.3	2.1	0.074	0.0	0.4	2.6	0.162	-0.8	0.1	1.4
Cer 18:0	0.034	0.3	-0.9	-1.9	0.031	0.2	-1.1	-2.4	0.453	-0.3	0.0	0.2
Cer 20:0	0.325	0.0	0.1	0.7	0.826	-0.1	0.0	0.0	0.162	-0.5	0.7	2.6
Cer 22:0	0.018	-0.4	0.9	2.7	0.146	0.0	0.6	1.5	0.118	-0.5	1.2	3.0
Cer 24:0	0.016	0.0	1.6	2.7	0.108	0.0	0.8	1.5	0.225	-0.8	0.0	0.8
Cer 24:1	0.025	0.0	1.5	1.9	0.393	0.0	0.0	0.8	0.418	-0.4	0.0	0.2
MHC 16:0	0.065	-0.4	-1.2	-0.5	0.004	-0.2	-3.6	-3.0	0.235	0.0	-0.7	-0.8
MHC 20:0	0.028	0.0	-1.8	-1.5	0.213	0.0	-0.6	-0.8	0.250	-0.3	0.2	0.9
MHC 22:0	0.081	-0.3	-1.6	-0.1	0.038	-0.2	-1.9	-1.2	0.235	-0.6	0.0	0.9
MHC 24:0	0.563	-0.1	-0.2	0.0	0.037	-0.3	-1.9	-1.2	0.165	-0.3	-1.5	-0.6
MHC 24:1	0.070	0.0	-1.3	-0.8	0.004	-0.5	-3.3	-3.3	0.162	0.0	-1.7	-1.8
DHC 24:1	0.395	-0.4	0.0	0.1	0.769	0.0	0.0	-0.2	0.332	-0.4	-0.6	0.0
SM 31:1	0.513	0.0	-0.1	-0.2	0.794	0.1	0.0	0.0	0.370	0.4	0.4	0.0
SM 34:1	0.071	0.0	-1.1	-1.1	0.794	0.0	0.0	-0.1	0.412	-0.4	-0.3	0.0
SM 35:1	0.007	0.0	-3.3	-3.0	0.019	0.0	-2.4	-2.0	0.227	-0.5	-0.9	-0.2
SM 36:1	0.009	0.6	-1.3	-3.3	0.060	0.0	-1.2	-1.7	0.410	-0.2	-0.5	0.0
SM 38:1	0.124	0.0	-1.0	-0.5	0.727	-0.1	0.0	0.1	0.410	-0.4	-0.3	0.0
SM 38:2	0.488	0.0	0.3	0.1	0.136	0.0	1.0	1.0	0.718	0.0	0.0	0.1
SM 39:1	0.809	0.0	0.0	0.0	0.806	0.1	0.0	0.0	0.322	-0.6	-0.3	0.1
SM 41:1	0.850	0.0	0.0	0.0	0.842	0.0	0.0	0.0	0.294	-0.4	-0.8	0.0
SM 41:2	0.630	-0.1	0.0	0.1	0.638	-0.1	0.0	0.2	0.422	-0.3	-0.4	0.0
SM 42:1	0.110	-0.4	0.3	1.0	0.191	0.0	0.4	1.2	0.385	-0.5	-0.2	0.0
PC 30:0	0.179	-0.1	0.2	0.8	0.993	0.0	0.0	0.0	0.255	-0.3	-0.9	-0.2
PC 31:0	0.021	-0.5	-2.3	-0.7	0.010	0.0	-3.3	-2.2	0.162	-0.1	-1.3	-1.1
PC 31:1	0.930	0.0	0.0	0.0	0.424	-0.4	-0.1	0.1	0.412	-0.3	-0.4	0.0
PC 32:0	0.007	-0.1	-3.6	-3.0	0.004	-0.2	-3.9	-3.9	0.162	0.1	-1.7	-1.2
PC 32:1	0.007	0.4	3.0	3.3	0.006	0.0	3.3	3.0	0.206	-0.4	0.2	1.0
PC 32:2	0.009	0.8	2.5	1.5	0.007	0.0	3.0	3.0	0.433	0.0	0.1	0.4
PC 32:3	0.348	-0.3	0.2	0.2	0.166	0.2	1.0	0.5	0.165	-1.9	-0.3	0.2
PC 33:0	0.024	-0.4	-3.3	-0.1	0.011	-0.1	-3.6	-1.7	0.162	-0.2	-1.6	-1.1
PC 33:1	0.050	0.0	1.2	1.4	0.334	-0.1	0.2	0.6	0.550	-0.2	-0.2	0.0
PC 33:2	0.083	-0.3	-1.3	-0.3	0.417	0.0	-0.3	-0.4	0.368	-0.2	-0.6	0.0
PC 34:0	0.422	-0.1	0.0	0.3	0.575	-0.1	0.0	0.2	0.516	-0.3	-0.1	0.0
PC 34:1	0.693	0.0	0.1	0.0	0.595	-0.1	-0.1	0.2	0.458	-0.2	-0.4	0.0
PC 34:2	0.064	0.0	-1.1	-1.2	0.570	-0.1	-0.2	0.0	0.550	-0.3	0.0	0.0
PC 34:3	0.383	0.0	0.3	0.3	0.038	0.0	1.9	1.6	0.474	-0.4	-0.1	0.1
PC 34:4	0.226	0.1	0.6	0.3	0.057	0.4	2.0	0.4	0.412	-0.4	-0.3	0.0
PC 34:5	0.007	0.4	3.3	3.0	0.022	0.0	2.4	1.9	0.722	-0.1	0.0	-0.1
PC 35:0	0.056	-1.5	-0.1	0.7	0.424	-0.3	0.1	0.2	0.165	-0.1	-1.5	-0.7
PC 35:1	0.349	-0.2	0.0	0.5	0.248	-0.6	0.0	0.6	0.322	-0.6	-0.4	0.0
PC 35:2	0.179	-0.9	0.0	0.4	0.461	-0.3	0.0	0.2	0.433	-0.6	0.0	0.1
PC 35:3	0.486	-0.1	0.0	0.3	0.595	0.0	0.1	0.1	0.475	-0.3	-0.3	0.0
PC 36:1	0.017	-0.8	0.8	2.5	0.236	0.0	0.5	0.9	0.283	-0.6	0.0	0.7
PC 36:2	0.025	-1.2	0.1	2.1	0.143	0.0	0.6	1.3	0.258	-0.4	0.1	0.8
PC 36:3	0.015	0.0	1.8	2.7	0.028	0.0	1.9	2.0	0.301	-0.1	0.1	0.8
PC 36:4a	0.082	-0.2	0.3	1.5	0.059	0.3	1.9	0.6	0.322	-0.1	0.3	0.5
PC 36:4b	0.007	0.4	-3.6	-3.3	0.004	0.3	-3.9	-3.9	0.174	0.0	-1.5	-0.7
PC 36:5	0.007	0.0	3.0	3.3	0.004	-0.1	3.6	3.6	0.192	-0.8	0.1	1.0
PC 36:6	0.007	0.3	3.6	3.3	0.004	0.1	3.9	3.9	0.322	-0.3	0.1	0.5
PC 37:4	0.007	0.2	-3.6	-2.7	0.015	0.0	-2.8	-2.0	0.192	-0.1	-0.9	-0.9
PC 37:5	0.350	-0.1	0.0	0.6	0.461	0.0	0.4	0.1	0.493	-0.4	0.0	0.1
PC 37:6	0.032	0.0	-2.0	-1.2	0.040	0.1	-1.3	-1.9	0.162	-0.3	-1.7	-0.6

Lipid species	6 weeks				10 weeks				16 weeks			
	P-value[a]	db/h vs. H/H[b]	db/db vs. H/H[b]	db/db vs. db/h[b]	*P*-value[a]	db/h vs. H/H[b]	db/db vs. H/H[b]	db/db vs. db/h[b]	*P*-value[a]	db/h vs. H/H[b]	db/db vs. H/H[b]	db/db vs. db/h[b]
PC 38:2	0.084	0.0	1.1	0.8	0.074	-0.1	0.6	2.0	0.692	0.0	0.0	0.2
PC 38:3	0.032	0.0	1.3	1.9	0.296	0.0	0.3	0.8	0.250	-0.1	0.4	1.0
PC 38:4	0.007	0.2	-3.0	-3.3	0.006	0.1	-2.6	-3.9	0.278	-0.1	-0.6	-0.6
PC 38:5	0.111	0.0	1.3	0.3	0.866	0.0	0.0	0.0	0.668	-0.2	0.0	0.0
PC 38:6a	0.154	-0.4	0.0	1.1	0.530	0.1	0.3	0.0	0.879	0.0	0.0	0.1
PC 38:6b	0.007	0.2	-3.6	-3.3	0.011	0.0	-2.4	-3.0	0.297	-0.3	-0.8	-0.1
PC 38:7	0.022	0.3	2.0	1.4	0.007	0.0	3.3	2.8	0.389	-0.1	0.1	0.6
PC 39:6	0.024	-0.8	-1.8	-0.7	0.017	0.0	-2.6	-2.0	0.322	-0.3	-0.6	-0.1
PC 39:7	0.668	0.0	-0.1	0.1	0.461	0.2	0.0	-0.3	0.562	0.1	-0.3	0.0
PC 40:5	0.209	0.0	0.4	0.6	0.321	0.0	0.2	0.7	0.165	-1.1	0.1	1.1
PC 40:6	0.017	0.2	-1.8	-2.1	0.417	0.0	-0.3	-0.4	0.422	-0.5	-0.1	0.1
PC 40:7	0.641	0.0	0.2	0.0	0.638	0.1	0.1	0.0	0.478	-0.3	0.0	0.2
PC(O-32:1)	0.117	0.0	1.0	0.6	0.453	0.0	0.2	0.4	0.717	-0.1	0.0	0.1
PC(O-34:1)	0.021	-1.0	-2.5	-0.1	0.017	-0.1	-2.4	-2.0	0.162	-0.3	-1.5	-0.7
PC(O-34:2)	0.076	-1.6	-0.3	0.1	0.194	-0.5	-1.0	0.0	0.364	-0.2	-0.3	-0.4
PC(O-35:4)	0.400	0.4	0.1	0.0	0.851	0.0	0.0	0.1	0.631	0.0	-0.2	-0.1
PC(O-36:0)	0.109	0.0	-0.9	-0.7	0.688	0.0	-0.1	-0.1	0.162	-0.6	-1.5	-0.5
PC(O-36:2)	0.721	-0.1	0.0	0.0	0.268	0.0	0.2	1.0	0.995	0.0	0.0	0.0
PC(O-36:3)	0.110	-1.1	-0.2	0.3	0.134	-0.2	-1.3	-0.4	0.181	-0.6	-1.1	-0.3
PC(O-36:4)	0.023	-0.3	-1.8	-1.4	0.004	-0.3	-3.6	-2.8	0.192	-0.1	-1.3	-0.4
PC(O-36:5)	0.267	0.4	-0.1	-0.3	0.814	0.0	0.0	0.0	0.322	-0.6	-0.3	0.1
PC(O-38:5)	0.021	0.0	-2.0	-1.7	0.004	-0.1	-3.6	-3.9	0.162	0.0	-1.0	-1.5
PC(O-40:6)	0.016	-0.7	-2.3	-1.1	0.015	0.0	-2.6	-2.2	0.291	-0.3	-0.8	-0.1
PC(O-40:7)	0.008	-0.2	-3.3	-2.3	0.004	-0.4	-3.9	-3.6	0.162	-0.1	-1.9	-1.4
PC(P-32:0)	0.708	0.0	-0.1	0.0	0.612	0.0	-0.1	-0.2	0.273	-0.3	-0.7	-0.3
PC(P-34:1)	0.509	-0.2	-0.1	-0.1	0.337	-0.7	0.0	0.1	0.192	-0.6	-0.9	-0.4
PC(P-36:2)	0.305	-0.8	0.0	0.1	0.319	-0.7	0.0	0.2	0.271	-0.3	-0.9	-0.1
PC(P-36:4)	0.082	0.4	-0.4	-1.1	0.872	0.0	0.0	0.0	0.322	-0.6	-0.3	0.0
PC(P-38:4)	0.104	0.0	-1.5	-0.3	0.191	-0.9	-0.4	0.1	0.322	0.0	-0.6	-0.4
PC(P-38:5)	0.055	-0.5	-1.5	-0.3	0.051	0.0	-0.9	-2.2	0.195	-0.1	-1.2	-0.6
PC(P-38:6)	0.008	-0.3	-3.3	-2.1	0.050	0.0	-1.5	-1.7	0.162	-0.2	-1.7	-0.7
PC(P-40:5)	0.013	-0.7	-3.0	-0.7	0.015	0.0	-2.8	-2.0	0.162	-0.6	-1.3	-1.0
PC(P-40:6)	0.041	0.0	-1.6	-1.2	0.028	0.0	-1.9	-2.0	0.165	0.0	-1.0	-1.2
LPC 16:0	0.460	0.3	0.1	0.0	0.337	0.1	0.5	0.3	0.718	0.0	0.0	0.1
LPC 16:1	0.007	0.6	3.6	3.3	0.011	0.0	2.8	2.6	0.162	0.0	1.1	1.6
LPC 18:0	0.778	0.0	0.0	0.0	0.248	1.0	0.2	0.0	0.474	0.0	0.1	0.4
LPC 18:1	0.112	0.0	0.8	0.8	0.123	1.2	0.7	0.0	0.918	0.0	0.0	0.0
LPC 18:2	0.021	0.0	1.3	2.5	0.358	0.2	0.5	0.0	0.773	-0.1	0.0	0.1
LPC 20:4	0.403	0.0	-0.1	-0.3	0.198	0.6	0.0	-0.8	0.381	0.0	-0.3	-0.4
LPC 22:6	0.264	0.8	0.0	-0.2	0.589	0.2	0.0	-0.1	0.819	0.0	0.0	-0.1
PE 32:0	0.546	-0.1	-0.2	0.0	0.281	0.0	-0.6	-0.5	0.550	-0.1	-0.2	0.0
PE 32:1	0.007	1.2	3.6	3.3	0.004	0.0	3.9	3.9	0.165	-0.1	0.6	1.5
PE 34:1	0.011	0.0	2.5	2.3	0.014	0.0	2.8	2.2	0.294	-0.9	0.0	0.3
PE 34:2	0.022	-0.1	1.3	2.3	0.015	-0.6	1.2	2.8	0.192	-1.5	0.0	0.5
PE 34:3	0.011	0.0	2.1	2.7	0.004	-0.1	3.6	3.9	0.192	-0.8	0.0	1.0
PE 35:1	0.087	-0.4	0.4	1.0	0.806	0.0	0.1	0.0	0.541	-0.3	0.0	0.0
PE 35:2	0.306	-0.1	0.3	0.3	0.446	-0.2	0.0	0.3	0.192	-1.6	-0.4	0.1
PE 36:0	0.202	0.5	0.0	-0.5	0.123	0.0	-1.1	-1.0	0.322	0.8	0.2	0.0
PE 36:1	0.046	0.1	1.6	1.0	0.191	0.0	0.7	0.9	0.271	-0.6	0.0	0.7
PE 36:2	0.042	0.0	1.3	1.5	0.282	0.1	0.1	1.0	0.177	-1.9	0.0	0.4
PE 36:3	0.086	0.0	0.7	1.4	0.059	0.0	1.5	1.5	0.322	-0.5	0.0	0.6
PE 36:4	0.075	0.0	0.9	1.2	0.223	-0.6	0.0	0.7	0.353	-0.8	0.0	0.1
PE 36:5	0.007	0.0	3.6	3.3	0.004	-0.3	3.6	3.9	0.258	-0.1	0.4	0.8
PE 38:3	0.349	0.0	-0.4	-0.2	0.526	-0.4	0.0	0.0	0.322	-0.6	0.0	0.2

Lipid species	6 weeks				10 weeks				16 weeks			
	P-value[a]	db/h vs. H/H[b]	db/db vs. H/H[b]	db/db vs. db/h[b]	*P*-value[a]	db/h vs. H/H[b]	db/db vs. H/H[b]	db/db vs. db/h[b]	*P*-value[a]	db/h vs. H/H[b]	db/db vs. H/H[b]	db/db vs. db/h[b]
PE 38:4	0.014	0.0	-1.8	-3.0	0.175	-0.1	-1.0	-0.5	0.301	-0.8	-0.2	0.1
PE 38:5	0.042	0.0	2.0	0.8	0.530	0.0	0.1	0.3	0.474	-0.4	0.0	0.1
PE 38:6	0.007	0.0	-3.3	-3.3	0.033	-0.6	-2.0	-0.8	0.176	-0.3	-1.5	-0.4
PE 40:5	0.716	0.0	0.1	0.0	0.483	-0.1	0.0	0.4	0.247	-1.2	-0.1	0.2
PE 40:6	0.008	0.4	-2.3	-3.0	0.173	-0.1	-0.9	-0.7	0.251	-0.3	-1.0	-0.1
PE 40:7	0.009	0.9	-1.2	-3.3	0.175	0.0	-0.6	-1.1	0.202	-0.2	-1.1	-0.4
PE(O-36:2)	0.306	-0.1	0.3	0.3	0.446	-0.2	0.0	0.3	0.192	-1.6	-0.4	0.1
PE(O-36:5)	0.472	0.0	-0.2	-0.3	0.014	-0.4	-1.9	-2.8	0.162	-0.8	-1.7	-1.0
PE(O-38:4)	0.021	-0.6	-2.5	-0.5	0.081	0.0	-1.3	-1.2	0.162	-0.8	-1.6	-1.0
PE(O-38:5)	0.884	0.0	0.0	0.0	0.884	-0.1	0.0	0.0	0.412	0.0	-0.3	-0.3
PE(O-40:6)	0.009	0.0	-3.6	-1.9	0.033	0.0	-2.0	-1.6	0.219	-0.7	-0.9	-0.1
PE(P-36:4)	0.349	0.0	-0.3	-0.3	0.010	-0.3	-2.0	-3.6	0.162	-0.6	-1.6	-1.0
PE(P-38:4)	0.022	-0.3	-2.5	-0.6	0.188	-0.1	-1.0	-0.4	0.118	-0.8	-2.8	-1.6
PE(P-38:5)	0.716	0.1	0.0	0.0	0.240	-0.4	-0.6	-0.1	0.235	-0.6	-0.9	-0.1
LPE 16:0	0.060	1.1	1.2	0.0	0.268	-0.1	0.3	0.7	0.451	-0.2	0.0	0.4
LPE 18:0	0.281	0.6	0.2	0.0	0.952	0.0	0.0	0.0	0.278	-0.5	0.0	0.7
LPE 18:1	0.007	3.0	2.5	0.7	0.055	0.0	1.7	1.2	0.322	0.0	0.3	0.6
LPE 20:4	0.087	1.2	0.7	0.0	0.393	0.6	0.1	0.0	0.902	0.0	0.0	0.0
LPE 22:6	0.063	1.5	0.0	-0.8	0.268	0.9	0.0	-0.3	0.474	0.0	-0.3	-0.2
PI 36:1	0.207	0.0	0.4	0.6	0.768	0.0	0.1	0.1	0.370	-0.1	0.1	0.6
PI 36:2	0.528	0.0	0.1	0.3	0.958	0.0	0.0	0.0	0.291	-0.5	-0.8	0.0
PI 38:2	0.009	-0.1	2.3	2.7	0.015	1.2	2.0	1.1	0.235	-0.1	0.4	1.0
PI 38:3	0.021	-0.2	1.2	2.3	0.102	0.1	1.2	1.0	0.162	-0.3	0.4	1.6
PI 38:4	0.096	0.3	-0.1	-1.5	0.720	0.0	-0.1	-0.1	0.294	-0.5	-0.6	-0.1
PI 40:4	0.015	-0.3	1.3	2.7	0.103	-0.2	0.5	1.5	0.162	-0.6	0.2	1.9
PI 40:5	0.022	0.0	2.0	1.7	0.049	-0.8	0.3	1.9	0.162	-0.7	0.1	1.5
PI 40:6	0.021	0.0	-1.3	-2.7	0.342	0.0	-0.6	-0.3	0.162	-0.4	-1.5	-0.6
PS 36:1	0.148	-0.2	-1.1	-0.1	0.102	-0.1	-1.2	-1.0	0.162	-0.3	-1.9	-1.0
PS 36:2	0.348	-0.3	0.0	0.4	0.247	-0.6	0.0	0.6	0.322	-0.6	-0.4	0.0
PS 38:3	0.624	0.0	0.0	0.2	0.417	-0.2	0.0	0.4	0.550	-0.2	0.0	0.1
PS 38:4	0.009	0.1	-2.5	-2.7	0.004	-0.6	-3.9	-2.8	0.215	-0.1	-0.9	-0.7
PS 38:5	0.009	0.1	2.3	3.0	0.004	-0.1	3.9	3.9	0.379	-0.1	0.0	0.6
PS 40:5	0.471	0.0	0.2	0.3	0.105	-1.3	0.0	0.7	0.478	-0.4	0.0	0.1
PS 40:6	0.121	0.0	-0.5	-1.1	0.123	-1.0	-0.9	0.0	0.322	-0.3	-0.8	0.0
PG 34:1	0.663	-0.2	0.0	0.0	0.306	-0.1	0.1	0.7	0.590	-0.1	-0.2	0.0
PG 34:2	0.349	-0.4	-0.1	0.1	0.879	0.0	0.0	0.0	0.389	0.0	-0.6	-0.1
PG 36:1	0.991	0.0	0.0	0.0	0.525	-0.2	0.0	0.1	0.514	-0.1	-0.3	0.0
PG 36:2	0.178	-0.1	-1.2	0.0	0.530	-0.2	-0.1	0.0	0.215	-1.0	-0.8	0.0
PG 36:3	0.703	0.0	0.1	0.0	0.337	0.1	0.7	0.1	0.723	0.0	-0.2	0.0
BMP 18:1/18:1	0.009	-0.1	2.1	3.3	0.105	-0.1	0.4	1.7	0.162	-0.4	0.1	1.8
CL 18:2/18:2/18:2/16:1	0.009	0.7	3.0	1.2	0.004	0.2	3.0	3.9	0.320	-0.1	0.3	0.6
CL 18:2/18:1/18:2/16:1	0.007	0.4	3.6	2.5	0.019	0.6	1.9	1.9	0.301	-0.4	0.1	0.6
CL 18:2/18:1/18:1/16:1	0.007	0.3	3.6	2.3	0.014	0.2	2.2	2.6	0.162	-0.6	0.9	1.3
CL 18:2/18:2/18:2/18:3	0.209	-0.8	0.0	0.3	0.424	0.0	0.2	0.4	0.258	-1.0	-0.5	0.0
CL 18:2/18:2/18:2/18:2	0.010	0.0	-2.5	-2.5	0.013	-0.2	-3.0	-1.7	0.397	-0.4	-0.3	0.0
CL 18:2/18:2/18:2/18:1	0.063	0.1	-0.4	-1.9	0.393	0.0	-0.2	-0.6	0.215	-0.9	-0.8	0.1
CL 18:2/18:1/18:2/18:1	0.285	0.5	0.0	-0.3	0.612	0.2	0.0	0.0	0.332	-0.4	-0.4	0.1
CL 18:1/18:1/18:1/18:2	0.800	0.0	0.0	0.0	0.461	0.3	0.0	-0.2	0.894	0.0	0.0	0.0
CL 18:2/18:2/18:2/20:3	0.716	0.0	-0.1	-0.1	0.867	-0.1	0.0	0.0	0.772	0.0	0.0	0.1
CL 18:2/18:1/18:2/20:3	0.009	0.0	-3.3	-2.1	0.075	-0.1	-1.6	-0.9	0.433	-0.5	-0.1	0.1
CL 18:2/18:1/18:2/20:2	0.008	-0.2	-3.3	-2.3	0.010	-0.4	-3.0	-1.9	0.291	-0.6	-0.6	0.0
CE 16:0	0.021	1.0	-0.4	-2.3	0.219	0.0	-0.7	-0.7	0.692	0.0	0.0	-0.2
CE 16:1	0.009	2.5	2.8	0.0	0.054	0.7	1.7	0.4	0.174	0.0	1.1	1.0
CE 17:1	0.076	1.5	0.1	-0.5	0.342	0.5	0.3	0.0	0.947	0.0	0.0	0.0

Lipid species	6 weeks				10 weeks				16 weeks			
	P-value[a]	db/h vs. H/H[b]	db/db vs. H/H[b]	db/db vs. db/h[b]	*P*-value[a]	db/h vs. H/H[b]	db/db vs. H/H[b]	db/db vs. db/h[b]	*P*-value[a]	db/h vs. H/H[b]	db/db vs. H/H[b]	db/db vs. db/h[b]
CE 18:0	0.007	2.1	-1.5	-3.3	0.028	0.3	-1.2	-2.2	0.773	-0.1	0.0	0.0
CE 18:1	0.009	1.8	-0.5	-3.0	0.103	1.2	0.0	-0.9	0.412	0.0	-0.2	-0.4
CE 18:2	0.070	0.5	-0.1	-1.5	0.656	0.1	0.0	-0.1	0.723	-0.1	0.0	0.0
CE 18:3	0.140	0.2	0.0	-1.4	0.452	0.5	0.1	0.0	0.990	0.0	0.0	0.0
CE 20:3	0.563	0.3	0.0	0.0	0.362	0.7	0.0	-0.1	0.888	0.0	0.1	0.0
CE 20:4	0.076	0.3	0.0	-2.1	0.337	0.5	0.0	-0.4	0.618	0.0	0.0	0.2
CE 22:5	0.219	0.1	0.7	0.2	0.906	0.0	0.0	0.0	0.322	0.0	0.6	0.3
COH	0.305	-0.1	-0.8	0.0	0.981	0.0	0.0	0.0	0.368	-0.7	0.1	0.1
DG 14:0/16:0	0.007	0.6	3.0	2.3	0.004	0.7	3.6	2.4	0.894	0.0	0.0	0.0
DG 14:0/18:1	0.007	0.7	3.6	2.3	0.004	0.5	3.9	3.6	0.322	0.0	0.4	0.6
DG 14:0/18:2	0.119	0.2	1.3	0.0	0.032	0.7	1.5	1.5	0.995	0.0	0.0	0.0
DG 16:0/16:0	0.028	0.6	2.0	0.5	0.221	0.1	0.7	0.5	0.397	0.0	-0.5	-0.2
DG 16:0/18:0	0.054	1.0	1.3	0.1	0.203	0.3	0.8	0.3	0.963	0.0	0.0	0.0
DG 16:0/18:1	0.034	0.9	2.0	0.1	0.166	0.1	0.9	0.6	0.949	0.0	0.0	0.0
DG 16:0/18:2	0.270	0.3	0.0	-0.6	0.624	0.2	0.0	0.0	0.389	0.0	-0.2	-0.6
DG 16:0/20:3	0.418	0.0	0.4	0.1	0.918	0.0	0.0	0.0	0.956	0.0	0.0	0.0
DG 16:0/20:4	0.049	0.4	-0.6	-1.5	0.028	0.2	-1.2	-2.4	0.516	0.0	-0.1	-0.4
DG 16:0/22:5	0.217	0.1	0.7	0.2	0.236	0.0	0.7	0.6	0.268	0.0	0.5	0.8
DG 16:0/22:6	0.294	0.1	-0.1	-0.6	0.947	0.0	0.0	0.0	0.604	0.0	0.1	0.2
DG 16:1/18:0	0.007	1.6	3.6	2.7	0.004	0.7	3.9	3.9	0.271	0.0	0.6	0.7
DG 16:1/18:1	0.007	1.3	3.6	2.5	0.004	1.1	3.9	2.8	0.225	0.0	0.6	1.0
DG 18:0/18:1	0.325	0.3	0.4	0.0	0.337	0.6	0.3	0.0	0.993	0.0	0.0	0.0
DG 18:0/18:2	0.096	0.5	-0.3	-1.0	0.285	0.6	0.0	-0.4	0.557	0.0	-0.2	-0.2
DG 18:0/20:4	0.009	0.8	-1.5	-3.0	0.082	0.2	-0.7	-1.5	0.192	0.0	-0.6	-1.3
DG 18:1/18:1	0.097	0.8	1.0	0.0	0.369	0.7	0.1	0.0	0.963	0.0	0.0	0.0
DG 18:1/18:2	0.055	0.7	-0.4	-1.4	0.307	0.8	0.0	-0.2	0.389	0.0	-0.2	-0.6
DG 18:1/18:3	0.306	0.3	0.0	-0.5	0.429	0.4	0.2	0.0	0.477	0.0	-0.1	-0.4
DG 18:1/20:3	0.952	0.0	0.0	0.0	0.756	0.1	0.0	0.0	0.875	0.0	-0.1	0.0
DG 18:1/20:4	0.076	0.3	-0.6	-1.1	0.814	0.0	0.0	-0.1	0.385	0.0	-0.4	-0.3
DG 18:2/18:2	0.019	0.2	-1.8	-1.9	0.175	0.7	-0.1	-0.7	0.179	0.0	-0.7	-1.3
TG 14:0/16:0/18:1	0.032	0.9	2.0	0.2	0.158	0.6	0.6	0.6	0.181	0.0	1.0	1.0
TG 14:0/16:0/18:2	0.016	0.9	3.0	0.3	0.037	0.2	1.7	1.5	0.162	0.0	1.5	1.8
TG 14:0/16:1/18:1	0.016	1.0	2.8	0.3	0.082	0.7	1.0	0.8	0.162	0.0	1.2	1.5
TG 14:0/16:1/18:2	0.055	0.9	1.6	0.0	0.247	0.2	0.5	0.6	0.165	0.0	1.0	1.3
TG 14:0/17:0/18:1	0.084	1.1	0.8	0.0	0.459	0.3	0.2	0.0	0.258	0.0	0.6	0.7
TG 14:1/16:0/18:1	0.045	1.0	1.8	0.0	0.240	0.1	0.6	0.6	0.165	0.0	1.1	1.3
TG 14:1/16:1/18:0	0.007	1.2	3.6	1.1	0.004	0.4	3.3	3.6	0.162	0.1	1.7	1.9
TG 14:1/18:1/18:1	0.024	1.2	2.1	0.0	0.161	0.7	0.7	0.3	0.162	0.0	1.2	1.4
TG 15:0/16:0/18:1	0.042	1.0	1.8	0.0	0.268	0.4	0.5	0.2	0.165	0.0	0.9	1.3
TG 15:0/18:1/18:1	0.055	1.8	0.1	-0.5	0.323	0.9	0.0	-0.1	0.431	0.0	0.4	0.2
TG 16:0/16:0/16:0	0.049	0.1	1.8	0.6	0.025	0.5	2.0	1.3	0.165	0.0	0.6	1.5
TG 16:0/16:0/18:0	0.560	0.0	0.2	0.1	0.247	0.6	0.5	0.2	0.283	-0.1	0.2	0.8
TG 16:0/16:0/18:1	0.081	1.0	1.0	0.0	0.464	0.5	0.1	0.0	0.225	0.0	0.7	0.9
TG 16:0/16:0/18:2	0.126	0.8	0.1	-0.6	0.500	0.4	0.0	-0.1	0.259	0.0	0.4	0.9
TG 16:0/16:1/17:0	0.087	0.8	1.1	0.0	0.318	0.4	0.4	0.1	0.235	0.0	0.8	0.7
TG 16:0/16:1/18:1	0.021	1.5	2.1	0.0	0.247	0.7	0.4	0.1	0.165	0.0	1.1	1.2
TG 16:0/17:0/18:1	0.114	1.0	0.6	0.0	0.530	0.4	0.0	0.0	0.322	0.0	0.4	0.6
TG 16:0/17:0/18:2	0.065	1.5	0.7	0.0	0.570	0.3	0.0	0.0	0.322	0.0	0.6	0.4
TG 16:0/18:0/18:1	0.299	0.9	0.1	0.0	0.459	0.6	0.0	-0.1	0.271	0.0	0.6	0.7
TG 16:0/18:1/18:1	0.048	2.0	0.5	-0.1	0.411	0.7	0.0	-0.1	0.322	0.0	0.6	0.4
TG 16:0/18:1/18:2	0.048	1.6	0.0	-1.1	0.424	0.5	-0.1	-0.1	0.550	0.0	0.2	0.1
TG 16:0/18:2/18:2	0.043	1.1	-0.1	-1.5	0.471	0.2	-0.1	-0.1	0.950	0.0	0.0	0.0
TG 16:1/16:1/16:1	0.009	1.0	3.6	0.6	0.004	0.1	3.3	3.6	0.162	0.0	1.9	1.9
TG 16:1/16:1/18:1	0.017	1.6	2.3	0.0	0.203	0.5	0.6	0.3	0.162	0.0	1.2	1.6

Lipid species	6 weeks				10 weeks				16 weeks			
	P-value[a]	db/h vs. H/H[b]	db/db vs. H/H[b]	db/db vs. db/h[b]	*P*-value[a]	db/h vs. H/H[b]	db/db vs. H/H[b]	db/db vs. db/h[b]	*P*-value[a]	db/h vs. H/H[b]	db/db vs. H/H[b]	db/db vs. db/h[b]
TG 16:1/17:0/18:1	0.060	2.0	0.4	-0.1	0.411	0.6	0.1	0.0	0.397	0.0	0.4	0.3
TG 16:1/18:1/18:1	0.023	2.0	1.5	0.0	0.236	1.0	0.3	0.1	0.162	0.0	1.2	1.2
TG 16:1/18:1/18:2	0.063	1.3	0.4	-0.5	0.446	0.6	0.1	0.0	0.304	0.0	0.6	0.6
TG 17:0/18:1/18:1	0.058	1.8	0.4	-0.2	0.393	0.7	0.0	-0.1	0.368	0.0	0.4	0.4
TG 18:0/18:0/18:1	0.930	0.0	0.0	0.0	0.417	0.7	0.0	0.0	0.192	-0.1	0.4	1.3
TG 18:0/18:1/18:1	0.115	1.5	0.0	-0.3	0.247	1.4	0.0	-0.1	0.474	0.0	0.2	0.3
TG 18:0/18:2/18:2	0.016	1.8	-0.3	-2.1	0.149	0.4	-0.3	-1.1	0.975	0.0	0.0	0.0
TG 18:1/18:1/18:1	0.055	2.0	0.3	-0.2	0.223	1.5	0.0	0.0	0.304	0.0	0.6	0.6
TG 18:1/18:1/18:2	0.050	1.3	0.0	-1.2	0.306	0.9	0.0	-0.2	0.855	0.0	0.1	0.0
TG 18:1/18:1/20:4	0.009	1.5	-1.2	-2.3	0.125	0.2	-0.4	-1.3	0.879	0.0	0.0	0.0
TG 18:1/18:1/22:6	0.017	1.3	-0.6	-2.1	0.362	0.1	-0.2	-0.6	0.903	0.0	0.0	0.0
TG 18:1/18:2/18:2	0.042	1.2	-0.1	-1.5	0.429	0.6	0.0	-0.1	0.950	0.0	0.0	0.0
TG 18:2/18:2/18:2	0.017	0.9	-0.9	-2.3	0.232	0.2	-0.2	-0.9	0.875	0.0	0.0	0.0

[a] *P*-value for the comparison of levels of each lipid species between genotypes at each age using the Kruskal Wallis test with Benjamini-Hochberg correction for multiple comparisons. $P < 0.05$ was considered significant (highlighted in pink).

[b] Post-hoc analysis was performed using the Mann Whitney *U* test with Dunn-Sidak correction for multiple group comparisons. Values were derived from the formula: sign(difference in median levels)*-log10(post-hoc *P*-value). Colour-coded values 1.3 to 2.0 (light red, $P = 0.05$-0.01) and > 2.0 (dark red, $P < 0.01$) indicate a significant increase relative to the reference group. Colour-coded values -1.3 to -2.0 (light green, $P = 0.05$-0.01) and < -2.0 (dark green, $P < 0.01$) indicate a significant decrease relative to the reference group.

Table S4.7 Relationship between genotype and skeletal muscle lipid species in female mice.

Lipid species	6 weeks				10 weeks				16 weeks			
	P-value[a]	db/h vs. H/H[b]	db/db vs. H/H[b]	db/db vs. db/h[b]	*P*-value[a]	db/h vs. H/H[b]	db/db vs. H/H[b]	db/db vs. db/h[b]	*P*-value[a]	db/h vs. H/H[b]	db/db vs. H/H[b]	db/db vs. db/h[b]
Cer 16:0	0.079	0.0	-0.8	-1.8	1.000	-0.4	0.0	0.4	0.865	-0.1	0.0	0.0
Cer 18:0	0.026	0.2	-1.4	-2.3	0.035	-2.0	-1.9	-0.1	0.211	0.0	-1.0	-0.8
Cer 22:0	0.633	0.1	-0.2	0.0	0.008	-2.9	0.0	3.0	0.649	-0.1	0.0	0.2
Cer 24:0	0.701	0.0	-0.1	-0.1	0.045	-2.2	0.0	1.3	0.934	0.0	0.0	0.0
Cer 24:1	0.081	0.0	-1.3	-1.2	0.084	-1.9	-0.1	1.0	0.844	0.0	-0.1	0.0
MHC 18:0	0.155	1.1	0.7	0.0	0.190	-1.5	-0.1	0.6	0.998	0.0	0.0	0.0
MHC 20:0	0.506	0.2	0.3	0.0	0.372	-1.2	-0.4	0.1	0.922	0.0	0.0	0.0
MHC 22:0	0.266	0.5	0.5	0.0	0.273	-1.3	-0.3	0.3	0.993	0.0	0.0	0.0
MHC 24:0	0.192	0.8	0.7	0.0	0.405	-1.0	-0.1	0.5	0.999	0.0	0.0	0.0
MHC 24:1	0.200	0.6	0.8	0.0	0.233	-1.4	-0.1	0.6	0.981	0.0	0.0	0.0
GM3 18:0	0.015	0.2	-2.3	-2.3	0.035	-2.4	-0.4	0.9	0.649	-0.2	0.0	0.1
SM 32:1	0.034	0.3	2.1	1.1	0.006	-2.9	0.6	3.9	0.452	0.0	0.1	0.5
SM 33:1	0.514	0.0	-0.1	-0.4	0.029	-2.2	-0.6	1.2	0.449	-0.5	-0.2	0.0
SM 34:1	0.960	0.0	0.0	0.0	0.008	-3.1	0.0	3.3	0.364	-0.5	0.0	0.4
SM 34:2	0.389	0.1	0.5	0.0	0.006	-3.1	0.6	3.9	0.146	-0.3	0.7	1.5
SM 35:1	0.104	-0.1	-1.4	-0.6	0.039	-2.4	-0.3	0.8	0.261	-0.3	-0.9	-0.1
SM 36:1	0.026	0.7	-0.5	-2.8	0.008	-3.0	-0.6	1.9	0.890	0.0	-0.1	0.0
SM 36:2	0.897	0.0	0.0	0.0	0.006	-3.3	0.0	3.9	0.503	0.0	0.2	0.3
SM 38:1	0.785	0.0	0.1	0.0	0.006	-3.1	0.5	3.6	0.364	0.0	0.0	1.1
SM 38:2	0.009	0.2	3.9	3.3	0.005	-2.5	3.9	3.9	0.146	0.0	0.7	1.9
SM 39:1	0.202	-0.8	0.0	0.7	0.008	-2.5	0.4	3.3	0.801	0.0	0.0	0.2
SM 41:1	0.814	0.0	0.0	-0.2	0.008	-2.5	0.0	3.9	0.870	0.0	0.1	0.0
SM 41:2	0.623	0.0	-0.1	-0.2	0.008	-2.9	-0.1	3.3	0.993	0.0	0.0	0.0
SM 42:1	0.539	0.2	0.1	0.0	0.180	-1.4	0.0	0.9	0.998	0.0	0.0	0.0
PC 24:0	0.170	0.4	-0.1	-1.2	0.037	-1.5	0.3	2.2	0.216	-0.3	0.2	1.0
PC 28:0	0.009	2.8	3.9	0.4	0.024	-0.7	1.0	3.3	0.419	-0.5	-0.2	-0.1
PC 29:0	0.876	0.0	0.0	0.0	1.000	-0.1	0.0	0.0	0.211	0.0	-0.8	-0.9
PC 30:0	0.241	0.8	0.1	-0.3	0.111	-2.0	-0.6	0.0	0.211	0.0	-0.8	-0.9
PC 31:0	0.012	0.0	-2.8	-3.0	0.024	-2.2	-2.2	-0.1	0.138	0.0	-1.9	-1.8
PC 31:1	0.652	0.1	0.1	0.0	0.441	-0.3	0.4	1.0	0.317	0.6	0.0	-0.5
PC 32:0	0.010	0.0	-3.3	-3.3	0.007	-3.3	-2.8	-0.6	0.146	0.1	-1.4	-1.9
PC 32:1	0.012	2.1	3.3	0.4	0.006	-2.9	2.2	3.9	0.261	0.0	0.7	0.7
PC 32:2	0.009	0.8	3.9	3.0	0.005	-3.3	3.9	3.9	0.146	0.0	1.0	2.0
PC 32:3	0.012	0.2	3.1	2.3	0.006	-1.6	3.6	3.9	1.000	0.0	0.0	0.0
PC 33:0	0.014	0.0	-2.4	-3.0	0.008	-3.1	-2.6	0.0	0.146	0.0	-1.3	-1.4
PC 33:1	0.017	0.1	-1.6	-2.8	0.012	-2.9	-0.4	1.7	0.179	0.0	-1.2	-1.0
PC 33:2	0.662	-0.1	-0.1	0.0	0.012	-2.5	0.1	2.8	0.605	-0.1	0.0	0.3
PC 34:0	0.093	0.0	-0.8	-1.5	0.013	-3.3	-1.1	0.3	0.540	-0.1	-0.2	-0.1
PC 34:1	0.114	0.7	-0.1	-1.2	0.012	-2.8	-0.8	1.5	0.590	0.0	-0.2	-0.2
PC 34:2	0.422	0.0	0.7	0.0	0.006	-3.3	0.0	3.9	0.261	0.0	0.2	1.3
PC 34:3	0.009	0.2	3.9	2.8	0.005	-2.9	3.9	3.9	0.146	0.0	0.8	1.9
PC 34:4	0.026	1.6	1.8	-0.5	0.060	-1.6	0.0	1.9	0.416	0.0	-0.2	-0.5
PC 35:0	0.177	0.0	-0.6	-1.0	0.081	-2.1	0.0	0.8	0.318	-0.2	-0.6	-0.2
PC 35:1	0.015	0.0	-2.1	-3.0	0.012	-2.8	-0.9	1.5	0.242	0.0	-0.7	-0.7
PC 35:2	0.740	-0.1	0.0	0.1	0.008	-2.9	0.3	3.3	0.458	-0.1	0.0	0.5
PC 35:3	0.452	-0.3	0.0	0.3	0.019	-0.7	2.2	2.4	0.993	0.0	0.0	0.0
PC 35:4	0.017	0.0	-2.4	-2.1	0.054	-1.9	-1.6	0.0	0.179	0.0	-1.2	-1.0
PC 36:1	0.676	0.0	0.0	-0.1	0.011	-2.8	-0.1	2.6	0.916	0.0	0.0	0.1
PC 36:2	0.255	0.0	0.2	0.9	0.006	-2.8	1.0	3.6	0.211	0.1	0.5	1.0
PC 36:3	0.717	0.0	-0.1	-0.1	0.008	-3.0	-0.1	3.0	0.449	0.0	0.0	0.7
PC 36:4a	0.015	0.3	3.3	1.1	0.006	-1.9	2.6	3.9	0.190	0.0	0.8	1.2
PC 36:4b	0.009	0.5	-3.1	-3.3	0.008	-2.2	-3.6	-1.3	0.146	0.0	-1.2	-1.5

Lipid species	6 weeks				10 weeks				16 weeks			
	P-value[a]	db/h vs. H/H[b]	db/db vs. H/H[b]	db/db vs. db/h[b]	*P*-value[a]	db/h vs. H/H[b]	db/db vs. H/H[b]	db/db vs. db/h[b]	*P*-value[a]	db/h vs. H/H[b]	db/db vs. H/H[b]	db/db vs. db/h[b]
PC 36:5	0.015	0.4	3.9	0.9	0.005	-2.8	3.0	3.9	0.146	0.0	1.0	1.8
PC 36:6	0.515	0.4	0.0	0.0	1.000	-0.4	-0.1	0.1	0.455	0.0	-0.2	-0.4
PC 37:4	0.012	0.0	-3.1	-3.0	0.049	-1.9	-1.7	0.0	0.149	-0.2	-1.2	-1.0
PC 37:5	0.076	0.0	-1.1	-1.5	0.020	-2.9	-1.0	0.3	0.616	-0.1	-0.2	-0.1
PC 37:6	0.015	0.0	-2.3	-2.8	0.117	-0.6	-1.9	-0.4	0.146	0.0	-1.3	-1.3
PC 38:2	0.693	0.0	0.0	0.2	0.033	-2.8	0.0	1.1	0.787	0.0	0.0	0.1
PC 38:3	0.717	0.0	0.0	0.2	0.007	-3.3	0.3	3.3	0.242	-0.2	0.2	1.0
PC 38:4	0.318	0.0	-0.3	-0.5	0.041	-2.0	-0.3	1.5	0.418	-0.5	0.0	0.2
PC 38:5	0.562	0.2	0.0	-0.2	0.037	-2.2	-0.1	1.5	0.261	0.1	0.0	1.1
PC 38:6a	0.859	0.0	0.0	0.0	0.036	-0.9	1.3	2.0	0.267	0.1	0.2	0.9
PC 38:6b	0.015	0.0	-1.8	-3.6	0.036	-0.6	-2.4	-1.3	0.211	0.0	-0.8	-0.9
PC 38:7	0.187	0.9	0.7	0.0	0.156	-0.5	0.4	1.7	0.401	0.3	0.4	0.1
PC 39:6	0.073	0.0	-1.5	-1.2	0.495	-0.9	-0.6	0.0	0.179	-0.5	-1.3	-0.5
PC 39:7	0.036	0.1	-1.1	-2.3	0.102	-0.6	-1.7	-0.7	0.149	0.0	-1.2	-1.3
PC 40:5	0.911	0.0	0.0	0.0	0.054	-2.1	0.0	1.3	0.146	-0.8	0.3	1.7
PC 40:6	0.204	0.0	-0.4	-1.0	0.665	-0.7	-0.6	0.0	0.525	-0.4	0.0	0.1
PC 40:7	0.150	0.1	-0.3	-1.3	1.000	-0.7	-0.2	0.0	0.948	0.0	0.0	0.0
PC(O-32:0)	0.032	0.0	-1.6	-2.1	0.013	-2.4	-3.0	0.0	0.138	-0.1	-2.2	-1.4
PC(O-32:1)	0.414	0.2	0.4	0.0	0.301	-1.2	0.0	0.7	0.971	0.0	0.0	0.0
PC(O-34:1)	0.183	0.0	-0.5	-1.0	0.021	-2.9	-1.0	0.3	0.146	0.0	-1.6	-1.0
PC(O-34:2)	0.513	0.0	-0.2	-0.2	0.054	-2.1	-0.1	1.1	0.416	-0.6	-0.2	0.0
PC(O-36:2)	0.562	0.0	-0.2	-0.2	0.077	-2.1	-0.3	0.6	0.386	-0.2	-0.6	0.0
PC(O-36:4)	0.019	0.0	-1.6	-3.0	0.008	-2.8	-3.6	-0.1	0.263	-0.7	-0.5	-0.1
PC(O-38:4)	0.016	-1.8	-2.4	-0.3	0.019	-2.5	-2.0	-0.1	0.412	-0.1	-0.7	-0.1
PC(O-38:5)	0.200	-0.8	-0.7	0.0	0.011	-2.9	-2.2	0.2	0.211	-1.1	0.0	0.7
PC(O-40:6)	0.222	0.0	-0.8	-0.4	0.224	-0.9	-1.5	0.0	0.787	0.0	-0.1	0.0
PC(O-40:7)	0.021	-0.3	-2.6	-1.2	0.024	-2.2	-2.2	0.0	0.528	-0.2	0.0	0.2
PC(P-32:0)	0.017	0.1	-1.3	-3.3	0.010	-2.1	-2.6	-1.3	0.146	0.0	-1.2	-1.6
PC(P-32:1)	0.413	0.4	0.0	-0.2	1.000	-0.2	0.1	0.4	0.711	-0.3	0.0	0.0
PC(P-34:1)	0.219	0.3	-0.1	-0.9	0.593	-1.0	-0.4	0.0	0.185	0.0	-0.9	-1.2
PC(P-34:2)	0.935	0.0	0.0	0.0	0.044	-2.3	-1.2	0.0	0.605	0.0	0.1	0.2
PC(P-36:4)	0.012	0.0	-2.8	-2.8	0.035	-1.1	-2.8	-0.4	0.468	-0.1	-0.3	-0.1
PC(P-38:5)	0.241	0.0	-0.3	-0.8	0.035	-2.4	-1.3	0.0	0.875	-0.2	0.0	0.0
PC(P-38:6)	0.054	0.0	-0.8	-2.5	0.035	-0.6	-2.4	-1.3	0.179	0.0	-1.1	-1.1
PC(P-40:5)	0.079	0.0	-1.5	-1.0	0.079	-1.8	-1.3	0.0	0.138	-1.3	-1.8	-0.8
PC(P-40:6)	0.105	0.1	-0.4	-1.6	0.179	-1.2	-1.1	-0.1	0.158	0.0	-1.3	-1.1
LPC 14:0	0.464	0.0	-0.2	-0.3	0.020	-2.4	0.0	2.2	0.922	0.0	0.1	0.0
LPC 16:0	0.104	0.0	-0.4	-2.0	0.078	-2.2	-0.3	0.4	0.993	0.0	0.0	0.0
LPC 16:1	0.979	0.0	0.0	0.0	0.006	-2.5	2.4	3.9	0.267	0.0	0.7	0.6
LPC 18:0	0.279	0.0	0.0	-1.6	0.014	-2.5	0.0	2.6	0.787	0.0	0.1	0.1
LPC 18:1	0.105	0.0	-0.6	-1.6	0.057	-1.2	0.4	1.9	0.751	0.0	0.2	0.0
LPC 18:2	0.617	-0.1	0.0	0.3	0.006	-3.3	0.3	3.9	0.317	0.0	0.5	0.6
LPC 20:4	0.135	-0.1	-0.8	-1.0	0.066	-2.1	-0.2	0.8	0.787	-0.2	0.0	0.0
LPC 22:6	0.034	-0.2	-1.6	-1.8	0.325	-1.4	-0.4	0.0	0.787	-0.1	0.0	0.0
PE 32:0	0.118	-0.4	-1.0	-0.5	0.224	-1.3	-0.9	0.0	0.138	-1.6	-2.4	-0.3
PE 32:1	0.413	0.3	0.4	0.0	0.133	-1.4	0.2	1.1	0.517	0.3	0.0	-0.2
PE 34:1	0.437	0.4	0.0	-0.1	0.013	-2.9	-0.1	1.9	0.929	0.0	0.0	0.1
PE 34:2	0.851	0.0	0.0	0.0	0.008	-3.0	0.0	3.6	0.528	0.0	0.1	0.4
PE 34:3	0.012	0.0	2.8	3.0	0.006	-2.1	2.2	3.6	0.138	-0.8	0.5	2.6
PE 35:2	0.076	-0.1	0.4	2.3	0.022	-2.0	0.1	2.6	0.446	-0.3	0.0	0.4
PE 36:1	0.255	-0.2	0.0	-1.1	0.023	-2.8	-0.2	1.1	0.934	0.0	0.0	0.0
PE 36:2	0.414	0.0	0.3	0.3	0.006	-3.3	0.3	3.9	0.216	0.0	0.3	1.2
PE 36:3	0.079	0.0	0.9	1.6	0.006	-3.0	1.0	3.9	0.179	0.0	0.4	1.8
PE 36:4	0.076	0.0	-1.6	-1.0	0.009	-2.9	-1.0	1.6	0.892	0.0	0.1	0.0

Lipid species	6 weeks				10 weeks				16 weeks			
	P-value[a]	db/h vs. H/H[b]	db/db vs. H/H[b]	db/db vs. db/h[b]	*P*-value[a]	db/h vs. H/H[b]	db/db vs. H/H[b]	db/db vs. db/h[b]	*P*-value[a]	db/h vs. H/H[b]	db/db vs. H/H[b]	db/db vs. db/h[b]
PE 36:5	0.015	0.0	3.1	1.8	0.005	-2.9	3.6	3.9	0.293	0.0	0.3	0.8
PE 38:3	0.864	0.0	0.0	0.0	0.018	-1.8	0.3	3.0	0.455	0.0	0.1	0.5
PE 38:4	0.839	0.0	0.0	0.0	0.028	-2.2	0.0	2.0	0.216	-0.2	0.0	1.4
PE 38:5	0.745	0.0	0.1	0.1	0.008	-3.0	0.0	2.8	0.211	0.1	0.0	1.6
PE 38:6	0.011	0.7	-2.4	-3.0	0.043	-1.9	-1.9	0.0	0.211	0.2	-0.4	-1.1
PE 40:5	0.070	0.2	-0.8	-1.8	0.043	-2.0	-1.3	0.3	0.926	0.0	0.0	0.0
PE 40:6	0.057	0.0	-1.4	-1.6	0.174	-1.8	-0.3	0.2	0.865	0.0	-0.1	0.0
PE 40:7	0.318	0.3	0.0	-0.5	0.047	-1.9	0.2	1.6	0.179	-0.5	0.1	1.5
PE(O-34:1)	0.364	0.3	0.0	-0.4	0.022	-2.9	-0.1	1.1	0.692	-0.1	-0.1	-0.1
PE(O-36:2)	0.209	0.9	0.2	-0.3	0.543	-1.0	-0.1	0.3	0.993	0.0	0.0	0.0
PE(O-38:5)	0.740	-0.2	0.0	0.0	0.066	-1.7	0.4	1.3	0.138	-0.7	0.8	2.2
PE(O-40:5)	0.651	0.0	-0.1	0.0	0.094	-2.4	-0.1	0.3	0.787	0.0	0.0	-0.2
PE(O-40:6)	0.073	0.0	-0.9	-1.8	0.614	-0.9	-0.2	0.2	0.998	0.0	0.0	0.0
PE(O-40:7)	0.318	0.2	-0.1	-0.6	1.000	-0.6	-0.1	0.3	0.993	0.0	0.0	0.0
PE(O-42:7)	0.821	0.0	0.0	0.0	1.000	-0.1	0.0	0.0	0.317	0.6	0.5	0.0
PE(P-34:1)	0.255	0.6	0.3	-0.1	0.623	-0.9	0.0	0.4	0.738	-0.1	0.0	0.2
PE(P-36:1)	0.667	0.1	0.0	-0.1	0.679	-0.9	-0.2	0.1	0.894	0.1	0.0	0.0
PE(P-36:2)	0.183	0.6	1.0	0.0	0.783	-0.7	0.0	0.5	0.922	0.0	0.0	0.0
PE(P-36:4)	0.231	-0.1	-0.8	-0.3	0.008	-2.4	-3.6	-0.2	0.343	-0.8	-0.2	0.0
PE(P-38:4)	0.318	0.0	-0.3	-0.6	0.550	-1.1	0.0	0.3	0.614	-0.1	0.0	0.2
PE(P-38:5)	0.643	0.0	-0.1	-0.1	0.072	-2.0	-0.9	0.1	0.993	0.0	0.0	0.0
PE(P-38:6)	0.015	0.3	-1.3	-3.6	0.024	-1.1	-2.4	-1.2	0.146	0.0	-1.2	-1.4
PE(P-40:5)	0.252	0.1	-0.3	-0.7	0.043	-2.0	-1.7	0.0	0.418	0.0	-0.3	-0.4
PE(P-40:6)	0.018	0.0	-2.3	-2.1	0.017	-2.4	-2.4	-0.1	0.196	0.1	-0.8	-1.0
LPE 16:0	0.091	0.4	-0.1	-1.8	0.123	-1.9	-0.4	0.2	0.971	0.0	0.0	0.0
LPE 18:0	0.172	0.2	-0.2	-1.2	0.120	-1.3	0.0	1.5	0.509	0.0	0.2	0.3
LPE 18:1	0.376	0.4	0.2	-0.1	0.212	-1.0	0.1	1.2	0.437	-0.1	0.2	0.3
LPE 22:6	0.036	0.0	-0.8	-3.0	0.124	-1.8	-0.9	0.0	0.319	-0.3	-0.7	-0.1
PI 32:0	0.090	0.1	-1.1	-1.1	0.377	-1.1	-0.6	0.0	0.267	-1.2	-0.1	0.1
PI 34:0	0.074	1.2	-0.1	-1.3	0.290	-1.0	0.0	1.0	0.389	-0.7	0.0	0.2
PI 34:1	0.081	0.8	-0.2	-1.5	0.233	-1.1	0.0	1.0	0.590	-0.2	0.0	0.2
PI 36:1	0.322	0.4	0.0	-0.5	0.089	-1.7	0.0	1.3	0.998	0.0	0.0	0.0
PI 36:2	0.789	0.1	0.0	0.0	0.008	-2.5	0.4	3.3	0.187	-0.7	0.1	1.3
PI 36:4	0.071	0.0	-1.4	-1.3	0.008	-3.0	-2.8	0.1	0.418	-0.2	-0.5	-0.1
PI 38:2	0.661	0.0	-0.1	-0.1	0.066	-1.5	0.1	1.7	0.449	0.0	0.2	0.4
PI 38:3	0.114	0.0	-0.9	-1.1	0.273	-0.9	0.0	1.2	0.317	0.0	0.7	0.4
PI 38:4	0.073	0.1	-1.3	-1.3	0.068	-2.0	-0.6	0.4	0.645	0.0	-0.1	-0.2
PI 38:5	0.318	0.0	-0.8	-0.1	0.013	-2.6	0.0	2.6	0.452	-0.1	0.0	0.6
PI 38:6	0.010	0.1	-3.1	-3.3	0.006	-2.9	-3.9	-0.8	0.138	0.1	-1.9	-1.8
PI 40:4	0.039	0.0	-2.1	-1.3	0.008	-2.8	-1.2	1.7	0.476	-0.1	0.1	0.4
PI 40:5	0.924	0.0	0.0	0.0	0.011	-2.5	0.0	3.3	0.261	-0.1	0.2	1.0
PI 40:6	0.009	0.3	-3.3	-3.6	0.019	-1.9	-2.8	-0.3	0.149	0.0	-1.0	-1.5
PS 36:1	0.209	0.5	0.8	0.0	0.294	-1.1	-0.1	0.6	0.776	0.0	0.0	0.1
PS 36:2	0.668	0.1	0.1	0.0	0.030	-2.4	-0.2	1.3	0.457	-0.2	0.0	0.4
PS 38:3	0.661	0.0	0.0	-0.3	0.007	-3.3	0.0	3.6	0.449	0.0	0.1	0.5
PS 38:4	0.953	0.0	0.0	0.0	0.014	-3.0	-0.3	1.5	0.261	-0.7	0.0	0.7
PS 38:5	0.863	0.0	0.0	0.0	0.140	-1.3	0.0	1.3	0.926	0.0	0.0	0.0
PS 40:5	0.799	0.0	0.0	0.0	0.008	-3.0	0.0	2.8	0.158	-0.2	0.2	1.8
PS 40:6	0.012	0.0	-2.8	-3.0	0.035	-2.4	-1.5	0.0	0.453	0.0	-0.2	-0.4
PG 32:0	0.440	0.0	-0.1	-0.5	0.072	-1.2	-1.9	-0.2	0.146	0.5	-0.2	-1.8
PG 34:1	0.570	0.3	0.0	0.0	0.007	-2.4	1.1	3.9	0.611	-0.3	0.0	0.1
PG 34:2	0.863	0.0	0.0	0.0	0.008	-1.9	1.9	3.6	0.649	-0.2	0.0	0.1
PG 36:1	0.192	0.6	0.8	0.0	0.290	-1.0	0.0	0.9	0.916	0.0	0.0	0.0
PG 36:2	0.513	0.2	0.3	0.0	0.011	-1.8	0.6	3.6	0.211	-0.3	0.0	1.4

Lipid species	6 weeks				10 weeks				16 weeks			
	P-value[a]	db/h vs. H/H[b]	db/db vs. H/H[b]	db/db vs. db/h[b]	*P*-value[a]	db/h vs. H/H[b]	db/db vs. H/H[b]	db/db vs. db/h[b]	*P*-value[a]	db/h vs. H/H[b]	db/db vs. H/H[b]	db/db vs. db/h[b]
CL 18:2/18:2/18:2/16:1	0.059	1.5	1.5	0.0	0.006	-2.0	1.9	3.9	0.138	0.0	1.5	3.0
CL 18:2/18:1/18:2/16:1	0.222	0.4	0.8	0.0	0.019	-1.0	0.7	3.6	0.455	0.0	0.2	0.4
CL 18:2/18:1/18:1/16:1	0.183	0.9	0.7	0.0	1.000	-0.1	0.0	0.2	0.419	0.0	0.6	0.2
CL 18:2/18:2/18:2/18:2	0.864	0.0	0.0	0.0	0.017	-2.1	0.1	2.8	0.190	0.0	0.2	1.7
CL 18:2/18:2/18:2/18:1	0.163	0.3	-0.3	-1.1	0.041	-2.5	-0.1	0.8	0.369	-0.5	-0.1	0.3
CL 18:2/18:1/18:2/18:1	0.146	0.3	-0.3	-1.1	0.035	-2.4	-0.2	1.1	0.261	-1.0	-0.3	0.1
CL 18:1/18:1/18:1/18:2	0.302	0.7	0.2	0.0	1.000	-0.2	0.1	0.6	0.419	-0.7	0.0	0.1
CL 18:2/18:2/18:2/20:3	0.814	0.0	0.0	-0.1	0.038	-2.1	-0.3	1.3	0.314	-0.3	0.0	0.7
CL 18:2/18:1/18:2/20:3	0.473	0.3	0.0	-0.3	0.045	-2.1	-0.6	0.8	0.416	-0.5	-0.3	0.0
CL 18:2/18:1/18:2/20:2	0.217	0.2	-0.2	-0.9	0.436	-1.0	-0.6	0.0	0.380	0.0	-0.5	-0.4
CL 18:2/18:2/18:2/20:4	0.778	0.0	0.0	-0.1	0.054	-1.8	0.0	1.7	0.190	-1.6	-0.2	0.2
CL 18:2/18:2/18:2/22:6	0.076	0.9	-0.2	-1.5	1.000	-0.3	-0.6	0.0	0.261	0.0	-0.5	-0.9
CL 18:2/18:1/18:2/22:6	0.180	-0.1	-1.1	-0.3	1.000	0.0	-0.2	-0.1	0.410	0.0	-0.3	-0.5
CE 18:0	0.661	0.0	-0.1	-0.2	0.047	-1.1	-2.2	-0.4	0.738	-0.1	0.0	0.1
CE 18:1	0.209	0.0	-0.7	-0.7	0.156	-1.1	-1.3	-0.1	0.924	0.0	0.0	0.0
CE 18:2	0.795	0.0	0.0	0.1	0.126	-1.5	-0.1	1.1	0.261	0.0	0.5	0.9
CE 20:4	0.312	0.0	-0.1	-0.9	0.291	-1.1	-0.1	0.7	0.211	0.0	0.2	1.4
CE 22:6	0.864	0.0	0.0	0.0	0.043	-0.6	0.3	3.6	0.146	0.0	1.0	2.2
COH	0.376	0.4	0.0	-0.4	0.037	-2.3	-0.4	0.9	0.926	0.0	0.0	0.0
DG 14:0/16:0	0.496	0.0	0.1	0.4	0.066	-1.2	0.3	1.9	0.616	-0.1	0.0	0.3
DG 14:0/18:1	0.103	0.0	0.6	1.8	0.091	0.0	1.5	1.9	0.211	0.0	0.6	1.2
DG 16:0/16:0	0.496	0.0	-0.1	-0.4	0.032	-2.3	-0.6	1.0	0.993	0.0	0.0	0.0
DG 16:0/18:1	0.523	0.0	0.1	0.4	0.145	-0.1	0.7	1.9	0.197	0.0	0.6	1.3
DG 16:0/18:2	0.617	0.0	0.0	0.3	0.196	-0.1	0.9	1.5	0.235	0.0	0.5	1.0
DG 16:0/20:4	0.502	0.3	0.0	-0.2	0.098	-1.7	0.0	1.2	0.787	-0.1	0.0	0.1
DG 16:0/22:5	0.102	0.0	1.6	0.6	0.008	-2.6	0.6	3.3	0.138	-0.8	0.8	2.2
DG 16:0/22:6	0.580	0.1	0.0	-0.2	0.068	-1.7	0.0	1.6	0.930	0.0	0.0	0.0
DG 16:1/18:1	0.038	0.0	1.5	2.0	0.015	0.1	2.8	3.0	0.146	0.0	1.0	2.2
DG 18:0/18:1	0.717	0.0	0.0	0.2	0.744	-0.1	0.4	0.8	0.416	0.0	0.3	0.4
DG 18:0/18:2	0.839	0.0	0.0	-0.1	0.595	-0.2	0.3	1.0	0.416	0.0	0.2	0.6
DG 18:0/20:4	0.574	0.1	0.0	-0.3	0.084	-2.1	-0.3	0.4	0.926	0.0	0.0	0.0
DG 18:1/18:1	0.594	0.0	0.1	0.2	0.325	0.0	0.9	1.1	0.211	0.0	0.4	1.2
DG 18:1/18:2	0.594	0.0	0.1	0.2	0.256	0.1	1.1	1.0	0.240	0.0	0.5	1.0
DG 18:1/18:3	0.076	0.0	0.7	2.1	0.050	0.1	1.9	2.0	0.179	0.0	0.7	1.4
DG 18:1/20:4	0.192	0.1	0.8	0.4	0.027	-0.4	2.0	2.4	0.196	-0.1	0.4	1.3
DG 18:2/18:2	0.389	0.0	0.2	0.5	0.145	0.3	1.3	1.1	0.267	-0.1	0.2	0.9
TG 14:0/16:0/18:1	0.076	0.0	0.8	2.0	0.013	-0.1	2.4	3.9	0.261	0.0	0.5	0.8
TG 14:0/16:0/18:2	0.015	0.0	2.6	2.5	0.008	-0.1	3.9	3.9	0.146	0.0	1.1	1.6
TG 14:0/16:1/18:1	0.015	0.1	2.6	2.1	0.008	0.0	3.9	3.9	0.146	0.0	1.0	1.8
TG 14:0/16:1/18:2	0.015	0.1	2.6	2.1	0.008	0.0	3.9	3.9	0.146	0.0	0.9	1.7
TG 14:0/17:0/18:1	0.211	0.0	0.4	1.1	0.019	-0.1	2.0	3.6	0.242	0.0	0.3	1.2
TG 14:0/18:0/18:1	0.256	0.0	0.2	1.1	0.043	-0.7	0.6	2.8	0.616	0.0	0.2	0.1
TG 14:0/18:2/18:2	0.099	0.0	0.5	2.1	0.010	-0.1	3.0	3.9	0.190	0.0	0.7	1.4
TG 14:1/16:0/18:1	0.015	0.1	2.4	2.3	0.008	0.0	3.9	3.9	0.146	0.0	0.9	1.7
TG 14:1/16:1/18:0	0.009	0.3	3.6	3.0	0.008	0.0	3.9	3.9	0.146	0.1	1.1	1.5
TG 14:1/18:0/18:2	0.034	0.1	1.6	2.0	0.008	0.0	3.9	3.9	0.158	0.0	0.8	1.6
TG 14:1/18:1/18:1	0.023	0.1	2.1	2.0	0.008	0.0	3.9	3.9	0.146	0.0	1.0	1.8
TG 15:0/16:0/18:1	0.294	0.0	0.3	0.8	0.051	-0.2	1.3	2.4	0.292	0.0	0.4	0.8
TG 15:0/18:1/18:1	0.462	0.0	0.2	0.3	0.042	-0.1	1.6	2.6	0.211	0.0	0.5	1.4
TG 16:0/16:0/16:0	0.255	0.0	0.2	1.1	0.015	-1.0	0.8	3.9	0.404	0.0	0.3	0.5
TG 16:0/16:0/18:0	0.444	0.0	0.0	0.7	0.055	-1.3	0.0	2.4	0.645	0.0	0.2	0.1
TG 16:0/16:0/18:1	0.222	0.0	0.4	1.0	0.017	-0.2	1.7	3.9	0.216	0.0	0.6	1.0
TG 16:0/16:0/18:2	0.255	0.0	0.3	1.0	0.019	-0.2	1.6	3.9	0.292	0.0	0.5	0.7
TG 16:0/16:1/17:0	0.130	0.0	0.5	1.6	0.013	-0.2	2.2	3.9	0.211	0.0	0.5	1.3

Lipid species	6 weeks				10 weeks				16 weeks			
	P-value[a]	db/h vs. H/H[b]	db/db vs. H/H[b]	db/db vs. db/h[b]	*P*-value[a]	db/h vs. H/H[b]	db/db vs. H/H[b]	db/db vs. db/h[b]	*P*-value[a]	db/h vs. H/H[b]	db/db vs. H/H[b]	db/db vs. db/h[b]
TG 16:0/16:1/18:1	0.042	0.0	1.6	1.6	0.008	-0.1	3.9	3.9	0.146	0.0	1.0	1.9
TG 16:0/17:0/18:0	0.266	0.0	0.4	0.7	0.033	-0.1	1.7	2.8	0.211	0.0	0.5	1.2
TG 16:0/17:0/18:1	0.241	0.0	0.4	0.9	0.024	-0.2	1.2	3.9	0.216	0.0	0.5	1.1
TG 16:0/17:0/18:2	0.222	0.0	0.4	0.9	0.017	-0.1	2.0	3.9	0.242	0.0	0.4	1.1
TG 16:0/18:0/18:1	0.414	0.0	0.1	0.8	0.066	-0.7	0.3	2.6	0.416	0.0	0.3	0.5
TG 16:0/18:1/18:1	0.318	0.0	0.3	0.7	0.037	-0.1	1.3	3.0	0.190	0.0	0.7	1.4
TG 16:0/18:1/18:2	0.269	0.0	0.4	0.7	0.019	0.0	2.0	3.6	0.211	0.0	0.5	1.3
TG 16:0/18:2/18:2	0.187	0.0	0.4	1.2	0.015	-0.1	2.2	3.9	0.196	0.0	0.6	1.4
TG 16:1/16:1/16:1	0.009	0.3	3.9	3.3	0.008	0.0	3.9	3.9	0.146	0.0	1.2	1.6
TG 16:1/16:1/18:0	0.099	0.0	0.7	1.8	0.008	-0.5	2.6	3.9	0.292	0.0	0.5	0.7
TG 16:1/16:1/18:1	0.012	0.2	2.8	2.5	0.008	0.0	3.9	3.9	0.146	0.0	1.2	1.7
TG 16:1/17:0/18:1	0.222	0.0	0.4	0.9	0.017	0.0	2.4	3.6	0.190	0.0	0.6	1.5
TG 16:1/18:1/18:1	0.076	0.0	1.3	1.3	0.008	0.0	3.6	3.9	0.146	0.0	0.8	2.1
TG 16:1/18:1/18:2	0.099	0.0	0.8	1.5	0.011	0.0	3.0	3.9	0.146	0.0	0.7	2.0
TG 17:0/18:1/18:1	0.502	0.0	0.2	0.2	0.132	-0.1	0.6	2.2	0.216	0.0	0.4	1.3
TG 18:0/18:0/18:1	0.570	0.0	0.0	0.5	0.223	-0.9	0.0	1.5	0.631	0.0	0.3	0.0
TG 18:0/18:1/18:1	0.421	0.0	0.1	0.7	0.089	-0.5	0.4	2.4	0.343	0.0	0.3	0.7
TG 18:0/18:2/18:2	0.488	0.0	0.2	0.3	0.039	-0.2	1.3	2.8	0.343	0.0	0.3	0.7
TG 18:1/18:1/18:1	0.676	0.0	0.1	0.1	0.110	0.0	0.9	2.2	0.261	0.0	0.4	1.0
TG 18:1/18:1/18:2	0.506	0.0	0.2	0.2	0.107	0.0	1.0	2.2	0.261	0.0	0.3	1.0
TG 18:1/18:1/20:4	0.200	0.0	0.4	1.1	0.021	0.0	2.4	3.0	0.211	0.0	0.5	1.3
TG 18:1/18:2/18:2	0.255	0.0	0.4	0.7	0.024	0.0	2.0	3.3	0.216	0.0	0.5	1.2
TG 18:2/18:2/18:2	0.222	0.0	0.4	0.9	0.015	0.0	2.6	3.6	0.233	0.0	0.4	1.2
TG 18:2/18:2/20:4	0.211	0.0	0.5	0.9	0.024	0.0	1.6	3.9	0.261	0.0	0.5	0.9

[a] *P*-value for the comparison of levels of each lipid species between genotypes at each age using the Kruskal Wallis test with Benjamini-Hochberg correction for multiple comparisons. $P < 0.05$ was considered significant (highlighted in pink).

[b] Post-hoc analysis was performed using the Mann Whitney *U* test with Dunn-Sidak correction for multiple group comparisons. Values were derived from the formula: sign(difference in median levels)*-log10(post-hoc *P*-value). Colour-coded values 1.3 to 2.0 (light red, $P = 0.05$-0.01) and > 2.0 (dark red, $P < 0.01$) indicate a significant increase relative to the reference group. Colour-coded values -1.3 to -2.0 (light green, $P = 0.05$-0.01) and < -2.0 (dark green, $P < 0.01$) indicate a significant decrease relative to the reference group.

Table S4.8 Relationship between genotype and left-ventricle lipid species in female mice.

Lipid species	6 weeks				10 weeks				16 weeks			
	P-value[a]	db/h vs. H/H[b]	db/db vs. H/H[b]	db/db vs. db/h[b]	*P*-value[a]	db/h vs. H/H[b]	db/db vs. H/H[b]	db/db vs. db/h[b]	*P*-value[a]	db/h vs. H/H[b]	db/db vs. H/H[b]	db/db vs. db/h[b]
Sph 18:1	0.419	-0.1	-0.4	-0.1	0.391	-0.3	-0.2	0.0	0.262	-0.1	0.1	1.0
Cer 16:0	0.378	-0.3	0.0	0.4	0.005	-2.2	0.1	1.9	0.969	0.0	0.0	0.0
Cer 18:0	0.026	-0.4	0.6	2.1	0.002	-2.6	0.3	2.6	0.200	-0.8	-0.4	0.2
Cer 20:0	0.020	-0.6	0.9	2.0	0.002	-1.2	1.3	3.0	0.300	-0.5	-0.3	0.1
Cer 22:0	0.070	-0.9	0.1	1.2	0.027	-1.0	0.1	1.7	0.660	0.0	-0.1	-0.1
Cer 24:0	0.169	-1.1	0.0	0.4	0.123	-0.9	-0.3	0.2	0.132	0.0	-0.8	-1.1
Cer 24:1	0.918	0.0	0.0	0.0	0.048	-1.3	0.1	0.9	0.554	0.0	-0.1	-0.2
MHC 22:0	0.158	-0.2	-1.3	-0.1	0.789	0.0	0.0	0.0	0.157	0.1	-0.4	-1.1
MHC 24:0	0.071	-0.1	-1.1	-1.0	0.129	0.0	-0.8	-0.6	0.074	-0.1	-1.4	-1.0
MHC 24:1	0.529	-0.3	-0.1	0.0	0.276	-0.4	-0.4	0.0	0.514	0.0	-0.3	-0.1
DHC 20:0	0.184	-0.4	0.0	1.0	0.524	0.0	0.1	0.2	0.387	0.5	0.1	-0.1
DHC 22:0	0.898	0.0	0.0	0.0	0.085	-0.3	0.3	1.2	0.645	0.1	0.0	-0.2
THC 18:0	0.749	-0.1	0.0	0.1	0.959	0.0	0.0	0.0	0.201	0.9	0.1	-0.4
GM3 18:0	0.086	0.0	-1.3	-0.7	0.020	-1.7	-1.3	0.0	0.653	0.2	0.0	0.0
GM3 20:0	0.020	0.0	-1.8	-1.8	0.150	0.0	-0.9	-0.5	0.302	0.0	-0.4	-0.6
GM3 22:0	0.004	0.0	-3.9	-2.8	0.002	-0.1	-3.0	-3.0	0.168	0.1	-0.3	-1.2
GM3 24:0	0.038	0.2	-0.9	-1.6	0.099	0.0	-0.9	-0.8	0.213	0.1	-0.1	-1.2
GM3 24:1	0.242	0.1	-0.7	-0.4	0.007	0.0	-2.8	-1.9	0.979	0.0	0.0	0.0
SM 31:1	0.771	0.0	0.0	0.0	0.392	-0.4	-0.1	0.0	0.984	0.0	0.0	0.0
SM 32:1	0.006	0.2	2.6	2.5	0.203	-0.1	0.2	0.7	0.493	0.0	0.4	0.1
SM 33:1	0.406	0.0	-0.2	-0.4	0.629	0.0	-0.1	-0.1	0.032	0.0	-1.6	-2.4
SM 34:0	0.158	-0.6	0.1	0.8	0.096	-1.0	0.0	0.6	0.412	-0.4	0.0	0.2
SM 34:1	0.267	-0.6	-0.2	0.1	0.109	-1.1	-0.4	0.0	0.253	0.0	-0.6	-0.6
SM 34:2	0.354	-0.5	-0.1	0.1	0.595	0.0	0.1	0.1	0.653	0.0	-0.2	0.0
SM 35:1	0.154	-0.8	-0.8	0.0	0.111	-0.7	-0.9	0.0	0.129	0.0	-0.8	-1.1
SM 36:1	0.717	-0.2	0.0	0.0	0.048	-1.7	-0.2	0.2	0.150	-0.1	-0.9	-0.7
SM 36:2	0.795	0.0	0.0	0.0	0.075	-1.3	0.0	0.6	0.400	-0.5	-0.1	0.1
SM 38:1	0.276	-0.8	-0.1	0.0	0.538	-0.2	0.0	0.1	0.326	-0.2	-0.7	0.0
SM 38:2	0.668	0.0	0.0	0.2	0.321	-0.1	0.1	0.4	0.419	-0.2	-0.4	0.0
SM 39:1	0.004	0.0	-3.3	-3.3	0.001	-2.0	-3.9	-1.2	0.032	0.1	-1.4	-2.2
SM 41:1	0.007	0.0	-3.1	-1.8	0.008	-1.0	-2.2	-0.8	0.035	0.0	-1.3	-2.5
SM 41:2	0.042	0.6	-0.9	-1.2	0.003	-0.7	-3.0	-1.7	0.104	0.0	-0.8	-1.3
SM 42:1	0.074	-0.2	-1.3	-0.7	0.024	-0.6	-2.2	-0.3	0.042	0.0	-1.5	-1.8
PC 24:0	0.232	0.0	-0.8	-0.4	0.047	-0.3	-1.9	-0.3	0.376	0.5	-0.2	0.0
PC 30:0	0.004	0.0	3.1	3.0	0.008	-0.3	1.9	2.0	0.647	-0.1	0.0	-0.1
PC 31:0	0.079	-0.8	-1.4	0.0	0.121	-1.0	-0.5	0.0	0.023	0.0	-2.4	-3.1
PC 31:1	0.117	0.0	0.7	1.1	0.321	-0.4	0.0	0.2	0.104	0.0	-1.0	-1.1
PC 32:0	0.020	0.0	-2.1	-1.5	0.001	-0.7	-3.9	-2.6	0.027	0.0	-1.8	-3.1
PC 32:1	0.003	0.1	3.9	3.6	0.001	-0.6	3.9	3.9	0.082	0.0	0.9	1.5
PC 32:2	0.003	-0.1	3.9	3.6	0.001	-0.5	3.3	3.9	0.044	-0.2	0.6	2.4
PC 33:0	0.067	-1.0	-1.3	0.0	0.020	-1.1	-1.7	-0.3	0.023	0.0	-2.7	-3.1
PC 33:1	0.060	-0.1	0.8	1.5	0.213	-0.9	0.0	0.2	0.066	0.0	-1.2	-1.5
PC 33:2	0.009	-0.6	1.8	2.1	0.010	-0.2	1.6	2.2	0.339	0.0	-0.1	-0.7
PC 34:0	0.107	0.0	-0.8	-1.0	0.026	-0.8	-1.9	-0.2	0.038	0.0	-1.3	-2.2
PC 34:1	0.007	0.0	3.9	1.3	0.010	-0.1	2.2	1.7	0.676	0.1	0.1	0.0
PC 34:2	0.003	-0.1	3.9	3.3	0.001	-0.5	3.9	3.9	0.677	0.0	0.1	0.1
PC 34:3	0.003	0.0	3.9	3.6	0.001	-0.3	3.9	3.9	0.032	0.0	1.5	2.4
PC 34:4	0.004	0.0	3.1	3.3	0.001	-0.5	3.9	3.9	0.032	-0.5	0.5	2.7
PC 35:0	0.035	-0.1	-1.8	-1.0	0.066	-1.7	-0.4	0.0	0.043	0.7	-0.7	-1.8
PC 35:1	0.354	-0.2	-0.6	0.0	0.109	-1.5	0.0	0.1	0.023	0.4	-1.5	-3.3
PC 35:2	0.005	-0.3	2.3	3.0	0.001	-1.9	1.7	3.3	0.205	0.0	-0.5	-0.8
PC 35:3	0.010	-0.1	1.9	2.3	0.001	0.0	3.9	3.9	0.575	0.3	0.0	0.0

Lipid species	6 weeks				10 weeks				16 weeks			
	P-value[a]	db/h vs. H/H[b]	db/db vs. H/H[b]	db/db vs. db/h[b]	*P*-value[a]	db/h vs. H/H[b]	db/db vs. H/H[b]	db/db vs. db/h[b]	*P*-value[a]	db/h vs. H/H[b]	db/db vs. H/H[b]	db/db vs. db/h[b]
PC 35:4	0.719	-0.1	0.0	0.1	0.158	-0.5	0.1	0.6	0.253	-0.3	-0.7	-0.1
PC 36:0	0.811	0.0	0.0	0.0	0.465	0.0	0.2	0.3	0.358	-0.3	-0.5	0.0
PC 36:1	0.004	0.3	3.3	2.5	0.001	-0.9	3.9	3.6	0.894	0.0	0.0	0.0
PC 36:2	0.003	0.0	3.9	3.6	0.001	-1.2	3.9	3.9	0.302	0.0	0.5	0.5
PC 36:3	0.003	0.0	3.9	3.6	0.001	-0.3	3.9	3.9	0.340	0.0	0.2	0.7
PC 36:4a	0.003	0.0	3.9	3.6	0.001	-0.4	3.9	3.9	0.300	0.0	0.2	0.7
PC 36:4b	0.590	0.0	0.2	0.1	0.008	-0.2	1.2	3.0	0.514	-0.4	-0.1	0.0
PC 36:5	0.003	0.0	3.9	3.6	0.001	-0.7	3.9	3.9	0.038	-0.1	1.2	2.2
PC 36:6	0.701	-0.1	0.0	0.1	0.091	-0.5	0.5	0.8	0.410	-0.3	0.0	0.4
PC 37:4	0.868	0.0	0.0	0.0	0.039	-1.1	0.1	1.2	0.094	-0.1	-1.2	-0.9
PC 37:5	0.181	-0.1	0.7	0.6	0.002	-0.3	3.9	3.0	0.807	0.0	0.0	0.1
PC 37:6	0.076	-0.6	-1.3	-0.2	0.151	0.0	-0.7	-0.6	0.358	-0.2	-0.5	0.0
PC 38:2	0.425	0.0	0.1	0.4	0.774	0.0	0.0	0.1	0.771	-0.1	0.0	0.0
PC 38:3	0.014	0.4	2.1	1.5	0.001	-0.8	3.3	3.6	0.384	0.0	0.1	0.5
PC 38:4	0.556	0.0	0.1	0.3	0.006	-0.8	0.7	3.0	0.770	-0.1	0.0	0.0
PC 38:5	0.089	0.0	1.3	0.8	0.002	-0.7	3.0	3.3	0.065	-0.2	0.6	1.9
PC 38:6a	0.005	0.1	3.9	1.8	0.002	0.0	3.9	3.6	0.279	0.0	0.3	0.8
PC 38:6b	0.047	-0.1	-1.6	-0.8	0.014	0.0	-1.7	-2.0	0.150	-0.1	-1.0	-0.6
PC 38:7	0.419	0.0	0.4	0.1	0.002	-0.1	3.6	3.0	0.419	-0.2	0.0	0.4
PC 39:6	0.060	-0.1	-1.9	-0.4	0.099	-0.8	-0.8	0.0	0.097	-0.2	-1.1	-0.9
PC 39:7	0.406	0.0	-0.7	0.0	0.847	0.0	0.0	0.0	0.917	0.0	0.0	0.0
PC 40:5	0.208	-0.7	0.0	0.6	0.121	-0.8	0.1	0.6	0.212	-0.7	0.0	0.7
PC 40:6	0.012	-0.2	-2.6	-1.3	0.002	0.0	-3.6	-3.9	0.046	-0.3	-1.5	-1.2
PC 40:7	0.559	0.0	-0.3	-0.1	0.219	-0.1	0.3	0.5	0.591	0.0	-0.1	-0.2
PC(O-30:0)	0.765	0.0	-0.1	0.0	0.541	-0.1	0.0	0.2	0.095	0.0	-1.1	-1.2
PC(O-32:0)	0.004	0.0	-3.3	-3.3	0.100	-0.2	-0.9	-0.6	0.023	0.1	-2.5	-2.9
PC(O-32:1)	0.075	0.4	1.3	0.4	0.007	-0.4	1.3	2.6	0.666	-0.2	0.0	0.0
PC(O-34:0)	0.243	-0.1	-0.6	-0.4	0.145	-0.1	-0.8	-0.4	0.023	0.4	-2.5	-2.2
PC(O-34:1)	0.004	0.0	-3.6	-3.3	0.083	-1.0	-0.7	-0.1	0.028	0.0	-1.8	-2.7
PC(O-34:2)	0.939	0.0	0.0	0.0	0.411	0.0	0.2	0.3	0.027	0.0	-2.2	-2.4
PC(O-34:3)	0.393	-0.2	0.0	0.4	0.392	0.0	0.1	0.5	0.205	0.0	-0.9	-0.5
PC(O-36:0)	0.248	-0.3	-0.8	0.0	0.363	0.0	-0.3	-0.4	0.032	0.1	-1.4	-2.4
PC(O-36:1)	0.659	0.0	-0.1	0.0	0.665	-0.1	0.0	-0.2	0.095	0.0	-1.1	-1.2
PC(O-36:2)	0.580	0.0	-0.1	-0.3	0.893	0.0	0.0	0.0	0.032	0.0	-2.0	-2.0
PC(O-36:3)	0.304	-0.3	-0.6	0.0	0.211	-0.7	0.0	0.3	0.038	0.0	-1.5	-1.9
PC(O-36:4)	0.852	0.0	0.0	0.0	0.068	-0.9	0.0	1.1	0.279	-0.2	-0.7	-0.1
PC(O-36:5)	0.313	0.0	0.7	0.2	0.119	-0.6	0.2	0.7	0.284	-0.8	-0.1	0.2
PC(O-38:4)	0.641	-0.1	0.0	0.1	0.859	0.0	0.0	0.0	0.083	0.0	-1.4	-1.0
PC(O-38:5)	0.588	0.0	0.2	0.1	0.027	-0.7	0.6	1.5	0.113	-0.4	0.2	1.4
PC(O-40:6)	0.235	-0.2	-0.9	0.0	0.627	0.0	-0.1	-0.1	0.046	-0.4	-1.8	-0.8
PC(O-40:7)	0.119	-0.1	-1.3	-0.3	0.524	-0.1	-0.1	0.1	0.540	-0.1	-0.2	-0.1
PC(P-32:0)	0.634	0.0	-0.2	-0.1	0.151	-0.4	-0.7	-0.1	0.028	-0.1	-1.9	-2.4
PC(P-32:1)	0.043	0.9	1.6	0.1	0.013	-0.1	2.0	1.7	0.557	0.0	0.4	0.0
PC(P-34:1)	0.230	0.0	0.8	0.3	0.560	0.0	0.2	0.0	0.677	0.0	0.0	-0.2
PC(P-34:2)	0.680	-0.2	0.0	0.0	0.372	0.0	0.3	0.2	0.148	-0.1	-1.0	-0.6
PC(P-34:3)	0.064	0.0	-1.1	-1.2	0.295	-0.3	-0.3	-0.2	0.193	0.0	-0.7	-0.8
PC(P-36:2)	0.593	0.1	0.0	-0.3	0.185	0.8	0.3	0.0	0.132	0.0	-0.6	-1.4
PC(P-36:4)	0.272	0.0	0.8	0.3	0.021	-0.5	0.9	1.7	0.302	-0.8	-0.1	0.0
PC(P-36:5)	0.006	0.0	3.6	1.8	0.002	0.0	3.6	3.3	0.114	-0.1	0.5	1.5
PC(P-38:4)	0.836	-0.1	0.0	0.0	0.574	0.0	0.2	0.1	0.410	-0.1	-0.5	0.0
PC(P-38:5)	0.412	0.0	-0.5	0.0	0.631	-0.2	0.0	0.0	0.376	-0.6	-0.2	0.0
PC(P-38:6)	0.090	-0.2	-1.4	-0.3	0.158	0.0	-0.6	-0.6	0.097	-0.7	-1.2	-0.3
PC(P-40:5)	0.147	-0.4	-1.1	0.0	0.556	0.0	-0.1	-0.3	0.032	-0.4	-2.4	-1.1
PC(P-40:6)	0.020	-0.5	-2.6	-0.3	0.034	0.3	-0.7	-1.6	0.023	-0.3	-2.2	-2.7

Lipid species	6 weeks				10 weeks				16 weeks			
	P-value[a]	db/h vs. H/H[b]	db/db vs. H/H[b]	db/db vs. db/h[b]	*P*-value[a]	db/h vs. H/H[b]	db/db vs. H/H[b]	db/db vs. db/h[b]	*P*-value[a]	db/h vs. H/H[b]	db/db vs. H/H[b]	db/db vs. db/h[b]
LPC 14:0	0.518	-0.2	0.1	0.2	0.096	-1.0	0.0	0.6	0.157	0.0	0.5	1.2
LPC 15:0	0.402	0.0	-0.3	-0.3	0.042	-0.4	-1.7	-0.3	0.677	0.1	0.0	-0.1
LPC 16:0	0.699	0.0	-0.1	-0.1	0.039	-0.7	-1.7	-0.1	0.872	0.0	0.0	0.0
LPC 16:1	0.004	0.2	3.6	3.0	0.007	-0.4	1.6	2.4	0.023	0.1	3.1	3.6
LPC 17:0	0.515	0.0	-0.4	0.0	0.114	-1.0	-0.6	0.0	0.376	0.1	-0.1	-0.5
LPC 17:1	0.939	0.0	0.0	0.0	0.091	-0.7	-1.0	-0.1	0.967	0.0	0.0	0.0
LPC 18:0	0.955	0.0	0.0	0.0	0.093	-1.0	-0.6	0.0	0.953	0.0	0.0	0.0
LPC 18:1	0.201	0.0	0.5	0.8	0.003	-1.8	0.9	2.6	0.321	0.0	0.2	0.7
LPC 18:2	0.018	0.0	1.9	1.8	0.001	-2.3	2.4	3.9	0.262	0.1	0.6	0.5
LPC 20:1	0.773	-0.1	0.0	0.0	0.179	-0.6	0.0	0.6	0.894	0.1	0.0	0.0
LPC 20:3	0.022	0.0	1.9	1.5	0.001	-3.1	3.3	3.9	0.138	0.1	0.3	1.4
LPC 20:4	0.556	0.0	0.1	0.3	0.001	-2.5	2.4	3.9	0.253	0.1	0.2	0.9
LPC 22:4	0.357	0.0	0.2	0.4	0.003	-0.7	1.0	3.9	0.616	0.0	0.1	0.2
LPC 22:5	0.195	-0.4	0.1	0.8	0.001	-2.5	1.5	3.9	0.038	0.1	1.1	2.2
LPC 22:6	0.339	-0.3	-0.4	-0.1	0.071	-1.8	-0.1	0.1	0.653	0.0	0.2	0.0
LPC(O-16:0)	0.016	0.2	-1.0	-2.8	0.005	-0.6	-3.0	-1.2	0.648	0.1	0.0	-0.1
PE 32:0	0.845	0.0	0.1	0.0	0.361	0.0	-0.2	-0.4	0.777	-0.1	0.0	0.0
PE 34:1	0.087	0.0	0.7	1.5	0.004	0.0	2.8	2.6	0.368	0.3	0.5	0.0
PE 34:2	0.003	0.0	3.9	3.6	0.001	0.0	3.9	3.9	0.579	0.0	0.2	0.1
PE 34:3	0.003	0.0	3.9	3.3	0.001	0.4	3.9	3.9	0.047	-0.1	0.7	2.4
PE 35:1	0.358	0.0	0.5	0.2	0.560	0.0	0.2	0.0	0.719	0.0	-0.2	0.0
PE 35:2	0.025	-0.2	1.3	1.8	0.001	-0.9	3.9	3.9	0.122	0.0	-0.5	-1.4
PE 36:1	0.399	0.1	0.5	0.0	0.219	-0.1	0.4	0.5	0.201	0.1	-0.4	-0.8
PE 36:2	0.003	0.0	3.9	3.6	0.001	-0.1	3.9	3.9	0.909	0.0	0.0	0.0
PE 36:3	0.003	0.0	3.9	3.6	0.001	-0.4	3.9	3.9	0.205	0.0	0.6	0.8
PE 36:4	0.003	0.0	3.9	3.6	0.001	0.0	3.9	3.9	0.038	-0.2	0.7	2.5
PE 36:5	0.003	0.6	3.9	3.6	0.001	0.0	3.9	3.9	0.027	0.0	2.4	2.2
PE 38:3	0.103	0.2	0.8	0.9	0.001	0.1	3.9	3.9	0.551	0.0	0.1	0.3
PE 38:4	0.003	0.1	3.9	3.6	0.001	-0.1	3.9	3.9	0.045	-0.2	0.8	2.0
PE 38:5	0.003	0.0	3.9	3.6	0.001	0.0	3.9	3.9	0.038	-0.7	0.5	2.2
PE 38:6	0.906	0.0	0.0	0.0	0.145	0.0	0.9	0.5	0.327	-0.4	-0.5	0.0
PE 40:5	0.031	0.0	1.5	1.5	0.006	-0.3	1.6	2.6	0.177	-1.1	-0.5	0.0
PE 40:6	0.765	0.0	-0.1	0.0	0.185	-0.1	0.6	0.4	0.150	-0.1	-1.0	-0.5
PE 40:7	0.918	0.0	0.0	0.0	0.004	0.0	3.0	2.2	0.541	-0.1	-0.2	0.0
PE(O-34:1)	0.160	0.0	0.9	0.4	0.191	-0.1	0.3	0.6	0.541	0.1	0.0	-0.2
PE(O-36:2)	0.408	-0.3	0.0	0.3	0.430	0.2	0.2	0.0	0.559	0.0	-0.1	-0.2
PE(O-36:3)	0.786	0.0	0.0	0.0	0.113	0.1	0.8	0.7	0.541	0.0	-0.1	-0.3
PE(O-36:4)	0.518	-0.1	0.0	0.3	0.003	0.1	2.8	2.8	0.669	-0.1	-0.1	0.0
PE(O-36:5)	0.658	0.1	0.1	0.0	0.576	-0.4	0.0	0.0	0.862	0.0	0.0	0.0
PE(O-38:4)	0.343	0.2	0.6	0.0	0.711	0.0	0.0	0.1	0.156	-0.2	-1.1	-0.3
PE(O-38:5)	0.003	0.0	3.9	3.6	0.001	-0.3	3.9	3.9	0.023	-0.2	2.0	3.6
PE(O-40:4)	0.984	0.0	0.0	0.0	0.574	0.1	0.0	-0.2	0.902	0.0	0.0	0.0
PE(O-40:5)	0.044	0.0	1.9	0.9	0.038	0.0	1.1	1.6	0.217	-0.5	0.0	0.8
PE(O-40:6)	0.485	-0.1	-0.4	0.0	0.284	0.0	0.3	0.4	0.285	0.1	-0.6	-0.3
PE(O-40:7)	0.939	0.0	0.0	0.0	0.027	-0.1	1.6	1.3	0.648	-0.1	0.0	0.1
PE(P-34:2)	0.104	0.0	1.1	0.7	0.071	0.0	1.1	1.0	0.514	0.1	0.5	0.0
PE(P-36:2)	0.483	-0.3	0.0	0.2	0.027	0.8	1.7	0.3	0.122	-0.1	-1.6	-0.2
PE(P-36:4)	0.004	0.0	3.6	2.5	0.002	-0.3	2.8	3.9	0.773	0.0	0.1	0.0
PE(P-38:4)	0.038	0.0	1.9	1.0	0.002	-0.4	2.8	2.8	0.648	0.0	-0.2	-0.1
PE(P-38:5)	0.008	0.0	2.4	2.3	0.004	0.0	2.8	2.6	0.540	-0.2	0.0	0.2
PE(P-38:6)	0.669	0.0	-0.1	-0.1	0.284	-0.1	0.1	0.6	0.125	-1.4	-0.7	0.0
PE(P-40:4)	0.224	-0.8	0.0	0.4	0.959	0.0	0.0	0.0	0.869	0.0	0.0	0.0
PE(P-40:5)	0.584	0.0	0.0	0.2	0.498	0.0	0.2	0.2	0.443	0.0	-0.3	-0.2
PE(P-40:6)	0.750	0.0	-0.1	0.0	0.859	0.0	0.0	0.0	0.038	-0.1	-2.0	-1.3

Lipid species	6 weeks				10 weeks				16 weeks			
	P-value[a]	db/h vs. H/H[b]	db/db vs. H/H[b]	db/db vs. db/h[b]	*P*-value[a]	db/h vs. H/H[b]	db/db vs. H/H[b]	db/db vs. db/h[b]	*P*-value[a]	db/h vs. H/H[b]	db/db vs. H/H[b]	db/db vs. db/h[b]
LPE 16:0	0.519	0.0	-0.1	-0.3	0.022	-0.2	-2.6	-0.6	0.469	0.4	0.2	0.0
LPE 18:0	0.975	0.0	0.0	0.0	0.194	-0.1	-0.9	-0.1	0.536	0.3	0.1	0.0
LPE 18:1	0.852	0.0	0.0	0.0	0.459	-0.1	-0.3	0.0	0.587	0.0	0.3	0.0
LPE 18:2	0.217	0.0	0.3	0.9	0.070	-0.6	0.1	1.3	0.279	0.7	0.3	-0.1
LPE 20:4	0.020	0.0	1.8	1.8	0.001	-2.4	2.6	3.9	0.099	0.3	1.0	0.9
LPE 22:5	0.018	0.0	1.4	2.3	0.001	-1.0	3.9	3.9	0.023	0.1	2.5	3.6
LPE 22:4	0.975	0.0	0.0	0.0	0.077	-1.3	-0.1	0.4	0.388	0.2	0.5	0.0
LPE 22:6	0.237	-0.7	-0.4	0.0	0.026	-2.3	-0.2	0.2	0.347	0.0	0.0	-0.9
PI 34:1	0.020	0.4	1.9	1.1	0.001	0.1	3.9	3.9	0.591	0.0	0.1	0.1
PI 36:1	0.069	0.8	1.3	0.2	0.021	-0.1	0.9	2.4	0.762	0.0	0.0	-0.1
PI 36:2	0.028	-0.2	1.1	1.8	0.026	-0.1	1.6	1.3	0.253	0.0	-0.5	-0.7
PI 36:3	0.003	0.3	3.9	3.0	0.001	0.3	3.9	3.9	0.151	0.0	0.7	1.1
PI 36:4	0.003	0.0	3.9	3.3	0.008	0.0	3.0	1.6	0.349	-0.3	-0.5	0.0
PI 38:2	0.020	0.0	2.1	1.5	0.238	0.0	0.4	0.5	0.651	0.2	0.0	0.0
PI 38:3	0.750	0.0	0.0	0.1	0.006	0.0	3.3	1.7	0.591	0.0	0.0	0.2
PI 38:4	0.419	0.0	0.1	0.4	0.126	-0.1	0.4	1.0	0.193	-0.8	-0.7	0.0
PI 38:5	0.003	0.3	3.9	3.6	0.001	-0.1	3.9	3.9	0.144	-0.2	0.2	1.4
PI 38:6	0.795	0.0	0.0	-0.1	0.690	-0.1	0.0	0.0	0.405	-0.4	0.0	0.2
PI 40:4	0.786	0.0	0.0	0.1	0.141	-0.1	0.2	1.1	0.579	-0.2	-0.1	0.0
PI 40:5	0.004	-0.5	2.6	2.8	0.004	-0.1	1.9	3.3	0.023	-0.8	1.4	3.1
PI 40:6	0.186	-0.2	-0.8	-0.3	0.028	-0.4	-1.6	-0.8	0.388	-0.2	-0.5	0.0
PS 36:1	0.181	0.0	-0.4	-1.0	0.018	-0.2	-1.7	-1.5	0.023	0.1	-1.6	-3.3
PS 36:2	0.004	-0.8	2.4	3.3	0.001	-1.9	1.3	3.6	0.902	0.0	0.0	0.0
PS 38:3	0.118	-0.3	0.3	1.1	0.185	0.0	0.3	0.9	0.750	0.0	-0.1	0.0
PS 38:4	0.276	0.0	0.4	0.5	0.204	-0.2	-0.2	0.6	0.307	0.0	-0.5	-0.5
PS 38:5	0.006	-0.1	2.3	2.8	0.002	0.0	3.6	3.9	0.082	-1.1	0.0	1.4
PS 40:5	0.020	-0.4	1.5	1.6	0.002	-0.8	1.6	3.6	0.273	-0.7	0.0	0.4
PS 40:6	0.719	-0.2	0.0	0.0	0.072	-0.5	-0.1	1.3	0.091	-0.4	-1.4	-0.5
PG 34:1	0.090	-0.2	0.4	1.3	0.027	0.0	1.7	1.3	0.660	0.0	0.1	0.1
PG 34:2	0.004	-0.4	2.3	3.6	0.002	0.0	3.9	3.0	0.902	0.0	0.0	0.0
PG 36:1	0.495	-0.3	0.0	0.1	0.139	-0.9	-0.3	0.1	0.253	0.0	-0.8	-0.3
PG 36:2	0.006	0.0	3.3	2.0	0.007	0.0	2.8	1.9	0.953	0.0	0.0	0.0
PG 36:3	0.006	0.0	2.1	3.6	0.003	0.0	2.6	3.0	0.384	0.2	0.5	0.0
BMP 16:0/18:1	0.786	0.0	0.1	0.0	0.372	-0.2	0.1	0.3	0.294	-0.1	0.4	0.5
BMP 18:1/18:1	0.196	0.1	0.9	0.2	0.318	-0.2	0.1	0.4	0.762	0.0	0.1	0.0
CL 18:2/18:2/18:2/16:1	0.003	1.5	3.9	2.5	0.001	0.0	3.9	3.9	0.032	0.0	1.8	2.4
CL 18:2/18:1/18:2/16:1	0.003	0.4	3.9	3.6	0.001	0.1	3.9	3.9	0.028	0.0	2.2	2.2
CL 18:2/18:1/18:1/16:1	0.022	0.9	1.6	0.9	0.624	-0.2	0.0	0.0	0.027	-0.2	0.9	3.6
CL 18:2/18:2/18:2/18:3	0.614	0.0	0.1	0.2	0.003	-0.2	2.2	3.3	0.869	0.1	0.0	0.0
CL 18:2/18:2/18:2/18:2	0.011	0.0	2.8	1.5	0.001	-0.2	3.9	3.6	0.660	0.0	0.0	0.2
CL 18:2/18:2/18:2/18:1	0.934	0.0	0.0	0.0	0.014	0.0	2.4	1.5	0.474	0.0	-0.4	-0.1
CL 18:2/18:1/18:2/18:1	0.529	-0.1	-0.2	0.0	0.121	0.3	-0.1	-1.0	0.604	0.0	-0.2	0.0
CL 18:1/18:1/18:1/18:2	0.525	0.0	-0.2	-0.2	0.129	0.4	1.0	0.0	0.917	0.0	0.0	0.0
CL 18:2/18:2/18:2/20:3	0.107	0.0	0.9	0.9	0.002	-0.1	3.0	3.0	0.418	-0.1	0.0	0.5
CL 18:2/18:1/18:2/20:3	0.746	0.0	0.0	0.1	0.125	0.0	1.1	0.5	0.591	-0.1	-0.2	0.0
CL 18:2/18:1/18:2/20:2	0.495	-0.3	-0.1	0.1	0.769	-0.1	0.0	0.0	0.179	0.0	-0.7	-0.9
CL 18:2/18:2/18:2/20:4	0.515	-0.1	0.0	0.4	0.004	-0.2	2.4	2.8	0.557	-0.3	-0.1	0.0
CL 18:2/18:1/18:2/20:1	0.310	-0.6	0.0	0.3	0.637	0.0	0.4	0.0	0.046	-0.4	-1.6	-0.9
CL 18:2/18:2/18:2/22:6	0.071	-0.3	-1.4	-0.4	0.174	0.0	-0.4	-0.8	0.128	0.0	-0.8	-1.1
CL 18:2/18:1/18:2/22:6	0.296	0.0	-0.8	-0.1	0.018	0.0	-1.6	-1.9	0.122	-0.1	-1.1	-0.7
CL 18:2/18:1/18:2/22:5	0.730	0.0	0.1	0.0	0.108	0.0	1.1	0.6	0.474	-0.2	-0.3	0.0
CL 18:2/22:6/18:2/20:3	0.562	-0.1	-0.2	0.0	0.030	0.3	-1.3	-1.2	0.575	-0.1	-0.1	-0.2
CE 18:1	0.267	0.1	0.6	0.3	0.169	0.0	0.3	1.0	0.618	0.0	-0.1	-0.1
CE 18:2	0.004	-0.1	2.8	3.6	0.002	-0.3	2.8	3.9	0.038	-0.5	0.5	2.5

Lipid species	6 weeks				10 weeks				16 weeks			
	P-value[a]	db/h vs. H/H[b]	db/db vs. H/H[b]	db/db vs. db/h[b]	*P*-value[a]	db/h vs. H/H[b]	db/db vs. H/H[b]	db/db vs. db/h[b]	*P*-value[a]	db/h vs. H/H[b]	db/db vs. H/H[b]	db/db vs. db/h[b]
CE 18:3	0.006	0.0	3.3	2.1	0.008	-0.1	1.7	2.4	0.373	-0.2	0.0	0.6
CE 20:3	0.213	0.1	0.8	0.2	0.026	-0.1	1.2	1.7	0.045	-0.2	1.1	1.8
CE 20:4	0.195	0.6	0.7	0.0	0.113	0.0	0.7	0.9	0.365	-0.2	0.0	0.6
CE 20:5	0.003	0.0	3.9	3.3	0.001	0.0	3.9	3.9	0.027	0.0	1.5	3.1
CE 22:6	0.502	0.0	0.3	0.1	0.003	-0.9	1.5	3.0	0.368	0.1	0.1	0.6
COH	0.593	0.2	0.0	0.1	0.196	-0.7	-0.1	0.3	0.269	0.0	-0.6	-0.5
DG 16:0/16:0	0.006	0.1	3.6	1.8	0.001	-2.1	3.9	3.9	0.063	0.0	0.9	1.9
DG 16:0/18:1	0.008	0.1	3.9	1.1	0.001	-1.3	3.9	3.9	0.032	-0.1	1.4	2.4
DG 16:0/18:2	0.047	0.0	2.4	0.4	0.001	-1.0	3.6	3.9	0.044	-0.1	0.9	2.2
DG 16:0/20:4	0.204	0.1	0.9	0.2	0.004	-0.1	2.2	3.0	0.798	0.0	0.0	0.1
DG 16:0/22:5	0.015	-0.1	1.5	2.3	0.001	-0.1	3.9	3.9	0.089	0.0	0.9	1.5
DG 16:0/22:6	0.773	0.0	0.0	0.1	0.051	0.0	1.0	1.5	0.578	-0.2	-0.2	0.0
DG 16:1/18:1	0.003	0.3	3.9	2.8	0.001	-1.8	2.8	3.9	0.027	0.0	1.8	3.1
DG 18:0/18:1	0.020	0.0	3.3	0.6	0.001	-1.7	2.8	3.9	0.104	0.0	0.6	1.5
DG 18:0/18:2	0.064	0.0	1.4	1.0	0.001	-1.3	3.9	3.9	0.483	0.0	0.1	0.5
DG 18:0/20:4	0.529	0.0	-0.2	-0.2	0.027	-1.6	-0.8	0.3	0.027	0.3	-1.3	-2.9
DG 18:1/18:1	0.016	0.4	3.3	0.3	0.001	-0.3	3.9	3.9	0.065	0.0	1.0	1.6
DG 18:1/18:2	0.023	0.3	3.1	0.2	0.001	-0.2	3.9	3.9	0.126	0.0	0.7	1.3
DG 18:1/18:3	0.008	0.0	3.6	1.3	0.001	-1.5	3.9	3.9	0.023	0.0	2.0	3.1
DG 18:1/20:3	0.226	0.0	0.5	0.7	0.002	0.0	2.8	3.6	0.578	0.0	0.2	0.2
DG 18:1/20:4	0.016	1.5	2.3	0.1	0.001	0.0	3.9	3.9	0.739	0.0	0.1	0.0
DG 18:2/18:2	0.177	0.1	1.3	0.0	0.002	0.0	3.3	3.9	0.412	0.0	0.2	0.4
TG 14:0/16:0/18:1	0.006	0.0	2.8	2.3	0.002	-0.1	2.6	3.9	0.037	-0.1	1.3	2.2
TG 14:0/16:0/18:2	0.018	0.0	2.1	1.6	0.004	-0.6	1.0	3.9	0.052	0.0	1.1	1.8
TG 14:0/16:1/18:1	0.006	0.0	3.3	2.0	0.003	-0.2	1.7	3.9	0.032	0.0	1.8	2.0
TG 14:0/16:1/18:2	0.011	0.0	2.3	2.1	0.002	-0.9	1.7	3.9	0.038	0.0	1.6	1.8
TG 14:0/17:0/18:1	0.022	-0.3	0.9	2.1	0.007	0.0	1.7	3.0	0.038	0.0	1.6	1.8
TG 14:1/16:0/18:1	0.008	0.2	3.1	1.3	0.010	0.0	1.3	3.0	0.038	0.0	1.8	1.8
TG 14:1/16:1/18:0	0.008	0.0	2.8	2.0	0.006	-0.3	0.8	3.9	0.032	0.0	1.8	2.4
TG 14:1/18:1/18:1	0.005	0.0	3.3	2.3	0.002	-0.2	2.2	3.9	0.023	0.0	2.5	2.9
TG 16:0/16:0/16:0	0.004	0.0	3.3	2.8	0.002	-0.9	1.9	3.9	0.144	-0.1	0.4	1.3
TG 16:0/16:0/18:0	0.006	0.0	3.1	2.1	0.002	-1.0	1.2	3.9	0.232	0.0	0.3	0.9
TG 16:0/16:0/18:1	0.004	0.0	3.9	2.1	0.002	-0.1	3.3	3.9	0.033	0.0	1.4	2.4
TG 16:0/16:0/18:2	0.007	0.0	3.1	2.0	0.002	0.0	2.8	3.9	0.066	-0.1	0.8	1.8
TG 16:0/16:1/18:1	0.004	0.0	3.6	2.8	0.002	-0.2	2.4	3.9	0.023	0.0	2.4	2.7
TG 16:0/17:0/18:1	0.011	0.0	2.3	2.1	0.003	0.0	3.0	2.8	0.038	0.0	1.6	1.8
TG 16:0/17:0/18:2	0.022	0.0	1.9	1.5	0.005	-0.1	1.5	3.6	0.065	0.0	1.0	1.6
TG 16:0/18:0/18:1	0.007	0.0	2.8	2.1	0.005	-0.2	1.1	3.9	0.091	-0.1	0.6	1.6
TG 16:0/18:1/18:1	0.007	0.2	3.3	1.5	0.003	0.0	2.2	3.9	0.032	0.0	1.6	2.4
TG 16:0/18:1/18:2	0.016	0.1	3.6	0.6	0.002	0.0	3.3	3.9	0.032	-0.1	1.6	2.0
TG 16:0/18:2/18:2	0.041	0.0	1.9	0.8	0.002	0.0	2.8	3.6	0.032	-0.1	1.9	2.0
TG 16:1/16:1/16:1	0.009	0.0	2.4	2.1	0.005	-0.2	1.1	3.9	0.027	0.0	2.4	2.2
TG 16:1/16:1/18:0	0.017	-0.2	1.9	1.6	0.004	0.3	1.3	3.9	0.144	-0.2	0.3	1.2
TG 16:1/16:1/18:1	0.005	0.0	3.3	2.3	0.004	0.1	1.5	3.9	0.023	0.0	2.7	3.1
TG 16:1/17:0/18:1	0.006	0.0	3.3	2.0	0.002	0.0	2.6	3.9	0.032	0.0	1.9	2.2
TG 16:1/18:1/18:1	0.004	0.1	3.9	2.5	0.002	-0.4	2.0	3.9	0.023	0.0	2.9	3.1
TG 16:1/18:1/18:2	0.004	0.0	3.6	2.3	0.002	-0.2	2.8	3.9	0.023	0.0	2.5	2.7
TG 17:0/18:1/18:1	0.050	0.0	1.3	1.3	0.094	-0.1	0.6	1.0	0.032	-0.1	1.6	2.2
TG 18:0/18:0/18:1	0.009	-0.1	2.8	1.8	0.004	-0.4	1.0	3.9	0.069	-0.1	0.5	2.0
TG 18:0/18:1/18:1	0.006	0.0	3.3	2.0	0.007	-0.1	1.1	3.9	0.042	0.0	1.3	1.9
TG 18:1/18:1/18:1	0.006	0.6	3.9	0.7	0.002	0.0	2.6	3.9	0.032	0.0	2.0	1.9
TG 18:1/18:1/18:2	0.037	0.1	2.4	0.4	0.003	0.0	2.6	3.6	0.045	-0.1	1.3	1.6
TG 18:1/18:1/20:4	0.007	1.6	3.1	0.3	0.021	0.0	1.5	1.9	0.143	0.0	0.9	0.9
TG 18:1/18:1/22:6	0.419	0.0	0.4	0.1	0.149	0.0	0.6	0.8	0.361	0.0	0.4	0.4

Lipid species	6 weeks				10 weeks				16 weeks			
	P-value[a]	db/h vs. H/H[b]	db/db vs. H/H[b]	db/db vs. db/h[b]	*P*-value[a]	db/h vs. H/H[b]	db/db vs. H/H[b]	db/db vs. db/h[b]	*P*-value[a]	db/h vs. H/H[b]	db/db vs. H/H[b]	db/db vs. db/h[b]
TG 18:1/18:2/18:2	0.059	0.2	1.9	0.3	0.002	0.0	3.0	3.3	0.044	0.0	1.6	1.5
TG 18:2/18:2/18:2	0.275	0.0	0.5	0.4	0.009	0.0	2.0	2.2	0.089	0.0	1.3	1.1
TG 18:2/18:2/20:4	0.417	0.3	0.3	0.0	0.811	0.0	0.0	0.0	0.288	-0.4	0.0	0.6

[a] *P*-value for the comparison of levels of each lipid species between genotypes at each age using the Kruskal Wallis test with Benjamini-Hochberg correction for multiple comparisons. $P < 0.05$ was considered significant (highlighted in pink).

[b] Post-hoc analysis was performed using the Mann Whitney *U* test with Dunn-Sidak correction for multiple group comparisons. Values were derived from the formula: sign(difference in median levels)*-log10(post-hoc *P*-value). Colour-coded values 1.3 to 2.0 (light red, $P = 0.05$-0.01) and > 2.0 (dark red, $P < 0.01$) indicate a significant increase relative to the reference group. Colour-coded values -1.3 to -2.0 (light green, $P = 0.05$-0.01) and < -2.0 (dark green, $P < 0.01$) indicate a significant decrease relative to the reference group.

Table S4.9 Relationship between genotype and adipose lipid species in female mice.

Lipid species	6 weeks				10 weeks				16 weeks			
	P-value[a]	db/h vs. H/H[b]	db/db vs. H/H[b]	db/db vs. db/h[b]	*P*-value[a]	db/h vs. H/H[b]	db/db vs. H/H[b]	db/db vs. db/h[b]	*P*-value[a]	db/h vs. H/H[b]	db/db vs. H/H[b]	db/db vs. db/h[b]
Sph 18:1	0.066	-0.2	0.4	1.3	0.151	0.9	0.3	0.0	0.692	-0.2	0.0	0.0
Cer 16:0	0.003	1.2	-2.1	-3.0	0.027	-0.4	-1.5	-1.3	0.824	0.0	0.0	0.0
Cer 18:0	0.003	0.0	-3.1	-3.3	0.020	0.0	-2.1	-2.0	0.647	0.1	0.0	-0.2
Cer 20:0	0.003	1.0	-3.9	-3.3	0.029	-0.2	-1.9	-0.8	0.634	0.0	0.0	-0.3
Cer 22:0	0.003	0.9	-3.3	-3.0	0.051	-0.3	-1.5	-0.4	0.971	0.0	0.0	0.0
Cer 24:0	0.003	0.6	-2.8	-2.7	0.020	-0.2	-1.9	-2.0	0.948	0.0	0.0	0.0
Cer 24:1	0.003	1.0	-3.9	-3.3	0.027	-0.2	-1.5	-1.6	0.598	0.0	-0.2	-0.1
MHC 16:0	0.102	-0.1	-1.4	-0.1	0.027	0.0	-2.3	-0.9	0.293	-0.2	-0.7	-0.1
MHC 22:0	0.082	-0.1	-1.1	-0.4	0.018	0.0	-2.9	-2.7	0.067	-0.8	-2.2	-0.8
MHC 24:0	0.021	-0.1	-1.8	-1.2	0.018	0.0	-3.1	-2.4	0.092	-0.7	-1.9	-0.3
MHC 24:1	0.069	-0.2	-1.3	-0.4	0.028	0.0	-1.8	-1.5	0.181	-0.5	-1.2	0.0
SM 32:1	0.004	-1.2	2.3	2.2	0.018	0.4	2.4	1.6	0.059	-0.1	3.3	2.9
SM 33:1	0.105	-0.4	-0.9	-0.1	0.276	0.0	-0.3	-0.6	0.440	0.0	-0.5	-0.1
SM 34:0	0.038	-1.3	0.0	1.3	0.099	0.2	1.0	0.4	0.161	-0.1	0.5	1.2
SM 34:1	0.115	-0.2	-0.9	-0.2	0.668	0.0	0.0	-0.2	0.129	-0.3	0.7	1.3
SM 34:2	0.219	0.1	0.7	0.1	0.115	0.1	0.8	0.7	0.082	0.2	1.8	1.3
SM 35:1	0.066	-1.6	-0.2	0.2	0.732	0.0	0.0	-0.1	0.920	0.0	0.0	0.0
SM 35:2	0.916	0.0	0.0	0.0	0.925	0.0	0.0	0.0	0.595	0.1	0.2	0.0
SM 36:1	0.168	-0.6	-0.1	0.4	0.415	0.2	0.2	0.0	0.996	0.0	0.0	0.0
SM 36:2	0.039	-0.6	0.4	1.5	0.051	0.7	1.2	0.3	0.529	0.1	0.3	0.0
SM 38:1	0.009	0.2	-1.6	-2.7	0.395	-0.1	-0.4	0.0	0.824	0.0	0.0	-0.1
SM 38:2	0.916	0.0	0.0	0.0	0.127	0.0	0.5	1.0	0.367	0.0	0.2	0.6
SM 39:1	0.149	-0.2	0.0	1.0	0.479	0.2	0.1	0.0	0.750	-0.1	0.0	0.1
SM 41:1	0.041	-0.2	0.8	1.3	0.045	0.9	1.2	0.2	0.464	0.0	0.2	0.3
SM 41:2	0.006	-0.1	2.4	2.4	0.029	0.9	1.3	0.6	0.211	0.1	1.1	0.2
SM 42:1	0.006	0.4	-2.1	-2.4	0.077	0.0	-0.9	-1.2	0.748	0.0	0.0	-0.1
PC 24:0	0.005	0.3	-2.1	-3.0	0.018	-1.6	-2.6	0.0	0.090	-0.5	-1.8	-0.8
PC 28:0	0.121	-0.6	0.0	0.9	0.653	-0.1	-0.1	0.0	0.163	-1.2	0.0	0.7
PC 30:0	0.011	-0.2	-2.6	-1.2	0.038	0.0	-1.8	-0.9	0.163	-0.1	-1.2	-0.6
PC 31:0	0.011	-0.3	-2.4	-1.3	0.018	0.0	-2.6	-1.8	0.073	-0.4	-2.0	-1.1
PC 31:1	0.075	-1.0	-0.8	0.0	0.094	-0.1	-1.5	-0.2	0.176	-0.8	-0.7	-0.2
PC 32:0	0.003	-0.1	-3.3	-2.7	0.018	-0.3	-2.9	-2.2	0.092	-0.1	-1.6	-1.2
PC 32:1	0.587	-0.2	-0.1	0.0	0.245	-0.2	0.0	0.7	0.696	0.0	-0.2	0.0
PC 32:2	0.013	-0.5	0.9	2.4	0.020	0.1	1.9	2.0	0.456	-0.2	0.0	0.4
PC 32:3	0.337	-0.2	0.0	0.4	0.154	0.2	0.8	0.2	0.497	0.0	0.1	0.3
PC 33:0	0.028	0.1	-1.6	-0.9	0.018	-0.1	-3.1	-1.5	0.067	-0.7	-2.0	-1.2
PC 33:1	0.003	0.0	-3.3	-3.0	0.032	-0.9	-1.5	-0.3	0.258	0.0	-0.7	-0.4
PC 33:2	0.004	0.1	-3.3	-2.4	0.019	-1.0	-2.1	-0.6	0.696	0.0	-0.2	0.0
PC 34:0	0.003	-0.5	-3.9	-2.2	0.018	-0.2	-3.4	-2.4	0.067	-0.5	-2.2	-1.4
PC 34:1	0.004	0.1	-2.8	-2.7	0.020	-0.7	-2.1	-0.8	0.178	0.0	-0.9	-0.7
PC 34:2	0.005	0.2	-2.4	-2.7	0.062	-0.4	-1.6	-0.1	0.748	0.0	0.0	-0.1
PC 34:3	0.014	0.1	-1.6	-2.0	0.080	-0.8	-1.0	0.0	0.949	0.0	0.0	0.0
PC 34:4	0.008	0.0	-2.4	-2.2	0.080	-0.4	-1.0	-0.4	0.384	0.0	-0.1	-0.7
PC 35:0	0.006	-0.3	-3.1	-1.6	0.027	-0.3	-2.1	-0.7	0.299	-0.1	-0.7	-0.2
PC 35:1	0.006	0.0	-2.8	-2.2	0.018	-0.6	-2.6	-1.5	0.207	0.0	-0.7	-0.7
PC 35:2	0.012	0.0	-2.1	-1.8	0.018	-0.9	-2.2	-0.8	0.952	0.0	0.0	0.0
PC 35:3	0.011	0.0	-2.1	-2.0	0.024	-0.8	-1.8	-0.6	0.547	0.0	-0.2	-0.2
PC 35:4	0.003	0.0	-3.6	-3.0	0.022	-0.5	-1.9	-0.9	0.228	0.0	-1.0	-0.3
PC 35:5	0.003	1.3	-3.1	-3.0	0.077	-0.1	-1.5	-0.3	0.192	0.1	0.0	-1.4
PC 36:0	0.089	-1.2	-0.4	0.1	0.837	0.0	0.0	0.0	0.456	-0.1	-0.5	0.0
PC 36:1	0.551	-0.1	0.0	0.2	0.491	0.1	0.2	0.0	0.392	0.0	0.0	-0.7
PC 36:2	0.053	0.4	-0.4	-1.3	0.314	-0.2	-0.6	0.0	0.765	0.1	0.0	-0.1

Lipid species	6 weeks				10 weeks				16 weeks			
	P-value[a]	db/h vs. H/H[b]	db/db vs. H/H[b]	db/db vs. db/h[b]	*P*-value[a]	db/h vs. H/H[b]	db/db vs. H/H[b]	db/db vs. db/h[b]	*P*-value[a]	db/h vs. H/H[b]	db/db vs. H/H[b]	db/db vs. db/h[b]
PC 36:3	0.003	0.3	-3.6	-3.0	0.025	-0.5	-1.9	-0.7	0.589	0.0	-0.1	-0.2
PC 36:4a	0.005	0.0	-3.1	-2.4	0.041	-0.5	-1.6	-0.3	0.384	0.0	-0.3	-0.4
PC 36:4b	0.003	0.4	-3.3	-3.3	0.020	-0.3	-2.4	-1.0	0.129	0.0	-1.0	-1.5
PC 36:5	0.017	0.2	-1.5	-1.6	0.154	-0.5	-0.7	0.0	0.576	0.0	-0.2	-0.2
PC 36:6	0.114	0.0	-0.8	-0.7	0.215	-0.5	-0.5	0.0	0.258	0.0	-0.8	-0.3
PC 37:4	0.003	0.1	-3.3	-3.3	0.018	-0.4	-2.6	-1.6	0.177	0.0	-0.7	-0.9
PC 37:5	0.007	0.1	-3.3	-1.6	0.033	-0.8	-1.1	-0.9	0.237	0.0	-0.7	-0.6
PC 38:2	0.021	0.0	-1.6	-1.5	0.909	0.0	0.0	0.0	0.852	0.0	0.0	0.0
PC 38:3	0.118	0.0	-0.7	-0.7	0.103	-0.9	-0.6	0.0	0.657	0.1	-0.1	-0.1
PC 38:4	0.003	0.1	-3.3	-3.3	0.018	-0.5	-2.6	-0.9	0.152	0.0	-1.1	-1.1
PC 38:5	0.003	0.1	-3.1	-3.3	0.048	-0.5	-1.1	-0.8	0.274	0.0	-0.3	-0.7
PC 38:6a	0.004	0.0	-2.6	-3.3	0.043	-0.6	-1.1	-0.8	0.161	0.0	-0.5	-1.5
PC 38:6b	0.004	0.0	-3.3	-2.4	0.026	-0.2	-2.2	-0.7	0.159	0.0	-0.5	-1.4
PC 38:7	0.042	0.0	-0.8	-1.5	0.178	-0.7	-0.4	0.0	0.305	0.0	-0.5	-0.5
PC 39:6	0.224	-0.1	-0.4	-0.4	0.050	0.0	-2.4	-0.3	0.299	0.0	-0.5	-0.4
PC 39:7	0.257	0.0	-0.5	-0.2	0.043	0.0	-0.9	-1.8	0.384	-0.3	-0.4	0.0
PC 40:5	0.242	-0.1	-0.6	-0.1	0.067	-0.2	-1.8	-0.1	0.407	-0.1	-0.2	-0.5
PC 40:6	0.417	0.0	-0.5	0.0	0.222	0.0	-0.9	-0.1	0.381	0.0	-0.1	-0.6
PC 40:7	0.009	0.0	-2.4	-2.0	0.036	-0.4	-1.8	-0.4	0.214	0.0	-0.5	-0.8
PC(O-30:0)	0.407	-0.1	-0.3	-0.1	0.195	0.0	-0.7	-0.4	0.067	-0.1	-2.4	-1.4
PC(O-32:0)	0.038	-0.4	-1.5	-0.5	0.018	0.0	-2.6	-2.4	0.067	-0.2	-2.4	-1.8
PC(O-32:1)	0.591	0.1	-0.1	0.0	0.319	0.0	-0.3	-0.4	0.809	0.0	-0.1	0.0
PC(O-34:0)	0.082	-0.5	-1.1	0.0	0.027	0.0	-1.5	-2.0	0.067	-0.3	-2.7	-1.5
PC(O-34:1)	0.143	-0.2	-0.9	-0.1	0.040	0.0	-1.0	-1.8	0.163	-0.4	-1.4	-0.1
PC(O-34:2)	0.551	0.1	0.2	0.0	0.411	0.0	-0.2	-0.4	0.199	-0.2	-0.8	-0.4
PC(O-34:4)	0.324	0.0	-0.3	-0.3	0.216	-0.3	-0.4	-0.3	0.829	0.0	0.0	0.0
PC(O-36:0)	0.188	-0.4	-0.6	0.0	0.397	0.0	-0.2	-0.4	0.149	-0.2	-1.6	-0.5
PC(O-36:1)	0.264	-0.4	-0.1	0.1	0.685	0.0	-0.1	-0.1	0.088	-0.3	-2.2	-0.7
PC(O-36:2)	0.474	-0.1	0.0	0.3	0.298	0.0	-0.4	-0.4	0.440	-0.1	-0.4	0.0
PC(O-36:3)	0.197	-0.1	-0.8	0.0	0.043	0.0	-1.2	-1.5	0.617	0.0	-0.3	0.0
PC(O-36:4)	0.045	0.0	-1.1	-1.2	0.018	0.0	-3.1	-2.4	0.085	-0.1	-1.3	-1.9
PC(O-36:5)	0.561	0.0	0.0	-0.2	0.685	0.0	-0.2	0.0	0.930	0.0	0.0	0.0
PC(O-38:4)	0.151	-0.1	-0.8	-0.2	0.022	0.0	-1.8	-2.0	0.092	0.0	-1.4	-1.5
PC(O-38:5)	0.149	0.0	-0.8	-0.3	0.020	0.0	-1.9	-2.0	0.497	-0.2	-0.2	0.0
PC(O-40:6)	0.290	-0.1	-0.4	0.0	0.033	0.0	-1.2	-1.8	0.128	-0.3	-1.5	-0.7
PC(O-40:7)	0.224	0.0	-0.6	-0.2	0.047	0.0	-1.0	-1.6	0.380	-0.3	-0.4	0.0
PC(P-32:0)	0.003	1.6	-3.3	-3.3	0.028	-0.2	-2.2	-0.6	0.159	0.0	-0.9	-1.0
PC(P-34:1)	0.003	1.3	-2.4	-3.3	0.033	-0.2	-1.9	-0.7	0.129	0.0	-1.3	-1.2
PC(P-34:2)	0.003	1.5	-2.6	-2.7	0.051	-0.1	-1.8	-0.5	0.299	0.1	-0.1	-0.7
PC(P-34:3)	0.021	-0.2	-1.8	-1.0	0.018	-0.3	-3.1	-3.0	0.178	0.0	-0.9	-0.7
PC(P-36:2)	0.004	0.0	-2.4	-3.3	0.032	-0.9	-1.6	-0.1	0.184	0.0	-0.6	-1.0
PC(P-36:4)	0.003	1.3	-3.1	-3.0	0.058	-0.1	-1.5	-0.6	0.173	0.1	-0.1	-1.4
PC(P-38:4)	0.014	0.0	-1.9	-1.6	0.018	0.0	-2.6	-2.0	0.159	-0.2	-0.9	-0.8
PC(P-38:5)	0.004	0.2	-2.1	-3.3	0.032	-0.1	-1.9	-0.8	0.245	0.0	-0.5	-0.7
PC(P-38:6)	0.003	1.5	-2.3	-3.0	0.077	0.0	-1.3	-0.6	0.274	0.0	-0.2	-0.8
LPC 14:0	0.275	0.0	-0.3	-0.4	0.628	0.0	-0.1	-0.1	0.696	0.0	-0.2	0.0
LPC 16:0	0.008	0.1	-1.9	-2.7	0.029	0.0	-1.8	-1.3	0.305	-0.1	-0.6	-0.2
LPC 16:1	0.832	0.0	0.0	0.0	0.087	0.4	1.2	0.1	0.852	0.1	0.0	0.0
LPC 17:0	0.143	-0.9	-0.4	0.0	0.749	0.1	0.0	0.0	0.809	0.0	0.0	0.0
LPC 18:0	0.684	0.0	-0.1	0.0	0.186	0.5	0.0	-0.7	0.720	0.0	-0.1	-0.1
LPC 18:1	0.075	0.2	-0.4	-1.2	0.348	0.1	-0.2	-0.3	0.330	0.0	-0.2	-0.7
LPC 18:2	0.081	0.2	-0.3	-1.2	0.391	0.0	-0.2	-0.2	0.440	0.2	0.0	-0.4
LPC 20:1	0.086	0.0	-0.8	-0.8	0.094	0.5	0.0	-1.5	0.267	0.0	-0.6	-0.4
LPC 20:3	0.075	0.3	-0.3	-1.2	0.345	0.0	-0.6	-0.1	0.647	0.1	0.0	-0.2

Lipid species	6 weeks				10 weeks				16 weeks			
	P-value[a]	db/h vs. H/H[b]	db/db vs. H/H[b]	db/db vs. db/h[b]	*P*-value[a]	db/h vs. H/H[b]	db/db vs. H/H[b]	db/db vs. db/h[b]	*P*-value[a]	db/h vs. H/H[b]	db/db vs. H/H[b]	db/db vs. db/h[b]
LPC 20:4	0.038	0.3	-0.8	-1.3	0.200	0.0	-0.5	-0.6	0.236	0.0	-0.2	-1.0
LPC 22:4	0.004	0.4	-1.9	-3.3	0.038	-0.3	-1.5	-0.8	0.173	0.2	-0.2	-1.1
LPC 22:5	0.165	0.0	-0.3	-0.8	0.726	0.0	0.0	-0.1	0.796	0.0	0.0	0.1
LPC 22:6	0.034	0.4	-0.8	-1.5	0.162	0.1	-0.5	-0.7	0.336	0.0	-0.2	-0.7
LPC(O-16:0)	0.622	-0.1	-0.1	0.0	0.263	0.4	0.0	-0.4	0.347	-0.3	-0.5	0.0
PE 32:0	0.007	-0.8	-2.8	-0.9	0.018	0.1	-2.4	-2.2	0.245	0.0	-0.7	-0.4
PE 32:1	0.003	-0.7	3.1	3.0	0.018	0.6	2.9	1.5	0.617	0.1	0.2	0.0
PE 34:1	0.035	0.0	-0.8	-1.8	0.236	-0.2	-0.6	-0.1	0.890	0.0	0.0	0.0
PE 34:2	0.075	0.0	-0.8	-1.2	0.728	0.0	0.1	0.0	0.336	0.2	0.7	0.0
PE 34:3	0.010	-0.9	0.9	2.4	0.018	0.5	3.4	0.9	0.087	0.3	1.6	1.2
PE 35:1	0.014	0.1	-1.6	-1.8	0.027	-0.3	-1.6	-1.2	0.687	0.1	0.0	-0.1
PE 35:2	0.025	0.0	-1.0	-2.0	0.900	0.0	0.0	0.0	0.750	0.0	0.1	0.1
PE 36:1	0.003	0.2	-3.6	-3.3	0.019	-0.3	-2.2	-1.5	0.245	0.1	-0.1	-1.0
PE 36:2	0.027	0.1	-0.7	-2.2	0.387	0.0	-0.5	0.0	0.342	0.4	0.5	0.0
PE 36:3	0.028	0.0	-1.3	-1.6	0.490	0.0	-0.2	-0.2	0.698	0.2	0.0	0.0
PE 36:4	0.004	0.0	-3.1	-2.7	0.057	-0.2	-1.5	-0.4	0.926	0.0	0.0	0.0
PE 36:5	0.908	0.0	0.0	0.0	0.186	-0.1	0.5	0.6	0.417	0.0	0.4	0.2
PE 38:3	0.005	0.0	-2.8	-2.4	0.018	-0.7	-2.4	-0.8	0.427	0.0	-0.3	-0.3
PE 38:4	0.003	-0.1	-3.9	-2.4	0.018	-0.1	-3.4	-1.6	0.155	0.0	-0.7	-1.4
PE 38:5	0.003	0.0	-3.6	-2.7	0.083	-0.1	-1.5	-0.2	0.668	0.0	0.0	-0.2
PE 38:6	0.008	0.0	-2.6	-2.0	0.122	-0.1	-0.8	-0.6	0.384	0.0	-0.3	-0.4
PE 40:5	0.050	-0.1	-1.3	-0.8	0.018	-0.4	-2.6	-1.2	0.159	0.0	-0.7	-1.3
PE 40:6	0.028	-0.2	-1.9	-0.5	0.029	0.0	-1.9	-1.2	0.144	0.0	-0.9	-1.4
PE 40:7	0.005	0.0	-3.3	-2.0	0.113	-0.1	-0.9	-0.5	0.214	0.0	-0.4	-1.0
PE(O-34:1)	0.012	0.0	-1.9	-2.2	0.018	-0.1	-3.1	-1.6	0.177	-0.1	-1.1	-0.4
PE(O-36:4)	0.003	0.4	-3.9	-3.3	0.018	0.0	-2.4	-2.7	0.144	0.0	-1.0	-1.3
PE(O-36:5)	0.003	1.5	-3.6	-3.0	0.154	0.0	-0.2	-1.5	0.990	0.0	0.0	0.0
PE(O-38:4)	0.028	-0.1	-1.5	-1.2	0.020	0.0	-1.8	-2.4	0.067	-0.3	-1.6	-1.8
PE(O-38:5)	0.030	0.0	-1.8	-0.9	0.027	0.0	-2.1	-1.2	0.930	0.0	0.0	0.0
PE(O-40:4)	0.084	-0.2	-1.3	-0.2	0.018	0.0	-1.5	-3.3	0.180	0.0	-1.0	-0.6
PE(O-40:5)	0.112	-0.6	-0.8	0.0	0.025	0.1	-1.3	-2.0	0.392	-0.3	-0.4	0.0
PE(O-40:6)	0.035	-0.4	-1.4	-0.7	0.045	0.0	-1.8	-0.8	0.440	-0.2	-0.3	0.0
PE(O-40:7)	0.014	0.0	-2.3	-1.5	0.069	0.0	-1.1	-1.0	0.184	-0.4	-1.0	-0.1
PE(P-34:1)	0.009	1.2	-0.9	-2.4	0.501	0.0	-0.2	-0.1	0.829	0.0	-0.1	0.0
PE(P-36:1)	0.886	0.0	0.0	0.0	0.728	0.0	0.0	-0.1	0.320	0.3	0.0	-0.6
PE(P-36:4)	0.003	1.3	-3.6	-3.0	0.036	0.0	-1.3	-1.5	0.696	0.0	-0.1	-0.1
PE(P-37:4)	0.675	-0.1	0.0	0.0	0.657	0.0	0.1	0.1	0.236	0.8	0.4	0.0
PE(P-38:4)	0.003	0.2	-3.3	-3.3	0.018	0.0	-2.2	-3.0	0.214	0.0	-0.4	-0.9
PE(P-38:5)	0.003	0.6	-3.3	-2.7	0.060	-0.1	-1.1	-1.0	0.576	0.0	-0.2	-0.2
PE(P-38:6)	0.003	0.6	-3.3	-3.3	0.077	0.0	-0.9	-1.2	0.696	0.0	0.0	-0.2
PE(P-40:4)	0.551	-0.1	-0.1	0.0	0.922	0.0	0.0	0.0	0.933	0.0	0.0	0.0
PE(P-40:5)	0.020	0.0	-1.8	-1.3	0.018	0.0	-2.2	-3.0	0.092	-0.8	-1.2	-1.2
PE(P-40:6)	0.003	-1.0	-3.3	-1.8	0.018	0.0	-3.1	-3.3	0.159	0.0	-0.7	-1.3
LPE 16:0	0.075	0.1	-0.4	-1.3	0.195	-0.1	-0.9	-0.1	0.813	-0.1	0.0	0.0
LPE 18:0	0.213	0.1	-0.1	-0.7	0.195	0.0	-0.6	-0.4	0.594	-0.2	-0.2	0.0
LPE 18:1	0.066	0.4	-0.1	-1.6	0.221	0.0	-0.7	-0.3	0.930	0.0	0.0	0.0
LPE 18:2	0.174	0.4	0.0	-0.7	0.391	0.1	0.0	-0.4	0.630	0.1	0.2	0.0
LPE 20:4	0.017	0.3	-1.0	-2.0	0.178	0.0	-0.6	-0.6	0.293	0.0	-0.5	-0.6
LPE 22:6	0.017	0.4	-0.9	-2.0	0.188	0.0	-0.6	-0.6	0.293	0.0	-0.3	-0.7
PI 34:1	0.012	0.3	-1.1	-2.7	0.072	-0.3	-1.0	-0.7	0.996	0.0	0.0	0.0
PI 36:1	0.004	0.4	-2.4	-3.0	0.042	-0.3	-1.3	-0.9	0.956	0.0	0.0	0.0
PI 36:2	0.145	0.1	-0.1	-1.0	0.131	-0.2	-1.0	-0.2	0.668	0.0	0.3	0.0
PI 36:3	0.290	0.0	0.0	-0.9	0.675	-0.1	0.0	0.1	0.270	0.2	0.7	0.1
PI 36:4	0.832	0.0	0.0	-0.1	0.820	0.0	0.0	0.0	0.668	0.1	0.0	-0.1

Lipid species	6 weeks				10 weeks				16 weeks			
	P-value[a]	db/h vs. H/H[b]	db/db vs. H/H[b]	db/db vs. db/h[b]	*P*-value[a]	db/h vs. H/H[b]	db/db vs. H/H[b]	db/db vs. db/h[b]	*P*-value[a]	db/h vs. H/H[b]	db/db vs. H/H[b]	db/db vs. db/h[b]
PI 38:3	0.075	0.1	-0.4	-1.3	0.195	0.0	-0.9	-0.2	0.361	0.1	-0.1	-0.6
PI 38:4	0.075	0.3	-0.4	-1.0	0.288	0.0	-0.7	-0.1	0.159	0.1	-0.7	-1.1
PI 38:5	0.775	0.0	0.0	-0.1	0.282	0.0	0.3	0.4	0.384	0.4	0.2	-0.1
PI 40:4	0.041	0.1	-0.8	-1.5	0.067	0.0	-1.5	-0.7	0.245	0.0	-0.5	-0.7
PI 40:5	0.165	0.1	-0.2	-0.8	0.414	-0.2	-0.2	0.0	0.497	0.1	-0.1	-0.3
PS 36:1	0.009	0.0	-2.4	-2.0	0.018	0.0	-2.4	-2.0	0.267	0.0	-0.6	-0.5
PS 36:2	0.003	0.4	-2.8	-3.0	0.026	-0.4	-2.1	-0.6	0.765	0.0	0.1	0.0
PS 38:3	0.038	0.0	-1.6	-0.8	0.150	0.0	-0.5	-1.0	0.571	-0.2	0.0	0.2
PS 38:4	0.229	0.0	-0.8	-0.1	0.642	0.0	0.0	-0.2	0.156	0.0	1.2	1.0
PS 38:5	0.091	-0.4	0.2	1.0	0.029	0.2	1.8	1.0	0.067	0.0	2.2	2.1
PS 40:5	0.035	-1.3	0.0	1.5	0.213	0.0	0.7	0.2	0.829	0.0	0.0	0.1
PS 40:6	0.065	-0.8	0.0	1.3	0.195	0.2	0.7	0.1	0.926	0.0	0.0	0.0
PG 34:1	0.003	-0.1	-3.9	-3.3	0.027	-0.4	-1.6	-1.2	0.174	0.0	-1.0	-0.7
PG 34:2	0.149	-0.1	-0.8	-0.2	0.846	0.0	0.0	0.0	0.238	0.0	-0.6	-0.6
PG 36:1	0.007	-0.3	-2.4	-2.0	0.020	0.0	-1.8	-2.2	0.133	-0.5	-1.2	-0.7
PG 36:2	0.003	0.3	-3.9	-3.3	0.027	0.0	-2.1	-1.2	0.417	0.1	-0.1	-0.4
BMP 18:1/18:1	0.684	0.0	-0.1	0.0	0.791	0.1	0.0	0.0	0.930	0.0	0.0	0.0
CL 18:2/18:2/18:2/16:1	0.607	-0.1	0.0	0.1	0.234	0.1	0.8	0.0	0.159	0.3	0.0	-1.7
CL 18:2/18:1/18:2/16:1	0.125	-0.6	-0.3	0.5	0.521	0.2	0.1	0.0	0.161	0.0	-0.9	-1.0
CL 18:2/18:2/18:2/18:2	0.003	0.1	-3.6	-3.3	0.018	-0.1	-3.1	-2.0	0.175	0.1	0.0	-1.6
CL 18:2/18:2/18:2/18:1	0.003	-0.4	-3.6	-2.7	0.018	0.0	-2.6	-2.4	0.115	0.0	-0.8	-1.8
CL 18:2/18:1/18:2/18:1	0.009	-0.2	-2.3	-2.0	0.018	-0.2	-2.4	-1.8	0.092	0.0	-1.5	-1.5
CE 14:0	0.142	0.0	0.8	0.5	0.019	1.0	2.6	0.1	0.129	1.1	1.3	0.2
CE 16:0	0.497	0.0	-0.2	0.0	0.194	0.7	0.0	-0.2	0.320	0.5	0.0	-0.4
CE 16:1	0.188	0.1	0.7	0.2	0.018	1.1	3.1	0.7	0.067	1.3	2.4	1.0
CE 18:0	0.850	0.0	0.0	0.0	0.027	1.4	1.5	0.0	0.501	0.5	0.0	0.0
CE 18:1	0.025	0.0	-1.4	-1.6	0.041	1.5	0.0	-0.8	0.267	0.2	0.9	0.0
CE 18:2	0.092	-0.2	0.3	1.0	0.058	0.7	1.3	0.0	0.258	0.0	0.9	0.2
CE 18:3	0.021	0.0	1.6	1.5	0.018	1.0	2.9	0.8	0.115	0.2	1.8	0.7
CE 20:3	0.337	0.0	0.2	0.4	0.052	0.6	1.6	0.0	0.356	0.0	0.6	0.2
CE 20:4	0.202	-0.2	0.1	0.6	0.094	0.7	1.0	0.0	0.459	0.1	0.5	0.0
CE 20:5	0.003	-0.1	3.3	3.0	0.018	0.7	2.4	1.8	0.092	0.0	2.0	1.0
CE 22:0	0.039	-0.5	0.8	1.2	0.018	1.9	1.6	0.9	0.299	0.0	0.7	0.4
CE 22:5	0.178	0.0	-0.3	0.7	0.018	0.8	3.1	1.5	0.440	0.0	0.2	0.3
CE 22:6	0.055	0.0	0.9	1.2	0.048	0.7	1.6	0.0	0.188	0.0	1.2	0.4
CE 24:0	0.040	0.0	1.4	1.0	0.024	0.8	1.5	1.0	0.152	0.0	1.4	0.8
COH	0.036	-0.1	-1.8	-0.5	0.688	0.1	0.0	-0.1	0.809	0.0	0.1	0.0
DG 14:0/16:0	0.045	0.0	1.5	0.8	0.027	0.9	1.8	0.1	0.155	0.4	1.5	0.2
DG 14:0/18:1	0.018	0.0	1.8	1.5	0.020	0.9	1.9	0.6	0.067	0.7	2.2	1.3
DG 14:0/18:2	0.019	0.0	1.8	1.5	0.020	0.9	1.9	0.7	0.067	0.5	2.0	1.6
DG 16:0/16:0	0.205	0.0	0.7	0.3	0.032	0.9	1.8	0.0	0.159	0.2	1.4	0.4
DG 16:0/18:0	0.143	0.0	0.8	0.5	0.028	0.9	1.8	0.1	0.159	0.2	1.5	0.3
DG 16:0/18:1	0.027	0.0	1.5	1.3	0.020	0.9	2.1	0.6	0.067	0.5	2.4	1.5
DG 16:0/18:2	0.018	0.0	1.8	1.5	0.020	0.9	1.9	0.8	0.067	0.4	1.9	1.7
DG 16:0/20:4	0.119	0.1	0.9	0.3	0.019	1.7	1.8	0.0	0.067	0.0	2.0	1.7
DG 16:1/18:0	0.014	0.1	1.9	1.6	0.018	0.8	2.2	1.3	0.067	0.5	2.4	1.6
DG 16:1/18:1	0.014	0.0	1.9	1.6	0.018	1.1	2.6	1.3	0.067	0.7	2.4	2.1
DG 18:0/18:1	0.039	0.0	1.4	1.0	0.027	0.8	2.1	0.1	0.090	0.5	1.8	0.9
DG 18:0/18:2	0.021	0.0	1.5	1.6	0.028	0.8	1.9	0.1	0.087	0.6	1.9	0.7
DG 18:0/20:4	0.104	0.0	0.9	0.6	0.026	1.7	1.1	0.0	0.685	0.0	0.0	0.3
DG 18:1/18:1	0.055	0.0	1.3	0.8	0.019	1.1	2.4	0.2	0.081	0.2	1.9	1.2
DG 18:1/18:2	0.050	0.0	1.4	0.8	0.020	1.1	2.2	0.2	0.068	0.4	2.0	1.2
DG 18:1/18:3	0.021	0.0	1.6	1.5	0.018	0.9	2.2	0.7	0.067	0.4	2.0	1.3
DG 18:1/20:0	0.036	0.0	1.3	1.3	0.036	0.7	1.9	0.0	0.115	0.8	1.5	0.4

Lipid species	6 weeks				10 weeks				16 weeks			
	P-value[a]	db/h vs. H/H[b]	db/db vs. H/H[b]	db/db vs. db/h[b]	*P*-value[a]	db/h vs. H/H[b]	db/db vs. H/H[b]	db/db vs. db/h[b]	*P*-value[a]	db/h vs. H/H[b]	db/db vs. H/H[b]	db/db vs. db/h[b]
DG 18:1/20:3	0.028	0.0	1.5	1.3	0.019	1.2	2.2	0.1	0.067	0.3	1.9	1.6
DG 18:1/20:4	0.279	0.0	0.5	0.1	0.018	1.8	2.2	0.0	0.092	0.1	1.8	1.0
DG 18:2/18:2	0.039	0.0	1.5	0.9	0.020	1.0	2.2	0.1	0.081	0.2	1.9	1.2
TG 14:0/16:0/18:1	0.011	-0.2	2.1	1.8	0.020	0.8	1.8	0.9	0.176	0.0	1.4	0.3
TG 14:0/16:0/18:2	0.014	0.0	1.9	1.6	0.018	0.8	2.1	1.3	0.161	0.0	1.3	0.6
TG 14:0/16:1/18:1	0.014	0.0	1.9	1.6	0.018	0.8	2.1	1.5	0.159	0.0	1.3	0.6
TG 14:0/16:1/18:2	0.014	0.0	1.9	1.6	0.018	1.0	1.9	1.5	0.159	0.0	1.3	0.7
TG 14:0/17:0/18:1	0.012	-0.2	1.9	1.8	0.022	0.7	1.8	1.0	0.204	0.0	1.1	0.4
TG 14:0/18:0/18:1	0.012	-0.3	2.1	1.6	0.027	0.6	1.8	0.6	0.245	0.0	1.1	0.1
TG 14:0/18:2/18:2	0.014	0.0	1.9	1.6	0.018	1.1	2.1	0.9	0.174	0.0	1.1	0.6
TG 14:1/16:0/18:1	0.014	0.0	1.9	1.6	0.020	0.8	1.8	1.2	0.160	0.0	1.3	0.6
TG 14:1/16:1/18:0	0.014	0.0	1.9	1.6	0.018	0.9	2.1	1.5	0.156	0.0	1.4	0.7
TG 14:1/18:1/18:1	0.014	0.0	1.9	1.6	0.018	0.9	2.1	1.5	0.155	0.0	1.4	0.7
TG 15:0/16:0/18:1	0.012	-0.2	2.1	1.6	0.020	0.8	1.8	0.9	0.189	0.0	1.2	0.3
TG 15:0/18:1/18:1	0.014	-0.1	1.9	1.6	0.020	0.8	2.1	0.8	0.176	0.0	1.1	0.6
TG 16:0/16:0/16:0	0.012	0.0	2.3	1.8	0.022	0.9	1.6	0.7	0.199	0.4	0.9	0.1
TG 16:0/16:0/18:0	0.017	-0.2	1.6	1.5	0.022	1.0	1.6	0.6	0.267	0.4	0.7	0.0
TG 16:0/16:0/18:1	0.009	-0.2	2.1	2.0	0.024	0.6	1.8	0.9	0.184	0.0	1.2	0.3
TG 16:0/16:0/18:2	0.013	-0.2	2.1	1.6	0.022	0.7	1.8	0.8	0.184	0.0	1.2	0.4
TG 16:0/16:1/17:0	0.012	-0.2	2.1	1.6	0.020	0.7	1.8	1.0	0.180	0.0	1.3	0.3
TG 16:0/16:1/18:1	0.014	0.0	1.9	1.6	0.018	0.9	2.1	1.3	0.159	0.0	1.4	0.6
TG 16:0/17:0/18:0	0.012	-0.1	2.1	1.8	0.029	0.8	1.5	0.5	0.222	0.2	0.9	0.2
TG 16:0/17:0/18:1	0.009	-0.3	2.1	2.0	0.022	0.7	1.8	0.9	0.180	0.0	1.3	0.3
TG 16:0/17:0/18:2	0.014	0.0	1.9	1.6	0.018	0.9	2.1	1.0	0.191	0.0	1.1	0.4
TG 16:0/18:0/18:1	0.009	-0.4	2.1	2.0	0.025	0.7	1.8	0.6	0.214	0.0	1.1	0.2
TG 16:0/18:1/18:1	0.017	0.0	1.9	1.5	0.020	0.8	1.9	0.9	0.159	0.0	1.3	0.6
TG 16:0/18:1/18:2	0.014	0.0	1.9	1.6	0.018	0.9	2.1	1.0	0.177	0.0	1.1	0.6
TG 16:0/18:2/18:2	0.014	0.0	1.9	1.6	0.018	0.9	2.1	1.0	0.177	0.0	1.1	0.6
TG 16:1/16:1/16:1	0.014	0.0	1.9	1.6	0.018	0.8	2.1	1.5	0.129	0.0	1.5	1.0
TG 16:1/16:1/18:0	0.014	-0.1	2.1	1.5	0.020	0.8	1.9	0.9	0.174	0.0	1.4	0.3
TG 16:1/16:1/18:1	0.014	0.1	1.9	1.6	0.018	0.9	2.1	1.5	0.140	0.0	1.5	0.9
TG 16:1/17:0/18:1	0.014	0.0	1.9	1.6	0.019	0.8	2.1	1.0	0.167	0.0	1.1	0.7
TG 16:1/18:1/18:1	0.014	0.0	1.9	1.6	0.018	0.9	2.1	1.5	0.155	0.0	1.4	0.7
TG 16:1/18:1/18:2	0.014	0.0	1.9	1.6	0.018	0.9	2.1	1.3	0.153	0.0	1.4	0.8
TG 17:0/18:1/18:1	0.014	0.0	1.9	1.6	0.020	0.8	1.9	0.8	0.161	0.0	1.3	0.6
TG 18:0/18:0/18:0	0.207	-0.4	0.1	0.4	0.048	0.9	1.5	0.0	0.569	0.1	0.2	0.0
TG 18:0/18:0/18:1	0.010	-0.4	2.1	1.8	0.029	0.7	1.8	0.4	0.236	0.1	1.0	0.2
TG 18:0/18:1/18:1	0.015	-0.1	2.1	1.3	0.020	0.7	1.9	0.8	0.164	0.1	1.4	0.4
TG 18:0/18:2/18:2	0.016	0.0	1.9	1.5	0.020	0.8	2.2	0.4	0.183	0.0	1.2	0.4
TG 18:1/18:1/18:1	0.017	0.0	1.9	1.5	0.020	0.9	1.9	0.8	0.159	0.0	1.3	0.6
TG 18:1/18:1/18:2	0.014	0.0	1.9	1.6	0.020	0.9	1.9	0.7	0.159	0.0	1.3	0.6
TG 18:1/18:1/20:4	0.014	0.1	2.1	1.6	0.018	1.3	2.4	0.9	0.159	0.1	1.2	0.7
TG 18:1/18:2/18:2	0.014	0.0	1.9	1.6	0.018	1.0	2.1	1.0	0.161	0.0	1.1	0.7
TG 18:2/18:2/18:2	0.014	0.0	1.9	1.6	0.018	0.8	2.1	1.2	0.164	0.0	1.0	0.7

[a] *P*-value for the comparison of levels of each lipid species between genotypes at each age using the Kruskal Wallis test with Benjamini-Hochberg correction for multiple comparisons. $P < 0.05$ was considered significant (highlighted in pink).

[b] Post-hoc analysis was performed using the Mann Whitney *U* test with Dunn-Sidak correction for multiple group comparisons. Values were derived from the formula: sign(difference in median levels)*-log10(post-hoc *P*-value). Colour-coded values 1.3 to 2.0 (light red, $P = 0.05$-0.01) and > 2.0 (dark red, $P < 0.01$) indicate a significant increase relative to the reference group. Colour-coded values -1.3 to -2.0 (light green, $P = 0.05$-0.01) and < -2.0 (dark green, $P < 0.01$) indicate a significant decrease relative to the reference group.

Table S4.10 Relationship between genotype and plasma lipid species in female mice.

Lipid species	6 weeks				10 weeks				16 weeks			
	P-value[a]	db/h vs. H/H[b]	db/db vs. H/H[b]	db/db vs. db/h[b]	*P*-value[a]	db/h vs. H/H[b]	db/db vs. H/H[b]	db/db vs. db/h[b]	*P*-value[a]	db/h vs. H/H[b]	db/db vs. H/H[b]	db/db vs. db/h[b]
Sph 18:1	0.659	0.0	0.0	-0.2	0.344	0.1	-0.1	-0.5	0.271	0.4	0.7	0.0
Cer 16:0	0.066	-0.2	1.1	0.8	0.316	0.0	0.5	0.5	0.035	-0.4	0.9	3.9
Cer 18:0	0.258	-0.2	-0.5	-0.1	0.682	0.1	0.0	0.0	0.795	0.0	0.1	0.0
Cer 20:0	0.173	-1.0	-0.2	0.0	0.317	0.0	0.5	0.4	0.035	-0.5	1.4	3.1
Cer 22:0	0.036	-1.1	0.1	1.5	0.283	0.1	0.5	0.3	0.036	-0.3	0.8	2.8
Cer 24:0	0.017	-1.2	0.4	2.0	0.219	0.0	0.6	0.7	0.106	-0.4	0.2	1.5
Cer 24:1	0.122	-0.8	0.0	0.8	0.282	0.2	0.5	0.2	0.449	-0.3	0.0	0.3
MHC 16:0	0.173	-1.0	-0.1	0.2	0.879	0.0	0.0	0.0	0.524	0.0	-0.2	-0.3
MHC 18:0	0.005	0.0	-2.8	-2.8	0.318	0.5	-0.1	-0.3	0.652	0.0	0.0	-0.2
MHC 20:0	0.154	-0.3	-1.0	0.0	0.216	1.0	0.0	-0.2	0.386	0.1	0.4	0.2
MHC 22:0	0.126	-1.0	0.0	0.5	0.672	0.2	0.0	0.0	0.486	0.0	0.3	0.2
MHC 24:0	0.032	-1.3	0.0	1.6	0.914	0.0	0.0	0.0	0.628	0.0	-0.2	-0.1
MHC 24:1	0.210	-0.7	-0.1	0.2	0.869	0.0	0.0	0.0	0.107	0.0	-1.0	-1.1
SM 31:1	0.015	0.0	1.9	2.0	0.047	0.2	1.7	1.0	0.263	0.0	0.4	0.8
SM 32:1	0.004	-0.7	1.9	3.6	0.021	0.6	2.4	0.8	0.056	0.0	1.0	2.1
SM 32:2	0.004	0.0	3.9	3.6	0.004	1.5	3.2	1.5	0.036	0.0	1.5	2.4
SM 33:1	0.026	-0.6	0.5	2.0	0.300	0.9	0.0	0.0	0.883	0.0	0.0	0.0
SM 34:1	0.018	-1.1	0.1	2.5	0.391	0.2	0.3	0.0	0.492	-0.1	0.0	0.4
SM 34:2	0.023	-1.2	0.1	2.0	0.221	0.4	0.5	0.2	0.363	0.0	0.2	0.8
SM 34:3	0.004	-0.8	1.9	3.3	0.014	0.9	2.2	1.1	0.035	0.0	1.8	2.6
SM 35:1	0.333	-0.2	-0.4	0.0	0.286	0.4	0.0	-0.5	0.746	0.0	0.0	-0.2
SM 35:2	0.865	0.0	0.0	0.0	0.474	0.6	0.0	0.0	0.757	0.0	0.0	-0.1
SM 36:1	0.018	0.0	-1.5	-2.1	0.232	0.2	-0.1	-0.9	0.500	0.0	-0.1	-0.4
SM 36:2	0.961	0.0	0.0	0.0	0.626	0.1	0.1	0.0	0.963	0.0	0.0	0.0
SM 36:3	0.492	0.0	0.3	0.1	0.291	0.1	0.5	0.3	0.178	0.0	0.5	1.0
SM 37:2	0.347	-0.3	-0.3	0.0	0.484	0.3	0.2	0.0	0.538	0.2	0.0	-0.2
SM 38:1	0.249	-0.1	0.1	0.7	0.552	0.1	0.2	0.1	0.040	0.0	1.5	1.9
SM 38:2	0.056	0.1	0.8	1.6	0.039	0.6	1.7	0.7	0.106	-0.2	0.3	1.6
SM 39:1	0.073	-0.4	0.1	1.6	0.063	0.8	1.3	0.3	0.144	-0.9	0.0	0.8
SM 41:1	0.024	-0.1	0.9	2.1	0.174	0.7	0.5	0.2	0.861	0.0	0.0	0.0
SM 41:2	0.014	-0.5	1.3	2.1	0.124	0.6	1.0	0.1	0.974	0.0	0.0	0.0
SM 42:1	0.056	-0.3	0.3	1.6	0.174	0.3	0.7	0.5	0.791	0.0	0.0	0.1
PC 24:0	0.320	-0.3	-0.3	-0.1	0.068	1.5	0.5	-0.1	0.998	0.0	0.0	0.0
PC 28:0	0.147	-0.8	0.0	0.6	0.067	0.1	1.5	0.9	0.652	0.1	0.0	0.1
PC 29:0	0.135	-0.9	0.0	0.6	0.022	1.7	1.7	0.0	0.757	0.0	-0.1	0.0
PC 30:0	0.115	-0.4	0.3	0.9	0.037	0.7	1.7	0.7	0.727	0.0	0.0	0.2
PC 31:0	0.054	-1.0	-1.1	0.2	0.450	0.4	0.1	0.0	0.535	0.0	-0.3	0.0
PC 31:1	0.630	-0.2	0.0	0.0	0.225	1.0	0.1	0.0	0.965	0.0	0.0	0.0
PC 32:0	0.033	-0.4	-1.9	-0.4	0.657	0.1	0.0	-0.1	0.605	0.0	-0.2	-0.1
PC 32:1	0.009	0.0	2.8	1.8	0.003	1.3	3.5	2.0	0.368	0.0	0.3	0.4
PC 32:2	0.009	0.0	2.8	1.8	0.021	0.5	2.0	1.3	0.172	0.0	0.4	1.1
PC 32:3	0.320	0.0	0.3	0.3	0.021	1.3	1.5	0.8	0.184	0.0	0.6	0.9
PC 33:0	0.043	-1.1	-1.1	0.3	0.696	0.1	0.1	0.0	0.652	0.1	-0.1	0.0
PC 33:1	0.023	-0.6	0.8	1.8	0.010	0.5	2.9	1.5	0.161	-0.2	0.1	1.3
PC 33:2	0.046	-0.9	0.0	1.6	0.121	0.6	1.0	0.2	0.091	-0.1	0.7	1.5
PC 33:3	0.106	0.0	0.9	0.7	0.058	0.3	1.7	0.6	0.188	0.0	0.8	0.7
PC 34:0	0.498	-0.3	0.0	0.0	0.626	0.2	0.0	0.0	0.991	0.0	0.0	0.0
PC 34:1	0.055	-0.1	1.0	1.1	0.091	0.2	1.3	0.6	0.406	0.0	0.2	0.5
PC 34:2	0.040	-0.3	1.0	1.2	0.024	0.7	1.9	0.9	0.038	-0.4	0.9	2.1
PC 34:3	0.033	0.0	1.3	1.6	0.005	0.9	3.2	1.9	0.151	0.1	0.8	0.9
PC 34:4	0.040	0.0	1.0	1.6	0.003	2.2	3.5	1.9	0.220	0.0	0.4	0.8
PC 34:5	0.014	0.0	1.9	2.0	0.003	1.1	3.5	3.5	0.221	0.0	0.4	1.0

Lipid species	6 weeks				10 weeks				16 weeks			
	P-value[a]	db/h vs. H/H[b]	db/db vs. H/H[b]	db/db vs. db/h[b]	*P*-value[a]	db/h vs. H/H[b]	db/db vs. H/H[b]	db/db vs. db/h[b]	*P*-value[a]	db/h vs. H/H[b]	db/db vs. H/H[b]	db/db vs. db/h[b]
PC 35:0	0.051	-1.3	0.0	1.1	0.398	0.2	0.4	0.0	0.643	0.0	0.0	0.2
PC 35:1	0.015	-0.8	0.8	2.1	0.040	0.1	2.0	1.0	0.196	-0.1	0.2	1.0
PC 35:2	0.012	-0.4	0.8	3.0	0.020	0.4	2.4	1.1	0.036	-0.3	0.9	2.4
PC 35:3	0.034	-0.4	0.5	1.8	0.006	1.3	3.5	0.8	0.106	-0.3	0.4	1.4
PC 35:4	0.348	-0.1	-0.4	-0.1	0.299	0.4	0.5	0.0	0.754	-0.1	-0.1	0.0
PC 36:0	0.436	-0.2	-0.1	0.2	0.271	1.0	0.1	0.0	0.831	0.0	0.0	0.0
PC 36:1	0.004	-0.4	2.8	3.3	0.045	0.5	1.4	1.0	0.117	0.0	0.8	1.3
PC 36:2	0.004	-0.9	2.1	3.6	0.024	0.4	2.0	1.1	0.035	-0.1	1.1	3.1
PC 36:3	0.004	-0.5	3.3	3.3	0.003	1.5	3.2	1.7	0.087	0.0	0.8	1.6
PC 36:4a	0.007	-0.3	1.8	2.8	0.003	0.8	3.5	2.9	0.035	-0.5	1.6	3.9
PC 36:4b	0.032	0.2	-0.8	-1.8	0.014	2.6	0.3	-0.5	0.714	0.0	-0.1	-0.1
PC 36:5	0.004	-0.1	3.6	2.8	0.003	1.5	3.5	2.9	0.271	0.0	0.3	0.8
PC 36:6	0.007	-0.2	2.8	2.0	0.003	2.3	3.5	3.5	0.149	0.0	0.6	1.3
PC 37:4	0.143	0.0	-0.8	-0.6	0.109	1.0	0.0	-0.9	0.449	0.0	-0.2	-0.4
PC 37:5	0.024	-0.5	0.7	2.0	0.109	1.1	0.7	0.0	0.566	-0.1	0.0	0.2
PC 37:6	0.205	-0.7	-0.4	0.0	0.422	0.1	0.5	0.0	0.363	0.0	0.1	0.8
PC 38:2	0.012	-0.5	0.8	2.8	0.101	0.5	1.0	0.5	0.818	0.0	0.0	0.1
PC 38:3	0.009	-0.4	1.4	2.5	0.030	1.0	1.5	0.6	0.161	0.0	0.8	0.8
PC 38:4	0.053	0.0	-0.9	-1.3	0.121	1.4	0.0	-0.2	0.752	0.0	0.0	-0.1
PC 38:5	0.006	-0.1	2.3	3.0	0.010	1.7	1.9	1.0	0.254	0.0	0.4	0.8
PC 38:6a	0.005	-0.3	3.6	2.0	0.003	2.1	3.5	1.5	0.106	0.0	0.7	1.6
PC 38:6b	0.259	0.0	-0.4	-0.4	0.200	1.1	0.2	0.0	0.838	0.0	0.0	0.0
PC 38:7	0.006	0.0	2.8	2.5	0.003	2.0	3.2	1.9	0.125	0.0	0.8	1.3
PC 39:6	0.091	-1.2	-0.1	0.4	0.258	0.4	0.6	0.0	0.384	0.0	0.2	0.5
PC 39:7	0.777	-0.1	0.0	0.0	0.007	0.5	3.5	1.5	0.268	-0.1	0.2	0.8
PC 40:5	0.004	-0.7	3.1	3.6	0.064	0.2	1.3	1.0	0.091	0.0	0.9	1.5
PC 40:6	0.865	0.0	0.0	0.0	0.291	0.6	0.3	0.1	0.517	0.0	0.1	0.4
PC 40:7	0.046	0.0	1.1	1.3	0.003	1.9	3.5	0.9	0.220	0.0	0.5	0.8
PC(O-30:0)	0.608	-0.1	0.0	0.1	0.113	0.3	1.4	0.2	0.727	0.0	0.1	0.1
PC(O-32:0)	0.093	-0.7	-1.0	0.0	0.712	0.0	0.0	-0.1	0.056	0.2	-1.3	-1.5
PC(O-32:1)	0.012	-1.0	1.1	2.0	0.004	0.0	3.5	3.5	0.386	0.0	0.2	0.6
PC(O-32:1)	0.014	-0.8	0.8	2.3	0.097	0.0	1.5	0.6	0.714	0.1	0.1	0.0
PC(O-34:0)	0.037	-0.5	-2.1	-0.1	0.375	0.2	0.0	-0.5	0.103	0.0	-1.1	-1.0
PC(O-34:1)	0.036	-1.2	-1.5	0.0	0.822	0.0	0.0	0.0	0.392	0.0	-0.4	-0.3
PC(O-34:2)	0.005	-1.6	0.7	3.3	0.045	0.2	1.9	0.9	0.041	-0.2	1.1	1.9
PC(O-34:3)	0.006	-1.8	0.2	3.3	0.017	0.0	2.9	1.7	0.791	0.0	0.1	0.0
PC(O-34:4)	0.055	-0.2	0.4	1.6	0.413	0.1	0.5	0.1	0.271	0.0	0.2	0.9
PC(O-35:4)	0.199	-0.3	0.0	0.7	0.626	0.0	0.1	0.1	0.991	0.0	0.0	0.0
PC(O-36:0)	0.064	-1.1	-0.9	0.0	0.271	0.3	0.6	0.0	0.587	-0.1	0.0	-0.3
PC(O-36:1)	0.543	0.0	0.0	0.3	0.406	0.4	0.2	0.0	0.368	-0.7	0.0	0.2
PC(O-36:2)	0.011	-0.9	0.4	3.0	0.028	0.6	2.2	0.6	0.386	-0.2	0.1	0.4
PC(O-36:3)	0.006	-1.1	1.0	3.0	0.101	0.1	1.4	0.6	0.268	0.0	0.4	0.8
PC(O-36:4)	0.297	-0.1	0.1	0.5	0.506	0.4	0.0	0.0	0.886	0.0	0.0	0.0
PC(O-36:5)	0.014	-0.1	1.9	2.0	0.026	0.6	2.2	0.7	0.035	0.0	1.9	2.8
PC(O-38:4)	0.504	-0.3	-0.1	0.0	0.427	0.3	0.3	0.0	0.429	-0.2	-0.4	0.0
PC(O-38:5)	0.298	-0.2	0.0	0.5	0.672	0.2	0.0	0.0	0.435	-0.4	0.0	0.2
PC(O-40:6)	0.143	-0.4	0.1	0.8	0.078	0.3	2.0	0.1	0.486	-0.2	0.0	0.3
PC(O-40:7)	0.320	-0.3	-0.3	0.0	0.868	0.0	0.0	0.0	0.991	0.0	0.0	0.0
PC(P-32:0)	0.320	-0.1	-0.5	0.0	0.363	0.6	0.0	-0.1	0.326	0.0	-0.2	-0.7
PC(P-32:1)	0.035	-0.5	0.3	2.0	0.082	0.6	1.4	0.2	0.963	0.0	0.0	0.0
PC(P-34:0)	0.608	-0.1	-0.1	0.0	0.660	0.1	0.1	0.0	0.293	-0.2	-0.7	-0.1
PC(P-34:1)	0.033	-1.1	0.0	2.0	0.579	0.1	0.2	0.0	0.522	-0.6	0.0	0.0
PC(P-34:2)	0.004	-1.5	1.3	3.6	0.041	0.0	1.7	1.5	0.035	-0.8	0.9	2.4
PC(P-34:3)	0.025	-0.1	0.8	2.3	0.122	0.2	1.4	0.3	0.464	-0.3	0.0	0.3

Lipid species	6 weeks				10 weeks				16 weeks			
	P-value[a]	db/h vs. H/H[b]	db/db vs. H/H[b]	db/db vs. db/h[b]	*P*-value[a]	db/h vs. H/H[b]	db/db vs. H/H[b]	db/db vs. db/h[b]	*P*-value[a]	db/h vs. H/H[b]	db/db vs. H/H[b]	db/db vs. db/h[b]
PC(P-36:2)	0.004	-2.0	0.9	3.6	0.006	0.4	3.5	1.9	0.478	-0.5	0.0	0.1
PC(P-36:4)	0.270	0.0	-0.8	-0.1	0.285	0.7	0.3	0.0	0.965	0.0	0.0	0.0
PC(P-36:5)	0.005	-0.5	1.4	3.6	0.054	0.1	1.4	1.4	0.053	-0.7	0.4	1.9
PC(P-38:4)	0.212	-0.9	0.1	0.0	0.502	0.0	0.3	0.1	0.122	0.2	-0.2	-1.6
PC(P-38:5)	0.445	-0.3	-0.1	0.0	0.344	0.3	0.5	0.0	0.818	0.0	0.0	0.1
PC(P-40:5)	0.259	-0.6	-0.1	0.1	0.188	1.0	0.2	0.0	0.449	0.0	-0.3	-0.3
PC(P-40:6)	0.035	-0.9	-1.6	-0.2	0.247	0.6	-0.1	-0.5	0.257	0.0	-0.5	-0.7
LPC 14:0	0.012	0.0	2.3	2.0	0.100	0.9	0.8	0.3	0.271	0.0	0.4	0.7
LPC 15:0	0.298	-0.1	0.1	0.6	0.534	0.2	0.0	-0.1	0.754	-0.1	0.0	0.0
LPC 16:0	0.143	0.0	0.5	0.9	0.570	0.2	0.1	0.0	0.218	0.0	0.4	0.9
LPC 16:1	0.006	0.1	2.8	2.3	0.014	0.7	2.4	1.1	0.077	0.0	1.0	1.6
LPC 17:0	0.071	0.0	0.8	1.2	0.657	0.1	0.1	0.0	0.086	-0.8	0.1	1.6
LPC 17:1	0.040	0.0	1.0	1.6	0.282	0.2	0.5	0.3	0.414	-0.1	0.0	0.6
LPC 18:0	0.093	0.0	0.7	1.1	0.528	0.1	0.2	0.0	0.061	0.0	1.1	1.8
LPC 18:1	0.029	-0.1	1.4	1.5	0.398	0.2	0.3	0.1	0.221	-0.1	0.2	1.0
LPC 18:2	0.037	-0.3	1.0	1.3	0.443	0.1	0.4	0.0	0.049	-0.1	1.1	1.9
LPC 18:3	0.021	0.0	1.5	2.0	0.443	0.0	0.3	0.2	0.181	0.0	0.6	0.9
LPC 20:0	0.007	-0.7	1.1	3.0	0.024	0.6	2.0	1.0	0.035	-0.2	1.9	3.9
LPC 20:1	0.024	-0.3	1.0	1.8	0.258	0.3	0.5	0.2	0.047	0.0	1.3	2.1
LPC 20:2	0.004	-1.3	1.6	2.8	0.215	0.0	0.8	0.5	0.161	-0.1	0.4	1.1
LPC 20:3	0.046	0.0	1.0	1.3	0.571	0.1	0.1	0.0	0.294	0.0	0.2	0.8
LPC 20:4	0.527	0.0	-0.1	-0.2	0.398	0.1	0.0	-0.5	0.714	0.0	0.0	0.2
LPC 20:5	0.006	0.0	2.6	2.8	0.203	0.0	0.7	0.6	0.220	0.0	0.5	0.8
LPC 22:0	0.019	-0.5	0.5	2.5	0.384	0.0	0.3	0.3	0.104	-0.1	0.5	1.5
LPC 22:1	0.094	-0.6	0.1	1.0	0.398	0.2	0.3	0.1	0.109	0.0	0.6	1.5
LPC 22:4	0.029	-0.4	1.3	1.3	0.872	0.0	0.0	0.0	0.328	-0.1	0.1	0.8
LPC 22:5	0.021	-0.2	1.5	1.6	0.879	0.0	0.0	0.0	0.139	-0.1	0.6	1.1
LPC 22:6	0.971	0.0	0.0	0.0	0.845	0.0	0.0	0.0	0.861	-0.1	0.0	0.0
LPC 24:0	0.025	-0.9	0.2	2.1	0.291	0.1	0.5	0.4	0.245	0.0	0.3	0.8
LPC(O-16:0)	0.618	0.0	0.0	0.2	0.532	0.3	0.1	0.0	0.447	0.0	0.1	0.4
LPC(O-18:0)	0.272	-0.4	0.0	0.4	0.726	0.1	0.0	0.0	0.818	0.0	-0.1	0.0
LPC(O-18:1)	0.458	0.0	0.1	0.3	0.931	0.0	0.0	0.0	0.542	-0.1	0.0	0.3
LPC(O-20:0)	0.320	-0.3	0.0	0.4	0.343	0.5	0.3	0.0	0.331	-0.4	-0.4	-0.1
LPC(O-22:0)	0.195	-0.7	0.0	0.4	0.532	0.0	0.1	0.3	0.895	0.0	0.0	0.0
LPC(O-22:1)	0.164	-0.5	0.0	0.8	0.532	0.0	0.3	0.1	0.447	0.0	0.1	0.5
LPC(O-24:1)	0.794	0.0	0.0	0.0	0.672	-0.1	0.0	-0.1	0.775	0.0	0.0	-0.1
PE 34:1	0.205	-0.6	-0.1	0.3	0.003	0.8	3.5	3.5	0.714	0.0	0.0	0.2
PE 34:2	0.040	-0.6	0.6	1.3	0.003	0.5	3.5	3.2	0.253	0.1	0.6	0.5
PE 36:1	0.193	-0.5	-0.1	0.4	0.018	0.0	2.0	2.2	0.429	0.0	0.3	0.4
PE 36:2	0.093	-0.4	0.2	1.1	0.003	1.1	3.5	3.5	0.117	0.0	0.8	1.3
PE 36:3	0.137	-0.8	0.0	0.7	0.003	1.7	3.5	3.2	0.176	0.0	0.5	1.1
PE 36:4	0.111	-1.0	-0.1	0.5	0.003	1.5	3.5	2.2	0.577	0.1	0.2	0.0
PE 38:3	0.320	-0.4	-0.1	0.2	0.003	0.4	3.5	3.5	0.397	0.0	0.4	0.2
PE 38:4	0.193	-0.6	-0.4	0.0	0.006	1.9	2.4	1.0	0.886	0.0	0.0	0.0
PE 38:5	0.249	-0.5	-0.2	0.1	0.008	0.7	2.9	1.7	0.571	0.0	0.4	0.0
PE 38:6	0.190	-0.7	-0.4	0.0	0.017	1.3	1.9	0.7	0.799	0.1	0.0	0.0
PE 40:5	0.287	-0.3	-0.4	0.0	0.010	0.2	2.4	2.4	0.363	0.0	0.3	0.5
PE 40:6	0.106	-0.7	-0.9	0.0	0.010	0.7	2.9	1.3	0.920	0.0	0.0	0.0
PE 40:7	0.156	-0.4	-0.8	0.0	0.045	0.6	1.4	0.9	0.831	0.0	0.0	-0.1
PE(O-34:1)	0.024	-1.8	0.0	1.5	0.123	0.3	1.0	0.4	0.035	0.0	2.4	1.9
PE(O-34:2)	0.011	-1.6	0.1	2.5	0.041	0.4	2.2	0.4	0.886	0.1	0.0	0.0
PE(O-36:2)	0.040	-0.5	0.5	1.5	0.134	0.5	0.9	0.2	0.617	-0.1	0.0	0.2
PE(O-36:3)	0.019	-0.3	0.8	2.3	0.132	0.1	1.4	0.3	0.775	-0.1	0.0	0.0
PE(O-36:4)	0.665	-0.1	0.0	0.0	0.724	0.1	0.1	0.0	0.746	0.0	0.0	-0.1

Lipid species	6 weeks				10 weeks				16 weeks			
	P-value[a]	db/h vs. H/H[b]	db/db vs. H/H[b]	db/db vs. db/h[b]	*P*-value[a]	db/h vs. H/H[b]	db/db vs. H/H[b]	db/db vs. db/h[b]	*P*-value[a]	db/h vs. H/H[b]	db/db vs. H/H[b]	db/db vs. db/h[b]
PE(O-38:4)	0.860	0.0	0.0	0.0	0.590	0.2	0.0	0.0	0.271	-0.6	0.1	0.4
PE(O-38:5)	0.094	-0.2	0.8	0.8	0.099	0.0	1.4	0.8	0.036	-0.2	0.9	2.4
PE(O-40:4)	0.450	-0.2	0.0	0.3	0.590	0.1	0.2	0.0	0.799	0.0	0.0	0.1
PE(O-40:5)	0.004	-1.3	1.6	2.8	0.064	0.7	1.3	0.5	0.363	0.0	0.2	0.7
PE(O-40:7)	0.503	-0.1	0.0	0.2	0.343	0.3	0.5	0.0	0.331	-0.3	0.0	0.6
PE(O-42:7)	0.690	0.0	0.0	-0.1	0.898	0.0	0.0	0.0	0.643	0.1	0.1	0.0
PE(P-36:1)	0.040	-0.5	0.5	1.5	0.134	0.5	0.9	0.2	0.617	-0.1	0.0	0.2
PE(P-36:2)	0.021	-0.5	0.8	2.1	0.021	0.0	1.7	2.4	0.174	0.0	0.8	0.8
PE(P-36:4)	0.218	-0.2	-0.8	0.1	0.672	0.0	-0.1	-0.1	0.623	-0.2	0.0	0.1
PE(P-38:4)	0.133	-0.5	-0.8	0.1	0.626	0.1	0.1	0.0	0.991	0.0	0.0	0.0
PE(P-38:5)	0.396	-0.1	-0.4	0.0	0.556	0.3	0.0	0.0	0.577	-0.1	-0.3	0.0
PE(P-38:6)	0.050	-0.1	-1.9	-0.4	0.845	0.1	0.0	0.0	0.895	0.0	0.0	0.0
PE(P-40:4)	0.007	-0.6	1.5	2.8	0.151	0.1	1.0	0.5	0.412	0.0	0.4	0.3
PE(P-40:5)	0.730	-0.2	0.0	0.0	0.203	0.8	0.4	0.0	0.838	0.1	0.0	0.0
PE(P-40:6)	0.421	-0.2	-0.3	0.0	0.291	0.2	0.7	0.0	0.754	0.3	0.0	0.0
LPE 16:0	0.147	-0.4	0.1	0.9	0.375	0.4	0.3	0.0	0.965	0.0	0.0	0.0
LPE 18:0	0.320	-0.1	0.0	0.5	0.406	0.2	0.3	0.1	0.524	0.0	0.1	0.3
LPE 18:1	0.006	-0.4	1.6	3.0	0.134	0.2	1.0	0.4	0.144	0.1	0.4	1.3
LPE 18:2	0.004	-0.6	2.1	3.3	0.130	0.0	0.8	1.0	0.035	-0.3	1.6	2.8
LPE 20:4	0.015	-0.1	1.6	2.1	0.488	0.0	0.3	0.2	0.263	0.0	0.3	0.8
LPE 22:6	0.091	0.0	0.4	1.5	0.863	0.0	0.0	0.0	0.729	0.0	0.0	0.2
PI 32:0	0.971	0.0	0.0	0.0	0.790	0.0	0.0	0.0	0.037	1.5	1.8	0.3
PI 32:1	0.004	0.0	3.3	3.3	0.014	0.2	2.4	1.9	0.035	0.0	1.6	2.6
PI 34:1	0.004	-0.9	2.1	3.6	0.078	0.5	1.1	0.6	0.040	-0.2	1.0	2.1
PI 36:1	0.004	-0.9	1.8	3.3	0.041	-0.1	1.5	1.5	0.035	-0.9	1.1	3.1
PI 36:2	0.004	-1.3	1.5	3.6	0.054	0.2	1.4	1.1	0.038	-0.2	1.1	2.1
PI 36:3	0.004	-1.1	2.4	3.6	0.028	0.2	2.0	1.3	0.053	0.0	0.9	2.1
PI 36:4	0.004	-0.6	2.4	3.6	0.027	0.1	2.0	1.5	0.062	0.0	0.9	1.9
PI 38:2	0.004	-0.5	2.8	3.6	0.011	0.0	2.9	2.2	0.149	0.0	0.8	1.0
PI 38:3	0.005	-0.7	1.5	3.3	0.299	0.1	0.5	0.4	0.156	0.0	0.5	1.1
PI 38:4	0.249	-0.2	0.1	0.5	0.328	0.3	0.3	0.1	0.262	0.0	0.4	0.8
PI 38:5	0.004	-0.3	3.3	3.6	0.006	0.3	3.5	2.2	0.121	0.0	0.7	1.4
PI 38:6	0.007	-0.5	1.3	3.0	0.061	0.0	1.5	1.1	0.056	-0.3	0.8	1.8
PI 40:4	0.011	-0.2	1.5	2.5	0.078	0.5	1.0	0.8	0.124	0.0	0.6	1.4
PI 40:5	0.004	-0.3	2.8	3.3	0.113	0.0	1.1	0.9	0.099	0.0	0.8	1.5
PI 40:6	0.147	-1.1	0.0	0.4	0.595	0.2	0.1	0.0	0.070	-0.8	0.1	1.6
LPI 18:1	0.065	-0.4	0.5	1.1	0.384	0.0	0.5	0.3	0.035	-0.2	1.4	2.8
LPI 18:2	0.070	-0.2	0.7	1.1	0.701	0.0	0.1	0.1	0.099	-0.5	0.6	1.1
LPI 20:4	0.396	0.0	0.3	0.2	0.970	0.0	0.0	0.0	0.587	-0.1	0.0	0.2
PS 38:4	0.135	-0.5	-0.9	0.0	0.844	0.0	0.1	0.0	0.339	0.0	-0.4	-0.5
PS 40:6	0.190	-0.3	-0.8	0.0	0.626	0.0	0.2	0.1	0.727	-0.1	-0.1	0.0
CE 14:0	0.004	-0.9	3.1	3.3	0.021	0.4	2.4	1.0	0.087	0.0	0.8	1.8
CE 15:0	0.009	-1.0	0.2	3.6	0.672	0.1	0.1	0.0	0.628	-0.2	0.0	-0.1
CE 16:0	0.255	-0.5	0.0	0.4	0.286	0.6	0.3	0.0	0.271	-0.7	0.0	0.4
CE 16:1	0.004	0.0	3.9	3.6	0.004	0.2	3.5	3.2	0.062	0.0	1.0	1.9
CE 16:2	0.007	0.0	2.3	2.8	0.058	0.2	2.0	0.5	0.775	0.0	0.0	0.1
CE 17:0	0.098	-0.4	0.0	1.5	0.571	0.3	0.0	0.0	0.203	-1.1	-0.4	0.0
CE 17:1	0.022	-0.8	0.4	2.1	0.200	0.6	0.7	0.0	0.389	-0.1	0.0	0.6
CE 18:1	0.085	-1.2	0.0	0.7	0.755	0.0	0.1	0.0	0.407	-0.3	0.0	0.4
CE 18:2	0.023	-0.2	0.8	2.3	0.282	0.0	0.6	0.4	0.035	-0.2	1.9	3.9
CE 18:3	0.006	-0.6	1.0	3.6	0.093	0.0	1.0	1.3	0.035	-0.4	1.3	3.3
CE 20:3	0.006	-0.1	2.3	2.8	0.064	0.4	1.4	0.6	0.429	0.0	0.3	0.4
CE 20:4	0.760	0.1	0.0	0.0	0.672	0.2	0.0	0.0	0.086	-0.1	0.2	2.4
CE 20:5	0.143	-0.4	-0.8	0.0	0.488	0.0	-0.2	-0.3	0.036	-1.6	-2.1	-0.1

Lipid species	6 weeks				10 weeks				16 weeks			
	P-value[a]	db/h vs. H/H[b]	db/db vs. H/H[b]	db/db vs. db/h[b]	*P*-value[a]	db/h vs. H/H[b]	db/db vs. H/H[b]	db/db vs. db/h[b]	*P*-value[a]	db/h vs. H/H[b]	db/db vs. H/H[b]	db/db vs. db/h[b]
CE 20:5	0.004	0.0	3.3	3.6	0.010	0.0	2.9	2.4	0.035	0.0	1.5	3.6
CE 22:4	0.007	-0.4	1.6	2.8	0.488	0.2	0.2	0.0	0.149	-0.1	0.5	1.0
CE 22:5	0.004	-0.9	3.9	3.6	0.022	0.0	2.2	1.7	0.035	0.0	1.4	3.9
CE 22:6	0.542	0.0	0.1	0.3	0.879	0.0	0.0	0.0	0.036	-0.1	0.8	2.8
CE 24:6	0.006	-1.0	0.8	3.3	0.215	0.0	0.5	0.8	0.461	0.0	0.1	0.4
COH	0.085	-0.4	0.4	1.0	0.117	0.0	1.3	0.7	0.363	-0.1	0.1	0.6
DG 16:0/16:0	0.035	0.0	1.8	0.9	0.113	0.1	1.4	0.5	0.500	0.0	0.3	0.2
DG 16:0/18:0	0.173	0.0	0.6	0.6	0.488	0.0	0.3	0.2	0.577	0.0	0.1	0.2
DG 16:0/18:1	0.030	0.3	1.5	1.1	0.003	1.3	3.5	1.7	0.102	0.0	1.0	1.3
DG 16:0/18:2	0.030	0.0	1.5	1.5	0.012	1.0	2.0	1.4	0.130	0.0	0.8	1.0
DG 16:1/18:1	0.005	0.3	3.6	1.8	0.003	1.0	3.5	2.9	0.038	0.0	1.6	1.9
DG 18:0/18:0	0.817	0.0	0.0	0.0	0.977	0.0	0.0	0.0	0.736	-0.1	-0.1	0.0
DG 18:0/18:1	0.025	0.0	1.9	1.2	0.010	1.2	2.7	0.7	0.271	0.0	0.6	0.5
DG 18:1/18:1	0.015	0.3	2.6	0.9	0.037	0.3	1.9	1.0	0.068	0.0	1.0	1.8
DG 18:1/18:2	0.016	0.0	2.4	1.3	0.057	1.0	1.3	0.3	0.109	0.0	0.8	1.4
DG 18:1/20:4	0.180	0.0	0.4	0.7	0.563	0.1	0.2	0.0	0.535	0.2	0.2	0.0
DG 18:2/18:2	0.035	0.1	1.5	1.1	0.286	0.4	0.4	0.1	0.221	0.0	0.7	0.7
TG 14:0/16:0/18:1	0.004	1.1	3.3	2.5	0.003	1.9	3.5	3.2	0.036	0.0	1.8	2.1
TG 14:0/16:0/18:2	0.004	1.0	3.3	3.3	0.003	1.7	3.5	3.5	0.036	0.0	1.8	1.9
TG 14:0/16:1/18:1	0.004	1.3	3.9	2.8	0.003	1.1	3.5	3.5	0.038	0.0	1.6	1.9
TG 14:0/16:1/18:2	0.004	0.7	3.3	3.3	0.003	0.9	3.5	2.9	0.036	0.0	1.9	1.8
TG 14:0/17:0/18:1	0.008	0.4	2.6	1.6	0.006	0.8	2.9	2.0	0.088	0.0	1.3	1.1
TG 14:0/18:2/18:2	0.004	1.1	2.8	2.8	0.008	0.6	2.7	2.0	0.056	0.0	1.4	1.6
TG 14:1/16:0/18:1	0.004	0.7	3.1	2.3	0.003	0.6	3.5	3.5	0.038	0.0	1.6	1.9
TG 14:1/16:1/18:0	0.004	1.8	3.9	3.6	0.003	2.0	3.5	3.5	0.036	0.1	1.8	1.9
TG 14:1/18:1/18:1	0.004	1.2	3.1	3.6	0.003	1.5	3.5	3.5	0.036	0.0	1.8	1.9
TG 15:0/16:0/18:1	0.004	0.4	2.8	2.5	0.003	1.3	3.5	2.7	0.038	0.0	1.6	1.9
TG 15:0/18:1/18:1	0.013	0.0	1.8	2.3	0.017	0.6	2.0	1.5	0.048	-0.1	1.1	1.9
TG 16:0/16:0/16:0	0.006	1.1	2.8	1.1	0.004	1.2	3.5	1.5	0.062	0.0	1.4	1.5
TG 16:0/16:0/18:0	0.016	0.8	2.4	0.4	0.008	1.0	3.5	0.6	0.052	0.0	1.3	1.9
TG 16:0/16:0/18:1	0.004	0.5	2.8	2.5	0.006	0.6	2.9	2.4	0.036	0.0	1.8	2.3
TG 16:0/16:0/18:2	0.008	0.3	2.4	2.0	0.009	0.7	2.7	1.7	0.036	-0.2	1.5	2.1
TG 16:0/16:1/17:0	0.005	0.7	2.8	2.1	0.004	0.8	3.2	2.2	0.065	0.0	1.4	1.4
TG 16:0/16:1/18:1	0.004	1.2	3.1	3.6	0.003	1.7	3.5	3.2	0.036	0.0	1.6	2.3
TG 16:0/17:0/18:1	0.008	0.0	2.4	2.3	0.022	0.3	2.0	1.4	0.036	0.0	1.8	2.3
TG 16:0/17:0/18:2	0.004	0.0	2.8	3.6	0.007	0.3	2.9	2.4	0.036	0.0	1.8	2.1
TG 16:0/18:0/18:1	0.018	0.1	2.4	1.0	0.044	0.2	1.7	1.0	0.035	0.0	2.1	3.6
TG 16:0/18:1/18:1	0.005	0.1	2.8	2.5	0.057	0.2	1.7	0.7	0.035	0.0	1.9	2.4
TG 16:0/18:1/18:2	0.009	0.2	2.1	2.3	0.174	0.4	0.8	0.2	0.043	-0.1	1.3	1.9
TG 16:0/18:2/18:2	0.017	0.3	1.8	1.6	0.247	0.4	0.5	0.1	0.091	-0.1	1.0	1.3
TG 16:1/16:1/16:1	0.004	1.5	3.9	3.6	0.003	1.5	3.5	3.5	0.036	0.1	1.9	1.9
TG 16:1/16:1/18:1	0.004	1.1	3.1	3.6	0.003	1.4	3.5	3.5	0.036	0.0	1.8	1.9
TG 16:1/17:0/18:1	0.004	0.0	2.8	3.6	0.007	0.3	2.7	2.7	0.035	-0.1	1.6	2.4
TG 16:1/18:1/18:1	0.004	0.8	3.1	3.6	0.003	1.1	3.5	2.7	0.035	0.0	1.9	2.4
TG 16:1/18:1/18:2	0.004	0.8	2.6	3.3	0.004	0.7	2.9	2.7	0.035	0.0	2.1	2.3
TG 17:0/18:1/18:1	0.005	0.0	2.8	2.8	0.118	0.1	1.0	0.7	0.035	0.0	2.4	2.8
TG 18:0/18:0/18:0	0.032	1.1	1.8	0.0	0.120	1.2	0.3	-0.1	0.427	0.0	0.3	0.3
TG 18:0/18:0/18:1	0.056	0.0	1.3	0.9	0.016	0.5	2.4	1.3	0.035	0.0	2.1	2.1
TG 18:0/18:1/18:1	0.102	0.0	0.9	0.7	0.045	1.1	1.3	0.3	0.035	0.1	2.3	3.6
TG 18:0/18:2/18:2	0.050	0.0	0.9	1.5	0.534	0.1	0.2	0.1	0.035	0.0	2.1	2.1
TG 18:1/18:1/18:1	0.018	0.0	1.9	1.6	0.017	1.0	2.0	0.8	0.035	0.0	2.1	2.6
TG 18:1/18:1/18:2	0.021	0.0	1.6	1.8	0.012	1.0	2.4	0.9	0.035	-0.3	1.6	2.4
TG 18:1/18:1/20:4	0.181	-0.7	-0.1	0.4	0.607	0.0	-0.1	-0.2	0.129	-0.1	0.8	0.9
TG 18:1/18:1/22:6	0.294	-0.3	0.0	0.5	0.960	0.0	0.0	0.0	0.213	0.0	0.5	0.8

Lipid species	6 weeks				10 weeks				16 weeks			
	P-value[a]	db/h vs. H/H[b]	db/db vs. H/H[b]	db/db vs. db/h[b]	*P*-value[a]	db/h vs. H/H[b]	db/db vs. H/H[b]	db/db vs. db/h[b]	*P*-value[a]	db/h vs. H/H[b]	db/db vs. H/H[b]	db/db vs. db/h[b]
TG 18:1/18:2/18:2	0.016	0.0	1.6	2.1	0.171	0.2	0.9	0.4	0.035	0.0	1.8	2.4
TG 18:2/18:2/18:2	0.036	0.0	1.3	1.5	0.175	0.1	0.9	0.4	0.036	-0.1	1.6	2.1
TG 18:2/18:2/20:4	0.298	-0.1	-0.4	-0.2	0.795	0.0	0.0	-0.1	0.124	0.0	0.8	1.3

[a] *P*-value for the comparison of levels of each lipid species between genotypes at each age using the Kruskal Wallis test with Benjamini-Hochberg correction for multiple comparisons. $P < 0.05$ was considered significant (highlighted in pink).

[b] Post-hoc analysis was performed using the Mann Whitney *U* test with Dunn-Sidak correction for multiple group comparisons. Values were derived from the formula: sign(difference in median levels)*-log10(post-hoc *P*-value). Colour-coded values 1.3 to 2.0 (light red, $P = 0.05$-0.01) and > 2.0 (dark red, $P < 0.01$) indicate a significant increase relative to the reference group. Colour-coded values -1.3 to -2.0 (light green, $P = 0.05$-0.01) and < -2.0 (dark green, $P < 0.01$) indicate a significant decrease relative to the reference group.

Table S6.1 Significance levels obtained for comparisons of fasting plasma lipid species between the four study groups.

	ANCOVA[a]	Ov-ob/IS vs. Lean/IS	Ov-ob/IR vs. Lean/IS	T2D vs. Lean/IS	Ov-ob/IR vs. Ov-ob/IS	T2D vs. Ov-ob/IS	T2D vs. Ov-ob/IR
Lipid species	**Corrected *P*-value[b]**	**Post-hoc *P*-value[c]**	**Post-hoc *P*-value[c]**	**Post-hoc *P*-value[c]**	**Post-hoc *P*-value[c]**	**Post-hoc *P*-value[c]**	**Post-hoc *P*-value[c]**
dhCer 16:0	9.49E-01 (+)	9.98E-01 (-)	9.88E-01 (-)	1.00E+00	1.00E+00	1.00E+00	9.99E-01 (+)
dhCer 18:0	1.81E-01 (+)	3.37E-01 (+)	6.17E-01 (+)	7.85E-02 (+)	9.99E-01 (-)	9.92E-01 (+)	8.72E-01 (+)
dhCer 20:0	3.75E-01 (+)	4.01E-01 (+)	1.00E+00	6.34E-01 (+)	6.51E-01 (-)	9.99E-01 (-)	8.30E-01 (+)
dhCer 22:0	6.75E-02 (+)	1.42E-01 (+)	6.21E-02 (+)	**3.14E-02 (+)**	1.00E+00	9.96E-01 (+)	1.00E+00
dhCer 24:0	3.75E-01 (+)	3.83E-01 (+)	4.96E-01 (+)	4.92E-01 (+)	1.00E+00	1.00E+00	1.00E+00
dhCer 24:1	1.11E-01 (+)	8.67E-01 (+)	8.91E-01 (+)	**3.38E-02 (+)**	1.00E+00	4.35E-01 (+)	3.50E-01 (+)
Cer 16:0	9.87E-01 (+)	1.00E+00	1.00E+00	1.00E+00	1.00E+00	9.99E-01 (+)	1.00E+00
Cer 18:0	**3.84E-02 (+)**	9.19E-01 (+)	2.17E-01 (+)	**6.95E-03 (+)**	8.65E-01 (+)	1.18E-01 (+)	7.43E-01 (+)
Cer 20:0	1.96E-01 (+)	7.97E-01 (+)	3.87E-01 (+)	8.53E-02 (+)	9.95E-01 (+)	7.72E-01 (+)	9.82E-01 (+)
Cer 22:0	2.89E-01 (+)	7.41E-01 (+)	1.50E-01 (+)	6.09E-01 (+)	9.31E-01 (+)	1.00E+00	9.53E-01 (-)
Cer 24:0	6.06E-01 (+)	9.07E-01 (+)	6.61E-01 (+)	1.00E+00	9.99E-01 (+)	9.83E-01 (-)	8.36E-01 (-)
Cer 24:1	4.66E-01 (+)	1.00E+00	9.99E-01 (+)	4.86E-01 (+)	1.00E+00	5.90E-01 (+)	7.51E-01 (+)
MHC 16:0	2.12E-01 (+)	3.27E-01 (-)	4.67E-01 (-)	1.17E-01 (-)	1.00E+00	9.99E-01 (-)	9.83E-01 (-)
MHC 18:0	3.75E-01 (+)	6.38E-01 (-)	5.00E-01 (-)	3.08E-01 (-)	1.00E+00	9.99E-01 (-)	1.00E+00
MHC 20:0	4.84E-01 (+)	7.04E-01 (-)	4.31E-01 (-)	8.17E-01 (-)	1.00E+00	1.00E+00	9.92E-01 (+)
MHC 22:0	2.63E-01 (+)	9.80E-01 (-)	3.74E-01 (-)	1.97E-01 (-)	8.83E-01 (-)	6.76E-01 (-)	1.00E+00
MHC 24:0	9.92E-02 (+)	7.65E-01 (-)	1.41E-01 (-)	**3.84E-02 (-)**	9.08E-01 (-)	5.96E-01 (-)	9.97E-01 (-)
MHC 24:1	6.67E-02 (+)	3.87E-01 (-)	**2.11E-02 (-)**	6.51E-02 (-)	8.20E-01 (-)	9.73E-01 (-)	9.98E-01 (+)
DHC 16:0	**3.64E-02 (+)**	7.28E-02 (-)	**8.16E-03 (-)**	5.68E-02 (-)	9.80E-01 (-)	1.00E+00	9.74E-01 (+)
DHC 18:0	2.36E-01 (+)	4.55E-01 (-)	3.36E-01 (-)	1.00E+00	1.00E+00	5.91E-01 (+)	4.29E-01 (+)
DHC 20:0	9.97E-01 (+)	1.00E+00	1.00E+00	1.00E+00	1.00E+00	1.00E+00	1.00E+00
DHC 22:0	4.34E-01 (+)	4.71E-01 (+)	1.00E+00	1.00E+00	5.91E-01 (-)	4.70E-01 (-)	1.00E+00
DHC 24:0	2.61E-01 (+)	9.54E-01 (+)	5.23E-01 (-)	9.99E-01 (-)	1.25E-01 (-)	7.69E-01 (-)	7.73E-01 (+)
DHC 24:1	**3.37E-02 (+)**	3.02E-01 (-)	**2.86E-03 (-)**	1.92E-01 (-)	4.79E-01 (-)	1.00E+00	5.08E-01 (+)
THC 16:0	**1.27E-03 (+)**	**1.82E-02 (-)**	**2.15E-04 (-)**	**2.72E-05 (-)**	7.57E-01 (-)	3.82E-01 (-)	9.97E-01 (-)
THC 18:0	**3.64E-02 (+)**	1.15E-01 (-)	3.29E-01 (-)	**4.66E-03 (-)**	9.97E-01 (+)	8.78E-01 (-)	4.90E-01 (-)
THC 20:0	**2.71E-02 (+)**	**4.04E-02 (-)**	**3.26E-02 (-)**	**5.39E-03 (-)**	1.00E+00	9.92E-01 (-)	9.94E-01 (-)
THC 22:0	**9.86E-03 (+)**	1.64E-01 (-)	**5.69E-03 (-)**	**9.42E-04 (-)**	8.24E-01 (-)	4.56E-01 (-)	9.97E-01 (-)

Lipid species	ANCOVA[a] Corrected *P*-value[b]	Ov-ob/IS vs. Lean/IS Post-hoc *P*-value[c]	Ov-ob/IR vs. Lean/IS Post-hoc *P*-value[c]	T2D vs. Lean/IS Post-hoc *P*-value[c]	Ov-ob/IR vs. Ov-ob/IS Post-hoc *P*-value[c]	T2D vs. Ov-ob/IS Post-hoc *P*-value[c]	T2D vs. Ov-ob/IR Post-hoc *P*-value[c]
THC 24:0	**1.46E-02 (+)**	3.00E-01 (-)	**3.15E-03 (-)**	**4.20E-03 (-)**	5.02E-01 (-)	5.63E-01 (-)	1.00E+00
THC 24:1	**5.63E-03 (+)**	7.74E-02 (-)	**1.14E-03 (-)**	**8.36E-04 (-)**	7.19E-01 (-)	6.64E-01 (-)	1.00E+00
GM3 16:0	**6.86E-03 (+)**	6.88E-02 (-)	**4.44E-04 (-)**	**6.00E-03 (-)**	5.62E-01 (-)	9.72E-01 (-)	9.47E-01 (+)
GM3 18:0	**1.70E-02 (+)**	6.83E-01 (-)	**3.19E-03 (-)**	**1.35E-02 (-)**	1.90E-01 (-)	4.25E-01 (-)	9.95E-01 (+)
GM3 20:0	5.33E-02 (+)	7.46E-01 (-)	**8.58E-03 (-)**	7.76E-01 (-)	2.92E-01 (-)	1.00E+00	1.78E-01 (+)
GM3 22:0	5.93E-01 (+)	1.00E+00	8.05E-01 (-)	9.04E-01 (-)	7.32E-01 (-)	8.31E-01 (-)	1.00E+00
GM3 24:0	5.97E-02 (+)	9.78E-01 (-)	**3.66E-02 (-)**	6.76E-02 (-)	2.60E-01 (-)	3.71E-01 (-)	1.00E+00
GM3 24:1	**2.62E-03 (+)**	6.08E-01 (-)	**5.84E-05 (-)**	1.10E-01 (-)	**1.42E-02 (-)**	9.49E-01 (-)	8.24E-02 (+)
SM 31:1	2.03E-01 (+)	9.65E-01 (+)	6.74E-01 (+)	9.30E-01 (-)	9.95E-01 (+)	4.35E-01 (-)	1.15E-01 (-)
SM 32:1	2.63E-01 (+)	1.00E+00	9.06E-01 (+)	7.70E-01 (-)	9.91E-01 (+)	5.32E-01 (-)	1.40E-01 (-)
SM 32:2	2.03E-01 (+)	5.12E-01 (+)	7.72E-01 (+)	9.96E-01 (-)	9.99E-01 (-)	1.94E-01 (-)	3.61E-01 (-)
SM 33:1	4.10E-01 (+)	9.98E-01 (-)	1.00E+00	5.93E-01 (-)	9.70E-01 (+)	9.01E-01 (-)	3.32E-01 (-)
SM 34:1	1.87E-01 (+)	7.27E-01 (-)	2.54E-01 (-)	9.62E-02 (-)	9.86E-01 (-)	8.62E-01 (-)	9.99E-01 (-)
SM 34:2	1.09E-01 (+)	8.95E-01 (+)	8.65E-01 (-)	3.88E-01 (-)	2.52E-01 (-)	**4.13E-02 (-)**	9.81E-01 (-)
SM 34:3	2.22E-01 (+)	9.60E-01 (+)	9.86E-01 (+)	6.98E-01 (-)	1.00E+00	1.91E-01 (-)	2.29E-01 (-)
SM 35:1	7.98E-01 (+)	9.95E-01 (-)	1.00E+00	8.72E-01 (-)	9.99E-01 (+)	9.97E-01 (-)	9.12E-01 (-)
SM 35:2	3.47E-01 (+)	1.00E+00	1.00E+00	5.12E-01 (-)	1.00E+00	3.45E-01 (-)	4.64E-01 (-)
SM 36:1	6.54E-01 (+)	1.00E+00	9.81E-01 (+)	7.14E-01 (+)	9.90E-01 (+)	7.70E-01 (+)	9.90E-01 (+)
SM 36:2	8.30E-01 (+)	8.87E-01 (+)	1.00E+00	9.91E-01 (+)	9.78E-01 (-)	9.98E-01 (-)	1.00E+00
SM 36:3	1.25E-01 (+)	9.67E-01 (-)	7.80E-01 (-)	**4.40E-02 (-)**	9.99E-01 (-)	3.11E-01 (-)	5.64E-01 (-)
SM 38:1	**1.05E-02 (+)**	1.00E+00	1.00E+00	**1.29E-02 (-)**	1.00E+00	**5.90E-03 (-)**	**3.69E-03 (-)**
SM 38:2	7.32E-01 (+)	1.00E+00	1.00E+00	8.98E-01 (-)	1.00E+00	7.80E-01 (-)	9.19E-01 (-)
SM 39:1	3.49E-01 (+)	9.67E-01 (-)	7.74E-01 (+)	9.42E-01 (+)	2.87E-01 (+)	4.67E-01 (+)	9.99E-01 (-)
SM 41:1	8.30E-01 (+)	1.00E+00	1.00E+00	9.43E-01 (-)	1.00E+00	9.87E-01 (-)	9.10E-01 (-)
SM 41:2	6.60E-01 (+)	9.64E-01 (-)	9.19E-01 (-)	6.01E-01 (-)	1.00E+00	9.88E-01 (-)	9.96E-01 (-)
SM 42:1	4.45E-01 (+)	1.00E+00	9.31E-01 (-)	6.64E-01 (-)	7.87E-01 (-)	4.30E-01 (-)	9.98E-01 (-)
PC 28:0	9.97E-01 (+)	1.00E+00	1.00E+00	1.00E+00	1.00E+00	1.00E+00	1.00E+00
PC 29:0	8.30E-01 (+)	9.51E-01 (+)	9.39E-01 (+)	9.43E-01 (+)	1.00E+00	1.00E+00	1.00E+00
PC 30:0	9.97E-01 (+)	1.00E+00	1.00E+00	1.00E+00	1.00E+00	1.00E+00	1.00E+00
PC 31:0	8.38E-01 (+)	9.98E-01 (+)	9.31E-01 (+)	9.40E-01 (+)	9.99E-01 (+)	9.99E-01 (+)	1.00E+00
PC 31:1	**3.64E-02 (+)**	9.95E-01 (+)	9.98E-01 (+)	8.52E-02 (-)	1.00E+00	**2.14E-02 (-)**	**2.12E-02 (-)**

Lipid species	ANCOVA[a] Corrected *P*-value[b]	Ov-ob/IS vs. Lean/IS Post-hoc *P*-value[c]	Ov-ob/IR vs. Lean/IS Post-hoc *P*-value[c]	T2D vs. Lean/IS Post-hoc *P*-value[c]	Ov-ob/IR vs. Ov-ob/IS Post-hoc *P*-value[c]	T2D vs. Ov-ob/IS Post-hoc *P*-value[c]	T2D vs. Ov-ob/IR Post-hoc *P*-value[c]
PC 32:0	**3.97E-02 (+)**	7.44E-01 (-)	**2.17E-02 (-)**	**2.12E-02 (-)**	4.87E-01 (-)	4.69E-01 (-)	1.00E+00
PC 32:1	3.49E-01 (+)	5.60E-01 (+)	8.22E-01 (+)	2.36E-01 (+)	9.99E-01 (-)	9.98E-01 (+)	9.41E-01 (+)
PC 32:2	7.64E-01 (+)	9.99E-01 (+)	9.99E-01 (+)	9.87E-01 (-)	1.00E+00	8.76E-01 (-)	8.48E-01 (-)
PC 32:3	7.98E-01 (+)	1.00E+00	9.99E-01 (-)	9.72E-01 (-)	9.99E-01 (+)	9.82E-01 (-)	8.09E-01 (-)
PC 33:0	5.32E-01 (+)	1.00E+00	9.60E-01 (-)	4.92E-01 (-)	9.97E-01 (-)	7.33E-01 (-)	9.61E-01 (-)
PC 33:1	6.84E-01 (+)	9.60E-01 (+)	6.37E-01 (+)	9.34E-01 (+)	9.93E-01 (+)	1.00E+00	9.94E-01 (-)
PC 33:2	1.09E-01 (+)	5.04E-01 (-)	9.82E-01 (-)	**4.51E-02 (-)**	9.37E-01 (+)	8.73E-01 (-)	2.24E-01 (-)
PC 33:3	8.03E-01 (+)	9.28E-01 (+)	8.80E-01 (+)	9.97E-01 (-)	1.00E+00	9.98E-01 (-)	9.94E-01 (-)
PC 34:0	1.54E-01 (+)	9.91E-01 (+)	8.89E-01 (-)	2.80E-01 (-)	5.37E-01 (-)	7.73E-02 (-)	9.26E-01 (-)
PC 34:1	5.65E-01 (+)	8.60E-01 (+)	1.00E+00	9.96E-01 (-)	7.89E-01 (-)	4.99E-01 (-)	9.99E-01 (-)
PC 34:2	**3.64E-02 (+)**	5.20E-02 (-)	9.88E-01 (-)	**2.61E-02 (-)**	2.64E-01 (+)	1.00E+00	1.28E-01 (-)
PC 34:3	7.94E-01 (+)	1.00E+00	1.00E+00	9.34E-01 (-)	1.00E+00	9.16E-01 (-)	8.80E-01 (-)
PC 34:4	7.90E-01 (+)	7.99E-01 (+)	9.72E-01 (+)	9.96E-01 (+)	9.99E-01 (-)	9.80E-01 (-)	1.00E+00
PC 34:5	5.56E-01 (+)	6.16E-01 (+)	9.31E-01 (+)	1.00E+00	9.95E-01 (-)	7.23E-01 (-)	9.68E-01 (-)
PC 35:0	2.63E-01 (+)	1.00E+00	1.00E+00	2.71E-01 (-)	1.00E+00	4.36E-01 (-)	2.73E-01 (-)
PC 35:1	8.30E-01 (+)	1.00E+00	9.95E-01 (+)	9.97E-01 (-)	1.00E+00	9.78E-01 (-)	8.73E-01 (-)
PC 35:2	**1.70E-02 (+)**	2.69E-01 (-)	7.90E-01 (-)	**1.38E-03 (-)**	9.71E-01 (+)	3.70E-01 (-)	5.03E-02 (-)
PC 35:3	8.71E-02 (+)	1.00E+00	9.90E-01 (-)	5.39E-02 (-)	9.97E-01 (-)	8.14E-02 (-)	2.21E-01 (-)
PC 35:4	9.07E-01 (+)	1.00E+00	1.00E+00	9.83E-01 (-)	1.00E+00	9.85E-01 (-)	9.87E-01 (-)
PC 35:5	6.89E-01 (+)	7.58E-01 (+)	9.25E-01 (+)	1.00E+00	1.00E+00	9.11E-01 (-)	9.86E-01 (-)
PC 36:1	6.75E-02 (+)	**4.20E-02 (+)**	5.76E-01 (+)	1.00E+00	7.75E-01 (-)	5.77E-02 (-)	6.50E-01 (-)
PC 36:2	9.18E-02 (+)	4.11E-01 (-)	1.00E+00	7.26E-02 (-)	5.99E-01 (+)	9.74E-01 (-)	1.13E-01 (-)
PC 36:3	6.18E-01 (+)	9.07E-01 (-)	1.00E+00	7.16E-01 (-)	9.63E-01 (+)	1.00E+00	8.06E-01 (-)
PC 36:4a	**2.08E-02 (+)**	3.20E-01 (-)	3.32E-01 (-)	**1.23E-03 (-)**	1.00E+00	2.94E-01 (-)	2.34E-01 (-)
PC 36:4b	8.59E-01 (+)	1.00E+00	1.00E+00	9.90E-01 (+)	9.95E-01 (-)	1.00E+00	9.20E-01 (+)
PC 36:5	5.93E-01 (+)	5.60E-01 (+)	1.00E+00	9.99E-01 (+)	8.01E-01 (-)	8.33E-01 (-)	1.00E+00
PC 36:6	2.36E-01 (+)	3.46E-01 (+)	1.00E+00	9.98E-01 (-)	4.24E-01 (-)	1.33E-01 (-)	9.96E-01 (-)
PC 37:4	5.58E-01 (+)	9.72E-01 (-)	8.62E-01 (-)	4.69E-01 (-)	1.00E+00	9.47E-01 (-)	9.94E-01 (-)
PC 37:5	5.91E-01 (+)	8.65E-01 (+)	1.00E+00	9.96E-01 (-)	9.52E-01 (-)	5.15E-01 (-)	9.76E-01 (-)
PC 37:6	1.20E-01 (+)	9.94E-01 (+)	9.47E-01 (-)	1.85E-01 (-)	6.79E-01 (-)	5.20E-02 (-)	7.29E-01 (-)
PC 38:2	3.00E-01 (+)	1.00E+00	6.32E-01 (-)	4.72E-01 (-)	5.56E-01 (-)	3.78E-01 (-)	1.00E+00

Lipid species	ANCOVA[a] Corrected *P*-value[b]	Ov-ob/IS vs. Lean/IS Post-hoc *P*-value[c]	Ov-ob/IR vs. Lean/IS Post-hoc *P*-value[c]	T2D vs. Lean/IS Post-hoc *P*-value[c]	Ov-ob/IR vs. Ov-ob/IS Post-hoc *P*-value[c]	T2D vs. Ov-ob/IS Post-hoc *P*-value[c]	T2D vs. Ov-ob/IR Post-hoc *P*-value[c]
PC 38:3	4.93E-01 (+)	8.42E-01 (+)	3.97E-01 (+)	8.17E-01 (+)	9.91E-01 (+)	1.00E+00	9.88E-01 (-)
PC 38:4	9.42E-01 (+)	9.81E-01 (+)	1.00E+00	1.00E+00	9.96E-01 (-)	9.96E-01 (-)	1.00E+00
PC 38:5	2.83E-01 (+)	6.07E-01 (+)	9.94E-01 (-)	9.90E-01 (-)	2.75E-01 (-)	2.12E-01 (-)	1.00E+00
PC 38:6a	**3.40E-02 (+)**	9.32E-01 (+)	9.34E-01 (-)	6.38E-02 (-)	3.98E-01 (-)	**4.94E-03 (-)**	4.33E-01 (-)
PC 38:6b	1.87E-01 (+)	8.94E-01 (+)	6.44E-01 (-)	8.73E-01 (-)	1.21E-01 (-)	2.26E-01 (-)	9.99E-01 (+)
PC 38:7	**3.64E-02 (+)**	8.10E-01 (+)	7.61E-01 (-)	1.39E-01 (-)	1.22E-01 (-)	**5.80E-03 (-)**	8.86E-01 (-)
PC 39:6	2.89E-01 (+)	1.00E+00	7.12E-01 (-)	3.45E-01 (-)	7.15E-01 (-)	3.33E-01 (-)	9.97E-01 (-)
PC 40:5	4.66E-01 (+)	4.02E-01 (+)	1.00E+00	9.73E-01 (+)	5.99E-01 (-)	8.83E-01 (-)	9.96E-01 (+)
PC 40:6	4.66E-01 (+)	4.85E-01 (+)	1.00E+00	1.00E+00	5.24E-01 (-)	7.14E-01 (-)	1.00E+00
PC 40:7	**3.29E-03 (+)**	1.00E+00	**3.59E-02 (-)**	**2.29E-03 (-)**	**2.63E-02 (-)**	**1.30E-03 (-)**	9.46E-01 (-)
PC(O-30:0)	1.11E-01 (+)	9.63E-02 (-)	2.42E-01 (-)	8.02E-02 (-)	9.99E-01 (+)	1.00E+00	9.98E-01 (-)
PC(O-32:0)	**2.71E-02 (+)**	**1.04E-02 (-)**	**2.83E-02 (-)**	**1.86E-02 (-)**	9.99E-01 (+)	1.00E+00	1.00E+00
PC(O-32:1)	7.33E-02 (+)	1.47E-01 (-)	**2.60E-02 (-)**	1.13E-01 (-)	9.90E-01 (-)	1.00E+00	9.90E-01 (+)
PC(O-32:2)	4.66E-01 (+)	4.31E-01 (-)	6.62E-01 (-)	7.23E-01 (-)	1.00E+00	9.98E-01 (+)	1.00E+00
PC(O-34:0)	8.78E-01 (+)	1.00E+00	1.00E+00	9.88E-01 (-)	1.00E+00	9.71E-01 (-)	9.69E-01 (-)
PC(O-34:1)	**5.01E-03 (+)**	**3.07E-02 (-)**	**1.39E-03 (-)**	**5.40E-04 (-)**	9.29E-01 (-)	8.16E-01 (-)	1.00E+00
PC(O-34:2)	**3.40E-02 (+)**	1.16E-01 (-)	2.11E-01 (-)	**3.46E-03 (-)**	1.00E+00	8.29E-01 (-)	5.93E-01 (-)
PC(O-34:4)	8.59E-01 (+)	9.71E-01 (-)	1.00E+00	9.43E-01 (-)	9.99E-01 (+)	1.00E+00	9.95E-01 (-)
PC(O-35:4)	7.53E-01 (+)	9.99E-01 (-)	1.00E+00	8.32E-01 (-)	1.00E+00	9.80E-01 (-)	8.50E-01 (-)
PC(O-36:0)	8.48E-02 (+)	1.49E-01 (+)	1.00E+00	9.92E-01 (-)	1.08E-01 (-)	**3.16E-02 (-)**	9.99E-01 (-)
PC(O-36:1)	5.48E-01 (+)	6.85E-01 (-)	7.62E-01 (-)	1.00E+00	1.00E+00	8.68E-01 (+)	9.09E-01 (+)
PC(O-36:2)	**2.01E-03 (+)**	**4.02E-02 (-)**	**2.92E-02 (-)**	**2.95E-05 (-)**	1.00E+00	2.34E-01 (-)	2.38E-01 (-)
PC(O-36:3)	6.75E-02 (+)	1.84E-01 (-)	2.39E-01 (-)	**1.47E-02 (-)**	1.00E+00	9.40E-01 (-)	8.65E-01 (-)
PC(O-36:4)	3.91E-01 (+)	5.30E-01 (-)	5.77E-01 (-)	3.55E-01 (-)	1.00E+00	1.00E+00	1.00E+00
PC(O-36:5)	8.30E-01 (+)	9.61E-01 (+)	9.70E-01 (+)	1.00E+00	1.00E+00	9.72E-01 (-)	9.76E-01 (-)
PC(O-38:4)	4.66E-01 (+)	5.11E-01 (-)	7.17E-01 (-)	5.18E-01 (-)	1.00E+00	1.00E+00	1.00E+00
PC(O-38:5)	**4.89E-02 (+)**	4.03E-01 (-)	**4.60E-02 (-)**	**1.32E-02 (-)**	9.32E-01 (-)	7.05E-01 (-)	9.99E-01 (-)
PC(O-40:7)	**3.34E-02 (+)**	9.20E-01 (-)	**2.75E-02 (-)**	**1.30E-02 (-)**	3.27E-01 (-)	1.86E-01 (-)	1.00E+00
PC(P-32:0)	**1.67E-02 (+)**	**2.27E-02 (-)**	**5.92E-03 (-)**	**5.13E-03 (-)**	9.99E-01 (-)	9.99E-01 (-)	1.00E+00
PC(P-32:1)	6.29E-02 (+)	8.80E-01 (-)	**4.95E-02 (-)**	**3.60E-02 (-)**	5.28E-01 (-)	4.32E-01 (-)	1.00E+00
PC(P-34:1)	**1.27E-03 (+)**	5.07E-01 (-)	**3.99E-04 (-)**	**1.23E-04 (-)**	8.28E-02 (-)	**3.23E-02 (-)**	1.00E+00

Lipid species	ANCOVA[a] Corrected *P*-value[b]	Ov-ob/IS vs. Lean/IS Post-hoc *P*-value[c]	Ov-ob/IR vs. Lean/IS Post-hoc *P*-value[c]	T2D vs. Lean/IS Post-hoc *P*-value[c]	Ov-ob/IR vs. Ov-ob/IS Post-hoc *P*-value[c]	T2D vs. Ov-ob/IS Post-hoc *P*-value[c]	T2D vs. Ov-ob/IR Post-hoc *P*-value[c]
PC(P-34:2)	**1.43E-03 (+)**	1.84E-01 (-)	**2.98E-03 (-)**	**2.56E-05 (-)**	6.62E-01 (-)	**4.87E-02 (-)**	7.30E-01 (-)
PC(P-34:3)	5.93E-01 (+)	1.00E+00 (-)	1.00E+00	6.92E-01 (-)	1.00E+00	7.80E-01 (-)	7.35E-01 (-)
PC(P-36:2)	**4.44E-04 (+)**	1.34E-01 (-)	**6.48E-04 (-)**	**3.63E-06 (-)**	4.46E-01 (-)	**1.81E-02 (-)**	6.97E-01 (-)
PC(P-36:4)	7.22E-01 (+)	1.00E+00	9.48E-01 (-)	7.76E-01 (-)	9.90E-01 (-)	9.03E-01 (-)	1.00E+00
PC(P-36:5)	6.71E-01 (+)	9.51E-01 (+)	9.33E-01 (+)	1.00E+00	1.00E+00	8.61E-01 (-)	8.12E-01 (-)
PC(P-38:5)	4.08E-01 (+)	1.00E+00	7.03E-01 (-)	3.89E-01 (-)	9.21E-01 (-)	6.63E-01 (-)	9.99E-01 (-)
PC(P-40:5)	6.44E-02 (+)	7.44E-01 (-)	**4.30E-02 (-)**	**3.43E-02 (-)**	6.58E-01 (-)	5.90E-01 (-)	1.00E+00
LPC 14:0	7.98E-01 (+)	9.49E-01 (+)	9.66E-01 (+)	1.00E+00	1.00E+00	9.50E-01 (-)	9.62E-01 (-)
LPC 15:0	7.63E-02 (+)	9.94E-01 (-)	4.17E-01 (-)	**2.59E-02 (-)**	8.45E-01 (-)	1.31E-01 (-)	7.98E-01 (-)
LPC 16:0	**1.25E-02 (+)**	9.32E-01 (-)	**1.11E-02 (-)**	**3.47E-03 (-)**	1.67E-01 (-)	6.33E-02 (-)	1.00E+00
LPC 16:1	1.10E-01 (+)	9.99E-01 (+)	2.11E-01 (-)	4.42E-01 (-)	1.05E-01 (-)	2.20E-01 (-)	9.98E-01 (+)
LPC 17:0	**1.70E-02 (+)**	5.90E-01 (-)	**2.31E-02 (-)**	**2.07E-03 (-)**	6.55E-01 (-)	1.79E-01 (-)	9.75E-01 (-)
LPC 17:1	**2.38E-02 (+)**	1.00E+00	5.80E-02 (-)	**2.35E-02 (-)**	8.31E-02 (-)	**3.00E-02 (-)**	1.00E+00
LPC 18:0	**3.82E-02 (+)**	1.00E+00	1.31E-01 (-)	**2.28E-02 (-)**	2.77E-01 (-)	5.48E-02 (-)	9.88E-01 (-)
LPC 18:1	**5.63E-03 (+)**	9.85E-01 (-)	**2.87E-03 (-)**	**4.12E-03 (-)**	**3.22E-02 (-)**	**3.72E-02 (-)**	1.00E+00
LPC 18:2	**1.83E-03 (+)**	1.89E-01 (-)	**5.99E-04 (-)**	**1.20E-04 (-)**	3.33E-01 (-)	1.31E-01 (-)	9.99E-01 (-)
LPC 18:3	8.30E-01 (+)	1.00E+00 (-)	9.94E-01 (-)	9.00E-01 (-)	9.99E-01 (-)	9.45E-01 (-)	9.99E-01 (-)
LPC 20:0	**2.56E-03 (+)**	9.98E-01 (-)	**2.00E-02 (-)**	**4.15E-03 (-)**	**7.38E-03 (-)**	**1.07E-03 (-)**	9.98E-01 (-)
LPC 20:1	**1.83E-03 (+)**	9.99E-01 (-)	**1.02E-03 (-)**	**2.14E-03 (-)**	**6.81E-03 (-)**	**1.06E-02 (-)**	1.00E+00
LPC 20:2	**1.41E-02 (+)**	9.09E-01 (-)	**3.56E-03 (-)**	**1.14E-02 (-)**	8.48E-02 (-)	1.81E-01 (-)	9.98E-01 (+)
LPC 20:4	9.18E-02 (+)	1.00E+00	5.34E-02 (-)	6.79E-01 (-)	7.83E-02 (-)	7.25E-01 (-)	6.79E-01 (+)
LPC 20:5	5.31E-01 (+)	8.62E-01 (+)	9.89E-01 (-)	1.00E+00	4.70E-01 (-)	6.97E-01 (-)	9.99E-01 (+)
LPC 22:0	**9.86E-03 (+)**	5.30E-01 (+)	3.44E-01 (-)	1.09E-01 (-)	**8.84E-03 (-)**	**1.11E-03 (-)**	9.96E-01 (-)
LPC 22:1	**5.49E-03 (+)**	1.00E+00	**2.67E-03 (-)**	8.93E-02 (-)	**1.55E-03 (-)**	**4.28E-02 (-)**	7.36E-01 (+)
LPC 22:5	**1.27E-03 (+)**	9.88E-01 (+)	**1.71E-03 (-)**	**1.38E-02 (-)**	**3.47E-04 (-)**	**2.16E-03 (-)**	9.75E-01 (+)
LPC 22:6	**8.62E-03 (+)**	9.64E-01 (+)	**8.18E-03 (-)**	3.66E-01 (-)	**1.02E-03 (-)**	6.70E-02 (-)	5.11E-01 (+)
LPC 24:0	**9.86E-03 (+)**	9.61E-01 (+)	1.16E-01 (-)	**2.69E-02 (-)**	**1.84E-02 (-)**	**2.55E-03 (-)**	9.96E-01 (-)
LPC 26:0	**1.27E-03 (+)**	1.00E+00	**1.49E-03 (-)**	**2.04E-03 (-)**	**1.56E-03 (-)**	**1.55E-03 (-)**	1.00E+00
LPC(O-16:0)	**2.56E-03 (+)**	6.95E-01 (-)	**8.22E-03 (-)**	**1.41E-04 (-)**	3.26E-01 (-)	**1.72E-02 (-)**	8.17E-01 (-)
LPC(O-18:0)	**3.40E-02 (+)**	9.80E-01 (-)	1.13E-01 (-)	**8.32E-03 (-)**	5.20E-01 (-)	7.51E-02 (-)	9.30E-01 (-)
LPC(O-18:1)	**1.67E-03 (+)**	9.67E-01 (-)	**7.70E-03 (-)**	**1.41E-04 (-)**	9.46E-02 (-)	**2.88E-03 (-)**	8.29E-01 (-)

Lipid species	ANCOVA[a] Corrected *P*-value[b]	Ov-ob/IS vs. Lean/IS Post-hoc *P*-value[c]	Ov-ob/IR vs. Lean/IS Post-hoc *P*-value[c]	T2D vs. Lean/IS Post-hoc *P*-value[c]	Ov-ob/IR vs. Ov-ob/IS Post-hoc *P*-value[c]	T2D vs. Ov-ob/IS Post-hoc *P*-value[c]	T2D vs. Ov-ob/IR Post-hoc *P*-value[c]
LPC(O-20:0)	**2.38E-02 (+)**	9.29E-01 (-)	**1.72E-02 (-)**	**9.84E-03 (-)**	2.31E-01 (-)	1.44E-01 (-)	1.00E+00
LPC(O-22:0)	**2.01E-02 (+)**	6.04E-01 (-)	**2.17E-02 (-)**	**2.86E-03 (-)**	6.26E-01 (-)	2.11E-01 (-)	9.90E-01 (-)
LPC(O-22:1)	**4.44E-04 (+)**	9.57E-02 (-)	**3.41E-05 (-)**	**1.49E-05 (-)**	1.25E-01 (-)	7.13E-02 (-)	1.00E+00
LPC(O-24:0)	2.80E-01 (+)	8.95E-01 (-)	1.79E-01 (-)	3.78E-01 (-)	8.49E-01 (-)	9.75E-01 (-)	9.99E-01 (+)
LPC(O-24:1)	**2.21E-02 (+)**	6.29E-01 (-)	**5.53E-03 (-)**	**1.21E-02 (-)**	3.06E-01 (-)	4.53E-01 (-)	1.00E+00
LPC(O-24:2)	**8.17E-05 (+)**	**3.85E-02 (-)**	**1.28E-06 (-)**	**9.29E-06 (-)**	**3.74E-02 (-)**	1.26E-01 (-)	9.90E-01 (+)
PE 32:0	4.71E-01 (+)	5.89E-01 (-)	1.00E+00	7.29E-01 (-)	7.58E-01 (+)	1.00E+00	8.44E-01 (-)
PE 32:1	**2.61E-02 (+)**	9.57E-01 (+)	3.46E-01 (+)	**3.12E-03 (+)**	9.14E-01 (+)	**4.62E-02 (+)**	3.83E-01 (+)
PE 34:1	1.09E-01 (+)	8.69E-01 (+)	2.14E-01 (+)	**4.13E-02 (+)**	9.11E-01 (+)	4.81E-01 (+)	9.87E-01 (+)
PE 34:2	5.89E-01 (+)	9.99E-01 (-)	8.69E-01 (+)	9.53E-01 (+)	6.51E-01 (+)	7.74E-01 (+)	1.00E+00
PE 34:3	4.58E-01 (+)	1.00E+00	6.74E-01 (+)	5.03E-01 (+)	8.85E-01 (+)	7.42E-01 (+)	1.00E+00
PE 35:1	3.66E-01 (+)	9.15E-01 (+)	2.43E-01 (+)	5.84E-01 (+)	8.94E-01 (+)	9.97E-01 (+)	9.93E-01 (-)
PE 35:2	3.94E-01 (+)	1.00E+00	4.40E-01 (+)	9.90E-01 (+)	3.69E-01 (+)	9.65E-01 (+)	8.35E-01 (-)
PE 36:0	9.83E-01 (+)	1.00E+00	1.00E+00	9.97E-01 (+)	1.00E+00	1.00E+00	1.00E+00
PE 36:1	**3.64E-02 (+)**	4.81E-01 (+)	**8.20E-03 (+)**	**3.28E-02 (+)**	5.16E-01 (+)	8.30E-01 (+)	9.95E-01 (-)
PE 36:2	2.89E-01 (+)	1.00E+00	2.17E-01 (+)	6.99E-01 (+)	4.43E-01 (+)	8.98E-01 (+)	9.65E-01 (-)
PE 36:3	7.98E-01 (+)	1.00E+00	9.74E-01 (+)	9.89E-01 (+)	8.87E-01 (+)	9.19E-01 (+)	1.00E+00
PE 36:4	6.34E-01 (+)	9.94E-01 (+)	9.81E-01 (+)	5.66E-01 (+)	1.00E+00	9.29E-01 (+)	9.56E-01 (+)
PE 36:5	1.80E-01 (+)	8.00E-01 (+)	8.60E-01 (+)	6.41E-02 (+)	1.00E+00	6.93E-01 (+)	5.65E-01 (+)
PE 38:3	1.71E-01 (+)	3.42E-01 (+)	2.38E-01 (+)	9.46E-02 (+)	1.00E+00	9.95E-01 (+)	9.99E-01 (+)
PE 38:4	3.18E-01 (+)	2.87E-01 (+)	6.57E-01 (+)	3.33E-01 (+)	9.95E-01 (-)	1.00E+00	9.98E-01 (+)
PE 38:5	4.66E-01 (+)	8.36E-01 (+)	9.73E-01 (-)	3.56E-01 (+)	9.99E-01 (-)	9.87E-01 (+)	8.63E-01 (+)
PE 38:6	7.00E-01 (+)	1.00E+00	1.00E+00	7.38E-01 (+)	1.00E+00	9.17E-01 (+)	8.68E-01 (+)
PE 40:5	8.48E-02 (+)	1.34E-01 (+)	2.93E-01 (+)	**2.72E-02 (+)**	9.99E-01 (-)	9.95E-01 (+)	9.12E-01 (+)
PE 40:6	2.52E-01 (+)	6.68E-01 (+)	4.07E-01 (+)	1.27E-01 (+)	1.00E+00	9.43E-01 (+)	9.94E-01 (+)
PE 40:7	8.30E-01 (+)	9.96E-01 (+)	1.00E+00	9.88E-01 (+)	9.60E-01 (-)	1.00E+00	9.03E-01 (+)
PE(O-34:1)	6.94E-01 (+)	1.00E+00	8.47E-01 (+)	1.00E+00	8.98E-01 (+)	1.00E+00	7.28E-01 (-)
PE(O-34:2)	1.82E-01 (+)	1.16E-01 (-)	9.98E-01 (-)	4.89E-01 (-)	3.48E-01 (+)	9.66E-01 (+)	8.14E-01 (-)
PE(O-36:2)	7.16E-01 (+)	9.05E-01 (-)	1.00E+00	8.96E-01 (-)	9.28E-01 (+)	1.00E+00	9.02E-01 (-)
PE(O-36:3)	3.11E-01 (+)	2.90E-01 (-)	1.00E+00	6.18E-01 (-)	5.37E-01 (+)	9.96E-01 (+)	8.30E-01 (-)
PE(O-36:4)	6.44E-01 (+)	7.05E-01 (-)	1.00E+00	9.81E-01 (-)	7.56E-01 (+)	9.86E-01 (+)	9.84E-01 (-)

Lipid species	ANCOVA[a] Corrected *P*-value[b]	Ov-ob/IS vs. Lean/IS Post-hoc *P*-value[c]	Ov-ob/IR vs. Lean/IS Post-hoc *P*-value[c]	T2D vs. Lean/IS Post-hoc *P*-value[c]	Ov-ob/IR vs. Ov-ob/IS Post-hoc *P*-value[c]	T2D vs. Ov-ob/IS Post-hoc *P*-value[c]	T2D vs. Ov-ob/IR Post-hoc *P*-value[c]
PE(O-36:5)	9.79E-01 (+)	1.00E+00	9.98E-01 (+)	1.00E+00	9.99E-01 (-)	1.00E+00	9.97E-01 (-)
PE(O-36:6)	3.46E-01 (+)	7.26E-01 (+)	2.94E-01 (+)	9.97E-01 (+)	9.92E-01 (+)	9.55E-01 (-)	5.84E-01 (-)
PE(O-38:4)	8.93E-01 (+)	9.57E-01 (-)	1.00E+00	9.93E-01 (-)	9.95E-01 (+)	1.00E+00	1.00E+00
PE(O-38:5)	7.76E-01 (+)	9.74E-01 (-)	9.99E-01 (+)	9.94E-01 (-)	8.54E-01 (+)	1.00E+00	9.12E-01 (-)
PE(O-40:4)	2.78E-01 (+)	5.24E-01 (+)	9.95E-01 (-)	9.99E-01 (-)	2.27E-01 (-)	2.51E-01 (-)	1.00E+00
PE(O-40:5)	9.79E-01 (+)	9.99E-01 (+)	9.96E-01 (+)	9.99E-01 (+)	1.00E+00	1.00E+00	1.00E+00
PE(O-40:6)	8.59E-01 (+)	9.65E-01 (+)	9.95E-01 (+)	9.41E-01 (+)	1.00E+00	1.00E+00	1.00E+00
PE(O-40:7)	8.30E-01 (+)	1.00E+00	9.80E-01 (-)	9.47E-01 (-)	9.87E-01 (-)	9.58E-01 (-)	1.00E+00
PE(O-42:7)	**3.49E-12 (+)**	**5.12E-10 (+)**	4.36E-01 (+)	**2.43E-12 (+)**	**1.07E-06 (-)**	8.81E-01 (+)	**1.90E-09 (+)**
PE(P-34:1)	8.30E-01 (+)	9.89E-01 (+)	9.87E-01 (+)	1.00E+00	1.00E+00	9.51E-01 (-)	9.40E-01 (-)
PE(P-34:2)	4.93E-01 (+)	6.33E-01 (-)	1.00E+00	9.98E-01 (-)	4.54E-01 (+)	9.07E-01 (+)	9.65E-01 (-)
PE(P-36:1)	8.30E-01 (+)	1.00E+00	8.92E-01 (+)	1.00E+00	9.88E-01 (+)	1.00E+00	9.62E-01 (-)
PE(P-36:2)	3.93E-01 (+)	5.67E-01 (-)	1.00E+00	8.81E-01 (-)	4.32E-01 (+)	9.96E-01 (+)	7.21E-01 (-)
PE(P-36:4)	3.90E-01 (+)	7.83E-01 (+)	2.65E-01 (+)	9.43E-01 (+)	9.78E-01 (+)	9.99E-01 (-)	8.17E-01 (-)
PE(P-37:4)	2.89E-01 (+)	9.97E-01 (+)	4.80E-01 (+)	9.98E-01 (-)	8.52E-01 (+)	9.21E-01 (-)	1.81E-01 (-)
PE(P-38:4)	8.57E-01 (+)	9.30E-01 (+)	9.82E-01 (+)	9.99E-01 (+)	1.00E+00	9.94E-01 (-)	1.00E+00
PE(P-38:5)	8.30E-01 (+)	1.00E+00	9.70E-01 (+)	1.00E+00	9.86E-01 (+)	1.00E+00	8.75E-01 (-)
PE(P-38:6)	8.30E-01 (+)	1.00E+00	9.47E-01 (+)	1.00E+00	9.96E-01 (+)	9.99E-01 (-)	9.08E-01 (-)
PE(P-40:4)	**3.17E-02 (+)**	**6.94E-03 (+)**	9.99E-01 (+)	9.89E-01 (+)	**2.82E-02 (-)**	**3.81E-02 (-)**	1.00E+00
PE(P-40:5)	7.39E-01 (+)	9.98E-01 (+)	1.00E+00	9.48E-01 (-)	9.73E-01 (-)	7.32E-01 (-)	9.96E-01 (-)
PE(P-40:6)	8.30E-01 (+)	1.00E+00	1.00E+00	9.75E-01 (-)	1.00E+00	9.01E-01 (-)	9.72E-01 (-)
LPE 16:0	**6.86E-03 (+)**	4.31E-01 (-)	**3.50E-04 (-)**	**1.50E-02 (-)**	9.83E-02 (-)	7.05E-01 (-)	7.67E-01 (+)
LPE 16:1	7.98E-01 (+)	1.00E+00	1.00E+00	8.89E-01 (+)	1.00E+00	9.51E-01 (+)	9.13E-01 (+)
LPE 18:0	1.28E-01 (+)	9.94E-01 (+)	3.10E-01 (-)	5.32E-01 (-)	1.16E-01 (-)	2.08E-01 (-)	9.99E-01 (+)
LPE 18:1	6.22E-01 (+)	7.47E-01 (-)	6.64E-01 (-)	9.25E-01 (-)	1.00E+00	9.99E-01 (+)	9.97E-01 (+)
LPE 18:2	1.70E-01 (+)	4.21E-01 (-)	2.99E-01 (-)	7.51E-02 (-)	1.00E+00	9.73E-01 (-)	9.92E-01 (-)
LPE 20:4	2.88E-01 (+)	1.00E+00	5.78E-01 (-)	2.40E-01 (-)	8.48E-01 (-)	4.79E-01 (-)	9.97E-01 (-)
LPE 22:5	6.77E-01 (+)	9.23E-01 (-)	8.52E-01 (-)	1.00E+00	1.00E+00	9.39E-01 (+)	8.61E-01 (+)
LPE 22:6	1.07E-01 (+)	1.00E+00	7.70E-02 (-)	6.50E-01 (-)	8.54E-02 (-)	6.21E-01 (-)	8.04E-01 (+)
PI 32:0	5.00E-01 (+)	9.99E-01 (+)	5.60E-01 (+)	6.70E-01 (+)	8.63E-01 (+)	9.19E-01 (+)	1.00E+00
PI 32:1	3.00E-01 (+)	9.43E-01 (+)	3.82E-01 (+)	2.30E-01 (+)	9.49E-01 (+)	8.37E-01 (+)	1.00E+00

Lipid species	ANCOVA[a] Corrected *P*-value[b]	Ov-ob/IS vs. Lean/IS Post-hoc *P*-value[c]	Ov-ob/IR vs. Lean/IS Post-hoc *P*-value[c]	T2D vs. Lean/IS Post-hoc *P*-value[c]	Ov-ob/IR vs. Ov-ob/IS Post-hoc *P*-value[c]	T2D vs. Ov-ob/IS Post-hoc *P*-value[c]	T2D vs. Ov-ob/IR Post-hoc *P*-value[c]
PI 34:0	7.63E-01 (+)	9.97E-01 (-)	9.75E-01 (+)	1.00E+00	8.00E-01 (+)	1.00E+00	8.89E-01 (-)
PI 34:1	4.41E-01 (+)	9.98E-01 (+)	4.01E-01 (+)	6.98E-01 (+)	7.59E-01 (+)	9.45E-01 (+)	9.98E-01 (-)
PI 36:1	7.39E-01 (+)	1.00E+00	8.57E-01 (+)	1.00E+00	7.99E-01 (+)	9.99E-01 (+)	9.33E-01 (-)
PI 36:2	1.22E-01 (+)	4.28E-01 (-)	9.98E-01 (-)	7.92E-02 (-)	7.71E-01 (+)	9.75E-01 (-)	2.08E-01 (-)
PI 36:3	4.66E-01 (+)	7.66E-01 (-)	9.70E-01 (-)	3.78E-01 (-)	9.98E-01 (+)	9.97E-01 (-)	8.87E-01 (-)
PI 36:4	9.46E-01 (+)	9.98E-01 (+)	9.99E-01 (+)	9.80E-01 (+)	1.00E+00	1.00E+00	1.00E+00
PI 38:2	7.22E-01 (+)	6.97E-01 (-)	9.70E-01 (-)	9.95E-01 (-)	9.94E-01 (+)	9.58E-01 (+)	1.00E+00
PI 38:3	9.97E-01 (+)	1.00E+00	1.00E+00	1.00E+00	1.00E+00	1.00E+00	1.00E+00
PI 38:4	8.93E-01 (+)	9.98E-01 (+)	9.99E-01 (+)	1.00E+00	9.51E-01 (-)	9.89E-01 (-)	1.00E+00
PI 38:5	4.27E-01 (+)	1.00E+00	9.43E-01 (-)	6.24E-01 (-)	8.09E-01 (-)	3.95E-01 (-)	9.94E-01 (-)
PI 38:6	8.12E-01 (+)	1.00E+00	9.99E-01 (-)	9.39E-01 (-)	9.93E-01 (-)	8.66E-01 (-)	9.97E-01 (-)
PI 40:4	7.64E-01 (+)	9.97E-01 (+)	9.89E-01 (+)	7.51E-01 (+)	1.00E+00	9.74E-01 (+)	9.88E-01 (+)
PI 40:5	8.30E-01 (+)	9.59E-01 (+)	9.66E-01 (+)	9.17E-01 (+)	1.00E+00	1.00E+00	1.00E+00
PI 40:6	9.79E-01 (+)	1.00E+00	1.00E+00	1.00E+00	1.00E+00	9.94E-01 (-)	1.00E+00
PS 36:1	**3.64E-02 (+)**	**1.02E-02 (+)**	9.78E-01 (+)	1.00E+00	9.12E-02 (-)	**2.56E-02 (-)**	9.99E-01 (-)
PS 36:2	8.71E-02 (+)	5.69E-02 (+)	9.98E-01 (-)	1.00E+00	1.99E-01 (-)	5.21E-02 (-)	9.97E-01 (-)
PS 38:3	6.43E-02 (+)	**4.03E-02 (+)**	1.00E+00	1.00E+00	6.53E-02 (-)	**4.70E-02 (-)**	1.00E+00
PS 38:4	5.05E-02 (+)	**2.22E-02 (+)**	1.00E+00	1.00E+00	5.57E-02 (-)	**4.50E-02 (-)**	1.00E+00
PS 38:5	8.26E-02 (+)	**4.68E-02 (+)**	9.98E-01 (-)	1.00E+00	1.62E-01 (-)	5.65E-02 (-)	1.00E+00
PS 40:5	1.25E-01 (+)	6.26E-02 (+)	9.99E-01 (+)	9.97E-01 (+)	1.99E-01 (-)	1.88E-01 (-)	1.00E+00
PS 40:6	9.18E-02 (+)	**3.66E-02 (+)**	9.97E-01 (+)	9.92E-01 (+)	1.45E-01 (-)	1.49E-01 (-)	1.00E+00
COH	8.30E-01 (+)	9.66E-01 (+)	1.00E+00	1.00E+00	9.27E-01 (-)	9.33E-01 (-)	1.00E+00
CE 14:0	7.47E-02 (+)	9.03E-01 (+)	**3.82E-02 (+)**	7.64E-02 (+)	4.27E-01 (+)	5.96E-01 (+)	1.00E+00
CE 15:0	2.18E-01 (+)	9.93E-01 (+)	1.03E-01 (+)	7.95E-01 (+)	4.04E-01 (+)	9.92E-01 (+)	7.43E-01 (-)
CE 16:0	2.58E-01 (+)	9.94E-01 (-)	4.19E-01 (+)	1.00E+00	1.69E-01 (+)	9.95E-01 (+)	3.71E-01 (-)
CE 16:1	1.64E-01 (+)	9.70E-01 (+)	1.40E-01 (+)	1.67E-01 (+)	6.26E-01 (+)	6.67E-01 (+)	1.00E+00
CE 16:2	1.22E-01 (+)	1.00E+00	1.13E-01 (+)	1.00E+00	1.22E-01 (+)	1.00E+00	1.42E-01 (-)
CE 17:0	9.87E-01 (+)	1.00E+00	9.99E-01 (+)	1.00E+00	1.00E+00	1.00E+00	1.00E+00
CE 17:1	5.44E-01 (+)	1.00E+00	7.62E-01 (+)	6.94E-01 (+)	8.60E-01 (+)	7.92E-01 (+)	1.00E+00
CE 18:0	4.71E-01 (+)	1.00E+00	7.89E-01 (+)	9.95E-01 (-)	8.78E-01 (+)	9.87E-01 (-)	3.65E-01 (-)
CE 18:1	1.91E-01 (+)	9.77E-01 (-)	3.77E-01 (+)	1.00E+00	9.94E-02 (+)	9.76E-01 (+)	3.33E-01 (-)

Lipid species	ANCOVA[a] Corrected *P*-value[b]	Ov-ob/IS vs. Lean/IS Post-hoc *P*-value[c]	Ov-ob/IR vs. Lean/IS Post-hoc *P*-value[c]	T2D vs. Lean/IS Post-hoc *P*-value[c]	Ov-ob/IR vs. Ov-ob/IS Post-hoc *P*-value[c]	T2D vs. Ov-ob/IS Post-hoc *P*-value[c]	T2D vs. Ov-ob/IR Post-hoc *P*-value[c]
CE 18:2	**3.64E-02 (+)**	5.39E-01 (-)	3.53E-01 (+)	9.19E-01 (-)	**9.52E-03 (+)**	9.88E-01 (+)	**3.12E-02 (-)**
CE 18:3	1.22E-01 (+)	1.00E+00	1.08E-01 (+)	1.00E+00	1.12E-01 (+)	1.00E+00	1.67E-01 (-)
CE 20:1	**1.27E-03 (+)**	**1.34E-02 (-)**	**9.79E-03 (-)**	**1.02E-05 (-)**	1.00E+00	2.94E-01 (-)	2.93E-01 (-)
CE 20:3	**2.38E-02 (+)**	9.96E-01 (-)	**1.51E-02 (+)**	7.73E-01 (+)	**4.65E-03 (+)**	4.11E-01 (+)	2.69E-01 (-)
CE 20:4	2.89E-01 (+)	9.79E-01 (-)	6.74E-01 (+)	9.97E-01 (+)	2.48E-01 (+)	1.00E+00	2.88E-01 (-)
CE 20:5	3.46E-01 (+)	1.00E+00	7.22E-01 (+)	9.72E-01 (-)	8.38E-01 (+)	9.42E-01 (-)	1.95E-01 (-)
CE 22:0	2.89E-01 (+)	8.17E-01 (+)	1.63E-01 (+)	5.08E-01 (+)	9.00E-01 (+)	9.99E-01 (+)	9.86E-01 (-)
CE 22:1	6.74E-01 (+)	9.04E-01 (-)	6.52E-01 (-)	9.11E-01 (-)	9.99E-01 (-)	1.00E+00	9.98E-01 (+)
CE 22:4	3.75E-01 (+)	9.51E-01 (-)	7.68E-01 (+)	1.00E+00	2.49E-01 (+)	9.73E-01 (+)	6.59E-01 (-)
CE 22:5	3.07E-01 (+)	1.00E+00	5.37E-01 (+)	9.99E-01 (+)	3.66E-01 (+)	1.00E+00	2.57E-01 (-)
CE 22:6	2.61E-01 (+)	9.83E-01 (-)	9.94E-01 (+)	4.77E-01 (-)	7.90E-01 (+)	9.29E-01 (-)	1.47E-01 (-)
CE 24:0	2.76E-01 (+)	9.05E-01 (+)	1.50E-01 (+)	4.77E-01 (+)	7.91E-01 (+)	9.90E-01 (+)	9.86E-01 (-)
CE 24:1	8.45E-01 (+)	1.00E+00	1.00E+00	9.08E-01 (+)	1.00E+00	9.90E-01 (+)	9.80E-01 (+)
CE 24:4	3.46E-01 (+)	2.95E-01 (-)	7.24E-01 (-)	3.82E-01 (-)	9.90E-01 (+)	1.00E+00	9.98E-01 (-)
CE 24:5	6.35E-01 (+)	6.11E-01 (-)	1.00E+00	9.99E-01 (-)	8.34E-01 (+)	8.73E-01 (+)	1.00E+00
CE 24:6	3.97E-01 (+)	9.96E-01 (-)	8.97E-01 (+)	7.37E-01 (+)	6.07E-01 (+)	3.78E-01 (+)	1.00E+00
DG 14:0/16:0	9.18E-02 (+)	1.00E+00	**4.73E-02 (+)**	5.49E-01 (+)	9.88E-02 (+)	7.03E-01 (+)	7.70E-01 (-)
DG 14:0/18:1	6.75E-02 (+)	1.00E+00	**2.59E-02 (+)**	8.04E-01 (+)	6.08E-02 (+)	9.14E-01 (+)	3.51E-01 (-)
DG 14:0/18:2	8.37E-02 (+)	1.00E+00	6.49E-02 (+)	1.00E+00	6.53E-02 (+)	9.99E-01 (+)	1.09E-01 (-)
DG 16:0/16:0	8.78E-02 (+)	1.00E+00	**4.16E-02 (+)**	6.36E-01 (+)	8.77E-02 (+)	7.79E-01 (+)	6.53E-01 (-)
DG 16:0/18:0	**3.84E-02 (+)**	1.00E+00	**1.32E-02 (+)**	6.75E-01 (+)	**2.46E-02 (+)**	7.52E-01 (+)	3.25E-01 (-)
DG 16:0/18:1	5.73E-02 (+)	9.99E-01 (+)	**1.61E-02 (+)**	7.60E-01 (+)	6.21E-02 (+)	9.49E-01 (+)	2.93E-01 (-)
DG 16:0/18:2	9.42E-02 (+)	1.00E+00	9.30E-02 (+)	1.00E+00	6.46E-02 (+)	9.97E-01 (+)	1.34E-01 (-)
DG 16:0/20:0	3.47E-01 (+)	7.04E-01 (-)	9.55E-01 (+)	9.99E-01 (-)	2.10E-01 (+)	9.09E-01 (+)	7.60E-01 (-)
DG 16:0/20:3	1.34E-01 (+)	9.99E-01 (+)	6.99E-02 (+)	5.65E-01 (+)	2.09E-01 (+)	8.40E-01 (+)	8.48E-01 (-)
DG 16:0/20:4	7.90E-02 (+)	1.00E+00	**3.20E-02 (+)**	6.04E-01 (+)	8.38E-02 (+)	8.00E-01 (+)	6.12E-01 (-)
DG 16:0/22:5	1.25E-01 (+)	9.95E-01 (+)	**4.78E-02 (+)**	7.63E-01 (+)	2.17E-01 (+)	9.83E-01 (+)	5.56E-01 (-)
DG 16:0/22:6	1.81E-01 (+)	9.89E-01 (+)	7.96E-02 (+)	6.07E-01 (+)	3.73E-01 (+)	9.63E-01 (+)	8.45E-01 (-)
DG 16:1/18:0	1.09E-01 (+)	9.82E-01 (+)	**3.47E-02 (+)**	5.17E-01 (+)	2.37E-01 (+)	9.49E-01 (+)	7.20E-01 (-)
DG 16:1/18:1	2.70E-01 (+)	9.60E-01 (+)	1.28E-01 (+)	8.99E-01 (+)	6.31E-01 (+)	1.00E+00	6.69E-01 (-)
DG 18:0/18:0	4.66E-01 (+)	7.61E-01 (-)	9.89E-01 (+)	1.00E+00	3.62E-01 (+)	9.26E-01 (+)	9.01E-01 (-)

Lipid species	ANCOVA[a] Corrected *P*-value[b]	Ov-ob/IS vs. Lean/IS Post-hoc *P*-value[c]	Ov-ob/IR vs. Lean/IS Post-hoc *P*-value[c]	T2D vs. Lean/IS Post-hoc *P*-value[c]	Ov-ob/IR vs. Ov-ob/IS Post-hoc *P*-value[c]	T2D vs. Ov-ob/IS Post-hoc *P*-value[c]	T2D vs. Ov-ob/IR Post-hoc *P*-value[c]
DG 18:0/18:1	**1.70E-02 (+)**	1.00E+00	**2.65E-03 (+)**	7.91E-01 (+)	1.20E-02 (+)	9.54E-01 (+)	6.74E-02 (-)
DG 18:0/18:2	5.39E-02 (+)	1.00E+00	**2.85E-02 (+)**	9.99E-01 (+)	5.27E-02 (+)	1.00E+00	5.96E-02 (-)
DG 18:0/20:4	7.63E-02 (+)	4.49E-01 (+)	**1.54E-02 (+)**	6.40E-01 (+)	6.95E-01 (+)	1.00E+00	3.89E-01 (-)
DG 18:1/18:1	6.08E-02 (+)	9.99E-01 (+)	2.41E-02 (+)	9.98E-01 (+)	1.01E-01 (+)	1.00E+00	6.66E-02 (-)
DG 18:1/18:2	1.09E-01 (+)	1.00E+00	3.51E-01 (+)	9.39E-01 (-)	2.09E-01 (+)	9.96E-01 (-)	**3.64E-02 (-)**
DG 18:1/18:3	1.86E-01 (+)	1.00E+00	1.77E-01 (+)	1.00E+00	2.99E-01 (+)	1.00E+00	1.63E-01 (-)
DG 18:1/20:0	1.32E-01 (+)	9.02E-01 (-)	4.11E-01 (+)	1.00E+00	5.85E-02 (+)	9.80E-01 (+)	2.02E-01 (-)
DG 18:1/20:3	5.63E-01 (+)	9.75E-01 (+)	5.07E-01 (+)	9.98E-01 (+)	9.58E-01 (+)	1.00E+00	8.02E-01 (-)
DG 18:1/20:4	8.79E-02 (+)	1.00E+00	5.43E-02 (+)	9.97E-01 (+)	8.01E-02 (+)	9.98E-01 (+)	1.50E-01 (-)
DG 18:2/18:2	1.64E-01 (+)	8.55E-01 (-)	9.86E-01 (+)	4.00E-01 (-)	4.44E-01 (+)	9.90E-01 (-)	8.88E-02 (-)
TG 14:0/16:0/18:1	**3.82E-02 (+)**	8.36E-01 (+)	**2.68E-02 (+)**	**1.82E-02 (+)**	4.34E-01 (+)	3.34E-01 (+)	1.00E+00
TG 14:0/16:0/18:2	1.25E-01 (+)	8.90E-01 (+)	1.07E-01 (+)	9.94E-02 (+)	7.24E-01 (+)	6.93E-01 (+)	1.00E+00
TG 14:0/16:1/18:1	1.47E-01 (+)	7.88E-01 (+)	1.33E-01 (+)	9.66E-02 (+)	8.83E-01 (+)	8.11E-01 (+)	1.00E+00
TG 14:0/16:1/18:2	4.18E-01 (+)	9.85E-01 (+)	2.96E-01 (+)	7.87E-01 (+)	7.94E-01 (+)	9.96E-01 (+)	9.71E-01 (-)
TG 14:0/17:0/18:1	**4.89E-02 (+)**	8.32E-01 (+)	**2.24E-02 (+)**	**3.81E-02 (+)**	3.99E-01 (+)	5.13E-01 (+)	1.00E+00
TG 14:0/18:0/18:1	**1.70E-02 (+)**	8.60E-01 (+)	**6.86E-03 (+)**	**7.95E-03 (+)**	1.73E-01 (+)	1.78E-01 (+)	1.00E+00
TG 14:0/18:2/18:2	4.66E-01 (+)	9.98E-01 (+)	3.60E-01 (+)	9.49E-01 (+)	7.28E-01 (+)	9.99E-01 (+)	8.95E-01 (-)
TG 14:1/16:0/18:1	6.09E-02 (+)	6.82E-01 (+)	5.95E-02 (+)	**2.11E-02 (+)**	7.96E-01 (+)	5.31E-01 (+)	1.00E+00
TG 14:1/16:1/18:0	1.66E-01 (+)	7.28E-01 (+)	3.28E-01 (+)	6.42E-02 (+)	9.96E-01 (+)	7.70E-01 (+)	9.80E-01 (+)
TG 14:1/18:0/18:2	**3.82E-02 (+)**	2.27E-01 (+)	**1.63E-02 (+)**	**1.63E-02 (+)**	9.13E-01 (+)	9.18E-01 (+)	1.00E+00
TG 14:1/18:1/18:1	2.57E-01 (+)	6.11E-01 (+)	1.46E-01 (+)	3.64E-01 (+)	9.73E-01 (+)	1.00E+00	9.97E-01 (-)
TG 15:0/16:0/18:1	**4.74E-02 (+)**	8.45E-01 (+)	**2.55E-02 (+)**	**3.00E-02 (+)**	4.12E-01 (+)	4.35E-01 (+)	1.00E+00
TG 15:0/18:1/18:1	5.73E-02 (+)	4.78E-01 (+)	**1.44E-02 (+)**	6.73E-02 (+)	6.50E-01 (+)	9.45E-01 (+)	9.90E-01 (-)
TG 16:0/16:0/16:0	**3.64E-02 (+)**	9.95E-01 (+)	**4.27E-02 (+)**	**2.78E-02 (+)**	2.00E-01 (+)	1.29E-01 (+)	1.00E+00
TG 16:0/16:0/18:0	**3.97E-02 (+)**	9.82E-01 (+)	**2.38E-02 (+)**	**4.78E-02 (+)**	1.79E-01 (+)	2.75E-01 (+)	1.00E+00
TG 16:0/16:0/18:1	**3.37E-02 (+)**	9.07E-01 (+)	**2.07E-02 (+)**	**1.68E-02 (+)**	2.91E-01 (+)	2.39E-01 (+)	1.00E+00
TG 16:0/16:0/18:2	1.18E-01 (+)	9.90E-01 (+)	6.62E-02 (+)	2.44E-01 (+)	3.19E-01 (+)	6.81E-01 (+)	9.90E-01 (-)
TG 16:0/16:1/17:0	**4.89E-02 (+)**	8.78E-01 (+)	**3.10E-02 (+)**	**3.03E-02 (+)**	4.15E-01 (+)	3.94E-01 (+)	1.00E+00
TG 16:0/16:1/18:1	7.63E-02 (+)	4.85E-01 (+)	5.88E-02 (+)	**3.29E-02 (+)**	9.23E-01 (+)	8.27E-01 (+)	1.00E+00
TG 16:0/17:0/18:0	**1.43E-02 (+)**	8.81E-01 (+)	**6.35E-03 (+)**	**5.81E-03 (+)**	1.49E-01 (+)	1.29E-01 (+)	1.00E+00
TG 16:0/17:0/18:1	**2.84E-02 (+)**	7.72E-01 (+)	**6.08E-03 (+)**	**3.00E-02 (+)**	2.19E-01 (+)	5.24E-01 (+)	9.91E-01 (-)

Lipid species	ANCOVA[a] Corrected *P*-value[b]	Ov-ob/IS vs. Lean/IS Post-hoc *P*-value[c]	Ov-ob/IR vs. Lean/IS Post-hoc *P*-value[c]	T2D vs. Lean/IS Post-hoc *P*-value[c]	Ov-ob/IR vs. Ov-ob/IS Post-hoc *P*-value[c]	T2D vs. Ov-ob/IS Post-hoc *P*-value[c]	T2D vs. Ov-ob/IR Post-hoc *P*-value[c]
TG 16:0/17:0/18:2	**4.89E-02 (+)**	5.26E-01 (+)	**1.98E-02 (+)**	**2.86E-02 (+)**	6.79E-01 (+)	7.62E-01 (+)	1.00E+00
TG 16:0/18:0/18:1	**1.70E-02 (+)**	8.76E-01 (+)	**3.27E-03 (+)**	**1.96E-02 (+)**	9.54E-02 (+)	3.04E-01 (+)	9.86E-01 (-)
TG 16:0/18:1/18:1	**2.80E-02 (+)**	3.70E-01 (+)	**7.45E-03 (+)**	**1.23E-02 (+)**	6.10E-01 (+)	7.22E-01 (+)	1.00E+00
TG 16:0/18:1/18:2	2.89E-01 (+)	9.70E-01 (+)	1.49E-01 (+)	7.26E-01 (+)	6.43E-01 (+)	9.97E-01 (+)	8.95E-01 (-)
TG 16:0/18:2/18:2	5.00E-01 (+)	1.00E+00 (+)	4.46E-01 (+)	9.75E-01 (+)	6.92E-01 (+)	9.98E-01 (+)	9.02E-01 (-)
TG 16:1/16:1/16:1	3.91E-01 (+)	6.99E-01 (+)	4.75E-01 (+)	3.41E-01 (+)	1.00E+00	9.98E-01 (+)	1.00E+00
TG 16:1/16:1/18:0	**4.82E-02 (+)**	8.50E-01 (+)	**2.24E-02 (+)**	**3.66E-02 (+)**	3.78E-01 (+)	4.78E-01 (+)	1.00E+00
TG 16:1/16:1/18:1	3.46E-01 (+)	5.90E-01 (+)	3.78E-01 (+)	3.16E-01 (+)	1.00E+00	1.00E+00	1.00E+00
TG 16:1/17:0/18:1	**4.89E-02 (+)**	4.63E-01 (+)	**1.52E-02 (+)**	**3.91E-02 (+)**	6.77E-01 (+)	8.76E-01 (+)	9.99E-01 (-)
TG 16:1/18:1/18:1	1.34E-01 (+)	1.57E-01 (+)	1.62E-01 (+)	1.19E-01 (+)	1.00E+00	1.00E+00 (+)	1.00E+00
TG 16:1/18:1/18:2	3.66E-01 (+)	7.62E-01 (+)	2.71E-01 (+)	4.94E-01 (+)	9.84E-01 (+)	1.00E+00 (+)	9.99E-01 (-)
TG 17:0/18:1/18:1	**2.01E-02 (+)**	2.94E-01 (+)	**2.03E-03 (+)**	**2.49E-02 (+)**	4.19E-01 (+)	9.22E-01 (+)	9.40E-01 (-)
TG 18:0/18:0/18:0	1.86E-01 (+)	9.77E-01 (+)	7.63E-02 (+)	6.60E-01 (+)	4.23E-01 (+)	9.88E-01 (+)	7.93E-01 (-)
TG 18:0/18:0/18:1	**1.69E-02 (+)**	9.16E-01 (+)	**1.37E-03 (+)**	1.20E-01 (+)	**3.93E-02 (+)**	7.03E-01 (+)	4.95E-01 (-)
TG 18:0/18:1/18:1	**6.86E-03 (+)**	7.70E-01 (+)	**3.96E-04 (+)**	**3.23E-02 (+)**	**3.20E-02 (+)**	5.45E-01 (+)	6.00E-01 (-)
TG 18:0/18:2/18:2	2.13E-01 (+)	9.80E-01 (+)	1.71E-01 (+)	2.64E-01 (+)	6.47E-01 (+)	7.73E-01 (+)	1.00E+00
TG 18:1/18:1/18:1	6.29E-02 (+)	7.68E-01 (+)	**2.63E-02 (+)**	5.43E-02 (+)	5.07E-01 (+)	6.85E-01 (+)	1.00E+00
TG 18:1/18:1/18:2	4.99E-01 (+)	9.60E-01 (+)	4.98E-01 (+)	5.96E-01 (+)	9.71E-01 (+)	9.89E-01 (+)	1.00E+00
TG 18:1/18:1/20:4	1.09E-01 (+)	5.72E-01 (+)	8.59E-02 (+)	6.09E-02 (+)	9.32E-01 (+)	8.81E-01 (+)	1.00E+00
TG 18:1/18:1/22:6	8.26E-02 (+)	7.90E-01 (+)	1.53E-01 (+)	**2.50E-02 (+)**	9.07E-01 (+)	4.58E-01 (+)	9.84E-01 (+)
TG 18:1/18:2/18:2	7.39E-01 (+)	1.00E+00	7.82E-01 (+)	9.38E-01 (+)	9.35E-01 (+)	9.91E-01 (+)	1.00E+00
TG 18:2/18:2/18:2	8.78E-01 (+)	1.00E+00	9.95E-01 (+)	1.00E+00	9.54E-01 (+)	1.00E+00	9.72E-01 (-)
TG 18:2/18:2/20:4	4.34E-01 (+)	9.61E-01 (+)	5.19E-01 (+)	4.04E-01 (+)	9.75E-01 (+)	9.36E-01 (+)	1.00E+00

Ov-ob, overweight-to-obese; IS, insulin sensitive; IR, insulin resistant; T2D, type 2 diabetic

[a] Analysis of covariance of each lipid species in the four groups, adjusted for age, sex, and systolic blood pressure, with [b]*P*-value corrected for multiple comparisons using Benjamini-Hochberg method.

[c] Post-hoc analysis was performed using the Mann Whitney *U* test with Dunn-Sidak correction for multiple group comparisons.

Bold type indicates $P < 0.05$, with positive or negative sign in brackets indicating direction of change of lipid species relative to latter group.

Table S6.2 Linear regression of lipid species with HOMA-IR in fasting plasma and steady-state clamp plasma.

	HOMA-IR[a] (fasting plasma)			HOMA-IR[a] (steady-state clamp plasma)		
Lipid species	**β-Coefficient (95% CI)[b]**	**Uncorrected *P*-value**	**Corrected *P*-value[c]**	**β-Coefficient (95% CI)[b]**	**Uncorrected *P*-value**	**Corrected *P*-value[c]**
dhCer 16:0	0.24 (-0.20 - 0.67)	2.87E-01	5.80E-01	0.45 (-0.09 - 0.99)	1.06E-01	2.60E-01
dhCer 18:0	0.10 (-0.39 - 0.60)	6.83E-01	8.77E-01	0.41 (-0.05 - 0.88)	8.89E-02	2.40E-01
dhCer 20:0	-0.16 (-0.50 - 0.19)	3.83E-01	6.66E-01	0.12 (-0.24 - 0.48)	5.05E-01	6.74E-01
dhCer 22:0	0.29 (-0.21 - 0.79)	2.63E-01	5.61E-01	0.21 (-0.19 - 0.60)	3.17E-01	5.12E-01
dhCer 24:0	0.09 (-0.29 - 0.48)	6.43E-01	8.47E-01	0.18 (-0.22 - 0.58)	3.88E-01	5.92E-01
dhCer 24:1	-0.01 (-0.39 - 0.37)	9.60E-01	9.76E-01	-0.01 (-0.51 - 0.50)	9.80E-01	9.90E-01
Cer 16:0	0.29 (-0.14 - 0.72)	1.94E-01	4.83E-01	0.30 (-0.03 - 0.62)	8.47E-02	2.31E-01
Cer 18:0	0.25 (-0.21 - 0.72)	2.95E-01	5.83E-01	0.75 (0.24 - 1.26)	**5.87E-03**	**3.02E-02**
Cer 20:0	0.11 (-0.40 - 0.61)	6.82E-01	8.77E-01	0.38 (0.03 - 0.73)	**3.74E-02**	1.31E-01
Cer 22:0	0.37 (-0.09 - 0.84)	1.21E-01	3.59E-01	0.40 (0.05 - 0.75)	**2.94E-02**	1.11E-01
Cer 24:0	0.28 (-0.14 - 0.69)	1.94E-01	4.83E-01	0.23 (-0.10 - 0.56)	1.74E-01	3.62E-01
Cer 24:1	0.06 (-0.35 - 0.46)	7.86E-01	9.12E-01	0.25 (-0.13 - 0.62)	2.07E-01	4.05E-01
MHC 16:0	0.12 (-0.27 - 0.51)	5.58E-01	8.03E-01	0.16 (-0.22 - 0.54)	4.22E-01	6.27E-01
MHC 18:0	0.12 (-0.29 - 0.53)	5.56E-01	8.03E-01	0.16 (-0.19 - 0.50)	3.75E-01	5.77E-01
MHC 20:0	0.07 (-0.35 - 0.50)	7.31E-01	8.96E-01	0.00 (-0.49 - 0.50)	9.88E-01	9.94E-01
MHC 22:0	-0.05 (-0.41 - 0.31)	7.78E-01	9.12E-01	0.02 (-0.38 - 0.43)	9.16E-01	9.41E-01
MHC 24:0	-0.09 (-0.54 - 0.36)	7.02E-01	8.88E-01	-0.09 (-0.57 - 0.38)	7.01E-01	8.08E-01
MHC 24:1	-0.12 (-0.49 - 0.26)	5.44E-01	8.02E-01	-0.18 (-0.66 - 0.30)	4.71E-01	6.58E-01
DHC 16:0	-0.12 (-0.44 - 0.21)	4.82E-01	7.77E-01	-0.44 (-0.90 - 0.03)	7.31E-02	2.11E-01
DHC 18:0	0.15 (-0.35 - 0.65)	5.52E-01	8.03E-01	0.17 (-0.32 - 0.66)	5.05E-01	6.74E-01
DHC 20:0	-0.07 (-0.61 - 0.47)	8.07E-01	9.14E-01	0.27 (-0.11 - 0.66)	1.70E-01	3.57E-01
DHC 22:0	-0.15 (-0.57 - 0.27)	4.98E-01	7.78E-01	0.13 (-0.28 - 0.54)	5.36E-01	6.98E-01
DHC 24:0	-0.24 (-0.57 - 0.08)	1.53E-01	4.19E-01	-0.14 (-0.58 - 0.30)	5.41E-01	6.98E-01
DHC 24:1	-0.30 (-0.57 - -0.02)	**3.89E-02**	1.97E-01	-0.41 (-0.77 - -0.05)	**3.07E-02**	1.13E-01
THC 16:0	0.02 (-0.49 - 0.53)	9.36E-01	9.65E-01	-0.05 (-0.62 - 0.51)	8.52E-01	9.06E-01
THC 18:0	0.44 (-0.09 - 0.97)	1.12E-01	3.47E-01	0.73 (0.10 - 1.37)	**2.83E-02**	1.09E-01
THC 20:0	0.08 (-0.36 - 0.52)	7.28E-01	8.96E-01	-0.35 (-0.85 - 0.16)	1.81E-01	3.69E-01
THC 22:0	-0.16 (-0.62 - 0.30)	5.00E-01	7.78E-01	-0.07 (-0.42 - 0.28)	6.80E-01	7.98E-01
THC 24:0	-0.30 (-0.85 - 0.25)	2.89E-01	5.80E-01	-0.24 (-0.68 - 0.21)	3.00E-01	5.01E-01

	HOMA-IR[a] (fasting plasma)			HOMA-IR[a] (steady-state clamp plasma)		
Lipid species	**β-Coefficient (95% CI)[b]**	**Uncorrected *P*-value**	**Corrected *P*-value[c]**	**β-Coefficient (95% CI)[b]**	**Uncorrected *P*-value**	**Corrected *P*-value[c]**
THC 24:1	-0.19 (-0.74 - 0.36)	4.95E-01	7.78E-01	-0.48 (-1.04 - 0.07)	9.52E-02	2.46E-01
GM3 16:0	-0.06 (-0.48 - 0.36)	7.82E-01	9.12E-01	-0.15 (-0.56 - 0.27)	4.90E-01	6.72E-01
GM3 18:0	-0.28 (-0.76 - 0.20)	2.53E-01	5.52E-01	-0.22 (-0.77 - 0.34)	4.48E-01	6.40E-01
GM3 20:0	-0.33 (-0.84 - 0.19)	2.20E-01	4.99E-01	-0.12 (-0.48 - 0.23)	4.95E-01	6.73E-01
GM3 22:0	-0.05 (-0.58 - 0.49)	8.60E-01	9.37E-01	0.18 (-0.31 - 0.68)	4.66E-01	6.54E-01
GM3 24:0	-0.13 (-0.52 - 0.26)	5.23E-01	7.93E-01	-0.36 (-0.84 - 0.13)	1.58E-01	3.47E-01
GM3 24:1	-0.47 (-0.86 - -0.08)	**2.33E-02**	1.36E-01	-0.45 (-0.88 - -0.02)	**4.33E-02**	1.48E-01
SM 31:1	0.22 (-0.24 - 0.68)	3.49E-01	6.37E-01	0.08 (-0.25 - 0.41)	6.25E-01	7.62E-01
SM 32:1	0.34 (-0.08 - 0.75)	1.19E-01	3.55E-01	0.31 (-0.25 - 0.86)	2.83E-01	4.88E-01
SM 32:2	-0.07 (-0.58 - 0.45)	7.99E-01	9.14E-01	-0.11 (-0.67 - 0.46)	7.12E-01	8.08E-01
SM 33:1	0.45 (0.00 - 0.90)	5.49E-02	2.41E-01	0.19 (-0.29 - 0.68)	4.43E-01	6.40E-01
SM 34:1	0.06 (-0.26 - 0.38)	7.15E-01	8.96E-01	-0.03 (-0.40 - 0.34)	8.73E-01	9.23E-01
SM 34:2	-0.16 (-0.75 - 0.43)	5.89E-01	8.22E-01	-0.31 (-0.89 - 0.28)	3.13E-01	5.12E-01
SM 34:3	0.07 (-0.36 - 0.51)	7.39E-01	8.96E-01	0.09 (-0.43 - 0.61)	7.27E-01	8.20E-01
SM 35:1	0.11 (-0.33 - 0.54)	6.24E-01	8.35E-01	0.24 (-0.26 - 0.74)	3.52E-01	5.57E-01
SM 35:2	0.12 (-0.36 - 0.60)	6.25E-01	8.35E-01	0.04 (-0.39 - 0.48)	8.41E-01	9.01E-01
SM 36:1	0.04 (-0.44 - 0.52)	8.79E-01	9.38E-01	0.16 (-0.31 - 0.64)	5.02E-01	6.74E-01
SM 36:2	-0.05 (-0.58 - 0.48)	8.63E-01	9.37E-01	-0.10 (-0.59 - 0.40)	6.99E-01	8.08E-01
SM 36:3	-0.10 (-0.65 - 0.46)	7.29E-01	8.96E-01	-0.08 (-0.59 - 0.44)	7.73E-01	8.47E-01
SM 38:1	0.42 (-0.06 - 0.90)	9.50E-02	3.12E-01	-0.09 (-0.65 - 0.46)	7.48E-01	8.35E-01
SM 38:2	0.29 (-0.18 - 0.75)	2.35E-01	5.22E-01	0.09 (-0.33 - 0.52)	6.66E-01	7.95E-01
SM 39:1	0.23 (-0.12 - 0.58)	2.06E-01	4.87E-01	0.40 (-0.06 - 0.86)	9.50E-02	2.46E-01
SM 41:1	0.20 (-0.23 - 0.63)	3.61E-01	6.45E-01	0.21 (-0.23 - 0.66)	3.47E-01	5.52E-01
SM 41:2	0.01 (-0.45 - 0.47)	9.54E-01	9.75E-01	-0.10 (-0.60 - 0.41)	7.04E-01	8.08E-01
SM 42:1	-0.05 (-0.42 - 0.31)	7.73E-01	9.12E-01	-0.11 (-0.47 - 0.26)	5.60E-01	7.11E-01
PC 28:0	0.05 (-0.15 - 0.26)	6.06E-01	8.29E-01	0.16 (-0.13 - 0.46)	2.78E-01	4.86E-01
PC 29:0	0.14 (-0.21 - 0.49)	4.44E-01	7.30E-01	0.24 (-0.18 - 0.65)	2.67E-01	4.79E-01
PC 30:0	0.19 (-0.20 - 0.58)	3.51E-01	6.37E-01	0.34 (-0.06 - 0.75)	1.03E-01	2.59E-01
PC 31:0	0.22 (-0.14 - 0.58)	2.41E-01	5.30E-01	0.35 (-0.02 - 0.71)	7.28E-02	2.11E-01
PC 31:1	0.22 (-0.19 - 0.63)	2.92E-01	5.80E-01	0.19 (-0.24 - 0.63)	3.86E-01	5.92E-01
PC 32:0	-0.20 (-0.67 - 0.27)	4.08E-01	6.91E-01	0.15 (-0.43 - 0.73)	6.12E-01	7.57E-01

	HOMA-IR[a] (fasting plasma)			HOMA-IR[a] (steady-state clamp plasma)		
Lipid species	**β-Coefficient (95% CI)[b]**	**Uncorrected *P*-value**	**Corrected *P*-value[c]**	**β-Coefficient (95% CI)[b]**	**Uncorrected *P*-value**	**Corrected *P*-value[c]**
PC 32:1	-0.10 (-0.47 - 0.27)	6.01E-01	8.26E-01	0.19 (-0.28 - 0.65)	4.36E-01	6.39E-01
PC 32:2	0.06 (-0.38 - 0.50)	8.02E-01	9.14E-01	0.19 (-0.32 - 0.71)	4.61E-01	6.52E-01
PC 32:3	0.05 (-0.37 - 0.46)	8.24E-01	9.19E-01	0.18 (-0.24 - 0.60)	4.07E-01	6.07E-01
PC 33:0	0.05 (-0.37 - 0.48)	8.00E-01	9.14E-01	0.10 (-0.33 - 0.52)	6.56E-01	7.88E-01
PC 33:1	0.00 (-0.40 - 0.39)	9.83E-01	9.89E-01	0.35 (-0.12 - 0.81)	1.50E-01	3.32E-01
PC 33:2	0.37 (-0.19 - 0.93)	2.01E-01	4.86E-01	0.43 (-0.15 - 1.01)	1.48E-01	3.31E-01
PC 33:3	0.13 (-0.32 - 0.58)	5.73E-01	8.12E-01	0.28 (-0.15 - 0.71)	2.15E-01	4.12E-01
PC 34:0	-0.08 (-0.52 - 0.36)	7.17E-01	8.96E-01	0.24 (-0.18 - 0.66)	2.65E-01	4.79E-01
PC 34:1	-0.07 (-0.51 - 0.37)	7.60E-01	9.07E-01	0.00 (-0.39 - 0.40)	9.81E-01	9.90E-01
PC 34:2	0.40 (0.01 - 0.80)	5.21E-02	2.39E-01	0.16 (-0.30 - 0.62)	4.97E-01	6.73E-01
PC 34:3	-0.06 (-0.50 - 0.38)	7.93E-01	9.14E-01	0.09 (-0.33 - 0.51)	6.76E-01	7.98E-01
PC 34:4	0.01 (-0.40 - 0.43)	9.46E-01	9.73E-01	0.22 (-0.20 - 0.63)	3.08E-01	5.08E-01
PC 34:5	-0.06 (-0.40 - 0.28)	7.33E-01	8.96E-01	0.02 (-0.32 - 0.36)	9.11E-01	9.39E-01
PC 35:0	0.23 (-0.11 - 0.57)	1.94E-01	4.83E-01	0.13 (-0.20 - 0.46)	4.48E-01	6.40E-01
PC 35:1	0.05 (-0.36 - 0.46)	8.23E-01	9.19E-01	0.13 (-0.19 - 0.45)	4.43E-01	6.40E-01
PC 35:2	0.27 (-0.22 - 0.77)	2.84E-01	5.79E-01	0.26 (-0.22 - 0.73)	2.93E-01	4.96E-01
PC 35:3	0.12 (-0.34 - 0.58)	6.12E-01	8.31E-01	0.18 (-0.28 - 0.64)	4.48E-01	6.40E-01
PC 35:4	0.21 (-0.23 - 0.65)	3.57E-01	6.41E-01	0.29 (-0.23 - 0.81)	2.79E-01	4.86E-01
PC 35:5	0.03 (-0.34 - 0.40)	8.80E-01	9.38E-01	-0.01 (-0.32 - 0.29)	9.41E-01	9.64E-01
PC 36:1	0.03 (-0.34 - 0.39)	8.83E-01	9.38E-01	0.18 (-0.32 - 0.69)	4.78E-01	6.63E-01
PC 36:2	0.54 (0.11 - 0.97)	**1.83E-02**	1.11E-01	0.23 (-0.14 - 0.60)	2.34E-01	4.37E-01
PC 36:3	0.20 (-0.28 - 0.69)	4.10E-01	6.91E-01	0.35 (-0.08 - 0.78)	1.13E-01	2.68E-01
PC 36:4a	0.03 (-0.43 - 0.49)	8.90E-01	9.41E-01	-0.03 (-0.39 - 0.33)	8.73E-01	9.23E-01
PC 36:4b	0.06 (-0.31 - 0.43)	7.63E-01	9.07E-01	0.04 (-0.50 - 0.58)	8.86E-01	9.26E-01
PC 36:5	-0.10 (-0.53 - 0.33)	6.47E-01	8.47E-01	-0.09 (-0.52 - 0.34)	6.84E-01	7.98E-01
PC 36:6	-0.22 (-0.68 - 0.23)	3.37E-01	6.28E-01	-0.16 (-0.64 - 0.32)	5.25E-01	6.93E-01
PC 37:4	0.14 (-0.30 - 0.58)	5.43E-01	8.02E-01	0.16 (-0.34 - 0.65)	5.39E-01	6.98E-01
PC 37:5	0.00 (-0.39 - 0.39)	9.95E-01	9.98E-01	-0.03 (-0.35 - 0.29)	8.47E-01	9.03E-01
PC 37:6	-0.12 (-0.50 - 0.26)	5.46E-01	8.02E-01	-0.04 (-0.41 - 0.32)	8.09E-01	8.77E-01
PC 38:2	-0.13 (-0.51 - 0.25)	4.99E-01	7.78E-01	-0.05 (-0.44 - 0.34)	8.11E-01	8.77E-01
PC 38:3	0.36 (-0.12 - 0.83)	1.47E-01	4.12E-01	0.53 (0.05 - 1.00)	**3.37E-02**	1.21E-01

	HOMA-IR[a] (fasting plasma)			HOMA-IR[a] (steady-state clamp plasma)		
Lipid species	**β-Coefficient (95% CI)[b]**	**Uncorrected *P*-value**	**Corrected *P*-value[c]**	**β-Coefficient (95% CI)[b]**	**Uncorrected *P*-value**	**Corrected *P*-value[c]**
PC 38:4	0.17 (-0.17 - 0.50)	3.38E-01	6.28E-01	0.14 (-0.42 - 0.71)	6.22E-01	7.62E-01
PC 38:5	-0.13 (-0.61 - 0.35)	5.95E-01	8.23E-01	-0.08 (-0.54 - 0.38)	7.40E-01	8.30E-01
PC 38:6a	0.08 (-0.38 - 0.54)	7.39E-01	8.96E-01	-0.12 (-0.61 - 0.36)	6.19E-01	7.62E-01
PC 38:6b	-0.26 (-0.68 - 0.15)	2.17E-01	4.99E-01	-0.26 (-0.75 - 0.22)	2.91E-01	4.95E-01
PC 38:7	-0.33 (-0.85 - 0.19)	2.15E-01	4.99E-01	-0.37 (-0.88 - 0.14)	1.63E-01	3.54E-01
PC 39:6	-0.13 (-0.53 - 0.27)	5.16E-01	7.90E-01	-0.18 (-0.59 - 0.23)	4.00E-01	6.00E-01
PC 40:5	-0.02 (-0.35 - 0.32)	9.22E-01	9.57E-01	0.10 (-0.39 - 0.58)	7.01E-01	8.08E-01
PC 40:6	-0.15 (-0.60 - 0.29)	5.09E-01	7.85E-01	-0.10 (-0.63 - 0.43)	7.06E-01	8.08E-01
PC 40:7	-0.34 (-0.84 - 0.16)	1.84E-01	4.81E-01	-0.27 (-0.70 - 0.16)	2.29E-01	4.30E-01
PC(O-30:0)	0.09 (-0.41 - 0.58)	7.34E-01	8.96E-01	0.13 (-0.34 - 0.60)	5.86E-01	7.33E-01
PC(O-32:0)	-0.01 (-0.41 - 0.39)	9.63E-01	9.76E-01	-0.01 (-0.43 - 0.40)	9.46E-01	9.66E-01
PC(O-32:1)	-0.14 (-0.74 - 0.47)	6.58E-01	8.55E-01	-0.30 (-0.89 - 0.29)	3.22E-01	5.18E-01
PC(O-32:2)	-0.10 (-0.48 - 0.27)	5.91E-01	8.22E-01	0.13 (-0.22 - 0.49)	4.64E-01	6.54E-01
PC(O-34:0)	0.06 (-0.46 - 0.57)	8.30E-01	9.19E-01	0.40 (-0.13 - 0.93)	1.46E-01	3.29E-01
PC(O-34:1)	-0.09 (-0.62 - 0.44)	7.44E-01	8.97E-01	-0.13 (-0.71 - 0.44)	6.54E-01	7.88E-01
PC(O-34:2)	0.12 (-0.35 - 0.59)	6.19E-01	8.35E-01	0.12 (-0.37 - 0.60)	6.39E-01	7.76E-01
PC(O-34:4)	-0.21 (-0.54 - 0.11)	2.04E-01	4.87E-01	-0.21 (-0.51 - 0.10)	1.89E-01	3.78E-01
PC(O-35:4)	-0.23 (-0.75 - 0.29)	3.89E-01	6.73E-01	-0.08 (-0.56 - 0.41)	7.53E-01	8.36E-01
PC(O-36:0)	-0.36 (-0.72 - 0.00)	5.55E-02	2.41E-01	0.00 (-0.31 - 0.31)	9.96E-01	9.96E-01
PC(O-36:1)	-0.01 (-0.42 - 0.40)	9.64E-01	9.76E-01	0.17 (-0.35 - 0.70)	5.21E-01	6.91E-01
PC(O-36:2)	0.14 (-0.40 - 0.68)	6.25E-01	8.35E-01	0.14 (-0.32 - 0.59)	5.62E-01	7.11E-01
PC(O-36:3)	0.21 (-0.28 - 0.71)	4.06E-01	6.91E-01	0.22 (-0.28 - 0.72)	3.92E-01	5.92E-01
PC(O-36:4)	0.06 (-0.37 - 0.48)	7.96E-01	9.14E-01	0.30 (-0.28 - 0.87)	3.18E-01	5.12E-01
PC(O-36:5)	-0.03 (-0.45 - 0.38)	8.77E-01	9.38E-01	-0.07 (-0.44 - 0.30)	7.09E-01	8.08E-01
PC(O-38:4)	0.22 (-0.24 - 0.69)	3.48E-01	6.37E-01	0.34 (-0.19 - 0.86)	2.12E-01	4.09E-01
PC(O-38:5)	0.04 (-0.46 - 0.54)	8.84E-01	9.38E-01	0.16 (-0.37 - 0.70)	5.57E-01	7.11E-01
PC(O-40:7)	-0.31 (-0.92 - 0.29)	3.17E-01	6.02E-01	-0.31 (-0.79 - 0.18)	2.23E-01	4.24E-01
PC(P-32:0)	-0.13 (-0.55 - 0.29)	5.40E-01	8.02E-01	-0.27 (-0.66 - 0.11)	1.68E-01	3.57E-01
PC(P-32:1)	-0.28 (-0.67 - 0.12)	1.73E-01	4.60E-01	-0.29 (-0.70 - 0.13)	1.78E-01	3.65E-01
PC(P-34:1)	-0.33 (-0.91 - 0.25)	2.69E-01	5.63E-01	-0.54 (-1.22 - 0.13)	1.22E-01	2.85E-01
PC(P-34:2)	-0.10 (-0.67 - 0.47)	7.41E-01	8.96E-01	-0.23 (-0.84 - 0.37)	4.56E-01	6.48E-01

	HOMA-IR[a] (fasting plasma)			HOMA-IR[a] (steady-state clamp plasma)		
Lipid species	**β-Coefficient (95% CI)[b]**	**Uncorrected *P*-value**	**Corrected *P*-value[c]**	**β-Coefficient (95% CI)[b]**	**Uncorrected *P*-value**	**Corrected *P*-value[c]**
PC(P-34:3)	-0.06 (-0.61 - 0.48)	8.26E-01	9.19E-01	-0.01 (-0.54 - 0.52)	9.58E-01	9.76E-01
PC(P-36:2)	0.07 (-0.50 - 0.65)	8.06E-01	9.14E-01	-0.24 (-0.91 - 0.44)	4.98E-01	6.73E-01
PC(P-36:4)	-0.02 (-0.54 - 0.49)	9.28E-01	9.60E-01	0.09 (-0.49 - 0.66)	7.69E-01	8.46E-01
PC(P-36:5)	0.03 (-0.27 - 0.32)	8.64E-01	9.37E-01	0.02 (-0.25 - 0.28)	9.01E-01	9.32E-01
PC(P-38:5)	-0.06 (-0.47 - 0.34)	7.55E-01	9.04E-01	-0.09 (-0.47 - 0.29)	6.48E-01	7.85E-01
PC(P-40:5)	-0.10 (-0.58 - 0.39)	6.92E-01	8.83E-01	-0.21 (-0.73 - 0.31)	4.32E-01	6.38E-01
LPC 14:0	0.02 (-0.39 - 0.43)	9.22E-01	9.57E-01	0.25 (-0.19 - 0.69)	2.73E-01	4.86E-01
LPC 15:0	-0.06 (-0.45 - 0.32)	7.50E-01	9.01E-01	0.09 (-0.33 - 0.51)	6.83E-01	7.98E-01
LPC 16:0	-0.20 (-0.73 - 0.32)	4.55E-01	7.44E-01	-0.08 (-0.46 - 0.30)	6.73E-01	7.97E-01
LPC 16:1	-0.41 (-0.87 - 0.04)	8.25E-02	2.97E-01	-0.32 (-0.87 - 0.23)	2.54E-01	4.63E-01
LPC 17:0	-0.11 (-0.51 - 0.28)	5.86E-01	8.22E-01	-0.08 (-0.58 - 0.43)	7.70E-01	8.46E-01
LPC 17:1	-0.37 (-0.83 - 0.10)	1.31E-01	3.72E-01	-0.22 (-0.68 - 0.25)	3.68E-01	5.68E-01
LPC 18:0	-0.16 (-0.72 - 0.40)	5.74E-01	8.12E-01	0.04 (-0.46 - 0.54)	8.81E-01	9.25E-01
LPC 18:1	-0.38 (-0.80 - 0.04)	8.64E-02	3.01E-01	-0.50 (-1.02 - 0.02)	6.32E-02	1.90E-01
LPC 18:2	-0.34 (-0.77 - 0.08)	1.19E-01	3.55E-01	-0.38 (-0.81 - 0.04)	8.20E-02	2.26E-01
LPC 18:3	-0.12 (-0.42 - 0.18)	4.42E-01	7.30E-01	-0.12 (-0.48 - 0.25)	5.41E-01	6.98E-01
LPC 20:0	-0.29 (-0.68 - 0.10)	1.48E-01	4.12E-01	-0.20 (-0.56 - 0.16)	2.84E-01	4.88E-01
LPC 20:1	-0.47 (-0.92 - -0.02)	**4.70E-02**	2.21E-01	-0.31 (-0.75 - 0.13)	1.68E-01	3.57E-01
LPC 20:2	-0.40 (-0.85 - 0.04)	8.08E-02	2.97E-01	-0.24 (-0.70 - 0.22)	3.15E-01	5.12E-01
LPC 20:4	-0.35 (-0.79 - 0.10)	1.31E-01	3.72E-01	-0.26 (-0.64 - 0.12)	1.92E-01	3.79E-01
LPC 20:5	-0.31 (-0.83 - 0.20)	2.38E-01	5.26E-01	-0.23 (-0.63 - 0.17)	2.73E-01	4.86E-01
LPC 22:0	-0.24 (-0.68 - 0.21)	3.06E-01	5.98E-01	-0.25 (-0.62 - 0.13)	2.05E-01	4.02E-01
LPC 22:1	-0.53 (-0.94 - -0.12)	**1.52E-02**	1.02E-01	-0.54 (-0.98 - -0.11)	**1.82E-02**	7.60E-02
LPC 22:5	-0.70 (-1.24 - -0.16)	**1.45E-02**	9.86E-02	-0.76 (-1.34 - -0.18)	**1.36E-02**	6.08E-02
LPC 22:6	-0.71 (-1.15 - -0.26)	**3.03E-03**	**3.37E-02**	-0.69 (-1.14 - -0.23)	**5.00E-03**	**2.73E-02**
LPC 24:0	-0.14 (-0.57 - 0.30)	5.47E-01	8.02E-01	-0.31 (-0.69 - 0.07)	1.15E-01	2.70E-01
LPC 26:0	-0.53 (-1.11 - 0.05)	8.01E-02	2.97E-01	-0.25 (-0.61 - 0.10)	1.69E-01	3.57E-01
LPC(O-16:0)	-0.22 (-0.78 - 0.34)	4.38E-01	7.28E-01	-0.04 (-0.56 - 0.48)	8.77E-01	9.25E-01
LPC(O-18:0)	-0.22 (-0.82 - 0.38)	4.76E-01	7.75E-01	0.05 (-0.47 - 0.58)	8.40E-01	9.01E-01
LPC(O-18:1)	-0.29 (-0.72 - 0.14)	1.94E-01	4.83E-01	-0.09 (-0.60 - 0.42)	7.32E-01	8.23E-01
LPC(O-20:0)	-0.27 (-0.83 - 0.29)	3.56E-01	6.41E-01	-0.32 (-0.87 - 0.23)	2.61E-01	4.74E-01

	HOMA-IR[a] (fasting plasma)			HOMA-IR[a] (steady-state clamp plasma)		
Lipid species	**β-Coefficient (95% CI)[b]**	**Uncorrected *P*-value**	**Corrected *P*-value[c]**	**β-Coefficient (95% CI)[b]**	**Uncorrected *P*-value**	**Corrected *P*-value[c]**
LPC(O-22:0)	-0.19 (-0.78 - 0.40)	5.35E-01	8.02E-01	-0.14 (-0.56 - 0.28)	5.07E-01	6.75E-01
LPC(O-22:1)	-0.37 (-0.83 - 0.10)	1.26E-01	3.66E-01	-0.50 (-0.90 - -0.09)	**2.03E-02**	8.29E-02
LPC(O-24:0)	-0.14 (-0.56 - 0.27)	5.01E-01	7.78E-01	-0.23 (-0.58 - 0.12)	2.11E-01	4.09E-01
LPC(O-24:1)	-0.28 (-0.68 - 0.13)	1.84E-01	4.81E-01	-0.30 (-0.65 - 0.06)	1.10E-01	2.66E-01
LPC(O-24:2)	-0.63 (-1.15 - -0.11)	**2.22E-02**	1.33E-01	-0.86 (-1.50 - -0.21)	**1.21E-02**	5.53E-02
PE 32:0	0.04 (-0.32 - 0.40)	8.31E-01	9.19E-01	0.43 (-0.01 - 0.87)	6.36E-02	1.90E-01
PE 32:1	0.17 (-0.15 - 0.48)	3.11E-01	5.98E-01	0.39 (0.01 - 0.77)	**4.87E-02**	1.58E-01
PE 34:1	0.21 (-0.16 - 0.57)	2.70E-01	5.63E-01	0.39 (0.05 - 0.72)	**2.96E-02**	1.11E-01
PE 34:2	0.26 (-0.04 - 0.55)	9.42E-02	3.12E-01	0.37 (0.07 - 0.67)	**2.11E-02**	8.38E-02
PE 34:3	0.18 (-0.17 - 0.52)	3.16E-01	6.02E-01	0.31 (-0.02 - 0.64)	7.16E-02	2.10E-01
PE 35:1	0.29 (-0.03 - 0.61)	8.01E-02	2.97E-01	0.48 (0.13 - 0.82)	**8.80E-03**	**4.27E-02**
PE 35:2	0.26 (-0.04 - 0.56)	9.15E-02	3.12E-01	0.39 (0.11 - 0.68)	**9.57E-03**	**4.57E-02**
PE 36:0	-0.40 (-0.86 - 0.05)	8.66E-02	3.01E-01	0.16 (-0.36 - 0.67)	5.57E-01	7.11E-01
PE 36:1	0.39 (0.02 - 0.77)	**4.62E-02**	2.21E-01	0.40 (0.08 - 0.72)	**1.88E-02**	7.74E-02
PE 36:2	0.30 (0.02 - 0.59)	**4.03E-02**	2.01E-01	0.37 (0.10 - 0.63)	**8.81E-03**	**4.27E-02**
PE 36:3	0.25 (-0.15 - 0.65)	2.26E-01	5.10E-01	0.41 (0.06 - 0.77)	**2.72E-02**	1.06E-01
PE 36:4	0.13 (-0.15 - 0.41)	3.70E-01	6.56E-01	0.31 (0.03 - 0.60)	**3.72E-02**	1.31E-01
PE 36:5	0.09 (-0.36 - 0.53)	6.99E-01	8.88E-01	0.28 (-0.05 - 0.60)	1.04E-01	2.60E-01
PE 38:3	0.15 (-0.14 - 0.45)	3.09E-01	5.98E-01	0.44 (0.10 - 0.78)	**1.38E-02**	6.08E-02
PE 38:4	0.08 (-0.20 - 0.37)	5.67E-01	8.12E-01	0.40 (0.05 - 0.75)	**3.01E-02**	1.12E-01
PE 38:5	0.14 (-0.34 - 0.62)	5.77E-01	8.13E-01	0.44 (0.00 - 0.88)	5.51E-02	1.75E-01
PE 38:6	0.04 (-0.33 - 0.41)	8.22E-01	9.19E-01	0.24 (-0.10 - 0.57)	1.69E-01	3.57E-01
PE 40:5	0.05 (-0.33 - 0.44)	7.87E-01	9.12E-01	0.38 (0.01 - 0.74)	**4.74E-02**	1.57E-01
PE 40:6	0.11 (-0.26 - 0.47)	5.70E-01	8.12E-01	0.35 (-0.07 - 0.77)	1.05E-01	2.60E-01
PE 40:7	-0.09 (-0.53 - 0.35)	6.93E-01	8.83E-01	0.22 (-0.27 - 0.71)	3.91E-01	5.92E-01
PE(O-34:1)	0.27 (-0.13 - 0.68)	1.95E-01	4.83E-01	0.31 (-0.20 - 0.82)	2.40E-01	4.45E-01
PE(O-34:2)	0.45 (-0.02 - 0.91)	6.65E-02	2.74E-01	0.43 (-0.07 - 0.93)	1.00E-01	2.53E-01
PE(O-36:2)	0.18 (-0.23 - 0.58)	3.92E-01	6.75E-01	0.04 (-0.47 - 0.54)	8.91E-01	9.26E-01
PE(O-36:3)	0.25 (-0.13 - 0.63)	1.98E-01	4.86E-01	0.28 (-0.08 - 0.64)	1.37E-01	3.12E-01
PE(O-36:4)	0.21 (-0.20 - 0.63)	3.12E-01	5.98E-01	0.31 (-0.12 - 0.73)	1.61E-01	3.52E-01
PE(O-36:5)	-0.03 (-0.47 - 0.42)	9.13E-01	9.56E-01	0.14 (-0.30 - 0.58)	5.41E-01	6.98E-01

	HOMA-IR[a] (fasting plasma)			HOMA-IR[a] (steady-state clamp plasma)		
Lipid species	**β-Coefficient (95% CI)[b]**	**Uncorrected *P*-value**	**Corrected *P*-value[c]**	**β-Coefficient (95% CI)[b]**	**Uncorrected *P*-value**	**Corrected *P*-value[c]**
PE(O-36:6)	0.12 (-0.22 - 0.47)	4.85E-01	7.77E-01	0.08 (-0.28 - 0.44)	6.60E-01	7.90E-01
PE(O-38:4)	0.14 (-0.32 - 0.60)	5.55E-01	8.03E-01	0.26 (-0.20 - 0.72)	2.76E-01	4.86E-01
PE(O-38:5)	0.21 (-0.15 - 0.57)	2.56E-01	5.55E-01	0.32 (-0.11 - 0.74)	1.49E-01	3.31E-01
PE(O-40:4)	-0.14 (-0.57 - 0.29)	5.34E-01	8.02E-01	0.24 (-0.20 - 0.67)	2.89E-01	4.95E-01
PE(O-40:5)	0.07 (-0.30 - 0.45)	7.07E-01	8.91E-01	0.14 (-0.30 - 0.59)	5.30E-01	6.98E-01
PE(O-40:6)	-0.01 (-0.37 - 0.35)	9.69E-01	9.78E-01	0.40 (-0.04 - 0.84)	7.88E-02	2.23E-01
PE(O-40:7)	-0.09 (-0.44 - 0.26)	6.12E-01	8.31E-01	-0.16 (-0.60 - 0.28)	4.86E-01	6.70E-01
PE(O-42:7)	-0.71 (-1.20 - -0.22)	**6.45E-03**	5.55E-02	-0.78 (-1.22 - -0.35)	**9.74E-04**	**7.23E-03**
PE(P-34:1)	0.11 (-0.36 - 0.58)	6.45E-01	8.47E-01	0.21 (-0.23 - 0.65)	3.54E-01	5.57E-01
PE(P-34:2)	0.52 (0.00 - 1.03)	5.40E-02	2.41E-01	0.51 (-0.02 - 1.03)	6.50E-02	1.92E-01
PE(P-36:1)	0.43 (-0.04 - 0.90)	8.23E-02	2.97E-01	0.12 (-0.29 - 0.54)	5.57E-01	7.11E-01
PE(P-36:2)	0.48 (0.03 - 0.94)	**4.37E-02**	2.15E-01	0.51 (-0.01 - 1.03)	6.19E-02	1.90E-01
PE(P-36:4)	0.21 (-0.29 - 0.72)	4.18E-01	7.02E-01	0.31 (-0.06 - 0.68)	1.07E-01	2.62E-01
PE(P-37:4)	0.05 (-0.40 - 0.49)	8.40E-01	9.26E-01	0.19 (-0.34 - 0.71)	4.91E-01	6.72E-01
PE(P-38:4)	0.07 (-0.41 - 0.55)	7.80E-01	9.12E-01	0.40 (-0.05 - 0.84)	8.49E-02	2.31E-01
PE(P-38:5)	0.13 (-0.35 - 0.61)	5.96E-01	8.23E-01	0.21 (-0.36 - 0.77)	4.75E-01	6.61E-01
PE(P-38:6)	0.02 (-0.33 - 0.37)	9.13E-01	9.56E-01	0.01 (-0.39 - 0.41)	9.75E-01	9.90E-01
PE(P-40:4)	-0.22 (-0.57 - 0.13)	2.29E-01	5.13E-01	-0.07 (-0.34 - 0.20)	6.12E-01	7.57E-01
PE(P-40:5)	-0.05 (-0.49 - 0.39)	8.22E-01	9.19E-01	-0.03 (-0.41 - 0.36)	8.93E-01	9.26E-01
PE(P-40:6)	-0.01 (-0.41 - 0.39)	9.50E-01	9.74E-01	0.00 (-0.45 - 0.45)	9.92E-01	9.95E-01
LPE 16:0	-0.53 (-1.11 - 0.06)	8.26E-02	2.97E-01	-0.09 (-0.66 - 0.48)	7.61E-01	8.41E-01
LPE 16:1	-0.06 (-0.50 - 0.38)	7.80E-01	9.12E-01	0.17 (-0.19 - 0.54)	3.61E-01	5.64E-01
LPE 18:0	-0.32 (-0.90 - 0.26)	2.81E-01	5.79E-01	0.16 (-0.24 - 0.55)	4.44E-01	6.40E-01
LPE 18:1	-0.07 (-0.47 - 0.33)	7.21E-01	8.96E-01	0.19 (-0.17 - 0.55)	3.00E-01	5.01E-01
LPE 18:2	-0.02 (-0.49 - 0.44)	9.18E-01	9.57E-01	0.22 (-0.19 - 0.63)	2.95E-01	4.97E-01
LPE 20:4	-0.05 (-0.57 - 0.48)	8.59E-01	9.37E-01	0.39 (0.03 - 0.75)	**3.86E-02**	1.34E-01
LPE 22:5	-0.04 (-0.47 - 0.39)	8.60E-01	9.37E-01	0.25 (-0.15 - 0.64)	2.25E-01	4.25E-01
LPE 22:6	-0.50 (-0.92 - -0.08)	**2.53E-02**	1.45E-01	-0.05 (-0.45 - 0.34)	7.97E-01	8.67E-01
PI 32:0	0.33 (0.02 - 0.64)	**4.46E-02**	2.16E-01	0.47 (0.08 - 0.86)	**2.08E-02**	8.36E-02
PI 32:1	0.11 (-0.22 - 0.45)	5.10E-01	7.85E-01	0.22 (-0.15 - 0.59)	2.41E-01	4.45E-01
PI 34:0	0.29 (-0.12 - 0.70)	1.67E-01	4.46E-01	0.38 (-0.08 - 0.84)	1.13E-01	2.68E-01

	HOMA-IR[a] (fasting plasma)			HOMA-IR[a] (steady-state clamp plasma)		
Lipid species	**β-Coefficient (95% CI)[b]**	**Uncorrected *P*-value**	**Corrected *P*-value[c]**	**β-Coefficient (95% CI)[b]**	**Uncorrected *P*-value**	**Corrected *P*-value[c]**
PI 34:1	0.21 (-0.20 - 0.61)	3.20E-01	6.03E-01	0.25 (-0.12 - 0.62)	1.89E-01	3.78E-01
PI 36:1	0.22 (-0.19 - 0.62)	3.09E-01	5.98E-01	0.16 (-0.18 - 0.50)	3.57E-01	5.60E-01
PI 36:2	0.19 (-0.16 - 0.54)	2.83E-01	5.79E-01	0.16 (-0.15 - 0.48)	3.06E-01	5.08E-01
PI 36:3	0.17 (-0.21 - 0.56)	3.73E-01	6.56E-01	0.21 (-0.12 - 0.53)	2.18E-01	4.15E-01
PI 36:4	0.17 (-0.20 - 0.54)	3.73E-01	6.56E-01	0.38 (0.02 - 0.73)	**4.27E-02**	1.47E-01
PI 38:2	0.29 (-0.13 - 0.70)	1.87E-01	4.83E-01	0.37 (-0.11 - 0.86)	1.40E-01	3.19E-01
PI 38:3	0.23 (-0.18 - 0.64)	2.79E-01	5.78E-01	0.33 (-0.03 - 0.70)	7.99E-02	2.24E-01
PI 38:4	0.15 (-0.28 - 0.58)	4.99E-01	7.78E-01	0.33 (0.00 - 0.66)	5.69E-02	1.77E-01
PI 38:5	-0.03 (-0.49 - 0.43)	9.03E-01	9.52E-01	0.27 (-0.12 - 0.65)	1.78E-01	3.65E-01
PI 38:6	0.12 (-0.36 - 0.60)	6.38E-01	8.47E-01	0.33 (-0.22 - 0.88)	2.46E-01	4.51E-01
PI 40:4	0.22 (-0.32 - 0.76)	4.23E-01	7.06E-01	0.43 (-0.12 - 0.99)	1.33E-01	3.05E-01
PI 40:5	0.14 (-0.24 - 0.51)	4.79E-01	7.76E-01	0.25 (-0.11 - 0.62)	1.82E-01	3.69E-01
PI 40:6	-0.04 (-0.48 - 0.40)	8.70E-01	9.38E-01	0.05 (-0.39 - 0.49)	8.26E-01	8.90E-01
PS 36:1	-0.49 (-1.00 - 0.02)	6.44E-02	2.69E-01	0.06 (-0.37 - 0.50)	7.77E-01	8.49E-01
PS 36:2	-0.38 (-0.83 - 0.08)	1.09E-01	3.42E-01	0.14 (-0.34 - 0.62)	5.66E-01	7.13E-01
PS 38:3	-0.42 (-0.83 - 0.00)	5.34E-02	2.41E-01	0.11 (-0.30 - 0.51)	6.04E-01	7.53E-01
PS 38:4	-0.42 (-0.85 - 0.02)	6.80E-02	2.75E-01	0.10 (-0.29 - 0.48)	6.25E-01	7.62E-01
PS 38:5	-0.44 (-0.90 - 0.03)	7.13E-02	2.80E-01	0.09 (-0.33 - 0.51)	6.69E-01	7.95E-01
PS 40:5	-0.39 (-0.87 - 0.09)	1.14E-01	3.50E-01	0.06 (-0.29 - 0.40)	7.53E-01	8.36E-01
PS 40:6	-0.26 (-0.64 - 0.13)	1.94E-01	4.83E-01	-0.02 (-0.36 - 0.32)	8.93E-01	9.26E-01
COH	0.00 (-0.45 - 0.45)	9.99E-01	9.99E-01	0.18 (-0.24 - 0.60)	4.00E-01	6.00E-01
CE 14:0	0.46 (0.10 - 0.83)	**1.70E-02**	1.07E-01	0.63 (0.30 - 0.97)	**5.11E-04**	**4.49E-03**
CE 15:0	0.58 (0.05 - 1.12)	**3.76E-02**	1.96E-01	0.73 (0.33 - 1.13)	**7.23E-04**	**5.62E-03**
CE 16:0	0.59 (0.21 - 0.96)	**3.77E-03**	**3.93E-02**	0.58 (0.17 - 0.99)	**8.14E-03**	**4.06E-02**
CE 16:1	0.27 (-0.03 - 0.57)	8.45E-02	3.00E-01	0.54 (0.19 - 0.90)	**4.14E-03**	**2.39E-02**
CE 16:2	0.64 (0.18 - 1.11)	**8.98E-03**	6.81E-02	0.83 (0.45 - 1.20)	**7.67E-05**	**2.02E-03**
CE 17:0	0.09 (-0.31 - 0.50)	6.53E-01	8.52E-01	0.51 (0.10 - 0.91)	**1.72E-02**	7.26E-02
CE 17:1	0.13 (-0.43 - 0.70)	6.46E-01	8.47E-01	0.31 (-0.15 - 0.78)	1.91E-01	3.79E-01
CE 18:0	0.35 (-0.06 - 0.76)	1.02E-01	3.21E-01	0.41 (0.01 - 0.80)	**4.79E-02**	1.57E-01
CE 18:1	0.66 (0.21 - 1.12)	**5.99E-03**	5.41E-02	0.54 (0.22 - 0.87)	**1.90E-03**	**1.25E-02**
CE 18:2	0.75 (0.40 - 1.11)	**1.09E-04**	**7.29E-03**	0.52 (0.33 - 0.72)	**4.25E-06**	**1.01E-03**

	HOMA-IR[a] (fasting plasma)			HOMA-IR[a] (steady-state clamp plasma)		
Lipid species	**β-Coefficient (95% CI)[b]**	**Uncorrected *P*-value**	**Corrected *P*-value[c]**	**β-Coefficient (95% CI)[b]**	**Uncorrected *P*-value**	**Corrected *P*-value[c]**
CE 18:3	0.33 (0.08 - 0.58)	**1.44E-02**	9.86E-02	0.50 (0.21 - 0.78)	**1.14E-03**	**8.29E-03**
CE 20:1	-0.14 (-0.53 - 0.25)	4.86E-01	7.77E-01	-0.09 (-0.59 - 0.40)	7.17E-01	8.12E-01
CE 20:3	0.56 (0.25 - 0.88)	**1.04E-03**	**2.14E-02**	0.57 (0.30 - 0.84)	**1.37E-04**	**2.58E-03**
CE 20:4	0.42 (0.13 - 0.70)	**5.93E-03**	5.41E-02	0.58 (0.34 - 0.83)	**2.64E-05**	**1.47E-03**
CE 20:5	0.27 (-0.09 - 0.64)	1.49E-01	4.12E-01	0.46 (0.15 - 0.77)	**5.16E-03**	**2.73E-02**
CE 22:0	0.40 (0.09 - 0.72)	**1.57E-02**	1.03E-01	0.28 (-0.04 - 0.60)	9.01E-02	2.41E-01
CE 22:1	-0.13 (-0.50 - 0.25)	5.21E-01	7.93E-01	-0.13 (-0.61 - 0.35)	5.86E-01	7.33E-01
CE 22:4	0.25 (-0.13 - 0.62)	2.00E-01	4.86E-01	0.54 (0.18 - 0.90)	**5.22E-03**	**2.73E-02**
CE 22:5	0.39 (0.04 - 0.74)	**3.21E-02**	1.76E-01	0.64 (0.27 - 1.01)	**1.39E-03**	**9.34E-03**
CE 22:6	0.32 (-0.08 - 0.72)	1.28E-01	3.69E-01	0.40 (0.19 - 0.61)	**4.78E-04**	**4.44E-03**
CE 24:0	0.31 (0.09 - 0.53)	**7.71E-03**	6.13E-02	0.30 (-0.05 - 0.66)	9.74E-02	2.48E-01
CE 24:1	0.09 (-0.33 - 0.52)	6.71E-01	8.69E-01	0.22 (-0.20 - 0.63)	3.09E-01	5.08E-01
CE 24:4	0.03 (-0.38 - 0.45)	8.74E-01	9.38E-01	-0.08 (-0.48 - 0.32)	7.06E-01	8.08E-01
CE 24:5	0.24 (-0.13 - 0.60)	2.08E-01	4.88E-01	0.41 (0.00 - 0.81)	5.55E-02	1.75E-01
CE 24:6	0.28 (-0.15 - 0.72)	2.11E-01	4.92E-01	0.60 (0.20 - 1.00)	**5.14E-03**	**2.73E-02**
DG 14:0/16:0	0.31 (0.13 - 0.49)	**1.36E-03**	**2.14E-02**	0.37 (0.18 - 0.55)	**2.82E-04**	**3.14E-03**
DG 14:0/18:1	0.43 (0.19 - 0.66)	**9.14E-04**	**2.04E-02**	0.27 (0.14 - 0.40)	**1.39E-04**	**2.58E-03**
DG 14:0/18:2	0.31 (0.12 - 0.50)	**2.22E-03**	**2.65E-02**	0.36 (0.17 - 0.54)	**3.65E-04**	**3.81E-03**
DG 16:0/16:0	0.26 (0.13 - 0.40)	**3.49E-04**	**1.43E-02**	0.32 (0.16 - 0.48)	**2.49E-04**	**3.07E-03**
DG 16:0/18:0	0.51 (0.28 - 0.73)	**5.69E-05**	**7.29E-03**	0.31 (0.16 - 0.46)	**1.35E-04**	**2.58E-03**
DG 16:0/18:1	0.43 (0.21 - 0.64)	**3.69E-04**	**1.43E-02**	0.31 (0.16 - 0.46)	**1.93E-04**	**3.07E-03**
DG 16:0/18:2	0.34 (0.14 - 0.53)	**1.18E-03**	**2.14E-02**	0.27 (0.13 - 0.41)	**6.09E-04**	**4.96E-03**
DG 16:0/20:0	0.71 (0.39 - 1.03)	**5.91E-05**	**7.29E-03**	0.65 (0.37 - 0.92)	**3.23E-05**	**1.54E-03**
DG 16:0/20:3	0.47 (0.21 - 0.74)	**1.10E-03**	**2.14E-02**	0.32 (0.15 - 0.49)	**4.84E-04**	**4.44E-03**
DG 16:0/20:4	0.42 (0.19 - 0.65)	**7.84E-04**	**2.04E-02**	0.38 (0.18 - 0.59)	**5.53E-04**	**4.65E-03**
DG 16:0/22:5	0.43 (0.14 - 0.73)	**5.65E-03**	5.39E-02	0.40 (0.17 - 0.62)	**1.34E-03**	**9.33E-03**
DG 16:0/22:6	0.33 (-0.06 - 0.71)	1.01E-01	3.20E-01	0.42 (0.11 - 0.73)	**1.03E-02**	**4.87E-02**
DG 16:1/18:0	0.35 (0.13 - 0.57)	**3.03E-03**	**3.37E-02**	0.31 (0.14 - 0.48)	**9.66E-04**	**7.23E-03**
DG 16:1/18:1	0.28 (0.04 - 0.53)	**2.95E-02**	1.67E-01	0.36 (0.15 - 0.56)	**1.27E-03**	**9.02E-03**
DG 18:0/18:0	0.19 (0.04 - 0.35)	**1.82E-02**	1.11E-01	0.41 (0.19 - 0.62)	**4.48E-04**	**4.44E-03**
DG 18:0/18:1	0.64 (0.35 - 0.94)	**1.06E-04**	**7.29E-03**	0.39 (0.21 - 0.57)	**7.86E-05**	**2.02E-03**

	HOMA-IR[a] (fasting plasma)			HOMA-IR[a] (steady-state clamp plasma)		
Lipid species	**β-Coefficient (95% CI)[b]**	**Uncorrected *P*-value**	**Corrected *P*-value[c]**	**β-Coefficient (95% CI)[b]**	**Uncorrected *P*-value**	**Corrected *P*-value[c]**
DG 18:0/18:2	0.38 (0.16 - 0.60)	**1.41E-03**	**2.14E-02**	0.35 (0.18 - 0.53)	**2.74E-04**	**3.14E-03**
DG 18:0/20:4	0.36 (-0.02 - 0.74)	6.84E-02	2.75E-01	0.44 (0.21 - 0.67)	**4.92E-04**	**4.44E-03**
DG 18:1/18:1	0.52 (0.21 - 0.83)	**1.78E-03**	**2.28E-02**	0.39 (0.20 - 0.57)	**1.57E-04**	**2.62E-03**
DG 18:1/18:2	0.39 (0.09 - 0.69)	**1.39E-02**	9.86E-02	0.38 (0.16 - 0.60)	**1.40E-03**	**9.34E-03**
DG 18:1/18:3	0.25 (0.02 - 0.47)	**3.82E-02**	1.96E-01	0.27 (0.09 - 0.44)	**4.94E-03**	**2.73E-02**
DG 18:1/20:0	0.66 (0.35 - 0.96)	**1.02E-04**	**7.29E-03**	0.54 (0.26 - 0.82)	**3.63E-04**	**3.81E-03**
DG 18:1/20:3	0.40 (-0.01 - 0.81)	6.24E-02	2.64E-01	0.44 (0.14 - 0.74)	**6.29E-03**	**3.18E-02**
DG 18:1/20:4	0.39 (0.11 - 0.67)	**8.43E-03**	6.54E-02	0.47 (0.17 - 0.77)	**3.52E-03**	**2.14E-02**
DG 18:2/18:2	0.20 (-0.03 - 0.43)	9.70E-02	3.15E-01	0.27 (0.07 - 0.47)	**1.20E-02**	5.53E-02
TG 14:0/16:0/18:1	0.40 (0.12 - 0.67)	**7.42E-03**	6.05E-02	0.69 (0.35 - 1.03)	**2.50E-04**	**3.07E-03**
TG 14:0/16:0/18:2	0.21 (0.02 - 0.41)	**3.35E-02**	1.77E-01	0.43 (0.15 - 0.71)	**3.74E-03**	**2.22E-02**
TG 14:0/16:1/18:1	0.20 (-0.02 - 0.43)	8.16E-02	2.97E-01	0.57 (0.20 - 0.95)	**4.35E-03**	**2.46E-02**
TG 14:0/16:1/18:2	0.18 (-0.03 - 0.38)	9.52E-02	3.12E-01	0.32 (0.05 - 0.59)	**2.48E-02**	9.76E-02
TG 14:0/17:0/18:1	0.53 (0.22 - 0.83)	**1.39E-03**	**2.14E-02**	1.04 (0.63 - 1.45)	**9.95E-06**	**1.11E-03**
TG 14:0/18:0/18:1	0.50 (0.22 - 0.77)	**9.11E-04**	**2.04E-02**	0.80 (0.45 - 1.15)	**4.72E-05**	**1.58E-03**
TG 14:0/18:2/18:2	0.23 (-0.03 - 0.49)	8.94E-02	3.08E-01	0.31 (0.00 - 0.62)	5.84E-02	1.81E-01
TG 14:1/16:0/18:1	0.28 (0.01 - 0.55)	5.02E-02	2.33E-01	0.57 (0.20 - 0.94)	**3.79E-03**	**2.22E-02**
TG 14:1/16:1/18:0	0.17 (-0.07 - 0.41)	1.63E-01	4.38E-01	0.40 (0.09 - 0.70)	**1.45E-02**	6.31E-02
TG 14:1/18:0/18:2	0.37 (0.04 - 0.70)	**3.22E-02**	1.76E-01	0.55 (0.20 - 0.91)	**3.44E-03**	**2.13E-02**
TG 14:1/18:1/18:1	0.22 (-0.04 - 0.49)	1.01E-01	3.20E-01	0.42 (0.09 - 0.75)	**1.50E-02**	6.40E-02
TG 15:0/16:0/18:1	0.43 (0.18 - 0.68)	**1.53E-03**	**2.14E-02**	0.76 (0.44 - 1.07)	**1.97E-05**	**1.37E-03**
TG 15:0/18:1/18:1	0.43 (0.15 - 0.72)	**4.00E-03**	**4.05E-02**	1.10 (0.62 - 1.58)	**4.57E-05**	**1.58E-03**
TG 16:0/16:0/16:0	0.35 (0.16 - 0.54)	**8.37E-04**	**2.04E-02**	0.56 (0.30 - 0.82)	**9.53E-05**	**2.12E-03**
TG 16:0/16:0/18:0	0.35 (0.17 - 0.53)	**4.33E-04**	**1.45E-02**	0.48 (0.24 - 0.72)	**2.57E-04**	**3.07E-03**
TG 16:0/16:0/18:1	0.38 (0.15 - 0.61)	**1.91E-03**	**2.36E-02**	0.75 (0.42 - 1.07)	**3.88E-05**	**1.58E-03**
TG 16:0/16:0/18:2	0.27 (0.10 - 0.44)	**3.53E-03**	**3.81E-02**	0.50 (0.24 - 0.77)	**4.73E-04**	**4.44E-03**
TG 16:0/16:1/17:0	0.45 (0.18 - 0.72)	**1.78E-03**	**2.28E-02**	0.91 (0.53 - 1.28)	**2.04E-05**	**1.37E-03**
TG 16:0/16:1/18:1	0.28 (0.00 - 0.57)	5.63E-02	2.41E-01	0.65 (0.25 - 1.05)	**2.70E-03**	**1.73E-02**
TG 16:0/17:0/18:0	0.48 (0.20 - 0.76)	**1.44E-03**	**2.14E-02**	0.61 (0.33 - 0.88)	**7.37E-05**	**2.02E-03**
TG 16:0/17:0/18:1	0.61 (0.29 - 0.93)	**5.19E-04**	**1.58E-02**	0.97 (0.60 - 1.35)	**6.02E-06**	**1.01E-03**
TG 16:0/17:0/18:2	0.40 (0.11 - 0.70)	**9.97E-03**	7.40E-02	0.82 (0.42 - 1.22)	**2.32E-04**	**3.07E-03**

	HOMA-IR[a] (fasting plasma)			HOMA-IR[a] (steady-state clamp plasma)		
Lipid species	**β-Coefficient (95% CI)[b]**	**Uncorrected *P*-value**	**Corrected *P*-value[c]**	**β-Coefficient (95% CI)[b]**	**Uncorrected *P*-value**	**Corrected *P*-value[c]**
TG 16:0/18:0/18:1	0.51 (0.25 - 0.77)	**3.03E-04**	**1.43E-02**	0.63 (0.32 - 0.93)	**2.28E-04**	**3.07E-03**
TG 16:0/18:1/18:1	0.37 (0.08 - 0.65)	**1.61E-02**	1.03E-01	0.84 (0.38 - 1.29)	**6.99E-04**	**5.56E-03**
TG 16:0/18:1/18:2	0.29 (0.03 - 0.54)	**3.32E-02**	1.77E-01	0.50 (0.12 - 0.88)	**1.25E-02**	5.63E-02
TG 16:0/18:2/18:2	0.18 (-0.01 - 0.37)	7.06E-02	2.80E-01	0.32 (-0.01 - 0.65)	6.37E-02	1.90E-01
TG 16:1/16:1/16:1	0.13 (-0.10 - 0.35)	2.70E-01	5.63E-01	0.33 (0.01 - 0.65)	**4.75E-02**	1.57E-01
TG 16:1/16:1/18:0	0.40 (0.12 - 0.67)	**6.48E-03**	5.55E-02	0.73 (0.34 - 1.11)	**5.57E-04**	**4.65E-03**
TG 16:1/16:1/18:1	0.10 (-0.06 - 0.27)	2.19E-01	4.99E-01	0.33 (0.02 - 0.64)	**4.46E-02**	1.51E-01
TG 16:1/17:0/18:1	0.43 (0.13 - 0.72)	**6.87E-03**	5.73E-02	0.99 (0.54 - 1.45)	**9.16E-05**	**2.12E-03**
TG 16:1/18:1/18:1	0.16 (-0.17 - 0.48)	3.50E-01	6.37E-01	0.60 (0.02 - 1.17)	**4.96E-02**	1.59E-01
TG 16:1/18:1/18:2	0.23 (-0.08 - 0.54)	1.54E-01	4.19E-01	0.35 (-0.03 - 0.74)	7.68E-02	2.19E-01
TG 17:0/18:1/18:1	0.53 (0.18 - 0.88)	**4.94E-03**	**4.85E-02**	0.93 (0.49 - 1.37)	**1.50E-04**	**2.62E-03**
TG 18:0/18:0/18:0	0.24 (-0.03 - 0.51)	9.29E-02	3.12E-01	0.19 (-0.15 - 0.54)	2.79E-01	4.86E-01
TG 18:0/18:0/18:1	0.34 (0.14 - 0.54)	**1.53E-03**	**2.14E-02**	0.42 (0.21 - 0.63)	**2.13E-04**	**3.07E-03**
TG 18:0/18:1/18:1	0.58 (0.28 - 0.87)	**3.85E-04**	**1.43E-02**	0.63 (0.32 - 0.94)	**2.24E-04**	**3.07E-03**
TG 18:0/18:2/18:2	0.18 (-0.05 - 0.42)	1.25E-01	3.66E-01	0.38 (0.04 - 0.73)	**3.35E-02**	1.21E-01
TG 18:1/18:1/18:1	0.58 (0.15 - 1.01)	**1.14E-02**	8.27E-02	0.58 (0.21 - 0.94)	**3.34E-03**	**2.11E-02**
TG 18:1/18:1/18:2	0.20 (-0.14 - 0.55)	2.60E-01	5.60E-01	0.31 (-0.05 - 0.67)	9.72E-02	2.48E-01
TG 18:1/18:1/20:4	0.29 (-0.07 - 0.65)	1.15E-01	3.50E-01	0.40 (-0.06 - 0.87)	9.48E-02	2.46E-01
TG 18:1/18:1/22:6	0.24 (-0.20 - 0.69)	2.90E-01	5.80E-01	0.31 (-0.32 - 0.93)	3.38E-01	5.40E-01
TG 18:1/18:2/18:2	0.13 (-0.10 - 0.36)	2.64E-01	5.61E-01	0.23 (-0.10 - 0.56)	1.76E-01	3.65E-01
TG 18:2/18:2/18:2	0.07 (-0.09 - 0.23)	3.78E-01	6.61E-01	0.14 (-0.16 - 0.44)	3.63E-01	5.65E-01
TG 18:2/18:2/20:4	0.29 (-0.03 - 0.60)	7.91E-02	2.97E-01	0.15 (-0.22 - 0.52)	4.34E-01	6.39E-01

HOMA-IR, homeostasis model assessment of insulin resistance

[a] Linear regression of HOMA-IR versus each lipid species in the three non-diabetic groups, adjusted for age, sex, BMI and systolic blood pressure.

[b] Beta-coefficient (95% confidence intervals) based on an interquartile range increase in predictor lipid species measurement.

[c] *P*-value corrected for multiple comparisons using Benjamini-Hochberg method. Bold type indicates $P < 0.05$.